Durham E-Theses

The behaviour of laterally loaded two-pile groups

Arta, Mahmood Reza

How to cite:

Arta, Mahmood Reza (1992) *The behaviour of laterally loaded two-pile groups*, Durham theses, Durham University. Available at Durham E-Theses Online: http://etheses.dur.ac.uk/6122/

The Behaviour of Laterally Loaded
Two-Pile Groups

Mahmood Reza Arta BSc, MSc

A Thesis Submittted for the degree of

Doctor of Philosophy

in the Faculty of Science, University of Durham

Applied Mechanics Group

School of Engineering and Computer Science

Faculty of Science

University of Durham

January 1992

1 6 OCT 1992

Abstract

The response of piles and two-pile groups to lateral loading has been studied by field tests and computationally. Due to the lack of field test data and because of uncertainty concerning the pile/soil system it has been suggested that further experimental studies of pile groups under lateral loading should be undertaken.

The research was conducted through a series of tests on vertical single piles and two-pile groups at various spacing and pile cap overhang heights, to identify the lateral stiffness, bending moment and axial force distribution. Attempts were also made to measure the in-situ total lateral soil pressure on the pile walls. Piles were designed to behave as "long" pile since most piles used in the U.K. are long and flexible. Piles were instrumented with strain gauges for measurement of bending moments and axial forces. Field tests were conducted in a sand trench using 4.0m long piles. A stiff steel pile cap was used to connect head of the two piles firmly together.

Linear elastic back analyses of single pile tests were carried out to estimate the soil modulus profile with depth. Thereafter comparisons were made between the field test results on two-pile groups, published analyses and also a three dimensional finite element analysis. Tests results showed that the lateral stiffness of a two-pile groups tends towards a limit as spacing increases. A similar result was found from predictive and finite element analyses. The ratio between the maximum pile shaft bending moment and horizontal force varied between dry and wet season, being greater in the latter. The ratio between maximum reverse bending moment and horizontal load increased as the pile spacing and the overhang increased. Similar results results were found by finite element analysis.

One of the main achievements in this research was the measurement of the axial forces in the vertical piles due to lateral loading. It was found that as the pile spacing increased and pile cap overhang height decreasd the peak axial forces per unit load decreased. Similar results were obtained by three dimensional finite element analysis.

Acknowledgements

Statement of Copyright

Declaration

No material from this thesis has previously been submitted for a degree at this or any other university.

For Mitra, Mahnaz, and Hessom

Table of Contents

CHAPTER THREE

Experimental Programme

CHAPTER FOUR

Field Test Series Results

CHAPTER FIVE

Back Analysis of the Single Pile Field Test and Prediction

CHAPTER SEVEN

Discussion

CHAPTER EIGHT

Conclusions and Recommendations

List of Figures

xvi

List of Tables

List of Plates

NOTATION

The following parameters are those generally used in this thesis

If others are used they will be defined following their appearance

A	Ratio of modulus of elasticity E_s of cohesionless soil to over burden pressure; pile cross section area
A_y, A_s, A_m, A_v & A_p	Non dimensional coefficients relating an applied lateral force to deflection, slope, moment, shear and soil reaction respectively
A_e	Equivalent cross section
$[ABC]$	The flexibility coefficient matrix
$[a]$	Geometric matrix; transformation matrix of pile
B	Breadth of the loaded area
B_y, B_s, B_m, B_v & B_p	Non dimensional coefficients relating an applied moment to deflection, slope, moment, shear and soil reaction respectively
b	Width of the pile section
C_y	Non dimensional coefficient giving the deflection of a pile depending on the degree of fixity
c_u	Undrained shear strength of soil
D	Flexural rigidity
D_r	Relative density of sand
d	Pile diameter
E_{ef}	Effective elastic modulus of pile $\left(\frac{E_p I_p}{\frac{\pi r^4}{4}}\right)$
E_m	Mean value of pressuremeter modulus of elasticity over characteristic length
E_p	Elastic modulus of pile

E_s Elastic modulus of soil

e Eccentricity of pile above ground line; distance between the point of intersection of resultant forces with the underside of the pile cap and the neutral axis

F_y, F_m & F_p Non dimensional coefficients relating an applied lateral force to deflection, moment and shear force

F_U, F_θ Deflection and rotation factors which allow for soil yield (F_U', F_θ' refer to non-homogeneous soils and F_{Uf} refers to fixed head pile)

$[F]$ Force matrix

f Frequency; depth to plastic hinge over which there is a soil reaction from a laterally loaded pile

G Shear modulus of soil

G^* Product of $G(1 + \frac{3\nu}{4})$

G_c Average value of G^* over active length of pile

H Horizontal or lateral load

H_F or H_R Horizontal loads in the front and rear piles

H_G Total horizontal load on pile group

H_{UF} Ultimate lateral load capacity of a fixed headed pile

H_u Ultimate lateral load capacity of a pile

H_{ur} The reduced ultimate lateral load capacity of a pile

h Thickness of pressure cell diaphram; product of $\frac{H}{c_u d^3}$

I_p Second moment of area of a pile

I_{UH}, I_{UM}, $I_{\theta H}$, $I_{\theta M}$, I_{UF} Poulos dimensionless deformation factors (' refers to non-homogeneous soils)

I_H, I_{HM}, I_{HM}, I_{MM}, I_{FH} Banerjee and Davies dimensionless deformation factors (' refers to non-homogeneous soils)

I_{uy}, $I_{\theta y}$, I_{ufy}, I_{my}	Budhu and Davies yielding influence factors
K	Product of $\frac{E_{ef}}{n_h d}$; gauge factor
$[K]$	Stiffness matrix system
KN	Pile flexibility factor for noncohesive soils $\frac{E_p I_p}{n_h L^5}$
KR	Pile flexibility factor for cohesive soils $\frac{E_p I_p}{E_s L^4}$
K_o	Coefficient of earth pressure at rest
$K_a \& K_p$	Coefficients of active and passive soil pressure
K_h	Coefficient of subgrade reaction related to a pile $(K_h = k_h.B)(kN.m^{-2})$
$K_{hi} \& K_{hf}$	Terzaghi coefficients of horizontal subgrade reaction related to a pile, initial and final values
K_q	Brinch Hansen's earth pressure coefficient
K_v	Coefficient of vertical subgrade reaction for a pile of width B.
k_h	Terzaghi's coefficient of horizontal subgrade reaction $(kN.m^{-3})$
L	Embedded length of a pile
L_e	Equivalent length of a pile
L_{eH}, L_{eM} & L_{UF}	Equivalent length of a pile with respect to loading and pile head condition
l_c	Critical length of a pile
l_m	Distance between the Maximum bending moment and ground surface.
M_f	Fixing moment
M_{max}	Maximum bending moment on the pile shaft

M_t	Moment on a free headed pile
M_u	Ultimate bending moment in a pile
M_{yield}	Yielding moment in a pile
M_x	Bending moment on a pile shaft at depth x
m	Rate of increase of soil shear modulus with depth
m^*	Product of $m(1 + \frac{3\nu}{4})$
N	Average number of blows over the embedded length of the pile from SPTs.
$N_q \& N_\gamma$	Bearing capacity factors
n	Number of piles in a group
n_h	Terzaghi's rate of increase of coefficient of horizontal subgrade reaction with depth $(kN.m^{-3})$
n_{hi}	Initial value of n_h at small strain
P	Resolved axial components of vertical load ; Focht at el(1973) factor
$[P]$	Load vector
P_u	The ultimate lateral resistance of soil
P_{ua}	The ultimate lateral resistance of soil near the ground surface
P_{ud}	The ultimate lateral resistance of soil at depth
P_x	Axial load on the pile at depth x
p	Soil reaction
Q	Resolved horizontal component

R	Characteristic length of pile for homogeneous soil, $R = \sqrt[4]{\frac{E_p I_p}{k_h}}$; Relative rigidity ratio $\frac{E_p}{E_s}$; Resultant of a horizontal and vertical load
R_G	Group reduction factor for axially loaded pile
R_o	Reference radius
R_R	Group reduction factor referring to load
R_U	Group reduction factor referring to displacement
R_{UH}, R_{UM} & R_{UF}	Group reduction factors with respect to loading and pile head fixity
r	Radius of pile
S	Shear force
s	Spacing between pile centrelines
$[s]$	Stiffness matrix
T	Characteristic length of pile for non-homogeneous soils, $T = \sqrt[5]{\frac{E_p I_p}{n_h}}$
U	Pile head displacement
U_e	Lateral displacement of single pile head determined by elastic continuum
U_{ef}	Elastic lateral displacement of a fixed headed pile
U_{efF} & U_{efR}	Elastic lateral displacements of front and rear piles
U_g	Lateral Ground line deflection
$\bar{U}_g$	Elastic lateral displacement of a pile at ground line from unit horizontal force
U_s	Lateral displacement of single pile head determined by p/u analysis
U_u	Ultimate lateral displacement of single pile head

$U_v, U_h \& \theta$ Vertical, horizontal displacement and rotation of pile head

U_y Pile head lateral displacement referring to non-linear analysis

u Pile deflection

u_o Ground line deflection of pile or pile group

u_{oi} Limiting deformation of pile for which n_{hi} applies.

V Vertical component of load on individual pile

w_{max} Maximum deflection at the centre of pressure cell diaphram

x Distance between the pile and the neutral axis ; depth below the ground

Y Focht et al factor

Z Non dimensional depth parameter $(\frac{z}{T})$

z Depth below ground line

z_f Distance to point of virtual fixity

α A rheological factor

$\alpha_{UF}, \alpha_{UH}, \alpha_{UM}$ Interaction factors for deformation and rotation caused by
$\& \ \alpha_{\theta H}$ lateral load and moment

β Relative stiffness of pile $(\sqrt[4]{\frac{k_h}{4E_p I_p}})$; angle from the direction of loading of the pile

γ Unit weight of soil (' refers to effective unit weight of soil)

$[\delta]$ Deflection matrix

δ_ε Change in strain

$[\Delta]$ Product matrix

ε Strain

ηl	Lateral efficiency factor
θ_e	Slope or rotation of pile head referring to elastic analysis
θ_g	Slope or rotation of pile head at ground level
θ_y	Slope or rotation of pile head referring to non-linear analysis
ν	Poisson's ratio
π	Mathematical constant
ρ_c	Factor giving relative homogeneity of soil
σ_{max}	Maximum stress
ϕ	Angle of shearing resistance (' refers to effective angle of shearing resistance)

CHAPTER ONE

Introduction

1.1-Piling Applications

The purpose of piling a foundation is to transmit forces through a weak stratum to a lower stronger stratum having sufficient bearing capacity to support the structure. Piling may be required to support vertical, lateral or uplift loads. In recent years the search for oil has been extended to deeper waters. A structure in deep water needs to be sufficiently strong to resist large lateral forces due to wave and wind loading. Lateral loads on structures may be due to various sources for example earthquakes in areas such as Iran and Japan, cable pull on transmission towers, in harbour structures such as jetties, in offshore structures, in earth retaining walls, in bridge abutments and in lock construction. These lateral loads may be grouped in the following forms;

1 -Static

2 -Transient

3 -Cyclic

4 -Others

Figure 1.1 illustrates some types of lateral loading on piled foundations. Static types of loading include earth pressure and drag from stream flow. Transient loading includes earthquakes, ship berthing, vehicle braking, impact and wind. Cyclic loading includes

earthquakes and wave loading. The last group of lateral loading includes consolidation of soil, and effects of shrinkage, creep and thermal change. Often, a foundation will carry predominantly vertical loads, with only light horizontal loads, (e.g a building with wind loading), while jetties and mooring dolphins may be exposed solely to horizontal loads. It is the latter case which is the specific topic of this work.

Partly as a result of the use of simple pinned frame analysis, design of pile groups to resist lateral loading has been incorporated the use of raked piles. Installation of such piles proved to be expensive and the alternative approach of using of vertical piles to resist lateral load was considered. The design of vertical piles to carry horizontal loads should give consideration to:

1 -Bending strength and stiffness of the piles

2 -Pile group geometry

3 -Resistance of the soil

4 -Induced axial loads

5 -Lateral deflection

A range of analytical methods have been developed over the years for analysis of this complex system, ranging from simple equivalent structures, to modern computational techniques incorporating non-linear soil behaviour.

When bearing piles are connected together by a pile cap their behaviour is different from that of a single pile. Piles are normally used in groups in foundations and are usually long. The behaviour of a pile group is complex and prediction of group behaviour based on that of a single pile can be unreliable, a contributary factor to this difficulty being a deficiency of knowledge of the intraction between piles within the group. Another major difficulty arises in choosing suitable soil parameters as functions of depth and of deflection.

Many researchers have addressed the soil structure interaction problem of piles

designed to carry lateral loads in bridge abutments , retaining walls, harbour structures, jetties and offshore structures. Winkler(1867) introduced the elastic spring medium and Hetenyi(1946) presented solutions for a beam on elastic foundation, Terzaghi(1955) derived the coefficient of subgrade reaction method, Reese and Matlock(1956) and Davison and Gill (1963) adopted p-y curves. Hansen(1961), and Broms (1964a and 1964b) presented solutions based on ultimate capacity. Poulos (1971a,1971b, 1973, 1975 and 1979), Banerjee(1978), Banerjee and Driscoll(1976), Banerjee and Davies(1978) and Budhu and Davies(1987 and 1988) presented elastic continuum methods. Randolph (1981) presented a solution based on finite element solutions by axisymmetric means for analysing laterally loaded single piles and pile groups. A fuller review of relevant published work is given in chapter two.

There are several computer programs available to analyses pile groups. Reese(1977) presented a program for analysing laterally loaded single piles based on the p/u method. There are programs for analysing laterally loaded pile groups such as SW Pile by Midland road construction unit, Minipont by Department of transport, PGROUP3.0 by Department of transport, PILYLD by Department of Environment, PIGLET by Randolph(1980), LAWPILE by Wood(1979) and DEFPIG by Poulos(1975).

There have also been model tests to simulate the behaviour of pile groups, e.g Selby and Poulos(1985), Hughes et al (1980), Arta (1986), Long (1987). Full scale tests are few e.g Kim and Brungraber (1976 and 1979).

Two particular problems in the analysis of laterally loaded pile groups are the uneven distribution of bending moments between the piles and the magnitudes of the induced axial forces in the piles. There has been some experimental evidence to suggest that the moments in leading piles exceed those in trailing piles as a function of pile spacing. When a pile group is laterally loaded the front pile attracts axial compression load while the trailing pile experiences uplift forces. These axial forces

in the piles may vary with pile spacing due to lateral loading. There is only limited experimental or theoretical verification of the magnitude of the above effects.

1.2-Research Objectives

In this research the aim was to investigate the behaviour of two-pile groups subjected to horizontal loading in near to full scale tests. Pairs of piles were placed at 3, 5, 8 and 12 pile width spacing and were connected by a steel cap to form a two-pile group. Two such pairs of piles were installed and were pulled towards each other in order to obtain the lateral stiffness of the two-pile group, the moments, axial forces and changes in lateral soil pressures. The lateral load was applied at 150, 300 and 400mm above the ground line to observe the above effects due to variation in eccentric horizontal loading. Single pile tests were conducted to obtain the soil modulus profile. The piles consisted of two channel sections, with instruments mounted on each channel. The channels were welded together to form a 154mm square box pile with a shoe at the bottom of the each pile to make the driveability of the pile easier. Each pile was instrumented internally with strain gauges for deduction of both bending moments and axial forces. Pressure cells were mounted on the pile walls to deduce the change in lateral soil pressure.

The total length of each pile was 4m, with a 0.2m shoe forming the tip of each pile. They were driven 3.35m into the ground in order that the pile would behave as a long flexible pile.

A trench was excavated 6 × 1 × 2.2m deep which was back-filled with building sand. Two stand pipes were placed in the sand trench in order to allow dewatering the trench by hand pump, and also to observe the water table level. The piles were driven into the sand trench and for a short distance into the clay beneath. The program of tests carried out and the results are presented in chapter three and four respectively.

Single pile tests were carried out to allow back analysis for the soil stiffness profile. The results from back analyses and predictive analyses are presented in chapter five.

None of the published analyses offered prediction of axial forces in the two-pile group so linear elastic finite element analyses of single piles and two-pile groups were undertaken using PAFEC package. The pile/soil systems were modelled to match the site conditions. The finite element analyses of single piles and two-pile groups are presented in chapter six.

In order to assess the validity of the test results they were compared with published "predictive" methods and finite element analyses as reported in chapter seven. Final conclusions are drawn in chapter eight.
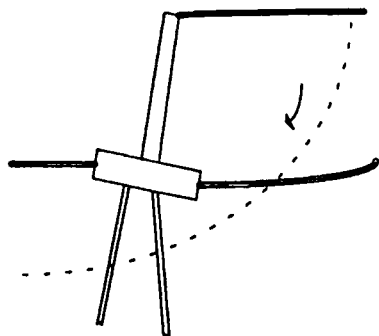
a) Active earth pressure on slope.
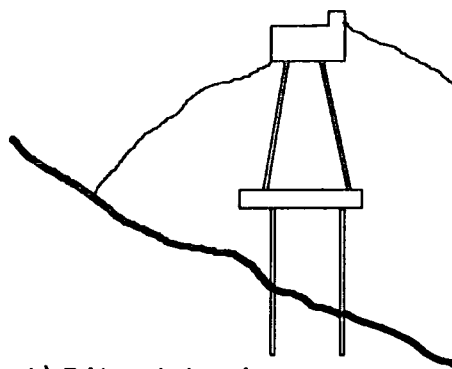
b) Bridge abutment
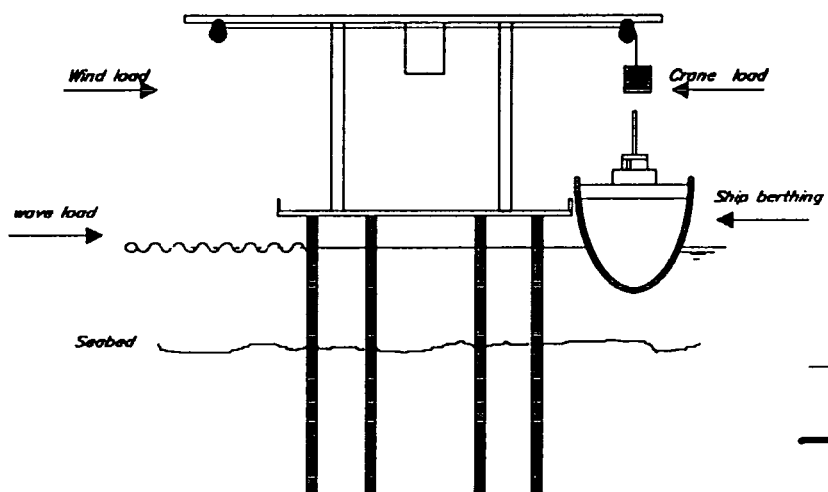
c) Jetty
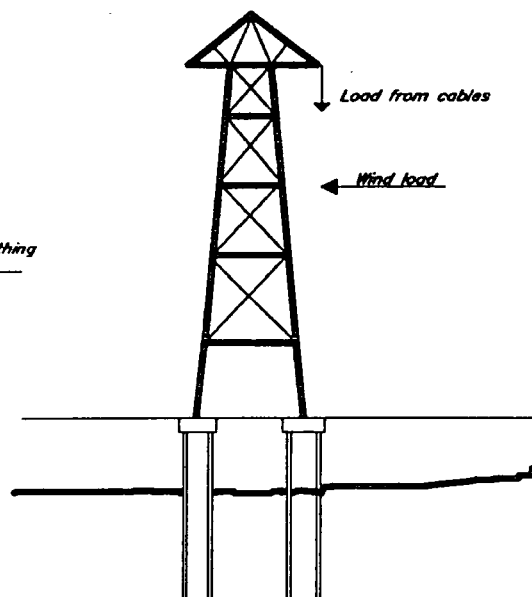
d) Electricity pylon
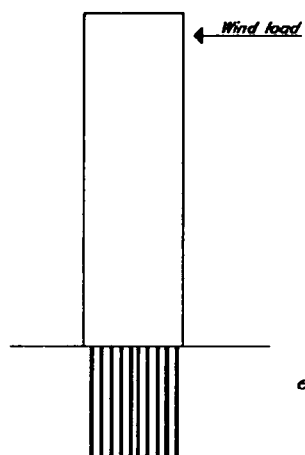
e) High rise building

Figure 1.1 Typical lateral loads on structures.

CHAPTER TWO

Literature Review

2.1-Introduction

The analysis of laterally loaded piles involves both the response of the soil to lateral movement of the pile and also the bending deflection of the pile. The soil offers resistance to the pile which is dependent on the stiffness of soil. The initial response of the soil is nearly linear elastic but, as the lateral deflection increases the soil starts to behave in a more plastic response and the stiffness reduces. Excessive deflection of the pile may result in yield of the pile which may be incorporated into an analytical solution. An analytical solution may assume a linear elastic soil continuum or an elastic-plastic soil. A number of analytical solutions have been developed by various authors to estimate the response of piles and pile groups which are laterally loaded. These analytical solutions have been developed in order to provide the design engineer with a realistic and economic method of dealing with laterally loaded piles.

Work in this area may be divided into two categories.

1 -The beam on elastic foundation solution which is based on work by Hetenyi (1946). The soil is modelled as a series of independent springs known as the Winkler model (see Figure 2.1). This method has been used to develop analytical solutions by Gleser(1953), Barbar (1953), McClelland and Focht (1958), Matlock

and Reese (1961) Reese (1971), Wood(1979) and others. Work on the Winkler soil method has also been extended to account for non-linear response of the soil. The non-linear analysis is based on developing p/u curves.

2 -The elastic continuum approach assumes that the soil is an elastic isotropic half space. Poulos (1971a, b, c) used the Mindlin (1936) solution for a single laterally loaded pile initially for a homogeneous soil. Poulos (1973) extended his solution to account for non-homogeneous soils. Banerjee and Davies (1978) used the Mindlin (1936) solution and extended the analytical solution into a heterogeneous soil, in which the soil stiffness increases linearly with depth. Randolph (1981) used a finite element axisymmetric method to develop elastic analysis for piles in both homogeneous and non-homogeneous soils. Budhu and Davies (1987 and 1988) also presented solutions based on the elastic continuum approach.

Both approaches have been used to develop methods of analysis for both single piles and pile groups under lateral load. The behaviour of a single pile differs from that of a group of piles. The difference is the single pile is not affected by any adjoining pile, whilst, in a group, piles interact. The behaviour of piles in a group is affected by the pile cap stiffness. Only a limited number of field tests on pile groups has been undertaken.

Toolan and Scotts (1979) presented a report on the use of laboratory and in-situ data to design piles under lateral loading. Elson(1985) presented a report on behalf of CIRIA which is a comprehensive review of the design of laterally loaded piles and pile groups.

In this chapter some of the published methods of analysis available for laterally loaded single piles and pile groups in both cohesive and non-cohesive soils are discussed, and later in this chapter reports are presented on some important lateral load tests on single piles and pile groups.

2.2-Horizontal Subgrade Modulus

Subgrade reaction is defined as the pressure per unit deflection of the surface of contact between the pile and the soil on which it bears and onto which it transfers the loads (see Figure 2.2).

Terzaghi(1955) presented his theory of horizontal subgrade reaction for a linear elastic soil material, assuming that the embedded length of the pile is supported by a series of discrete springs along the pile where the stiffness of a spring is defined by;

$$k_h = \frac{p}{u} \tag{2.1}$$

where k_h is the coefficient of subgrade reaction (units of kNm^{-3}), p is the horizontal soil pressure and u is the horizontal displacement. In the following text k_h will be replaced by K_h (units of $kN.m^{-2}$) which is the coefficient of subgrade reaction related to pile width ($K_h = k_h.B$) which is the product of k_h and B, where B is the breadth of the pile.

When a pile is displaced laterally in cohesive soils there will be a progressive consolidation under a maintained horizontal load. As displacement u increases the coefficient K_h decreases with time and both u and K_h will approach limiting values. Terzaghi(1955) recommended the use of the higher values of K_h for design. Work by Ranjan et al (1977) on model tests gave a relation using the Reese and Matlock(1969) solution of

$$u = \frac{A_y H}{(E_p I_p)^{\frac{1}{4}} K_{hi}^{\frac{3}{4}}} \tag{2.2}$$

where

$$\frac{K_{hf}}{K_{hi}} = [\frac{u_i}{u_f}]^{\frac{4}{3}} \tag{2.3}$$

where u_i is immediate deflection at the ground surface and u_f is final deflection at the ground surface.

The ratio of $\frac{K_{hf}}{K_{hi}}$ is not a constant quantity but increases as load approaches

ultimate. Ranjan et al (1977) recommended that the Broms (1964a) proposal for values of K_h may lead to erroneous results (see equation 2.19 and 2.20).

Carter and Booker(1981) studied the consolidation of a soil due to lateral loading on a pile. They presented their analysis in terms of time as well as displacements and excess pore pressure and used superposition to obtain a solution. They studied two different piles with different embedded length to radius ratio. They concluded using finite element analysis that as the time progressed the increases in lateral displacement in both cases were nearly equal despite the difference in embedded lengths.

If a pile is displaced horizontally in a cohesion-less soil, the values of u and k_h are effectively independent of time, and for a modulus of elasticity of cohesion-less soil increasing approximately in simple proportion to depth, Terzaghi presented:

$$k_h = \frac{n_h \times z}{B} \tag{2.4}$$

where n_h is the rate of increase of horizontal subgrade reaction with depth for piles embedded in sand. The values of n_h suggested by Terzaghi are tabulated in tables T2.1a and T2.1b.

Various authors have reported values of n_h from back-analyses of field tests with values up to five times larger than Terzaghi's values. Reese et al (1974) suggested that Terzaghi's data should be adopted as a lower limit and equation 2.5 be used for an upper limit.

$$n_h = 0.19D_r^{1.16}(MN/m^3) \tag{2.5}$$

where D_r is the relative density of the cohesion-less soils.

Garassino et al (1976) suggested relationships for non-linear behaviour of piles at high loads of:

$$n_h = n_{hi} \times \left(\frac{u_o/B}{u_{oi}/B}\right)^b \tag{2.6}$$

or

$$K_h = K_{hi} \times \left(\frac{u_o/B}{u_{oi}/B}\right)^b \tag{2.7}$$

where

$$K_{hi} = k_{hi} \times B \tag{2.8}$$

Values of b range from -0.5 to -0.7 for normally consolidated clay or for sand. Garassino et al (1976) prepared charts for values of u_{oi} which were presented in the above reference.

Pressuremeter tests have also been adopted to determine horizontal subgrade reaction values. Menard et al (1968) proposed an equation for the values of the horizontal subgrade reaction using the pressuremeter modulus,

$$\frac{1}{K_h} = \frac{1}{6E_m}\left[\frac{1.3R_o}{r}\left(\frac{2.65r}{R_o}\right)^\alpha + \alpha\right] \tag{2.9}$$

where E_m is the mean value of the pressuremeter modulus of elasticity over the characteristic length of the pile, $R_o = 0.3m$ and α is a rheological factor varying between 1.0 to 0.5 for clay, 0.67 to 0.33 for silt and 0.5 to 0.33 for sand.

The initial soil modulus of subgrade reaction may be related to the self boring pressuremeter modulus using an empirical factor;

$$K_{hi} = 1.6 \text{ to } 2.0E_m$$

Jamiolkowski and Lancelotta (1977) presented similar values. Poulos(1980) suggested that;

$$K_h = 0.8E_m/B \tag{2.10}$$

Terzaghi (1955) has suggested the use of a vertical plate bearing test to obtain the horizontal subgrade reaction. This test can only be conducted in clay, as it is not possible in practice to do such a test in cohesion-less soil. The Navy design Manual (1982) suggested a similar relation to obtain K_h;

$$k_h = f\frac{z}{B} \tag{2.11}$$

where f is the same as n_h

Francis (1964) suggested values for K_h using vertical bearing capacity factors as;

$$K_h = [(1885.08\gamma B N_\gamma) + (3770.16\gamma z N_q)] \qquad (2.12)$$

The value of elastic modulus E_s which may be used to estimate K_h has been suggested by Bowles(1982);

$$K_h = 0.8 \text{ to } 1.3\frac{E_s}{B} \qquad (2.13)$$

Audibert and Nyman (1977) carried out laboratory tests and in-situ tests and they presented the following equation ;

$$K_h = \frac{1}{A + By} \qquad (2.14)$$

where

$$A = \frac{0.145U_u}{\gamma_z N_q} \qquad (2.15)$$

and

$$B = \frac{0.855}{\gamma_z N_q} \qquad (2.16)$$

where U_u is the ultimate displacement and N_q is the bearing capacity factor given by charts.

For a short pile Sogge(1981) proposed;

$$k_h = 314.18 \text{ to } 4712.7 \times \frac{z}{B} \qquad (2.17)$$

where z is the pile depth and B is the pile width.

Based on field test data on timber piles in cohesion-less soil, Robinson(1979) observed that K_h is independent of pile width and he presented a relationship between n_h and standard penetration resistance (N). Robinson's results were a function of relative density and magnitude of applied horizontal force. Values obtained by Robinson suggested that the recommended values of n_h by Terzaghi(1955) were a lower bound.

Alizadeh (1969), Alizadeh and Davisson(1970) and Barton(1982) suggested that n_h is a function of pile deflection, especially when pile deflection is small. As deflection increases n_h approaches a limiting value.

Based on field test SPT results Bushan and Askari (1968) presented the following relationship for n_h and deflection

$$Log n_h = 0.82 + Log N - 0.62 Log \frac{U}{B} \qquad (2.18)$$

where N is the average number of blows over the embedded length of the pile in SPT and $\frac{U}{B}$ is the ratio of pile displacement to pile width as a percentage. Based on Decourt's (1991) experience in Brazil he suggested that;

$$E_s = 2N = 160c_u \qquad (2.19)$$

He also suggested that from 0.8mm plate bearing tests the vertical subgrade reaction k_v is;

$$k_v = 2.5N \qquad (2.19a)$$

and the k_h is;

$$k_h = \frac{k_v}{2} = 1.25N \qquad (2.19b)$$

where n_h is equal to N for submerged sand and n_h is equal to 1.6N for dry sand. Broms(1964a) suggested that if $L \geq 5B$ then,

$$K_h = 120c_u..... \text{ for long term loading.} \qquad (2.20)$$

$$K_h = 20c_u....... \text{ for short term loading.} \qquad (2.21)$$

Terzaghi (1955) suggested that

$$n_h = \frac{A\gamma}{1.35} \qquad (2.22)$$

where A is denoted ratio between modulus of elasticity E_s of cohesionless sand and overburden pressure ($p = \gamma z$) and γ is the unit weight of sand.

Reese and Matlock (1956) presented a solution to obtain n_h;

$$n_h = \frac{4.42(H_g)^{1.667}}{U_g^{1.667} E_p I_p^{0.667}}$$ (2.23)

where U_g is the pile deflection at the ground line and $E_p I_p$ is the flexural stiffness of pile.

Pise(1977) carried out experimental tests on model piles and found that

$$K_h = n_h z^{\frac{2}{3}}$$ (2.24)

Parikh and Pal (1981) carried out plain strain finite element analysis to determine

$$K_h = \frac{H}{U\,B}$$ (2.25)

where H is the horizontal load, U pile head displacement and B width of the pile section. Their work included a parametric study. They extended the finite element plain strain analysis to deal with two-pile groups. They reported that the K_h obtained was less than for an isolated pile. The K_h values were modified by the relative rigidity ratio $(R = \frac{E_p}{E_s})$, where E_p and E_s are the elastic modulus of pile and soil respectively.

2.3-Ultimate Lateral Resistance of a Single Pile

In determining the ultimate lateral resistance of a pile, it is necessary to classify the pile as short and rigid or long and flexible.

A pile can be designated as "rigid" if the induced deformation and bending moments are significant over its whole length. A pile can be designated as "flexible" if the induced deformation and bending moment are confined to the upper part of the pile and the overall length of pile does not significantly affect the response of the pile.

To determine whether a pile behaves as rigid or as flexible, one must obtain the stiffness factors R or T for particular combinations of pile and soil. For stiff over-consolidated clay a stiffness factor R is;

$$R = \sqrt[4]{\frac{E_p I_p}{k_h}}$$ (2.26)

For normally-consolidated clay and for granular soil the stiffness factor T;

$$T = \sqrt[5]{\frac{E_p I_p}{n_h}}$$ (2.27)

where $E_p I_p$ is the flexural stiffness of pile, k_h is the horizontal subgrade modulus and n_h is the rate of increase of horizontal subgrade modulus with depth.

When R or T has been estimated the behaviour of a pile can be related to embedded length L. T and R have a unit of length, and if the length of the pile L is divided by T or R a non-dimensional ratio is derived which is called depth coefficient Z. If Z is less than 2 the pile behaves as rigid and if the Z is greater than 4 the pile behaves as flexible. Values of Z with respect to soil types can obtained in Elson's (1985) report for cohesive and non-cohesive soils. The T value and R values can also be calculated from SPT's. Dacourt(1991) suggested that;

$$T = \sqrt[5]{\frac{E_p I_p}{N}} ...\text{for submerged sand}$$ (2.28)

$$T = \sqrt[5]{\frac{E_p I_p}{1.6\ N}} ....\text{for dry sand}$$ (2.29)

$$R = \sqrt[4]{\frac{E_p I_p}{N}} .... \text{ for clay}$$ (2.30)

where N is the average number of blows of the SPT over the length of the embedded length of the pile. Pise (1977) based on his experimental analysis suggested that;

$$T = (\frac{E_p I_p}{n_h})^{4.67}$$ (2.31)

Brinch Hansen (1961) presented solutions to predict the ultimate resistance of short rigid piles. His methods are applicable to both layered and uniform soil. His method which considers that the resistance of a rigid element to rotation about a point is obtained by the sum of the moment of the soil resistance above and below that point.

Poulos and Davies (1980) used a similar approach to obtain ultimate lateral resistance of a pile by taking into account Brom's (1964a) theory of lateral resistance of soil. He presented charts to obtain the ultimate lateral resistance of piles for both cohesive and non-cohesive soils. In using his charts for piles in non-cohesive soil, the P_u would be calculated at the middle of the pile rather than the toe of the pile.

Broms (1981) presented charts to predict the ultimate lateral resistance of a pile in cohesive soil. These charts are related to undrained shear strength c_u, the pile width B and ratio $\frac{L}{B}$ of embedded length to width.

Broms assumed that over the depth of 1.5B below the ground surface is a zone of zero pressure to represent the effect of soil shrinkage away from the pile. To predict the depth of zero shear and obtain the maximum bending moment for a unrestrained pile (see Figure 2.3a) the following equations may be used;

$$f = \frac{H}{9c_u.B} \tag{2.32}$$

$$M_{max} = H(e + 1.5B + 0.5f) \tag{2.33}$$

From equilibrium, at the point of zero shear the pile bending moment

$$M_{max} = 2.25c_uB(L - 1.5B - f)^2 \tag{2.34}$$

If the pile is short and restrained against rotation (see Figure 2.4a) at the ground surface then

$$M_{max} = \frac{1}{2}9c_uB(L^2 - 2.25B^2) \tag{2.35}$$

Broms (1964b) suggested that for short piles in cohesion-less soil the soil (see Figure 2.5a and 2.6a) reaction at any depth

$$P_u = 3\gamma'zK_p \tag{2.36}$$

where γ' is the effective unit weight of sand and

$$K_p = \frac{1 + sin\phi'}{1 - sin\phi'} \tag{2.37}$$

where ϕ' is the effective angle of friction of the soil.

While Brom's solution is good for soils with K_p of about 3, Fleming et al (1985) refer to work by Barton(1982) and suggest that

$$P_u = K_p{}^2 \gamma' z \qquad (2.38)$$

is a better approximation for naturally occurring sand, because values of K_p are normally greater than 3, so that this equation may give an improved estimation of P_u.

Reese et al (1974) also suggested that in considering the soil reaction distribution with depth, allowance should be made for a wedge type failure near ground surface. The solution for wedge type failure is used in chapter 5 for back analysis and construction of p/u curves.

For a rigid pile in cohesion-less soil (see Figure 2.5a and 2.6a) Broms(1964b) suggested that H_u may be predicted by,

$$H_u = \frac{1/2 B L^3 K_p \gamma'}{(e+L)} .... \text{ free-headed} \qquad (2.39)$$

$$H_u = \frac{3}{2} B \gamma L^2 K_p .... \text{ fixed-headed} \qquad (2.40)$$

For a flexible pile a statics approach may be used to predict the H_u :

$$H_u = \frac{M_u}{(e+z_f)} .... \text{ free-headed} \qquad (2.41)$$

$$H_u = \frac{2 M_u}{(e+z_f)} .... \text{ fixed-headed} \qquad (2.42)$$

where z_f is the point of virtual fixity, which for granular soil or stiff clay can be taken as 1.5m, and 3.0m for soft clay or silt measured from ground level.

Broms(1981) also presented solutions for predicting ultimate moments of resistance and ultimate lateral resistance of a long pile (see Figure 2.3b) in cohesive soil;

$$M_{max} = H(e + 1.5B + \frac{f}{2}) .... \text{ free-headed} \qquad (2.33 \ .bis)$$

$$H_u = \frac{2M_u}{1.5B + (f/2)} \text{.... fixed-head} \tag{2.43}$$

For a flexible pile in cohesion-less (see Figures 2.5b and 2.6b) soil;

$$M_{max} = H(e + 0.67f) \text{.... free-headed} \tag{2.44}$$

$$H_u = \frac{2M_u}{e + 0.54\sqrt{\frac{H_u}{\gamma B K_p}}} \text{.... fixed-headed} \tag{2.45}$$

$$f = 0.82\sqrt{\frac{H}{\gamma B K_p}} \tag{2.46}$$

Broms (1981) presented charts to obtain H_u and M_u.

2.4-Analysis of Laterally Loaded Single Piles and Pile Groups

The lateral behaviour of piles is governed by the stiffness of the soil. The stiffness of the soil may vary from one type to another, but in general the stiffness of soil may be constant with depth, may vary linearly with depth or may step change with change in soil stratum. There are numerical solutions to analyse laterally loaded piles according to its soil stiffness. Some solutions used in design of lateraly loaded piles are presented here to predict lateral deflection, rotation, bending moment, shear force and soil reaction.

There are basically three different types of approach used to predict deflection due to lateral loading of a pile as follows;

1-Cantilever method

2-Winkler soil method

3-Elastic continuum method

Each method has its advantages and disadvantages. The cantilever method ignores the resistance of soil over the length of the pile but gives tolerable results very economically. The Winkler soil method models the soil as a series of discrete springs with a constant stiffness for individual springs. This method ignores the shear resistance between the springs but gives fairly accurate results for both cohesive and

non-cohesive soils. The elastic continuum method gives the most accurate results, but when dealing with soil whose stiffness varies with depth the solution is difficult. These two prefered methods may incorporate non-linearity of soil stiffness.

2.4.1-Cantilever Method

This method is usually used for flexible piles rather than short rigid piles. This method can be used to estimate lateral deflection of the pile head for both free head or fixed headed piles. The first step in using this method is to select an arbitrary depth below the ground line z_f. This distance below the ground line is usually 1.0 to 1.5m. From this depth down to the base the pile is assumed to be fully restrained then an equivalent length of pile is obtained by adding the z_f to the free standing part of the pile e. Using simple cantilever theory and ignoring soil reaction the head deflection is ;

$$U = \frac{H \ (e \ + z_f)^3}{3E_pI_p}\ ......\text{free head} \qquad (2.47)$$

$$U = \frac{H \ (e \ + z_f)^3}{12E_pI_p}\ ......\text{fixed head} \qquad (2.48)$$

where E_pI_p is the flexural stiffness of the pile and e is the eccentricity of applied horizontal load above the ground line.

Davisson and Robinson (1965) presented solutions for flexible piles partially embedded in both cohesive and non-cohesive soils. They used beam on elastic foundation theory and also subgrade modulus to model an equivalent cantilever beam. Their solutions were in non-dimensional form. Lee (1968) used Davisson and Robinson's solution to analyses his model tests. He found a reasonable agreement.

2.4.2-Winkler Method

This method is widely used in design of piles. The governing equation using this method is the solution for a beam on elastic foundation proposed by Hetenyi (1946). The solution is coupled with the Winkler method and the differential equation is

solved (see Figure 2.1).

$$E_p I_p . \frac{du^4}{dx^4} + \frac{P_x \, du^2}{dx^2} - p = 0 \tag{2.49}$$

where $E_p I_p$ is the flexural stiffness of pile, u is lateral deflection, x is the vertical distance from ground level (positive downwards), P_x is the axial load on the pile at the depth x and p is soil resistance. For cohesive soils $p = k_h u$ and for non-cohesive soils $p = n_h u$. The fourth order differential equation can be solved numerically by finite difference using a standard computer program, eg that presented by Reese(1977). In most engineering situations a lateral load test on a single pile is needed to give values of p for use in the equation. The boundary equation predicts deflection at the ground line and zero deflection at the pile tip. In order to measure ground parameters a pile may be strain gauged to measure the bending moment. Bending moment data is smoothed by using polynominal least squares curve fitting techniques. From the smoothed bending moment curves values of deflection and soil pressure are obtained by;

$$u = \int \int \frac{M_x}{E_p I_p} . dx \tag{2.50}$$

$$p = \frac{d^2 \, M_{(x)}}{dx^2} \tag{2.51}$$

This technique gives a set of p/u curves which can then be used to evaluate pile behaviour. Reese et al (1974) used data from Mustang island to present a solution to evaluate p/u curves numerically by assuming wedge failure of the non-cohesive soil. Reese et al(1975) also used data from tests in Austin Texas to develop a numerical solution to evaluate p/u curves for cohesive soil. Murchison and O'Neill(1985) and Gazioglu and O'Neill(1985) presented solutions to evaluate p/u curves for non-cohesive and cohesive soil respectively.

The beam on elastic foundation theory developed by Hetenyi(1946) has been used by Gleser (1953) Barbar(1953), Reese and Matlock (1956), Matlock and Reese (1961),

Davisson and Gill (1963), Reddy and Valsangkar (1968), Matlock (1970), Reese et al (1975) Pise (1977) and Allen and Reese (1980) to present solutions to laterally loaded piles. Gleser(1953) presented a solution to predict pile head deflection and rotation for a free headed pile, in cohesive soil

$$U = (\frac{H}{K_h dL}) I_{UH} + (\frac{H}{K_h dL^2}) I_{UM} \tag{2.52}$$

$$\theta = (\frac{H}{K_h dL}) I_{\theta H} + (\frac{M}{K_h dL^2}) I_{\theta M} \tag{2.53}$$

For a fixed head pile

$$U = (\frac{H}{K_h dL}) I_{UF} \tag{2.54}$$

where I_{UH}, I_{UM}, $I_{\theta H}$, $I_{\theta M}$ and I_{UF} are deflection and rotation influence factors depending on the type of loading and pile head condition.

For non-cohesive soil the deflection and rotation can also be predicted by changing the term K_h to $n_h L$.

Reese and Matlock (1956) presented a non-dimensional solution to predict the deflection, rotation, bending moment, shear force and soil reaction along the embedded length of the pile and their numerical solutions are as follows;

For a free-headed pile

$$u = \frac{A_y H T^3}{E_p I_p} + \frac{B_y M t T^3}{E_p I_p} \tag{2.55}$$

$$\theta = \frac{A_s H T^3}{E_p I_p} + B_s M t T^3 \tag{2.56}$$

$$M = A_m H T + B_m M t \tag{2.57}$$

$$S = A_v H + B_v M t \tag{2.58}$$

$$p = \frac{A_p H}{T} + \frac{B_p M t}{T^3} \tag{2.59}$$

For a fixed-headed pile

$$u = \frac{F_y H T^3}{E_p I_p} \tag{2.60}$$

$$M = F_m HT \tag{2.61}$$

$$S = F_p \frac{H}{T} \tag{2.62}$$

For a long flexible pile, Matlock and Reese (1961) suggested the following equation;

$$u = C_y \frac{HT^3}{E_p I_p} \tag{2.63}$$

where

$$C_y = A_y \frac{MtB_y}{HT} \tag{2.64}$$

The Reese and Matlock solutions contain various coefficients A_y, B_y, A_s, B_s, A_m, B_m, A_v, B_v, A_p, B_p, F_y, F_m and F_p which are tabulated in their papers.

Broms (1981) proposed limit solutions to predict the head displacement at ground surface for a laterally loaded pile based on horizontal subgrade reaction;

For a long free-headed pile

$$U_g = \frac{2H\beta(e\beta + 1)}{K_h B} \dots\dots \text{ for cohesive soil} \tag{2.65}$$

$$U_g = \frac{2.4H}{n_h^{0.6} E_p I_p^{0.4}} \dots\dots \text{ for cohesion-less soil} \tag{2.66}$$

For a long fixed-headed pile

$$U_g = \frac{0.93H}{n_h^{0.6} E_p I_p} \dots\dots \text{ for a cohesion-less soil} \tag{2.67}$$

$$U_g = \frac{H}{K_h B} \dots\dots \text{ for cohesive soil} \tag{2.68}$$

where

U_g is the Pile displacement at ground surface

H is horizontal force

$E_p I_p$ is stiffness of pile

B is pile diameter or width

L is embedded length of the pile

K_h is coefficient of horizontal subgrade reaction

n_h Terzaghi rate of increase of coefficient of horizontal subgrade reaction with depth

e is distance from the loaded point to the ground surface

and

$$\beta = \sqrt[4]{\frac{k_h}{4EI}} \qquad (2.69)$$

Broms (1981) presented charts which may be used to predict pile head deflection.

Davisson and Gill (1963) proposed solutions to predict pile head deflection U_g and pile head rotation θ_g at the ground surface. The solutions were based on horizontal subgrade reaction;

$$U_g = \frac{1.35H\lambda^3}{E_p I_p} \qquad (2.70)$$

where

$$\lambda = \sqrt[4]{\frac{EI}{K_h}} \qquad (2.71)$$

These equations may be recorded as;

$$K_h = \frac{1.49H^{1.333}}{U_g E_p I_p^{0.333}} \qquad (2.72)$$

$$\theta_g = \frac{H_g}{K_h \lambda^2} \qquad (2.73)$$

The p/u criteria are based on the results of lateral load tests in homogeneous soils, coupled with earth pressure theory. Many researchers have reported that the p/u criteria offers a realistic method of analysis.

2.4.3-Elastic Continuum Method

Elastic continuum methods have been used by Poulos (1971a, 1971b, 1971c, 1973, 1975 and 1980), Butterfield and Banerjee(1971), Banerjee and Driscoll(1976), Bannerjee and Davis(1978), Randolph(1981), Budhu and Davies(1987 and 1988) and Verruijt and Kooijmaan(1989) to analyse laterally loaded piles. Most authors used boundary

integral equations to model the soil as an elastic continuum and ignored the horizontal shear stresses on the side of the pile. Randolph (1981) used an axi-symmetric finite element analysis using similar assumptions. This method analyses an elastic pile embedded in an elastic half space. The use of an elastic analysis gives lower values of deflection, rotation of the pile head and moment than found in practice. This is because the soil tangent modulus used in the analysis from triaxial tests adopts an upper bound of soil stiffness. Because of their significance the solutions by Poulos and Randolph are next considered in more detail. The Poulos (1971a,b,c, 1973, 1975 and 1979) and Randolph(1981) solutions for a laterally loaded single pile have been extended to analyse groups of laterally loaded piles by use of interaction factors.

2.4.3.1-Poulos(1971) Method

Poulos developed solutions in which the pile is assumed to be a thin rectangular vertical strip of width d, length L and constant flexural stiffness $E_p I_p$. He simplified his solutions by ignoring the horizontal shear stresses between the soil and the side of the pile and divided the piles into n+1 elements, each element of a length δ except for the bottom and top elements of the pile which have a length of $\frac{\delta}{2}$,and a uniform stress P acting on each element (see Figure 2.7) The soil was assumed to be an homogeneous-isotropic semi-infinite elastic material, with elastic modulus E_s and Poisson's ratio ν_s and the soil is unaffected by the presence of the pile. Poulos also assumed that the soil at the back of the pile does not separate and the horizontal displacements of soil and the pile are equal. He proposed that the displacements u_e for all central points of the elements over the length of the embedded pile are;

$$u_e = \frac{d}{E_s(I_s)p} \qquad (2.74)$$

where I_s is the dimensionless soil displacement influence factor.

Mindlin(1936) presented solutions to evaluate the displacements and stresses at any point depth below the ground surface. Douglas and Davis(1964) integrated the

Mindlin solution to give the horizontal displacement of a point within a semi-infinite half space caused by a horizontal point load within the mass. Poulos(1971a) used these solutions to present equations to obtain the pile head deflection and rotation. He also introduced coefficients KR and KN which are given by;

$$KR = \frac{E_p I_p}{E_s L^4}....\text{pile in cohesive soils} \qquad (2.75)$$

$$KN = \frac{E_p I_p}{n_h L^5}....\text{pile in non-cohesive soils} \qquad (2.76)$$

where n_h is the rate of increase of soil elastic modulus with depth, for a free head pile under horizontal loading H and moment M.

Assuming the soil is linear elastic and the soil modulus is constant with depth, the following equations would predict pile head lateral displacement U_e and rotation θ_e ;

$$U_e = \left(\frac{H}{E_s L}\right) I_{UH} + \left(\frac{M}{E_s L^2}\right) I_{UM} \qquad (2.77)$$

$$\theta_e = \left(\frac{H}{E_s L^2}\right) I_{\theta H} + \left(\frac{M}{E_s L^3}\right) I_{\theta M} \qquad (2.78)$$

For a fixed head pile the displacement of the pile head is given by;

$$U_{ef} = \left(\frac{H}{E_s L}\right) I_{UF} \qquad (2.79)$$

In addition it may be necessary to obtain displacement above the level of ground surface or at the point of application of the horizontal load and the solution is given by;

$$U_e = \left[\left(\frac{H}{E_s L}\right)\left(I_{UH} + \frac{e}{L} I_{UM}\right)\right]$$
$$+\left[\left(\frac{He}{E_s L^2}\right)\left(I_{\theta H} + \frac{e}{L} I_{\theta M}\right)\right] + \left[\frac{He^3}{3 E_p I_p}\right] \qquad (2.80)$$

If the soil elastic modulus increases linearly with depth then the pile head displacement and the rotation for a free head pile is given by;

$$U_e = \left(\frac{H}{n_h L^2}\right)(I'_{UH} + \left(\frac{e}{L}\right) I'_{UM}) \qquad (2.81)$$

$$\theta_e = \left(\frac{H}{n_h L^3}\right)\left(I'_{\theta H} + \left(\frac{e}{L^4}\right)I'_{\theta H}\right) \tag{2.82}$$

and for a fixed head pile

$$U_{ef} = \left(\frac{H}{n_h L^2}\right)I'_{UF} \tag{2.83}$$

In equations 2.77 to 2.83 $'e'$ is the eccentricity of horizontal load, I_{UH} and I_{UM} are the influence factors for deflection caused by horizontal load and moment respectively, and $I_{\theta H}$ and $I_{\theta M}$ are the influence factors for rotation caused by horizontal load and moment respectively. From reciprocal theory I_{UM} and $I_{\theta M}$ are equal.

The suffices I and I' refer to influence factors for the soil with constant soil modulus with depth and linear varying soil modulus with depth respectively and n_h now refers to rate of increase of soil elastic modulus. Poulos(1971a) presented charts to determine influence factors and yield factors.

2.4.3.2-Randolph(1981) Method

Randolph(1981) presented solutions for a laterally loaded pile based on elastic continuum analysis by finite-elements to model the pile in an elastic medium. The pile and soil were modelled by an axisymmetric mesh to obtain rotation and displacement for both homogeneous soil and for soil with modulus proportional to depth.

For homogeneous soil, pile head deflection and rotation are given by;

$$U_e = 0.25\frac{H}{G^*r}\left(\frac{E_{ef}}{G^*}\right)^{\frac{-1}{7}} + 0.27\frac{M}{G^*r^2}\left(\frac{E_{ef}}{G^*}\right)^{\frac{-3}{7}} \tag{2.84}$$

$$\theta_e = 0.27\frac{H}{G^*r^2}\left(\frac{E_{ef}}{G^*}\right)^{\frac{-3}{7}} + 0.8\frac{M}{G^*r^3}\left(\frac{E_{ef}}{G^*}\right)^{\frac{-5}{7}} \tag{2.85}$$

For non-homogeneous soil with shear modulus increasing with depth the pile head deflection and rotation are given by;

$$U_e = 0.54\frac{H}{m_*r^2}\left(\frac{E_{ef}}{m_* r}\right)^{\frac{-3}{9}} + 0.60\frac{M}{m^*r^3}\left(\frac{E_{ef}}{m^* r}\right)^{\frac{-5}{9}} \tag{2.86}$$

$$\theta_e = 0.60\frac{H}{m^*r^3}\left(\frac{E_{ef}}{m^* r}\right)^{\frac{-5}{9}} + 1.13\frac{M}{m_*r^4}\left(\frac{E_{ef}}{m^* r}\right)^{\frac{-7}{9}} \tag{2.87}$$

He combined equation 2.84 and 2.86 (2.85 and 2.87) to give general solutions for laterally loaded piles in any type of soil medium, and the solution for ground line deflection and rotation is given by;

$$U_e = \frac{(E_{ef} / G_c)^{\frac{1}{7}}}{\rho_c} \left[0.27H(\frac{l_c}{2})^{-1} + 0.3M(\frac{l_c}{2})^{-2} \right] \tag{2.88}$$

$$\theta_e = \frac{(E_{ef} / G_c)^{1/7}}{\rho_c} \left[0.3H(\frac{l_c}{2})^{-2} + 0.8(\rho_c)^{\frac{1}{2}}M(\frac{l_c}{2})^{-3} \right] \tag{2.89}$$

From equation 2.84 to 2.89 E_{ef} is the effective elastic modulus of pile

$$E_{ef} = \left(\frac{E_p I_p}{\frac{\pi r^4}{4}} \right) \tag{2.90}$$

G^* is the product of shear modulus G

$$G^* = G(1 + \frac{3\nu}{4}) \tag{2.91}$$

r is the radius of pile, m^* is the product of rate of increase of shear modulus for non-homogeneous soil m

$$m^* = m(1 + \frac{3\nu}{4}) \tag{2.92}$$

Randolph correlates the deflection of the pile at the ground to the critical slenderness ratio and with stiffness ratio given by

$$(\frac{l_c}{r}) = 2(\frac{E_p}{G^*})^{\frac{2}{7}} \tag{2.93}$$

$$(\frac{l_c}{r}) = 2(\frac{E_p}{m^*})^{\frac{2}{9}} \tag{2.94}$$

G_c is the characteristic shear modulus at $\frac{l_c}{2}$ and the parameter ρ_c is

$$\rho_c = \frac{G^*_{z=l_c/4}}{G^*_{z=l_c/2}} \tag{2.95}$$

Randolph suggested that, for a fixed head pile , the fixing moment may be predicted by;

$$M_f = -\left[\frac{0.375}{(\rho_c)^{\frac{1}{2}}} \right] H(\frac{l_c}{2}) \tag{2.96}$$

Randolph(1981) reports that, the maximum bending moment occurs at a depth of about $\frac{Lc}{4}$ for homogeneous soil and $\frac{Lc}{3}$ for soil with modulus proportional to depth, and if a suitable shear modulus for the soil is chosen, his equations, together with his charts may be used to estimate the pile head displacement, rotation and induced bending moment under working load conditions. The maximum bending moment in the pile shaft is given by;

$$M_{max} \approx (\frac{0.1}{\rho_c})Hl_c \tag{2.97}$$

2.4.3.3-Banerjee and Davies(1978) Method

Solutions for predicting pile head deflection and rotation at the ground line for a laterally loaded pile by Banerjee and Davis(1978) are as follows;

For a free headed pile

$$U_e = (\frac{H}{E_{(L)}L})I_H + (\frac{M}{E_{(L)}L^2})I_{HM} \tag{2.98}$$

$$\theta_e = (\frac{H}{E_{(L)}L^2})I_{HM} + (\frac{M}{E_{(L)}L^3})I_{MM} \tag{2.99}$$

for a fixed head pile the ground line deflection is given by;

$$U_e = (\frac{H}{E_{(L)}L})I_{FH} \tag{2.100}$$

The I_H, I_{HM}, I_{MM} and I_{FH} are the influence factors and can be obtained from the above reference. The $E_{(L)}$ is the soil modulus at the pile toe.

2.4.3.4-Budhu and Davies(1978 and 1988) Method

Budhu and Davies (1987 and 1988) presented a solution to predict lateral displacement and rotation of a laterally loaded pile head. They presented sets of equations to calculate the influence factors. There was no interpolation of a curve to obtain influence factors like Poulos (1971a and 1971b) and Banerjee and Davies(1978). The solutions are as follows;

For a free headed pile

$$U_e = \frac{H}{n_h d^2}I_{UH} + \frac{M}{n_h d^3}I_{UM} \tag{2.101}$$

$$\theta_e = \frac{H}{n_h d^3} I_{\theta H} + \frac{M}{n_h d^4} I_{HM} \qquad (2.102)$$

For a fixed head pile the ground line deflection

$$U_{ef} = \frac{H}{n_h d^2} I_{FH} \qquad (2.103)$$

where n_h is the rate of increase in soil modulus, d is the pile diameter and I_{UH}, I_{UM}, $I_{\theta H}$, $I_{\theta M}$ and I_{UF} are the influences factors. To calculate the influence factors the following equations are used;

$$I_{UH} = 3.2 K^{\frac{-3}{9}} \qquad (2.104)$$

$$I_{UM} = I_{\theta H} = 5.0 K^{\frac{-5}{9}} \qquad (2.105)$$

$$I_{\theta M} = 13.6 K^{\frac{-7}{9}} \qquad (2.106)$$

$$I_{FH} = 1.4 K^{\frac{-3}{9}} \qquad (2.107)$$

where K is the pile/soil stiffness ratio and is given by;

$$K = \frac{E_{ef}}{n_h d} \qquad (2.108)$$

E_{ef} is calculated from equation 2.90. The fixing moment M_f for a laterally loaded pile is given by

$$M_f = -H \, d \, I_{MF} \qquad (2.109)$$

where

$$I_{MF} = 0.4 K^{\frac{2}{9}} \qquad (2.110)$$

The maximum bending moment M_{max} occurs at depth l_m and is given by;

$$\frac{l_m}{d} = 0.53 \ K^{\frac{2}{9}} \qquad (2.111)$$

$$M_{max} = I_{MH} \ H \ d \qquad (2.112)$$

where

$$I_{MH} = 0.3 \ K^{\frac{2}{9}} \qquad (2.113)$$

2.5-Elastic and Elastic-Plastic Analysis of Laterally Loaded Single Pile

The non-linear analysis of laterally loaded piles takes account of the non-linear relationship between the lateral soil pressure and deflection of the pile. There are basically two different approaches to take into account the non-linearity.

The first approach is the construction of p/u curves. Using the beam-on-elastic-foundation theory and horizontal subgrade theory a series of p/u curves is constructed as has already been discussed in section 2.3.2. There are several types of analysis to construct p/u curves. Madhav et al (1971), Kubo(1965), Matlock(1970), Reese(1974, 1975 1977), Reese and Welch(1975), Frydman et al (1975), Baguelin et al(1978), Sullivan et al (1979) Murchison and O'Neill (1985) and Gazioglu and O'Neill(1985) have presented solutions to develop p/u curves. There are several computer programs available to develop p/u curves.(eg Reese 1977).

The second type of approach for analysing non-linear behaviour of pile head deflection and rotation for a laterally loaded single pile is to modify an elastic continuum analysis.

2.5.1-p/u Curve Method

In order to construct p/u curves along the pile length, a wedge type failure of soil near the ground surface is assumed with a plastic response of the soil well below the ground level. In order to estimate the wedge failure near the ground surface and well below the ground level it is first necessary to know the soil properties including the shear strength of the soil, the effective angle of friction of the soils the unit weight of the soil, the water table level and the stress/strain relationship of the soil. Having obtained these variables the soil resistance at selected depth is calculated corresponding to the deflected shape of the pile. When the construction of p/u curves is completed the horizontal subgrade reaction can be obtained. Then the non-linear behaviour of pile deflection, rotation, moment, shear force and soil pressure is obtained. The references mentioned above can be used to construct p/u curves.

2.5.2-Elastic Continuum Method

Using this method the elastic deflection and the rotation of the pile head is first predicted and then a yielding influence factor is used to scale the deflection for a given horizontal load. Poulos(1971a and 1971b) and Budhu and Davies (1987 and 1988) presented solutions to obtain the yielding factors.

2.5.2.1-Poulos Method

From linear elastic and elastic-plastic analyses of laterally loaded piles Poulos (1971a and 1971b) introduced yielding factors for pile head deflection F_u and rotation F_θ. The yielding influence factors are in direct relation to applied horizontal load H and ultimate lateral resistance of pile H_u ($\frac{H}{H_u}$). Poulos(1971) presented charts for F_u and F_θ. In order to use the charts the length to diameter ratio has to be known. Interpolation is needed to obtain the yielding factors which may result in minor errors in pile head deflection, but it is one of the useful tools in nonlinear analysis. Having obtained yielding factors then they are multiplied by the elastic deflection or rotation of the pile under the same loading condition so that;

$$U_y + \theta_y = U_e \ F_u + \theta_e \ F_\theta \tag{2.115}$$

$$U_{yf} = U_{ef} \ F_{uf} \tag{2.116}$$

2.5.2.2-Budhu and Davies Method

This method uses a similar technique for nonlinear analysis except the yielding influence factors can be interpolated from charts or calculated arithmetically from the following formula;

$$I_{uy} = 1 + \frac{h \ - \ 14.0K^{0.32}}{40k^{0.53}} \tag{2.117}$$

$$I_{\theta y} = 1 + \frac{h \ - \ 14.0K^{0.32}}{54k^{0.53}} \tag{2.118}$$

$$I_{ufy} = 1 + \frac{h \ - \ 32.0K^{0.43}}{105k^{0.54}} \tag{2.119}$$

$$I_{My} = 1 + \frac{h - 8.0K^{0.32}}{96k^{0.48}} \qquad (2.120)$$

$$I_{uy} = 1 + \frac{h - 30.0K^{0.32}}{312k^{0.56}} \qquad (2.121)$$

where $k = K/1000$, $h = H/cd^3$ for cohesive soil or $h = H/n_h d^3$.

2.6-Lateral Analysis of Pile Groups

In practice piles are normally used in groups rather than singly. In the U.K. piles are normally long and flexible.

The behaviour of pile groups under lateral loading differs from that of a single pile. The lateral load may be distributed unevenly among the piles, the lateral deflections of the piles may vary slightly and front piles may carry more loads than centre and rear. There are few methods available for the analysis of lateral behaviour of pile groups. It should be mentioned that the measured response of full scale piles in group action under lateral loading is not well documented. However Elson (1985) presented his report on behalf of CIRIA, Poulos(1971b) and Randolph(1981) presented numerical analyses based on modified elastic continuum analysis, Reese and Matlock (1970) presented a modified subgrade reaction solution.

Kim and Brungraber(1976) and Brown et al (1987 and 1988) conducted full scale tests, Matlock(1980) Schmidt(1981),and Uromeihi(1985) reported field test results on lateral behaviour of pile groups. Model tests have been reported by Hughes et al(1980), Selby and Poulos(1985), Selby and Parton (1987), Pise (1982), Sung Ho and Maddison (1989), Arta(1986), Long (1987) and Hotoinhs and Nakatani(1991) on the lateral behaviour of pile groups. Later in this section some of the reported cases of field tests and model tests will be presented.

Basically there are three methods available to analyse lateral behaviour of pile groups as follows;

1 - Static Method

2 - Winkler Soil Method

3 - Elastic Continuum Method

2.6.1-Static Analysis Method

The static analysis of a pile group can be used to determine forces and moments in individual piles. There are two approaches to the solution. The first approach is that the soil resistance offered by the soil medium is totally ignored and the problem is solved by a polygon of forces or by resultant forces taking moments about the centre of the pile group. The second approach to the problem is a stiffness or a flexibility method in which the piles in the group are fixed at a distance below the ground, sometimes described as the equivalent-bent method.

In the first method the load on individual piles in a group of vertical piles can be estimated by taking moments about the neutral axis of the pile group. This method can be used for lateral loading or combined axial and lateral loading. The vertical component V of the load on each individual pile would give rise to an inclined thrust R , where R is the resultant of a horizontal load H and vertical (axial load) W can be given as ;

$$V = \frac{W}{n} + \frac{We\hat{x}}{\sum \hat{x}^2} \qquad (2.122)$$

where $'e'$ is distance between the point of the intersection of R with underside of the pile cap and the neutral axis of the pile group. $\hat{x}$ is distance between the pile and the neutral axis.

The 'Polygon of force' is a graphical solution of forces. It can be used to estimate the force in each pile in a group with up to three planes of raked piles.

The stiffness method is based on structural stiffness analysis and can offer reasonable prediction of pile head forces and moments. This method is used because piles in a group are generally symmetrical with respect to the vertical. The problem can often be treated as two dimensional rather than three dimensional. This method is similar to the structural method but by judicious estimation of lateral pile stiffness,

gives improved estimates of pile head forces and cap displacements. This method has been used to analysis pile group loading by, Turzynski(1967), Sawko(1968), Reddy and Ramasamy(1976), Poulos(1980), Randolph and Poulos(1982), Selby and Wallace(1986). Using this method the equivalent length of the pile must be obtained for either vertical or raked piles. Poulos(1980) presented solutions to estimate the equivalent length of laterally loaded piles.

The stiffness method involves a pile stiffness matrix $[s]$, a system stiffness matrix $[K]$ the load vector $|P|$, and deflection vector $|\delta|$, so that $|P| = [K].|\delta|$ The matrix $[a]$ is the transformation matrix for the pile, then;

$$[\Delta] = [a] \cdot |\delta| \qquad (2.123)$$

where $|\delta|$ is a column vector of the unknown displacement. The forces in the piles are given by;

$$[F] = [s].[\Delta] = [s].[a].[\delta] \qquad (2.124)$$

The global load to local load is given by;

$$[P] = [a]^T.[F] \qquad (2.125)$$

2.6.1.1-Poulos Static Analysis Method

Poulos(1980) adopted his theory elastic continuum(1971b) to present solutions for piles in the group. His method gave a major improvement in available methods. Figure 2.8a shows the pile group which is subjected to vertical, horizontal and moment loading. Figure 2.8b shows the pile cap supported by a frame in which the columns are fixed end free standing and the columns are of equivalent length L_e and equivalent cross section A_e. There are several methods to determine the L_e and A_e. This depends upon the condition of loading. Poulos suggested the following equations to obtain the L_e and A_e for different conditions of loading (see Figure 2.9):

$$L_{eH} = L\sqrt{3I_{UH}KR\ R_{UH}}... \text{ for condition a} \qquad (2.126)$$

$$L_{eM} = L\sqrt{2I_{UM}KR\ R_{UM}}... \text{ for condition b} \qquad (2.127)$$

$$L_{UF} = \sqrt[3]{12I_{UF}\ KR\ R_{UF}}... \text{ for condition c} \qquad (2.128)$$

for condition d and e

$$\left(\frac{L_e}{L}\right)^3 + 1.5\frac{M}{HL}\left(\frac{L_e}{L}\right)^2 = 3KR\left(R_{UH}I_{UH} + \frac{M}{HL}I_{UM}R_{UM}\right) \qquad (2.129)$$

For case d, $(L_e = L_{e1})$ $M = He$. For case e $(L_e = L_{e2})$ then

$$M = -HL\left[\frac{I_{\theta H}KR\ R_{\theta H} + 1/6(\frac{e}{L})^2}{I_{\theta M}\ KR\ R_{\theta M} + 1}\right] + He \qquad (2.130)$$

The A_e of a free standing pile is defined by:

$$A_e = \frac{L_e + e}{\frac{I_{Rs}}{d}\frac{E_p}{E_s} + \frac{e}{A}} \qquad (2.131)$$

If the L_e is required then

$$L_e = \frac{L_e A}{A_e} \qquad (2.132)$$

The L_e and A_e can be used for vertical piles as well as raked piles. The I_{UH}, I_{UM}, $I_{UF}, I_{\theta H}$ and $I_{\theta M}$ are the influence factors depending on the condition of loading, and they are discussed in section 2.3. The $R_{UH}, R_{UM}, R_{UF}, R_{\theta H}$ and $R_{\theta M}$ are group reduction factors which will be discussed in section 2.5.2. The I is the influence factor and R_s is the settlement ratio for axial loading which is defined by Poulos and Davies(1980). The KR is defined by equation 2.75 for a pile in soil of constant modulus. In the case of piles in soil in which the soil modulus increases with depth KN can be used instead KR. KN is defined by equation 2.75 and 2.76.

If the pile is raked in the group the the first step is to resolve the forces by;

$$P = V\ cos\psi + H\ sin\psi \qquad (2.133)$$

$$Q = H\ cos\psi - V\ sin\psi \qquad (2.134)$$

where ψ is the angle of a raked pile. The axial and normal displacement of a raked pile can be resolved into vertical and horizontal components. In order to do this, it is assumed that the lateral load does not influence axial displacement and vice versa. Poulos presented sets of solutions to obtain the vertical and horizontal displacement and rotation of the groups.

Poulos used his interaction theory and assumed that the interaction factor for a vertical pile and a raked pile in the group was the same, and introduced equivalent pile spacing if in the pile group the piles are raked. Based on those assumptions he presented the following solution for a two-dimensional pile group containing batter piles in the form of a matrix equation;

$$\begin{bmatrix} A_v & B_v & C_v \\ A_h & B_h & C_h \\ A_\theta & B_\theta & C_\theta \end{bmatrix} \cdot \left\{ \begin{array}{c} V \\ H \\ M \end{array} \right\} = \left\{ \begin{array}{c} U_v \\ U_h \\ \theta \end{array} \right\} \tag{2.135}$$

where V, H and M are vertical horizontal and moment loading on the pile head, U_v, U_h and θ are the vertical and horizontal displacement and rotation of pile head. The flexibility coefficients in the matrix, ABC can be obtained from Poulos(1980).

2.6.2-Winkler Soil Model

The application of this method to pile groups is not generally recommended. It is more appropriate for analysing laterally loaded single piles.

The application to a group is not straight forward but the effect of pile spacing on the subgrade modulus should be considered. Several authors investigated the reduction of subgrade modulus due to pile interaction within a group; generally for pile spacing of more than eight diameters no reduction is needed, for three diameter spacing a reduction of 25% is appropriate.

The application of a Winkler soil model for analysis of a pile group is as follows. If the piles in the group are partially embedded and the head is free to rotate then the first step is to divided the total horizontal load (H_g) by the number of piles (n) in the group. The applied moment (M) to the pile is the horizontal load on each individual

pile times the distance (e) between the ground line and the applied horizontal load.

$$H = \frac{H_g}{n} \quad \text{and} \quad M = H\,e \qquad (2.136)$$

The next step is to obtain the stiffness factors T and R which are defined by equation 2.26 and 2.27 for appropriate soil conditions. The Z_{max} is obtained by dividing the length of the pile by T or R. The Z_{max} factor is used to determine the coefficients for horizontal load and bending moment. Using equation 2.55 to 2.59 the deflection, rotation, bending moment, shear force and soil pressure are obtained. If the pile head is fixed a similar procedure is conducted except that the maximum shear occurs at the top of each pile in the group.

If the piles are battered in the group the equivalent length is used as described in a previous section. The equivalent head displacement found from the cantilever beam is equated as;

$$\frac{H L_e{}^3}{3 E_p I_p} = \frac{H T^3 A_y}{E_p I_p} + \frac{M T^3 B_y}{E_p I_p} \qquad (2.137)$$

2.6.3-Elastic Continuum Analysis Methods

Poulos(1971) and Randolph(1981) have extended their work to analysis of pile groups based on elastic continuum and they introduced reduction factors based on interaction effects of neighbouring piles. The reduction factor is defined as the fractional increase in deformation of one pile due to the presence of a similarly loaded neighbouring pile. Poulos considered two identical, equally loaded piles, and adopted the same method of analysis as for a single pile, except that there is now another soil-displacement influence factor (see Figure 2.10) The spacing and the angle of departure play an important part in choosing the value of reduction factor. Poulos presented charts to obtain these factors in the above reference. They have six characteristics

1 -The factors decrease with increase in spacing and are greater for angle of departure for 0° than for 90° (the angle of departure is angle from the direction of loading of the pile).

2 -the factors increase with embedded length to diameter ratio.

3 -As the pile stiffness factor KR increases so do the factors.

4 -The factors for horizontal loading are greater than for moment, for free head piles.

5 -The displacement factors are greater than the corresponding rotational factors for a free head pile.

6 -For horizontal loading only, values of interaction factors for fixed head piles are greater than the corresponding values for the displacement interaction factor for a free head pile.

The KR and KN are the pile flexibility factors depending on the type of soil modulus and they are defined by equation 2.75 and 2.76 and for soil modulus constant with depth and varying with depth respectively. Most of Poulos' reduction factors presented are for KN. But he proposed $KR = KN$ in his charts. He also suggested that the use of KR instead KN would result in an over-estimate of pile head displacement and rotation.

Randolph(1981) presented solutions to obtain interaction factors for displacement of free head piles and fixed head piles. His reduction factors α for homogeneous and non-homogeneous soils and for different pile stiffness ratios are ;

$$\alpha_{UF} = 0.6\rho_c(\frac{Ep}{G_c})^{\frac{1}{7}}\frac{r}{s}(1 + cos^2\beta).... \text{ fixed headed} \qquad (2.138)$$

$$\alpha_{UH} = 0.5\rho_c(\frac{Ep}{G_c})^{\frac{1}{2}}\frac{r}{s}(1 + cos^2\beta).... \text{ free headed} \qquad (2.139)$$

$$\alpha_{\theta H} = \alpha_{UM} = \alpha_{UH}^2 \qquad (2.140)$$

$$\alpha_{\theta M} = \alpha_{UH}^3 \qquad (2.141)$$

$$\alpha_{UH} = 0.8\alpha_{UF} \qquad (2.142)$$

Randolph compared his expressions for interaction factors with Poulos' interaction factors for piles in homogeneous soil. He reported that the agreement is normally

good, for piles in line with the applied load, but at close spacing they tend to give conservative values compared with Poulos values. He suggested that this may because Poulos treated the pile as a thin strip for the integral equation. This tends to increase the amount of soil between piles compared with circular piles, therefore leading to lower interaction factors at close spacings.

Poulos(1971b) used the superposition principal to analyse the displacement and rotation of any general pile group subjected to lateral loading and moment.

In using this solution throughout the group two important points should be considered as follows;

1 -Each pile in the group displaces equally.

2 -Each pile carries equal horizontal load and moment.

Having considered these two points Poulos expressed the displacement of the k_{th} pile in the group as;

$$U_k = \bar{U_H}\Big[\sum_{\substack{j=1 \\ j \neq k}}^{n}\Big(H_j.\alpha_{UHkj}\Big) + H_k\Big] \qquad (2.143)$$

$$H_g = \sum_{j=1}^{n} H_j \qquad (2.144)$$

where

$\bar{U_H}$ is the unit reference displacement; that is the displacement of a single free headed pile due to unit lateral load,

H_j is the load on pile j

α_{UHkj} is the value of α_{UH} for two piles, corresponding to the spacing between piles k and j and the angle β between the direction of lateral loading and the line joining the centres of piles k and j

H_g is the total horizontal load.

From the above equation and considering the horizontal equilibrium with H_g, the unknown pile load and group displacement may be estimated. This condition applies

only when the piles are displaced equally but if the load is equally shared then the displacement of each pile may be estimated directly.

In a group of piles the displacement may be expressed as a group reduction factor R_R, defined as the ratio of the group displacement to the displacement of a single pile carrying the same average load or moment as the group,

$$R_R = \frac{U_g}{\bar{U} H_g} \tag{2.145}$$

or

$$R_R = \frac{1}{n}\Big(\sum_{\substack{j=1 \\ j \neq k}}^{n} \alpha_{jk} + 1\Big) \tag{2.146}$$

where $\bar{U}$ is the unit reference displacement, U_g is the group displacement, n is the number of piles, α_{jk} interaction factor. Poulos refered to unit-reference displacement u_g as the surface displacement. If we consider that elastic conditions exist in the soil Poulos suggested R_R and R_u are related by;

$$R_U = R_R{}^n \tag{2.147}$$

Poulos (1975) suggested that the R_U is the more useful quantity, but in examining the behaviour of various groups theoretically, the use of R_R has some advantage, since as with R_g, R_R always lies within the range 1 to $\frac{1}{n}$. He presented various values of R_R depended upon the loading, head deflection and rotation. These values can be obtained from the above reference.

Poulos(1975) has studied the behaviour of square pile groups and based upon the use of reduction factor R_R he reported that;

1 -The outer piles carry more load than the centre piles.

2 -As the spacing increases the load becomes more uniformly distributed.

3 -The pile group stiffness increases with the number of piles in the group

4 -The non-uniformity of load distribution generally becomes more pronounced as K_R and $\frac{L}{d}$ increases.

The values of influence factors reduction factors depend on KN, KR and l/d.

Focht et al(1973) presented a rational solution for lateral performance of pile groups. Their argument is that near to the surface, soil around most piles is strained well into the plastic zone and the application of an elastic half space solution cannot be used for piles and pile groups. However below plastic strain the elastic theory may be computed to combine the subgrade reaction theory with elastic half space and they suggested that the equation 2.148 should be as follows;

$$U_k = \bar{U_H}\Big[\sum_{\substack{j=1 \\ j \neq k}}^{n}\big(H_j . \alpha_{UHkj}\big) + R.H_k\Big] \qquad (2.148)$$

where

$$R = \frac{U_s}{U_e} \qquad (2.149)$$

where U_s is the deflection of a single isolated pile determined by p/u curve analysis and U_e is the elastic deflection determined by elastic half space. They presented a solution to modify p/u data by introducing 'Y' and 'P' factors to take into account an increase in deflection due to a neighbouring pile in a group.

2.7-Nonlinear Analysis For Load/Deflection Curves

Poulos(1975) presented solutions for an approximate prediction of load /deflection curves for pile groups, with three assumptions to be considered;

1 -The group reduction factors R_R remain constant even up to failure load.

2 -The reduced ultimate lateral load capacity H_{ur} of each pile is

$$H_{ur} = \eta_l H_u \qquad (2.150)$$

where η_L is the lateral efficiency factor and H_u is the ultimate lateral load capacity of a single pile. The η_l is considered to remain equal for all piles in the group.

3 -In the group of piles all piles deflect equally, so that the load- deflection curve for the group is determined by computing the curve for a single pile having an

ultimate load H_{ur}, and multiplying the ordinates of this curve by the number of piles in the group.

Poulos(1975) suggested that for a free headed pile group in a soil with constant Es the ground-line deflection u_G is;

$$U_g = \frac{\frac{H_g}{LE_s}\left(R_{RUH}I_{UH} + \frac{e}{L}R_{RUM}I_{UM}\right)}{F_u} \qquad (2.151)$$

where F_u is the yielding displacement factor (see section).

If it is required to obtain the deflection at the point of application of horizontal load then;

$$U_g = \frac{\frac{H_g}{L^3E_s}\left(L^2 R_{RUH}I_{UH} + eL R_{RUM}I_{UM}\right)}{F_u} + \frac{\left(L R_{R\theta H}I_{\theta H} + e^2 R_{R\theta M}I_{\theta M}\right)}{F_{\theta u}} \qquad (2.152)$$

where R_{RUH} is Group reduction factor for deflection caused by horizontal load, R_{RUM} is Group reduction factor for deflection caused by moment. $R_{R\theta M} = R_{R\theta H}$ and is the group reduction factor for rotation caused by moment.

For pile groups in soil with linearly varying E_s, a similar equation can be determined. It is necessary to replace E_s by n_h L, I_{UH}, I_{UM} and $I_{\theta M}$ are replaced by I'_{uH}, I'_{UM} and $I'_{\theta M}$ and F_U and F_θ are replaced by F'_U and F'_θ. Similar expressions can be obtained for fixed head pile groups by replacing the appropriate factor.

2.8-Scale Model Tests

Model pile group tests have been conducted by various researchers to investigate the lateral behaviour of pile groups. Model pile group tests with lateral loading have been carried out by Gleser(1953), Prakash and Saran(1967), Druery and Ferguson(1969), Oteo(1972), Singh(1979), Selby and Poulos(1980) Selby and Parton(1987) Hughes et al(1981) Pise(1982), Arta(1986), Long(1987) and Sung Ho and Maddison(1989).

Poulos(1971,1973,1975,1977), Randolph(1981), Banerjee and Davies(1978) and Budhu and Davies (1987 and 1988) have used model tests results for comparison with their analytical solutions.

Model pile tests are conducted in such a way that the pile geometry is scaled down and the tests are carried out in a tank of sand or clay. Because of the gravitational effect the results obtained from model tests are not applicable to full scale piles because the soil insitu stressses are not correctly scaled. The influence factors or reduction factors obtained from model tests are generally greater than those at full scale.

Details of model tests are not reported here due to their limited value. In the next sections some full scale lateral load tests on single piles and pile groups are discussed.

2.9-Full Scale Lateral Loading Case Histories on Single Pile and Pile Groups

The work presented in this section are the results of large scale or field test investigations undertaken by various researchers on the behaviour of laterally loaded single piles and pile groups. The tests may be classified into two groups;

1-tests in cohesive soil

2-tests in non-cohesive soil

There is limited field test data available on laterally loaded pile groups, although a few valuable results are available for testing of analytical solutions.

Basically lateral single pile tests are conducted to study the behaviour of the pile/soil system in terms of pile head stiffness and pile shaft bending moment. A useful objective is to determine the soil modulus profile. Various researchers have conducted tests on pile groups in order to study group lateral stiffness and pile shaft moments. It unfortunate that very few workers have reported induced axial forces due to lateral load. Reddaway and Elson (1982) was a valuable exception which will be discussed later in this section.

2.9.1-Lateral Load Single Pile Tests in Non-Cohesive Soil

Reese et al(1974) conducted free head lateral load tests on two single piles in

a dense sand in Mustang Island (U.S.A). The piles were 610mm in diameter, and lateral loading was applied to the pile head as both static and cyclic loading. From the collected data they determined the soil stiffness characteristics and the deflected shape of the pile. Based on passive wedge failure theory, they proposed a method for developing p/u curves for sand. The agreement between the field test results and the proposed method was good. They reported values of n_h about twice as large as those recommended by Terzaghi(1955). Recommended values of n_h from static and cyclic loading are tabulated in table T2.1.

2.9.2-Lateral Load Single Pile Tests in Cohesive Soil

Reese et al(1975) carried out further tests on similar single piles installed in stiff clay. The tests were conducted to the North East of Austin Texas adjacent to U.S highway 290. From the experimental results they developed similar solutions to construct p/u curves for laterally loaded piles in cohesive soil.

Matlock(1970) carried out lateral load tests on a single steel pile 323mm in diameter and 12.8m long. The pile was installed in normally consolidated clay in lake Austin, Texas. The pile head condition was fixed and static and cyclic lateral load was applied to the pile head. He presented a solution to predict the ultimate resistance by assuming flow around a pile in the horizontal plane. He correlated his method with the field tests and good agreement was obtained for determining load/deflection and bending moment diagrams. His solution contained empricial factors. In his work he reported that in rapid cyclic loading the period at rest does not provide any restoration of soil resistance since there are no significant forces that would tend to refill the cavity found near the top of the pile. Filling the cavity with slurry did not have any effect on consolidating forces, but filling the cavity with granular material improved the resistance.

Price and Wardle(1979) conducted a series of tests on single piles in London clay. The piles were 0.168m in diameter and 5.1m long. Their main study was to observe

the deflection of the pile at different times of year. They measured the deflection of the pile from an adjacent trench by means of probes. Static and cyclic loading was applied to the pile head. They also investigated the response of an adjacent pile due to lateral loading of the first pile. From their results they concluded that the deflected shape of the pile changes due to seasonal effects. This has an effect on the horizontal subgrade reaction when the piles are statically or cyclically loaded. Monitoring of the adjacent pile showed that the unloaded pile was effected by movements of the adjacent laterally loaded pile.

Price and Wardle(1981) also compared the lateral response of an H pile section and a tubular pile having the same vertical bearing capacity. From results they obtained they found that the H-section pile deflected 40% more than the tubular pile under static loading and the tubular pile carried more lateral load in cyclic horizontal loading than H-section pile. Different values of soil stiffness were used to represent the behaviour of the two piles, which were difficult to derive from the site investigation report. Finite element and p/u curve techniques were used to compare the deflected shape of the pile and close agreement was achieved.

Lord and Davis(1979) conducted lateral load tests on driven piles in chalk near Brighton. They carried out horizontal plate bearing tests using a $450 \times 450mm^2$ plate to obtain the horizontal soil modulus. They then carried out lateral testing on a 800mm diameter pile which had a wall thickness of 20mm. From back analysing the pile test results they obtained the horizontal soil modulus. Different values of soil modulus were obtained from the horizontal plate test and the back analysis. The values of soil modulus obtained from the plate test were higher than from the back analysis of the pile tests. They concluded that the pile driving reduced the soil modulus and the plate test results were of limited use in predicting the lateral behaviour.

Alizadeh (1969) carried out lateral tests on two instrumented timber piles. He

reported that the soil modulus decreased sharply as the pile head deflection increased and at about 12.5mm deflection of the pile head the soil modulus reaches a limiting value. Similar results have been reported by Fleming et al (1980) who referred to work by Barton (1982).

Alizadeh and Davisson (1970) carried out a series of test on piles of different size and cross section in the Arkansas river project. They reported findings similar to those of Alizadeh's (1969) test except that lateral load test was carried out on different sized piles. The values of soil modulus they obtained differed from one type of pile to another.

Odone et al(1979) conducted lateral load tests on two single point mooring piles in the North Sea. The main pile diameter was 2.7m with wall thickness of 32 to 75mm. Two submarine pipe lines were connected to the bottom of the piles and delivered oil from two platforms. The piles were designed to resist lateral loading caused by a ship of 250 tonnes resulting in 1.0m deflection at the point of lateral load application. For both single mooring piles the observed deflection and tilt at maximum load were greater than predicted by up to 20 percent. The movement of the piles above the sea was observed on video camera. During load application maximum displacement was 12mm. In order to compare the stiffness behaviour of the two structures both before and after test the natural frequencies were measured to be 0.5Hz and 0.45Hz respectively. The stiffness of such structures is proportional to the square of natural frequency, so that a 10% reduction in frequency implied a 10% reduction in stiffness. Finite element analysis was used for both towers and the results obtained were in close agreement with the measured values.

2.9.3-Lateral Loaded Pile Group Field Tests

Holloway(1981) conducted an eight-pile group test in sand in a flood plain 1.7km downstream of Ellis Island. The piles were 14 inch diameter timber. The piles were driven at 0.9m centres , and the pile arrangement was 2 × 4 piles, driven 10.7m into

the sand. A reinforced concrete cap (2.13m × 3.96m × 1.83m thick) was cast with the piles embedded 0.61m into the reinforced concrete cap. The cap was cast 0.91m above the ground to form a gap between the base of the cap and ground surface. This gap allowed measurements of deflection, strain and inclination of the piles. A constant vertical load was maintained throughout the tests when the piles groups were loaded laterally. Details of the testing arrangement are shown in Figure 2.11 The pile group was loaded to failure defined as a deflection rate in excess of 0.25mm/hr. They obtained load/deflection curves and bending moment and shear force diagrams for the pile group. They compared the measured data with a program by O'Niell et al(1977). The program over-estimated lateral displacement by about 30%. The measured shaft bending moments of a front pile and a rear pile agreed closely with computed values. However the reverse bending moments under the base of the cap were not in agreement with the computer program. They found that the front pile carried greater shear force and moment than the rear pile. They recommended that the computer program by O'Neill et al(1977) should allow for relaxing the pile cap fixity and for stiffening the modelled soil.

Kim and Brungraber(1976) carried out extensive full scale lateral loading tests on three six-pile groups and on two single piles. The tests were conducted in Bucknell Campus farm in Lewisburg U.S.A. The soil was cohesive where the tests were conducted. Each pile was 12.2m long and strain gauged to determine bending strain along the piles during lateral loading tests. Slope indicators were also used to determine the slope of the piles. Each pile group contained six identical H piles. Two of the pile groups contained vertical piles only, (see Figure 2.12) with 1.2m spacing (group 1) and 0.9m spacing (group 2)and by third group piles were spaced at 0.9m (group 3) but two of the front piles were vertical and the remaining four piles were battered (1:3 slope). One of the isolated single piles was vertically installed while the other one was battered (1:3 slope). Each pile group was capped with 1.2m thick insitu

concrete. The concrete cap was extended 0.6m beyond the centre of any pile. The piles extended 0.3m into the cap. The cap was in contact with the ground surface.

One objective of their research was to relate the behaviour of isolated single piles to the behaviour of pile groups in static and cyclic loading.

The loading arrangement was intended to simulate that of a bridge abutment comprising vertical dead load and a lateral load and then applied incrementally to simulate the back filling process. One additional vertical load was applied to simulate the traffic load (live load). They also studied the effect of cyclic loading on the single piles and pile groups.

Three series of tests were conducted on the single pile and pile groups A, B and C at different times of the year. After each series there was a time delay to allow recovery of the soil/pile system. Comparisons were made between the three series.

Tests results showed that the deflection of pile groups in series B were greater than series A, by as much as 100 percent. In series B and C the pile group deflections were nearly the same for all the three groups. Regarding the spacing of the pile groups, the lateral deflection of the group 1 was less than group 2 and less than the isolated vertical pile. Group 1 deflected less than group 2 which means that the wider pile spacing gave greater lateral resistance in the groups. Group 1 was capable of resisting lateral load of 4.2 times that of the isolated vertical single pile and group 2, 2.3 times that of the isolated vertical single pile. The effect of cyclic loading was that the pile group stiffness was reduced by 22%.

The effect of battered piles in the group was studied in group 3. An isolated single battered pile showed deflection of 6 times that of the group 3.

They found that the maximum bending moment in the single pile was 5 times greater than those in group 1 and three times greater than in group 2. This means that as the spacing increased the maximum bending moment in pile group tends

toward that of a single pile.

Their main findings were that the stiffness of the pile group increased with pile spacing, the cyclic loading reduced the lateral stiffness by up to 22%, the stiffness of groups of battered piles was greater than of the vertical pile groups, and the maximum moments in piles at close spacing were greater than those in the single pile.

Gleser(1976) and Matlock(1976) criticised these tests by Kim and Brungraber (1976) because no account was taken that some the piles were bent about the minor axis and also because the resistance of the soil offered to the concrete pile cap was not considered.

Kim et al(1979) extended the work to conduct a fourth series of tests on piles and pile groups (series D). They removed the soil under the pile cap for 100mm and conducted similar tests as piles and pile groups as in series A, B and C except that a higher load was applied to the piles and pile groups. Their findings were as follows;

The removal of the soil beneath the pile cap had little effect on lateral resistance of pile groups. The removal of soil just below the cap reduced the lateral resistance and the maximum moments rose to twice those occurring when the pile cap was touching the soil surface. The bending stresses in the battered pile were higher in series D, but lower than in the vertical group piles. The effect of increasing pile spacing increased the lateral resistance.

Matlock et al (1980) conducted a series of field tests on circular pile groups in soft clay in Harvey, Louisiana. Each circular (154mm diameter) pile was composed of two sections, a 9.14m tube welded to a lower 4.57m, so the total length of each was 13.71m (see Figure 2.13). Static and cyclic loading was applied during 6 field tests, two on single piles and four on groups. The first pile group contained 5 piles at 3.4 pile diameter spacing and the second pile group contained 10 piles at 1.8 diameter pile spacing. The lateral load was applied at two different points above the ground to simulate a fixed head situation. The piles were instrumented to measure the bending

moments. They observed the failure of the soil around the piles.

Tests on single piles showed that the cyclic loading curves diverged from the static test by a reducing increment. In cyclic loading the position of maximum bending moment moved lower down the pile shaft and the bending moment reduced due to the cyclic loading. Observation of the soil around the pile showed an egg shaped cavity indicating a plastic zone. The soil in the front of the single pile was slightly raised to the horizontal extent of one pile diameter. The egg shaped cavity extended to several pile diameters below ground level.

Tests on a five-pile group showed that in the static test series, superposition of the soil strain in the single pile test occurred. A small distinct mound developed but for the five-pile group, the limits of displaced soil were more extensive. The mound that developed was related more to the group diameter than the diameter of individual pile. No cavity was created around the group as a whole but egg shape cavities again formed around the individual piles similar to the single pile tests. At the limits of deflection the curves indicated a general reduction of resistance due to cyclic loading. The front pile did not shield those at the rear as often supposed. The bending moments in piles in the group were the same as in the single pile. This was the same for both static and cyclic loading. This indicated that the piles acted individually. The position of positive maximum bending moment increased in depth in cyclic loading. The deflection was greater than for the single pile test.

In tests on ten-pile groups only half the piles were instrumented because of the expensive instrumentation. The total group reaction was estimated by assuming symmetrical distribution of load to the pile group. There was not a clear pattern of horizontal load sharing in the group but, there was clear uniformity of bending moment in the pile group. It was suggested that, in the restrained head case shear is more sensitive than bending moment to variation in soil resistance. The egg shaped separation was evident in the pattern of the group. The progressive decrease in lateral

resistance was seen in cyclic loading.

The maximum deflection for the ten-pile group was greater than for the five-pile group. However bending stresses or lateral resistance per pile were greater than for individual piles. The strain field would have lead to an increase in deflection especially for cyclic loading. The nonlinear behaviour of the soil was evident throughout the tests. The cyclic loading deflection was greater than in the static loading condition. The cyclic deflection curves departed from static at about 12.5mm deflection.

Reddaway and Elson(1982) undertook on behalf of CIRIA a comprehensive instrumentation excercise to monitor the behaviour of a bridge abutment in Newhaven on the A259 road (see Figure 2.14). They assumed a dead load on the bridge, and back fill on the abutment giving a lateral load equivalent to $5kN$. They compared the measured forces, deflection and rotation with 4 methods for analysing pile groups;

1-Static method

2-Stiffness method

3-Poulos method

4-PGROUP program

The comparisons were made for front, middle and rear piles. The above solutions all gave reasonable predictions of the load effects. The static method gave a close agreement on the distribution of the loads between the piles in comparison with the measured values and reasonable predictions were achieved using the above methods, for the measured deflection. The Poulos method for the prediction of deflection was the closest to the measured value. Rotation measurement cannot be compared because measurements from the site were not available. They also measured the axial force induced into the piles by the loading and used the stiffness method to compare; close agreement was found with the measured values. It is worth mentioning here that this is a rare example of work in which axial forces were measured and it forms

a valuable contribution to the subject.

Brown et al (1987) tested a large scale group of nine steel-pipe piles 43 ft long. The spacings between the piles were approximately 3 diameters. The pile group was subjected to two-way cyclic lateral loading. They also carried out a single pile test so that the results of the pile group test could be compared. The pile heads were free to rotate. The test was conducted in saturated stiff over-consolidated clay in Houston Texas. The behaviour of the pile group was non-linear. Their findings were as follows;

1 -The deflection of the group of piles was greater than that of the single pile for the first cycle of loading and similarly for 100 cycles of loading. The deflection of the single pile at 100 cycles of loading was very close to the first cycle on the pile group.

2 -The ratios of the first cycle pile head deflection to the 100 cycle deflection and first cycle maximum moment to 100 cycle maximum moment were traced against the lateral load. They found that as the load increased so did these ratios

3 -The distribution of load was measured and they found that the front row of piles carried more load than the middle row of piles which carried more that the back row of piles.

4 -The moments were measured along the pile length and it was found that the front row of piles carried greater moments than the middle row of pile and the position of the maximum moment was closer to the surface than in the middle row of piles. The middle row piles carried more moment than the back row piles and the position of the maximum bending moment was closer to the surface than in the back row piles.

5 -They also presented p/u curves in respect to each row of piles and found that the p/u curves were greater for the front row than the middle row which were

greater than the back row.

Brown et al (1988) carried out research on the nine pile group as in (1987). The piles were not extracted from the ground but the soil around the piles was excavated and was back filled with the sand. Similar measurement trends were recorded, with respect to lateral deflection, force and moment distribution and p/y curves. The p/u curves were different in the sand than in the clay but the treands were the same. They recommented multi level p/u curves. They compared the response of the pile in the group to the single pile and reported that the loss of efficiency of the piles in the group was due to the shadowing effect. They also reported that the lateral loading densified the sand around the single pile and pile groups. Ismael(1988) suggested that the loess sand may densify under lateral loading, but not cemented sands. Reese(1988) who is co-reporter in Brown et al(1988) agreeed with Ismael (1988). Prakash(1988) also referred to Brown et al(1988) and criticised their choice of A and B coefficient factors because the load was applied a foot above the ground rather than at the ground level.

2.10-Discussion

In this chapter some of the available methods of analysis for lateral loading were presented. Overall, it has been noted that the soil stiffness controls the lateral behaviour of the piles so it is important to set up a proper soil stiffness model. It has been mentioned by various authors (eg Poulos(1980), Broms(1964a and 1964b) Davisson and Gill (1963) Davisson (1970)) that the lateral behaviour of piles is governed primarily by the stiffness of soil near the ground line. Davisson and Gill(1963) suggested that soil in the region of 0.2R to 0.4R depth controls the load/deflection behaviour. The soil near the ground line may lose or gain stiffness due to an increase or decrease in soil moisture content. It has been presented by Price and Wardle(1979) that the lateral stiffness of a pile changes due to seasonal variation in ground properties. In the above reference the estimated pile capacity using subgrade modulus should be carefully selected to take into account the effect of seasonal changes. The

soil modulus may be under estimated due to elevated water table level. Ramasamy (1989) recommended that the observed load/deflection of the pile head should not be used directly to estimate the lateral capacity. However observed load/deflection should be used to take into account the possible changes in ground conditions. The lateral capacity of piles in a group may also be reduced due to spacing of the piles (see section 2.4)

It is also an important factor that the ultimate lateral resistance of a pile is well established. Barton (1982) carried out model tests, considering P_u varying with depth and compared results from Broms(1964b) and Reese et al(1956). Fleming et al(1985) reported that close to the soil surface P_u is $K_p\gamma'z$, but below about 1.5B, however, P_u closely follows the variation given by equation 2.34. Okahara and Nakatani (1991) found results for P_u similar to Broms'(1964b). Reese and Matlock (1956), Reese(1971) and other authors have presented solutions to take into account the failure of soil in front of the pile. It should be mentioned that the shadowing effect of the wedge type failure in a pile group is not well established.

The elastic continuum approach in analysing laterally loaded single piles is well established but, although the method can take into account the distribution of load in a pile group it is not entirely satisfactory because it assumes that the outer piles always carry the greater lateral load and the inner piles carry less. It has been demonstrated by Hughes et al (1980), Arta(1985), Long(1987) and Pise(1979) in model pile tests that the front piles carry more than the trailing piles, as was shown also by Uromeihy (1986), Brown et al(1987) Brown et al (1988).

2.11-Analyses Appropriate To The Test Programme.

From the many analytical and empirical solutions discussed in this chapter, it is necessary to identify those which are appropriate to the proposed test programme. Analysis is required for a pile which would behave as a long pile in a sand by using recommended values of n_h (see section 3.2.3). As tests are intended to be conducted

in a sand trench it is essential to determine the sand properties by conducting labratory tests and insitu tests and by back analysis of single pile test results. The most reliable and appropriate analyses of laterally loaded single piles and pile groups initially for linear elastic soil behaviour and then for elastic-plastic soil properties are those by Poulos, Randolph, Banerjee & Davies , Budhu & Davies and Reese & Matlock. Poulos solution uses charts based on boundary element solution for laterally loaded single piles and pile groups with both linear and non-linear soil behaviour, in cohesive and non-cohesive soils. Randolph presents equations based on a finite element axi-symmetric analysis for single piles and pile groups, taking into account vertical variation in soil properties. Banerjee & Davies present charts also based on an analytical solution to determine laterally loaded pile behaviour in a layered soil. Budhu & Davies also present explicit equations for an analytical solution similar to Poulos for linear and non-linear models of behaviour, as well as charts. Reese & Matlock present solutions based on the characteristic length of the pile for both cohesive and non-cohesive soils by employing the Winkler soil model, and a p/u analysis for non-linear behaviour of the soil. These several solutions will be used initially in back analysis of single pile results to deduce soil properties then to predict the behaviour of two-pile groups (Randolph and Poulos). Having completed the field tests series comparison will be made between the field tests and various analytical predictions using values of n_h obtained mentioned above. In addition a fully three dimensional finite element analysis will be used to model the soil/pile group to include pile cap tilting and pile interaction, in order to estimate lateral stiffness of the pile two-pile group, lateral soil pressure changes, and bending and axial effects on the piles. The finite element computations will then be compared with the field tests results and theoritical analyses for two-pile groups.

2.12-Conclusions

The following conclusions are presented here for the different types of analysis

and case histories.

1 -A single pile test is essential to back analyse the soil stiffness profile.

2 -The different methods presented here may be adopted to estimate the lateral response of both single piles and pile groups.

3 -The elastic continuum method offers a better understanding of pile soil interaction than the p/u method.

4 -The elastic continuum method does not present a good method for distribution of lateral load among piles in a group.

5 -Computer programs available for analysing single piles and pile groups have been reviewed by Elson(1985).

6 -The methods available for laterally loaded single pile and pile groups presented in this chapter will be used to design a pile which would behave as a long flexible pile.

7 -The available methods will be used to determine values of n_h by back annlysis of the field tests series on single pile.

8 -The Values of n_h obtained from back analyses will be used to predicted the behaviour of two-pile group.

9 -Comparison will be undertaken to quantify the observed results and predictive results.

10- More work should be undertaken towards understanding lateral load and moment distribution in pile groups because the mechanism of soil response to lateral loading in pile groups is not fully understood. It is particularly important to measure axial loads and moments in large scale pile group tests.
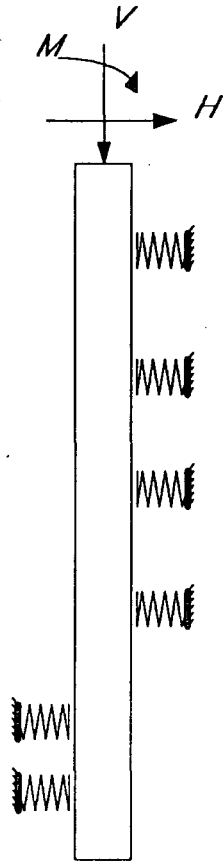
Figure 2.1 Soil/pile model used as Winkler spring system.
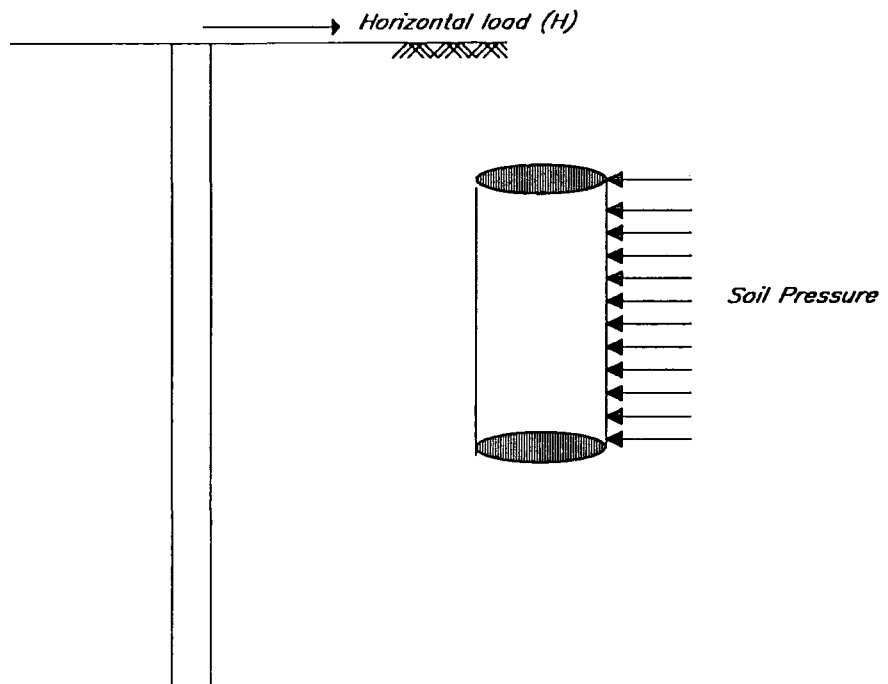
Figure 2.2 Laterally loaded single pile.
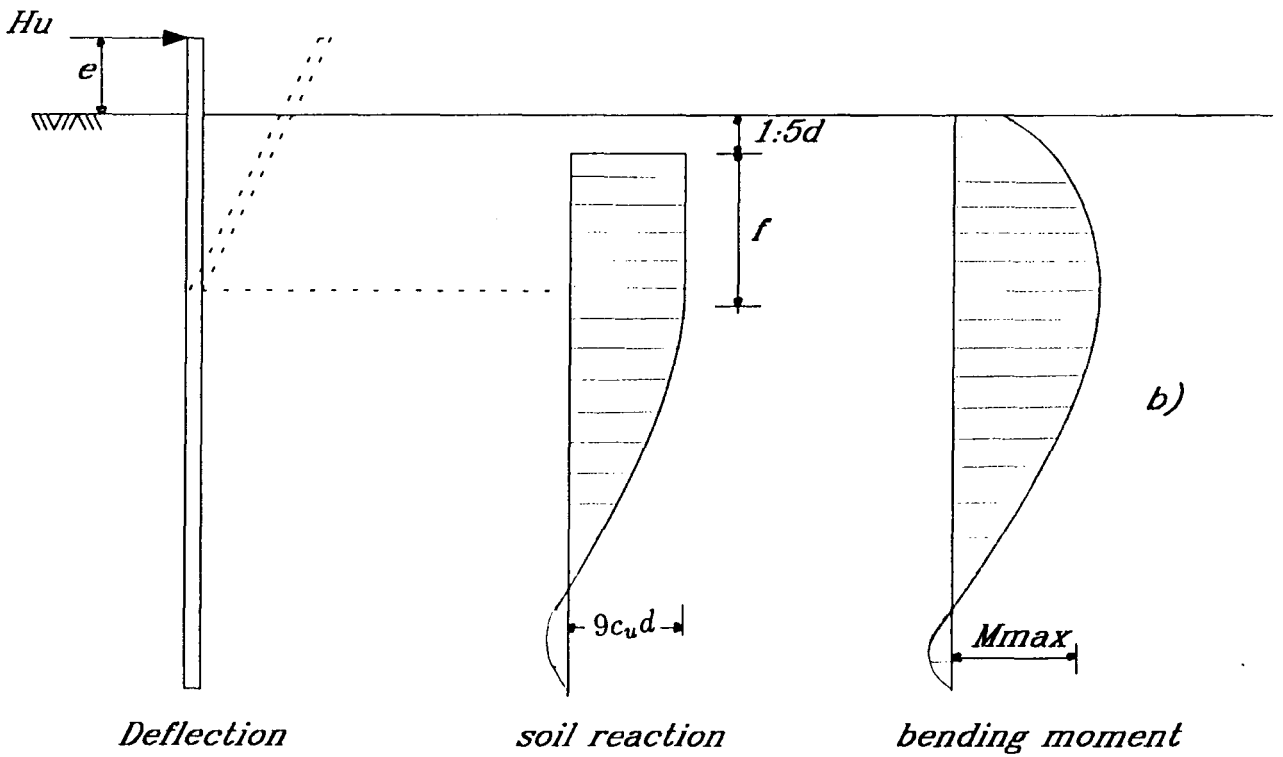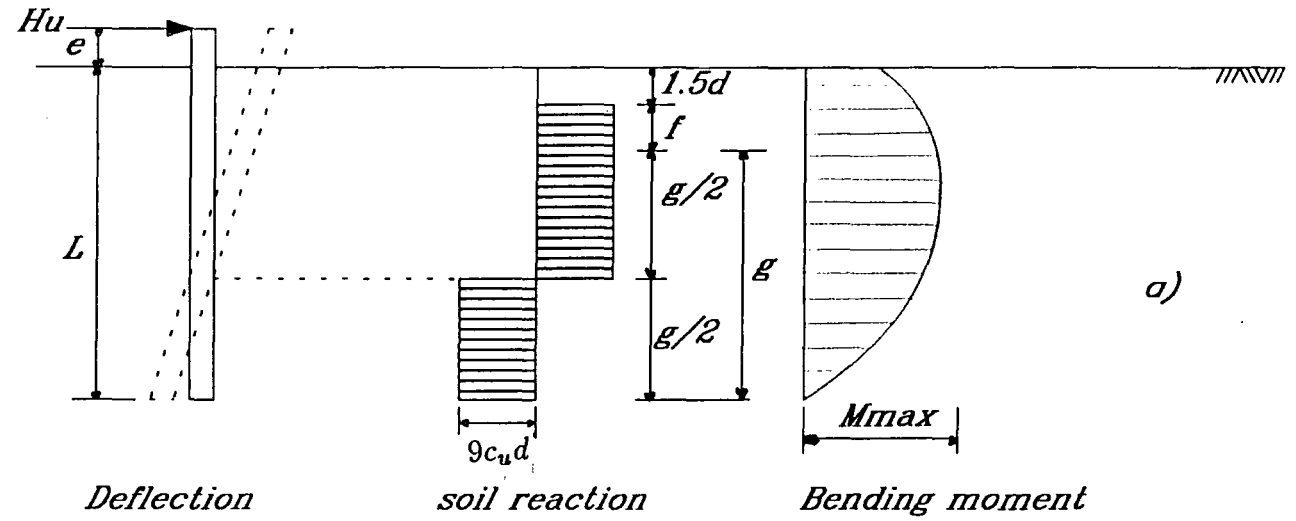
Figure 2.3 Laterally loaded free head single pile in cohesive soil;
(a) short pile: (b) long pile (after Broms, 1964a).
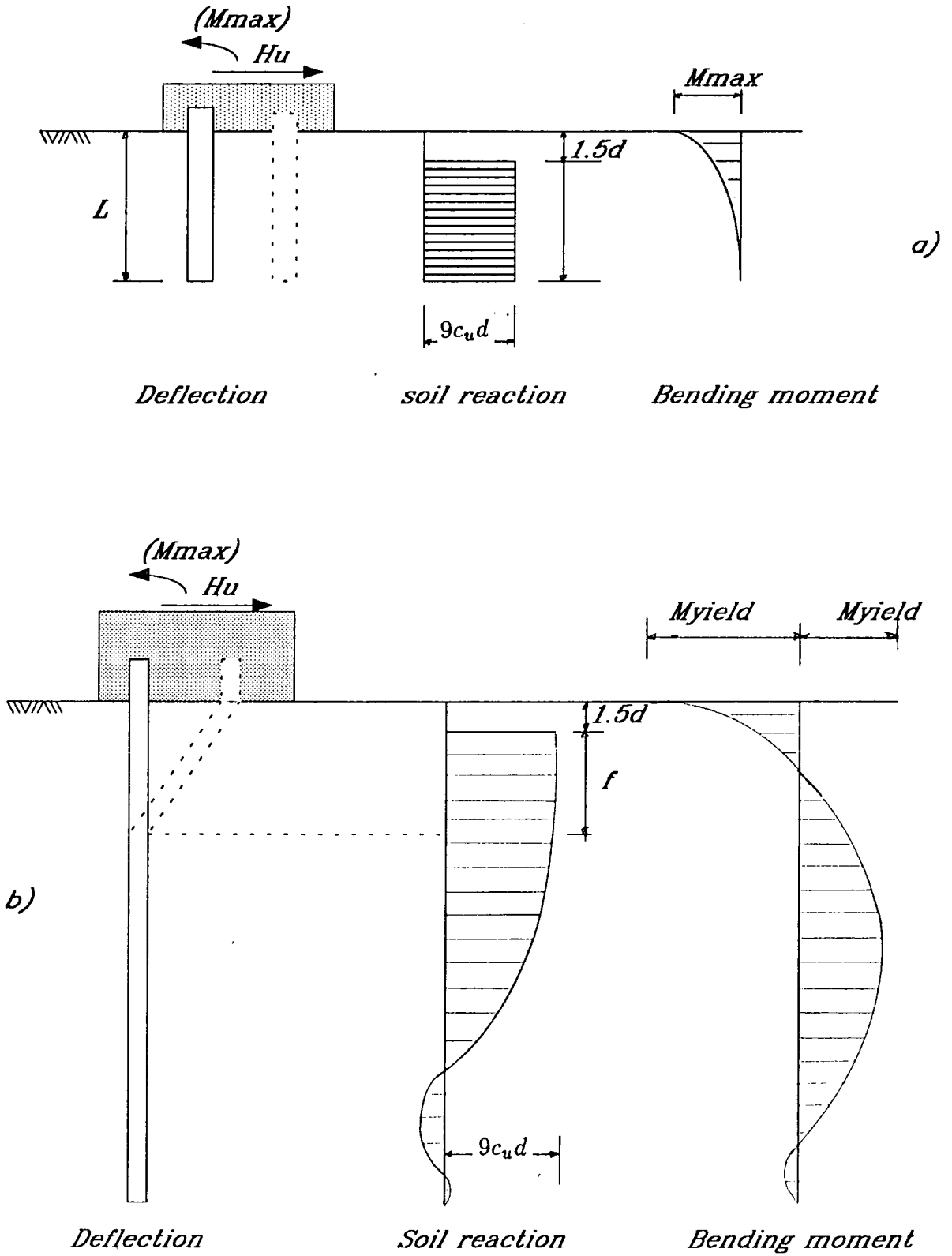
Figure 2.4 Laterally loaded fixed head single pile in cohesive soil:
(a) short pile: (b) long pile; (after Broms 1964a).
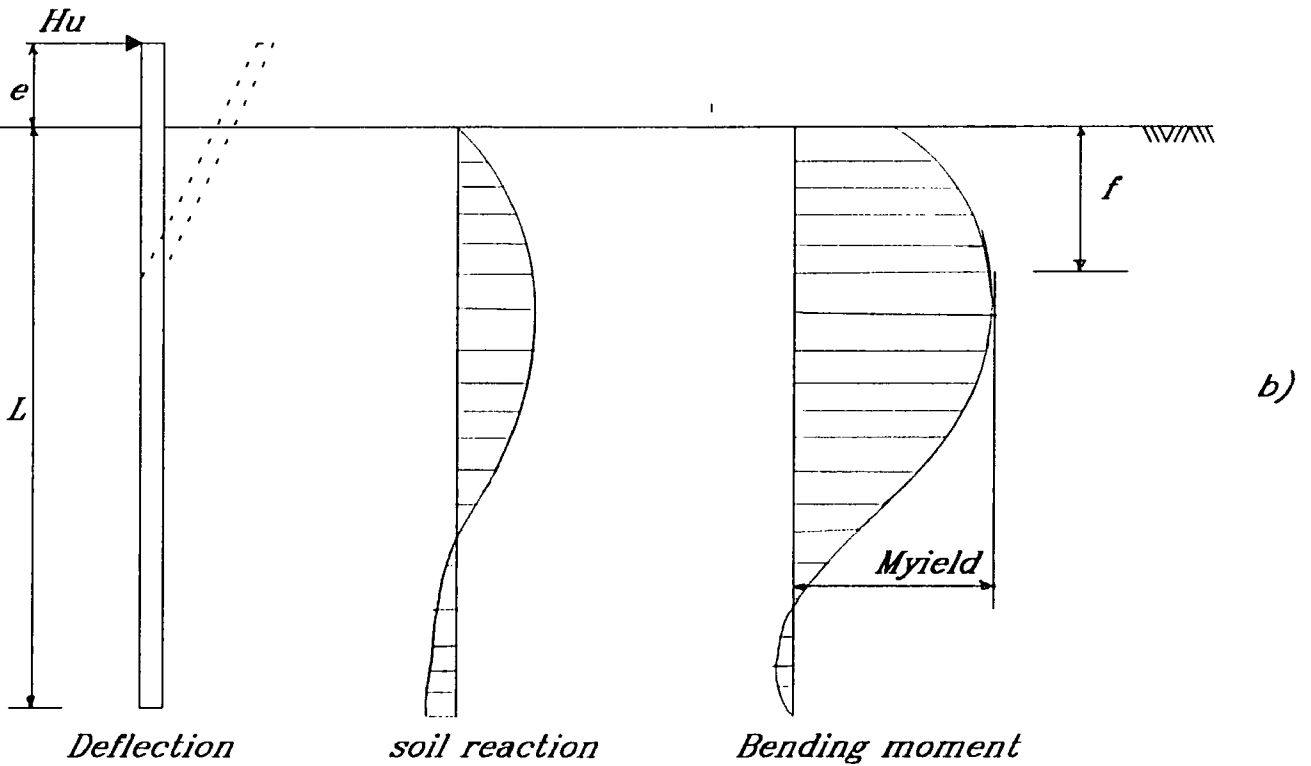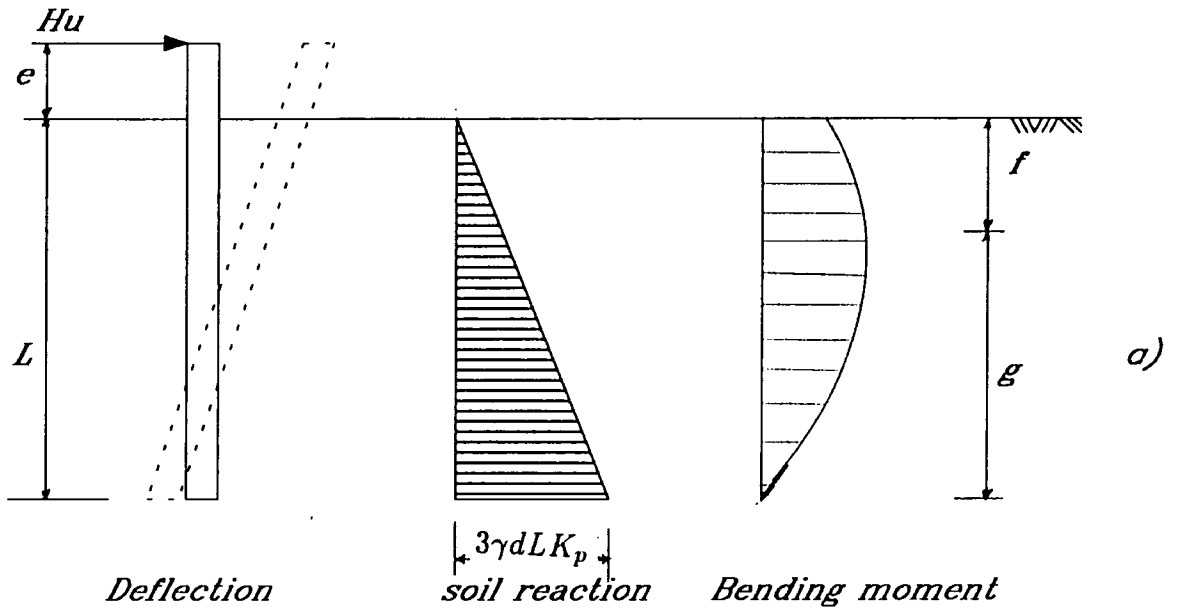
Figure 2.5 Laterally loaded free head single pile in cohesionless soil:
(a) short pile: (n) long pile : (after Broms 1964b).

(Mmax)

Hu

Mmax

L

$3\gamma dLK_p$

a)

Deflection   *soil reaction*   *Bending moment*

(Myield)

Hu

Myield   *Myield*

f

b)

$3\gamma df K_p$

Deflection   *Soil reaction*   *Bending moment*
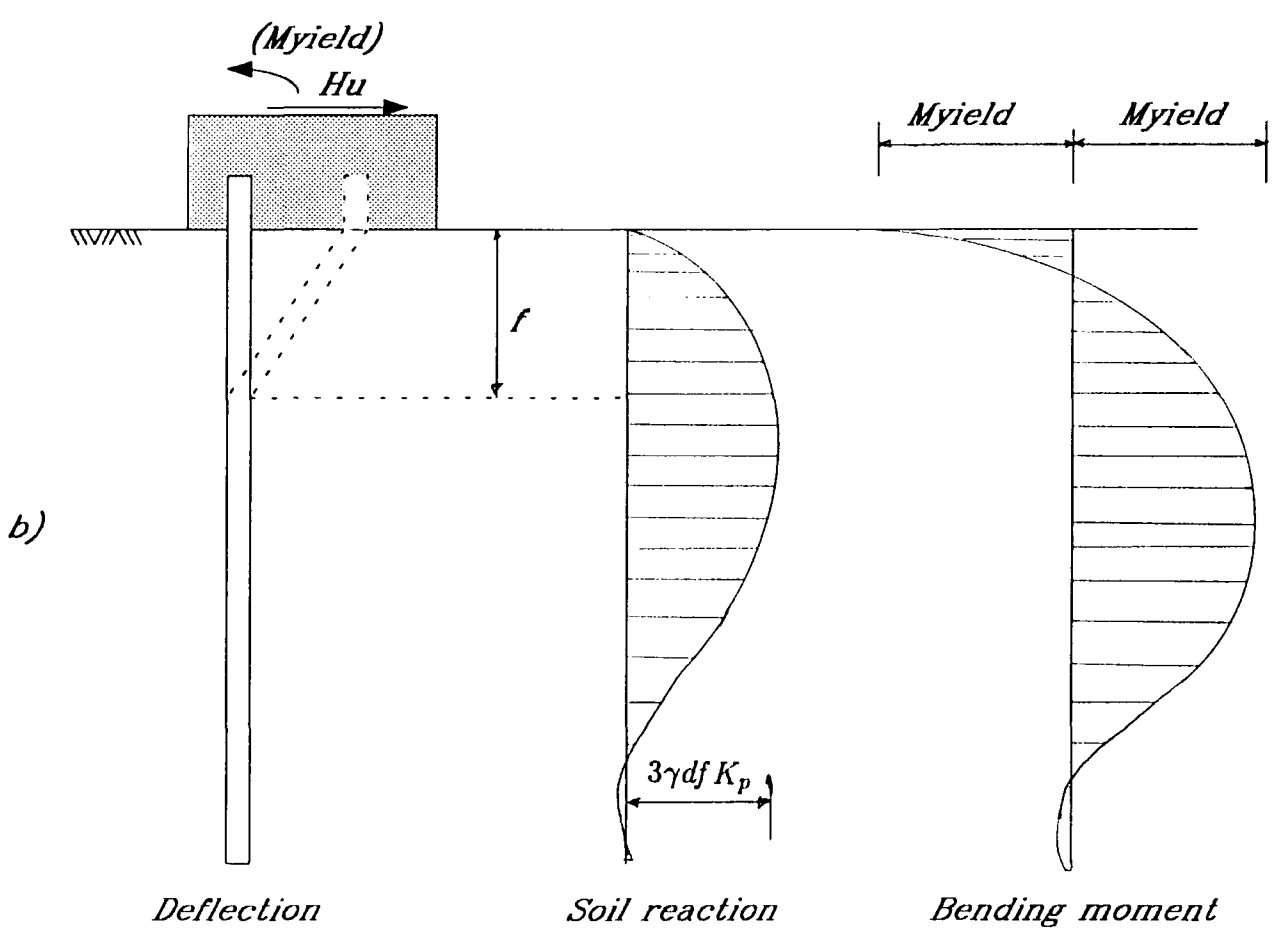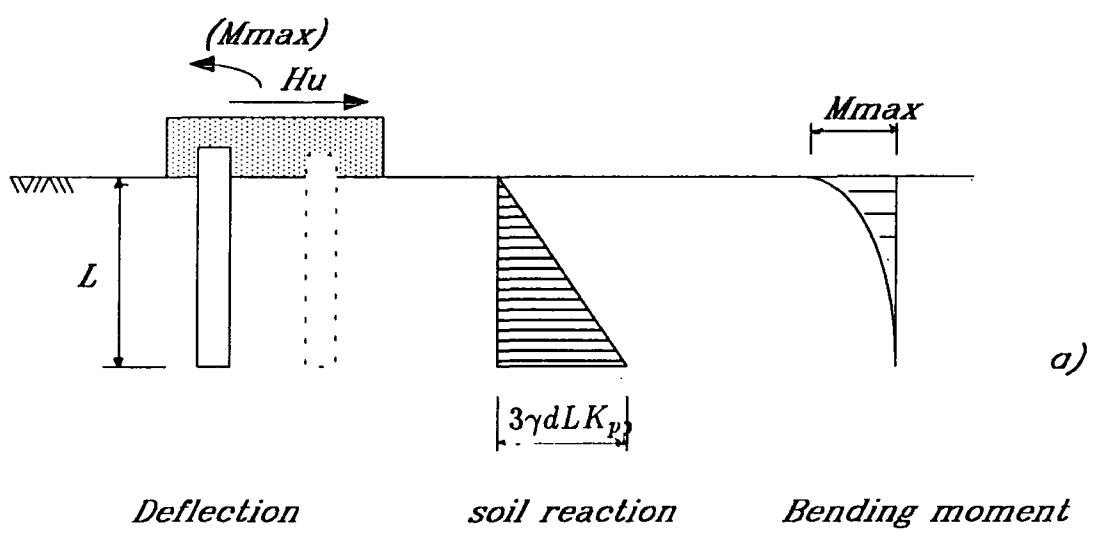
*Figure 2.6 Laterally loaded fixed head single pile in cohesionless soil
(a) short pile : (b) long pile (after Broms 1964b).*
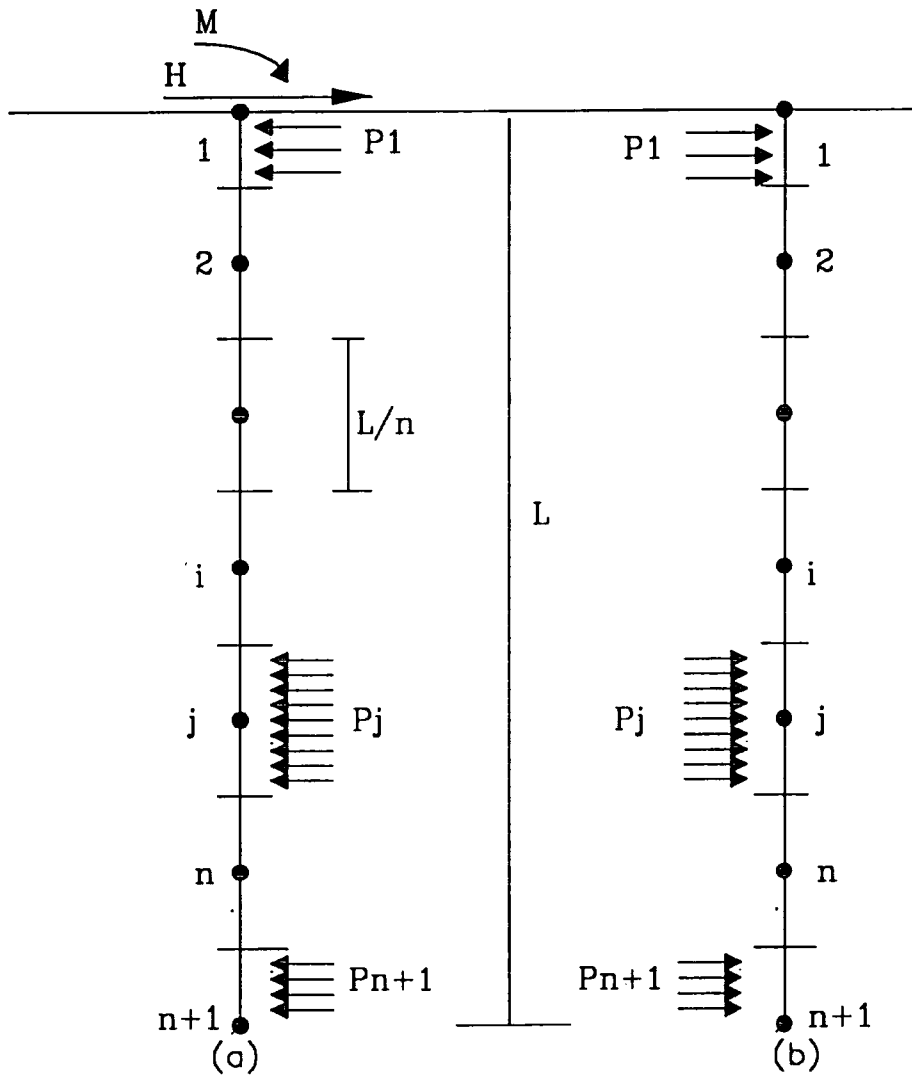
*Figure 2.7 Stresses acting on the floating pile: (a) pile, (b) soil
adjacent to the pile. (after Poulos 1971a).*
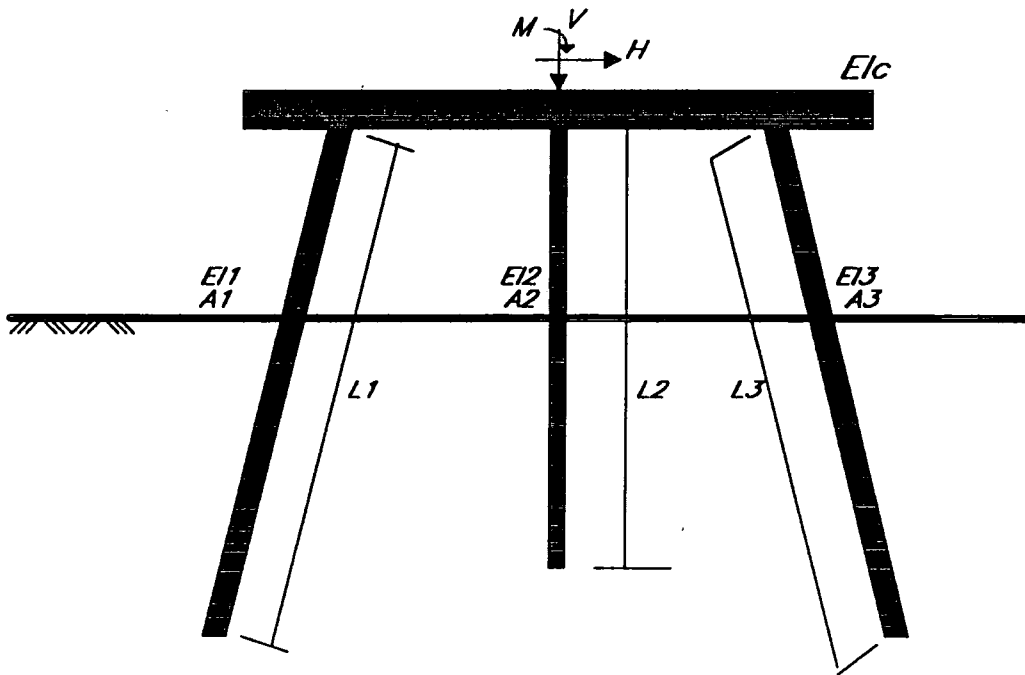
Figure 2.8a The actual pile group (after Poulos 1980).
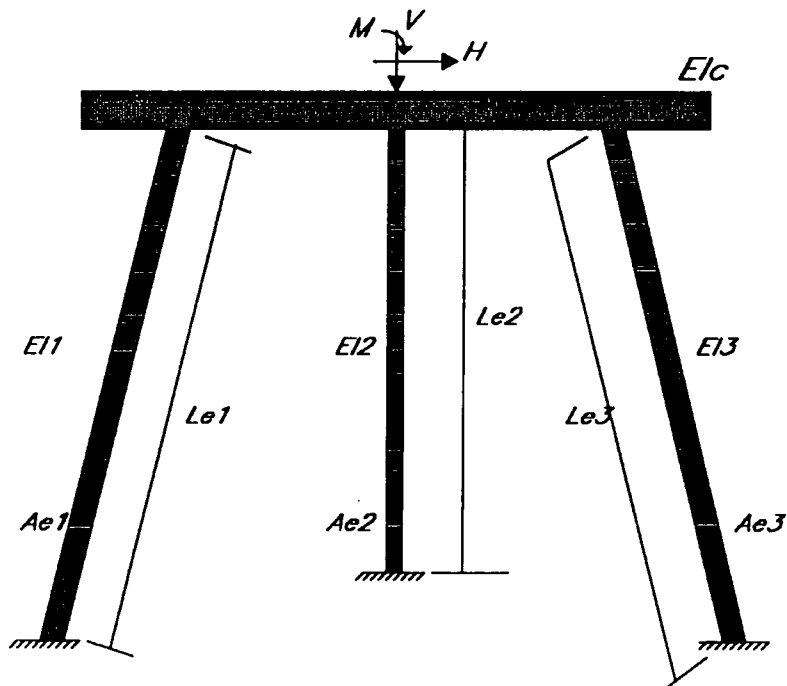
Figure 2.8b The equivalent bent method (after Poulos 1980).
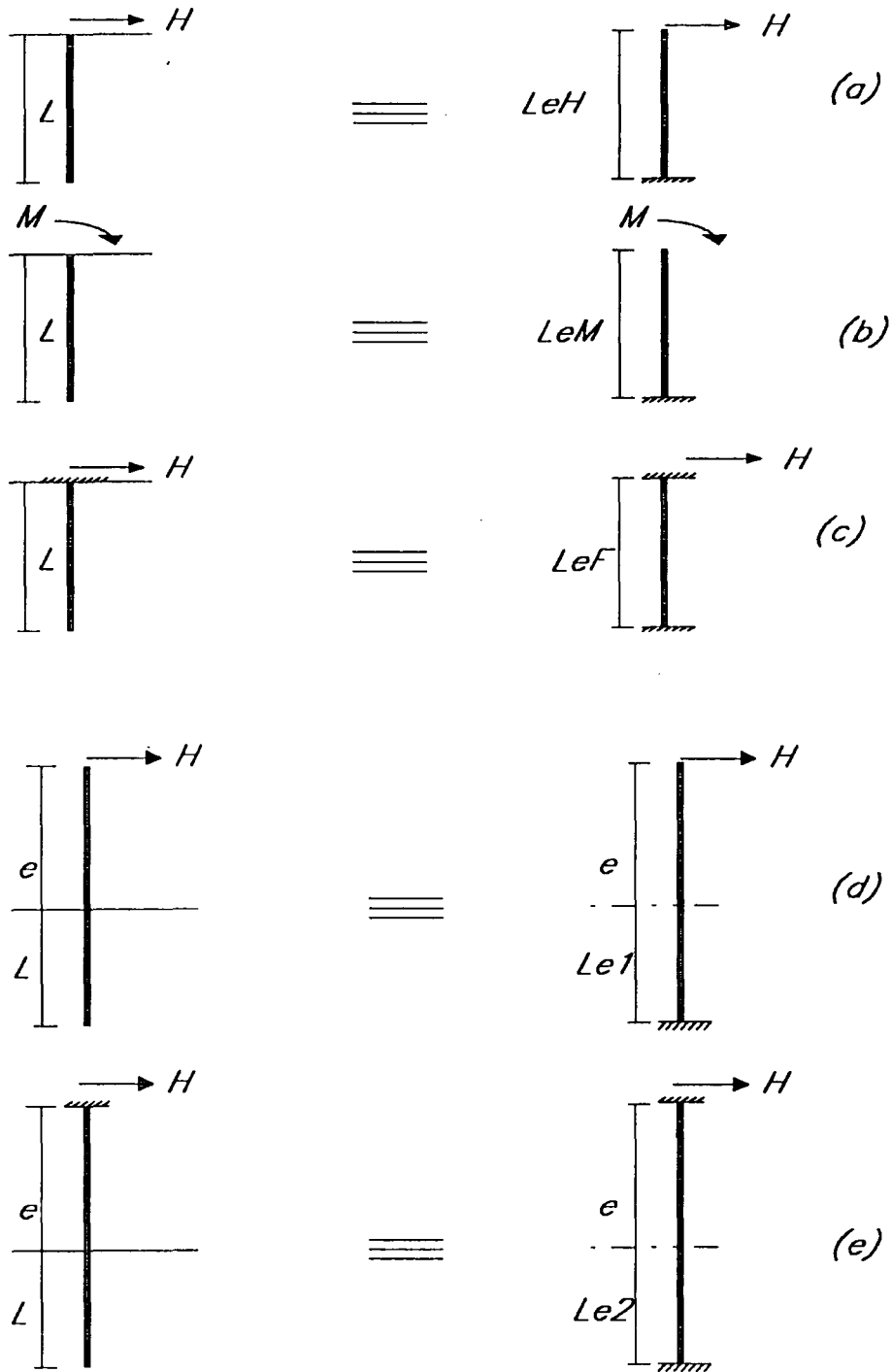
Figure 2.9 The equivalent cantilevers for laterally loaded piles.
(after Poulos and Davis 1980)
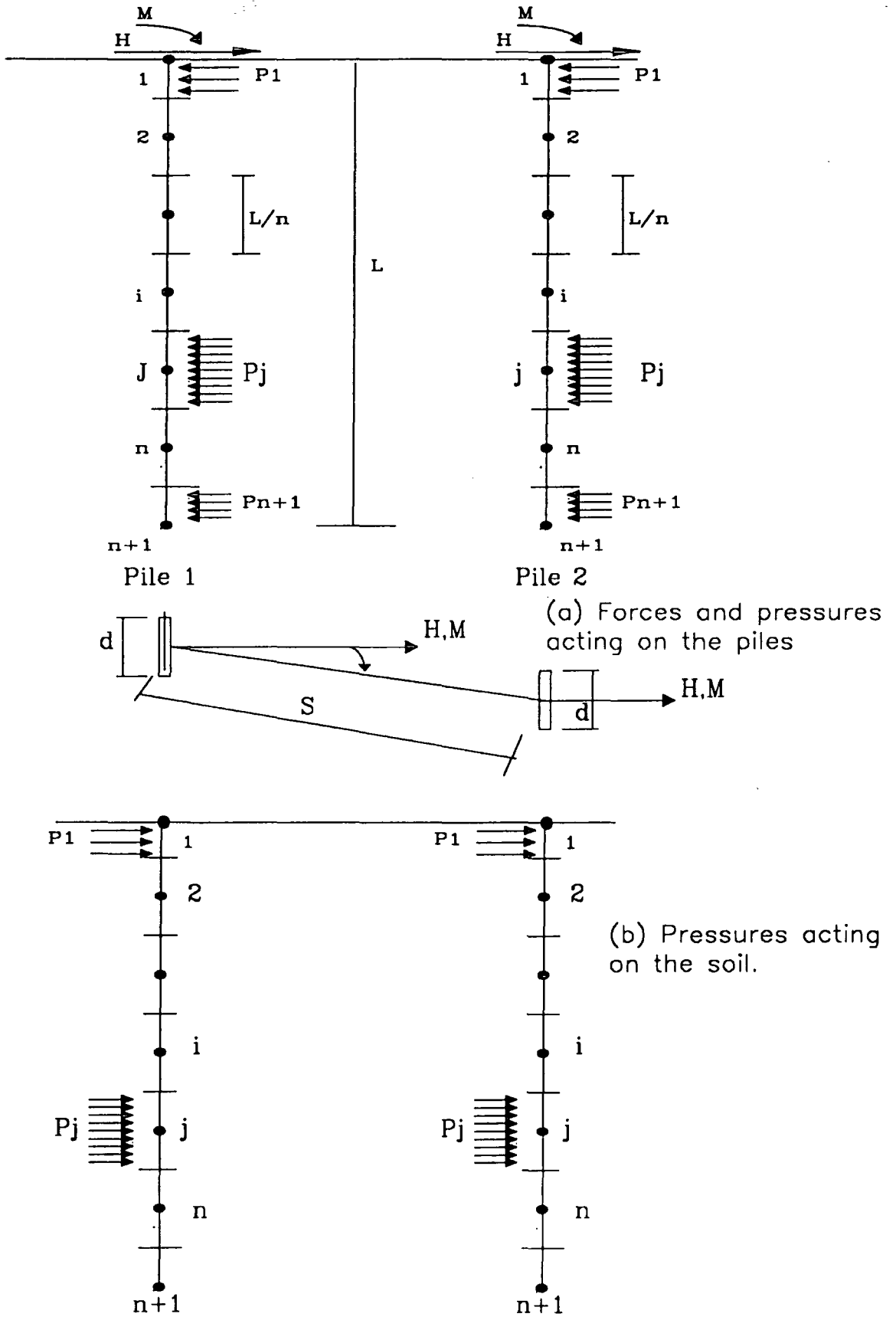
Figure 2.10 Two piles laterally loaded (after Poulos 1971b).
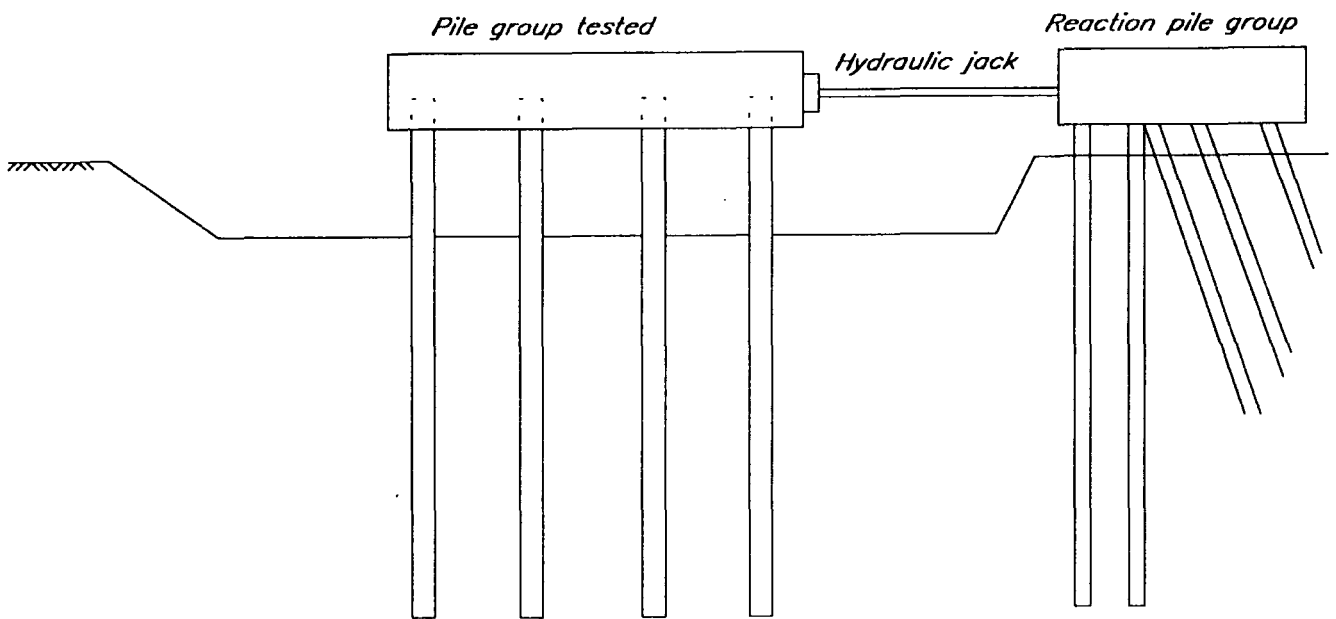
Figure 2.11 Pile group setup (after Holloway at el)

Group 1   Group 2   Group 3
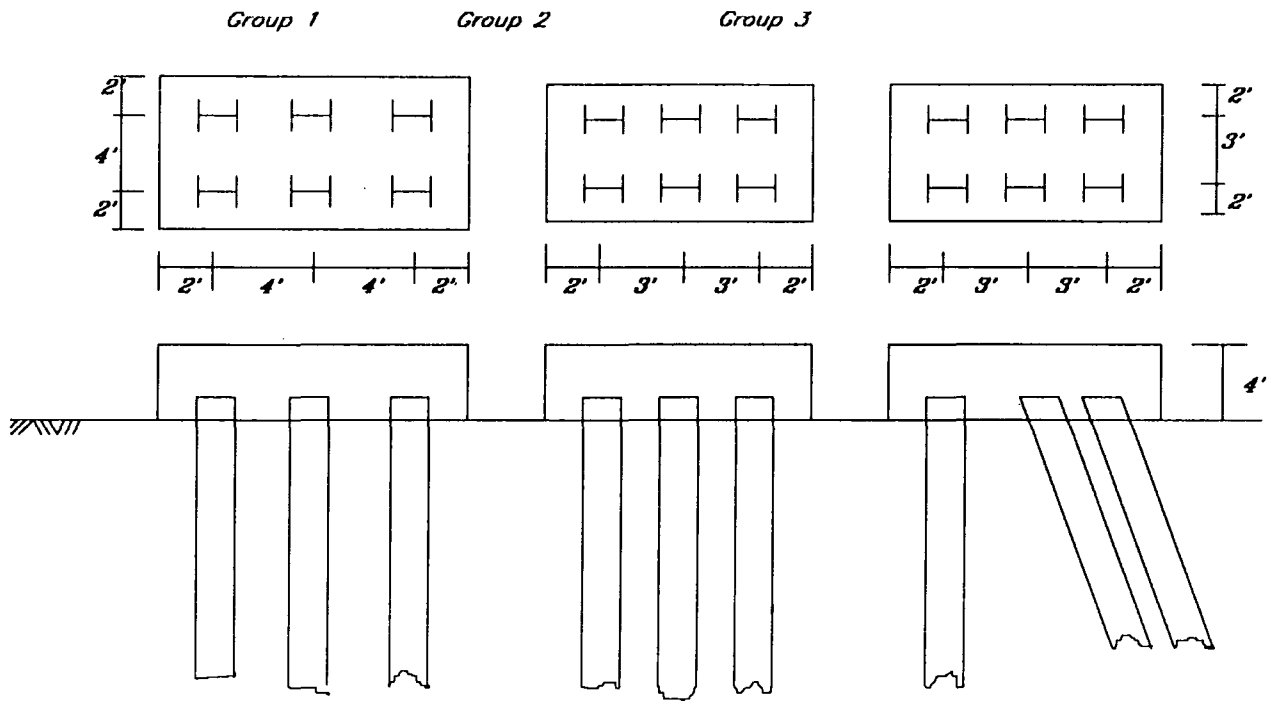
(a) plan view and elevation of pile groups
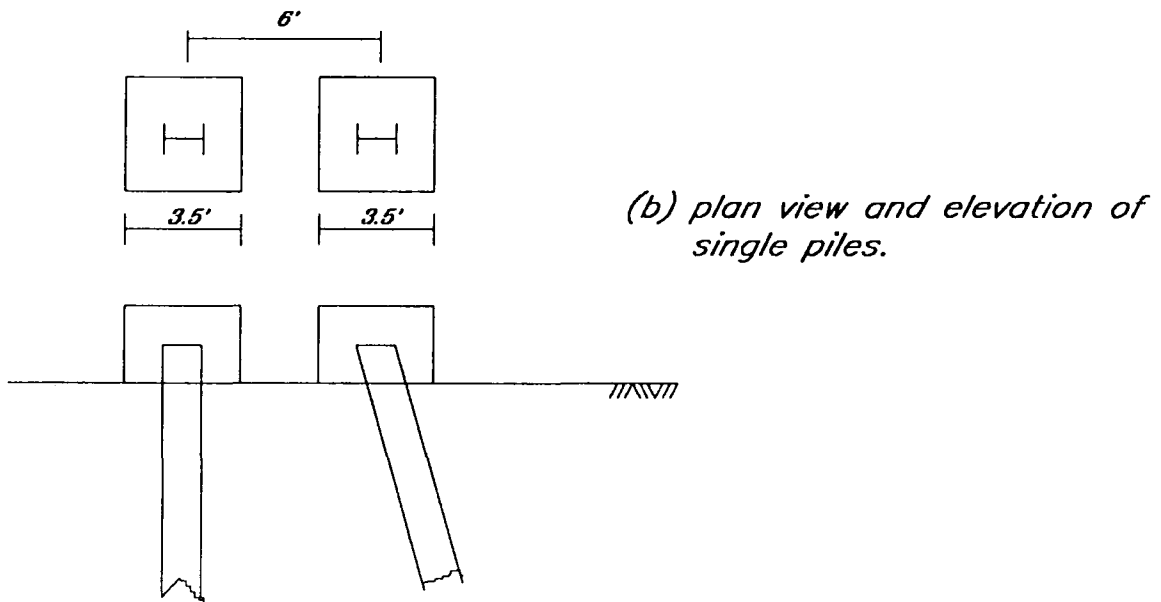
(b) plan view and elevation of single piles.

Figure 2.12 Pile layout and elevations (after Kim and Brungraber 1976).
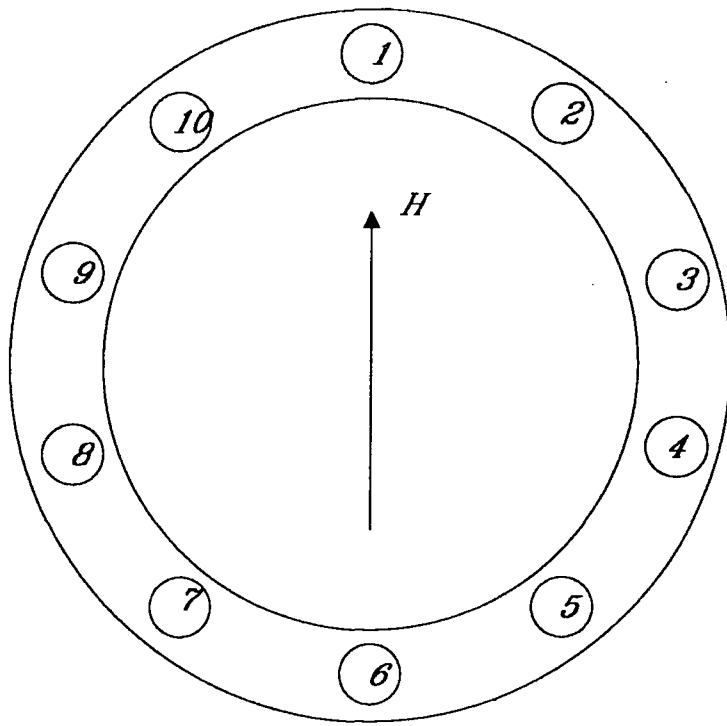
Figure 2.13 Pile group plan layout (after Matlock et al 1980).

(a) Plan view
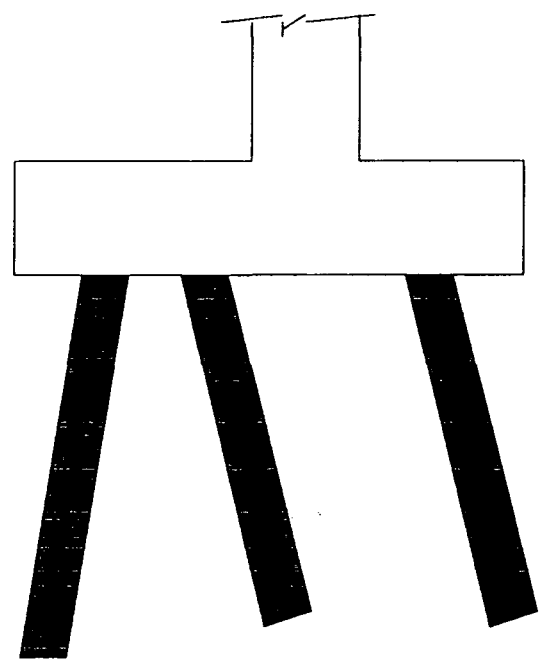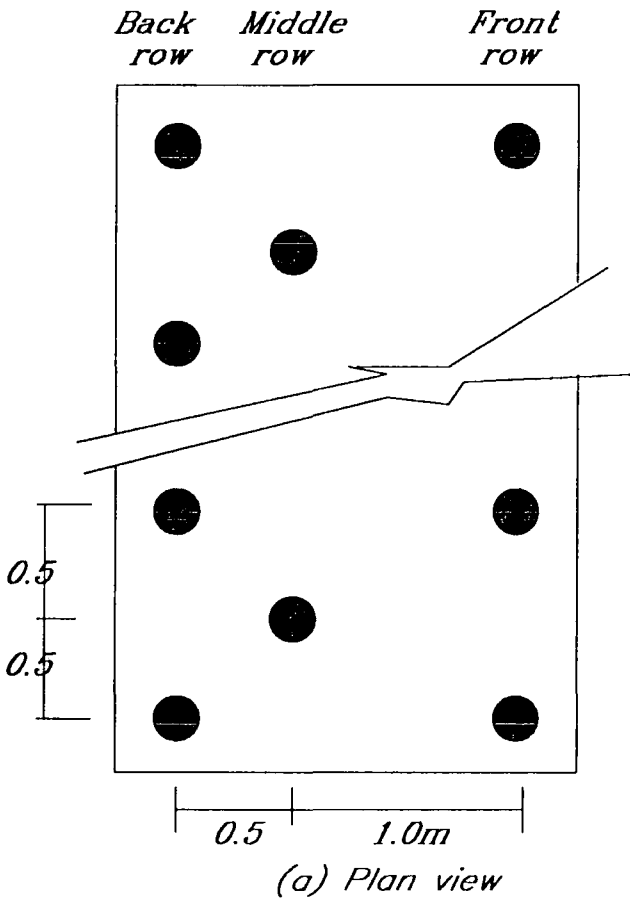
(b) Elevation view

Figure 2.14 Plan and elevation view of the pile group (after
Reddaway and Elson 1982).

Table T2.1a

Recommended values of K_h for cohesive soil

Consistancy	Stiff	Very stiff	Hard
Undrained cohesive strength c_u kNm^{-2}	100-200	200-400	> 400
Range of K_h $MN.m^{-2}$	18-36	36-72	> 72
Recommended K_h $MN.m^{-2}$	27	54	108

Table T2.1b

Recommended values of n_h for cohesion-less soil

Relative density	Loose	Medium dense	Dense
n_h for dry or moist soil MNm^{-3}	2.5	7.5	20.0
n_h for submerged (Terzaghi) soil (Terzaghi) $MN.m^{-3}$	14.0	5.0	12.0
n_h for submerged soil (Reese et al) $MN.m^{-3}$	5.3	16.3	34.0

CHAPTER THREE

Experimental Programme

3.1-Introduction

Model testing has often been used for studying the response of piled foundations to both axial and lateral loading and at small scale it is cheap to conduct. Work by Hughes et al (1980), Selby and Poulos (1985), Whitaker(1971), Arta(1986) and others on model piles and pile groups has contributed to the understanding of pile/soil systems, but these model tests do not fully represent the nature of pile/soil systems at full scale. Pile and soil dimensions can be scaled down but the gravitational force and consequential soil behaviour will not be in correct proportion.

There has been little field test data to allow comparison of model tests with full scale field test results. The objective of this study was to investigate the response of laterally loaded single pile and two-pile groups at various pile spacings and cap overhangs by undertaking a series of field tests at a realistic scale. In the test series it was important to investigate the characteristic behaviour of load/deflection of pile head and pile cap, bending moment and axial force distribution along the length of the pile, and the soil pressure distribution on the front and back of each pile along the embedded length of the pile.

In order to gain these objectives piles were constructed of two steel channel sec-

tions welded together to form a box section. This allowed installation of instruments on the flanges of each channel section before welding.

It was decided to conduct the test series in a sand trench, filled with yellow Permian sand. Prior to each test the upper layers of sand were removed, replaced and compacted. In addition the sand trench was dewatered by hand pump from two stand-pipes at the corners.

Each pile was erected using a winch fixed to a tripod above the sand trench, and driven into the ground by 50 and 100kg drop weights. The piles were limited to a maximum of 4.5m in length because of the height of the tripod.

Piles were tested either as single piles or as two-pile groups, in response to lateral loads. In the case of the two-pile groups, the pile heads were connected by a steel cap.

3.2-Choice of Pile Length

In their design piles may be regarded as either rigid or flexible. The measure of flexibility Zmax is a function of the elastic modulus of the pile, the second moment of area, the soil properties, and the pile length (see section 3.2.4). Piles with a value of Zmax greater than 4 are defined as being flexible. The flexible pile condition is more often encountered than the rigid pile case. The induced deformations and bending moments in a flexible pile are confined to the upper part of the pile and the lower embedded length of the pile has little effect on the pile head response to lateral load. Conversely, the response of a rigid pile is pure tilting. Piles in deep foundations are usually flexible and so it was important to design a flexible pile by calculating the flexibility function to be greater then 4 (see section 3.2.4).

3.2.1-The Pile Cross Section

Each pile consisted of two cold-rolled steel channel 'C' sections welded together to form a hollow square box section. The steel was supplied by Brockhouse Berry plc, of

Bromsgrove, UK. The overall length of the each channel section was 4m. The choice of a box section comprising two C section channels allowed installation of gauges on the inside faces of the flanges of the box. The gauges and leads were thus in a protected environment during driving and testing. The toe of the pile comprised a 200mm long pointed shoe for easier drivability. Figure 3.1 shows the dimensions of the pile cross section. The piles were classified as large displacement piles and so the soil around the pile would be disturbed during driving. The pile was very heavy to handle and was capable of carrying a high compressive load during installation.

During welding it was necessary to protect the wiring and gauges by employing a heat shield on the inside of the pile cavity. Also the heat inside the pile cavity due to welding was reduced by applying a constant flow of air from a high pressure source at one end of the pile. This had the added benefit of removing fume from inside the pile. Care had to be taken during welding to avoid bowing which might occur if one side were welded along its whole length in a single operation. Bowing was prevented by using a systematic pattern of welding in which small sections from each side and each end of the pile were welded alternately.

3.2.2-Elastic Modulus of Pile

Because the material properties of the cold rolled channel section were unknown, tests had to be conducted in order to determine the elastic modulus of the steel. Samples $15 \times 200 \times 5.5mm$ thick were cut from a channel section in order to conduct a cantilever bend test. Two electrical resistance strain gauges were mounted on the top and bottom surfaces of the sample 100mm away from the free end of the cantilever. The sample was clamped firmly to a mounting block and the bending strains were recorded in response to tip loading. From simple bending theory the bending stresses were calculated at the point of the measured strains ,and by plotting the calculated bending stresses against measured bending strains a linear relationship was found. The slope of the curve gave the elastic modulus of the steel to be 210GPa. Figure 3.2

shows the cantilever dimensions and the stress/strain relation of the pile material.

3.2.3 -Second Moment of Area of the Pile Section

As the piles consisted of two cold rolled channel C sections the second moment of area, I, of the pile section had to be calculated. The pile cross section was assumed to consist of flat plates with square corners, and the second moment of area was calculated by the parallel axes theorem. No allowance was made for cut-outs or for shear lag across the flanges. The second moment of area of the pile was calculated to be $1.39 \times 10^{-5} \ m^4$. Figure 3.3 shows the assumed cross section of the pile and Table 3.2 shows the calculation for the second moment of area of the pile.

3.2.3-Pile Behaviour

As discussed in section 3.2 it was required to design a pile which would behave in a flexible manner. The second moment of area and the elastic modulus of the pile were determined as described in section 3.2.2 and 3.2.3. The behaviour of the pile was described by equation 2.27 which was used to obtain the stiffness factor T for a pile in normally consolidated clay or granular soils. The soil modulus was assumed to increase linearly with depth. Terzaghi(1955) proposed that for normally consolidated soil the rate of increase of horizontal subgrade reaction n_h for dry or moist soil is approximately 2500,7500 and 20000 kNm^{-3} for loose, medium and dense sand respectively. As the yellow sand in lightly compacted state would fall into the loose to medium category the n_h value was taken as 5000 kNm^{-3} for an estimate of stiffness factor. Using Terzaghi's approximation the following calculations were undertaken

$$T = \sqrt[5]{\frac{EpIp}{n_h}} \qquad (2.27bis.)$$

where

T is the Stiffness factor

EpIp is the flexural stiffness of pile

Ep is the elastic modulus of pile $= 210 GPa$

Ip is the Second moment of area of pile $= 1.39 \times 10^{-5} \ m^4$

n_h is the rate of increase of horizontal subgrade reaction profile, 5000 kNm^{-3}

therefore

$$T = \sqrt[5]{\frac{2.1 \times 10^8 \times 1.39 \times 10^{-5}}{5000}}$$

giving a stiffness factor T $= 0.862$

Reese and Matlock (1956) defined pile behaviour in terms of a depth coefficient Zmax. If Zmax is less than 4 the pile will behave as rigid but if Zmax is greater than 4 it may be considered to be flexible. Here,

$$Z_{max} = \frac{L}{T} = \frac{3.35}{0.862} = 3.87 \tag{3.1}$$

Z_{max} is close to 4 and therefore the pile should behave in a predominately flexible manner.

3.3-Pile Instrumentation

The primary parameters to be measured in the lateral loading tests were the pile head displacements, the bending moments and the axial forces in the piles and soil pressure distribution along the embedded length of the pile. It was also hoped that axial loads in the piles could be measured. It was necessary to evaluate the several types of instrument available. To obtain bending moment values at various positions along the length of the pile electrical resistance strain gauges (ERSG) or vibrating wire strain gauges (VWSG) could be used. For soil pressure measurement a special pressure cell had to be manufactured in the Durham University workshops.

3.3.1-Electrical Resistance Strain Gauges (ERSG)

The ERSG is a strain measuring device which shows changes in electrical resis-

tance proportional to strain in the gauged material. ERSG's are manufactured in various sizes and configurations, and a standard single gauge commonly has a resistance of about 120 Ohm and a gauge factor of about 2.1. The resistance change in response to strain is caused partly by the changes in geometry and partly by a change in resistivity.

Small changes in resistance are measured by use of a wheatstone bridge. Strain gauges may be connected into a bridge circuit to make a quarter, half or full active bridge. Strain readings were recorded manually using strain bridge model HW1-D which is calibrated to read directly in microstrain ($\mu\varepsilon$). The bridge was connected to a switching box to allow scanning of up to 23 channels. One disadvantage of ERSG's is their susceptibility to moisture. They must be kept well sealed from moisture intrusion. Also during scanning, the strain gauges may drift because electrical resistance changes in the wire due to the heating effect of the electric current (see Horowitz and Hill (1989)) introduce errors in the true strain readings. The apparent resistance changes caused by temperature changes can be eliminated using the dummy gauge method. The active gauge is mounted on the surface of the material and a dummy gauge is mounted on an unstrained separate sample of the same material, exposed to the same environment as the active gauge. Since the dummy and active gauges are in the same conditions the effect of the temperature changes upon the active gauge is cancelled. Thus the measured resistance change represents only the strain imposed on the active gauge.

3.3.2-Vibrating Wire Strain Gauges (VWSG)

The VWSG is a versatile mechanically mounted strain gauge which was developed originally by the Road Research Laboratory and measures strains slightly eccentric to the surface of a structural member. On steel surfaces the gauge may be attached either by bolting, by welding or by means of epoxy or other types of adhesive. Fixing to a concrete surface is achieved either by bolting to grouted-in studs or by adhesives.

In operation (see Figure 3.4) the VWSG uses a high tensile steel wire, in tension between the two end mounting blocks, to sense the variation in surface strain over the gauge length. This strain variation developes a correspounding change in tension in the wire which is detected by the change in frequency. A plucking coil is mounted in the protective enclosing tube surrounding the wire. A current pulse fed to the coil shock-excites the wire which then oscillates at a frequency determined by the wire tension. A variation in strain is thus converted to change in frequency of oscillation of the wire, observations of which are made by measuring the output from the coil which now acts as a pickup device.

The robust construction minimises the risk of mal-function of the gauge due to mishandling. The low gauge profile and the small number of mechanical joints in its construction ensure low transmission of eccentric strains to the gauge axis, but where bending of the structure is sufficient to induce errors, two gauges mounted back-to-back on opposite sides of the member allow bending strains to be eliminated.

A square law relationship exists between strain change and the observed frequency change.

$$\delta\varepsilon = K(f_1^2 - f_2^2) \tag{3.2}$$

where

K is gauge factor $K = 3.0 \times 10^{-3}$,

$\delta\varepsilon$ is change in strain,

f_1 is datum frequency in hertz,

f_2 is frequency after loading structure in hertz.

Preliminary testing of a tensioned gauge was needed before conducting the main test series. The clamp pin in the end block from which the tension wire emerges was released by unscrewing the socket screw in the block connecting the gauge to the strain measuring unit. The wire was then retensioned, taking care not to kink or

overstress the wire. At a plucking voltage of 24 volts a clear note should be heard. The wire was then clamped. The frequency recorded depends on the wire length and on the tension in the wire. The gauge was now ready for use in testing.

Very small strains of 0.5×10^{-6} can readily be measured, whilst at the other extreme the overall strain range measuring capacity is about $3000\varepsilon_\mu$. The VWSG's have excellent long term stability and are unaffected by lead length or deterioration of contact resistance in the interconnecting circuit. They are robust, easy to handle and install and may be adapted for mounting on different types of surface.

3.3.3-Initial Testing of ERSG and VWSG

Initially it was decided to use both ERSG's and VWSG's to determine bending strain along the length of the pile. As ERSGs are able to measure surface strain directly while VWSG measure eccentric strains, these strains had to be compared to observe the linear relation between the surface and eccentric strain. This test was conducted on a steel plate by mounting VWSG's on both sides of the steel plate and mounting ERSG's underneath the centre of the VWSG's on both sides. This test was conducted by cantilever tests as shown in Figure 3.5. The cantilever test was conducted and the bending strains were recorded and plotted against bending moment. The relationship between bending strain and bending moment was found for individual strain gauges (see Figure 3.6) and these relationships were plotted against the cross-section of the steel plate. It was found that the relationship between the surface strain and eccentric strain was linear through the cross section of steel plate (see Figure 3.7).

Several of the available VWSG's had to be modified, repaired and tested in order to record correct bending strains. Also a stability test was conducted on the VWSG's during pile driving. This test was carried out by mounting a VWSG on a 80mm square box section of length of 1.0m. Readings were recorded before and after a weight was dropped on to the prototype pile head, and it was found that the VWSG

readings were not affected by impact driving.

3.3.4-Locations of VWSG and ERSG in The Pile

Figure 3.8 illustrates the positions of the VWSG's and ERSG's along the length of a pile. In total 42 VWSG's were used, but due to a lack of sufficient numbers of VWSG's it was decided to use ERSG's also. In addition the ERSG's would act as a back-up system in case of failure of any of the VWSG's.

3.3.5-Design of Pressure Cell

It was considered to be an important contribution to the test series to record changes in lateral earth pressure along the embedded length of the pile due to lateral movement of the pile. The pressure cells were required to have a high degree of resistance to corrosion and to have a high yield stress. Stainless steel satisfied these conditions. It was decided to use stainless steel type 306A, which has yield stress of 463MPa and a recommended working stress of 340MPa.

The ultimate lateral earth pressure P_u on a pile was estimated by using Brom's equation;

$$P_u = 3 \times \gamma' \times z \times K_p \quad (kPa) \qquad (2.36 \ bis)$$

where

γ' is effective unit weight of soil

z is depth below the surface

K_p is Rankine passive coefficient $\frac{1+\sin\phi}{1-\sin\phi}$

ϕ is angle of shear resistance of soil

It was assumed that the maximum pressure would develop at the middle of the embedded length of the pile. Using Brom's solution and assuming values for γ of 18 kNm^{-3} , for ϕ of 35° , z of $\frac{3.55m}{2}$ and K_p of 3.7, then P_u would be 354MPa. For design of the pressure cells the circular plate was assumed to be uniformly loaded by P_u. The maximum deflection develops at the centre of the plate which was found

using (see Timoshenko and Woinowsky-Krieger(1959)):

$$w_{max} = \frac{P_u r^4}{64D} \qquad (3.3)$$

where r is the radius of circular plate and D is the flexural rigidity

$$D = \frac{Eh^3}{12(1 - \nu^2)} \qquad (3.4)$$

where E is elastic modulus of material 210GPa and ν is Poisson's ratio (0.33).

The maximum stress at the boundary of a plate is

$$\sigma_{max} = \frac{3P_u r^2}{4h^2} \qquad (3.5)$$

therefore

$$P_u = \sigma_{max} \frac{4h^2}{3r^2} \qquad (3.6)$$

Using the above solution a suitable thickness of a plate with a diameter of 20mm was obtained (see table T3.2).

It was decided to manufacture a pressure cell with a diaphragm thickness of 0.7mm with a radius of 10mm (see Figure 3.9), and a 3mm electrical resistance strain gauge was mounted on the internal surface of the diaphragm. A disc shaped adaptor was manufactured into which the diaphragm was threaded. To calibrate each pressure cell, the cell was screwed in reverse direction into the adapter which was held in a jig to facilitate testing. Air pressure was then applied to the device and the strain reading on the pressure cell diaphram was recorded (see Plate 3.1). The pressure cell had to be modified to meet design requirements and the final thickness of pressure cell was chosen to be approximately 0.4mm. Finally 48 pressure cells were manufactured and each pressure cell had to be individually calibrated because of small differences in the diaphragm thickness. The relationship between the applied pressure and the strain readings from the electrical strain gauges was recorded and the results of these tests are tabulated in table 3.3. To mount pressure cells in the front and back faces

of each pile, the pile was counterbored at specific distances (see Figure 3.9b) and the disc shaped adapters were held in position by four screws. The centre of the adapters were threaded to accept the pressure cell and the pressure cells were screwed in the centre of each adapter assembly. Care had to be taken in order to align the ERSG's in line with the vertical axis of the pile otherwise the ERSG's on the pressure cell diaphragm would not give the true lateral earth pressure. Each pressure cell assembly was sealed to make it water tight with silicon sealant. Also the ERSG's were protected by silicon rubber to exclude moisture. Figure 3.9b illustrates the positions of pressure cells along the length of the pile. Plate 3.2 illustrates the pressure cells on the pile.

3.3.5.1-Apparent Strains on the Pressure Cell

When the pressure cells were firmly fixed to the pile, they became part of the pile member, and bending of the pile might cause changes in strain on the pressure cells. This false reading may occur when there is no applied pressure on the cells and the pile is simply bent as a beam. Three point load tests were conducted on individual piles and some pressure cells showed small apparent strains due to bending. When the pile was bent in sagging the bottom section of the pile would go into tension and the top into compression. It was important to investigate whether apparent strain would be seen if the member was inverted. The results showed small but different apparent strains. The pressure cells which were affected due to the simple bending were identified and the relationship between the apparent strain on the pressure cell and the adjacent strain gauges was obtained. During actual testing the strain on the pressure cell had to be compared with the results obtained in simple three point load tests and the false strain had to be deducted from the actual testing results. Figure 3.10 shows the pile in the three point load test. Figure 3.11 shows relationships between the apparent strain and adjacent strain gauges on the pile sections for the pressure cells which were affected in simple bending.

3.3.5.2-Stability Test on the Pressure Cell

A stability test had to be conducted to determine the effect of pile driving on the pressure cells. A pressure cell assembly was mounted on the same box section used to investigate the effect of driving on the VWSG's. The test was conducted in the same manner as for the VWSG's. The results showed no effect on the pressure cell device during pile driving.

3.4-Leakage Tests On the Piles

As each pile consisted of two channel sections welded together to form the piles, inspection was necessary to eliminate any pin holes along the welded joints. This was necessary so that the piles, when installed would not fill with ground water. A blanking plate was secured to the end of the pile to enable an internal air pressure to be applied enabling an inspection of the welded joints (see Figure 3.12). Leakage holes were found by applying soapy water on the welded joints and more welding was done to eliminate the leaks.

3.5-Testing Site

Tests were to be carried out at Hollingside-lane in ground owned by Durham University, about 3 kilometres to the South East of Durham City.

3.6-Ground Conditions

The ground conditions consisted of top soil, sub soil,then weathered clay becoming firm yellow clay. Figure 3.13 shows a borehole log.

3.7-Sand Trench

It was decided to conduct all tests in a sand trench. A trench was excavated 6m long by 1.2m wide and 2.1m deep and was back filled with compacted yellow permian sand. Two stand pipes were placed in corners of the trench for dewatering and to observe the water table level (see Figure 3.14) This trench was used for all the tests.

3.8-Soil Testing

Testing of the condition of the sand in the trench was undertaken by cone pene-tration tests. Samples of sand were stored for later laboratory testing. Collection of clay samples from below the excavation was dangerous because the trench was un-supported. Therefore results of previous tests on the clay by Uromeihy (1986) on the same clay of the same site were used. Minor variations in sampling were not critical because in this pile test series the lateral movement of the pile was largely restricted to the upper portion of the pile within the sand trench, so that the clay affected axial loads only. The following tests were conducted on the sand.

3.8.1-Triaxial Testing

Sand samples were collected in standard U100 tubes from the sand trench for drained triaxial tests to determine the elastic modulus E and angle of shearing resis-tance ϕ. Three sand samples 200mm long by 100mm diameter were tested at three different effective confining pressures of 50,100 and 150kPa respectively. Each sample was inserted in a rubber membrane, and placed inside the triaxial cell. Water was used as the confining fluid and the sample was saturated for 24 hours. A B value was measured as the increase in pore water pressure divided by the increase in cell pressure. When the B value exceeded 0.95 the effective confining pressure was set. Drainage was allowed from top and bottom of the sample and the volume of water displaced during consolidation was measured and the percentage of volume change was calculated. Figure 3.15 shows percentage of volume change against square root of time. When there was no further volume change consolidation was complete.

At increments of vertical strain, measurements of vertical stress and vertical dis-placement were recorded. Figure 3.16 shows the relationship between the axial stress and percentage of axial strain for three different samples tested. From these relation-ships the elastic modulus of soil E was found to be 14MPa. The peak axial stresses at failure for all three samples were obtained. Mohr circles were drawn for the three

different peak axial stresses at failure and the confining pressures. Figure 3.17 shows the circles and the envelope. It was found that the angle of shearing resistince of the sand was 36.5^o and the sand had no cohesion.

3.8.2-Sieve Analysis of The Yellow Sand

Sieve analysis tests was carried out to determine the sand grading. The test complied with BS 1377: Part 2 : 1990, Figure 3.18 shows the grading of the sand and the sand is uniformly graded with less than 10% silt.

3.8.3-Sand Replacement Density Testing

As the trench was exposed to the environment, control of the sand density become difficult so the standard sand replacement test was carried out on the sand in the trench to determine the in-situ density, in compliance with BS 1377:Part 9:1990. Three locations were tested so as to give an average density of the sand. The average unit weight for the three tests was 19 kNm^{-3}.

3.8.4-Compaction Testing

Compaction tests were carried out to determine the sand dry density for a given compactive effort and for different moisture contents. The test complied with BS 1377:Part 4:1975,with the 2.5kg rammer falling through a height of 0.3m. Figure 3.19 shows the variation of the sand density with the moisture content. It can be seen that up to 12% moisture content the dry density increased with moisture content, but further increase in moisture decreased the dry density. The optimum moisture content for the sand was 12% and the maximum dry density was 17 kNm^{-3}. During these tests the cone penetrometer was inserted into the cylinder of compacted sand and the cone resistance was recorded after completion of each test for the different moisture contents and densities. Figure 3.20a shows the relationship between unit weight and the cone penetrometer reading for each test. Figure 3.20b shows the relationship between moisture content and the cone penetrometer reading for each

test. It was intended that this correlation would help to determine the sand density on site.

3.8.5-Cone Penetrometer Testing

To control sand density in the sand trench was difficult due to variable weather conditions through dry or rainy spells as the trench was exposed to the environment. The cone penetrometer was used to estimate the density after recompaction. The cone penetrometer consisted of a 1m long stainless steel rod with an end cone of 60°. The rod was marked at a regular intervals so that the readings could be taken at various distances during penetration. The top end of rod was threaded to accommodate a proving ring to determine the axial load on the rod. Above the proving ring a handle was attached for pushing the rod in the soil. Plate 3.3 shows a cone penetrometer during testing. The cone penetrometer proving ring was calibrated (see Figures 3.20a and 3.20b). Before each test the cone penetrometer was pushed into various parts of the sand trench and the readings on the proving ring were recorded for various intervals on the cone penetrometer rod.

It was intended that the reading on the penetrometer would be correlated with the compaction test values as described in section 3.7.4.

3.9-Dewatering The Sand Trench

Before each test ground water level table in the sand trench was observed. If the water level was above the bottom of the sand trench, the trench was dewatered from the stand-pipes at corners of the trench by inserting a hose pipe in the stand pipe and connecting the hose pipe to a hand pump. The pump had to be primed by pouring water into its out-let and continuing pumping. Once the pump was primed the water would start flowing out of its out-let, and hand pumping was continued until there was no standing water in the stand-pipes. This practice was repeated several times until there was no water left in the sand trench.

3.10-Method of Pile Driving

Each pile was erected, carefully positioned and aligned using a winch on a tripod and a long spirit level to set the piles vertical about both axes. The pile was secured firmly with rope. The pile was driven using a simple drop hammer which was raised above the centre of the pile and dropped using a quick release device. During driving, the spirit level was employed to recheck that the pile was vertical. A steel cap was made and placed on the head of the pile to limit damage during installation. Two drop hammers were available consisting of steel bar weighing either 50 or 100kg. At the start of the pile installation, the 50kg weight was used but later the 100kg weight was used to increase the impact energy. The hammer was suspended from a steel cable running over a pulley to a winch. This arrangement was supported on strong tripod which was carefully aligned above the centre of the pile head. The hammer was dropped under free fall to strike the pile head using the quick release device. When the hammer was dropped a rope was attached to the hammer to prevent the hammer from falling to the ground after the stike. Piles were driven through the sand in the trench and down into the clay. Plate 3.4 shows the method of driving.

3.11-Lateral Loading Device for a Single Pile

To apply horizontal load normal to the axis of the vertical pile a reaction pile was driven parallel to the vertical pile outside the sand trench. Load was applied by means of a stirrup shaped assembly, consisting of two channel sections. Two 8mm holes were drilled in the channels 200mm apart to accommodate two 7mm tension rods. Tapered wedges in barrels secured the tension rods to the stirrup. A manually operated hydraulic jack, consisting of a jack unit and a pump unit, was used to apply horizontal load. The jack was set up between the flange and the end plate of the stirrup. Figure 3.21a shows the loading device assembly.

To determine the load applied to the pile head, electrical resistance strain gauges were mounted on the tension rods to measure the strains. As the relationship between

the tension in the rods and strain readings was unknown, a 250mm long sample of similar rod was gauged and was tested in a Denison machine. Figure 3.21b shows the relationship between applied load and strain. A best fit line is drawn through the points giving a gradient of $0.0056 kN$/microstrain.

An advantage of using a stirrup shape loading device was that load could be applied at any distance above the ground simply by raising or lowering the assembly. Care had to be taken to ensure that the loading was applied normal to the axis of the vertical pile.

3.12-Deflection and Rotation Measuring System

The tests were displacement controlled rather than load controlled. The pile head or pile cap deflection was measured by a linearly variable differential transformer (LVDT). To measure the lateral movements of pile head and pile cap a light dexion frame was mounted in the ground outside of the sand trench, so that the frame would be unaffected by disturbed soil surrounding the pile. An LVDT was mounted on a dexion frame and set up touching the pile head.

All LVDT's were precalibrated for displacement using a micrometer calibration device. The LVDT's were energised by a 10 volt stablised supply. Calibrations were conducted to relate displacements to change in voltage. Figure 3.22 shows the relationship between displacement and voltage for the two LVDT's used.

To measure pile head rotation two LVDT's were placed on a dexion frame at different heights above the ground. The head rotation was obtained from the difference between the two LVDT's and the distance between the LVDT's.

To measure pile head rotations of the cap in two-pile group tests, a light dexion frame was mounted outside the sand trench, two pairs of dial gauges were mounted on the dexion frame for each pile, and the head rotations were obtained by taking the difference between dial gauge readings divided by the distance between gauges.

3.13-Design of The Pile Cap for Two-Pile Groups

As this work was particularly concerned with the distribution of load between piles in a two-pile group, a pile cap was needed to connect the two piles together to form a rigid frame. It was required to design a pile cap which would rigidly connect the two piles at any overhang and at variable pile spacing.

The pile cap was constructed from two longitudinal C section beams with cross frames, the same channel sections as were used to construct the piles, and of steel cleats which were bolted to each beam. The beams were then clamped to the pile head, see Figure 3.23a

It was necessary to estimate the horizontal load required to deflect the pile cap by 20mm and then to check the pile cap capacity. Using Brom's solution, the horizontal load required to deflect a single pile by 20mm was estimated to be 100kN. It was suggested in section 2.3 that Brom's solution is conservative. Using elastic solutions by Poulos with interaction factors for a fixed head two-pile group with 12 pile width spacing, the horizontal load was about 100kN. A computer program solution by Selby and Wallace (1985) which was based on a simple stiffness method, suggested that the head moment on each pile would be about 47kNm.

Having estimated the horizontal load and the pile head moment and assuming that the head moment would occur at the centre of the pile head, the design of the pile cap was as follows (see Figure 3.23b).

Horizontal force required is assumed to be 100kN, lever arm is 115mm, so shear force on bolts due to connection moment is;

$$Sm = \frac{47 \times 10^3}{8 \times 115} = 51kN \tag{3.7}$$

Shear force on bolts due to horizontal force is;

$$Sh = \frac{100}{8} = 12.5kN \tag{3.8}$$

Total shear force per interface on bolts is;

$$St = Sm + Sh = 63.5KN(Maximum) \tag{3.9}$$

Using 24mm diameter high strength friction grip (H.S.F.G) bolts (BS 4395:part 1 and 2; 1969), permissible shear load per interface is 66.5kN and applied shear load per interface is 63.5kN, therefore the bolts are sufficient.

Area required per bolt is;

$$A = \frac{12.5 \times 10^{-3}}{115} = 108.7mm^2 \tag{3.10}$$

available area per bolt is;

$$A_b = 72 \times 90 = 6480mm^2 \tag{3.11}$$

Plate thickness required is;

$$t = \frac{108.7}{(72 - 26)} = 2.3mm \tag{3.12}$$

8mm plate thickness would be adequate. It has been assumed that the H.S.F.G bolts would support the load connection, but the bars across the angles should be checked against bending stress. Load on each cross bar is ;

$$H_{bar} = \frac{100}{4} = 25kN \tag{3.13}$$

taking moments about point x therefore ;

$$25 \times 0.038 = 0.95kNm \tag{3.14}$$

allowable stress is $115Nmm^{-2}$, $Ixx = Iyy = 116cm^4$ for angle L $89 \times 89 \times 9.4mm$ thickness ;

$$\sigma = \frac{MY}{Ixx} = \frac{0.95 \times 0.045}{116} = 36.4Nmm^{-2} \tag{3.15}$$

as $\frac{115}{36.4} > 1$ the angle would not fail due to bending stress.

3.14-Loading Device for Two-Pile Groups.

To exert horizontal force on the cap of a two-pile group, a hydraulic jack assembly was used. The hydraulic jack, centrally mounted on a 16mm high tensile rod was used to exert pull on the pile cap toward a second two pile group. The rod was anchored by tapered wedges in a barrel where it passed through a C section bracket on one pile cap. The other end of the rod passed through a hole in a C section bracket on the opposing pile cap. The jack was locked between the back of the C section bracket on the tapered wedge on the free moving end of the rod, so that when the jack was extended by pressure, the pile caps were drawn towards each other. Figure 3.23a shows the loading assembly (see also Plate 3.5).

To determine the load applied to the pile head, electrical resistance strain gauges were mounted on the anchored rod to measure the strains. As the relationship between the tension in the rods and strain readings was unknown, the rod was tested in a Denison machine. Figure 3.24 shows the relationship between applied load and strain. A best fit line was drawn through the points giving a gradient of 0.021KN/microstrain.

3.15-Test Series.

A preliminay test series was undertaken on single pile. The main test programme was carried out on two-pile group, with variation in pile spacing and in cap overhang height.

3.15.1-Single Pile Test Series.

The pile was 4m long with a 200.0mm shoe, and 3.55m of the pile length was driven in the sand trench, leaving 650mm clear of the ground. A 2m reaction pile was driven outside the sand trench in line with the long axis of the trench directly across from the vertical single pile. The loading device was assembled as described in section 3.10, 500mm above the sand trench.

Datum readings of the strain gauges were recorded before loading the pile head.

The pile head was displaced 3,6,9,12,15 and 20mm horizontally. The loads in the tension bars were recorded for each deflection. After the final load the tensions in the bars were released and a cycle of loading and unloading up to 20mm pile head displacement was repeated four times. At the final cycle of loading the strain gauges on the tension bars and on the pile were recorded to compare the effect of cyclic loading to static loading. Rather than extracting the pile and refilling the sand trench for each test the soil around the pile was removed, replaced and compacted (see Plate 3.6).

3.15.2-Two-Pile Group Test Series.

For each test a second pile was driven in the sand trench in the same manner as the single pile at a set distance from the first and a loading assembly was attached to the pile heads as discribed in section 3.13.

Datum readings of the strain gauges were recorded before loading the pile cap. The pile cap was displaced 3,6,9,12,15 and 20mm horizontally. The load on the tension bar was recorded for each deflection. After the final load the tension on the bar was released and a cycle of loadings and unloading up to 20mm pile head displacement was repeated four times. At the final cycle of loading the strain gauges on the tension bar and on the pile were recorded to compare the effect of cyclic loading to static loading. Rather than extracting the piles and refilling the sand trench for each test the soil around the piles was removed, replaced and compacted.

In order to investigate the effect of pile separations on lateral loading, these tests were repeated for 3, 5, 8 and 12 pile width spacing. The effect of the cap overhang was investigated by simply lowering or raising the cap height of the loading assembly to 150, 300 and 400mm for each pile spacing case. Plate 3.7 shows test conditions on the site.

3.16-Pile Extraction.

As the piles had to be extracted from the sand trench and to be reused for a different pile spacing, concrete blocks were placed on each side of a pile and the head of the pile was clamped by angle cleats. Two hydraulic jacks were placed on each side of the pile and were slowly pumped simultaneously to overcome the shaft friction. The pile was then slowly lifted from the sand trench. The cable from the winch on the tripod was tied to the pile head to prevent the pile from sliding back in its hole. Plate 3.8 shows the method used to extract the pile from the sand trench.

3.17-Discussion

Throughout this section piles were designed in such a manner that their behaviour would be flexible. The instrumention was carefully chosen in according with the research requirements. Each pile before installation was tested and checked to ensure the reliability of the datas during actual field tests. After installation of the piles it was found that many of the WVSG's were not responding due to heavy pile driving and only piles number 3 and 4 were used for data collection while piles number 1 and 2 were used as a reaction two-pile group. One of the difficulties arising during early tests was the seepage of ground water into the single pile. This was overcome by dewatering inside the first pile installed and conducting leakage tests on piles number 2, 3 and 4. During the first single pile test it was also found that the pressure cells gave unreliable results and also, more care was taken during instrumentation of the pressure cells on the second, third and fourth piles. Throughout testing it was found that the handling of the piles during driving was very difficult. A relationship was found to determine the insitu unit weight of the sand using cone penetrometer, but it should be noted that this relation must be used carefully with allowance for the wet and dry seasons. After installation of all the piles the main test on two-pile groups were conducted and results are presented in chapter 4.
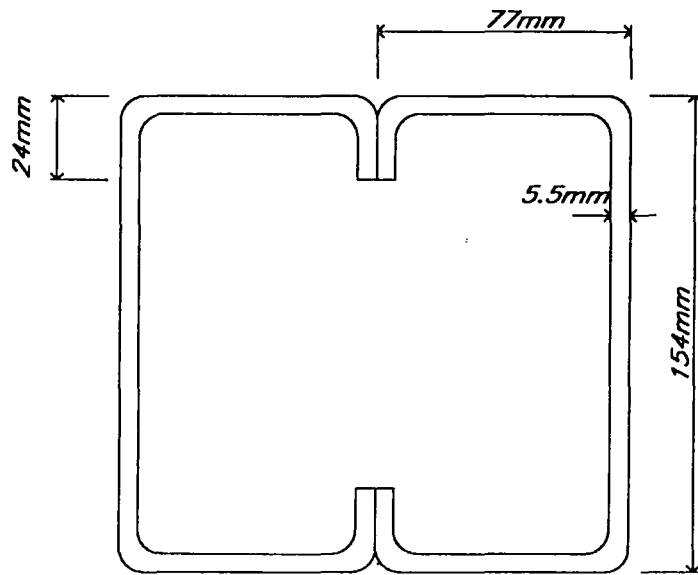
Figure 3.1 The dimensions of the pile cross section
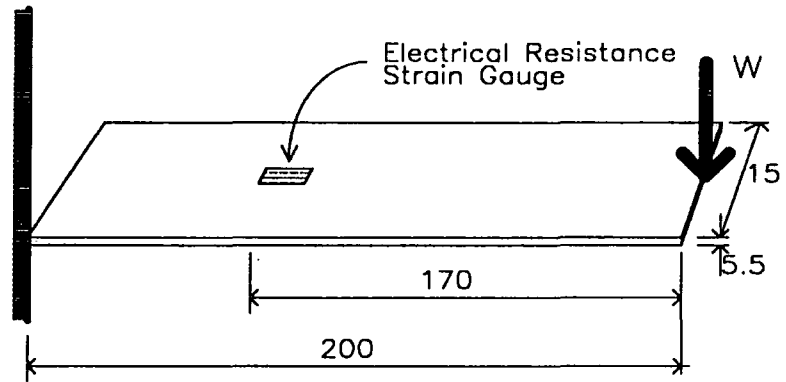
Fugure 3.2a The cantilever beam dimensions in mm.
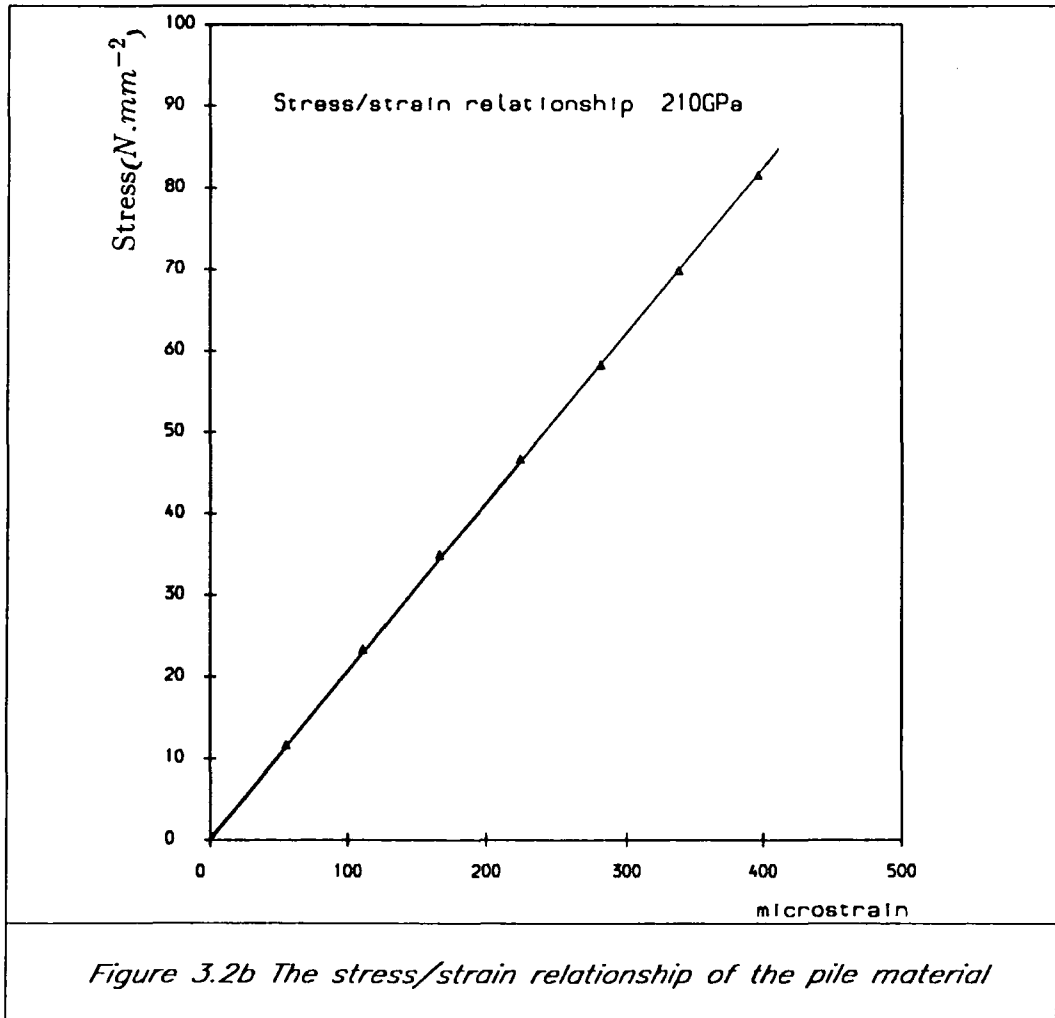
Figure 3.2b The stress/strain relationship of the pile material
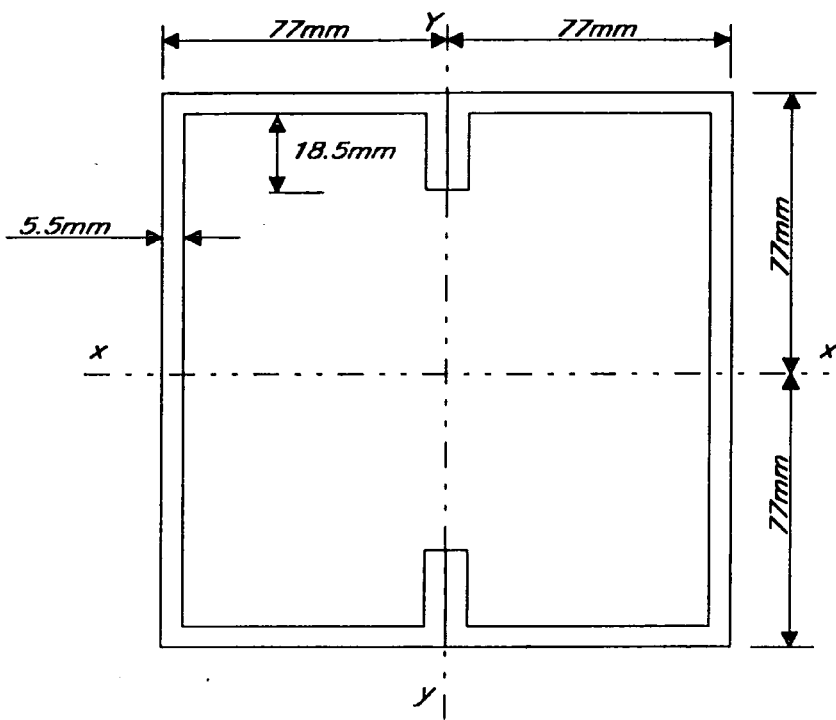
Figure 3.3 Assumed pile cross section

(a) Plan view

(b) side view

Plucking Coil assy

Locking Collar

Wire Tension Adjuster

tension wire

End Mounting
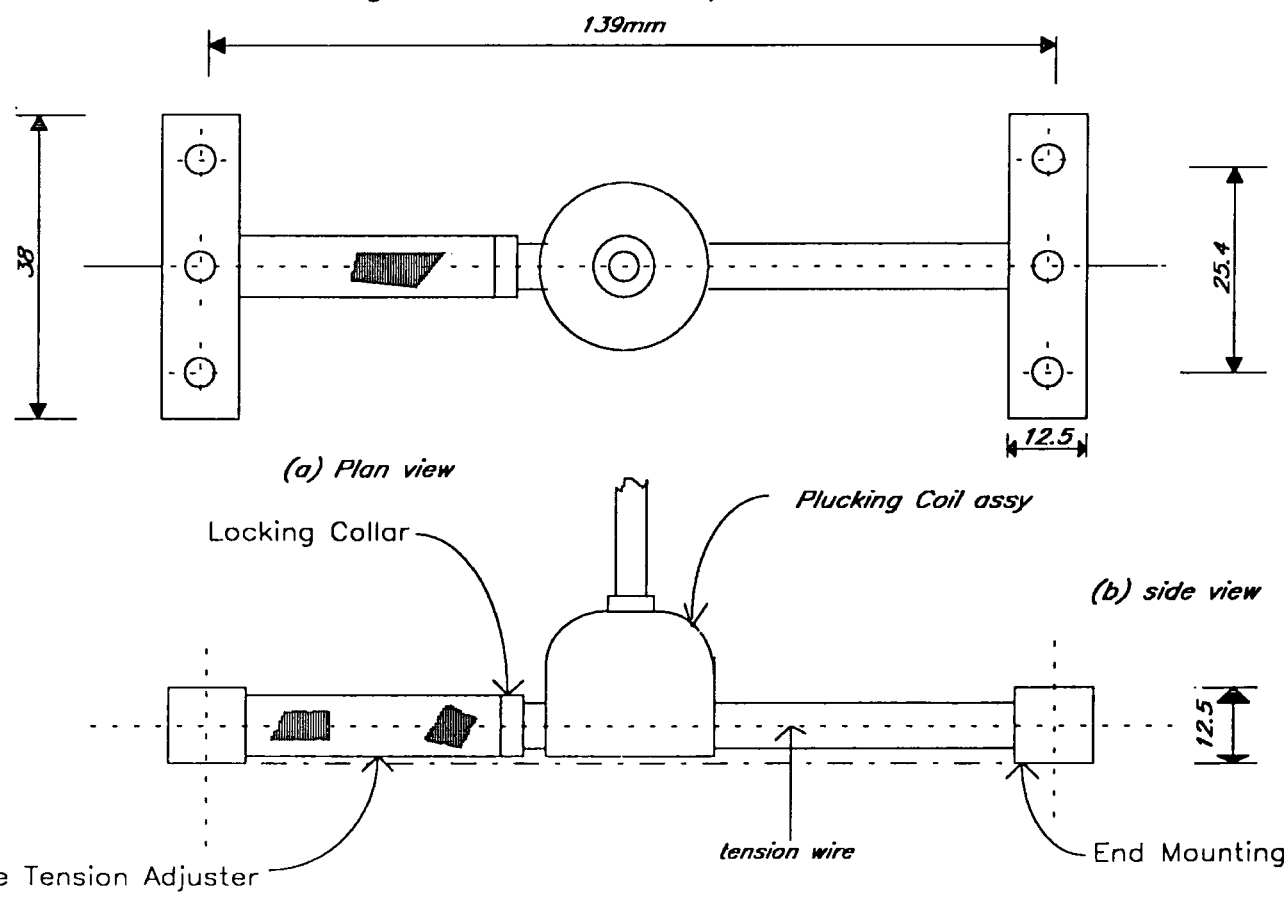
Figure 3.4 The plan and side view of VWSG's

VWSG and ERSG
at the top of the
cantilever beam

W

VWSG and ERSG
at the bottom of the
cantilever beam

L
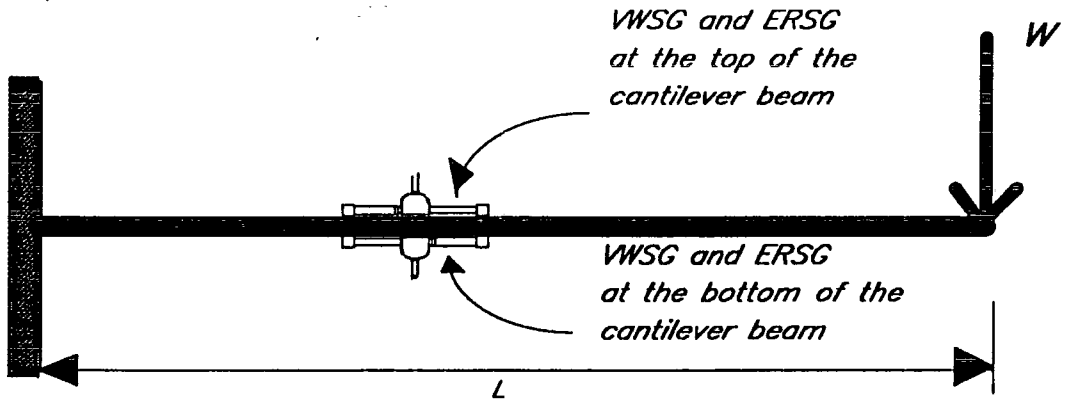
Figure 3.5 The calibration test conducted on VWSG and ERSG
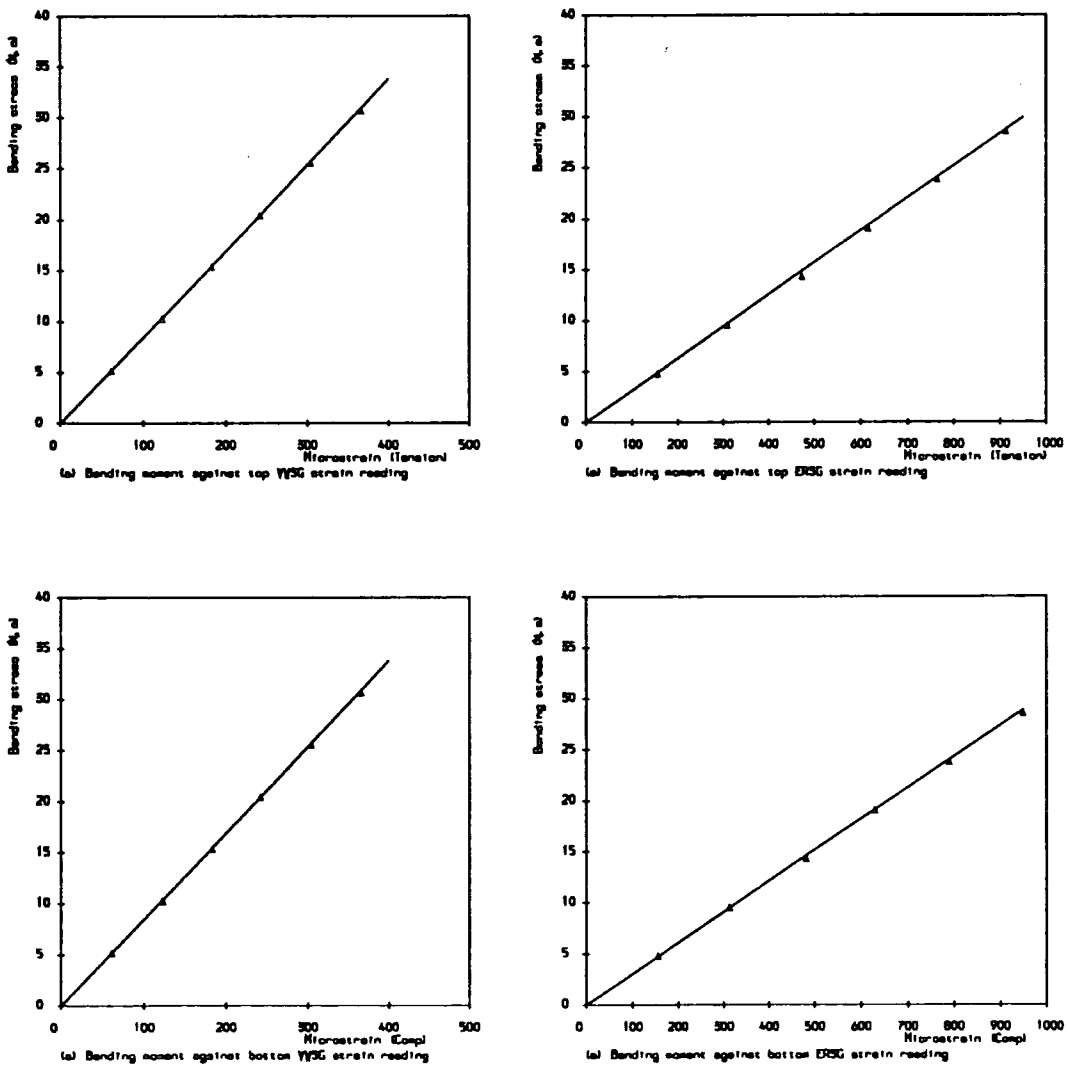
Figure 3.6 Bending moment and strain relationships of VWSG and ERSG

Figure 3.7 Linear relationship of eccentric and surface strain.
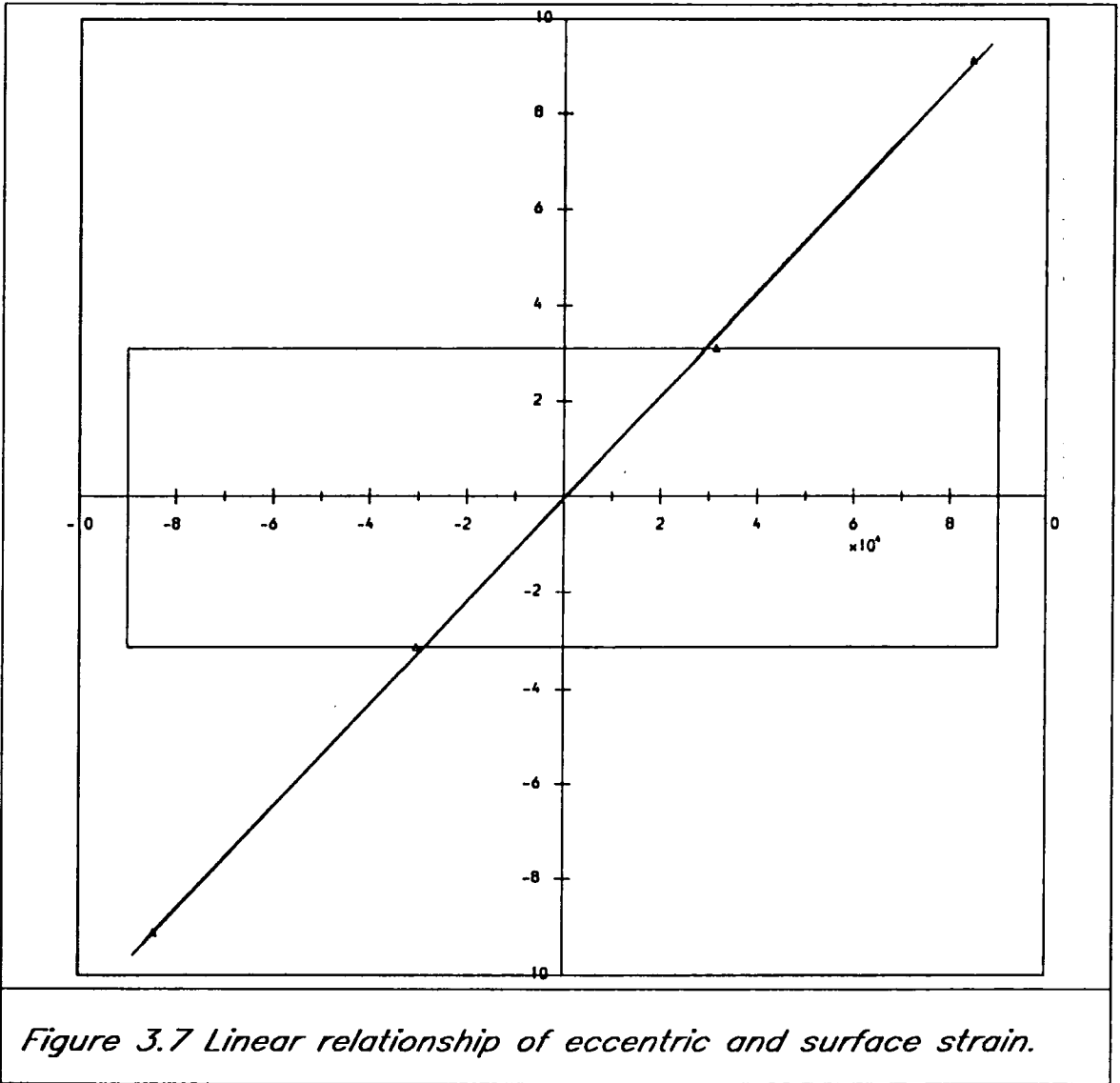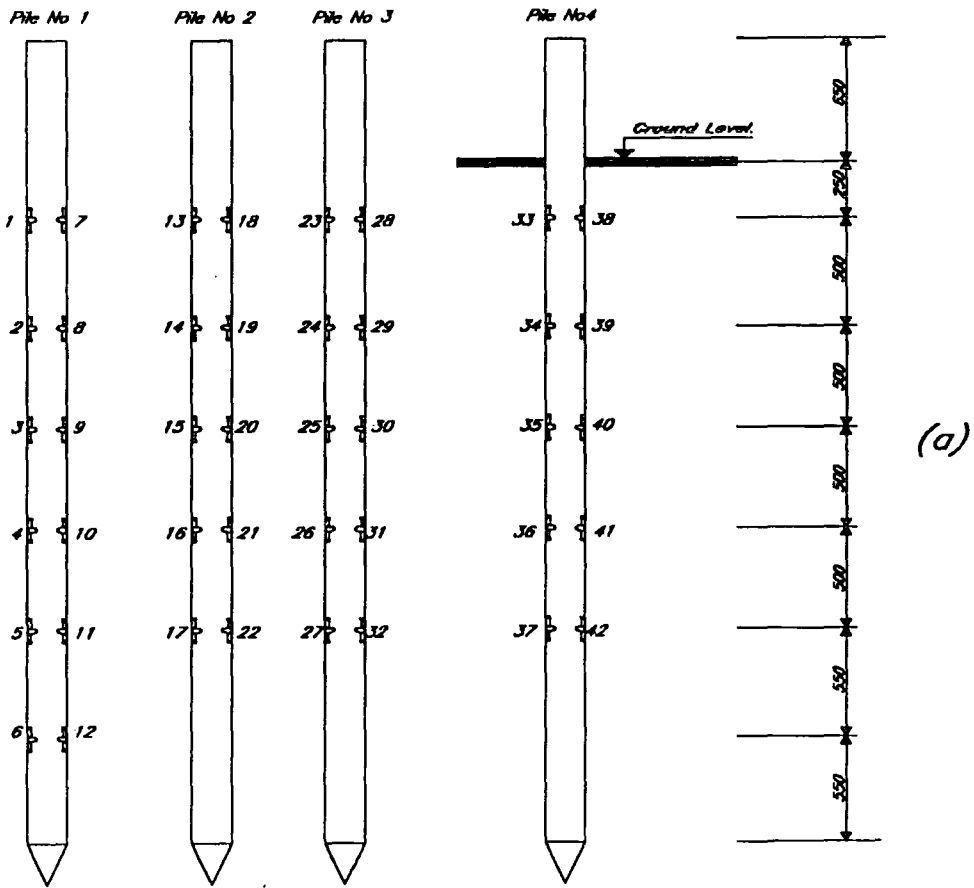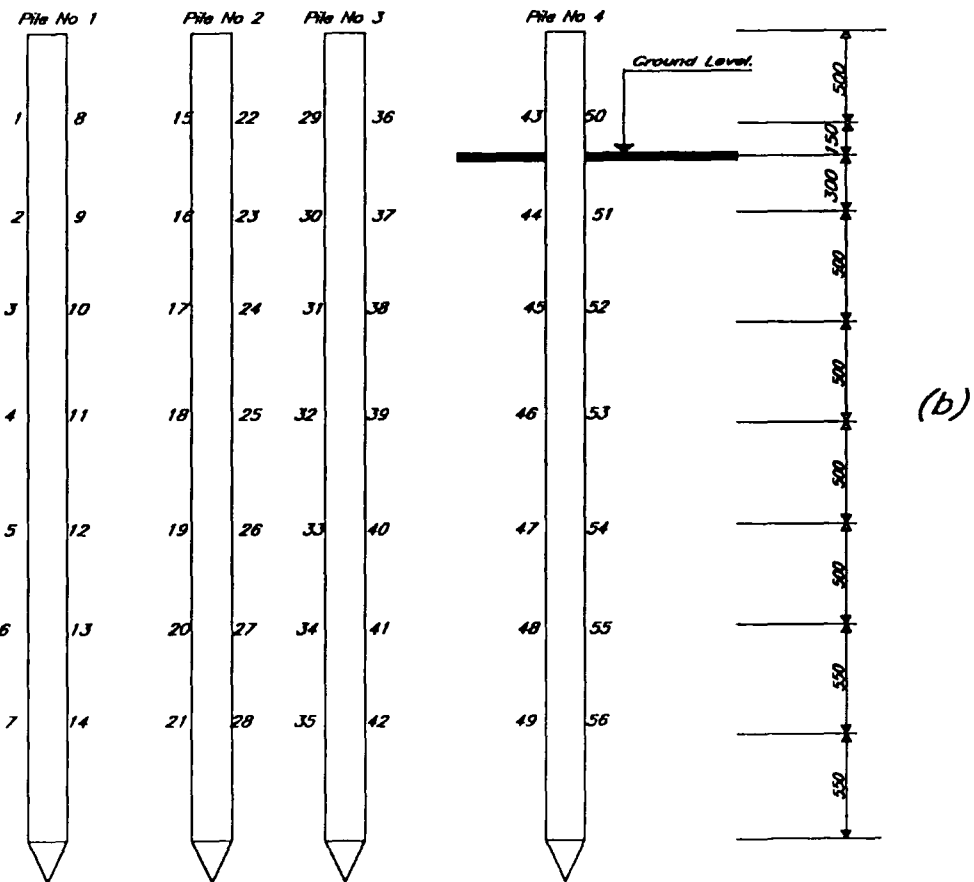
Figure 3.8 Location of (a) VWSG's and (b) ERSG's on the piles.
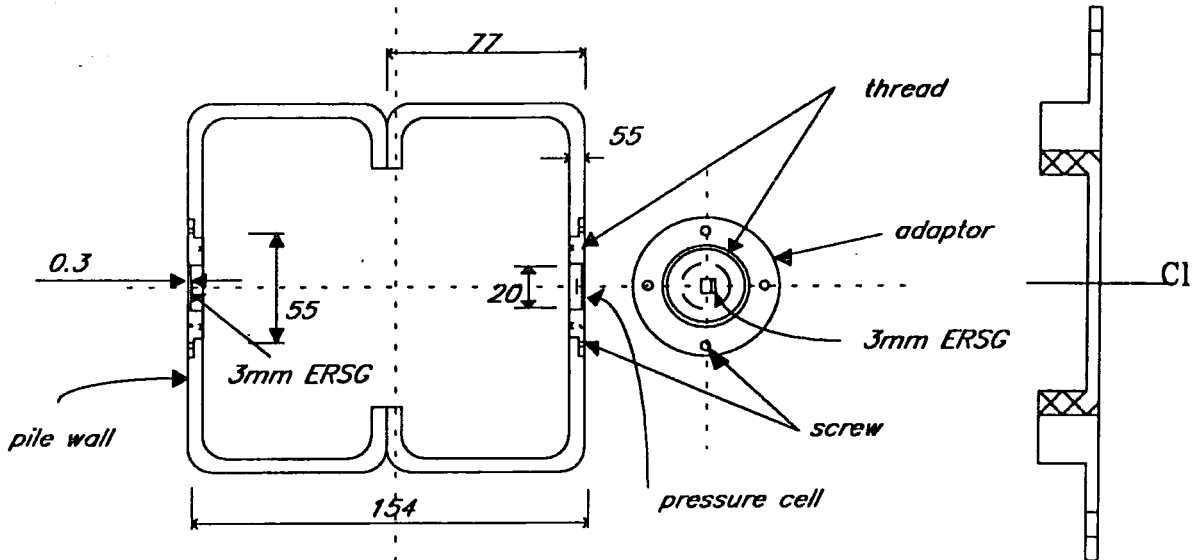
(a) Detail of pressure cell
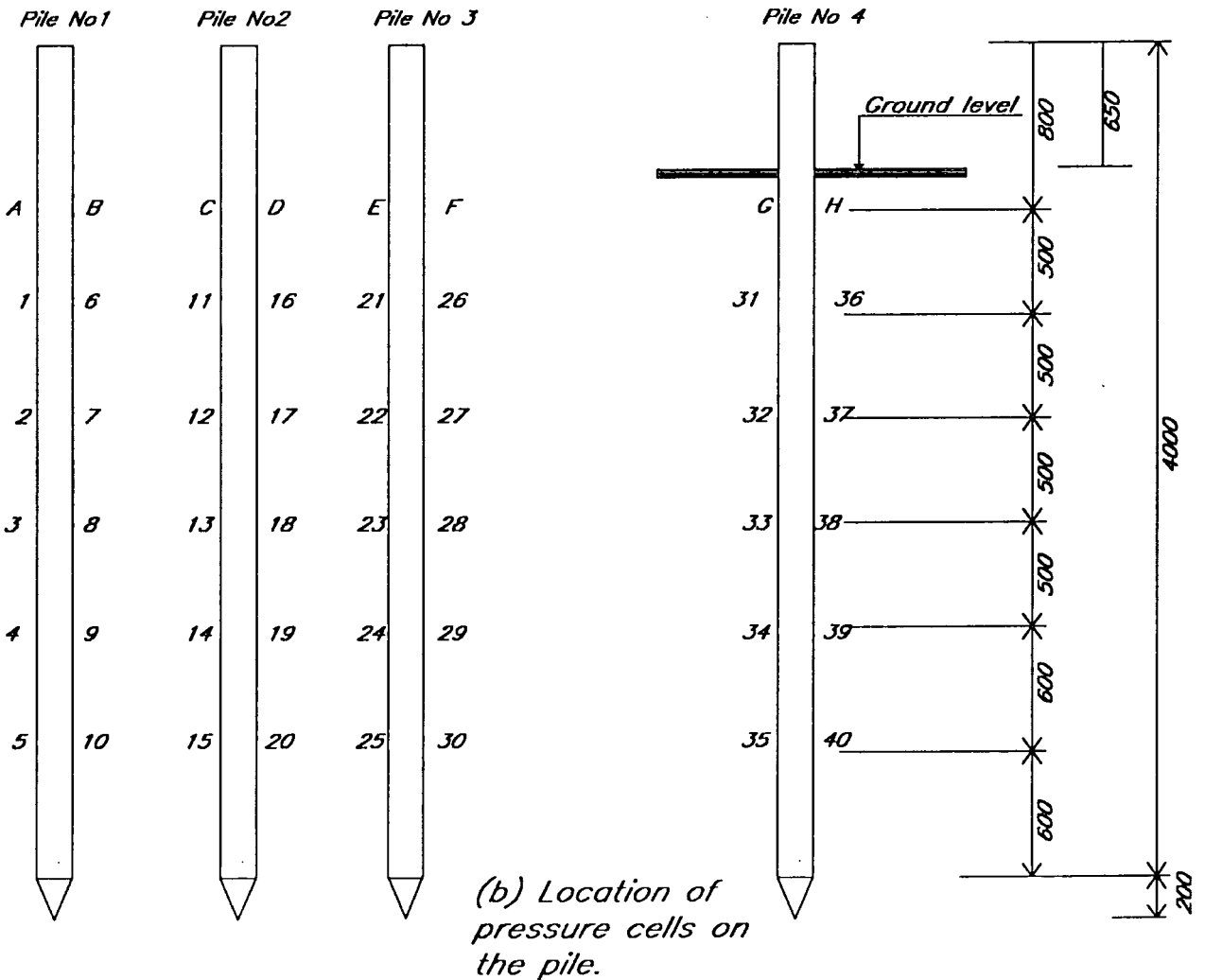
(b) Location of pressure cells on the pile.

Figure 3.9 Details of pressure cells and locations on the piles.
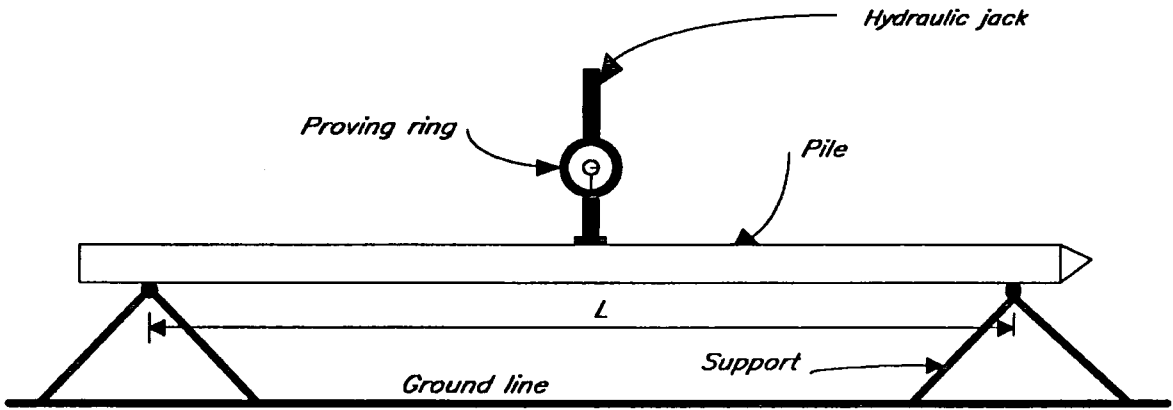
Figure 3.10   Three point bend test on the pile
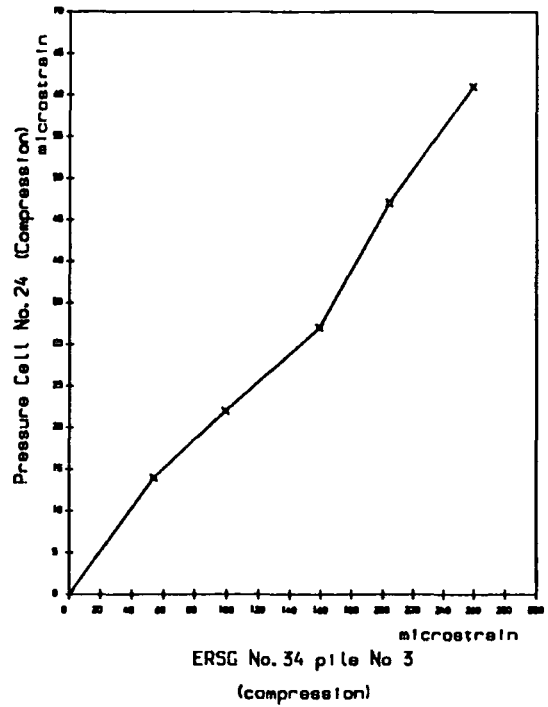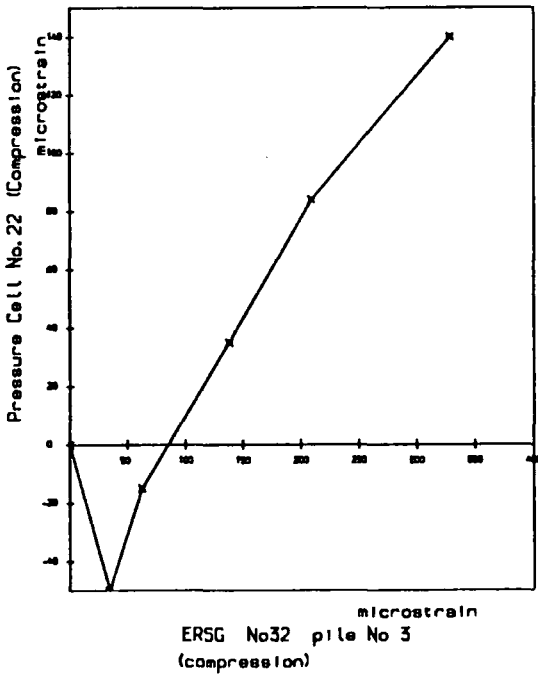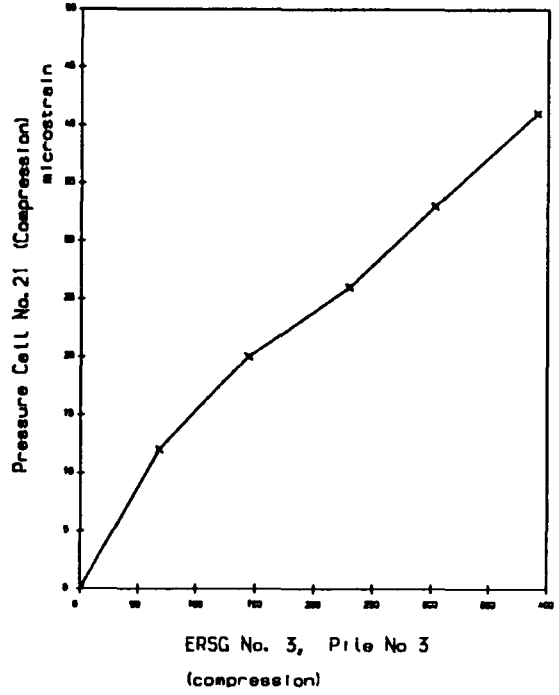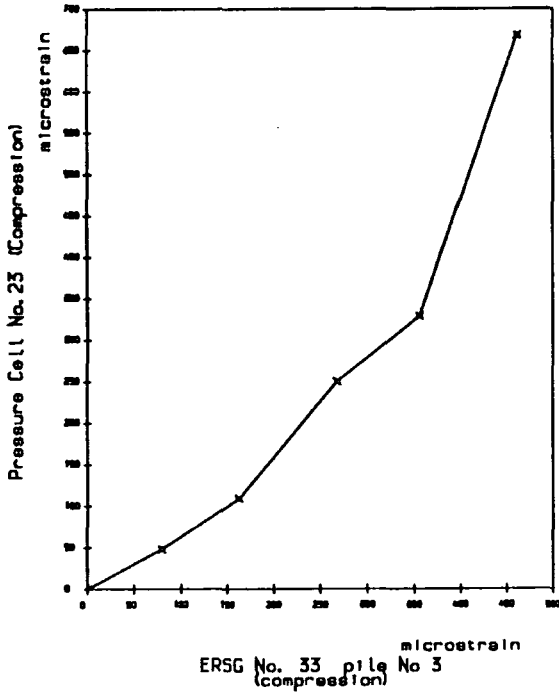
Figure 3.11 Apparent strain on the pressure cells.

Top seal plate

Rubber seal

Tension bar

Clamping plate

Air inlet

Pile wall

Tubes used to erect the piles
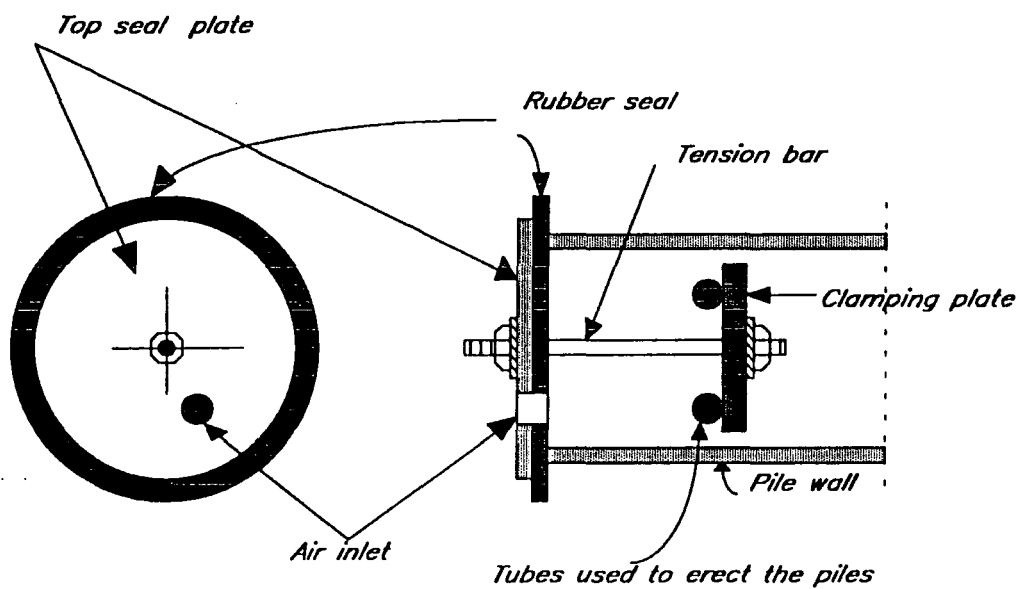
Figure 3.12 Illustration of leak detection system.
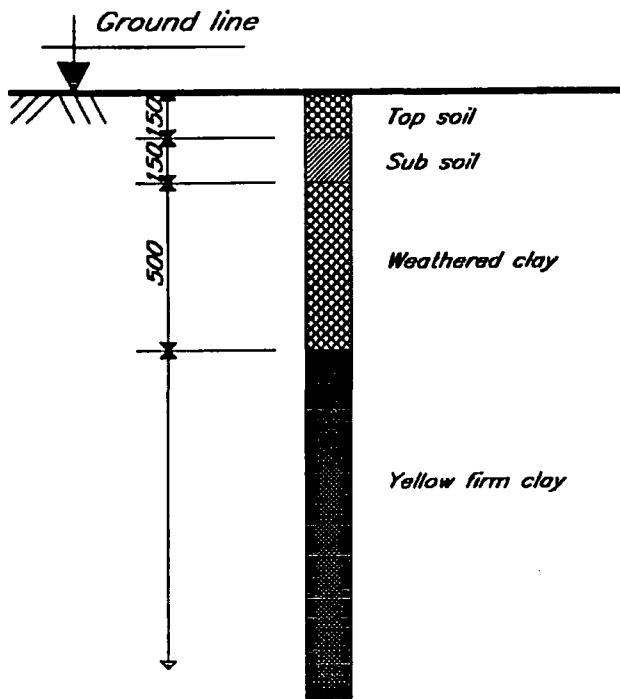
Figure 3.13 Borehole log of the Hollingside-lane site.

(a) Plan view

stand pipe
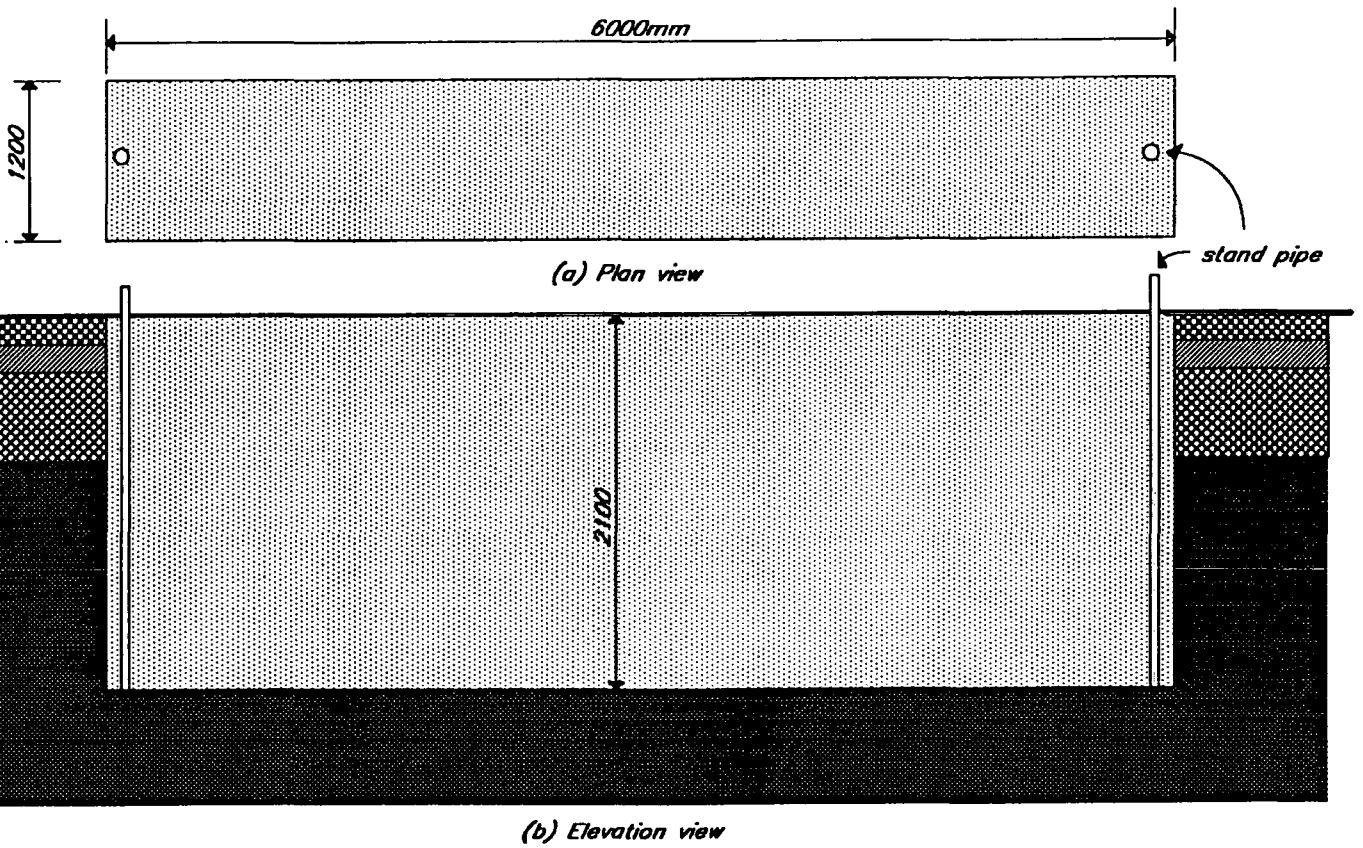
(b) Elevation view

Figure 3.14 Plan and elevation views of the sand trench
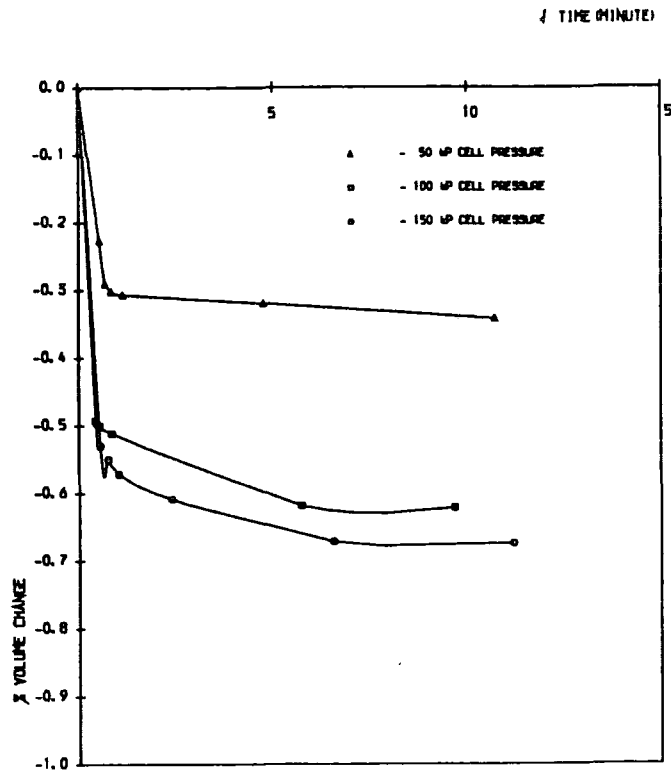
Figure 3.15 Plot of percentage volume change againt time.
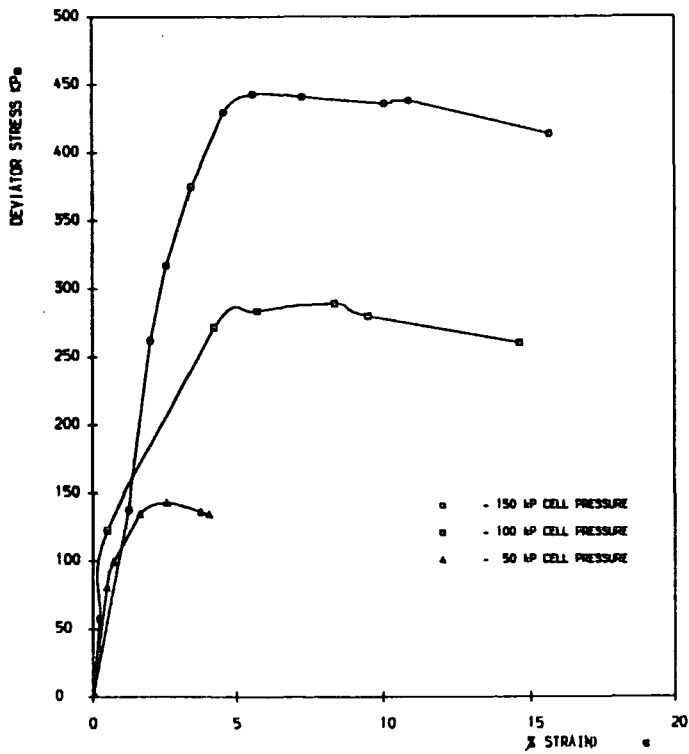
Figure 3.16 stress/strain relationship of the sand.
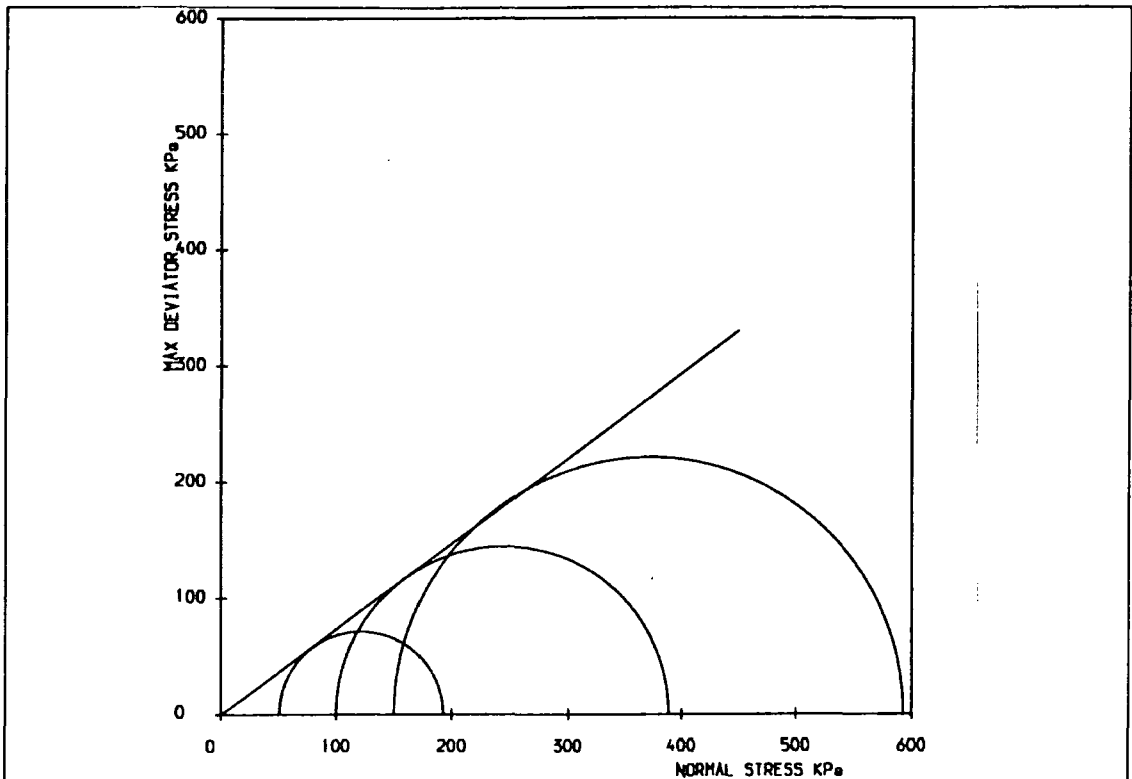
Figure 3.17 PLot of Mohr circles and envelope.
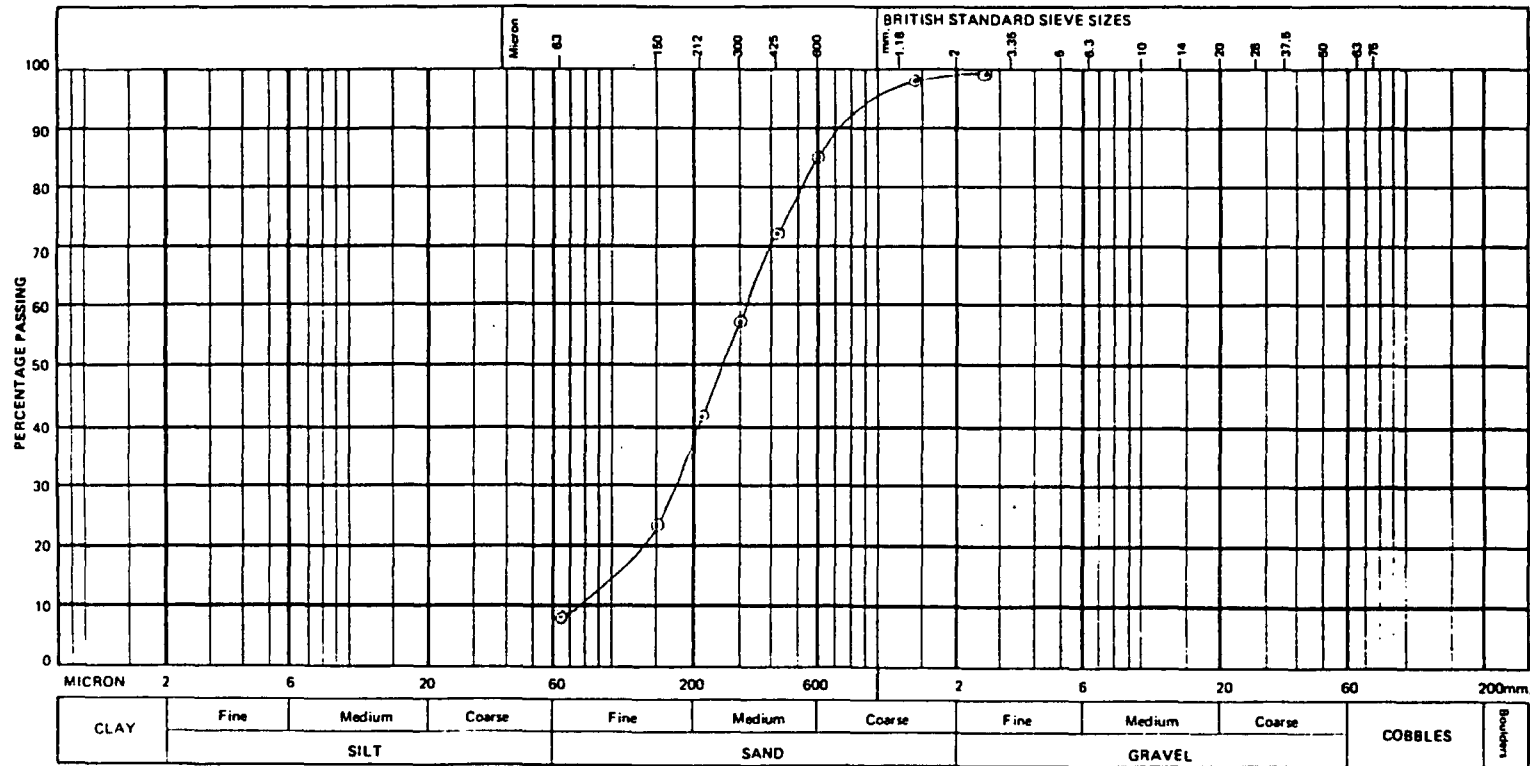
Figure 3.18 Particle size distribution of sand
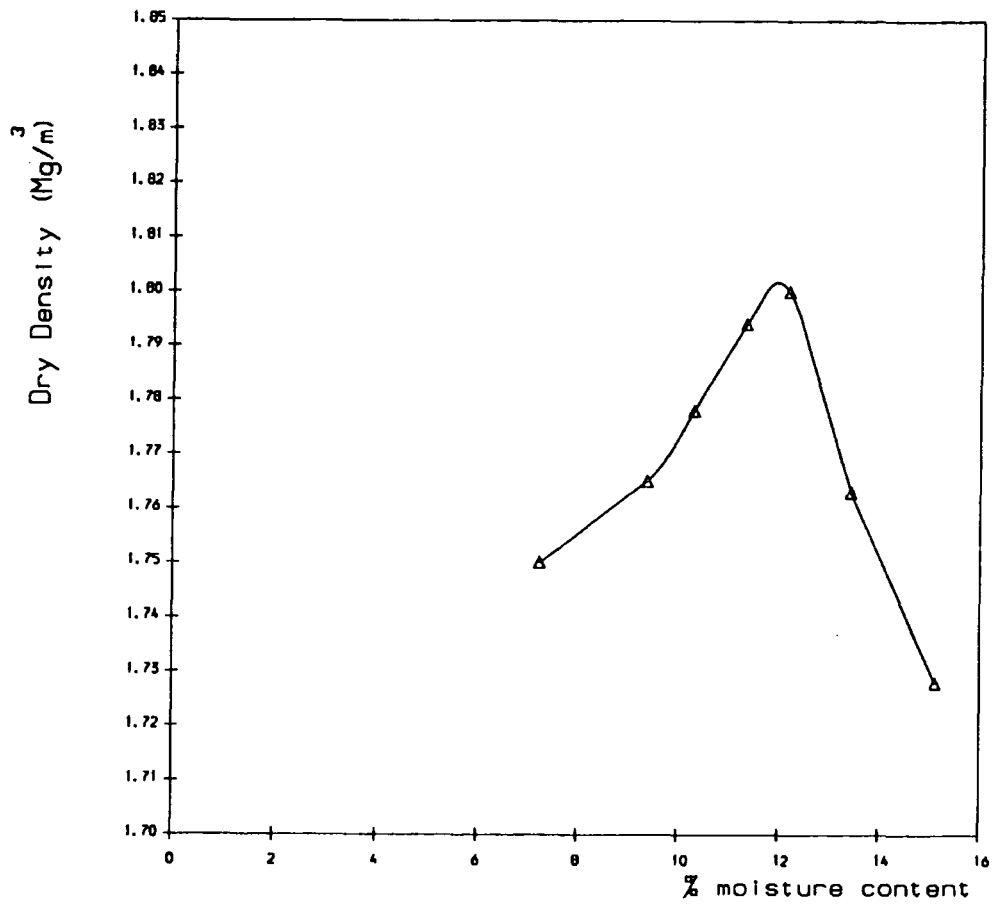
Figure 3.19 Compaction test on sand.
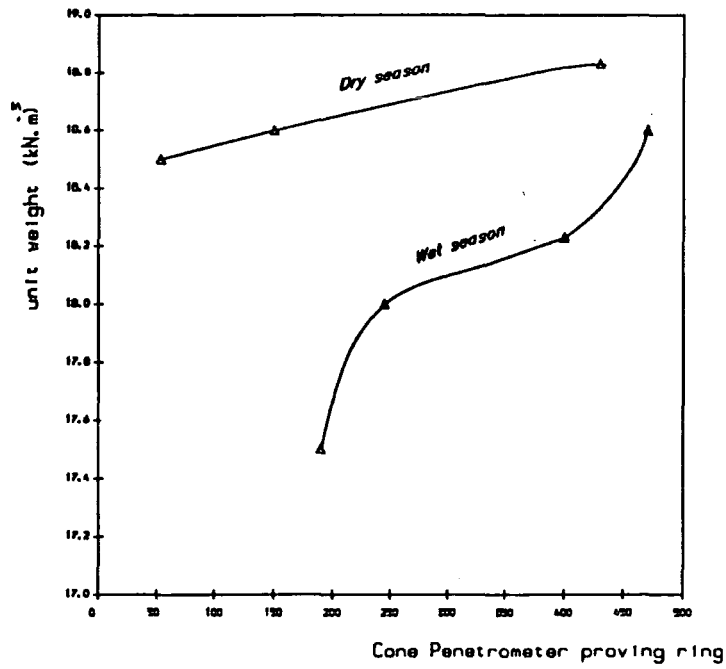
Figure 3.20a Calibration of cone penetrometer.
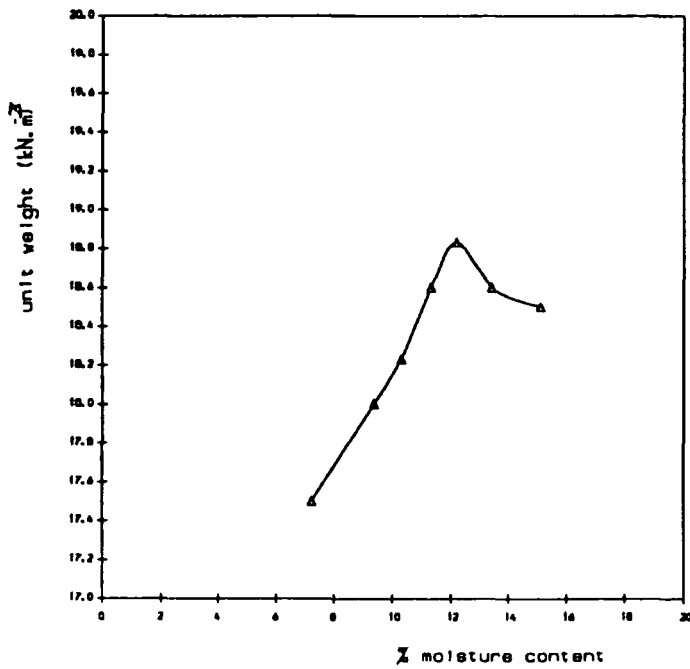
Figure 3.20b Calibration of cone penetrometer.
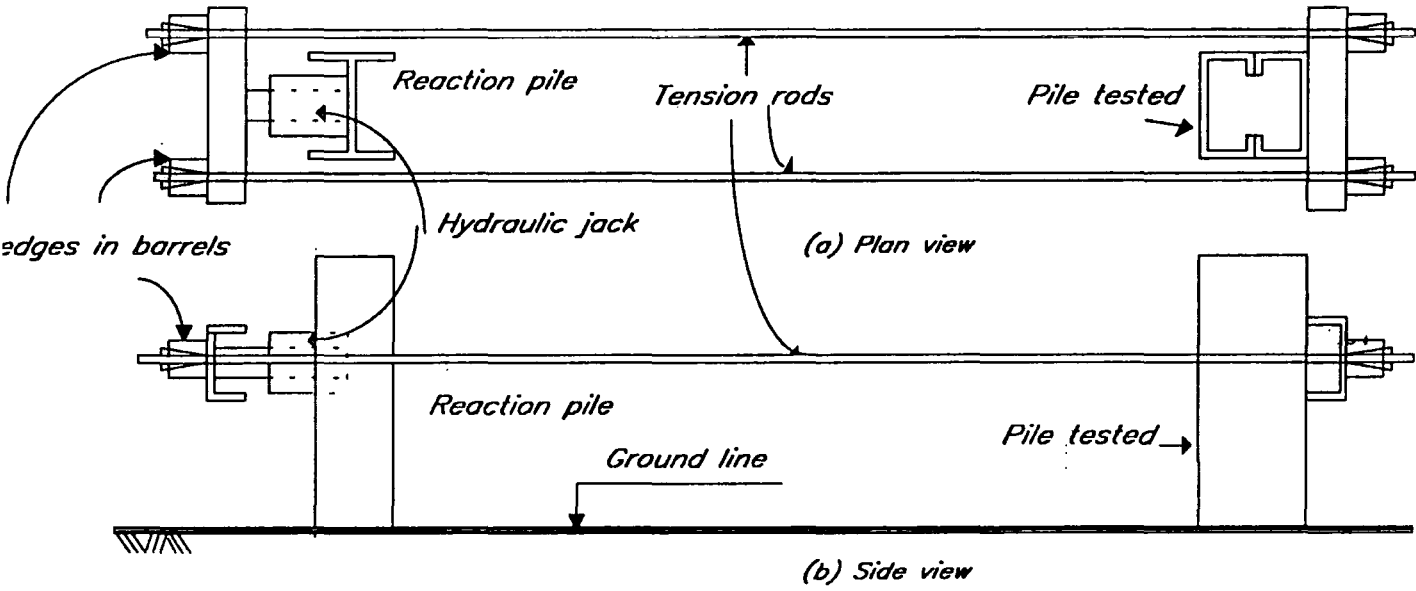
Figure 3.21a The loading device assembly for single pile tests
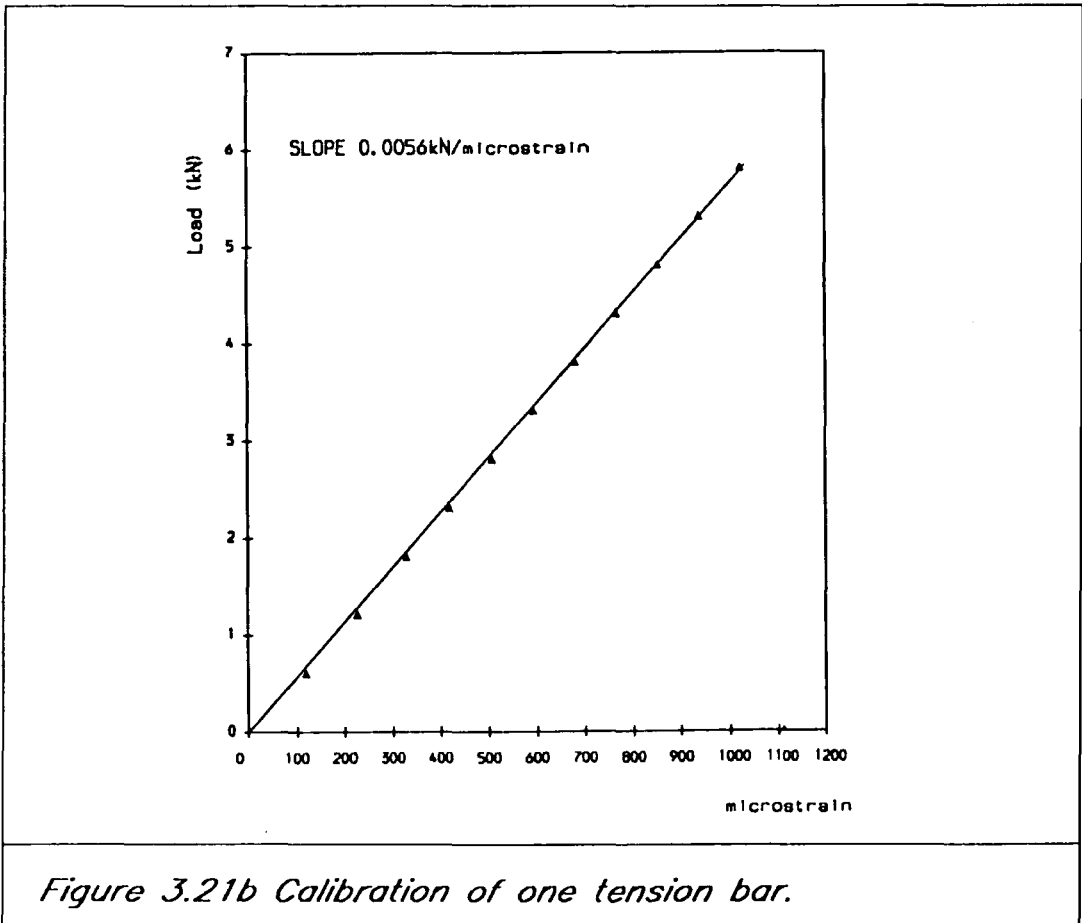
Figure 3.21b Calibration of one tension bar.
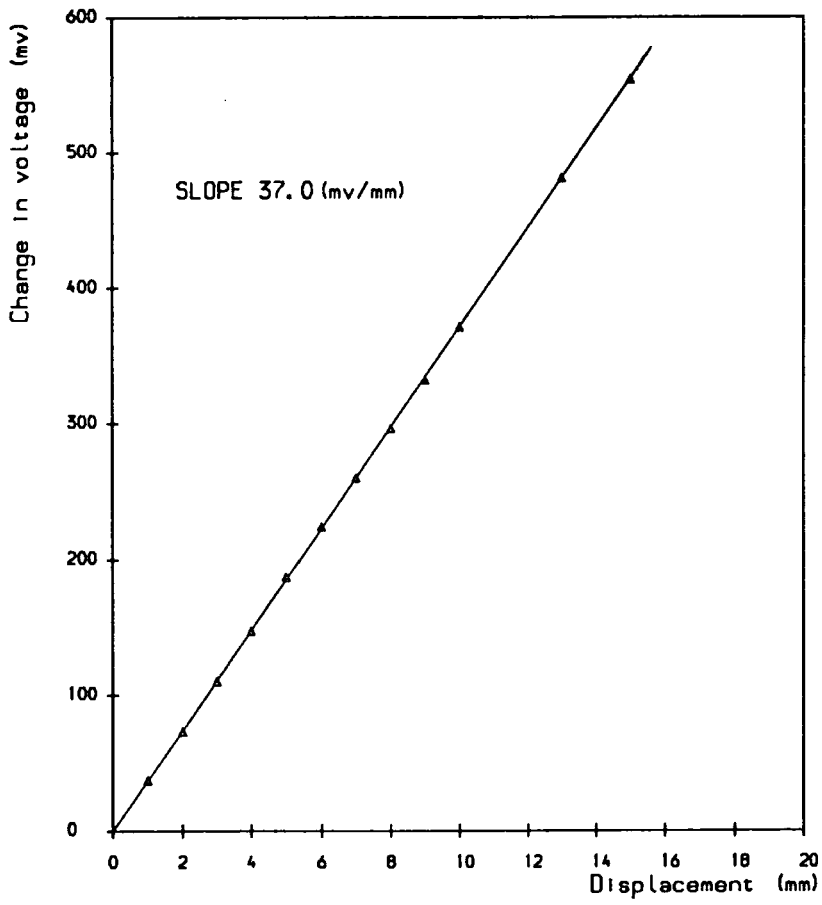
Figure 3.22 Calibration of LVDT.
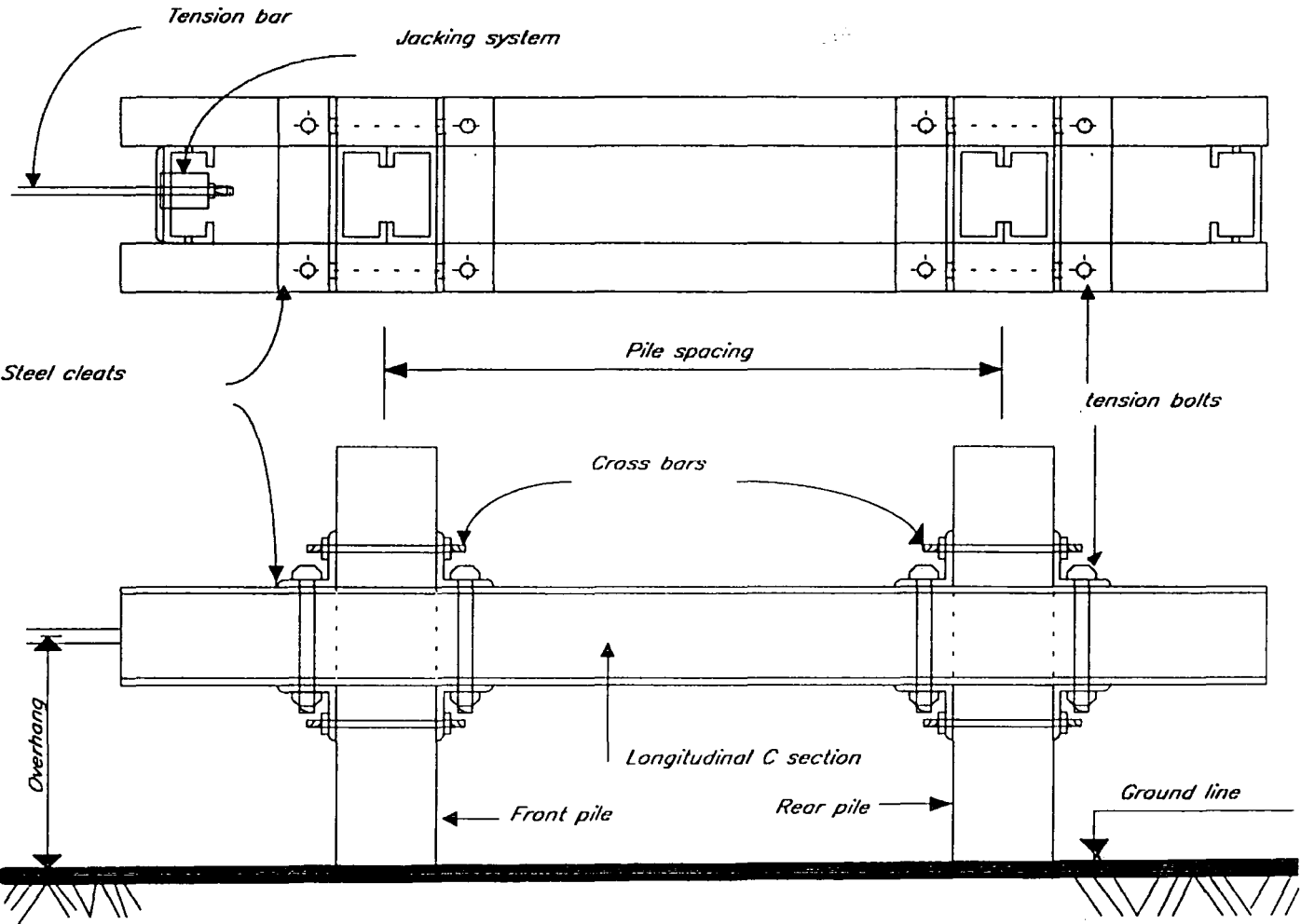
Figure 3.23a The plan and elevation view of two—pile group assembly
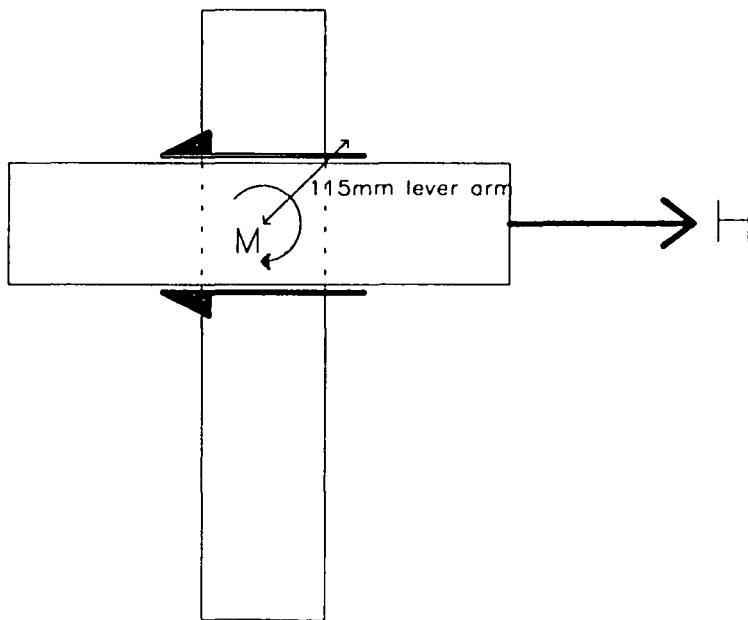
Figure 3.23b The forces and moments on the pile/cap junction
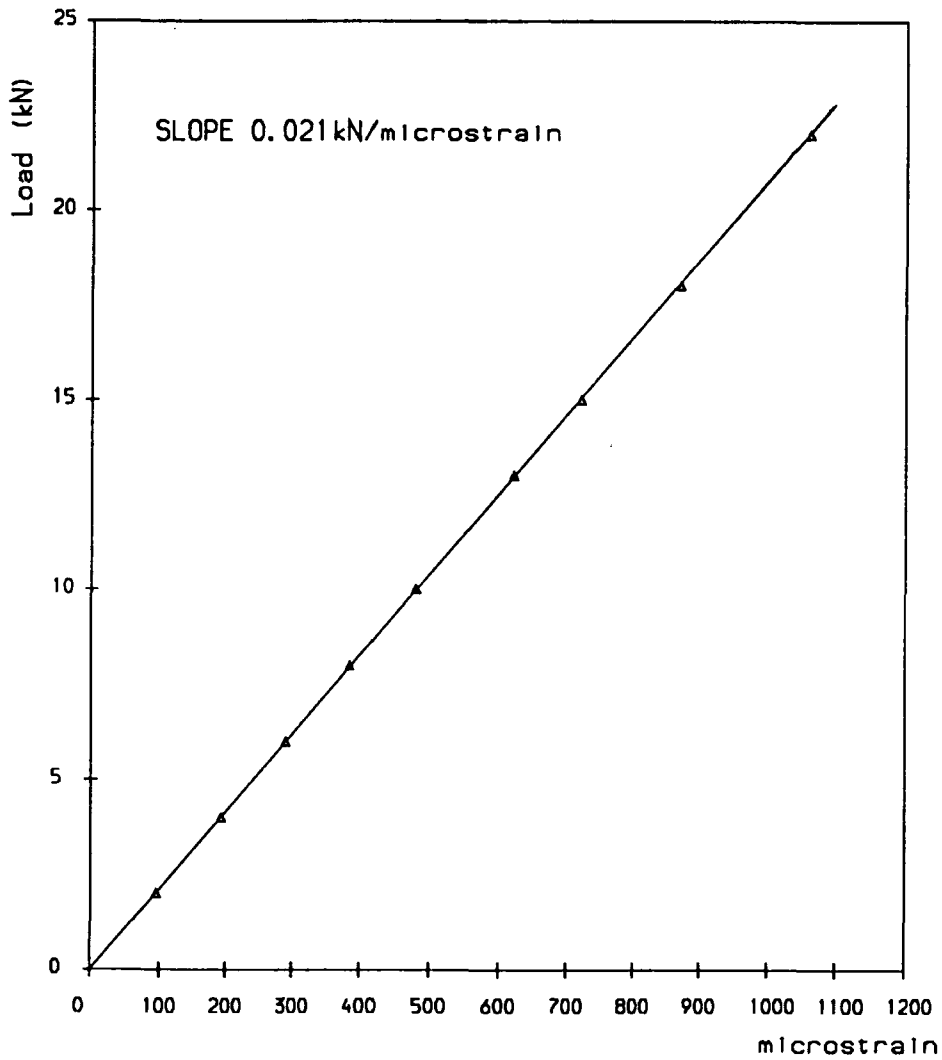
Figure 3.24 Calibration of tension bar used in two-pile group test.
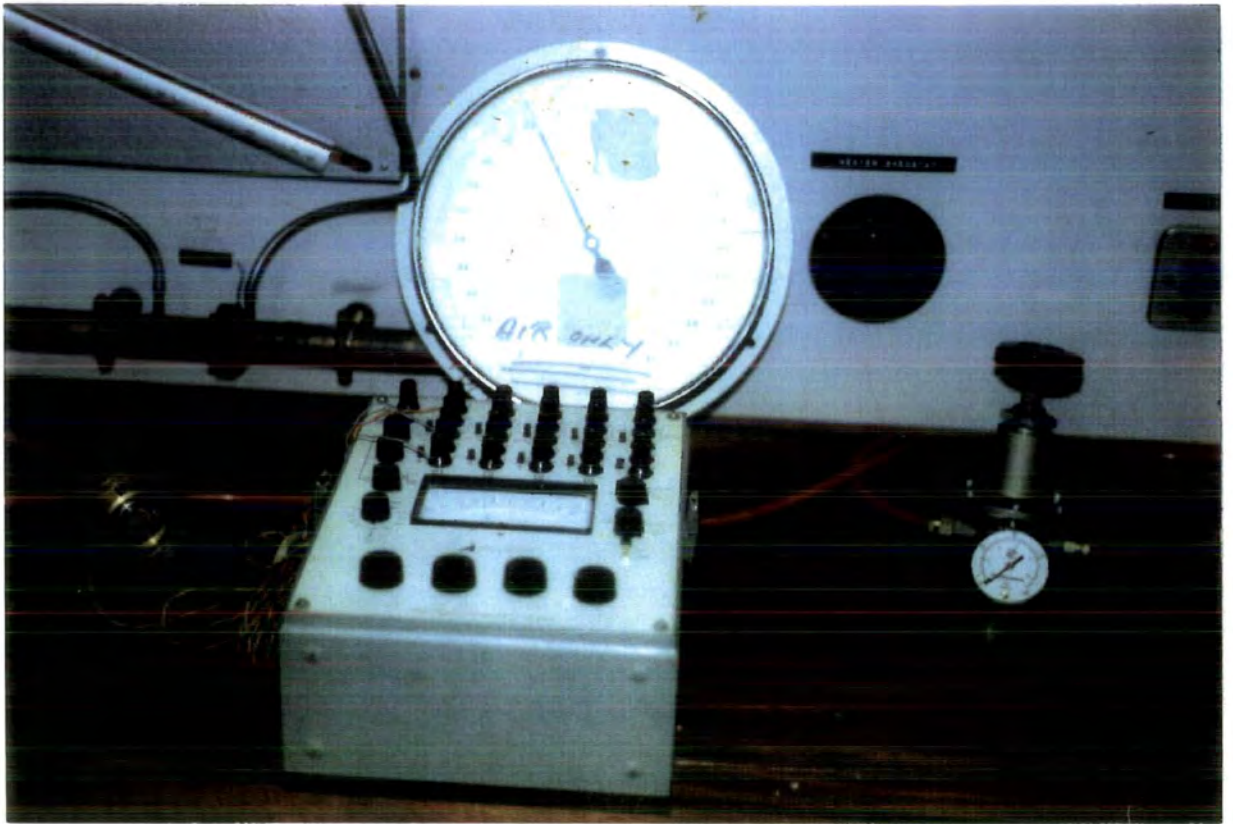
Plate 3.1   Calibration of pressure cell.
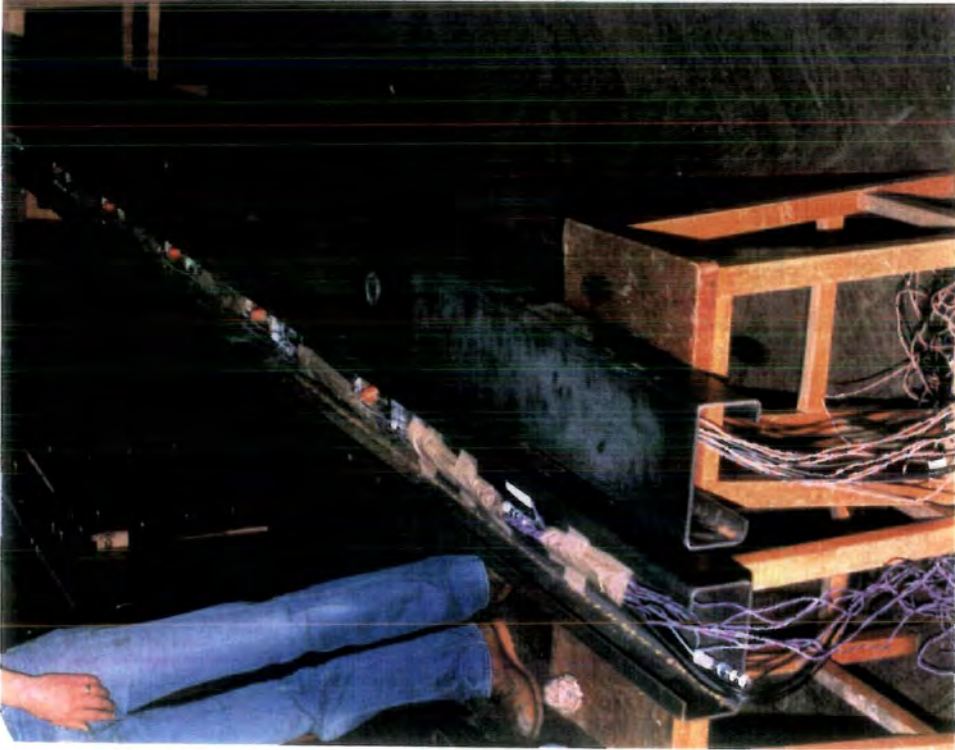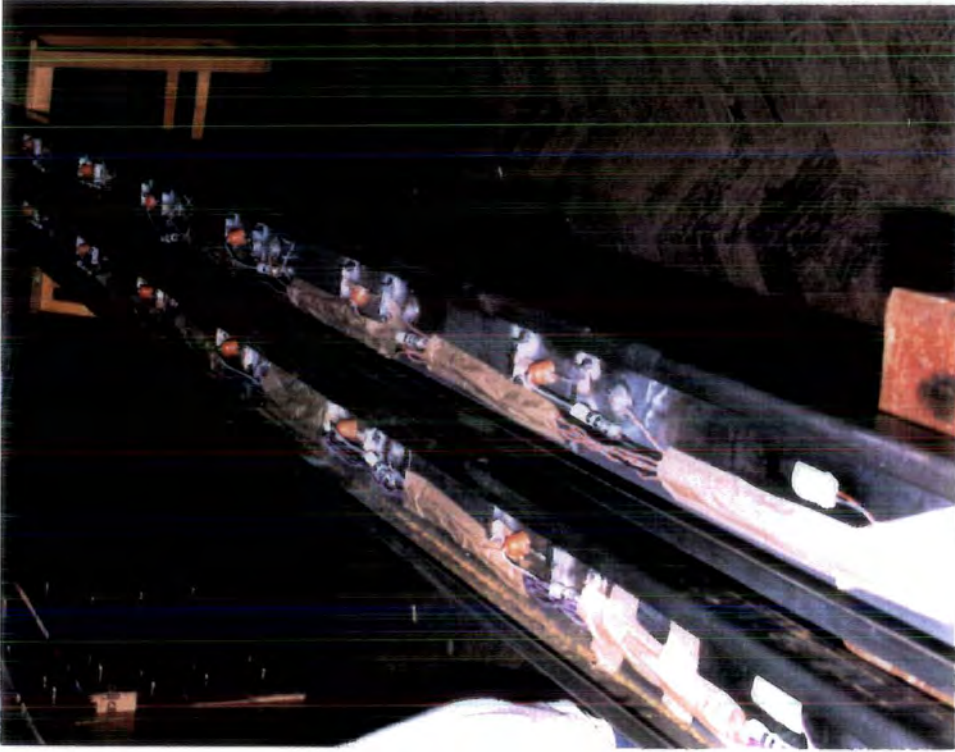
Plate 3.2 Pressure cells location
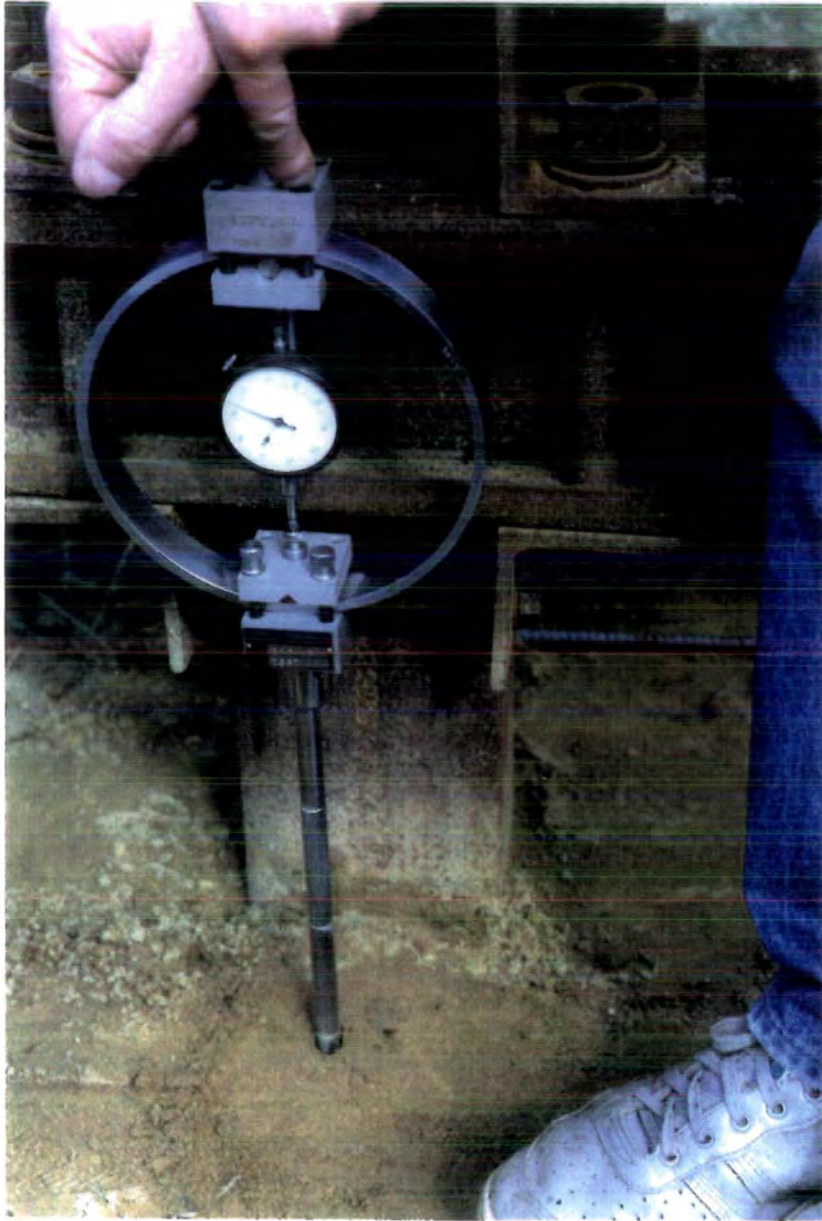
Plate 3.3 Cone penetrometer.

Plate 3.4   Pile driving technique.
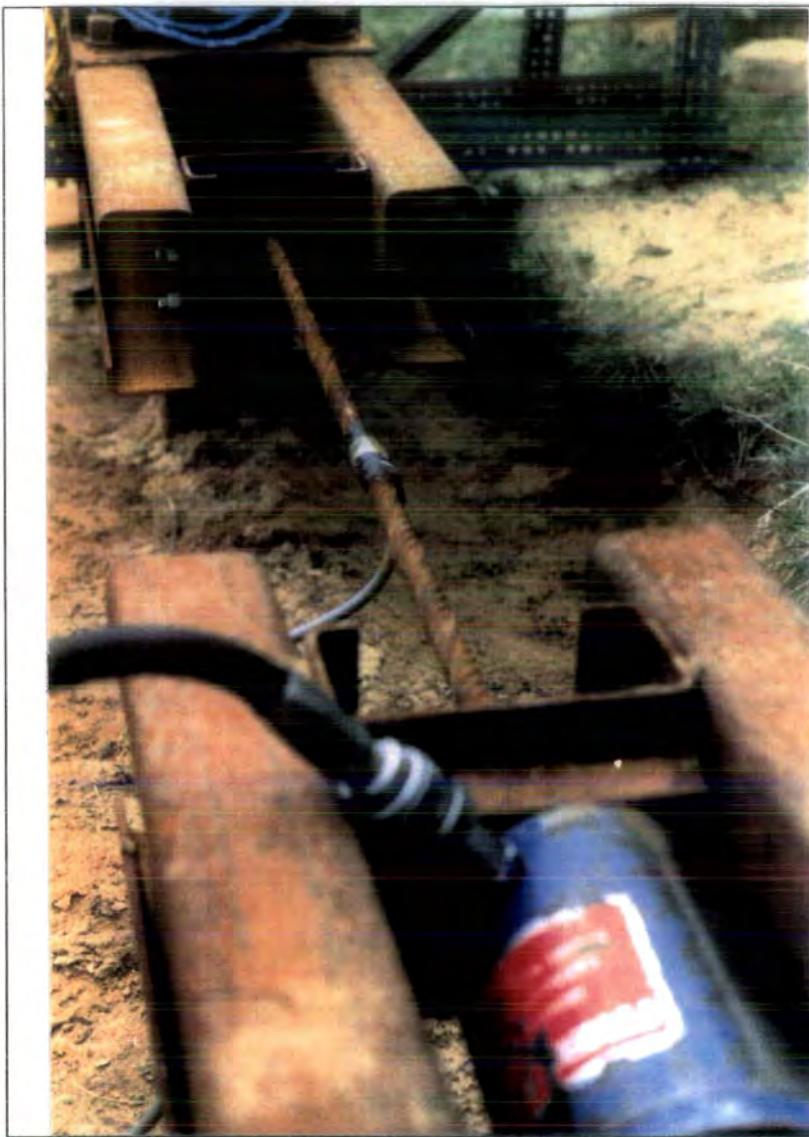
Plate 3.5 Pile cap loading assembly.

Plate 3.6 Excavation of sand around a pile.
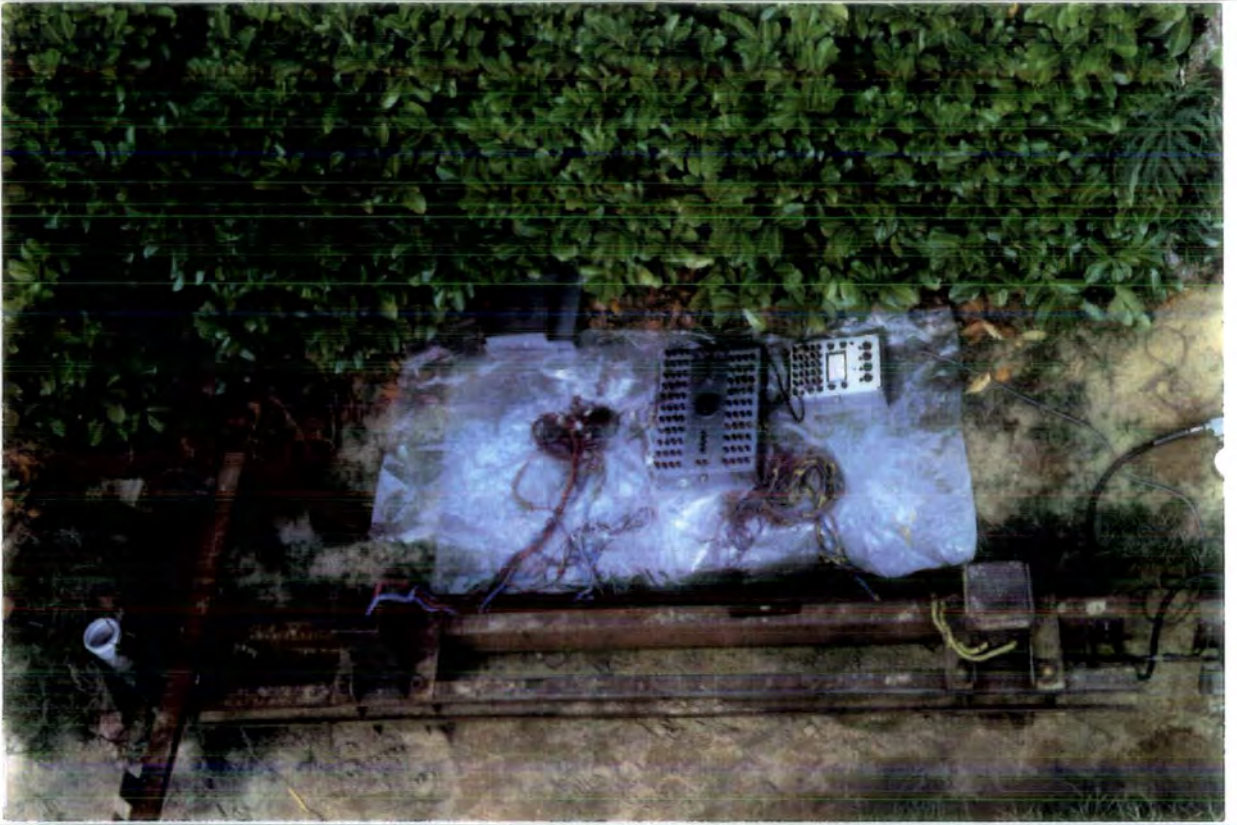
Plate 3.7 Two-pile groups test layout.

Plate 3.8 Pile extraction technique.

Table T3.1

Calculation of the second moment area of the pile cross section

segment	Distance from neutral axis (y) m	Area (a) m^2	$a.y^2$ m^4	I_{GG} m^4	$I_{GG} + ay^2$ m^4
A	-74.25×10^{-3}	7.865×10^{-4}	4.336×10^{-6}	1.9826×10^{-9}	4.338×10^{-6}
A'	74.25×10^{-3}	7.865×10^{-4}	4.336×10^{-6}	1.9826×10^{-9}	4.338×10^{-6}
B	0	8.47×10^{-4}	0	1.6739×10^{-6}	1.6739×10^{-6}
B'	0	8.47×10^{-4}	0	1.6739×10^{-6}	1.6739×10^{-6}
c	-67.75×10^{-3}	2.035×10^{-4}	9.34×10^{-7}	5.804×10^{-9}	9.34×10^{-3}
c'	67.75×10^{-3}	2.035×10^{-4}	9.34×10^{-7}	5.804×10^{-9}	9.34×10^{-3}
Σ		3.674×10^{-3}	1.05×10^{-5}	3.4×10^{-6}	1.39×10^{-5}

Table T3.2

Calculation for pressure cell diaphram thickness

h mm	Equation 3.6 kPa	Equation 3.3 mm
0.2	45.3	0.051
0.3	102.0	0.115
0.4	181.0	0.204
0.5	283.0	0.318
0.6	408.0	0.460
0.7	555.0	0.625
0.75	637.5	0.717
0.8	725.0	0.816
0.9	918.0	1.030
1.0	1133.0	1.270

Table T3.3 Calibration of pressure cells

Pressure Cell No.	Applied Pressure (kN.m^2)									$\frac{kN/m^2}{\mu}$
	20	40	60	80	100	120	140	160	180	
1	23	46	69	93	116	141	168	193	221	0.83
2	11	21	33	43	54	66	77	90	101	1.78
3	11	21	32	42	52	62	75	88	98	1.84
4	22	49	77	104	134	159	189	213	241	0.76
5	22	48	75	99	125	152	177	204	230	0.79
6	13	27	40	55	70	85	100	118	132	1.45
7	12	24	38	52	66	82	96	111	126	1.44
8	15	30	45	61	79	97	115	133	152	1.22
9	18	38	58	78	100	123	146	168	190	0.96
10	25	46	69	95	121	145	172	201	226	0.80
11	19	39	59	81	104	125	147	172	194	0.95
12	13	26	40	58	76	96	116	136	156	1.27
13	63	120	188	253	320	378	440	498	554	0.35
14	16	34	52	70	90	112	131	152	170	1.07
15	19	38	56	76	95	114	134	150	173	1.05
16	21	44	64	84	106	128	152	174	198	0.91
17	14	30	48	67	86	106	127	149	172	1.33
18	18	57	87	115	145	177	208	240	270	0.68
19	24	46	69	93	120	145	174	200	229	1.06
20	25	53	80	107	136	165	195	225	255	0.73
21	12	24	36	48	61	75	88	103	117	1.56
22	24	50	75	101	128	154	182	208	234	0.78
23	24	50	76	103	129	156	184	213	242	0.76
24	15	31	49	66	84	103	123	143	163	1.15

Table T3.3 Calibration of Pressure Cells (continued)

Pressure Cell No.	Applied Pressure (kN.m^2)									$\frac{kN/m^2}{\mu}$
	20	40	60	80	100	120	140	160	180	
25	12	28	43	59	78	90	107	124	140	1.29
26	10	21	33	44	57	69	82	97	111	1.72
27	13	27	44	61	81	99	119	136	156	1.29
28	17	33	52	70	89	107	126	145	163	1.13
29	34	67	99	134	172	208	250	289	330	0.57
30	17	34	53	72	90	108	127	149	170	1.08
31	8	16	24	33	42	52	63	75	87	2.24
32	9	18	27	34	44	54	65	75	85	2.14
33	28	55	84	112	140	167	197	226	256	0.71
34	25	48	76	100	130	156	184	213	241	0.76
35	15	31	48	62	80	98	117	136	153	1.20
36	58	120	180	238	297	355	412	467	520	0.35
37	15	31	47	66	87	107	132	164	187	1.03
38	33	70	107	149	190	232	277	320	336	0.51
39	24	46	69	100	145	174	200	225	252	0.80
40	17	34	53	70	90	108	125	145	165	1.10
A	17	35	55	74	95	115	137	160	182	1.03
B	13	28	44	61	77	91	108	125	140	1.31
C	13	29	46	65	85	107	131	157	179	1.09
D	11	23	34	45	56	68	80	93	105	1.71
E	15	33	51	69	87	106	127	148	166	1.09
F	15	31	48	65	84	101	120	138	155	1.18
G	13	25	37	50	63	76	90	104	117	1.56
H	16	34	56	75	98	115	136	159	183	1.09

CHAPTER FOUR

Field Test Series Results

4.1-Introduction

The lack of homogeneity in the soil is a large factor in determining the complex non-linear behaviour of the soil/pile group system. The geometry of the soil/pile group system also contributes to the non-linearity of the Load/Deflection characteristic behaviour because the upper part of the pile near the surface of the soil is less confined compared to the deeper part of the pile. The soil near the surface yields at low pressure, the yield depending on the stress-strain (σ/ε) relationship of the soil. Leyden (1971) calls this zone the *Plastic Zone* and below the plastic zone the soil acts as an elastic continuum. Fleming et al (1985) described the flow of the soil around a cylindrical pile, in which the soil is assumed to behave as rigid plastic. This non-linear behaviour causes uneven distribution of bending moments among the piles in a group, which indicates that the lateral load is not equally shared in the pile group.

As a direct effect of the horizontal loading each pile is deformed, producing a bending moment along the pile length. The maximum moment occurring in the pile shaft or immediately below the pile cap should not exceed the yielding moment of the pile. As the pile group is displaced laterally axial forces are produced in each pile, compression in the front pile and tension in the rear pile. There has been little attention given in research to measurement of the axial forces in the pile except

Reddaway(1982) who measured axial forces on a pile group. It would be an important contribution to the piling industry if the magnitude of axial forces in the piles under lateral load could be measured in full scale tests.

In this chapter results are presented of a series of field tests conducted to investigate the effect of static and the cyclic horizontal loading on a single pile and on two-pile groups at different spacing and overhang. In the two-pile group field tests the main aims were to investigate the distribution of moment between the front and the rear pile, the axial force distribution, lateral stiffness of the two pile group and lateral soil pressure changes as the pile group responded to horizontal loading. Several potential difficulties arise in the measurement of bending and axial strains, of soil pressure and of soil density. Accurate but robust gauges and instrumentation are required, and a repeatable soil bed condition is required. Strain were measured by gauges mounted inside the box section. The soil density was measured both by sand replacement technique or cone penetration as discussed in chapter three sections 3.8.3, 3.8.4 and 3.8.5. It was difficult to maintain the same density for all test series because the sand trench was exposed to rain water and variation in moisture content of the sand affected the test results. As the test site was an exposed open area sometimes tests had to be abandoned due to rainfall and the expensive equipment had to be well protected on the site.

4.2-The Objective of The Field Tests

The primary objective was to study the lateral behaviour of single pile and two pile groups at near full scale in a sand trench and to investigate the effect of pile spacing and overhang.

4.3-The Method of Study

Various field tests were conducted on single pile and two-pile groups to study the behaviour quantitatively. Each pile group was subjected to deflection controlled loading cycles at varying pile spacing and overhang. Tables of tests conducted on

single pile and on two-pile groups are presented in tables T4.1 and T4.2 respectively, showing number of tests, dates, overhangs, measures soil density and water table level.

The field tests were designed with the purpose of measuring the effect of various pile group geometries on the following types of behaviour in response to horizontal loading;

1 -Pile group lateral deflection

2 -Pile head rotation

3 -Pile bending moment

4 -Pile Axial forces

5 -Lateral soil pressure

4.3.1-Pile Deflection

In order to observe the head of the single pile or pile cap deflection characteristics, the horizontal load and deflection were measured as described in section 3.10, 3.11 and 3.13. A typical load/deflection curve during a test is shown in Figure 4.1. To conclude the investigation of the deflection behaviour, the stiffness of the pile head or pile cap had to be obtained from the load/deflection curves. The stiffness is calculated by the gradient of the load/deflection curve. Due to the non-linear behaviour of load and deflection two stiffnesses were calculated;

1 -Tangential stiffness from the initial deflection, equivalent to elastic behaviour of the pile/soil system at small strains.

2 -Secant stiffness based on a deflection of 20.0mm at the pile head, reflecting the strain softening of the soil in front of the pile.

4.3.2-Pile Head Rotation

The non-linear behaviour of a pile/soil system can be demonstrated by the load /pile head rotation curve. The methods used to obtain data for load/rotation curves

in the cases of single piles and pile groups are described in sections 3.11 and 3.12. Typical load/pile head rotation curves showing non-linear behaviour in the case of single pile and two pile groups are shown in Figure 4.2.

It was assumed that the pile cap stiffness was sufficient to constrain the two piles to deflect and tilt by the same amount. This was found to be the case, by careful measurements.

4.3.3-Pile Bending Moments

When a vertical pile is horizontally loaded the pile bends and produces a bending moment along its length. The bent shape of the pile would indicate whether the pile is a fixed head or free headed pile. Care should be taken in design not to design a pile beyond its maximum yielding value.

As the pile is bent, somewhere along the shaft a maximum positive bending moment is produced. In the case of fixed headed piles the reverse (negative) bending moment value occurs at the pile head, while the maximum (positive) bending moment occurs some distance down the pile shaft. These values are of particular interest in this work as they can be used to draw conclusions on the distribution of the load in the case of two pile groups.

When two piles are firmly connected by a pile cap and are horizontally loaded, the distribution of the moments between two piles can be described by the ratio of the maximum positive bending moment values along the pile shaft between the front and the rear pile. The bending moment values along the pile length were determined as described in section 3.3. It was for this purpose that strain gauges were mounted on the inner surface of the pile. To determine bending moments along the pile length, simple bending theory was used. As there were two strain gauges on opposite sides of the interior of the piles (see Figure 3.4) at specific distances along the pile length, the average bending strains were determined for each recording. The average bending

strains were used to determine the bending moment value for each specific distance.

$$M = \frac{I.E.\varepsilon_v}{Y}$$
(4.1)

where

M bending moment value

I the second moment of the area of the pile cross section

E elastic modulus of the pile

ε_v average bending strain

Y distance from the neutral axis to the measured bending strain.

As the VWSG's and ERSG's were measuring the eccentric bending strain and the surface bending strain along the pile length respectively, the Y value which is used in the above equation to determine the bending moment value would be different for WVSG's and ERSG's. In order to have constant Y value in the equation 4.1, the eccentric bending strain could be converted to surface bending strain using the linear relationship existing through the pile cross section as described in section 3.3.3 using equation 4.2. Using this relationship equation 4.3 is formed to calculate the surface bending strain from the eccentric bending strain;

$$\frac{\varepsilon_1}{d_1} = \frac{\varepsilon_2}{d_2}$$
(4.2)

where

ε_1 eccentric bending strain

ε_2 surface bending strain

d_1 distance from neutral axis to the measured eccentric bending strain

d_2 distance from neutral axis to the measured surface bending strain

therefore;

$$\varepsilon_2 = \frac{\varepsilon_1.d_2}{d_1}$$
(4.3)

Figure 4.3 shows a typical example of bending moment diagrams for the front and the rear piles.

4.3.4-Axial Force

When a single vertical pile is bent there will be negligible induced axial force. However when pile groups are laterally loaded the piles in the front are loaded in compression while the rear piles carry uplift force. These down-ward and up-ward forces must be equal so that vertical equilibrium is satisfied. In order to measure the axial forces along the piles the same measured strains were employed here as those used to determine the bending moment values. The sum of the compression and tension bending strains indicates whether the pile is in compression or in tension and the axial force on the pile may be determined by simply multiplying the sum of the bending strains for the specific distances along the pile by the pile cross sectional area and its elastic modulus. It must be emphasised here that to determine axial forces in the pile shaft is very difficult because they are deduced from small differences in electrical resistance strain gauge recordings.

$$F = (\varepsilon_T + \varepsilon_C).E.A \tag{4.4}$$

where

F is the axial force

ε_T bending strain indicating tension

$-\varepsilon_C$ bending strain indicating compression

E is the elastic modulus of the pile

A the area of the pile cross section.

Using the above equation axial forces in the pile were determined. Small differences in strain indicated large axial forces in the piles with some consequential errors. Figure 4.4 shows a typical example of an axial force diagram.

4.3.5-Lateral Soil Pressure

When a vertical pile is horizontally loaded the lateral soil pressure in front of the pile increases from its static pressure to a limiting pressure near the surface while in deeper zones the pressure continues to increase. At the back of the pile the lateral soil pressure decreases from its static pressure. Many authors such as Broms assume that the ultimate lateral soil resistance on a vertical pile is three times its lateral passive pressure and Barton(1982) suggests that the ultimate lateral resistance (P_u) on a vertical pile is $P_u = k_p^2 \gamma z d$. Poulos(1971) and Randolph(1981) assume that the soil adheres to the back of the pile. Having placed instrumentation at the front and back of each pile with pressure cells these assumptions were investigated in the test series. The methods used to determine lateral soil pressure from the pressure cells are described in section 3.3.5. It was also hoped to investigate lateral soil pressure between the front pile and the rear pile in the case of two pile groups. A problem occurred during testing due to heavy pile driving, and some of the strain gauges on the pressure cells did not respond. Figure 4.5 shows a typical soil pressure distribution along the embedded length of the pile.

4.4-Description of The Effect of Pile Spacing on The Two-Pile Groups

Five important effects that had to be investigated in respect to pile spacing (3, 5, 8 and 12 pile width) and overhangs are as follows;

1 -The distribution of bending moments in the two-pile groups.

2 -The distribution of axial forces in the two-pile groups.

3 -The distribution of change in lateral soil resistance.

4 -The lateral stiffness of two-pile groups.

5 -The tilting of the piles head in the two-pile group tests.

4.5-Test Results On The Single Piles

When the construction of the first pile was completed, the installation of the

single vertical pile in the sand trench and of the reaction pile were undertaken as described in section 3.10. Four separate tests were conducted on a single pile.

The single pile tests were free head tests allowing rotation at the pile head above the ground. It was not possible to conduct a fixed head single pile test because of the impracticality of restraining the head of the pile against rotation.

The objective of the single pile tests was to determine the behaviour of the pile/soil system for back analysis to determine the soil modulus profile. It should be mentioned here that the load/deflection curve refers to lateral load 500mm above the ground and pile deflection 70mm above the ground, for all four tests. The stiffness quoted for the purpose of back analysis and prediction analysis for the single pile was in accordance with the site geometry using the above definition.

Throughout the tests on the single pile, load/deflection, load/rotation, bending moments and lateral soil pressures were determined and the relevant Figures are presented in appendix A (Figures A.1 to A.4)

From tests conducted on the single piles, the best fit curve through the load/deflection data is shown in Figure 4.6 for the first cycle of lateral loading. From the initial portion of the load/deflection curve (see Figure 4.6), the tangent stiffness was calculated as $1.75MN.m^{-1}$ and the secant stiffness for 20mm pile head deflection was calculated as $0.825MN.m^{-1}$.

In order to obtain relationships between the maximum bending moment on the pile shaft, the horizontal force and pile head deflection, the maximum pile shaft moments were determined from the bending moment diagrams, and a summary of horizontal force, deflection and Max.BM are tabulated in Table T4.3. Figures 4.7 and 4.8 shows the relationships Max.BM/Horizontal force and Max.BM/pile head deflection respectively. It was found that the first relationship was effectively linear for all four tests, with a value of $0.69kNm.kN^{-1}$. To establish the relationship between the Max.BM and deflection, data was collected and plotted and it was found that this

relationship was non-linear (see Figure 4.8), varying between 1150 and $590kNm.m^{-1}$.

The soil pressures measured on the pressure cells were plotted down the embedded length of the pile. It was found that the lateral soil pressure in front of the pile increased for loading and the lateral pressure at the back of the pile reduced for each successive stage. The maximum observed pressure change was $450kPa$, see Figure A2.c

4.5.1-Test Difficulties On Single Piles

Various problems occurred during the testing procedure although they did not affect the results significantly. These problems may be discussed in the relation with the following factors;

Some of the VWSG's were damaged during heavy pile driving and so a full profile of results could be obtained only by recourse to the ERSG readings. Ground water was found to penetrate inside the pile. Fortunately through good installation of the ERSG's the moisture did not affect the majority of test results. By inserting a hose inside the pile the water at the bottom of the pile was pumped out continuously. This leakage was due to pin holes created during welding the two channel 'C' sections together to form the pile. In construction of later piles leakage tests were conducted as described in section 3.4 for preventing ground water getting inside the piles. It was found difficult throughout the tests to control the load so as to maintain constant increments of pile head deflection.

4.5.2-Conclusion From The Single Pile Tests.

Throughout the four single pile tests the following observations were obtained;

1 -The load/deflection was non-linear.

2 -The tangent stiffness was greater than the secant stiffness.

3 -The relationship between the Max.BM and the lateral load was linear.

4 -The relationship between the Max.BM and the deflection was non-linear.

5 -The lateral soil pressure in front of the pile increased as the load increased and the lateral pressure at the back of the pile reduced as the load increased. Caution must be excercised in drawing any conclusion on the results obtained from the pressure cells.

4.6-Test Results On Two-Pile Groups

When the construction of additional piles was completed, tests on two-pile groups were conducted. The two-pile group spacings were 3,5,8 and 12 pile width centre to centre of each pile. The overhang of the pile cap on the two pile group was chosen to be 150, 300 and 400mm. Piles were firmly connected by a stiff pile cap and were horizontally loaded as described in section 3.14. The deflection on the two-pile group tests refers to the deflection measured at the point of application of lateral load to the two-pile groups.

Throughout the tests on two-pile groups load/deflection curves, load/pile head rotation curves, bending moment diagrams, axial force diagram and lateral soil pressure diagrams were obtained and are presented in Figure A.5 to A.35 in appendix A. It must be mentioned here that the soil lateral pressures obtained were unreliable and no conclusion could be drawn. This was purely due to the presence of axial forces on the piles wall which are discussed in detail later in this section.

4.6.1-Lateral Stiffness of Two-Pile Groups

In order to assess the results of load/deflection curves for various pile separations and overhangs in terms of a two-pile group lateral stiffness, both tangent and secant stiffnesses were calculated in the same manner as for the single pile. In some cases the load/deflection curve had to be extrapolated slightly to obtain the group secant stiffness due to insufficient deflection of the pile cap in the test. Table T4.8 shows the calculated stiffness values for all overhangs and pile separations. Some of the calculated values were unrealistic and after repeat testing were ignored when calculating the average values. However even ignoring these spurious values some of the averaged

values were still anomalous, particularly that for 8 pile width spacing. Another factor which made the lateral stiffness calculated from load/deflection differ from similar tests was the variation of soil stiffnesses. As the tests were conducted at different time of the year the seasonal effect played an important factor which will be discussed in section 4.7. Despite the variability of the stiffnesses calculated the variation of lateral stiffness of two-pile groups is presented in Figure 4.9. Figure 4.9 shows the relationship between the group stiffness and the pile separation for all three overhangs. The effect of increasing the pile spacing was to increase group stiffness while increasing pile cap overhang reduced group stiffness. The secant stiffnesses were less than the tangent stiffnesses due to the softening effect of the soil near the surface. After the first cycle of lateral loading, the two-pile groups were unloaded and four cycles of lateral loading was applied in order to investigate the effect. It was found that the residual lateral stiffness of two-pile groups was reduced by 20% approximately (see Tables T4.4 to T4.7).

4.6.2-Pile Head Rotation of The Two-Pile Groups

The rotation of each pile head caused by horizontal load gave an indication of the degree of fixity of each pile into the pile cap. The pile head rotation was measured when the pile cap was at 400mm overhang. The relevant results are shown in Figures A.41 To A.47 in appendix A.

In assessment of the fixity of each pile head, results obtained from load/rotation measurement confirmed that the pile head condition was nearly fully fixed.

4.6.3-Bending Moment Distribution in The Two-Pile Groups

To draw a conclusion on the distribution of the moment between the front pile and rear pile, the maximum bending moment (Max.BM) values on the pile shaft were obtained from bending moment diagrams for each recorded stage and for all the tests. These values of overhang, horizontal force, deflection, Max.BM, and ratio, were tabulated in test number order for each of the seven stages. Tables T4.4, T4.5, T4.6

and T4.7 give these values for pile separations of 3,5,8 and 12 pile width respectively.

A number of graphs are presented to establish how the moments are distributed between the front and rear of the pile. Figures A.36 to A.39 in appendix A indicate the relationship between the ratio of Max.BM in the front and rear piles and the deflection for the various overhang and pile separations. A best-fit straight line was drawn to obtain the ratio of moments for a deflection of 20mm for each case. These ratios were plotted together against their corresponding values of pile separation. The distribution of these ratios are scattered and this is due to primarily the variation of soil stiffness, as the tests were conducted at different times of the year. The soil stiffness was reduced during wet times of the year and increased during the dry periods. This effect can be seen in Figure 4.12. Despite the variability of the soil stiffness it can be suggested that the distribution of these ratios can best be represented by their mean value of 1.08 as shown on the Figure 4.10. In Figure 4.10 also the time of the year when the tests were conducted is shown. It must emphasised here that the soil stiffness affects the distribution of the moments between the front pile and rear pile.

The reverse (negative) moment occurred directly beneath the pile cap. Assessment of reverse moments beneath the pile cap in respect to pile spacings and overhangs was very difficult because of the following reasons;

1 -No direct ERSG's reading could be obtained on the pile shaft directly beneath the pile cap.

2 -The ERSG's reading on the pile shaft near the pile cap were rejected because of the local effects.

3 -From bending moment diagrams the magnitude of reverse moment varied from one test to another because of the variable fixity of pile to pile cap.

4 -The variation of soil density and seasonal effects.

In order to draw conclusions on the values of reverse bending moment the reverse bending moment values were obtained from bending moment diagrams by extrapolation. It should be mentioned here that some of the reverse bending moment values were unrealistic and were ignored.

Using the above method to obtain reverse moment values three sets of graphs are presented. Figure 4.11a shows the relationship between the magnitude of the averaged reverse bending moment per unit horizontal load for the final cyclic loading against the pile spacing. Figure 4.11b shows the relationship between the magnitude of the averaged reverse bending moment over the final stage of first cyclic loading against pile spacing. Figure 4.11c shows the relationship between the magnitude of the averaged reverse bending moment over the final stage of pile cap displacement against pile spacing.

From these three figures it can be concluded that the reverse moment increased as the size of the overhang increased and increased with pile spacing. The magnitude of reverse bending moment increased from the first stage of loading to final stage of cyclic loading. The conclusions drawn are based on extrapolated values of bending moment curves to beneath the pile cap. These results obtained may be considered rather unreliable as there were not accurate readings possible at the pile/cap junction.

The relationship between the maximum bending moment and the lateral load on the two-pile groups in respect to pile spacing and overhangs was investigated. The average maximum bending moment was plotted against lateral load and a best fit line was drawn through the point for the range of overhangs and pile spacings. It was found that this relationship is linear. Four graphs had to be presented to draw conclusions on the relationship between the average maximum bending moment to lateral load ratio. These graphs are presented in appendix A Figures A.40a to A40d. The gradients in, $(kNm)(kN^{-1})$, were calculated and are tabulated in table T4.9.

The average maximum bending moment ratio between the front and the rear

pile for each stage of strain gauge recording were calculated. Figure 4.12 shows the relationship between the average maximum bending moment between the front and rear piles and lateral load on the two-pile group against pile spacing. It was found in Figure 4.12 that the values of maximum bending moment/horizontal load ratio were scattered due to seasonal effects. It can be seen that in tests during summer time when the soil is dry the soil stiffness is greater than during the winter when the moisture content of the soil is high. The magnitude of bending moment increased as the soil stiffness decreased and and vice versa. During dry times the magnitude of average maximum bending moment to horizontal load for 150, 300 and 400mm overhangs were 0.25, 0.32 and $0.38kNm.m^{-1}$ respectively regardless of the pile spacing. During wet times the magnitude of average maximum bending moment to horizontal load for 150, 300 and 400mm overhangs were 0.17, 0.22 and $0.23kNm.m^{-1}$ respectively regardless to the pile spacing. In both the summer and winter time this magnitude increased with increase in pile cap overhang but the increase in pile spacing had little effect (see Figure 4.12).

The magnitude of the reverse bending moment must also have been affected by the variation of soil stiffness as was the magnitude of the maximum bending moment. The effect of variation of soil stiffness on the reverse moment cannot be confirmed because there were no direct readings at the pile/cap junctions and the bending moment curves were extrapolated.

4.6.4-Axial Force Distribution on The Two-Pile Groups

Axial forces were calculated as described in section 4.3.4 and plotted for the front and rear pile. These show that the front pile was in compression, while the rear pile was in tension, and the values of the force were almost equal but of opposite sign. As the overhang increased so the axial forces on the pile increased. This data is presented in Figures A.5c to A.35c in appendix A. There was insufficient data to produce better graphs, but from the limited data recorded these conclusions were drawn. In some

tests it was not possible to determine a reliable axial forces diagram and for those tests, results have not been presented.

In order to assess the results of axial forces on the piles for various pile spacing and pile cap overhang on the two-pile groups peak axial force values were obtained from axial force diagrams for each stage of strain gauge recording. The peak axial forces values obtained sometimes were unreliable and had to be ignored. These unreliable axial force values were due primarily to difficulty in reading small strain differences between large, but nearly similar, readings. The axial force reaches its peak value near the ground surface so those values which were almost equal between the ground line and 1.0m approximately below the ground were collected from axial force diagrams. The peak axial force value was divided by the corresponding lateral load to give the peak axial force per unit lateral load on the two-pile group. A number of values for each pile cap overhang and spacing were obtained and the average value was calculated. The calculated average peak axial force per unit lateral load for various pile spacing and overhangs are tabulated in table T4.10.

An analysis of these results was made using a simple regression technique. First it was assumed that the peak axial force per unit lateral load (f) could be approximated using a linear combination of terms involving pile spacing (s) and overhang (e). Thus

$$f \approx g(s, e) = a_1 + a_2 s + a_3 e + a_4 se \qquad (4.5)$$

A measured deviation D of the points f_i from the function $g(e, s)$ was defined as follows;

$$D = \sum_{i=1}^{N} \left[f_i - g(s_i, e_i) \right]^2 \qquad (4.6)$$

The distance between the points and function was squared to eliminate the problem of sign. One effect of this is to weight the function in favour of points which deviate a long way from the general trend.

Using the above method one can minimize the function given by equation 4.6 as

shown below:

$$\frac{\partial D}{\partial a_1} = 0 = 2 \left[\sum_{i=1}^{N} \left(f_i - a_1 - a_2 s_i - a_3 e_i - a_4 s_i e_i \right)(-1) \right] \qquad (4.7a)$$

$$\frac{\partial D}{\partial a_2} = 0 = 2 \left[\sum_{i=1}^{N} \left(f_i - a_1 - a_2 s_i - a_3 e_i - a_4 s_i e_i \right)(-s) \right] \qquad (4.7b)$$

$$\frac{\partial D}{\partial a_3} = 0 = 2 \left[\sum_{i=1}^{N} \left(f_i - a_1 - a_2 s_i - a_3 e_i - a_4 s_i e_i \right)(-e) \right] \qquad (4.7c)$$

$$\frac{\partial D}{\partial a_4} = 0 = 2 \left[\sum_{i=1}^{N} \left(f_i - a_1 - a_2 s_i - a_3 e_i - a_4 s_i e_i \right)(-se) \right] \qquad (4.7d)$$

These partial differentials are evaluated by substituting equation 4.5 into 4.6 and differentiating with respect to each of the four unknown coefficients. Expanding and rearranging equations 4.7 in matrix form gives;

$$\begin{bmatrix} N & \sum s & \sum e & \sum se \\ \sum s & \sum s^2 & \sum se & \sum s^2 e \\ \sum e & \sum se & \sum e^2 & \sum se^2 \\ \sum se & \sum s^2 e & \sum se^2 & \sum s^2 e^2 \end{bmatrix} \cdot \begin{Bmatrix} a_1 \\ a_2 \\ a_3 \\ a_4 \end{Bmatrix} = \begin{Bmatrix} \sum f \\ \sum fs \\ \sum fe \\ \sum fse \end{Bmatrix} \qquad (4.8)$$

Note that for simplicity the limits have been omitted from the sums in equation 4.8. Solving for a_1, a_2, a_2 and a_4 produced;

$$f \approx 0.356 + 0.012s + 5.42e - 0.203se \qquad (4.9)$$

Obviously the term in s is small compared to the other terms and so the procedure was repeated with $a_2 = 0$ to give;

$$f \approx 0.444 + 5.14e - 0.164se \qquad (4.10)$$

As previously suggested the least squares fit analysis outlined will tend to bias the function toward points which deviate a long way from the trend. It is evident from Figure 4.13 that the value for f obtained for an overhang of 300mm and spacing of 3 pile width does not match the general trend, and so the analysis was repeated with this point excluded. The new equation is now:

$$f \approx 0.462 + 5.46e - 0.202se \qquad (4.11)$$

The average maximum peak axial force per unit lateral load was calculated to be $2.54kN.kN^{-1}$ for 3 pile width spacing at 400mm overhang. The average minimum peak axial force per unit lateral load from site test results was calculated to be $0.88kN.kN^{-1}$ for 12 pile width spacing at 150mm overhang (see table T4.10). This shows the reduction of about 400% when the pile are widely spaced and the overhang is reduced compared with piles at close spacing which carry greatest axial force. In order to draw conclusions regarding the average peak axial force per unit lateral load, values were plotted against pile spacing and a best line was drawn through the points for each of the overhangs. It was found that the value for 3 pile width spacing 150mm overhang was unrealistic due to difficulties with the readings and did not fit the trend of the other values.

Finally it may be concluded that the peak axial force per unit load decreases with increase in pile spacing provided that overhang is non-zero, and increased with increase in pile cap overhang (see Figure 4.13). One of the deductions from equation 4.11 is that, as the overhang increases the peak axial force increases. The equation also suggests that if the overhang is zero the prediction of the peak axial force is not a function of pile spacing. The proposed equation 4.11 takes into account the variation of both overhang and pile spacing.

The effect of reduction or increase in soil stiffness or density on the peak axial forces on the pile shaft cannot be confirmed because of lack of evidence. Figure 4.13 showed that the smooth reduction of peak axial forces with pile spacing occurred despite the tests have been conducted at different times of the year.

4.6.5-Lateral Soil Pressure Distribution on The Two-Pile Groups

The data for lateral soil pressure obtained from the pressure cells embedded in the length of the pile cannot be presented because they were unrealistic. This was purely due to existence of axial forces within the pile wall which interfered with the pressure cell readings since the pressure cell diaphrams were very thin. For these

reasons these data were not reliable at all and are not presented.

In the field tests tension cracks appeared in the surface indicating wedge shape failure of the soil near the ground (see Plate 4.1).

4.7-Test Difficulties on Two-Pile Groups

Various problems occurred during testing which are described in four categories;

1-Instrumentation

2-Alignment

3-Variation of soil density

4-Test results

6-Axial forces

1 -Many of the VSGW's were damaged during driving and therefore the ERSG's were used to obtain the bending strains along the piles. As discussed in section 3.3.1 the ERSG's showed drift, but this problem was overcome by recording the bending strains at uniform rate. Even so some of the ERSG's failed to recorded sensible bending strains but there were sufficient data to draw bending moment diagrams. Also there were enough data to obtain axial forces on the piles. Several strain gauges on some of the pressure cells failed to record strains and pressure cell readings were unrealistic. Ground water was not a problem inside the piles because they were constructed to be water proof.

2 -Overall the alignment of the piles caused some difficulty. Despite care in alignment some degree of rotation occurred during the installation of the pile for the 8 pile width spacing tests. The instrumented pile group was off-set approximately by 80mm through its centreline with the reaction pile. The test could not be conducted unless the pile group were displaced in line with the centreline. The problem was overcome by attaching a 12mm thick plate to the front of the pile cap and placing the jack in the web of the 'C' section. The 'C' section as de-

scribed in section 3.14 was placed horizontally to form a pile cap. A slot hole was made through the thick plate in front of the reaction pile group cap to accept the tension bar. For driving piles at twelve pile width spacing guide rails were used to prevent misalignment. After completion of tests on the three pile width spacing, the rear pile was selected to be extracted from the sand trench. During extraction of the pile, the pile failed in bending because, as the pile was displaced horizontally by a JCB to overcome the friction force the allowable horizontal force was exceeded and the pile failed. A new pile had to be constructed to continue the testing program. Unfortunately the construction of the new pile delayed testing.

3 -The crude way used to control the soil density was to relate the cone penetrometer reading to the compaction test conducted on the same sand (see section 3.7.4). This method gave an indication of unit weight of the sand after compaction and before the tests. As the site was exposed to the environment the sand trench could not had been protected against rainfall. During rainfall the soil moisture content and water table level increased although dewatering of the sand trench was conducted before any test. The moisture content of the soil could increase and consequently the soil stiffness stiffness was reduced. It was found that during spring and winter time the tests conducted had a greater maximum bending moment to horizontal load ratio than in the summer times or during dry seasons. Similar effects were obtained on the lateral stiffness of the pile groups. Bad weather caused severe problems. During set up or testing all the measurement instrumentation had to be protected from rainwater. This was achieved by placing a plastic sheet over the instruments. Sometimes tests or pile driving had to be abandoned due to bad weather. Figure 4.14 shows the variation of the average soil unit weight throughout the field tests on two-pile groups.

4 -Although the maximum horizontal deflection of the pile cap was selected to be 20.0mm for all the group tests, it was found that to control the pile cap load to

maintain the appropriate deflection was difficult. Sometimes the pile cap could not be displaced 20mm and sometimes it was displaced more than 20.0mm, by over-extension of the ram of the jack. Although any obvious gaps were filled between barrel and the wedges on the tension bar, such gaps were still a problem in some tests, so maximum care was taken during the initial applied load to close up any gaps. Inaccuracy of the pressure gauge on the hydraulic pump did not effect the horizontal load since this was measured on the tension bar. From load/deflection curves it was difficult to obtain a good tangent stiffness from two-pile groups, because of the early non-linear behaviour despite care in the curve fitting technique. The minimum bending moments obtained from the bending moment diagrams were extrapolation of the curves since there was no direct strain gauge reading at pile/cap junctions.

5 -In order to obtain axial forces in the pile the strain gauges reading used to determine bending moment values were used also to obtain axial forces. To obtain axial forces was very difficult due to the small differences in strain. In some cases the axial forces could not be obtained for every section of the pile due either to the failure of the gauges or unreliablity of the recording.

4.8-Discussion On Two-Pile Group Tests

In conducting near to full scale tests on two-pile groups there proved to be considerable difficulties in relation to preparation of the tests, conducting tests, data collection and analysis and presentation of the results. However from the tests conducted on two-pile groups some of the results obtained were of considerable interest particularly because both axial forces and moment distributions were measured simultaneously. In this section the major deductions are presented.

In the two-pile group tests the head condition lay between free and fixed because of cap tilt, and some lack of rigidity in the pile to cap joint. The lateral stiffness of a two-pile group depends on the head conditions and the soil stiffness as well as

pile spacing and cap overhang. Some variation of soil stiffness was inevitable between test. Also in the early portion of a load/deflection curve selecting a reliable tangent stiffness was difficult. However despite the variation of soil stiffness, it was clear that the stiffness of two-pile groups increased as the pile spacing increased. This is due to the broader frame,and the reduction in shielding effect offered by the front pile to the back pile. The lateral stiffness of the two-pile group did also increase as the pile cap overhang was reduced. This is simply due to the fact that the eccentric distance (and therefore moment) is reduced as is the above ground sway, and so a greater force is needed to deflect the pile group. The effect of cyclic loading on the two pile groups was also observed. It was found that the strain softening effect during cyclic lateral loading reduced the two-pile group stiffnesses by some 20% after first cycles.

The effect of seasonal soil stiffness variation was also evident in the measured shaft bending moments. It was found that when the tests were conducted during dry summer spells the bending moments were greater than in tests conducted during wetter periods. It was not possible to deduce a trend of behaviour between the maximum bending moment to horizontal load ratio and pile spacing. However as the cap overhang increased the maximum bending moment to horizontal load ratio increased in tests during both dry and wet periods (see Figure 4.12).

The ratio of front pile moment to rear pile moment was calculated, but no clear trend was observed as a function of either pile spacing or cap overhang. The ratio of maximum bending moment between the fronts and rear piles was calculated regardless of pile spacing and overhang as a mean value of 1.08. The scatter of values was clearly a function of seasonal variation in soil stiffness also. (see Figure 4.10).

The magnitude of reverse bending moment immediately beneath the pile cap was found to increase with pile spacing and cap overhang. However caution must be excercised because there were no direct readings of strain gauges at the pile/cap joint, and the strain gauges near at the pile cap experienced local effects. Hence the

results obtained regarding the magnitude of reverse moment were by extrapolation of the bending moment diagrams. In extrapolating the bending moment diagrams some values were found to be unreliable and had to rejected.

Cyclic loading was found to increase the reverse moment. Cyclic loading also increased the maximum bending moment in the pile shafts of the two-pile groups.

Deduction of the axial forces from strains measured on the site was a difficult exercise. It was found that the axial forces in the piles were almost equal in the rear pile and the front pile but of opposite sign. The front pile was under compression while the rear pile was in tension. Axial force in the pile shaft was almost constant between pile cap and some 1.0m below the ground line. From analysis of the data collected it was found that the axial forces in the two-pile groups decreased with increase in pile spacing and increased with increase in pile cap overhang. Compound regression of the data was used to propose an equation describing the peak axial force per unit lateral load.

The deduction of both axial forces and bending moments due to lateral load on the pile group was considered to be a central theme of this work, which has seldom been achieved at a realistic scale.

The relationship between the lateral soil pressure and lateral loading could not be established for the reasons described in section 4.5.1. In some cases results from the pressure cells indicated that the lateral soil pressure in front of the pile increased and at the back of the pile lateral soil pressure reduced with the pile deflection, but comprehensive reliable data were not achieved.

4.9 Conclusions From Two-Pile Groups Tests Results

The following conclusions can be drawn from the tests on two-pile groups.

1 -The lateral stiffness of a two-pile group increased as the pile spacing increases.

2 -The lateral stiffness of a two-pile group increased as the pile cap overhang de-

creased.

3 -The cyclic lateral loading reduced the lateral stiffness by 20% after first cycle

4 -The mean ratio of maximum bending moment between the front and rear pile was calculated to be 1.08 for the several different overhangs and pile spacings.

5 -The cyclic lateral loading increased the magnitude of moments.

6 -The relationship between the maximum bending moment and lateral load was linear.

7 -The maximum bending moment/horizontal load was nearly a constant with pile spacing but increased with pile cap overhang.

8 -The reverse bending moment increased with pile spacing and pile cap overhang.

9 -The soil stiffness affected the magnitude of the moments but had little effect on the axial forces in the piles.

10 -The axial forces indicated that the front pile was in compression and the rear pile in tension.

11 -The axial force increased with pile cap overhang and decreased with pile spacing

12 -An equation was proposed to describe the average peak axial forces within the two-pile group.

13 -The lateral soil pressure distribution could not be investigated because the axial forces within the pile wall corrupted the pressure cell readings.

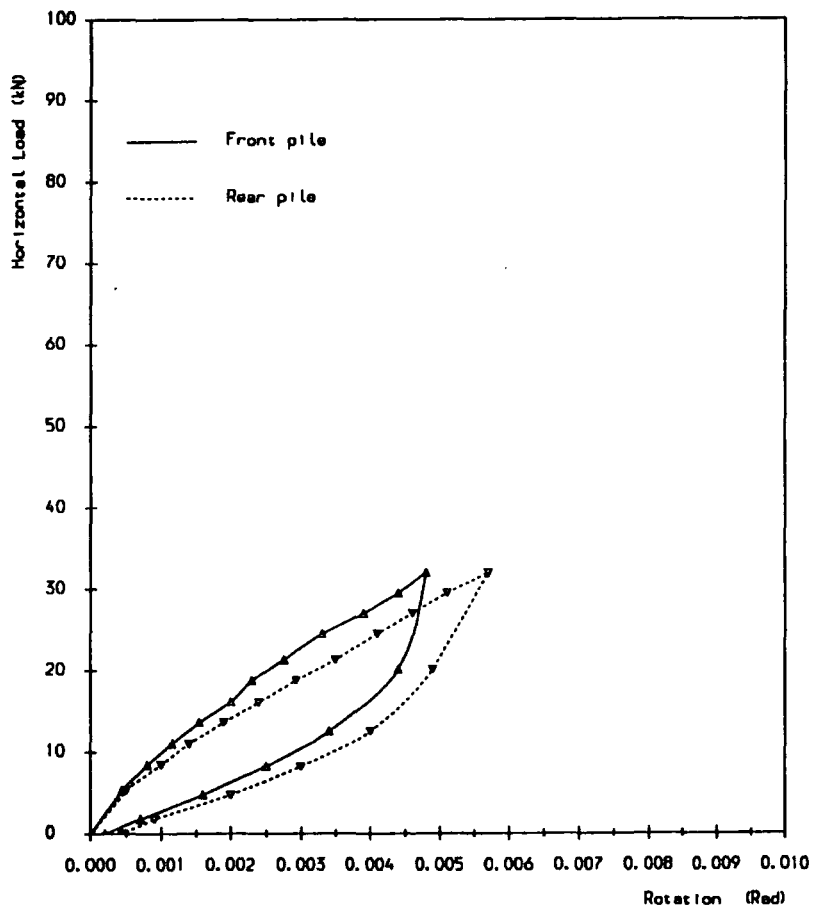Plate 4.1 Tension cracks in front of the pile.

Figure 4.1 A typical load/deflection curve of a two-pile group.
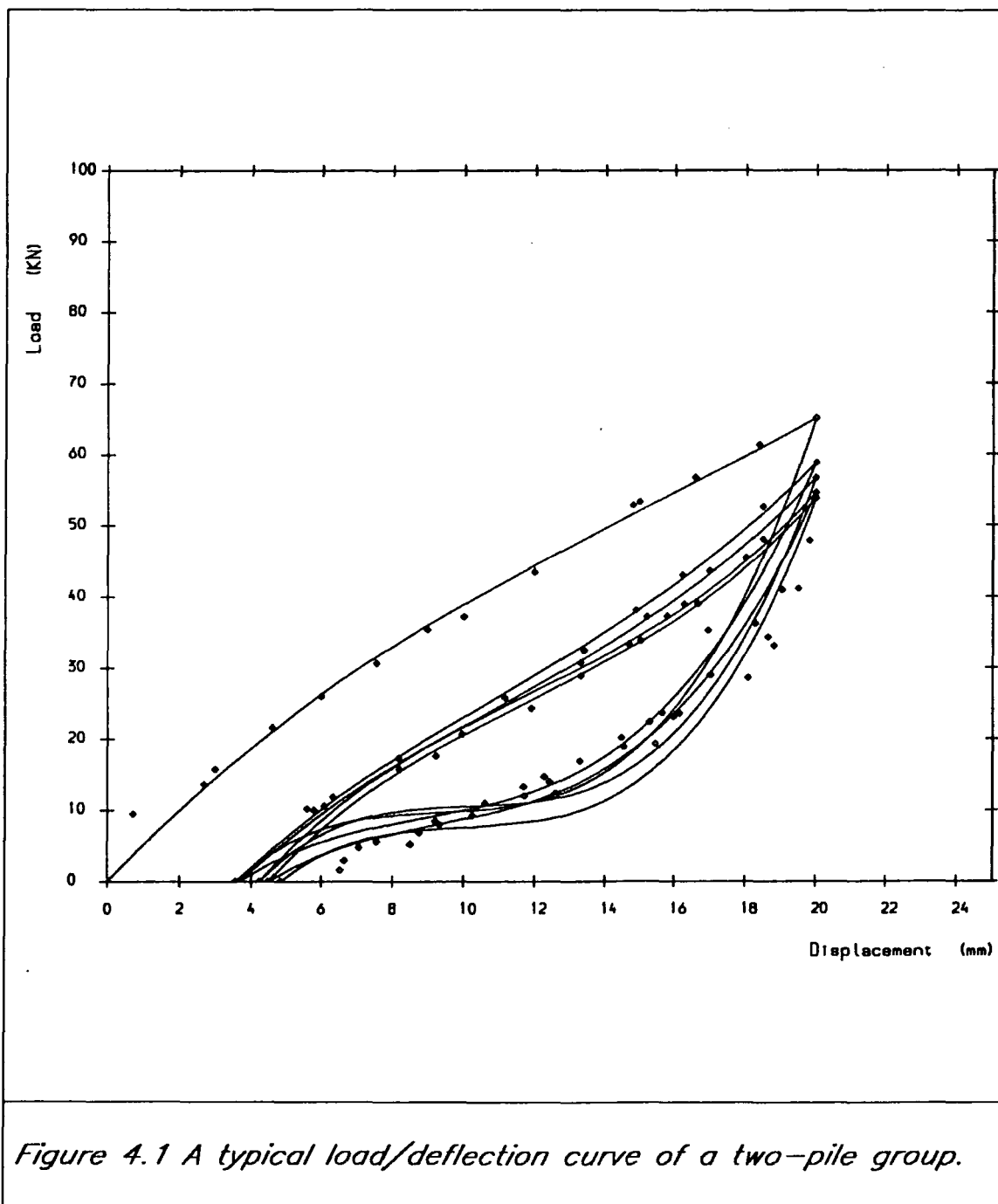
Figure 4.2 A typical load/pile head rotation curve.

BENDING MOMENT (kNm)

DEPTH (m)

-------- Rear pile
———— Front pile

1 = 3.00mm Pile cap Defl.
2 = 6.00mm Pile cap Defl.
3 = 9.00mm Pile cap Defl.
4 = 12.00mm Pile cap Defl.
5 = 15.00mm Pile cap Defl.
6 = 20.00mm Pile cap Defl.
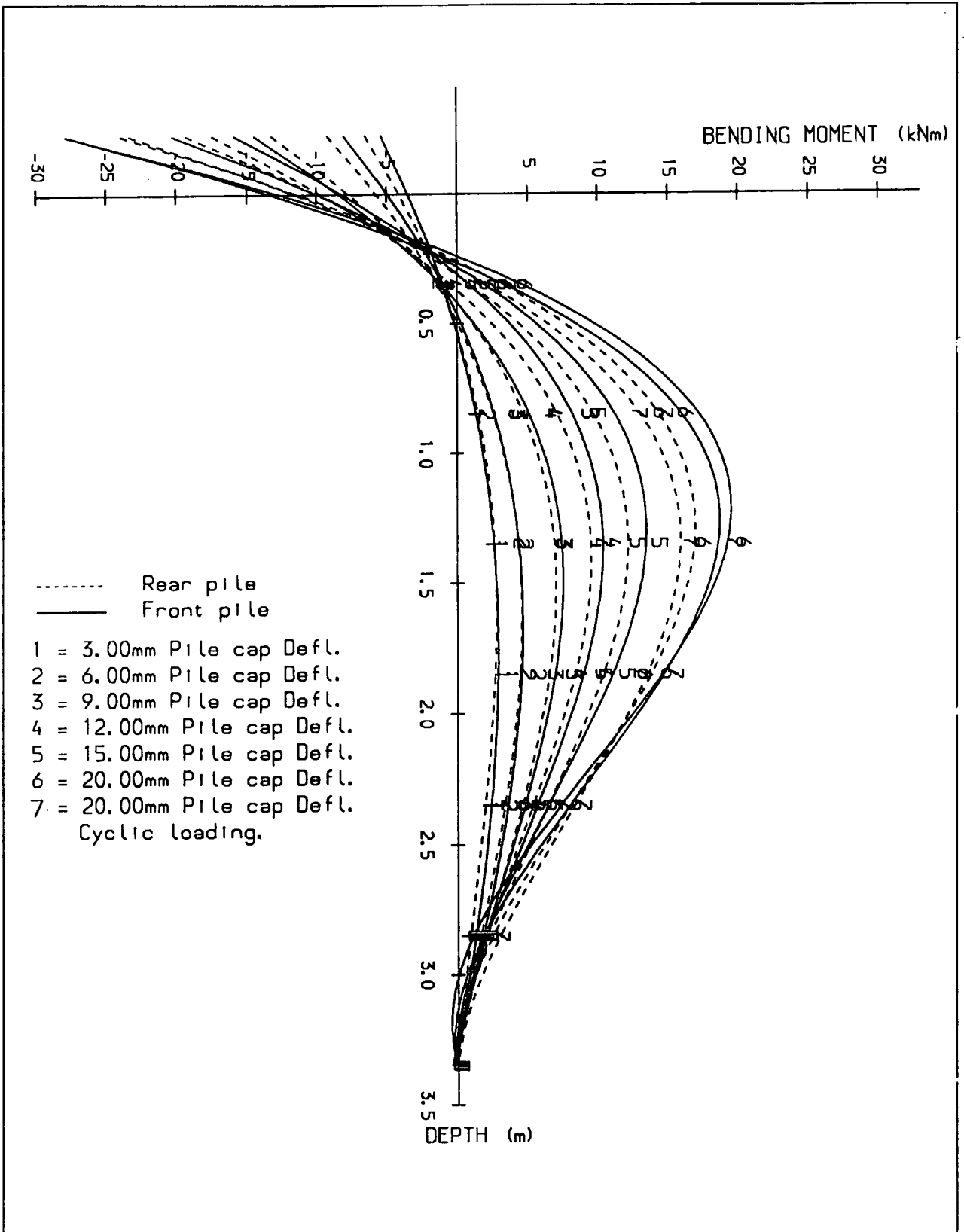7 = 20.00mm Pile cap Defl.
    Cyclic loading.

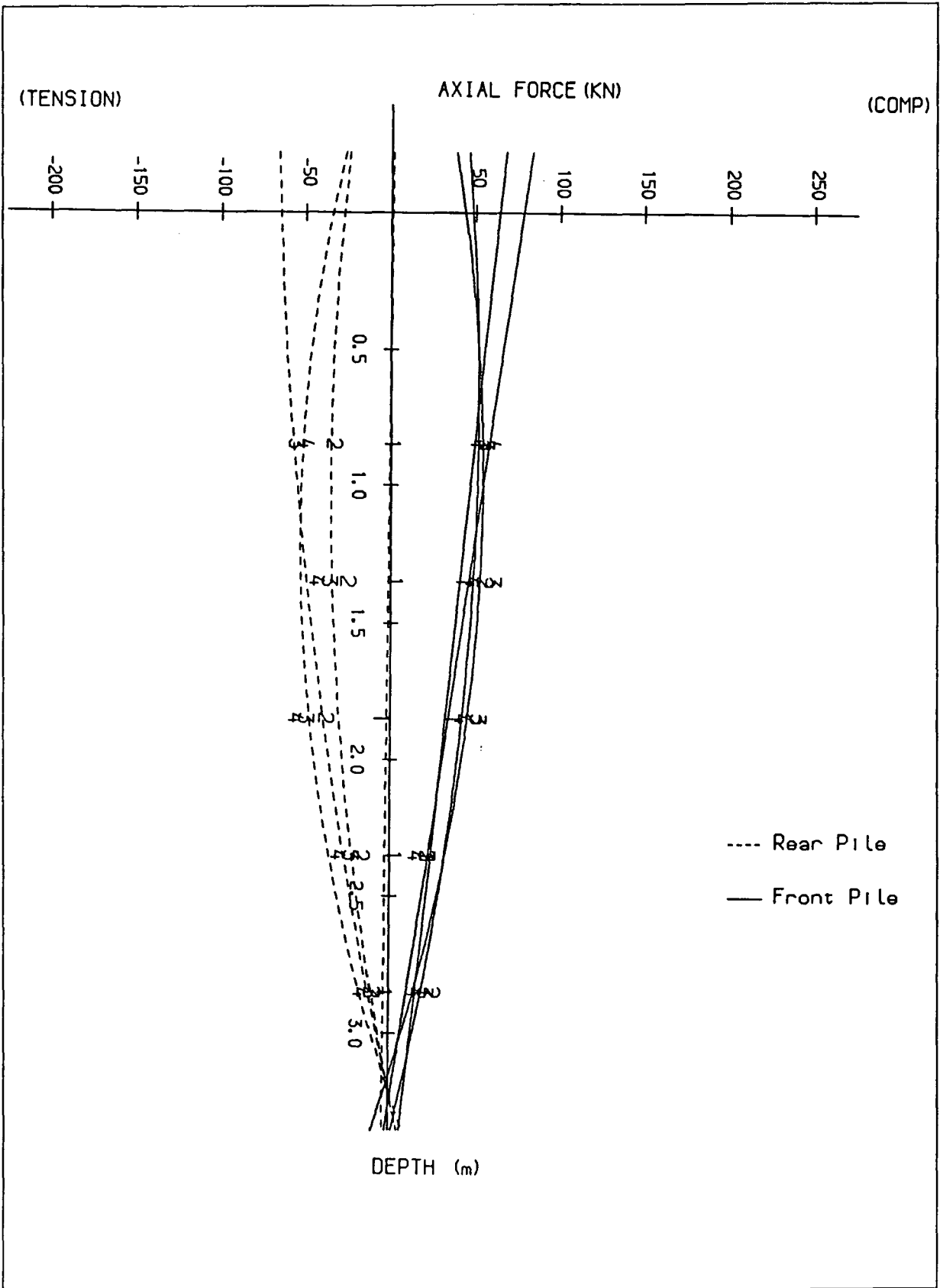*Figure 4.3 A typical bending moment diagram*

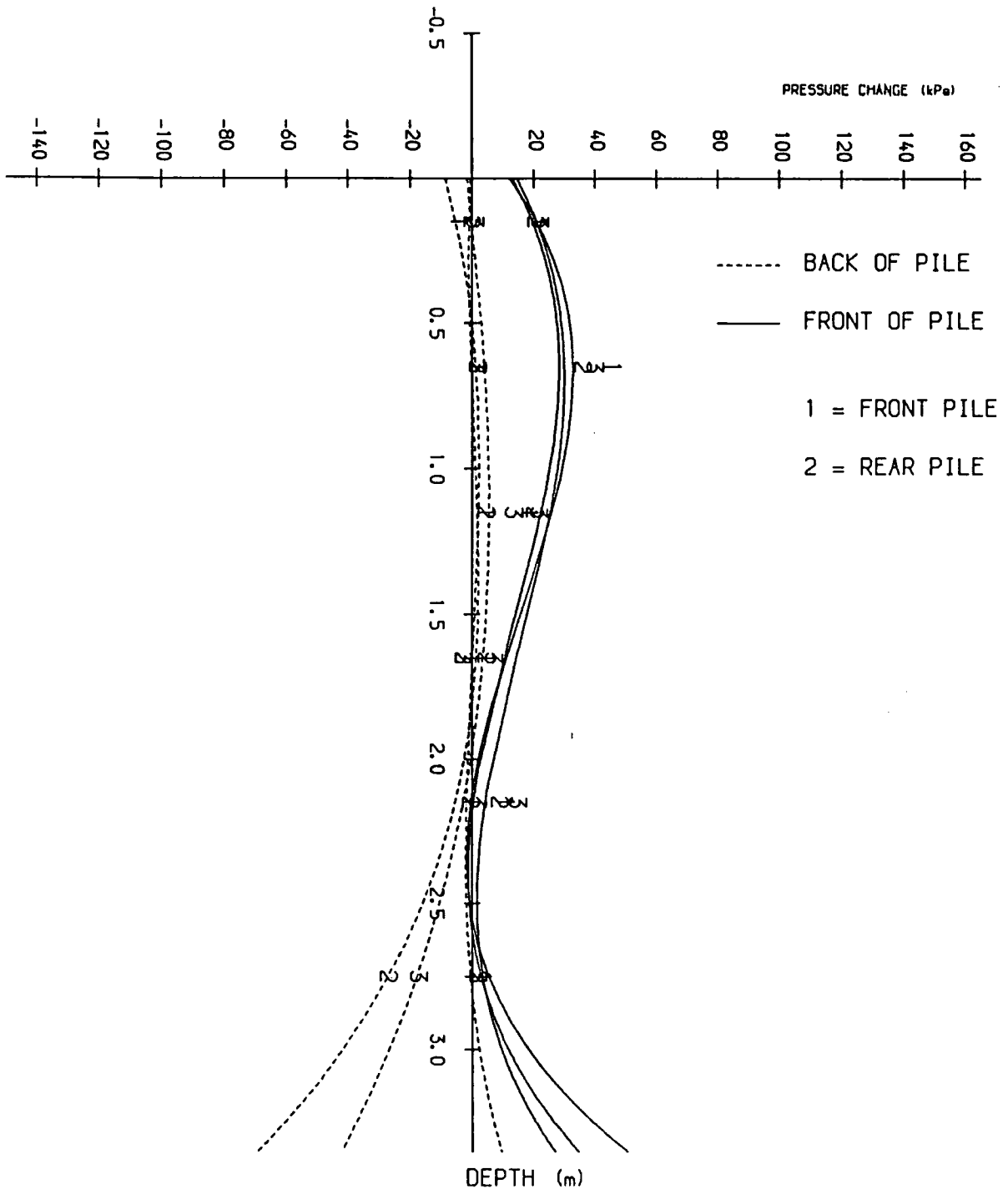Figure 4.4 A typical axial force diagram.
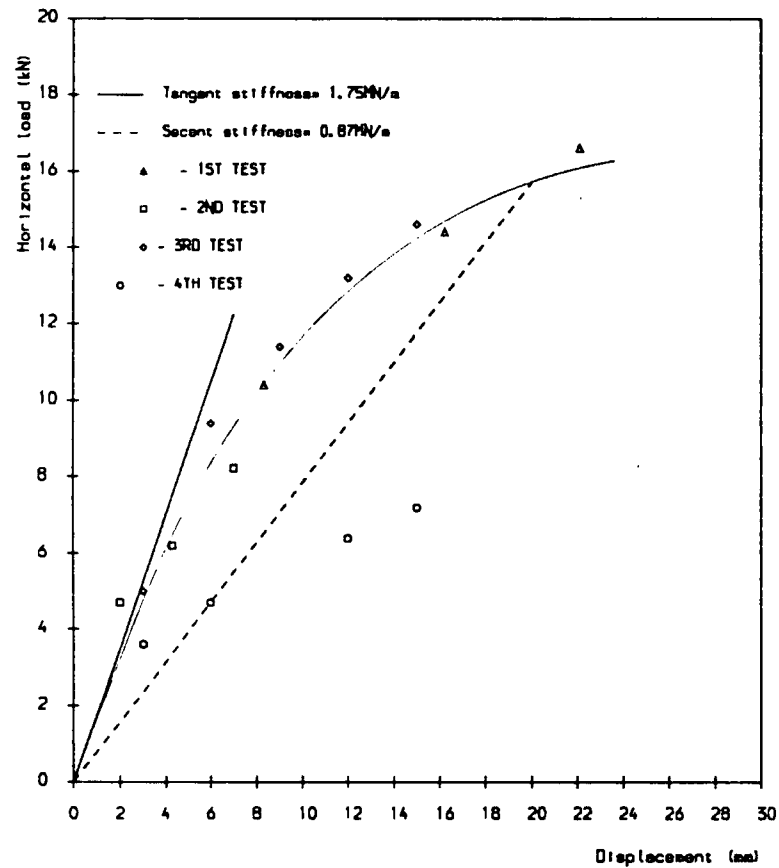
Figure 4.5 A typical lateral soil pressure change.

Figure 4.6 Average load/deflection curve for single pile tests.
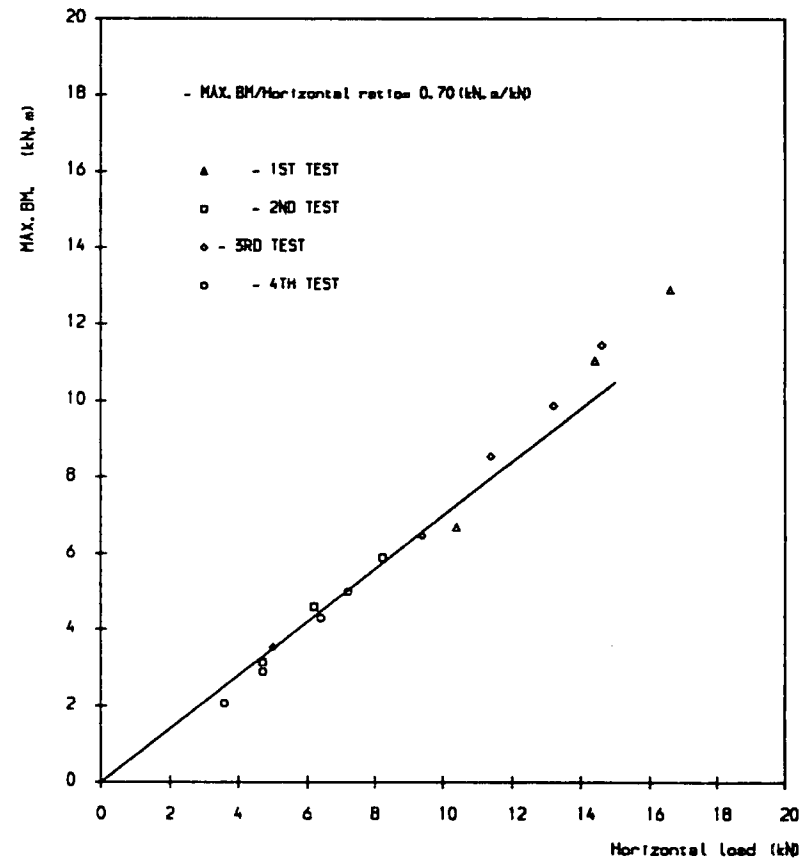
Figure 4.7 Maximum bending moment against horizontal load for single pile tests.

150
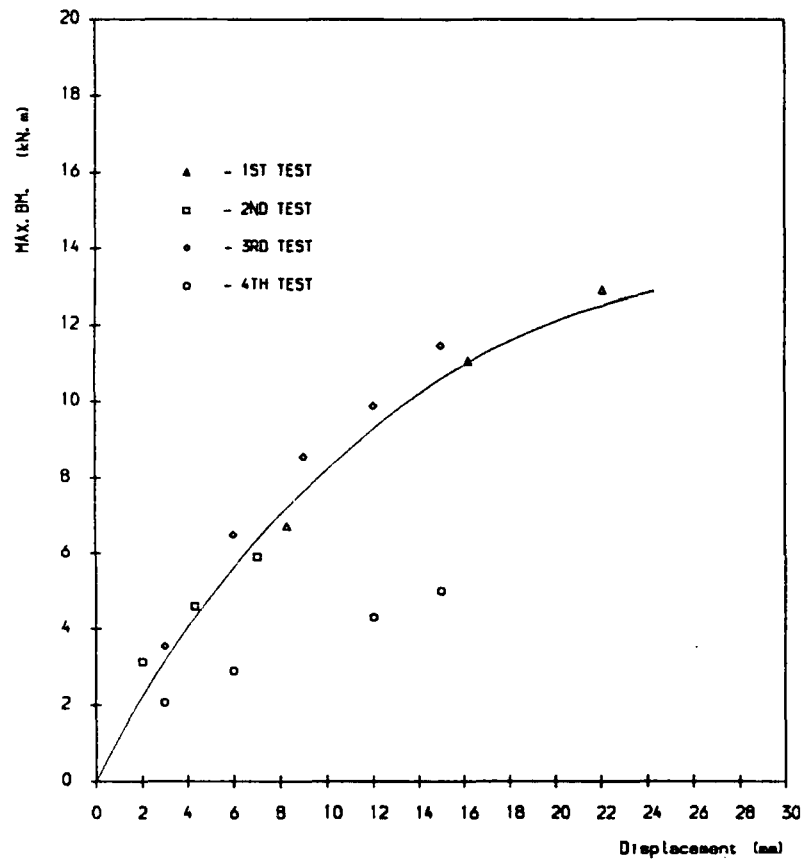
Figure 4.8 Maximum bending moment against pile
head displacement of the single pile tests.
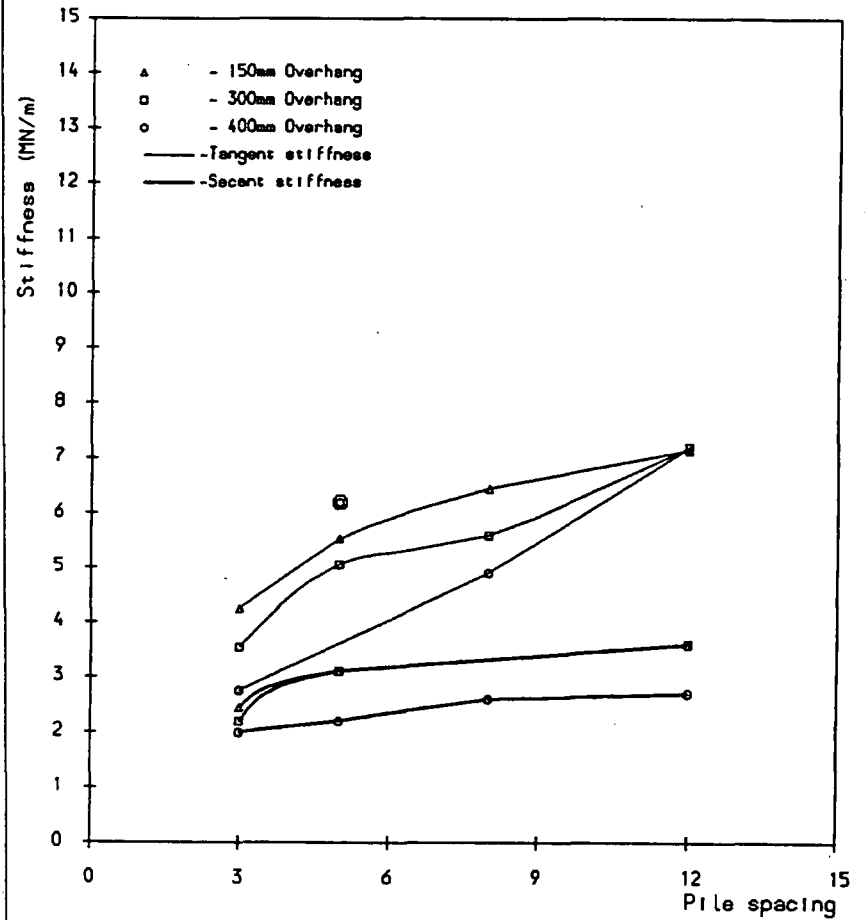
Figure 4.9 Tangent stiffness of two-pile groups
against pile spacing.
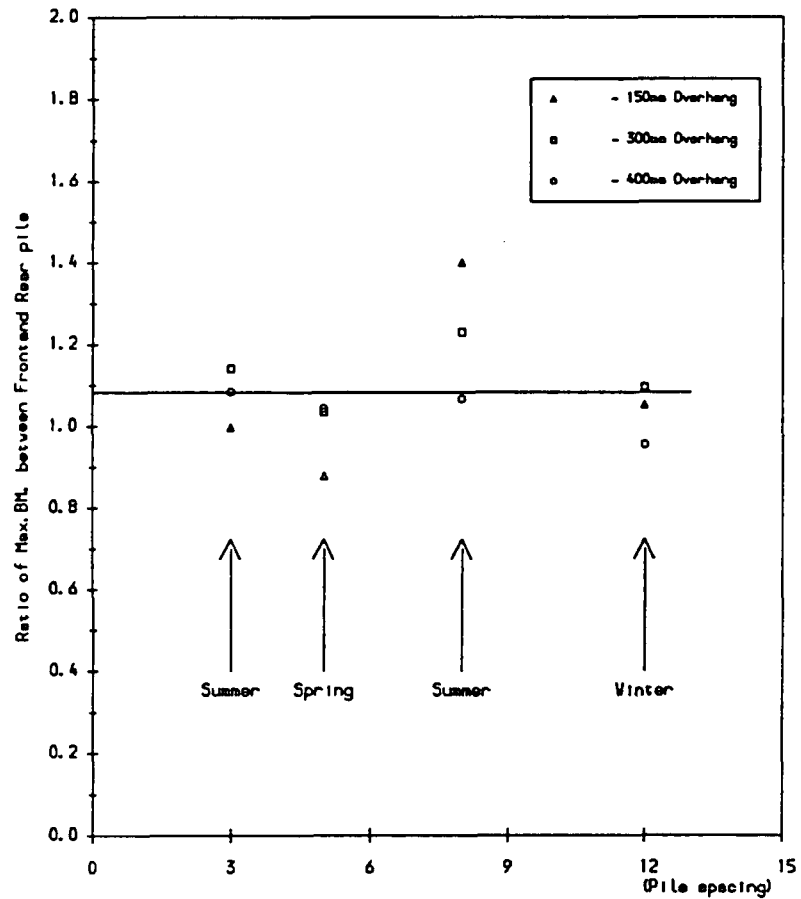
Figure 4.10 Ratio of maximum bending moment between front and rear pile for 20mm pile cap deflection against pile spacing.
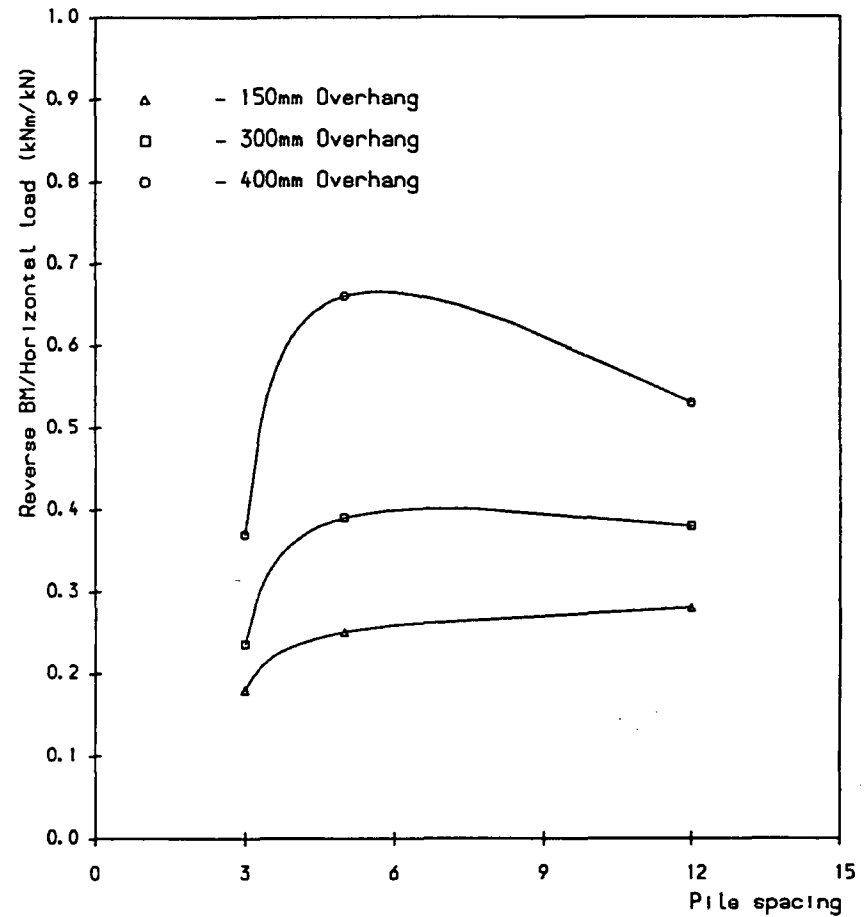
Figure 4.11a Reverse bending moment/horizontal cyclic load ratio against pile spacing.
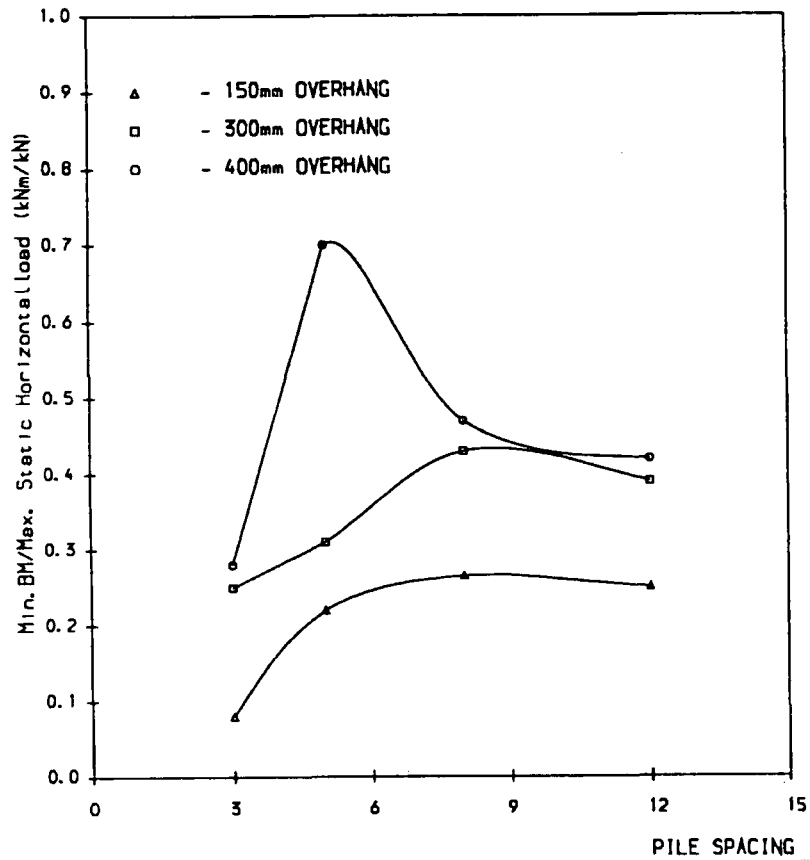
Figure 4.11b Reverse bending moment/horizontal load for final stage of first cyclic loading against pile spacing.
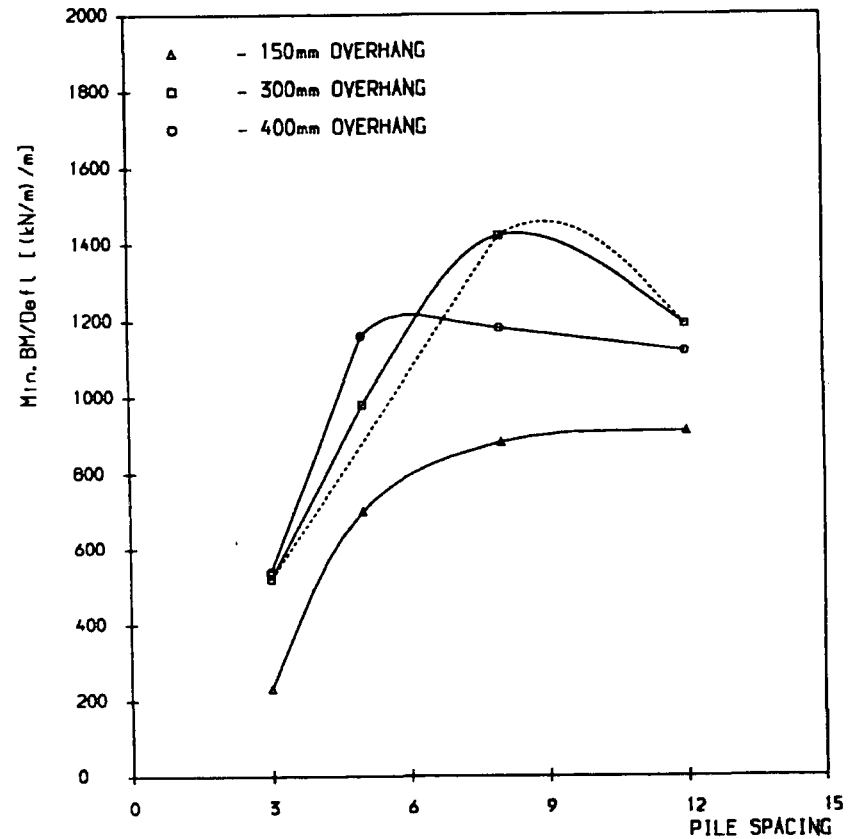
Figure 4.11c Reverse bending moment/final stage of pile cap deflection against pile spacing.
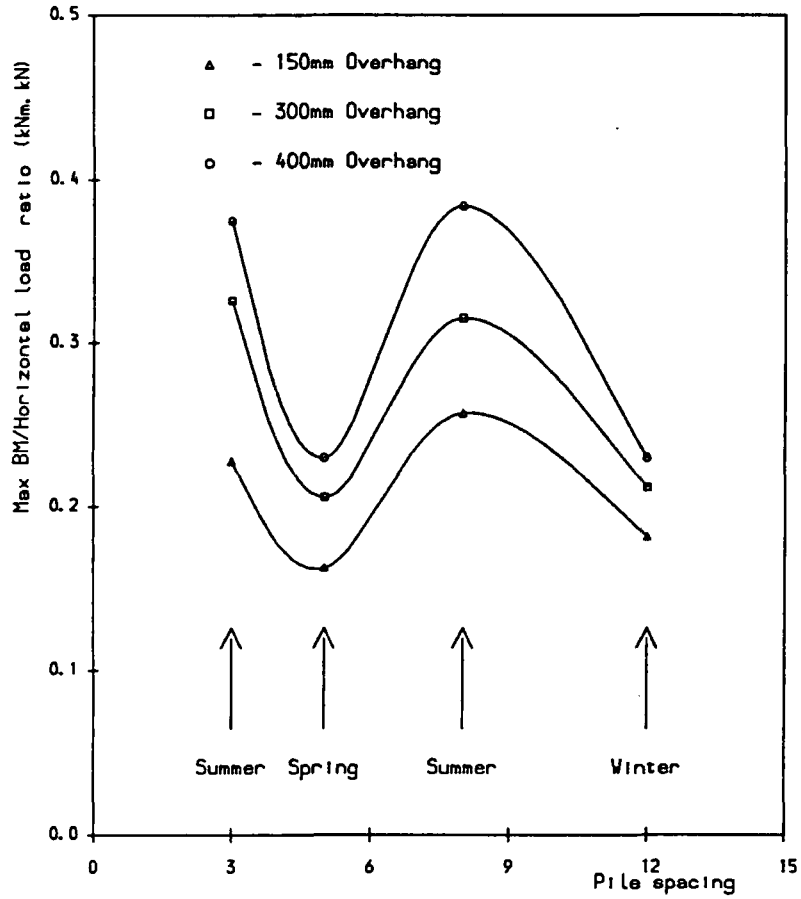
Figure 4.12 Plot of maximum bending moment/horizontal
load ratio against pile spacing.

Figure 4.13 Plot of peak axial force per unit load against
pile spacing.

Figure 4.14 Variation of sand unit weight during tests and pile spacing.

Table T4.1 Single pile general information			
Test No.	Date	Density $kN.m^{-3}$	Water-level m
1	20/7/87	18.7	.48
2	27/7/87	18.2	.50
3	7/8/87	18.9	.52
4	17/8/87	17.1	.20

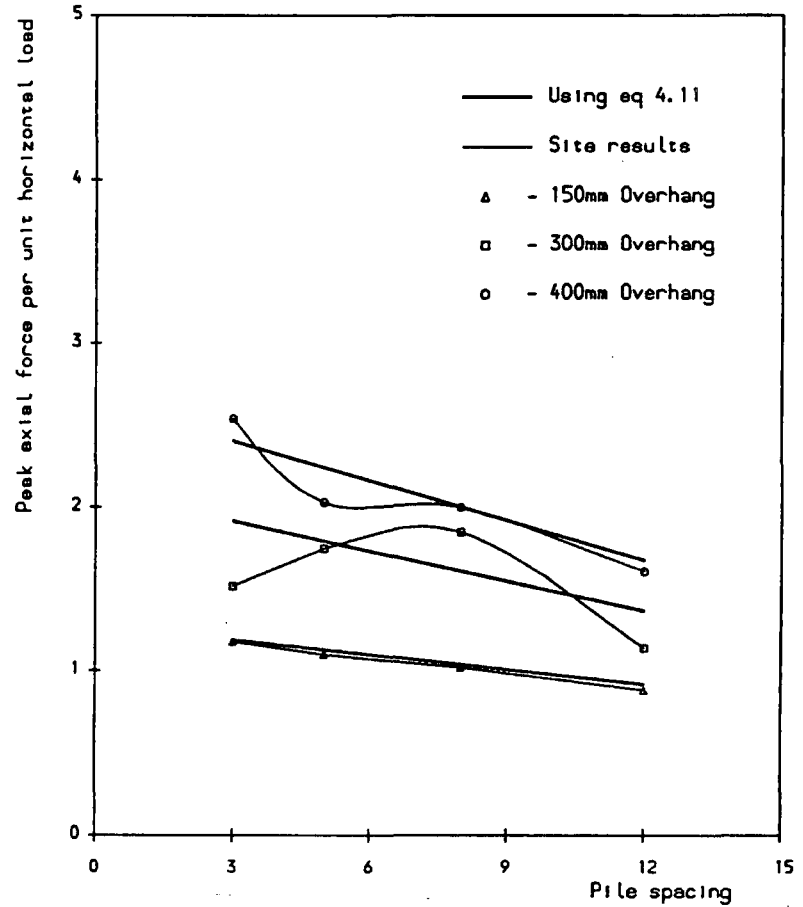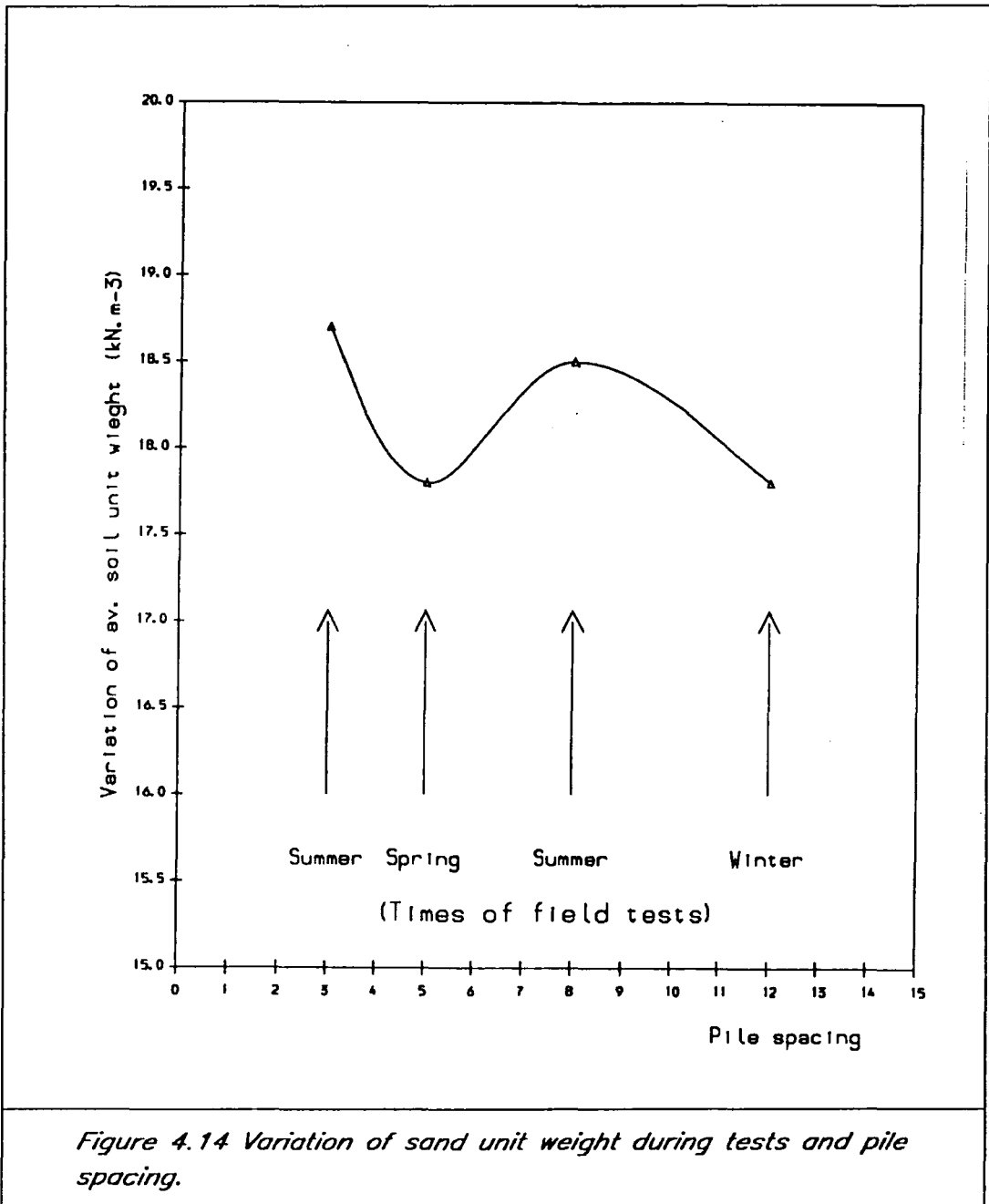| Test No.	Overhang mm	Pile width spacing	Date	Unit weight kN.m^{-3}	Water-level
			Table T4.2 General information on two-pile group tests		
1	150	3	9/2/88	18.7	.48
2	150	3	12/2/88	18.6	.50
1	300	3	19/2/88	18.6	.52
2	300	3	4/3/88	18.8	.50
1	400	3	8/3/88	18.7	.48
2	400	3	10/3/88	18.7	.50
3	400	3	18/3/88	18.5	.50
4	400	3	13/4/88	-	.40
5	400	3	14/5/88	-	.45
1	150	5	15/8/88	18.2	.48
2	150	5	24/8/88	17.9	.50
3	150	5	26/8/88	18.0	.52
4	150	5	13/10/88	17.8	.30
5	150	5	14/10/88	17.7	.35
1	300	5	7/9/88	18.0	.50
2	300	5	12/9/88	17.9	.48
1	400	5	23/9/88	17.5	.50
2	400	5	30/9/88	17.3	.50
3	400	5	2/10/88	-	.50
4	400	5	3/10/88	-	.50
1	150	8	18/3/89	18.7	2.10
2	150	8	31/3/89	18.5	2.10
3	150	8	17/4/89	18.6	2.10
1	300	8	27/4/89	18.1	2.10
2	300	8	5/5/89	18.2	2.10
1	400	8	11/5/89	18.6	2.10
2	400	8	23/5/89	18.6	2.10
3	400	8	30/5/89	18.7	2.10
4	400	8	31/5/89	18.8	2.10
4	400	8	3/6/89	-	2.10
1	150	12	7/8/89	17.6	2.10
2	150	12	15/8/89	18.6	2.10
1	300	12	21/8/89	18.1	2.10
2	300	12	27/8/89	17.6	2.10
1	400	12	1/9/89	17.4	2.10
2	400	12	6/9/89	17.6	2.10
2	400	12	12/9/89	-	2.10
2	400	12	14/9/89	-	2.10

Test No	Stage One			Stage Two			Stage Three			Stage Four			Stage Five			Stage Six Cyclic Loading		
	Load kN	Defl mm	Max.BM kN.m	Load kN	Defl mm	Max.BM kN.m	Load kN	Defl mm	Max.BM kN.m	Load kN	Defl mm	Max.BM kN.m	Load kN	Defl mm	Max.BM kN.m	Load kN	Defl mm	Max.BM kN.m
1	10.40	8.30	6.74	14.40	16.22	11.05	16.60	22.10	12.9									
2	4.70	2.00	3.14	6.22	4.30	4.60	8.22	7.00	5.90									
3	5.00	3.00	3.54	9.40	6.00	6.48	11.40	9.00	8.55	13.20	12.00	9.88	14.60	15.00	11.46	15.40	20.0	12.30
4	3.60	3.00	2.07	4.70	6.00	2.90	6.40	12.00	4.30	7.20	15.00	5.00				3.40	22.00	6.45

Table T4.3 Summary of the single pile test results

Table T4.4 Summary of the three pile width spacing test results

Description		Stage 1					Stage 2					Stage 3					Stage 4				
Test No.	Over-hang	H	Defl.	Max.BM.		Ratio	H	Defl.	Max.BM.		Ratio	H	Defl.	Max.BM.		Ratio	H	Defl.	Max.BM.		Ratio
	mm	kN	mm	Front	Rear	F/R	kN	mm	Front	Rear	F/R	kN	mm	Front	Rear	F/R	kN	mm	Front	Rear	F/R
1	150	23.8	8.95	9.2	7.1	1.30	36.8	14.76	11.0	10.0	1.10	39.4	17.70	12.3	11.9	1.03					
2	150	16.1	4.10	4.62	4.70	0.98	26.4	7.90	7.60	7.20	1.06	41.1	12.70	10.00	13.00	0.77	49.2	18.5	15.60	16.40	0.95
1	300	14.5	4.79	4.0	4.6	0.87	24.5	9.66	8.0	8.6	0.93	35.7	16.50	16.0	14.2	1.13	45.4	22.14	20.1	17.4	1.15
2	300	12.4	4.00	5.95	2.62	2.27	21.2	8.00	9.63	5.50	1.75	29.4	12.00	10.20	8.12	1.26	37.3	16.00	13.20	10.70	1.23
1	400	10.6	4.00	3.3	2.9	1.14	16.5	8.00	5.5	5.3	1.04	22.0	12.00	7.9	7.7	1.03	28.2	16.00	10.3	10.3	1.00
2	400	12.4	4.00	2.8	3.1	0.90	21.6	8.00	4.9	4.9	1.00	31.3	12.00	7.8	7.4	1.05	35.2	14.70	10.0	8.9	1.12
3	400	11.0	4.00	3.80	3.00	1.27	20.0	8.00	7.03	5.60	1.25	29.4	12.00	10.00	8.60	1.16	37.9	16.00	13.00	11.50	1.13

Summary of the three diameter test results (Contd.)

Description		Stage 5					Stage 6					Stage 7					Remarks
Test No	Over-hang	H	Defl.	Max.BM.		Ratio	H	Defl.	Max.BM.		Ratio	H	Defl.	Max.BM.		Ratio	
	mm	kN	mm	Front	Rear	F/R	kN	mm	Front	Rear	F/R	kN	mm	Front	Rear	F/R	
1	150											29.3	18.37	11.5	11.1	1.04	
2	150											29.8	18.50	13.2	14.2	0.93	
1	300											33.2	22.00	15.7	15.6	1.00	
2	300	46.9	22.00	16.2	13.4	1.21						35.0	22.00	14.4	12.6	1.14	
1	400	37.7	22.0	14.7	14.3	1.03						31.4	22.00	13.7	13.0	1.05	
2	400											31.7	15.00	10.0	8.7	1.15	
3	400	46.3	22.00	17.1	15.4	1.11						36.3	22.00	14.6	13.4	1.09	

Table T4.5 Summary of the five pile width spacing test results

Test No.	Over-hang mm	Stage 1 H kN	Defl. mm	Max.BM. Front	Rear	Ratio F/R	Stage 2 H kN	Defl. mm	Max.BM. Front	Rear	Ratio F/R	Stage 3 H kN	Defl. mm	Max.BM. Front	Rear	Ratio F/R	Stage 4 H kN	Defl. mm	Max.BM. Front	Rear	Ratio F/R
1	150	23.5	3.15	3.6	3.4	1.06	34.1	6.30	5.65	5.7	0.99	39.0	8.70	7.5	7.1	1.05	45.7	11.60	8.5	8.7	0.98
2	150	15.6	3.07	2.30	2.80	0.82	24.2	6.00	3.95	4.70	0.84	34.1	8.93	5.60	7.00	0.80	44.7	11.86	7.30	8.90	0.82
3	150	7.6	3.20	2.20	2.10	1.05	13.6	6.20	3.90	4.00	0.98	19.0	9.20	5.20	6.00	0.87	25.7	12.10	6.90	8.00	0.86
4	150	16.1	3.00	2.75	2.82	0.98	23.1	6.00	4.80	4.80	1.00	31.5	8.00	6.60	7.00	0.94	38.3	12.00	8.80	9.20	0.96
5	150	15.8	3.00	2.86	2.86	1.00	26.0	6.00	4.90	4.85	1.01	35.4	9.00	7.20	7.00	1.03	43.5	12.00	9.50	9.10	1.04
1	300	17.3	3.00	2.77	2.65	1.04	25.0	6.00	4.51	4.51	1.00	31.6	9.00	6.00	6.10	0.98	38.5	12.00	8.20	8.30	0.99
2	300	18.0	3.84	2.20	2.40	0.92	23.2	5.72	4.00	4.00	1.00	32.9	9.08	5.60	5.40	1.04	42.5	12.00	7.00	7.20	0.97
1	400	19.2	4.08	3.04	3.02	1.01	22.2	6.93	4.60	4.50	1.02	28.7	13.74	6.40	6.30	1.02	32.9	17.27	10.30	10.60	0.97
2	400	17.1	3.80	3.0	2.8	1.07	23.2	6.80	4.5	4.4	1.02	26.4	12.00	7.5	7.3	1.06	30.6	15.00	9.5	9.1	1.04

Summary of the five diameter test results (Contd.)

Test No	Over-hang mm	Stage 5 H kN	Defl. mm	Max.BM. Front	Rear	Ratio F/R	Stage 6 H kN	Defl. mm	Max.BM. Front	Rear	Ratio F/R	Stage 7 H kN	Defl. mm	Max.BM. Front	Rear	Ratio F/R	Remarks
1	150	52.25	14.40	11.3	11.1	1.02	58.6	19.10	13.3	13.3	1.00	44.85	18.90	12.6	11.5	1.10	
2	150	53.4	14.80	9.5	11.3	0.84	64.0	18.50	13.2	14.4	0.92	47.5	18.50	10.7	12.2	0.88	
3	150	33.8	15.00	9.4	9.9	0.95	45.0	20.00	12.9	13.1	0.98	38.0	20.00	11.2	12.0	0.93	
4	150	45.53	15.00	10.7	11.4	0.94	56.5	20.00	13.9	14.4	0.96	59.5	20.00	13.0	13.7	0.95	
5	150	53.3	15.00	11.8	11.4	1.04	65.1	20.00	15.4	15.0	1.03	53.8	20.00	13.6	14.0	0.97	
1	300	45.9	15.00	10.0	10.0	1.00	58.5	20.00	12.4	12.5	0.99	49.8	20.00	12.0	11.8	1.02	
2	300	52.4	15.00	9.40	8.9	1.06	66.7	20.00	13.00	11.6	1.12	50.0	20.00	10.30	10.3	1.00	
1	400	34.0	20.67	12.5	12.0	1.04	40.3	26.80	16.6	15.5	1.07	31.2	26.80	15.5	15.0	1.03	
2	400	37.1	20.00	13.3	12.10	1.10						30.1	20.00	13.4	12.30	1.09	

Table T4.6 Summary of the eight pile width spacing test results

Description		Stage 1					Stage 2					Stage 3					Stage 4				
Test No.	Over-hang mm	H kN	Defl. mm	Max.BM. Front	Rear	Ratio F/R	H kN	Defl. mm	Max.BM. Front	Rear	Ratio F/R	H kN	Defl. mm	Max.BM. Front	Rear	Ratio F/R	H kN	Defl. mm	Max.BM. Front	Rear	Ratio F/R
1	150	16.9	3.00	4.34	2.70	1.60	24.6	6.00	7.30	4.70	1.55	33.2	9.00	10.40	7.10	1.46	43.7	12.00	12.90	9.30	1.39
2	150	14.0	3.00	3.54	3.00	1.18	24.5	6.00	6.80	5.30	1.28	31.5	9.00	11.10	8.60	1.29	38.2	12.00	13.90	11.10	1.25
3	150	18.8	3.00	5.40	4.20	1.28	28.2	6.00	10.70	8.20	1.30	37.0	9.00	15.10	11.30	1.33	41.8	12.00	19.60	15.10	1.30
1	300	16.6	3.00	3.88	3.40	1.14	24.3	6.00	8.40	7.10	1.18	31.2	9.00	10.00	8.50	1.17	38.9	12.00	13.30	11.30	1.18
2	300	13.4	3.00	4.00	3.70	1.08	21.0	6.00	7.00	6.00	1.17	29.4	9.00	9.00	8.00	1.13	39.9	12.00	11.60	9.80	1.18
1	400	19.1	3.00	4.20	5.20	0.81	28.6	6.00	7.20	9.10	0.79	36.0	9.00	11.40	13.40	0.85					
2	400	12.2	3.00	3.20	3.00	1.06	17.0	6.00	6.40	6.30	1.02	20.8	9.00	8.70	7.90	1.10	28.5	12.00	11.00	10.20	1.08
3	400	13.0	3.00	2.95	3.30	0.89	19.3	6.00	5.20	6.30	0.82	24.4	9.00	8.10	8.80	0.92	27.7	12.00	10.70	10.80	0.99
4	400	21.0	3.00	6.00	5.60	1.07	29.8	6.00	7.90	7.70	1.03	37.7	9.00	11.30	10.80	1.05	45.7	12.00	16.40	16.60	0.99

Summary of the eight diameter test results (Contd.)

Description		Stage 5					Stage 6					Stage 7					Remarks
Test No	Over-hang mm	H kN	Defl. mm	Max.BM. Front	Rear	Ratio F/R	H kN	Defl. mm	Max.BM. Front	Rear	Ratio F/R	H kN	Defl. mm	Max.BM. Front	Rear	Ratio F/R	
1	150																
2	150																
3	150																
1	300																
2	300																
1	400																
2	400																
3	400																
4	400																

Table T4.7 Summary of the twelve pile width spacing test results

Test No.	Over-hang mm	Stage 1 H kN	Defl. mm	Max.BM. Front	Max.BM. Rear	Ratio F/R	Stage 2 H kN	Defl. mm	Max.BM. Front	Max.BM. Rear	Ratio F/R	Stage 3 H kN	Defl. mm	Max.BM. Front	Max.BM. Rear	Ratio F/R	Stage 4 H kN	Defl. mm	Max.BM. Front	Max.BM. Rear	Ratio F/R
1	150	17.6	3.00	3.11	3.50	0.89	25.6	6.00	5.90	6.10	0.97	33.2	9.00	8.50	9.30	0.91	39.7	12.00	11.60	11.50	1.01
2	150	26.1	3.00	2.94	3.90	0.76	34.5	6.00	5.00	6.60	0.84	38.0	9.00	7.60	8.30	0.92	50.4	12.00	11.50	12.00	0.96
1	300	14.0	3.00	2.90	2.85	1.02	25.8	6.00	4.60	4.30	1.07	28.7	9.00	7.00	6.60	1.06	37.7	12.00	10.20	9.50	1.07
2	300	24.5	3.00	2.90	2.80	1.05	28.4	6.00	4.60	4.60	1.00	36.7	9.00	7.60	7.00	1.09	45.6	12.00	10.40	9.60	1.08
1	400	15.8	3.00	2.90	2.30	1.03	19.4	6.00	4.50	4.00	1.13	33.6	9.00	6.70	6.50	1.04	42.4	12.00	8.60	9.20	0.93
2	400	26.7	3.00	2.20	3.10	0.71	30.5	6.00	4.60	5.90	0.78	36.7	9.00	6.00	7.40	0.81	44.5	12.00	8.10	9.90	0.82

Summary of the twelve diameter test results (Contd.)

Test No	Over-hang mm	Stage 5 H kN	Defl. mm	Max.BM. Front	Max.BM. Rear	Ratio F/R	Stage 6 H kN	Defl. mm	Max.BM. Front	Max.BM. Rear	Ratio F/R	Stage 7 H kN	Defl. mm	Max.BM. Front	Max.BM. Rear	Ratio F/R	Remarks
1	150	57.0	15.00	14.40	14.10	1.02	72.0	20.00	18.10	18.30	0.99	60.9	20.00	17.30	16.80	1.03	
2	150	56.1	15.00	14.60	14.50	1.01	71.4	20.00	21.00	19.00	1.10	60.2	20.00	18.80	17.60	1.07	
1	300	55.9	15.00	13.00	12.10	1.07	62.1	20.00	18.10	16.80	1.08	59.0	20.00	17.30	16.00	1.08	
2	300	55.0	15.00	13.50	12.20	1.11	69.3	20.00	19.50	17.00	1.15	63.5	20.00	18.70	16.00	1.17	
1	400	42.4	15.00	10.80	11.50	0.94	51.8	20.00	15.60	14.10	1.11	49.9	20.00	15.70	14.60	1.08	
2	400	48.3	15.00	10.80	12.50	0.86	54.6	20.00	15.40	17.30	0.89	48.0	20.00	14.30	16.90	0.84	

Table T4.8 Summary of stiffnesses calculated from two-pile group field tests series																	
Description		3 Pile Width				5 Pile Width				8 Pile Width				12 Pile Width			
Test No.	Over-hang	Stiffness (MN/m)				Stiffness (MN/m)				Stiffness (MN/m)				Stiffness (MN/m)			
	mm	Tan.	Av.	Sec.	Av.	Tan.	Av.	Sec.	Av.	Tan.	Av.	Sec.	Av.	Tan.	Av.	Sec.	Av.
1	150	4.2		2.2		7.3*		3.2		6.5		2.9		6.00		3.60	
2	150	4.3	4.25	2.7	2.45	5.5		3.0		4.8 *	6.45	2.7 *	2.9 **	8.3	7.15	3.6	3.6
3	150					2.5*	5.53	2.8	3.1	6.4		2.75 *					
4	150					6.1		2.9									
5	150					5.0		3.1									
1	300	3.2		2.2		5.6		2.9		7.3 *		2.75*		4.85		3.1	
2	300	3.9	3.55	2.2	2.2	4.5	5.05	3.25*	2.9	5.6	5.6	2.8*	2.8**	9.7	7.20	3.5	3.3
1	400	2.7		1.8		6.2*		2.2		8.1*		2.6		5.0		2.65	
2	400	3.5*	2.75	2.1	2.0	6.2*	6.2**	2.25	2.2	7.7*		1.9*		9.4	7.20	2.70	2.7
3	400	2.8		2.0						4.9	4.9	1.8*	2.6				
4	400									7.9*		2.6					

* : Not good data
** : data ignored
tangent (Tan.)
average (Av.)
Secant (Sec.)

Table T4.9 Summary of average maximum bending moment horizontal load ratio for two-pile groups				
Overhang (mm)	3 Pile width spacing	5 Pile width spacing	3 Pile width spacing	12 Pile width spacing
150	0.288	0.163	0.257	0.182
300	0.326	0.206	0.315	0.212
400	0.375	0.230	0.384	0.230

Table T4.10 Summary of average peak axial force per unit horizontal load for two-pile groups				
Overhang (mm)	3 Pile width spacing	5 Pile width spacing	3 Pile width spacing	12 Pile width spacing
150	1.18	1.10	1.02	0.88
300	1.52	1.75	1.85	1.44
400	2.54	2.03	2.00	1.61

CHAPTER FIVE

Back Analysis of The Single Pile Field test and Predicted Analysis of Single Pile and Two-Pile Groups

5.1-Introduction

There has been a trend in analyses of piles under axial and lateral loading away from a combination of empirical and experimental towards the theoretical. This has occurred because of a search for greater economy in piling design in the construction industry. It has forced researchers to develop theoretical analyses which may help to reduce the cost of deep foundations.

In this chapter results from the lateral load tests on single piles (free head) will be used in back analyses by theoretical solutions to obtain values for the rate of increase in soil modulus with depth (n_h). Because fixed head single pile tests were not feasible the n_h values obtained from free head single pile tests will be used to predict the behaviour of fixed headed piles, although there may be a difference between the n_h values for fixed and free head piles owing to the different deflection profile involved. The n_h values obtained from back analysis of the single pile tests will be used to predict the behaviour of two-pile groups. In predicting the behaviour of two-pile groups the pile head condition is assumed to be fixed. It was found that assuming a fixed pile head over-estimated the lateral stiffness of the two-pile group, as it was found from the field tests that the cap fixity is neither truly fixed or free. However

a comparison between the field tests and various analytical predictions using the n_h values obtained as above is presented.

Some of the methods available for analysis of laterally loaded single piles and pile groups discussed in Chapter Two are used to back analyse the results obtained from the single pile field tests series and predict the behaviour of two-pile group based on the values of n_h obtained from the back analysis of the single pile. The analysis is based at first on linear elastic theory and then on elastic-plastic soil properties.

For all the different types of analysis, it is assumed that the soil modulus increases linearly with depth. To obtain the rate of increase in soil modulus, the behaviour of a single free head pile case was back analysed. The obtained modulus profile is then used to predict the maximum bending moment in the pile shaft of a free headed pile and the lateral stiffness of a fixed headed pile.

The elastic-plastic analyses of a single free head pile is then undertaken, incorporating yielding of the soil, using p/u curves and also using yielding factors by Poulos(1973) and by Budhu and Davies(1988).

The elastic analysis of two-pile groups is undertaken using methods by Poulos(1975), and by Randolph(1981). The elastic-plastic analysis of two-pile groups is based on the yielding factor method by Poulos(1975 and 1979).

5.2-Elastic Back Analysis of a Single Pile.

In order to assess the accuracy of the available methods of analysis of a single vertical pile under horizontal loading two main functions had to be considered. These were the lateral stiffness of the pile and the maximum bending moment occurring in the pile shaft due to the horizontal load applied to the pile head.

In the field test the single pile was installed in the 2.1m deep sand trench, and penetrating into the clay beneath. The hollow square pile was $154mm \times 154mm$ and the embedded length was 3.35m. It would be reasonable to assume that the soil

modulus increased linearly with depth, as the maximum bending moment occurred within the sand layer and the lateral behaviour of pile was governed by the soil near the ground surface.

Throughout the single pile tests the deflection of the pile head was measured at 70mm and 400mm above the surface of the sand trench. Most of the available methods used here predict the pile head deflection and pile head rotation at the ground line. As the deflection was measured above the ground line, the additional deflection caused by rotation was added to the ground line deflection, ignoring curvature in the free standing portion of the pile.

5.2.1- Reese and Matlock(1964) Method

In order to obtain the rate of increase of soil modulus with depth, equations 2.55 and 2.56 were combined to predicted the lateral deflection of the pile 70mm above the ground line.

$$U_e = \frac{A_y H T^3}{E_p I_p} + \frac{B_y M T^2}{E_p I_p} + 70 \times 10^{-3} [\frac{A_s H T^2}{E_p I_p} + \frac{B_s M T}{E_p I_p}] \qquad (5.1)$$

where

U_e is the Elastic pile head deflection

A and B are coefficients relating to lateral force and moment loading, respectively

T is the characteristic length for nonhomogeneous soil

$E_p I_p$ is the flexural stiffness of pile

H and M are lateral force and moment loading.

Values of A_y, A_s, B_y and B_s at the ground line were obtained from Elson(1985) and they are 2.44, -1.62, 1.62 and -1.75 respectively for a stiffness factor (T) of 1.0.

The head deflection and shaft moment due to a horizontal load applied to the pile head were measured throughout four single pile tests. Equation 5.1 is a cubic equation in terms of T which was solved using Newton's method. Each successive

approximation was obtained by subtracting the value of the equation using the previous results for T divided by the value of the gradient, from the previous value of T.

$$T' = T - \frac{f(T)}{f'(T)} \tag{5.2}$$

Having obtained values for the T factor by back analysis equation 2.27 is rearranged to obtain the rate of increase of soil modulus (n_h) , as

$$n_h = (\frac{EI}{T^5}) \tag{5.3}$$

Curves for n_h versus deflection for four single pile tests are shown in Figure 5.1. The n_h values obtained from tests number 1 2 and 3 gave close agreement but, test number 4 gave lower value. A value of $3000kN.m^{-3}$ for n_h is derived for linear elastic analysis. Using equation 5.1 the elastic stiffness of a single free head pile is calculated to be $1.75MN.m^{-1}$ (see figure 4.6), with a maximum pile moment to head load ratio of 0.7kN.m/kN (see figure 4.7). Using this value of n_h would give the elastic stiffness of a fixed headed single pile as $3.07MN.m^{-1}$.

5.2.2- Poulos(1971) Method

The initial nearly linear portion of measured deflection/load curve for the first three tests was approximately $1.75MN.m^{-1}$ (see figure 4.6). As the deflection was measured 70mm above the ground line the theoretical expression should include the deflection due to head rotation as well as the ground line deflection. As previously, it is assumed that the soil modulus increases linearly with depth, and ignoring bending curvature of the free standing part of the pile, then the deflection at 70mm above the ground is given by (see equation 2.81 and 2.82)

$$U_e = \frac{H}{n_h L^2}(I'_{UH} + \frac{e}{L}I'_{UM}) + 70 \times 10^{-3}[\frac{H}{n_h L^3}(I'_{\theta H} + \frac{e}{L}I'_{\theta M})] \tag{5.4}$$

Therefore;

$$U_e = \frac{H}{n_h L^2}I'_{Ua} \tag{5.5}$$

where

$$I'_{Ua} = (I'_{UH} + \frac{e}{L}I'_{UM}) + \frac{70 \times 10^{-3}}{L}(I'_{\theta H} + \frac{e}{L}I'_{\theta M}) \qquad (5.6)$$

Substituting $\frac{U}{H}$,e and L from field test results gives

$$n_h = 155.9 I'_{Ua} \qquad (5.7)$$

the components of influence factor I'_{Ua}, I'_{UH}, I'_{UM}, $I'_{\theta H}$ and $I'_{\theta M}$ are functions of flexibility factor KN and are tabulated in Poulos(1975). Using the calculated value of I'_{Ua}, n_h may be calculated using equation 5.7. The results shown in table T5.1.

Another relationship between n_h and KN is obtained using equation 2.76.

$$n_h = \frac{EI}{KNL^5} \qquad (5.8)$$

Substitution of appropriate values for the pile gives;

$$n_h = \frac{6.92}{KN} \qquad (5.9)$$

Therefore, for different incremental values of KN two independent values of n_h can be computed using equations 5.7 and 5.9. If these values are then plotted on the same axis, as in Figure 5.2 the intersection gives the required value of KN and n_h to be 5.5×10^{-4} and $13 MN.m^{-3}$ respectively.

Using the obtained values of KN and n_h the influence factor for a fixed head pile I_{UF} in the sand is found to be 22.0. Substituting the obtained value into equation 2.83, the elastic stiffness of the fixed headed pile for 20.0mm pile head deflection is found to be $6.08 MN.m^{-1}$.

$$U_{ef} = \frac{H.I'_{UF}}{n_h L^2} \qquad (2.83.bis)$$

Therefore;

$$\frac{H}{U_{ef}} = \frac{n_h L^2}{I'_{UF}} = \frac{13.0 \times 3.35^2}{22.0} = 6.08 MN.m^{-1}$$

5.2.3- Randolph(1981) Method

The application of the theory by Randolph for a free headed single pile is as follows. Using equation 2.86 and 2.87 for back analysis, the first step in using the Randolph solution is to obtain the effective elastic modulus which would represent the pile as a solid circular pile with radius r=0.077m.

$$E_{ef} = \frac{E_p I_p}{\frac{\pi r^4}{4}} = 1.06 \times 10^8 \qquad (2.90.bis)$$

Using the initial portion of the measured load/deflection curves and substituting the appropriate values in equations 2.86 and 2.87 gives the soil stiffness m^* proportional with depth as $3.14 MN.m^{-1}$. Assuming that the Poisson's ratio v is 0.3 rearranging equation 2.92, The rate of increase of soil shear modulus m was found to be

$$m = \frac{m^*}{1 + \frac{3v}{4}} = 2.56 MN.m^{-3} \qquad (5.10)$$

It should be noted that, Randolph characterized the performance of a pile by shear modulus m and Poisson's ratio v.

5.2.4- Other Methods

Various other solutions were used for back analysis. A summary of these solutions is shown in table T5.2. In this table the values of n_h, pile head stiffness for free and fixed headed piles and ratio of maximum bending moment to the horizontal load are shown. Comparisons between the site test results obtained and the analytical solutions are discussed in chapter seven.

5.3.-Non Linear Analysis of Single Piles

The relationship between horizontal load and pile head deflection is nonlinear in practice. Several techniques have been developed to account for this non-linearity, and for a soil modulus varying linearly with depth, including those by Poulos(1971), Reese(1974) and Budhu and Davies(1987). Reese's solution is based on p/u curves while Poulos and Budhu and Davies introduced a yielding factor into their elastic

analyses to account for yielding of the soil. These three different analytical solutions are now used to analyse the non-linear behaviour of a horizontally loaded single, free headed pile.

5.3.1- Reese (p/u) Method

In order to construct a series of p/u curves for the pile shaft the unit weight of soil was measured ($18kNm^{-3}$) and the angle of friction was measured in triaxial tests ($36.5°$). The appropriate coefficient of earth pressure at rest (K_o) is assumed to be 0.5 for granular soil. The following solutions are based on an analysis of wedge type failure of soil (see Reese 1971).

The ultimate resistance near the ground surface was calculated using;

$$P_{un} = \gamma x[b\,(K_p - K_a) + x\sin\beta[K_p\tan\alpha + K_o\,(\tan\phi - \tan\alpha)]] \qquad (5.11a)$$

The ultimate resistance well below the ground surface was calculated using;

$$P_{ud} = d\gamma x[K_p{}^3 + 2K_o\tan\phi(K_p{}^2 + 1) - K_a] \qquad (5.11b)$$

where $\phi = 36.5°$,$\alpha = \frac{\phi}{2}$, $\beta = 45° + \alpha$, $K_a = \tan^2(45° - \alpha)$ and $K_p = \tan^2(45° + \alpha)$.

Figure 5.3 shows the relationship between the ultimate resistance of soil with depth using equations 5.11a and 5.11b. The intersection P_{ux} indicates that the ultimate soil resistance above the intersection point should be calculated using equation 5.11a and below this point using equation 5.11b, taking the smaller values as the governing ultimate resistance (P_u).

Various depths were selected to develop p/u curves (0.15, 0.3, 0.5, 0.8, 1.2, 1.6, 2.1,2.7 and 3.0m). In order to draw p/u the curves the early portion of deflection corresponding to ultimate soil resistance was calculated ;

$$\frac{p}{u} = k_h = n_h\,\frac{z}{B} \qquad (5.12)$$

The soil resistance value for corresponding u is obtained using;

$$p = P_u \ \tanh\left(\frac{n_h \ z \ u}{P_u}\right) \tag{5.13}$$

Using equation 5.13 the p/u curves for the various depths mentioned above were calculated. Figure 5.4 shows the family of the p/u curves predicted using equation 5.13. The curves are in the form of hyperbolic curves.

In order to construct a load/deflection curve for the pile, p/u curves were used. The procedure for developing the load/deflection curve can be found in Tomlinson (1977). The method which is extremely tedious to use can be summarised as follows. An approximate value of n_h is chosen from a set of recommended values for the different types of soil. Using equation 2.27 a first approximation for T is obtained. The deflected shape of the pile u is determined from equation 2.55. Using equation 5.13 a series of p/u curves are determined at several depths. From these curves the profile of soil secant modulus is constructed and a new n_h is obtained. Equation 2.27 is used again to calculate a second value for T. This process is repeated a second time from the beginning using the new value of n_h. A graph of trial T and computed T is drawn and a better approximation for T is obtained by finding the intersection of this graph with the 45° line. The process may have to be repeated (i.e. a new deflected shape of pile is calculated etc.) until the value of T remains constant. Figure 5.5 shows the load/deflection curve using subgrade reaction theory.

5.3.2-Poulos Method

The elastic theory of Poulos can be extended to account for non linear behaviour of the load/deflection curves. The application of his theory used to predict the load/deflection curves is as follows

In section 5.2.2 the rate of increase in soil modulus n_h with depth was found to be $13.0 MN.m^{-3}$ and $KN = 5.5 \times 10^{-4}$. Equation 2.115 was used to predict the

load/deflection curve 70mm above the ground line;

$$U_y = \frac{\frac{H}{n_h L^2}(I'_{UH} + \frac{e}{L}I'_{UM})}{F'_u} + \frac{70 \times 10^{-3}(\frac{H}{n_h L^3}(I'_{\theta H} + \frac{e}{L}I'_{\theta M}))}{F'_\theta} \qquad (5.14)$$

where F'_u and F'_θ are the yield displacement factor and yield rotation factor respectively. Values of I'_{UH}, $I'_{UM} = I'_{\theta H}$ and $I'_{\theta M}$ are 57, 170 and 800. Substituting the appropriate values in equation 5.14 then;

$$U_y = \frac{5.646 \times 10^{-4}H}{F'_u} + \frac{4.145 \times 10^{-5}H}{F'_\theta} \qquad (5.14a)$$

For $\frac{e}{L}$ the ultimate load H_U for failure of the soil is found (see Poulos(1981)) to be ;

$$\frac{H_u}{P_u dL} = 0.221 \qquad (5.15)$$

where P_u is the ultimate pressure half way along the embedded length of the pile. Broms(1964b) suggested that the ultimate pressure would be $3K_p\gamma'z$, giving P_u of 158.2kPa. Substituting the appropriate value in equation 5.15, the ultimate lateral load is found to be 18.0kN. The calculation for the load/deflection curve is shown in table T5.3 (For more information on values of F'_u and F'_θ see Poulos and Davies (1980). Figure 5.5 shows the predicted load/deflection curve.

5.3.3-Budhu and Davies Method

The application of the Budhu and Davies(1988) theory for developing load deflection curves is similar to the Poulos solution except that in their method there is no interpolation to determine influence factors and yielding factors. The application of their theory revealed that the rate of increase of soil modulus with depth was back analysed to be $8.0MN.m^{-3}$. Using equations 2.101 and 2.102 the elastic displacement U_e was calculated for horizontal loads of 1, 3, 5, 7, 10 and 15kN. Having obtained the linear load/deflection curve the next step is to obtain the yielding factor for displacement and rotation I_{uy} and $I_{\theta y}$. To determine these yielding factors h had to be defined;

$$h = \frac{H}{K_p\gamma'd^3} \qquad (5.16)$$

To calculate I_{uy} and $I_{\theta y}$ the following equations were used (see Budhu and Davies (1988);

$$I_{uy} = 1 + \frac{h - k^{0.35}}{6k^{0.65}} \qquad (5.17)$$

$$I_{\theta y} = 1 + \frac{h - k^{0.35}}{11.0k^{0.65}} \qquad (5.18)$$

where k is defined as $K/1000$ and

$$K = \frac{E_{ef}}{n_h d} \qquad (2.108.bis)$$

where E_{ef} is the effective elastic modulus of a solid circular section pile obtained from equation 2.90. The nonlinear behaviour of the load/deflection 70mm above the ground is calculated using;

$$U_y = U_e I_{uy} + \theta_e I_{\theta y} 70 \times 10^{-3} \qquad (5.19)$$

The calculation for the load and deflection are tabulated in table T5.4. Figure 5.5 shows the load/deflection curve.

5.4- Elastic Analysis of Two-Pile Groups

Two analytical solutions are used for analysing a two-pile group;

1 -Poulos(1971b) solution

2 -Randolph(1981) solution

In both analyses two identical, equally loaded piles are considered although the solutions can be extended for analysing larger groups of piles.

5.4.1- Poulos Solution

The application of Poulos' solution involves the calculation of the horizontal displacement of a two-pile group due to a horizontal load at the ground level. The two piles in the group were assumed to be rigidly connected together, so that the top of each pile displaces equally. The pile cap was assumed to be rigid and the pile to

behave as a fixed headed pile. From back analysis of the single pile test (see section 5.2.2) the rate of increase in soil modulus was found to be $13.0 MN.m^{-3}$ and the flexibility factor KN was found to be 5.5×10^{-4}. For a fixed headed pile the ground-line deflection is found by equation 2.83. It is assumed that the soil will remain linear elastic. The unit displacement U_{ef} for a single fixed headed pile may be calculated for $L/d = 22$, $KN = 5.5 \times 10^{-4}$ and $I_{UF} = 24.0$ Therefore ;

$$\frac{U_{ef}}{H} = \frac{24.0}{13000 \times 3.35^2} = 1.51 \times 10^{-4} m.kN^{-1} \qquad (5.20)$$

For elastic conditions, there is one unknown horizontal load in the group. The load in the front pile H_F is equal to load in the rear pile H_R, and therefore the displacement at ground line is given by;

$$U_{eF} = [H_F(1 + \alpha_{UF12})]\frac{U_{ef}}{H} \qquad (5.21a)$$

$$U_{eR} = [H_R(1 + \alpha_{UF21})]\frac{U_{ef}}{H} \qquad (5.21b)$$

For the condition of equal displacement of both piles $(U_{eF}/H = U_{eR}/H)$, and also from equilibrium;

$$H_G = H_F + H_R \qquad (5.22)$$

where H_G is the total applied horizontal load. It should be sufficiently accurate to assume L/d=25 and $KN = KR$. Poulos charts for various values of KN can be used to obtain interaction factors. Interaction factor values for $KN = 1 \times 10^{-3}$ and $KN = 1 \times 10^{-4}$ were linearly interpolated to obtain interaction factors for $KN = 5.5 \times 10^{-4}$. The relavent interaction factors are obtained for appropriate pile spacing in Poulos(1971). The unit displacement $\frac{U_{ef}}{H}$ is obtained from equation 5.20.

Substituting the appropriate values in equation 5.21a and 5.21b for front pile rear piles, and assuming that pile displacement is 20.0mm, the horizontal load for 20.0mm pile cap displacement is found. Then simply multiplying the horizontal load

on the front or rear pile by 2 the H_G is obtained. Table T5.5 shows the relavent interaction factors and the total horizontal load on the two pile groups for 20.0mm pile cap displacement. Figure 5.6 shows the lateral stiffness of two-pile groups.

5.4.2- Randolph Solution

The application of the elastic finite element theory by Randolph can be extended to deal with response of laterally loaded pile groups by the use of interaction factors. In section 5.2.3 the rate of increase of soil shear modulus m with depth was found by back analysis of the single pile test to be $2.56MN.m^{-3}$. The critical length L_c is calculated to be;

$$L_c = 2r(\frac{E_p}{m^*r})^{\frac{2}{9}} = 2.76m \tag{5.23}$$

Using L_c gives characteristic shear modulus of;

$$G_c = (m \times \frac{L_c}{2})(1 + \frac{3v}{4}) = 4331.0 kN.m^{-2} \tag{5.24}$$

The critical length of pile (L_c) is slightly greater than the embedded length of pile, but it should be mentioned here again that, the 0.2m shoe at the bottom of the pile is not included in the total embedded length. The L_c used will not cause significant error.

As the piles were firmly fixed to the pile cap the interaction factor for fixed head condition is calculated by;

$$\alpha_{UF} = 0.6\rho_c(\frac{E_p}{G_c})^{\frac{1}{7}}.\frac{r}{s}(1 + \cos^2 \beta) \tag{2.138.bis}$$

the departure angle $\beta = 0^o$ and ρ_c is;

$$\rho_c = \frac{G_{c@z=\frac{L_c}{4}}}{G_c \quad @z=\frac{L_c}{2}} = 0.5 \tag{2.95.bis}$$

where G_c is calculated from equation 5.24 and ρ_c is the ratio of characteristic shear modulus calculated from equation 2.95 for L_c of 3.4m and $\frac{L_c}{4}$.

Substituting the appropriate values in equation 2.138 the interaction factor is then determined. For a fixed headed pile, the fixing moment is given in equation 2.96. Substituting in equation 2.88 the displacement of the pile head for a fixed headed pile is;

$$U_{ef} = \frac{(\frac{E_p}{G_c})^{\frac{1}{7}}}{\rho_c G_c}[0.27H(\frac{L_c}{2})^{-1} - (\frac{0.375}{\rho_c^{\frac{1}{2}}})0.3H(\frac{L_c}{2})(\frac{L_c}{2})^{-2}] \tag{5.25}$$

Substitution of the appropriate values gives a unit displacement of;

$$\frac{U_{ef}}{H} = 1.31 \times 10^{-4} \tag{5.26}$$

Assuming 20.0mm pile head deflection and for linear elastic conditions the horizontal loads on the front pile and the rear pile are equal. Thus the displacement at ground level is given by;

$$U_{efF} = [H_F(1 + \alpha_{UF_{12}}) \times 1.31 \times 10^{-4}] \tag{5.27a}$$

$$U_{efR} = [H_R(1 + \alpha_{UR_{21}}) \times 1.31 \times 10^{-4}] \tag{5.27b}$$

The total horizontal load on the two pile group is $H_G = H_F + H_R$. For 20.0mm pile cap displacement the values of H_G for different pile spacing are tabulated in table T5.6 with the calculated interaction factors. Figure 5.6 shows the lateral stiffness of two-pile groups.

5.4.3- Prediction of Maximuum Bending moment in Two-Pile Groups.

The maximum bending moment occurs either in the pile shaft or at the pile/cap connection. For the condition of complete pile head fixity the maximum bending moment occurs at the pile head/cap connection (reverse moment). The Poulos and Davies (1981) and Randolph (1981) charts both suggest that the maximum reverse bending moment/horizontal load ratio is constant with pile spacing, at 0.301 and 0.4501 $kN.m.kN^{-1}$ respectively.

5.5- Prediction of Load/Deflection Curve For Two-Pile Groups.

Poulos developed a procedure for predicting load/deflection curves for pile groups.

His procedure can be implemented to predict load/deflection for any pile group configuration.

In order to calculate ultimate lateral resistance of a fixed headed two-pile group with no rotation at the pile head, it is first necessary to know the ultimate lateral resistance H_{UF} of a fixed head single pile. To calculate H_{UF}, Brom's(1964) dimensionless solution is used. He presented a relationship between ultimate lateral resistance $\frac{H_{UF}}{K_p d^3 \gamma'}$ and yield moment $\frac{M_{yield}}{K_p d^4 \gamma'}$. The M_{yield} is calculated from simple bending theory. Using a yield stress σ_{yield} of cold rolled steel of about $300 N mm^{-2}$, and from theory and the known second moment value (I) of the pile the M_{yield} is:

$$M_{yield} = \frac{\sigma_{yield} I}{y} = \frac{3.0 \times 10^5 \times 1.39 \times 10^{-5}}{71.5 \times 10^{-5}} = 58.3 kN.m \qquad (5.28)$$

Thus;

$$\frac{M_{yield}}{K_p d^4 \gamma'} = \frac{58.3}{3.93 \times 0.154^4 \times 8} = 3300 \qquad (5.29)$$

From the dimensionless solution (reference 12) for $\frac{M_{yield}}{K_p d^4 \gamma'}$ equal to 3000 the $\frac{H_{UF}}{K_p d^3 \gamma'}$ is found to be 500 therefore;

$$H_{Ul} = 500 \times 3.93 \times 0.154^3 \times 8 = 57.4 kN \qquad (5.30)$$

Assuming that the two piles in the group carry similar load, the ultimate lateral resistance of the two-pile group is 114.8kN. Using equation 5.20 the unit displacement of a fixed headed pile $\frac{U_{ef}}{H}$ is 1.51×10^{-4}. Using equation 5.21a or 5.21b the deflection of the two-pile group under a constant load H_{Ug} is calculated for various pile spacings. It was found that the deflections of the two-pile group for 3, 5, 8 and 12 pile width spacing gave factors (F_d) of 1.50, 1.38, 1.28 and 1.20 respectively greater than for the single fixed headed pile for the same load on each pile. The F_d gives the lateral efficiency (ηl) of the two pile group $(\frac{1}{F_d})$. The ηl values for pile spacing of 3, 5, 8 and 12 width are calculated to be 0.664, 0.72, 0.766 and 0.833 respectively.

Assuming the validity of calculated ηl and applying the ηl values to the ultimate lateral load capacity of the two-pile group H_{ug} would result in reductions in ultimate lateral load on the two-pile group. The group reduction factor (R_{RUF}) is obtained from charts presented by Poulos(1975). The R_{RUF} remain constant up to $H_u g$ and for 3, 5 and 8 pile width are 0.439, 0.373, and 0.334 respectively. For 12 pile width spacing the R_{RUF} was found to be 0.304 by extrapolating Poulos charts. It would be justifiable to assume that the $KR = KN$ when R_{URF}'s were obtained for $KN = 10 \times 10^{-4}$.

From back analysis of the single pile tests using Poulos solution the rate of increase of soil modulus n_h was estimated to be $13000kN.m^{-3}$. With this assumption and the calculated ηl and R_{RUF} Poulos solution was used to calculate ground line deflection $U_g y$ for a fixed headed pile group in a soil with linear varying soil modulus;

$$U_{gy} = [\frac{\frac{H_g(R_{RUF}.I'_{UF})}{n_h L^2}}{F'_{UF}}] \tag{5.31}$$

where F_{UF} is the yielding deflection factor for single pile, for $\frac{H_u}{nH_u\eta l}$. Table T5.7 shows the appropriate values used to calculate interaction factors, lateral efficiency factor and reduction factor.

The results of calculations of ground line load/deflection curves for the two-pile groups are tabulated in table T5.8. Figure 5.7 shows the load/deflection curves for the four cases. The calculation of load/deflection curves for the four cases above the ground is not possible because for a fixed headed pile the rotation θ at the head is zero. Thus there is no additional deflection caused by the rotation on the head of the pile. Figure 5.8 shows the variation of secant lateral stiffness of two-pile groups with pile spacing.

5.6-Discussion

In this chapter some of the available methods of analysis for laterally load piles and pile groups were used. In order to calculate the rate of increase of soil modulus with depth back analyses of the single pile test results were conducted. To calculate the

rate of increase of soil modulus with depth n_h, linear elastic analysis were conducted. It was found that the calculated rate of increase of soil modulus depends upon the method used. It was found that n_h values decreased as the pile head deflection increased for all the tests using equation 5.1. The sharp decrease in n_h value would imply early failure of the soil over the upper embedded length of the pile. The back analysed trends of n_h are similar to results by Alizadeh(1969) and Barton(1982) as reported by Fleming et al(985). The soil modulus values obtained were used to predict the maximum moment on the pile shaft for a free headed pile and lateral stiffness of a fixed headed pile for linear elastic condition. It was found that the maximum bending moment/horizontal force ratio predicted using the methods of Poulos(1971a), Randolph(1981), Budhu and Davis(1988) and Banerjee(1978) are in close agreement while Reese and Matlock over-estimated the bending moment/lateral force ratio(see table T5.2). The predicted lateral stiffness values of a fixed head single pile using Poulos(1971a), Randolph(1981) and Budhu and Davies(1988) methods were in close agreement, but not these of Reese and Matlock(1969) and Banerjee and Davies.

Throughout these analyses it was found that linear elastic continuum methods provided better prediction than subgrade reaction methods, for single piles.

The non-linear predictions of load/deflection were conducted based upon the elastic continuum approach by Poulos(1971a , 1973 and 1975) and Budhu and Davies(1988) and the p/u method. It was found that elastic continuum method using Budhu and Davies predicted better results than Poulos (see Figure 5.5). The p/u method was more laborious to apply than elastic continuum methods and the prediction was not the same. The prediction of load/deflection curve using the p/u method underestimate the lateral load by up to 20%. It has been suggested by Brown et al (1988) that the loose sand densifies under lateral pressure, which causes the n_h value to be under estimated. However at the early portion of the load/deflection curve, the p/u method gave close agreement with Poulos(1971a and 1973) and Budhu and Davies.

Poulos(1971b, 1973, 1975 and 1979) and Randolph(1981) methods were used to predicted the linear elastic stiffness of two-pile groups (see Figure 5.6) for various pile spacings. It was found that Poulos interaction factors were higher than Randolph's but Poulos prediction provided better results (see tables T5.6 and T5.7). The maximum bending moment occurred in the pile/cap connection and it was found that the maximum bending moment (reverse bending moment) was constant with pile spacing. The maximum bending moment calculated using Poulos(1971b) and Randolph (1981) assumed that the pile cap is fixed and there is no head rotation.

The non-linear estimation of the load/deflection curve for the two-pile groups was undertaken using Poulos(1975) method. The load/deflection curve for 3, 5, 8 and 12 pile width spacing for zero overhang for two-pile groups were reasonably good. In order to determine the reduction in lateral stiffness of two-pile groups, secant stiffnesses for 20.0mm pile cap deflection were calculated. Figure 5.8 shows secant lateral stiffnesses of two-pile groups for 20.0mm deflection of the pile cap. It was found that the elastic and plastic lateral stiffness of two-pile groups increased with pile spacing. The secant stiffnesses calculated were for zero pile cap overhang. The axial forces on the two pile groups could not be predicted numerically, because there is not an available method to predict axial forces induced into the piles in pile groups due to lateral forces. Prediction of axial forces can be made by computer programs such as DEFPIG,PGROUP and PIGLET, but unfortunately the computer programs were not available to the author.

5.7-Conclusions

In this chapter the following conclusions were obtained using back analysis and prediction analysis of single piles and two-pile groups.

1 -The calculated profile of soil modulus varied depending on the method used for back analysis.

2 -The elastic continuum method suggested that the piles considered in this study

were long flexible piles while the subgrade reaction method suggested that the piles were intermediate between long and short.

3 -The elastic continuum method provided better prediction of maximum bending moments/horizontal load ratio and lateral stiffness of a fixed head single pile.

4 -The elastic continuum method with interaction factors provided good prediction for lateral stiffness of the two pile groups.

5 -The lateral stiffnesses of the two-pile groups computed by the elastic continuum method increased as the pile spacing increases; the trend is correct.

6 -The reverse bending moment/horizontal load ratio were constant with pile spacing.

7 -The axial load on the two-pile groups could not be predicted by any available published manual method.
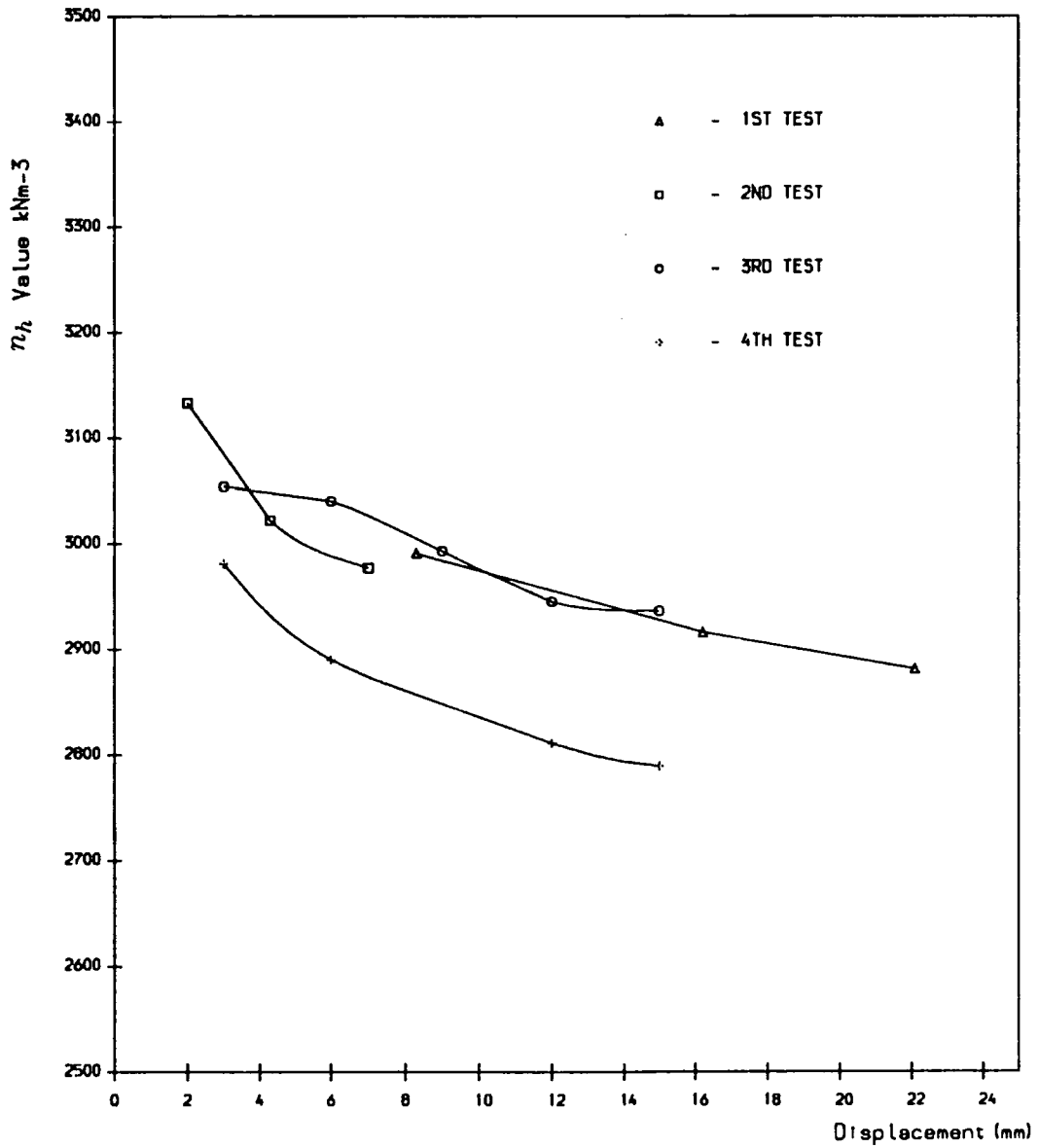
Figure 5.1 Variation of soil modulus profile with pile head deflection
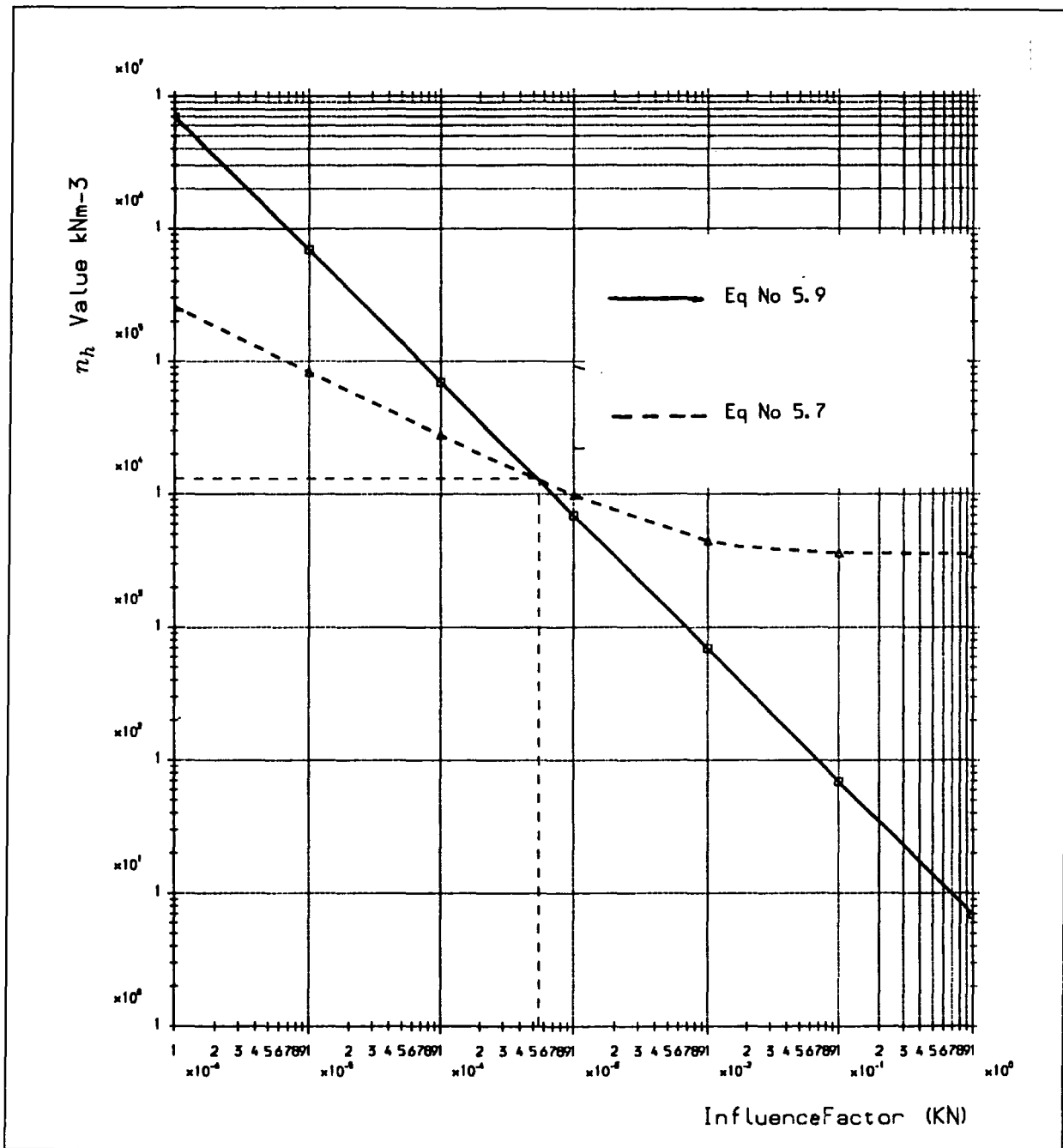
Figure 5.2 Plot of n_h values against KN values.
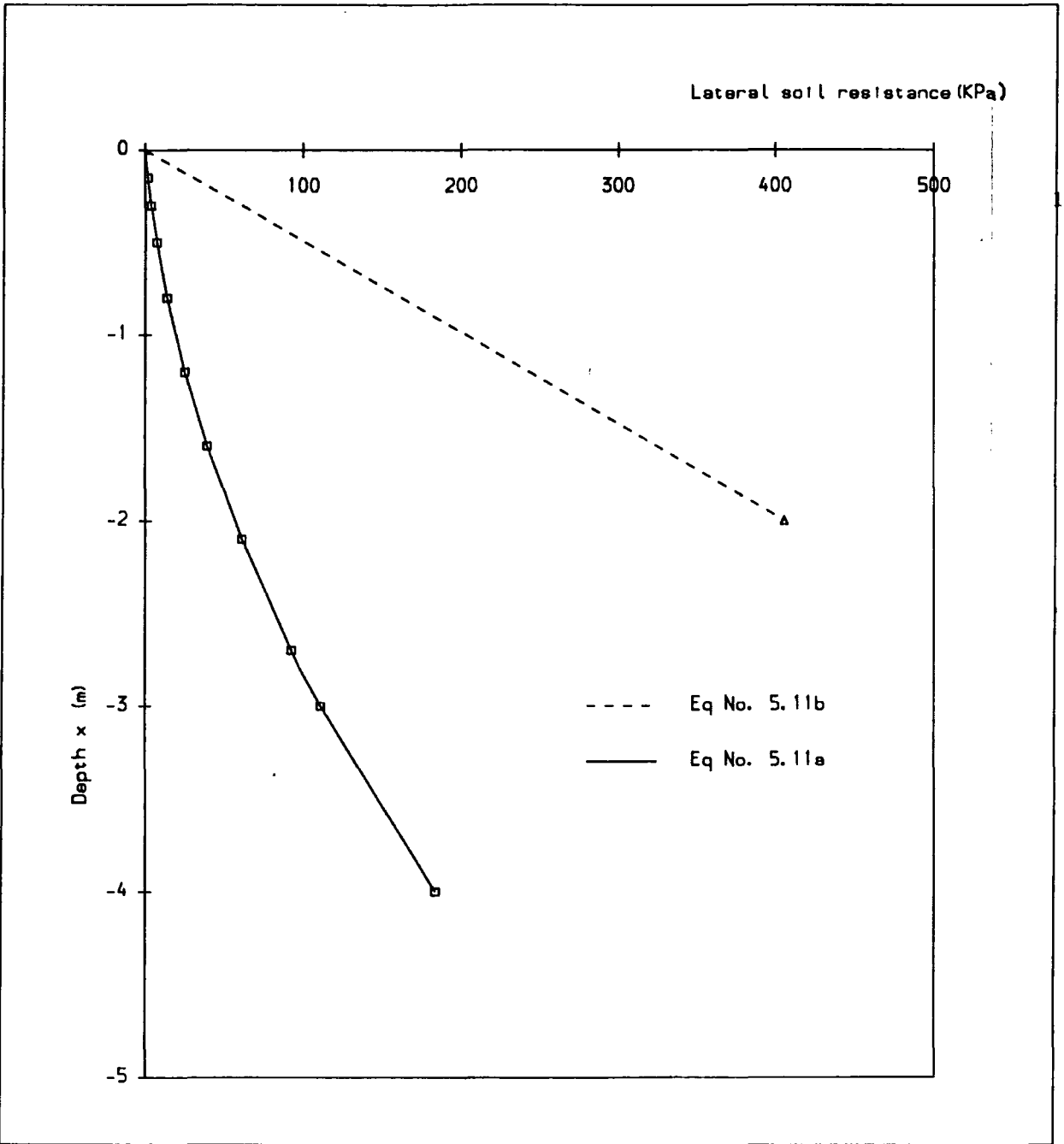
Figure 5.3 Lateral soil resistance against depth.
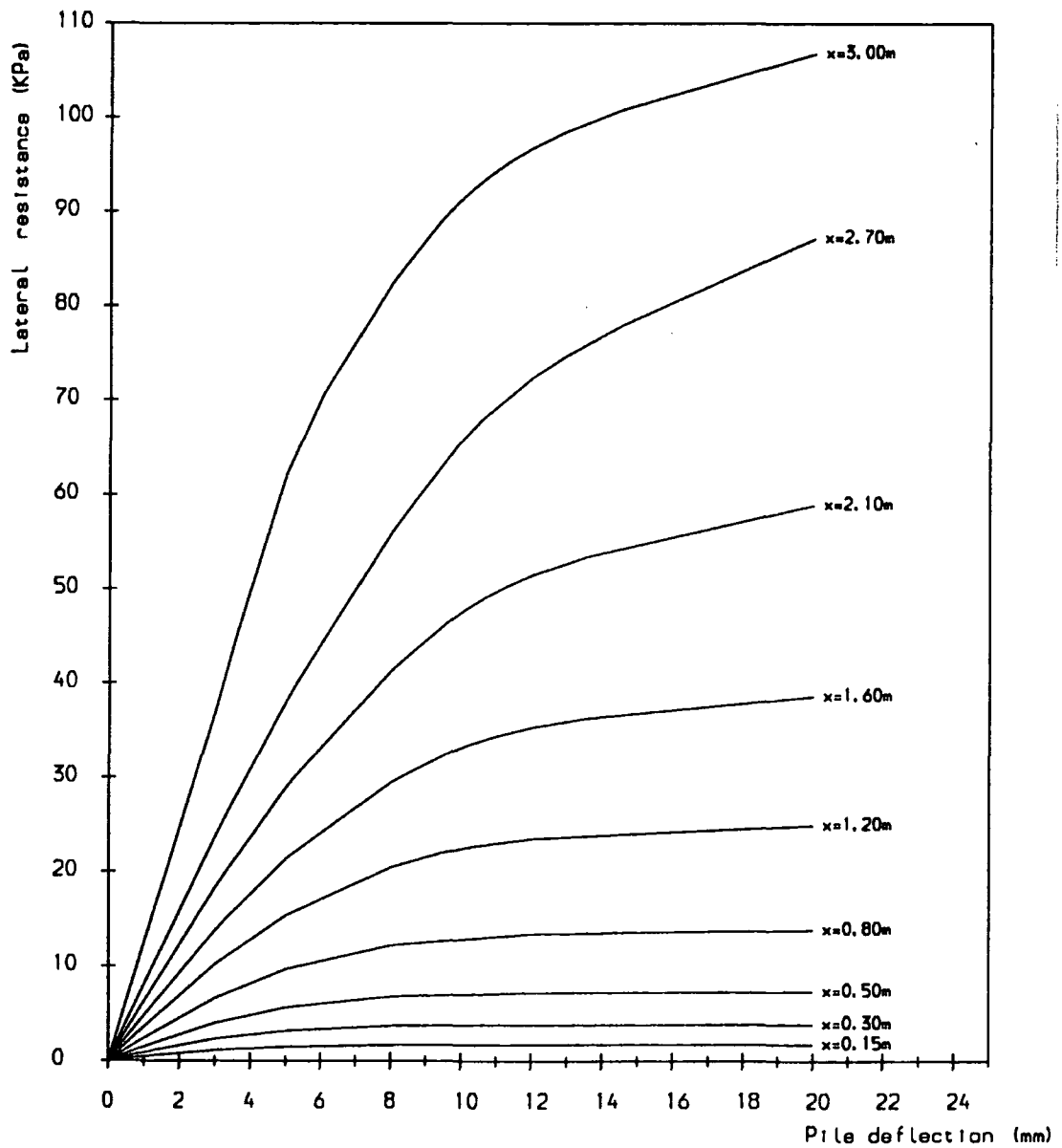
Figure 5.4 Lateral soil resistance against pile deflection(p/u curves).
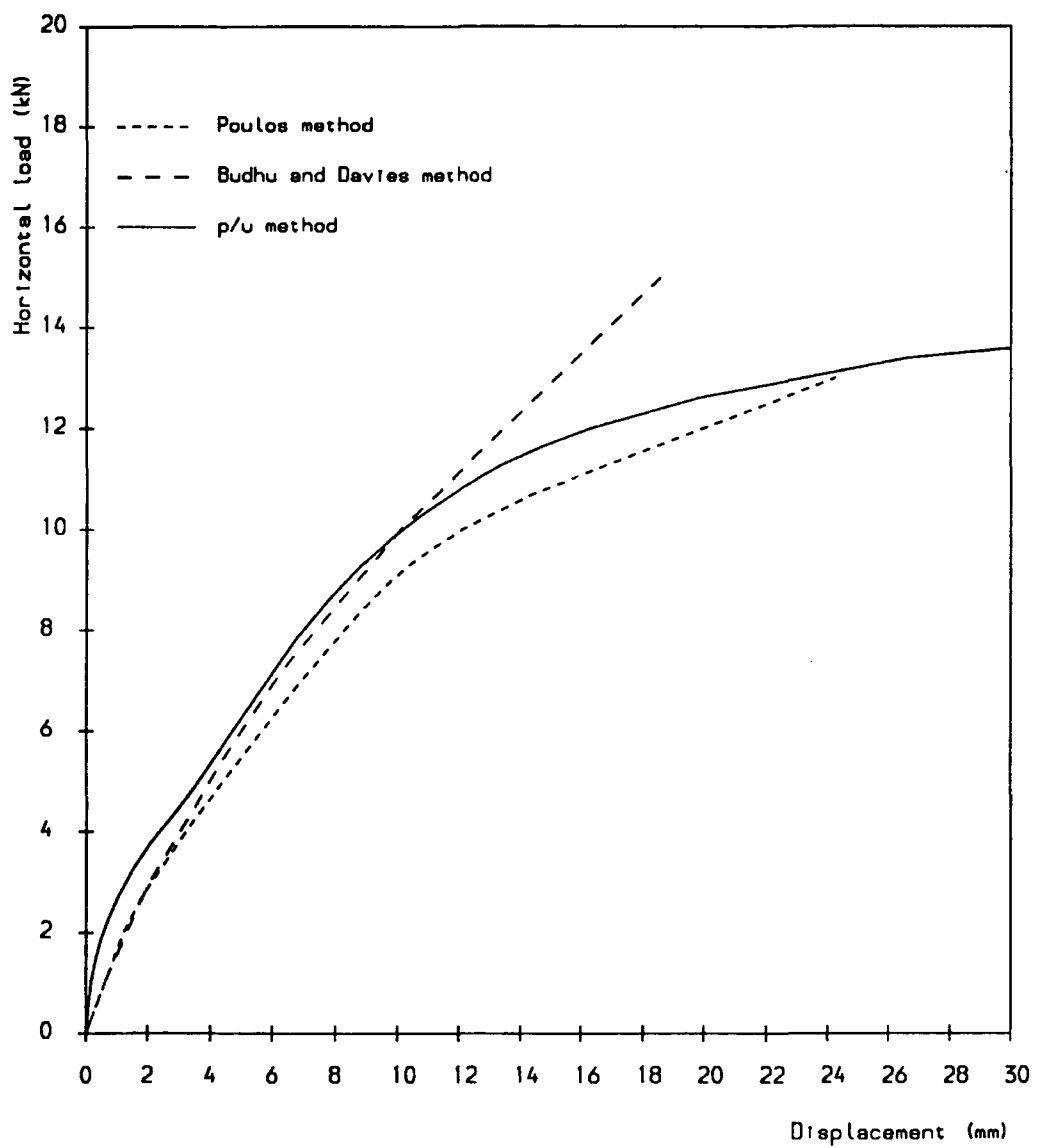
Figure 5.5 Predicted load/deflection curves.
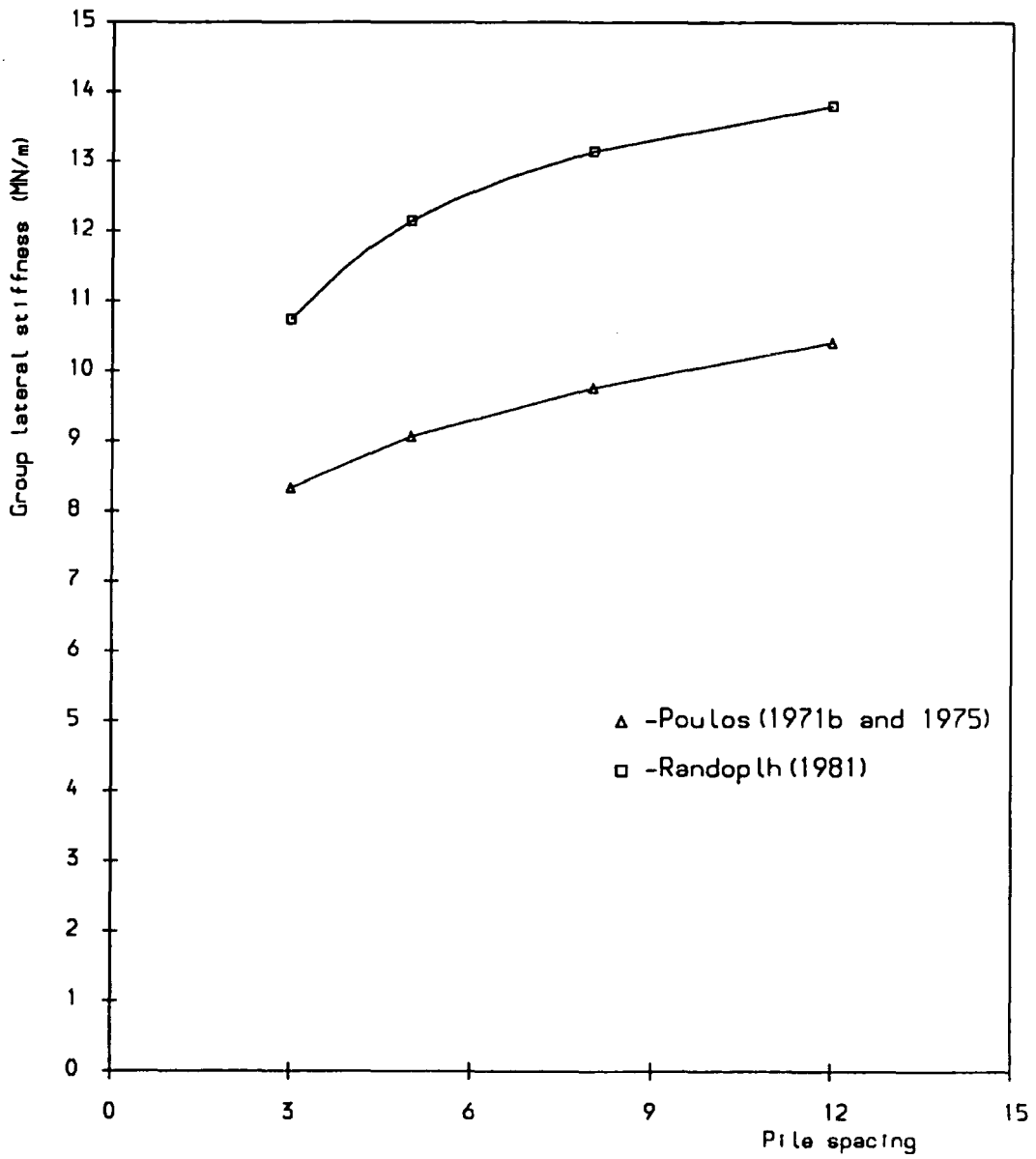
Figure 5.6 The lateral stiffness of two–pile groups against pile spacing.
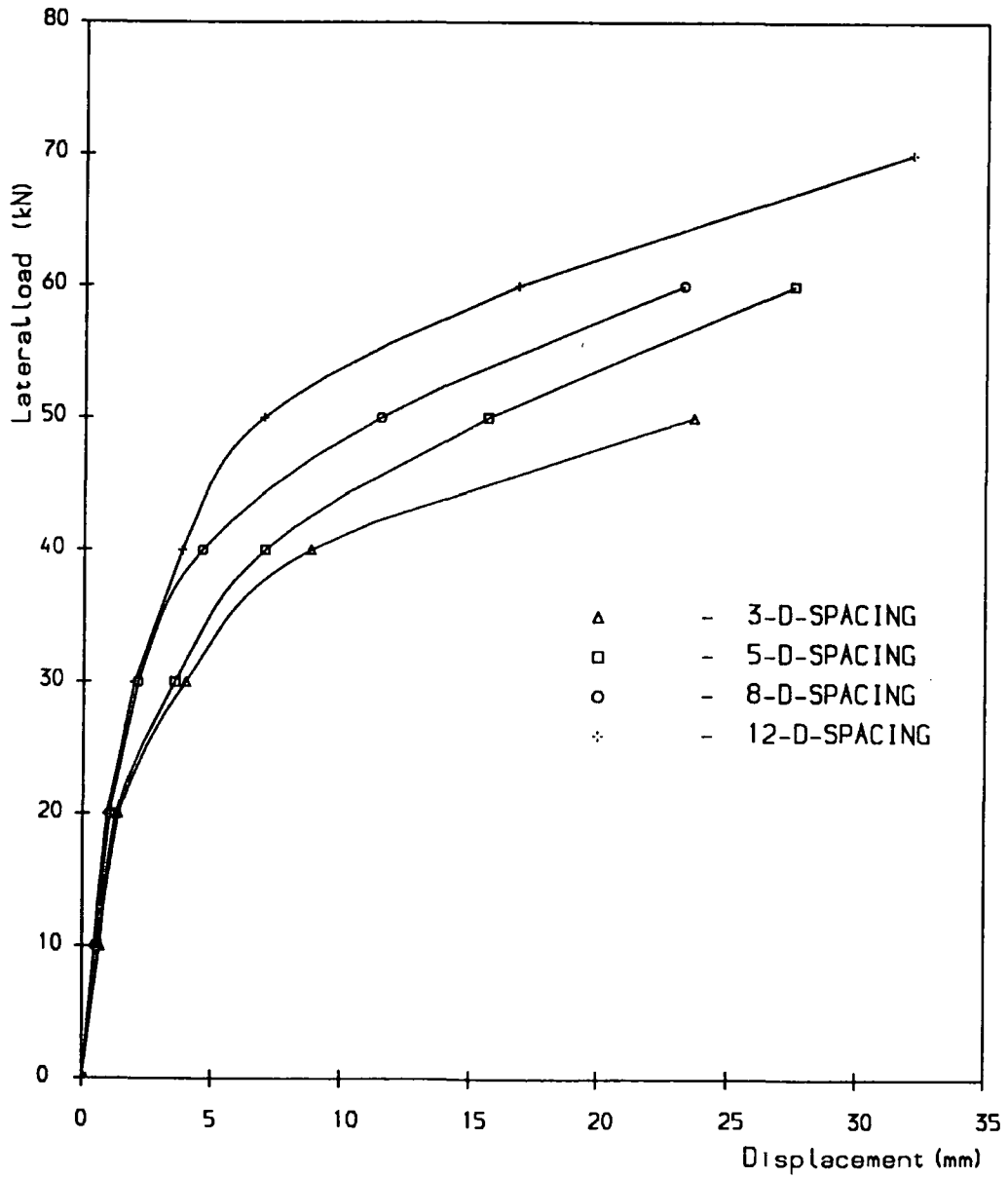
Figure 5.7 Predicated load deflection curves for two-pile groups.
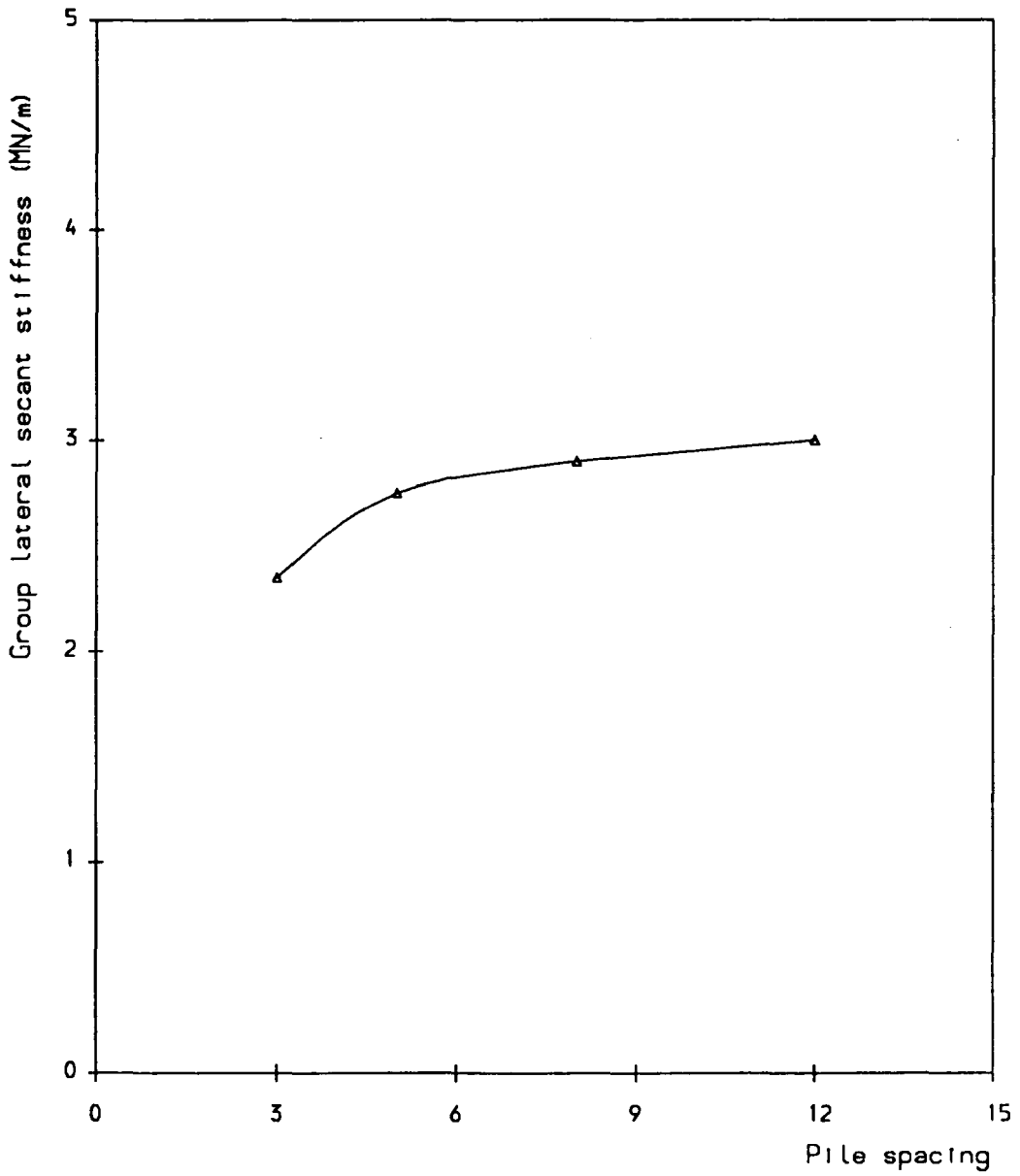
Figure 5.8 Variation of secant stiffnesses of two-pile groups with pile spacing.

Table T5.1 Determination of n_h using two alternative methods

Poulos (1971a)

KN	I'_{UH}	$I'_{UM} = I'_{\theta H}$	$I'_{\theta M}$	I'_{Ua}	$n_h = 155.9 I'_{Ua}$ (kNm^{-3})	$n_h = \frac{6.92}{KN}$ (kNm^{-3})
10^{-6}	531.0	4830.0	93500.0	1644.4	256362.0	6918470.000
10^{-5}	231.0	1410.0	16300.0	529.7	82580.0	691847.000
10^{-4}	103.0	384.0	2710.0	176.8	27563.0	69184.700
10^{-3}	43.6	103.0	437.0	62.5	9744.0	6918.470
10^{-2}	22.7	32.6	81.8	28.5	4443.0	691.847
10^{-1}	19.4	22.2	35.3	23.3	3632.5	69.184
10^{00}	19.0	21.5	30.2	22.8	3554.5	6.918

Table T5.2 Pile properties back analysed and predicted in the literature

	Site	Reese and Matlock (1960)	Poulos (1971)	Randolph (1981)	Budhu and Davis (1987)	Banerjee and Davies (1978)
n_h $(MN.m^{-3})$		3.07	13.00	2.56*	8.00	5.5
Elastic Stiffness (free head) $(MN.m^{-1})$	1.75	1.75	1.75	1.75	1.75	1.75
Elastic Stiffness (fixed head) $(MN.m^{-1})$		3.07	6.08	7.64	5.98	5.14
Max.BM/ H (free head) (kNm/kN)	0.68	1.02	0.60	0.63	0.58	0.65

* Shear modulus profile.

Table T5.3 Load/deflection calculation (Poulos (1975))

H (kN)	$\frac{H}{H_u}$	F'_u	F'_θ	U_y (mm)
2	0.111	1.00	1.00	1.21
4	0.222	0.75	0.89	3.20
7	0.388	0.605	0.76	6.92
10	0.554	0.490	0.70	12.11
13	0.831	0.315	0.56	24.26

Table T5.4 Load/deflection calculation (Budhu & Davies (1988))

H (kN)	U_e (mm)	U_θ	h	I_{uy}	$I_{\theta y}$	U_y
1	0.536	0.035	9.25	1.0414	1.0047	0.593
3	1.602	0.106	27.75	1.2118	1.0243	2.057
5	2.680	0.177	46.25	1.3822	1.0438	3.890
7	3.752	0.248	64.75	1.5526	1.0634	6.090
10	5.360	0.354	92.50	1.8082	1.0930	10.080
15	8.04	0.531	138.75	2.2342	1.1416	18.570

Table T5.5 Tangent stiffness prediction for two-pile groups

Poulos (1971b)

Pile Width Spacing	α_{UF}	H_G (kN)	Group stiffness $MN.m^{-1}$
3	0.50	166.6	8.33
5	0.38	181.1	9.06
8	0.28	195.3	9.76
12	0.20	208.3	10.41

Table T5.6 Tangent stiffness prediction for two-pile groups

Randolph (1981)

Pile Width Spacing	α_{UF}	H_G (kN)	Group stiffness $(MN.m^{-1})$
3	0.423	214.8	10.74
5	0.254	243.0	12.15
8	0.159	263.0	13.15
12	0.106	276.0	13.80

Table T5.7 Interaction factor analysis for two-pile groups

Pile Width Spacing	α_{UF}	Displacement factor F_d	ηl	R_{RUF}
3	0.500	1.500	0.666	0.439
5	0.380	1.380	0.720	0.373
8	0.280	1.280	0.766	0.334
12	0.200	1.200	0.833	0.304

| Table T5.8 | | | | | | | | | | | | | | | |
| Summary of load/deflection curve calculation for two-pile groups | | | | | | | | | | | | | | | |
3 Pile width spacing				5 Pile width spacing				8 Pile width spacing				12 Pile width spacing			
Load (H_g) (kN)	$\dfrac{H_g}{2H_{UI}\eta l}$	F'_{UF}	Defl (mm)	Load (kN)	$\dfrac{H_g}{2H_{UI}\eta l}$	F'_{UF}	Defl (mm)	Load (kN)	$\dfrac{H_g}{2H_{UI}\eta l}$	F'_{UF}	Defl (mm)	Load (kN)	$\dfrac{H_g}{2H_{UI}\eta l}$	F'_{UF}	Defl (mm)
10.0	0.130	1.00	0.66	10.0	0.120	1.00	0.56	10.0	0.114	1.00	0.50	10.0	0.105	1.00	0.46
20.0	0.260	0.98	1.35	20.0	0.242	0.90	1.25	20.0	0.230	0.98	1.03	20.0	0.210	1.00	0.92
30.0	0.390	0.50	3.97	30.0	0.363	0.65	2.59	30.0	0.340	0.63	2.40	30.0	0.310	0.70	1.96
40.0	0.520	0.30	8.82	40.0	0.480	0.32	7.03	40.0	0.450	0.38	6.60	40.0	0.420	0.48	3.82
50.0	0.660	0.14	23.64	50.0	0.600	0.18	15.62	50.0	0.570	0.22	11.44	50.0	0.520	0.33	6.94
				60.0	0.726	0.15	22.50	60.0	0.682	0.13	23.25	60.0	0.627	0.17	16.18
												70.0	0.732	0.10	32.09

CHAPTER SIX

Finite Element Analysis

6.1-Introduction

In recent years Finite Element Analysis has been used in various engineering problems and has enabled engineers to solve a range of complex problems. The technique was first developed for structural analysis, and the theory of the finite element technique can be obtained in many text books (eg Rocky at el (1975) and Zienkiewicz and Taylor(1991)). Finite element analyses of piles in soil are presented by Ottaviani(1975), Randolph(1981), Justo et al.(1987), Smith and Griffiths(1988) and more recently by Chehade et al (1991) and Selby and Arta (1991) to deal with laterally loaded piles. Today powerful computer packages such as Program for Automatic Finite Element Calculation (PAFEC75) have been developed which are capable of analysing 1, 2 and 3 dimensional problems with various types of element. The package uses the Virtual Work theory to evaluate nodal displacements due to applied load vectors, then from the nodal displacements the strains and stresses are calculated.

The PAFEC package is available in the Newcastle MTS system and was used to analyse a single pile and two-pile groups in a granular soil using a fully 3 dimensional model. The manner in which the input data were constructed was in accordance with the PAFEC 75 manual, and is briefly described in section 6.6.

The finite element model was developed for comparison with a series of field tests reported in chapter 4. Several steps had to be taken in order to construct and verify a model for single pile and two-pile groups. The finite element analysis was linear elastic , but attempts could be made to incorporate soil plasticity by reducing soil modulus values.

Because of the high computer cost (CPU Time) for analysing a 3 dimensional model the problem was halved by taking a plane of symmetry through the centre line of the model. A typical finite element analysis of a two-pile group needed approximately 3000 second to complete the analysis. Initially the soil model approximated an isotropic linear elastic half space with a soil modulus varying linearly to the depth of 2.1m and below 2.1m to 4.0m with a constant soil modulus. The boundary conditions for the model are described in section 6.4.1.

6.2-Finite Element Pile Model

Because of the geometrical problem of the actual hollow pile section, the web of the pile shaft was modelled by twenty noded isotropic solid brick elements which occupied the full cross section of the hollow box, with 3 degrees of freedom at each node. The flanges were modelled by plane stress elements which had 8 nodes. Both axial stiffness EA_a and web flexural shear stiffness EI_a of the actual pile had to be correctly modelled by these elements.

Having satisfied the axial stiffness using brick elements plus flange elements , the elastic bending modulus E_m of each brick element was of equivalent web stiffness to the web of the box section see Figure 6.1.

$$E_m = E_s \frac{area \ of \ web}{area \ of \ brick \ element} \tag{6.1}$$

$$E_m = 2.1 \times 10^{11}.\frac{(143 \times 5.5 \times 2) + (18.5 \times 11 \times 2)}{154 \times 154} = 1.75 \times 10^{10} Nm^{-2}$$

Having obtained the E_m, The flexural bending stiffness EI_a of the hollow pile had to be equal to the model pile. In order to satisfy this condition the flange thickness (t)

had to be calculated;

$$EI_a = EI_m \qquad (6.2)$$

$$2.92 \times 10^{11} = (1.75 \times 10^{10} \times \frac{0.154^4}{12}) + (0.154 \times t \times (77 \times 10^{-3})^2 \times 2)$$

From the above calculation the thickness of the flange elements (t) had to be 5.3mm thick. The flange element had 2 degrees of freedom at each node. These flange plane stress elements were linked to the web elements at the corner nodes. The total length of embedded model pile was 3.35m for all the analysis.

6.2.1-Finite Element Pile Model Testing

The pile shaft model bending behaviour had to be tested in order to investigate the accuracy of the pile model. A cantilever beam model ($0.154m \times 0.154m$) and $2.0m$ long was constructed in which the beam had the same linear elastic modulus as the model pile and same plate element thickness calculated in equation 6.2 were used to model the flanges of the box and were attached to the top and bottom of the beam (see figure 6.2). To obtain the deflection and the bending stresses along the cantilever beam for a 20.0kN load at its free end simple cantilever beam theory was used. Bending stresses and deflections were calculated for 200mm intervals along the beam. Using a similar load, PAFEC 75 was used to obtain the similar results on the model pile. Two different types of brick element were used: 8 and 20 noded, and also two types of plate element were used: 4 and 8 noded elements. It was found that the 20 noded brick element and 8 noded plate element model gave significantly better results than 8 noded brick element and 4 noded plate element because they offered linear strain rather than constant strain. These results were then compared with the cantilever beam theory and it was found that the pile was modelled accurately. Table T6.1 shows the values obtained from cantilever beam theory and finite element analysis based on 20 noded brick and 8 noded plate elements for both deflection and bending stress. As it can be seen from table T6.1 the results obtained by finite element analysis were in close agreement with the cantilever beam theory, thus the

final model of the pile was made of 20 noded brick elements and 8 noded plane stress elements. The advantage of using a 20 noded brick element is that it gives more accurate results than the 8 noded one, but the package needed more CPU time to analyse a 20 noded brick element than 8 noded brick element because of the larger number of degrees of freedom. The F.E model was suitably accurate for analysis of the pile shaft. It should be mentioned that the aspect ratio used in finite element analysis of the cantilever beam was an important factor, with an aspect ratio of less than 2 to 1 giving the best results.

Finally, the pile shaft was constructed using prism elements type 37110 with 3 degrees of freedom at each of 20 nodes and the flanges of the pile using plane stress elements type 36210 with 2 degrees of freedom at each of 8 nodes.

6.3-Finite Element Pile Cap Model

Figure 3.23a (chapter 3) illustrated the two C sections used to connect the two piles together with the help of angles, tension bolts and cross bars. As the finite element analyses were based on a half model with the plane of symmetry taken through the central line of the piles it was necessary to model the pile cap in a manner such that the bending stiffness was equal to that of the plates used in the site pile cap. The method used to model the pile cap of the C section was to use simple plate elements to be 6.0mm thick. The type of element used in modelling the pile cap was the 8 noded plane stress element with 2 degrees of freedom at each node, element type 36210 from the PAFEC 75 manual.

6.4-Finite Element Soil Modelling

The three dimensional twenty noded isoparametric brick element type 37110 which has 3 degrees of freedom at each node was chosen from the PAFEC manual to model the pile and so the same brick element was chosen to model the soil. The reason for choosing similar elements was to achieve compatible nodal connection. There were three points which had to be considered very carefully in order to

represent the soil in the model.

6.4.1-boundary conditions

As the site trench filled with sand was of limited dimensions within a stiff clay, it was necessary to know how far from the pile the boundaries should be fixed so that the soil elements at the boundary would observe negligible pressure change. It was assumed that the boundary should be 1.5m away from the front face of the front pile and 1.5m away from the back face of the rear pile in the direction of pile cap displacement, the side boundary was assumed to be 0.67m away from the plane of symmetry and the depth of the boundary was 4.0m below the surface. The distance to the boundary was the same for 3,5,8 and 12 pile width spacing of the pile groups and single pile in order to achieve negligible pressure change on the boundary. For a typical finite element run pressures at the front of the pile and at 1.5m away from the front pile was found to be 47.4 and 7.55kPa respectively. This indicated that the pressure near the boundary was sufficiently small for the boundary position to be acceptable.

6.4.2-Restraints on the Boundary Planes

Nodal displacement restraints were necessary on the boundary planes to prevent nodal displacements in the three orthogonal direction (i.e X,Y,Z). The front and rear boundaries were restrained in these three directions X,Y and Z. The nodes on the plane of symmetry were restrained in the direction Y only, and finally the nodes at the bottom were restrained in three directions X,Y and Z. The nodal restraints were the same for 3,5,8 and 12 pile width spacings and for all pile caps overhang (150,300 and 400mm) and also for single pile analysis.

6.4.3-Number of Layers and Modulus Values

It was necessary to divide the model into a number of layers in order to allow reasonable representation of the soil stiffness profile, and to determine values for

deflection, bending stress and soil pressure at various depths on the piles. It was decided to divide the model into 11 layers, and Figures 6.3 and 6.4 illustrate the plan and three dimensional views of single pile and two-pile group models respectively.

As a Gibson soil modulus varies linearly with depth and PAFEC does not allow the modulus to vary within a pafblock, (See Figure 6.5), it was necessary to choose a mean value for each layer. To obtain a correct number of mean values to be given in the soil layers, the mean values were attributed to an increasing number of layers for each PAFEC run and the slopes of the load/deflection response for single pile were plotted against the number layers (See Figure 6.6). It was found that increasing the number of layers of elements above six, had negligible effect on the pile load/deflection behaviour. The convergence test was monotonic and appeared to have approached within 3 percent of an asymptotic value when four layers were used. In the main analyses six values were used in the soil model for single pile and two-pile group analyses.

6.5-Soil Modulus Values in Finite Element Model

The soil modulus values are a most important parameter in constructing a representative model of the soil/pile system and had to be carefully chosen to represent the characteristic behaviour of the soil. Two techniques were considered to evaluate the soil modulus values as follows;

6.5.1-Triaxial Test Results

"Undisturbed" sand samples were collected in U100 tubes from the site and were tested at three different cell pressures (50,100 and 150KPa). The stress and strain relationships for 3 different cell pressure showed the sand tangent modulus to be 14MPa. In the triaxial tests the soil modulus changed little with the cell pressure. Several attempts were made to conduct triaxial tests at very low cell pressures, but each attempt failed due to collapse of the specimen. It has been suggested by various authors that the Poisson's ratio of sand is of the order of 0.3 and this value was used

in the finite element models.

6.5.2-Load/Deflection Curve

The non-linear characteristic behaviour of the soil was deduced from the load-deflection curves from single pile tests. Back analyses of these results were also used to evaluate the soil modulus profile based on tangent and secant stiffnesses.

In a free head single pile test the load was applied 500mm above the ground line and the deflection was measured 70.0mm below the ground line. The finite element model of the single pile was in accurdance with the site geometry. The initial tangent stiffness (Ktan) was $1.75MNm^{-1}$ with a secant stiffness (Ksec) of $0.87MNm^{-1}$ for 20mm deflection of the pile head. A constant value of maximum bending moment to lateral load ratio $(Max.BM/H)$ was $0.70kN.m/kN$. A trial and error technique was used for the single pile model by varying the soil modulus to obtain the same values of tangent stiffness (Ktan) and $Max.BM/H$ as the single pile test in the field. Figure 6.5 shows that the moduli were defined in relation to the bottom of the sand trench. Five mean values were attributed to sand layers and a single modulus attributed to the clay. It was assumed that the clay modulus was constant while the sand modulus (Gibson soil) varied linearly with depth. The elastic modulus profile for the sand increased from zero at the soil surface to 17MPa at the bottom of the sand, and was taken to be 22MPa in the clay.

Attempts can be made to obtain a secant stiffness (Ksec-m) from the finite element model by back analysis from the single pile test secant stiffness (Ksec). This gives a reduced soil modulus profile, but cannot be applied to pile groups, which have a different deflection mode.

It can be seen from the two different approaches that the soil modulus for the sand is dependent upon its condition and upon the testing mode. For a linear elastic finite element analysis the soil modulus profile obtained from the tangent stiffness of the single pile tests load/deflection (see Figures 4.6 and 4.7 in chapter 4) curve and

Max.BM/H was used.

6.6-Finite Element Single Pile Model

Figure 6.3a and 6.4a illustrate the plan and three dimensional views of the single pile and the soil boundary. The model had to be modified several times in order to satisfy the true nature of the pile soil interaction. The list of the module headers which had to be used in PAFEC 75 to construct and analyse the model are as follows;

Title

1-Nodes

2-Pafblocks

3-Mesh

4-Plates.and.Shells

5-Material

6-Displacements.Prescribed

7-Restraints

8-Stress.Element

9-In.Draw

10-Out.Draw

11-End.of.Data

Each module begins with a header which is called the module record, after which is a record giving headings for the columns which form the remainder of the module. This is called the contents record. For each type of module there is a standard default layout for the columns which is used if the content card is abbreviated. A constant property record can be inserted between the module card and the content card. The data can now be tabulated, but the data within each row of a module must be separated by commas or by spaces. A control module can be used to select primary

routes for the calculation (eg. Plane.Strain). PAFEC75 manual gives in detail the manner in which the input data should be tabulated.

6.7-Finite Element Two-Pile Group Model

Figure 6.3b illustrates the plan view of the two-pile group and the soil boundary. Figure 6.4b shows a 3 dimensional view of the model of a two-pile group. The model had to be modified several times although it was constructed basically in same manner as for the single pile, but with the addition of a pile cap. The number of elements in a two-pile group varied from 836 to 1056 with degrees of freedom varying from 11672 to 15017.

6.8-Required Analysis Using PAFEC75

The PAFEC 75 Finite Element analysis level 6.1 can analyse the whole model and give the results for all nodal stresses in selected Pafblocks only. It was found to be unnecessary to calculate all the stresses in every Pafblock, and so the Pafblocks were grouped and in the Stress.Element module only those groups in which stresses were required were listed for output to files or the printer.

6.9-Control Module

Primary selection of the calculation is defined in a special module known as CONTROL. The economical print known as ECON.PRINT was used to limit the very long print out of analysed results. For a 3 dimensional plastic analysis the 'PLASTIC' and 'SNAKE' modules may to be used in the control module. The 'PLASTIC' module is used in the control module when an elastic-plastic analysis is required, and the Snake module is used in 3 dimensional elastic/plastic analysis.

6.10-Batch Job

Using batch mode in the MTS system is the same as copying the job control command to the MTS system which emulates a card reader feeding the job for execution. A large job like a 3 dimensional finite element analysis is usually run overnight when

the system is quiet.

The cost of the computer time for analysing a 3 dimensional finite element analysis was reduced by using the plane of symmetry along the centre line of the model. Even so, the PAFEC program does not allocate enough temporary memory resource to allow analysis of the half space model, and so the PAFEC.BIG command or instruction had to be used. The PAFEC.BIG enables the user to create large temporary memory files for the analysis, and four temporary files had to be created in the BATCH file. The results from the PAFEC.BIG run were output to an intermediate file from which specific information was copied in batch mode to a temporary file and then printed at the Durham Computer Centre. The reason for having the last temporary file was to reduce the quantity of printed output and eliminate unwanted results. A copy of the batch file is shown in Figure 6.7.

6.11-F.E Linear Elastic Analysis of Single Pile and Two-Pile groups

The linear elastic analysis of single piles and two pile groups is based on modelling of the pile/soil, which has been described in previous sections. From back analysis of a single pile the profile of linear elastic modulus of the sand is taken as zero at the ground surface to 17MPa at the bottom of the sand trench as in section 6.5.2 describing the Soil/Pile system, and mean values were attributed to the appropriate layers in the sand trench. The linear elastic modulus of the clay was taken as 22MPa. The pile/soil model used in this analysis has already been described in section 6.2.

From these analyses the lateral stiffnesses, deflection, bending moments, axial forces and lateral soil pressure were obtained.

6.11.1-Finite Element Elastic Analysis of Single Pile Model (Free Head)

The load on the single pile model was applied as an imposed 26.0mm lateral displacement, at 500mm above the ground line to simulate the same condition as on the site. The load required to displace 26.0mm at 500mm above the ground

line was $36.9kN$ and the displacement at ground line was recorded as 21.0mm. The lateral stiffness K_{g1} of a single pile was measured as $1.75MN.m^{-1}$. Figure B.1a in appendix B shows the deflected shape of the pile. The bending moment diagrams and lateral soil pressure diagrams in front of and behind the single pile due to lateral head displacement of 26mm are presented in Figures B.1b to B.1c in appendix B. The maximum positive bending moment value in the pile shaft was 26.5kN.m, giving maximum bending moment to lateral load ratio of 0.72kN.m/kN. The maximum bending moment occurred at 1.7m below the ground line. The bending moment diagram was almost the same as the site results on the single pile. The lateral soil pressure in front of and behind the pile was equal as is to be expected in linear elastic analysis.

6.11.2-Finite Element Elastic Analysis of a Fixed Head Single Pile

The finite element analysis of a fixed headed pile was also conducted to investigate its maximum and reverse moment and lateral stifness under the same soil modulus profile as for single pile. To simulate a fixed head laterally loaded pile, load was applied as an imposed 26mm displacement at two different locations on the pile head above the ground.

Figures B.2a to B.2c show deflection, bending moment and lateral soil pressure diagrams in appendix B. From finite element analysis the lateral stiffness of a fixed head pile is calculated to be $3.98MN.m^{-1}$. From the bending moment diagram the maximum and reverse bending moments in the pile shaft and head were estimated to be 27.5 and -57.9kN.m respectively, due to lateral displacement of 26mm. The Max.BM/H and Rev.BM/H were calculated to be 0.27 and -0.56kN.m/kN respectively.

6.11.3-Finite Element Linear Elastic Analysis of Two-Pile Groups

The finite element linear elastic analyses of the two-pile groups were based on the linear elastic modulus profile of the soils obtained from back analysis of single pile

tests (see section 6.11.1). The purpose was to analyse the pile groups at the early stage of the loading when the soils parameters behave in a linear elastic manner and assuming the soil is in a similar condition as for the single pile model. 12 cases were considered, pairs of piles at 3,5,8 and 12 pile width spacing with three levels of cap overhang 150,300 and 400mm above the soil surface.

"Loading" was applied as an imposed horizontal pile cap deflection of standardized 20.0mm, for which load was computed. This facilitated comparison of bending moment, axial force and soil pressure changes.

6.11.3.1-Lateral Stiffness of Two-Pile Groups

Figures B.3a to B.14a in appendix B illustrate the deflected shapes of the two-pile groups. The primary response of the two-pile group to an in line horizontal load is of horizontal sway. The front pile settles under the induced downward force while the rear pile is lifted. This condition was observed for all 12 cases studied. The lateral deflected shape of the pile shafts was identical for all cases studied, and so only one detailed plot is shown. There is of course a linear relationship between the load and pile cap deflection from the finite element analyses. The lateral stiffness of a two-pile group (K_{2g}) is described as ;

$$K_{2g} = \frac{Horizontal\ load}{Horizontal\ displacement\ of\ the\ pile\ cap}$$

From finite element analysis the horizontal loads were obtained for 20.0mm pile cap displacement and the K_{2g} were calculated for all 12 cases. The results are tabulated in table T6.2. Figure 6.8 shows the lateral stiffness of two-pile groups against pile spacing, and it can be seen that;

1-The stiffness is greater with lower pile cap overhang.

2-The stiffness increases with increase in pile spacing.

From the deflected shape of the two-pile groups (Figures B.3a to B.14a in appendix

B) it can be seen that there is a small rotation or tilting of the pile cap. The pile head is not fully restrained and thus the head fixity compared with a fixed head single pile lies between the free head and fixed head condition as a function of overhang and spacing.

6.11.3.2-Bending Moment in Two-Pile Groups

The bending moment diagrams are shown in Figures B.3b to B.14b in Appendix 'B' for all 12 cases. The maximum bending moment occurred in the pile shaft at about half of the pile length below the ground line. The reverse bending moment occurred directly beneath the pile cap. As linear elastic conditions and symmetry prevail the bending moments in front and rear piles are equal. Table 6.3 shows the computed reverse and maximum bending moment values. In order to investigate the effect of pile spacing and overhang on the reverse and maximum bending moment, tabulated values in the above table were used. The maximum and reverse bending moments are plotted against pile spacing in Figure 6.9a and 6.9b respectively.

It can be seen from Figure 6.9a that the maximum bending moment hardly changes with overhang and pile spacing. There is of course greater bending curvature on the pile as the overhang increases, but only a small amount.

It can be seen from Figure 6.9b that the reverse bending moment increases with overhang and pile spacing.

The reactions for 20.0mm displacement were computed for all 12 cases and the reverse and maximum bending moments were obtained for prescribed 20mm displacement (see tables T6.3 and T6.4).

If instead the deflection, reverse and maximum bending moment values are calculated for a constant load of, for example 40kN, then a different picture of trends will emerge; see table T6.4. In this case for constant load the maximum bending moment in the pile shaft decreases with pile spacing but increases with pile overhang (see

Figure 6.10a). The reverse bending moment increases with pile spacing and decreases with cap overhang (see Figure 6.10b).

The maximum and reverse bending moments to horizontal load ratio are tabulated in table T6.5.

Figures 6.11a and 6.11b show plots of the ratio of the maximum and reverse bending moments to horizontal load as functions of pile spacing and overhang. It can be seen that the ratio for maximum moment increases with spacing and overhang, while the ratio for reverse moment reduces with pile spacing and overhang.

6.11.3.3-Axial forces in Two-Pile Groups

From computed stresses in the elements comprising the front and back of each pile the induced axial force is calculated. Referring to the deflected shape of a two-pile group horizontal load applied to the pile cap caused axial downward force in the front pile and uplift force on the rear pile. Figures B.3c to B.14c in appendix B shows the axial force diagrams for all 12 cases. The axial force is shed into the soil by some end bearing and by shaft friction. Vertical equilibrium of the pile cap is satisfied. The peak axial force occurs directly beneath the pile cap and is obtained from axial force diagrams. If the peak axial force is divided by the applied force, the peak axial force per unit load is obtained, see table T6.6. Figure 6.12 shows the peak axial force per unit load against the pile spacing. The axial load increases slightly with pile cap overhang and rapidly decreases with pile spacing.

6.11.3.4-Lateral Soil Pressure, Two-Pile Groups

Figures B.3d to B.14d in appendix B show the soil pressure changes on the pile shaft for all 12 cases. The soil gives resistance to the horizontal movement of the pile causing lateral pressure against the pile shaft. As linear elastic conditions prevail the compression on the front face of the front pile is equal to the tension on the rear face of the rear pile and the same for the inner faces. There is a negligible pressure

change with pile spacing and overhang for given 20mm displacement. In Gibson soil the pressure in the front of the front pile reaches a maximum value at about 1.2m below the ground line.

6.11.4-Finite Element Model Pile Cap Stiffness Reduction

In reality, total fixity between piles and pile cap is not achieved, and some relaxation may occur at the pile/cap joint. In order to investigate the consequences of reduced stiffness in the joint, the stiffness of the whole pile cap in the finite element models was reduced by 50% (reducing plate element thickness to 3.0mm from 6.0mm). This was expected to reduce the negative bending moment and increase the maximum bending moment in the pile shaft. Figure B.15a shows the bending moment diagram of a two-pile group at 3 pile width spacing in which the plate elements of pile cap were reduced from 6.0mm to 3.0mm. It can be seen that the maximum bending moment hardy changed in comparison with Figure B.5b. However the reverse bending moment is decreased in the pile cap by about 3% . This small reduction is negligible and no more further analysis was undertaken into this effect.

6.12-Nonlinear Analysis of Two-Pile Groups

When a material is subjected to loading its response may be described, simplistically, as comprising two forms. At very small strains, the behaviour may be nearly linear elastic such that if the material is loaded and unloaded the fibres of the material recover their original size and shape, and the relationship between the stresses and the strains during loading is linear. At large strains plastic behaviour may occur in which the fibres of the material are stressed into the plastic range of the material and the fibres of the material do not recover the original arrangement after unloading; the relationship between stress and strain during loading is typically convex upwards, corresponding to strain softening.

The previous finite element analyses of the site tests were linear elastic, which is appropriate to the initial part of the load/deflection curve. At higher loads the soil

behaves in a non-linear manner and in addition separation occurs between the backs of the piles and soil. In linear elastic finite element analyses the soil adheres to the back of the pile. In practice the non-linear behaviour of load/deflection results in a reduction in lateral stiffness and a re-distribution of bending moment between the piles which indicates non-uniform distribution of lateral load in a pile group.

Stress/strain relations from triaxial tests provided input data to PAFEC 75 of values for yield stress and also the values for the elastic and plastic moduli(see Figure 6.13). In analysing a 3 dimensional elastic-plastic problem PAFEC requires "SNAKES" and "PLASTIC" modules and also three external modules in data preparation:

1-Plastic.Material

2-Incremental

3- Yielding.Element

Before starting this analysis it was important to investigate how the analysis would respond, because of the high computer costs in running a 3 dimensional problem. Data for a 3 dimensional model was prepared, the stress/strain relationship in the material was specified, the analysis of this model was undertaken. However the results from PAFEC75 did not show correctly the specified stress/strain relationship during loading (see Figure 6.13) and it was concluded that with the PAFEC version available, it was not possible to analyse elastic-plastic behaviour and separation in full 3 dimensional system, with a very large number of degrees of freedom.

A semi-iterative procedure was conducted by manually reducing the soil moduli in areas of high strain, and allowing separation to occur where induced tensile stresses exceeded K_o values. This demonstrated that a strain softening model can be built-up, provided that detailed soil stress/strain information is available.

6.13-Discussion

Using PAFEC 75 package in linear elastic finite element analysis of a single pile, the pile/soil system was adequately modelled to match the stiffness and maximum bending moment of the site results. This provided a soil stiffness profile by back analysis. Larger finite element models were then built-up to derive the detailed behaviour of two-pile groups such as were tested on site. Detailed comparisons between the finite element and site recorded stiffnesses and bending moments are discussed in chapter seven.

6.14-Conclusions

The following conclusions were obtained from the linear elastic finite element analyses

1 -The pile/soil system was adequately modelled based on back analysis of the single pile site test.

2 -The stiffness of two-pile groups increases with the pile spacing and decreases with the pile cap overhang.

3 -The maximum bending moment in the pile shaft hardly varies with pile spacing and overhangs for prescribed 20mm pile cap deflection. However for a constant horizontal load, the maximum bending moment reduces with pile spacing and increases with pile cap overhang.

4 -The reverse bending moment increases with pile spacing and overhangs for either constant horizontal load or prescribed pile cap displacement.

5 -The maximum bending moment/horizontal load ratio reduces with pile spacing and increases with pile cap overhang.

6 -The reverse bending moment/horizontal load ratio increases with pile spacing and overhang increase.

7 -The peak axial force/horizontal force ratio decreases with pile spacing and in-

creases with pile cap overhang.

8 -Using PAFEC 75 package in linear elastic analysis of single pile and two-pile groups was satisfactory, but no satisfactory elastic-plastic analysis was achieved.

2
154mm 20 noded prism elements

5.3mm 8 noded plane stress elements
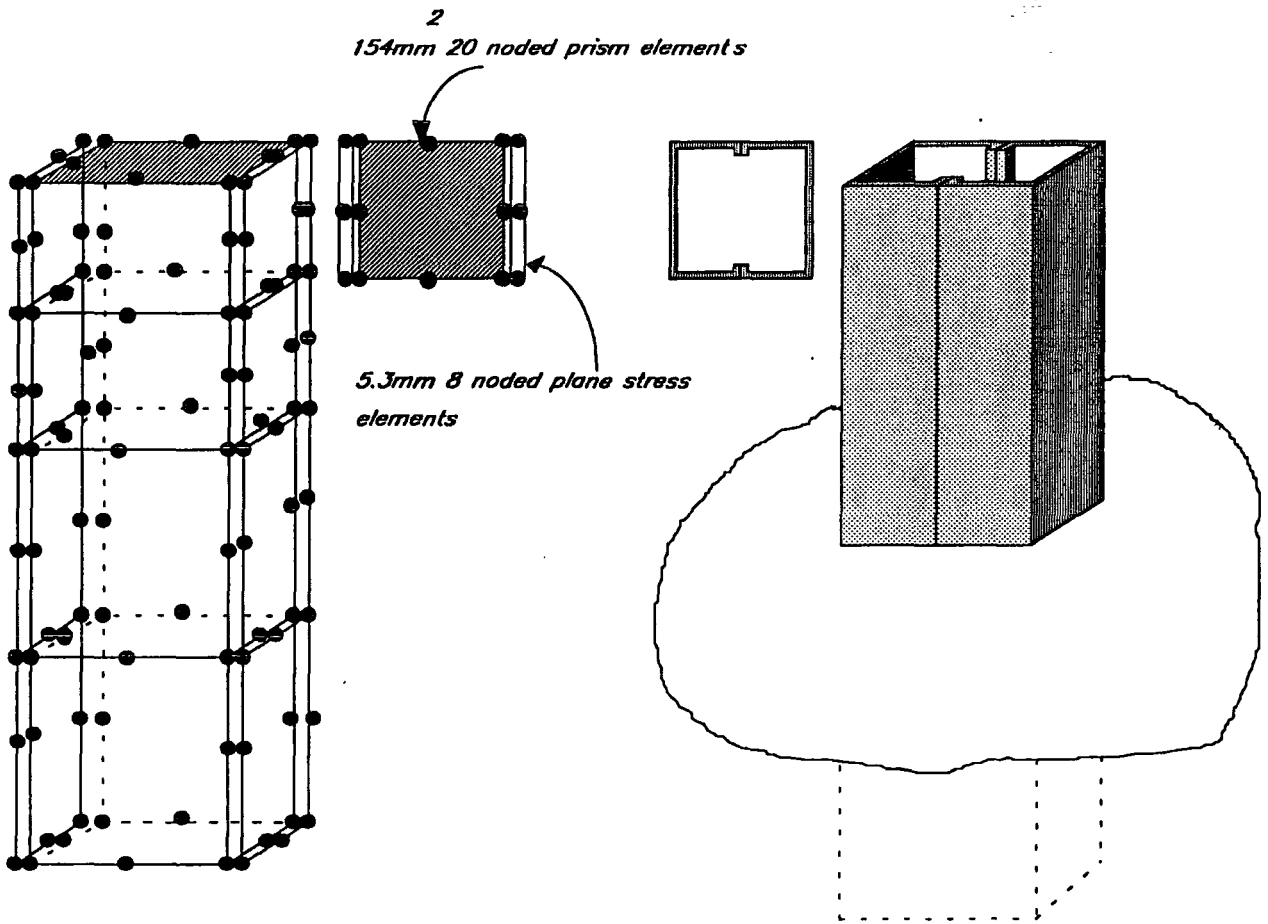
Figure 6.1 Finite element model of pile shaft.

5.3mm plane stress element

Load

Solid shaft
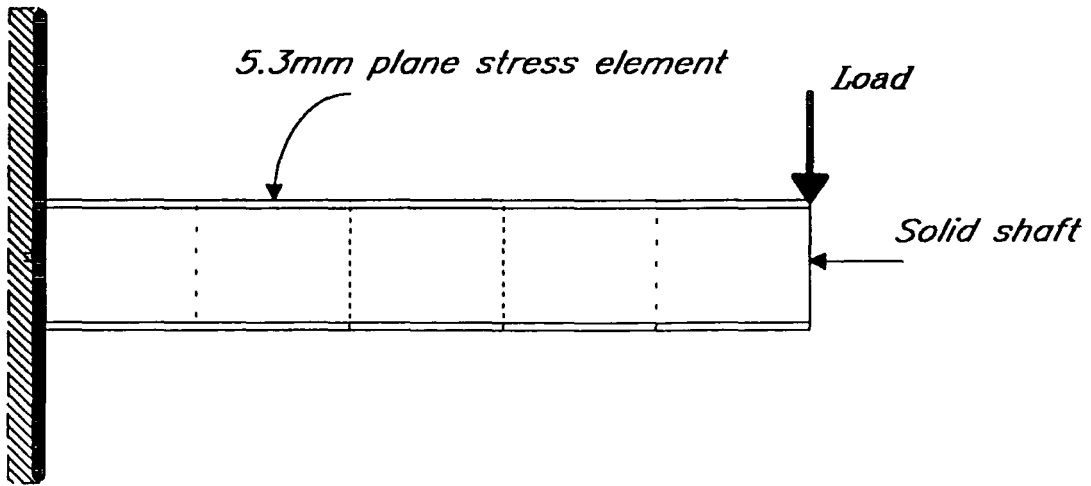
Figure 6.2 Finite element cantilever beam.
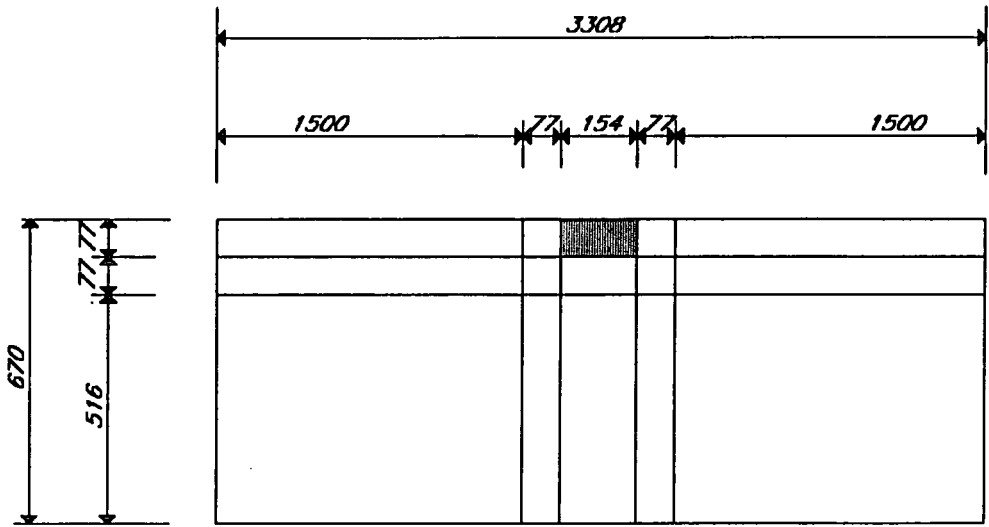
a) Plan view of single pile
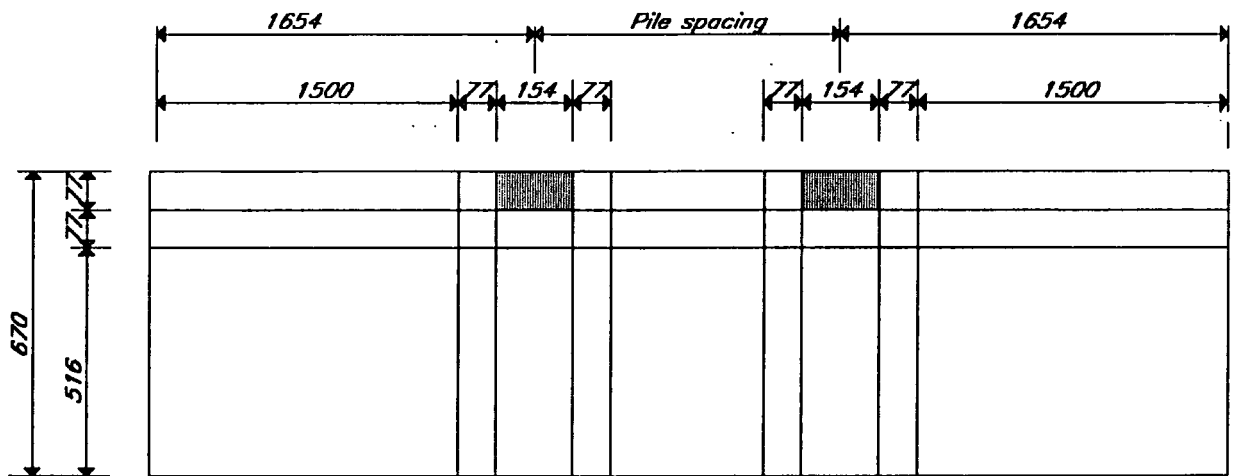
b) Plan view of two-pile groups

Figure 6.3 Finite element plan view of pile/soil model (all dimensions in mm).
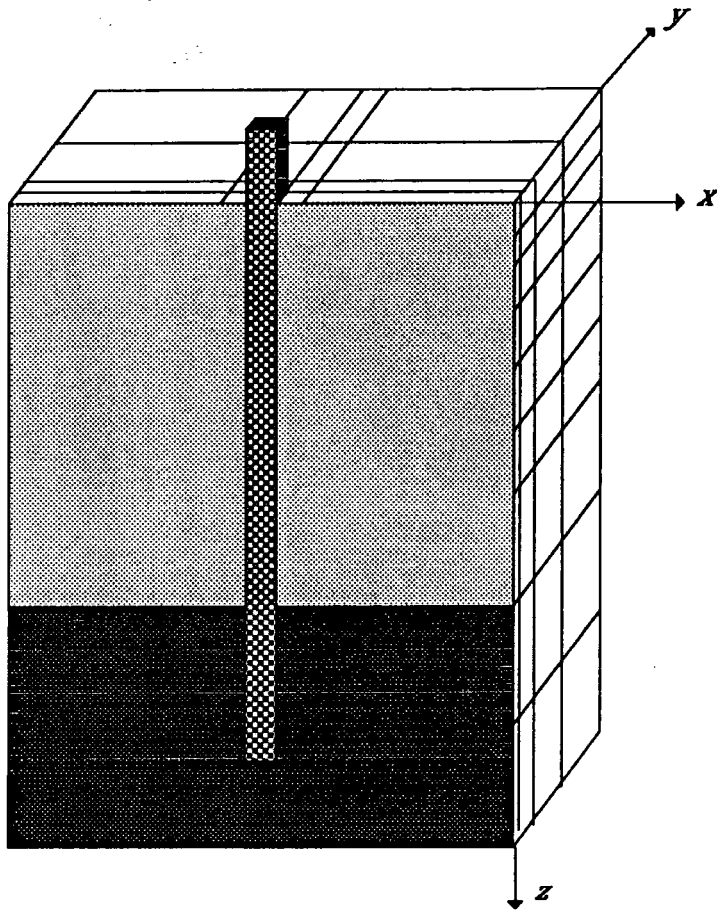
a) Single pile model
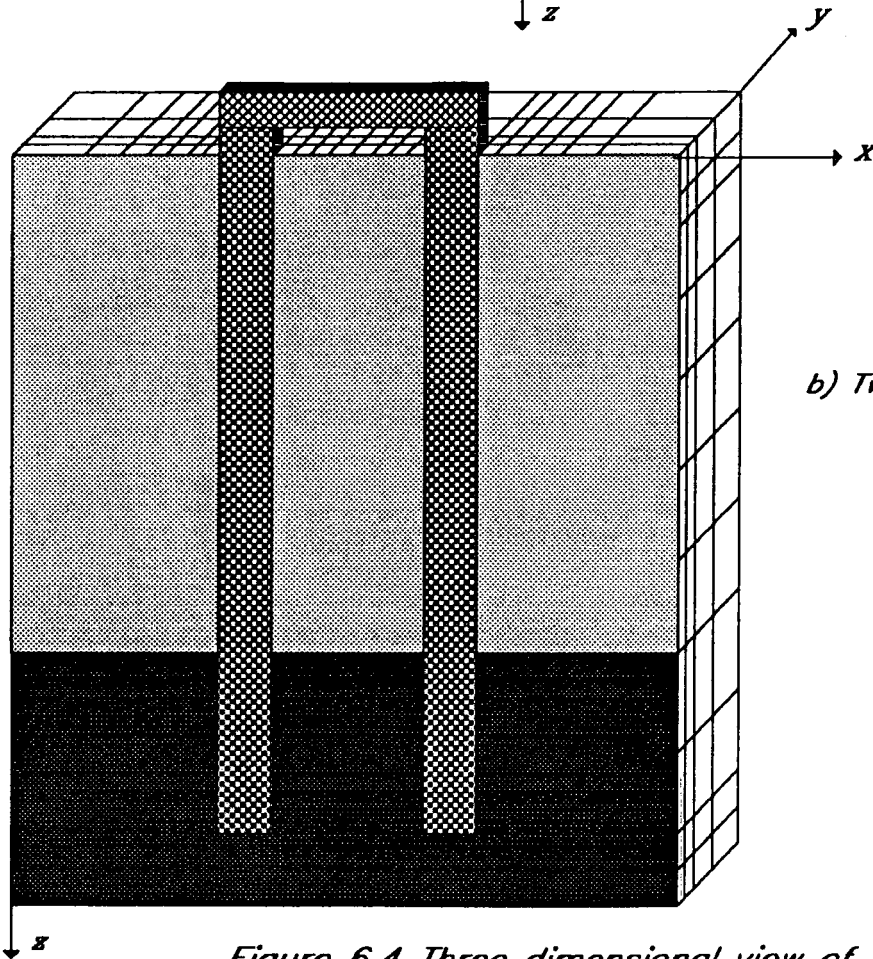
b) Two-pile group model

Figure 6.4 Three dimensional view of pile/soil models.
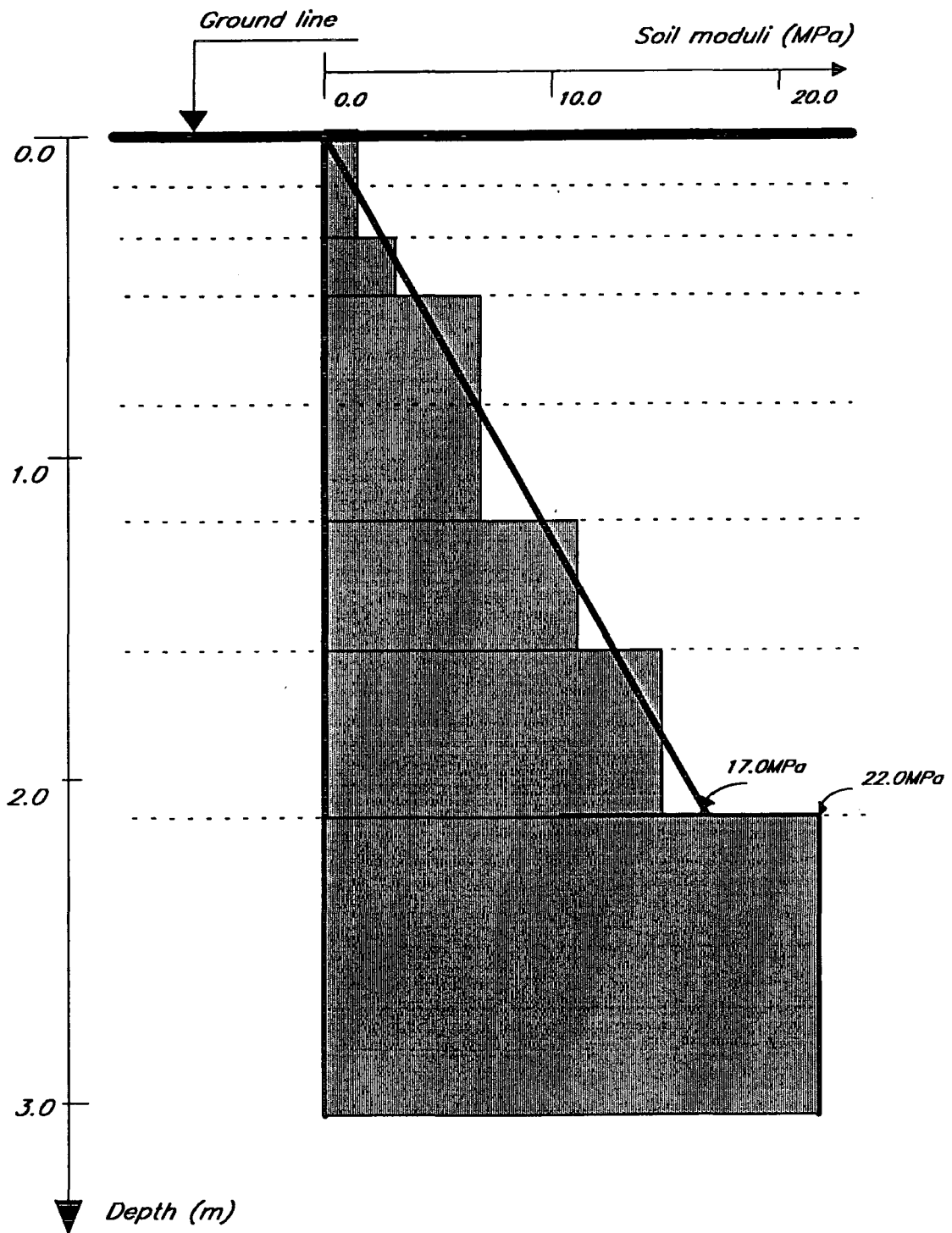
Figure 6.5 Finite element soil moduli profile.
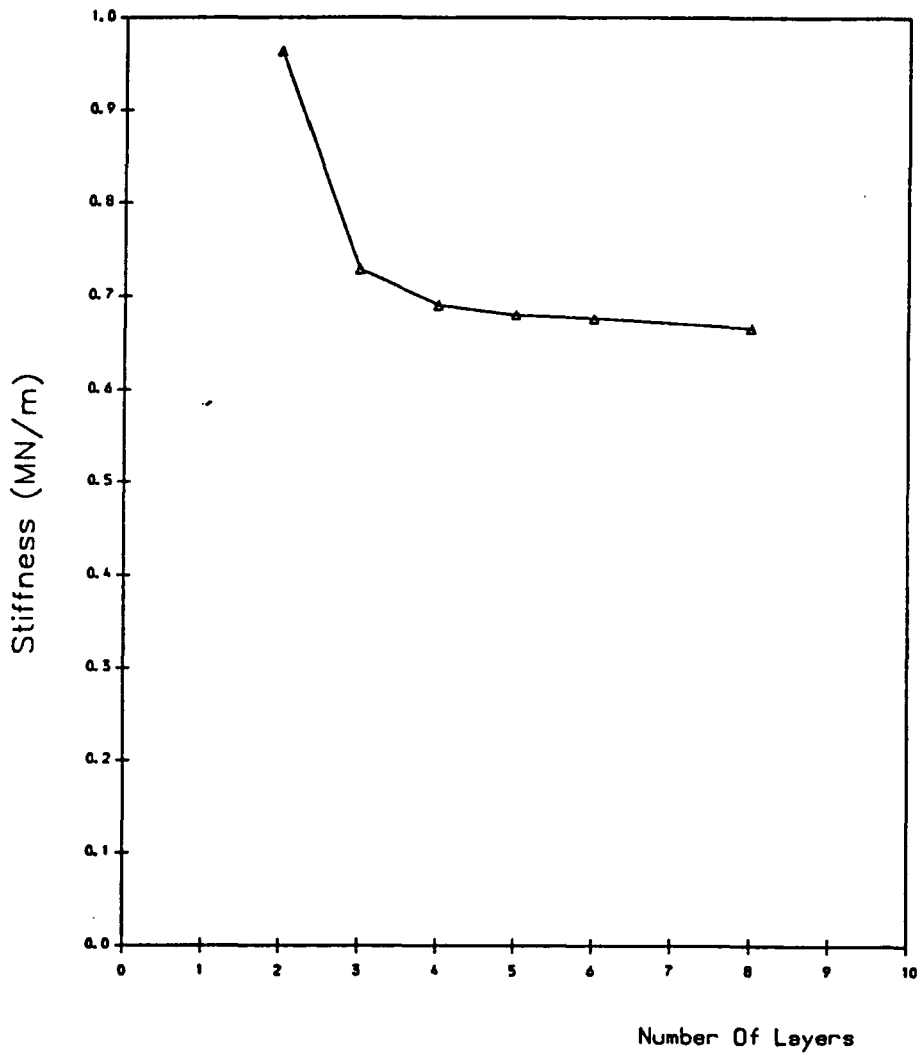
Figure 6.6 Plot of load/deflection against number of layers.

```
$SIG GLP1  t=40000 P=3500
PASSWORD
$CR  -P000001 SIZE=9000P
$CR  -P000002 SIZE=9000P
$CR  -P000004 SIZE=9000P TYPE=SEQ
$CR  -P000013 SIZE=9000P
$CR  3DS400
$ R * PAFEC.BIG SCARDS=3DS4-ELS SPRINT=3DS400 PAR=SIZE=1310720
$C 3DS400(1,1200)  -3DS4
$C 3DS400(3500,4200) -3DS4(*L+1)
$C 3DS400(5200,6520) -3DS4(*L+1)
$SET PROUTE=DURHAMLP
$LIST -3DS4 *PRINT*
$SINGOFF
```

Figure 6.7 A copy of a batch job.

Figure 6.8 Stiffness of two-pile groups against pile spacing for 20.0mm pile cap deflection.
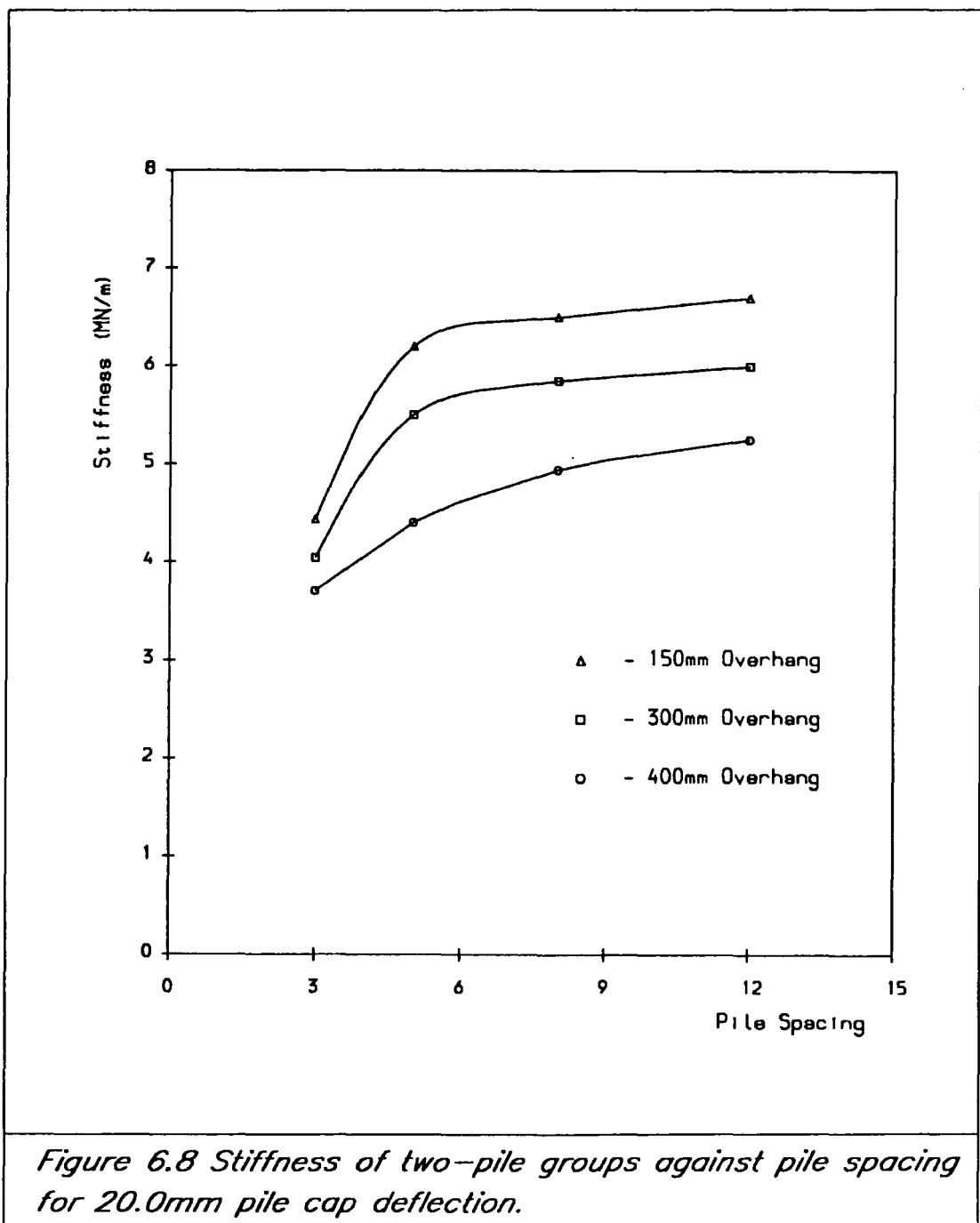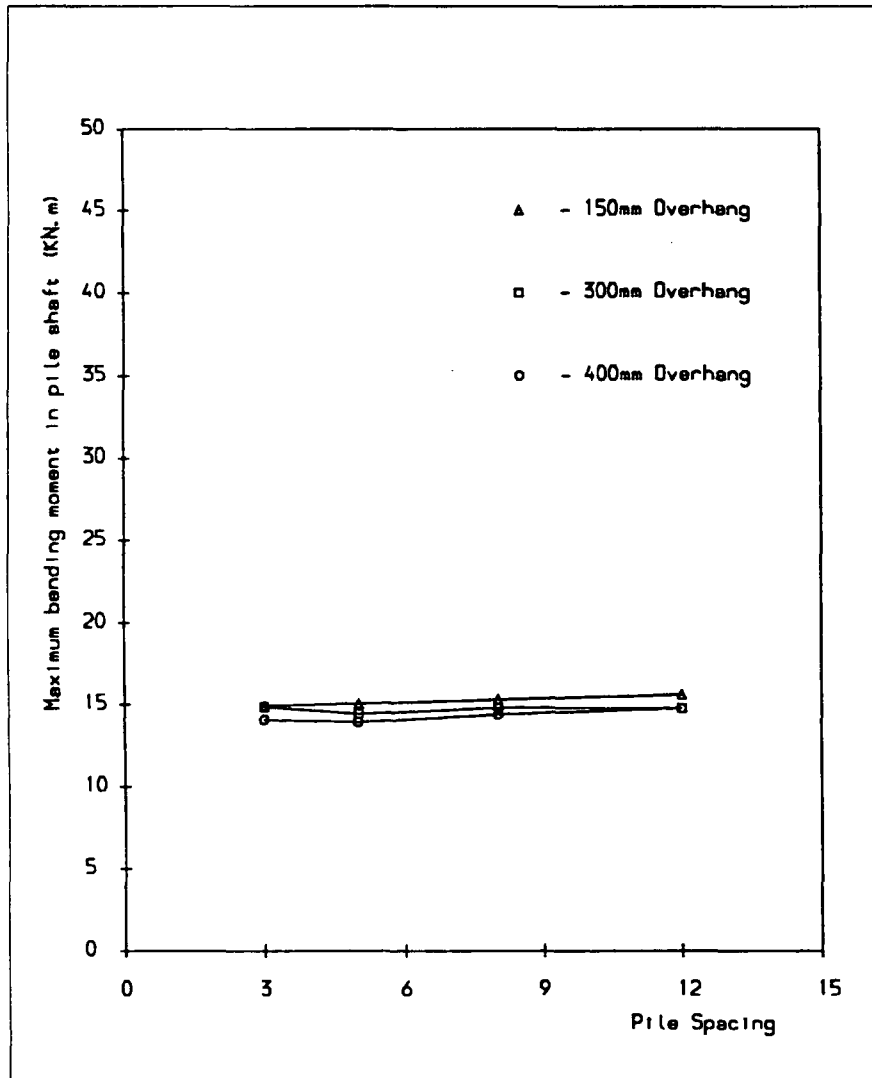
Figure 6.9a· Plot of maximum bending moment for 20.0mm pile cap deflection against pile spacing
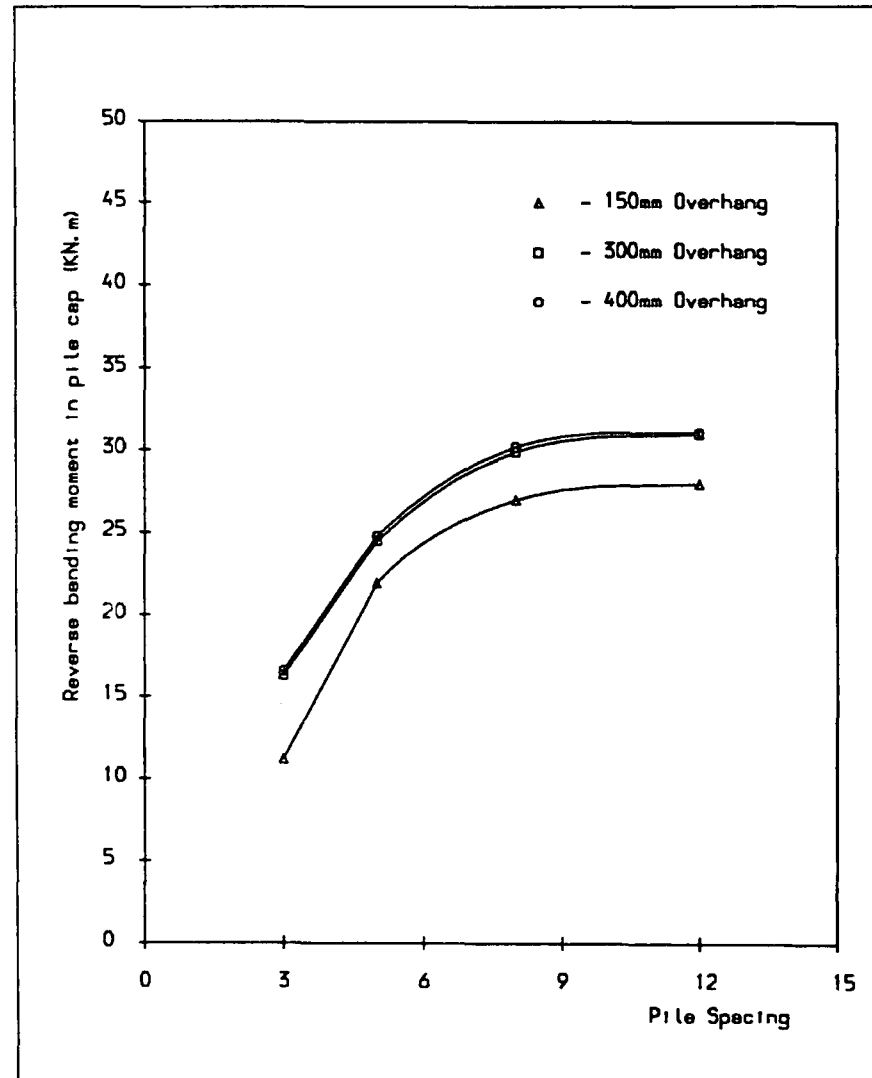
Figure 6. 9b Plot of reverse bending moment for 20.0mm pile cap deflection against pile spacing.
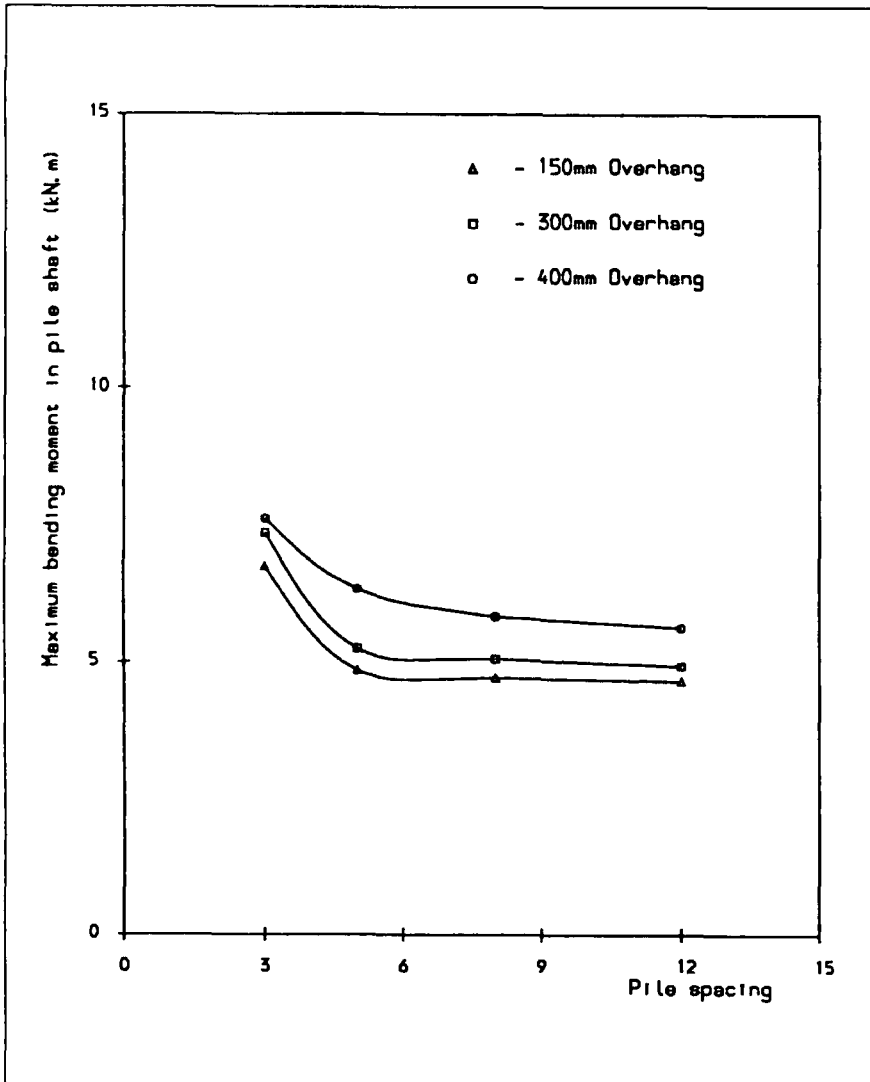
Figure 6.10a Plot of maximum bending moment for constant load (40kN) against pile spacing.
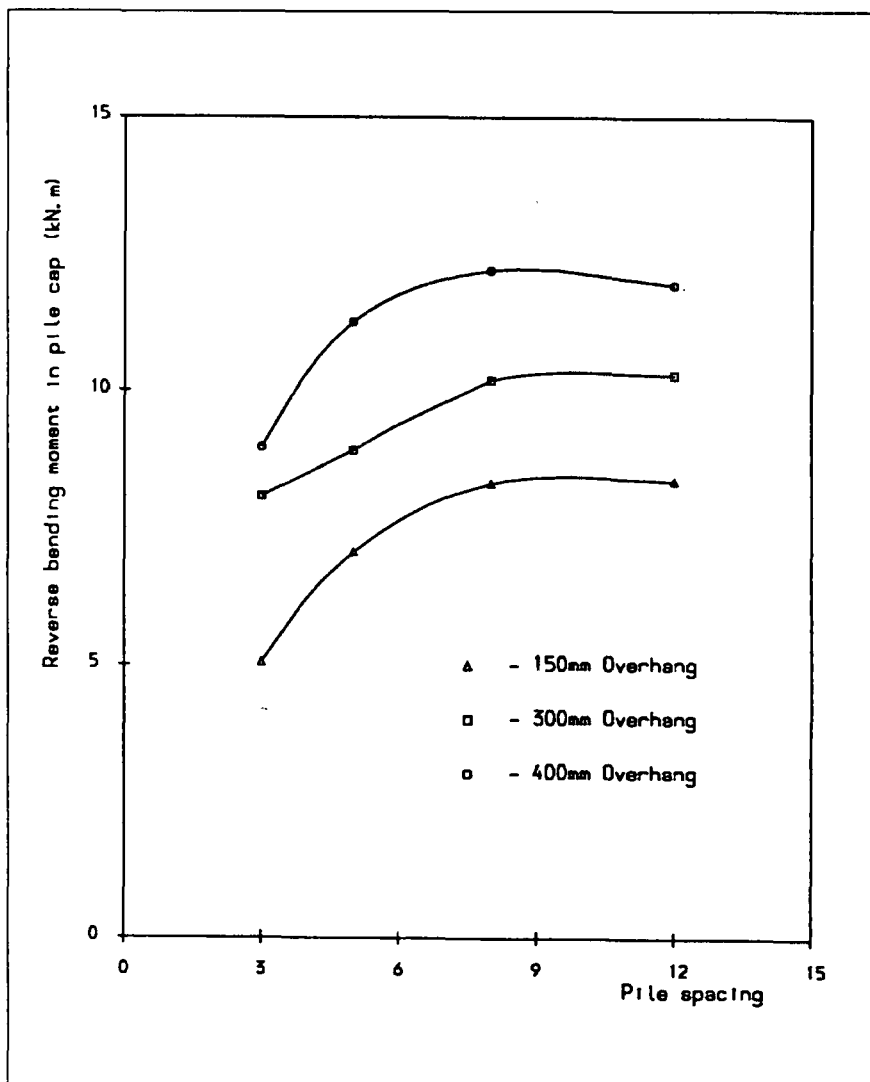
Figure 6.10b Plot of reverse bending moment for constant load (40kN) against pile spacing.
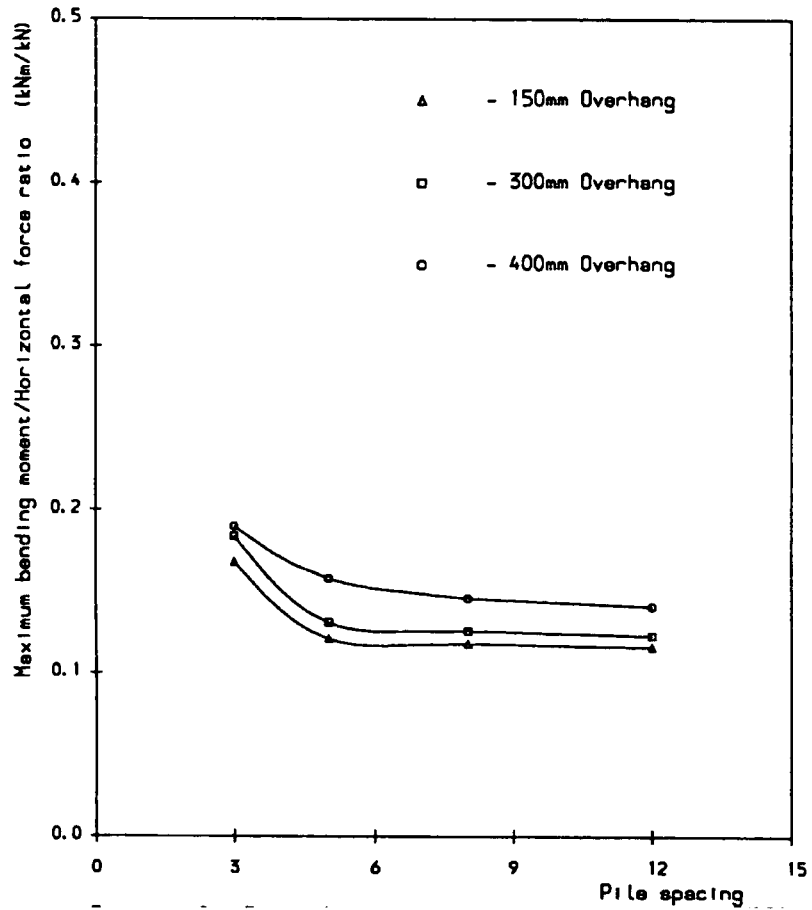
Figure 6.11a· Plot of maximum bending moment/horizontal load ratio against pile spacing.
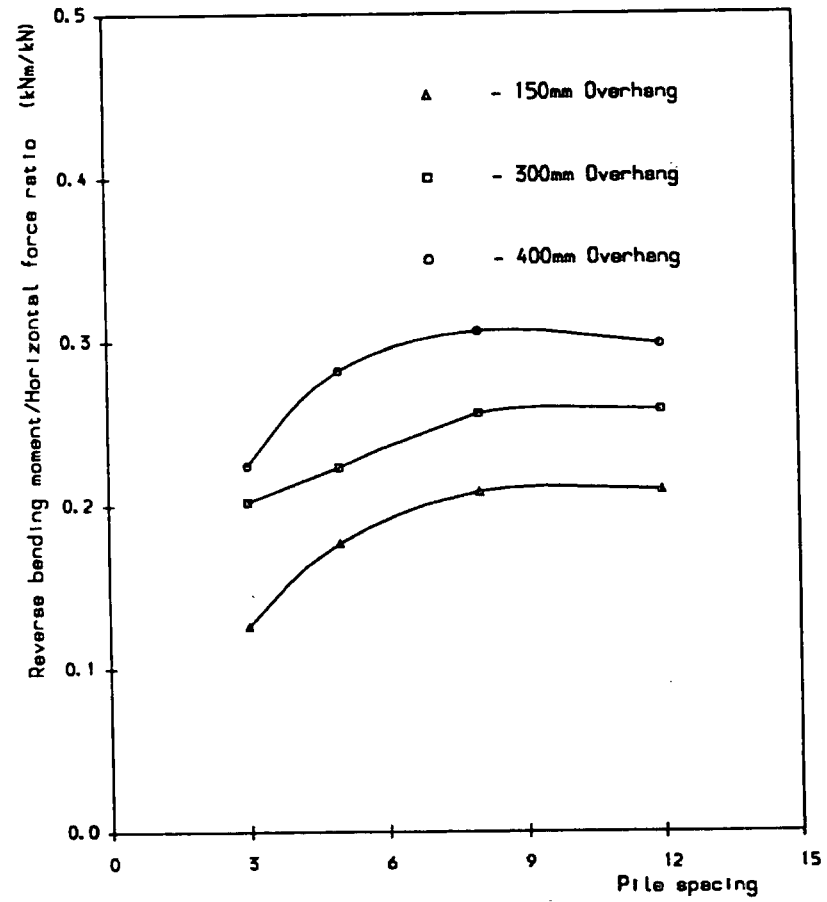
Figure 6.11b Plot of reverse bending moment/horizontal load ratio against pile spacing.
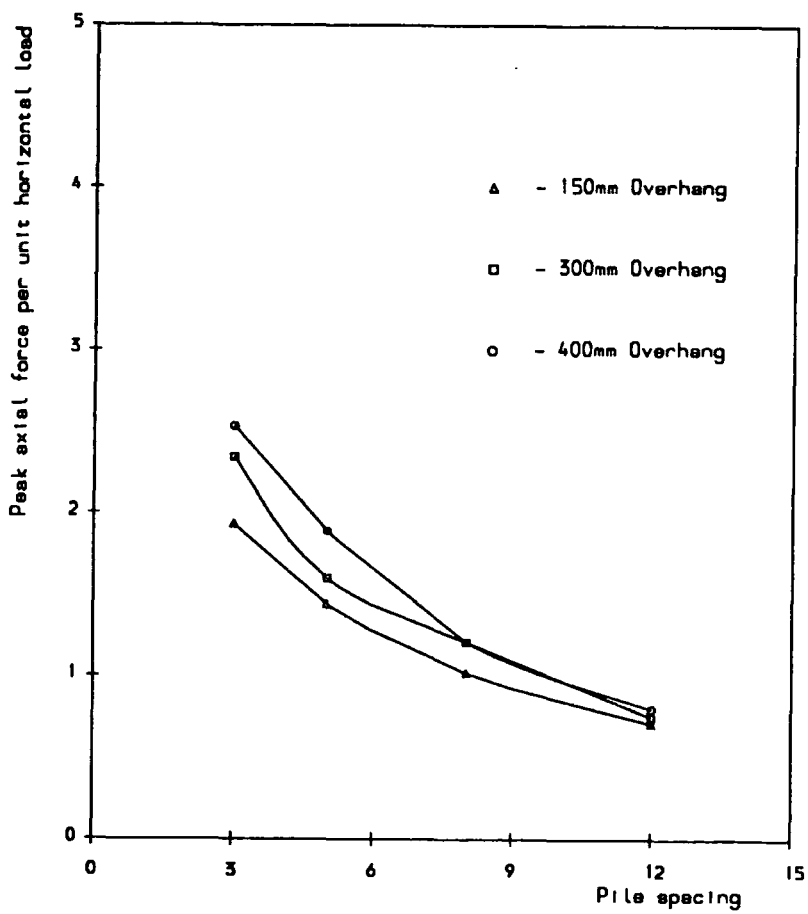
Figure 6.12 Plot of peak axial force per unit horizontal force against pile spacing.
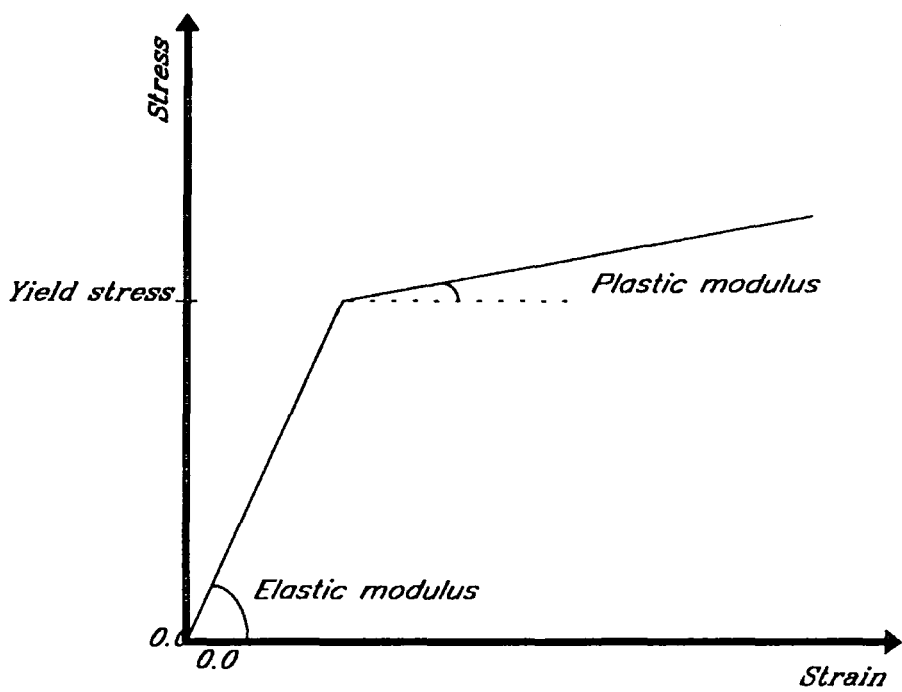
Figure 6.13 Stress/strain relationship.

Table T6.1

Summary of F.E cantilever beam results 20 noded prism element and 8 noded plane stress element											
Theory	Bending stress Nm^{-2}										
	D^*=2.0m	D=1.8	D=1.6m	D=1.4m	D=1.2m	D=1.0	D=0.8	D=0.6	D=0.4	D=0.2	D=0.0
F.E analysis	33.40	24.80	17.20	16.05	13.5	11.35	9.06	6.78	4.53	2.26	0.0
Cantilever beam	22.10	19.90	17.70	15.50	13.30	11.08	8.86	6.64	4.43	2.21	0.0
Deflection (mm)											
F.E analysis	0.0	0.46	1.44	2.86	4.60	6.80	9.27	11.90	14.77	17.70	20.73
Cantilever beam	0.0	0.36	1.02	2.26	3.80	5.71	7.89	10.29	13.80	15.50	18.27

D^* is distance from free end of the cantilever

Table T6.2

Summary of lateral stiffness of two-pile groups for 20.0mm pile cap deflection					
Overhang (mm)	Unit	lateral load and lateral stiffness			
		3 pile width spacing	5 pile width spacing	8 pile width spacing	12 pile width spacing
150	kN	88.60	124.00	130.00	134.00
	MNm^{-1}	4.43	6.20	6.50	6.70
300	kN	80.80	110.00	117.00	120.00
	MNm^{-1}	4.04	5.50	5.85	6.00
400	kN	74.00	88.00	98.80	105.00
	MNm^{-1}	3.70	4.40	4.94	5.25

Table T6.3

Summary of reverse and maximum bending moments for two-pile groups for 20.0mm pile cap deflection					
Overhang (mm)	sign	Bending moment values (kNm)			
		3 pile width spacing	5 pile width spacing	8 pile width spacing	12 pile width spacing
150	maximum	14.93	15.05	15.30	15.60
	reverse	-11.20	-21.90	-27.00	-28.00
300	maximum	14.85	14.44	14.80	14.80
	reverse	-16.30	-24.50	-29.90	-31.00
400	maximum	14.08	13.94	14.40	14.78
	reverse	-16.60	-24.80	-30.20	-31.10

table T6.4

Summary of reverse and maximum bending moments for two-pile groups for 40kN force					
Overhang (mm)	sign	Bending moment values (kNm)			
		3 pile width spacing	5 pile width spacing	8 pile width spacing	12 pile width spacing
150	maximum	6.74	4.85	4.71	4.65
	reverse	-5.05	-7.06	-8.31	-8.36
300	maximum	7.35	5.25	5.06	4.93
	reverse	-8.07	-8.91	-10.20	-10.30
400	maximum	7.61	6.33	5.83	5.63
	reverse	-8.97	-11.27	-12.20	-11.95

Table T6.5

Summary of reverse and maximum bending moments horizontal load ratio for two-pile groups					
Overhang (mm)	sign	Bending moment values (kN.m/kN)			
		3 pile width spacing	5 pile width spacing	8 pile width spacing	12 pile width spacing
150	maximum	0.168	0.121	0.118	0.116
	reverse	-0.126	-0.177	-0.208	-0.209
300	maximum	0.184	0.131	0.126	0.123
	reverse	-0.202	-0.223	-0.256	-0.258
400	maximum	0.190	0.158	0.146	0.141
	reverse	-0.224	-0.282	-0.306	-0.298

Table T6.6

Summary of peak axial force per unit horizontal load				
Overhang (mm)	Peak axial force per unit load			
	3 pile width spacing	5 pile width spacing	8 pile width spacing	12 pile width spacing
150	1.93	1.44	1.02	0.71
300	2.34	1.60	1.21	0.75
400	2.53	1.89	1.21	0.80

CHAPTER SEVEN

Discussion

7.1-Introduction

In this chapter results obtained from field tests, back analysis, various predictive analyses and finite element analyses will be compared and discussed. Comparisons will be made between the observed values, analytical predictions and finite element analyses. The summary and discussion will divided into two sections as follows;

1-Single piles

2-Two-pile groups

There will be a brief summary of results obtained from the field test series, back analysis, predictive analyses and finite element analyses.

7.2-The Response of Singles Pile To Lateral load

The aim of conducting free headed single pile tests was to obtain the soil modulus profile which would be used for predictive analysis of a fixed headed single pile and for the major objective of two-pile group analysis.

The measured load/deflection curves were non linear and the curves were not totally repeatable due to changes in water table level, soil stiffness profile and to a much lesser extent in the soil density. The initial portions of load/deflection curves were nearly linear, so the data from the load/deflection measurements were plotted

for all four single pile tests and a common curve was fitted through the data of the first, second and third test. The data from the fourth test was considered to be non-representative because of a marked reduction in stiffness due to an increase in water table level. The initial portion of this mean curve gave a tangent stiffness of $1.75kN.m^{-1}$ for the single pile.

The relationship between the maximum bending moment and lateral load was almost linear. The ratio was approximately $0.70kN.m.kN^{-1}$ The maximum bending moment on the pile shaft occurred typically at 1.2m, which was well within the sand trench, because the sand trench was nearly 14 pile widths deep (2.1m). Throughout the single pile test series (free head) the lateral behaviour was dominated by the response of the sand. For this reason it was also decided to assume that the soil modulus (E_s) increased linearly with depth even through the pile tip was in clay. The relation between the maximum bending moment and deflection was non-linear, (see figure 4.1) showing the soil modulus reduced at high strain.

Based on the initial part of the load/deflection curve representing elastic behaviour back analysis was then undertaken to obtain the soil modulus profile n_h, and also shear modulus (m). However these values were found to vary substantially depending upon the method adopted. The soil modulus values obtained using different solutions were used to calculate the maximum bending moment in the pile shaft, each giving a different value. The ratio of maximum bending moment to applied lateral load assuming linear elastic properties was compared with the observed ratio from the single pile field test series. The ratio between the theoretical values and field maximum bending moments varied from 0.58 to 1.02. The best agreement was obtained using the solution proposed by Banerjee and Davies(1978) which gives a good prediction compared to the field test results(see table T5.2 chapter 5).

Several linear elastic analyses also provided values for the lateral stiffness of a fixed head pile. Two of the values, those of Budhu and Davies(1987) and Poulos(1971a)

gave almost the same results. Randolph's(1981) method appeared to over estimate the lateral stiffness and Reese and Matlock appear to under estimate the lateral stiffness with values of 7.64 and $3.07MN.m^{-1}$ respectively. Banerjee and Davies (1978) prediction of lateral stiffness of a fixed head pile may be considered reliable because the stiffness obtained was similar to that by Poulos(1971a).

The non-linear form of the lateral stiffness of a single pile was estimated using both the p/u method and the elastic continuum method by quoted coefficients. It was found that the elastic continuum method by Poulos(1973) under estimated by 30% compared with the site values and Budhu and Davies(1988) by 10% compared with the site value. The p/u method also under estimated site values by 24%. Budhu and Davies(1987) method gave the closest prediction of the site values (see Figure 7.1).

In the site tests the initial portion of load/deflection of the pile head gave a lateral stiffness of $1.75MN.m^{-1}$. In finite element analysis the single pile was modelled according to the site geometry. The match in lateral stiffness was achieved by varying the soil modulus until the finite element model gave the same lateral stiffness as the field results. Having obtained the correct soil modulus, the maximum bending moment/horizontal load ratio in the pile shaft was predicted using finite element analysis to be $0.72kNm.kN^{-1}$. The finite element linear elastic analysis over estimated the maximum moment/horizontal load ratio by 3% compared with the bending moment/horizontal load ratio observed in the field series on the single piles. This supported the fact that the single pile model constructed closely represented the pile/soil system.

7.3-The Response of Two-Pile Groups To Lateral Load

The main objective of the programme of field testing was to investigate the response of two-pile groups to lateral load with respect to pile spacing and cap overhang height. The tests were conducted to determine the lateral stiffness of two-pile groups,

bending moment distribution, the maximum bending moment/horizontal load, the reverse bending moment/horizontal load, effect of cyclic loading on lateral stiffness and bending moment, lateral soil pressure changes and axial force distribution. Predictive analyses were undertaken to investigate the above effects, but unfortunately there was no analysis available to investigate the axial forces induced into the two-pile groups. Some of the predictive analyses could not take into account the effect of pile cap overhang. Linear elastic finite element analyses were also undertaken to investigate the above effects. The linear elastic finite element analysis was built-up from the single pile/soil model and the two-pile group finite element model geometry was in accordance with field tests.

In the following section the results obtained from the field test series, predictive analyses and finite element analysis will be presented and compared. The analysis is basically divided into two-groups;

1 -Linear elastic (Tangent)

2 -Non-linear (Secant)

The linear elastic analysis is based on the initial portion of the load/deflection curves while the non-linear is based on 20mm pile cap deflection.

7.3.1.-The Tangent stiffness of Two-Pile Groups

The tangent stiffnesses (Ktan) of two-pile groups were obtained from the initial portion of the load/deflection curves for various pile spacing and overhangs. The Ktan represented the linear elastic behaviour of the pile and soil at low strain. The calculated Ktan are tabulated in table T7.2. The tabulated values of Ktan are the average values calculated for the particular tests. In some tests the calculated values of Ktan were unreliable and were not used in averaging because the accuracy at small deflections was not good. Figure 7.2 shows the average values of Ktan in respect to two-pile group spacings and overhangs.

Back analyses of single pile tests were conducted to determine the soil modulus profile using several different methods. The obtained soil modulus profiles refer to a free headed pile. These modulus profiles were used to predict the linear elastic response of laterally loaded two-pile groups at various pile spacings. The solutions by Poulos(1971,1973,1975) and Randolph(1981) were used to obtain interaction factors. These predictions do not take account of tilting of the pile cap or of cap overhang, and also they are based on slightly different pile sections. Poulos(1971b) assumed the pile to be a rectangular thin beam while Randolph assumed that the pile was a solid circular section with a radius of r. The Poulos(1971b) and Randolph predictions showed that the Ktan increased with the pile spacing. The differences in Ktan values obtained using their solutions were due to the determined interaction factors. At close spacing the interaction factor difference is not significant but, as the spacing increases the difference in interaction factors increases. The values of interaction factors are tabulated in table T7.1.

The linear elastic finite element analyses of the behaviour of two-pile groups showed that an increase in pile spacing increased the lateral stiffness of the two-pile group and also that an increase in overhang decreased the lateral stiffness, as was observed in the site results. In comparing the Ktan values obtained in finite element analysis with the Ktan values obtained from site results and from the predictive analyses, the Ktan values tended toward an upper limit at large spacings as did the Poulos and Randolph Ktan curves. The Ktan values obtained by finite element gave the closest agreement with the site results because an accurate model of the pile/soil system was used and tilt of the pile cap in a two-pile group was incorporated so that induced axial forces were assessed. In comparing the finite element Ktan values with the predictive analyses the Poulos and Randolph curve over-estimated the Ktan partly because their values were for zero overhang. The extrapolation of finite element Ktan curves for zero overhang showed that the error due to this effect was approximately

20%. The Poulos prediction of Ktan gave a better agreement with the finite element solution than the Randolph solution by some 15% (see Figure 7.2). The calculated average values of Ktan from load/deflection curves, predictive methods and by finite element are tabulated in table T7.2

It should be noted that the published Randolph and Poulos values are for zero pile cap overhang and they do not incorporate pile cap tilting while the site Ktan values incorporate pile cap tilting. The soil moduli obtained from back analysis refer to the free head pile condition and so some errors may be introduced when they are used in prediction analysis for a fixed head condition since the deflected profile of a pile is different in the free head and fixed head conditions. It should recognised that calculation of Ktan values from the site load/deflection curves was a difficult task because the accuracy of the load/deflection measurements was low for small deflections. The variations observed on site with different pile spacing were affected by seasonal changes in soil properties (soil density and soil moisture).

7.3.2-Secant stiffness of Two-Pile Groups

The secant stiffnesses (Ksec) were calculated from the load/deflection curves for a 20mm pile cap deflection, representing some non-linearity of soil behaviour. In some tests direct Ksec values could not be derived because the pile group could not be deflected to 20mm, so an extrapolation procedure was adopted, particularly for the eight pile width spacing tests. The calculated Ksec values are tabulated in table T7.3. Only Poulos (1975) offered predictive charts for the non-linear behaviour of two-pile groups. Poulos' method was used to produce load/deflection curves and the secant stiffnesses were calculated from the load/deflection curves (of zero overhang) for 20mm pile cap deflection. Values of Ksec are tabulated in table T7.3.

The p/u method was not used to predict the Ksec because in utilising the p/u method a factor is required to take into account pile-interaction. A non-linear finite element analysis could not be undertaken partly because of the excessive computer

time required for a three dimensional iterative solution, and also because of a lack of a knowledge of the soil stress/strain curves at large compressive strains and also in tension. Site tests showed wedge shape zones bounded by tension cracks, indicating that a realistic finite element analysis would be difficult and expensive.

The comparison between the Ksec from the site results and by Poulos' prediction is in very good agreement and the maximum error is within 15% of the site values Ksec for 150mm overhang. However extrapolation of the site results to zero pile cap overhang does not improve the error. Both site and Poulos Ksec curves showed that at large pile spacing the Ksec tends toward a limiting value. This close agreement suggests that the non-linear prediction method by Poulos performs well even though pile cap tilt is not included. Figure 7.3 shows the distribution of Ksec values from site and by Poulos prediction with respect to pile spacing and overhang heights. It should be mentioned here that the calculated Ksec for 8 pile width spacing at 150 and 300mm pile cap overhang did not give good results because an extrapolation technique was needed to calculate the Ksec for 20mm pile cap displacement.

7.3.3-Cyclic Effect on Secant Stiffness of Two-Pile Groups

The effects of limited cyclic loading were investigated by applying 5 cycles of lateral loading in all tests except for the eight pile width set. The primary effect of a small number of cycles of loading was the reduction of lateral secant stiffness by approximately 20%. The values of Ksec for the first and cycles fifth of loading are tabulated in table T7.4. No analysis was available for cyclic loading.

7.3.4-Bending Moments on The Two-Pile Groups

In order to assess the pile bending moments within the two-pile groups in respect to pile spacing and overhang height the following parameters were investigated: the ratio of maximum shaft bending moment/horizontal load (Max.BM/H), reverse bending moment/horizontal load (Rev.BM/H), and the bending moment distribution between the front and rear pile.

7.3.4.1-Maximum Shaft Bending Moment/Horizontal Load

Throughout this investigation it was found that the ratio of maximum shaft bending moment/horizontal load was effectively linear. In the field test series on the two-pile groups it was found that the maximum bending moment/horizontal load ratio was strongly affected by seasonal changes, the max.BM/H ratio being higher during a dry season than a wet season. The Max.BM/H ratio was found almost constant regardless of pile spacing but, as the pile cap overhang increased so did the Max.BM/H ratio (see Figure 7.4). Finite element analysis of the maximum bending moment/horizontal load showed that for a constant cap deflection of 20.0mm the maximum bending moments in the pile shafts were nearly constant $(20kN.m)$ for various pile spacings and overhangs. When the results were investigated for a constant horizontal load of $40kN$, these results showed that the maximum bending moment/horizontal load ratio decreased with the pile spacing and increased with the pile cap overhang. Figure 7.4 shows the variation in the maximum bending moment/horizontal load values with respect to pile spacing and overhang height.

The site values of Max.BM/H differed from the finite element analysis by around 50% which was due partly to the seasonal effect that caused the Max.BM/H of the site to be greater than the finite element values because in the finite element model the soil modulus was deduced from single pile tests undertaken in a wet season. In order to try to discount the seasonal effect a mean value for each different overhang was calculated which then showed a trend with respect to overhang similar to that from finite elements. The variation of site Max.BM/H with pile spacing could not be deduced because it was lost within the seasonal variations. In finite element analysis the Max.BM/H values reduced with pile spacing towards a lower bound and increased with increase in pile cap overhang.(see Figure 7.4). The values of Max.BM/H ratio from the field tests and finite elements are tabulated in table T7.5.

7.3.4.2-Reverse Bending Moment/Horizontal Load

The reverse moment reaches its maximum just beneath the pile cap. In order to investigate this effect with increase in pile spacing and overhang, extrapolation was required to obtain the maximum reverse moment beneath the pile cap. The extrapolation of the bending moment diagram was necessary because direct readings could not be obtained at the pile/cap junction due to local effects. Figure 7.5 shows the site values of Rev.BM/H with respect to pile spacing and overhang. The solutions using Poulos' and Randolph coefficients indicates that the Rev.BM/H is constant and does not increase with pile spacing. The finite element results showed the correct trend of Rev.BM/H increasing with pile spacing, although the estimates were lower than the site values except for very close pile spacings. An erroneous point occurred for five pile width spacing and 400mm overhang caused either by extrapolation technique or by an instrumentation problem. The values of Rev.BM/H from field tests results, finite element and Poulos' method are tabulated in table T7.6.

7.3.4.3-Cyclic Loading Effects on Reverse Bending Moment/Horizontal Cyclic Load

The effects of cyclic loading on Rev.BM/H load was investigated by comparing the averaged maximum reverse moment/horizontal load ratio from first cycle of loading to the final cyclic loading. The comparison is shown in Figure 7.6. Despite the scatter of Rev.BM/H values for static loading a pattern does emerge. Both static and cyclic values of Rev.BM/H are tending toward a maximum as spacing increases, and the cyclic moments are generally larger than the equivalent static values because the soil modulus is modified by cyclic loading. Taking into account the unrealistic points and ignoring these values it can be suggested that the cyclic loading has increased the Rev.BM/H ratio by typically 25% from the static values.

7.3.4.4-Bending Moment Distribution Between Front and Rear Pile

The degree of unequal distribution of moments was investigated by determining

the ratio of the maximum positive bending moments in the shafts of the front and rear piles. The ratios obtained from field test series failed to show a clear trend. This was due to the seasonal effects and imperfect control on soil density. However the mean overall ratio calculated was 1.08 for all the results obtained from two-pile group tests. The mean ratio suggested that the front pile typically attracted a shaft moment of 8% higher than in the rear pile. This ratio was similar to that obtained by Arta(1986) in model tests. A similar effect of unequal distribution has been reported by Brown et al (1987 and 1988) on nine-pile group tests and Long(1987) on his model piles. Both Brown et al(1987 and 1988) and Long(1987) reported that the distribution of moments are in respect to rows of piles in the pile groups. This ratio is in disagreement with the theories of the elastic continuum by Poulos (1971b, 1973 and 1975) and Randolph(1981) which propose that the piles in a two-pile group would carry equal load effects and moment effects, as is obtained also by linear elastic finite element analysis.

7.3.4.5-Seasonal Effect on Bending Moment

In the field tests series on the two-pile groups it was found that the maximum positive bending moment/horizontal load ratio was strongly effected by seasonal changes, with high Max.BM/H ratios during a dry season. The seasonal changes in the Max.BM/H ratio were found to be dominant by comparison with the effect of pile spacing. Conversely, the reverse bending moment/horizontal load ratio did not appear to be affected by seasonal changes.

7.3.5-Axial Forces In Two-Pile Groups.

When two-pile groups are laterally loaded the front piles attract axial compression while the rear piles carry tensile or uplift force. The magnitude of the induced axial forces is of considerable significance with respect to pile group design. Very few large scale tests of laterally loaded pile groups have been undertaken in which axial load has been measured and so it was felt that the determination of the axial force distribution

would be of some significance. The axial forces along the length of the front and rear piles were determined from the recorded strains in the pile walls. The axial forces in the front pile and the rear pile were found to be nearly equal but of opposite sign. This indicated that equilibrium was satisfied during the field tests, and gave credibility to the measurements.

The variation of the axial forces in the two-pile groups with respect to pile spacing and overhang height was investigated in such a manner that the average peak axial forces in the two-pile groups were determined from axial force diagrams and the average peak axial forces were divided by the corresponding lateral load to give the average peak axial force per unit load. The average peak axial forces per unit load found were found to decrease with pile spacing and to increase with an increase in pile cap overhang height. A family of straight lines was determined and equations were derived to describe the average peak axial forces in the two-pile groups. Values of induced axial load were typically 2.5 times the applied lateral load for 3 pile width spacing and 400mm pile cap overhang height and 0.9 times the lateral load for 12 pile width spacing and 150mm pile cap overhang height (see Figure 7.7).

In the linear elastic finite element analyses the axial forces were determined in the pile shafts, which showed that the axial force in each pile reaches its peak beneath the pile cap. Nearly similar results were obtained from the field tests series. Figure 7.7 shows the comparison between the peak axial forces per unit load obtained from the field tests results and finite element results. Both results showed that the peak axial force per unit load decreases with pile spacing and increases with pile cap overhang heights. The finite element results showed only small changes with overhang while the field tests showed greater sensitivity. Although the discrepancies between the site values and finite element forces vary from just a few percent, up to some 70% the acquisition of realistic axial loads should not be underestimated. The values of average peak axial force per unit horizontal load from field test and finite elements

are tabulated in table T7.7.

7.3.6-Lateral Soil Pressure Changes

An attempt was made to measure total lateral soil pressure against the pile walls. Unfortunately no reliable results were obtained because axial forces in the pile wall caused the diaphragms of the pressure cells to buckle and to give unrealistic results.

In linear elastic finite element analysis, the lateral soil pressures on the outer faces of the piles in the group were equal but of different sign. The inner face pressures were also equal but of opposite sign (see Figures B.3d to B.14d in appendix B). The lateral soil pressures on the outer faces were greater than on the inner faces. The lateral pressure was not effected by pile group spacing or overhang, for the imposed displacement of 20mm to the pile cap. It is unfortunate that there were no reliable results of the soil pressure from the site, preventing any comparisons.

7.4-Evaluation of Results

Despite the variations in the results obtained from the field test series, predictive analyses based on charts by Poulos and Randolph gave values of lateral deflection and moments which were generally within 50% of the site values. The predictions may be considered reasonable because these two methods provide comprehensive charts and equations for analysis of laterally loaded pile groups. Some error in prediction of Ktan and bending moments is due the fact that the methods do not allow pile cap tilting. The predictions can only assume that the pile head is either fully restrained or free to rotate. No estimates are possible of induced axial forces. The results on the site showed that the pile fixity condition lay between the free and fixed condition. The other main source of error lay with the soil modulus profile adopted, which was based on back analysis of a free headed single pile. The soil modulus profile obtained from a free headed pile test may not accurately reflect the profile for a fixed headed pile due to the different pile deflection profile. Also in back analysis a simple linear soil modulus profile was assumed which may not be a good description of site conditions.

In addition the soil modulus profile was seen to vary at the site with seasonal effects as previously discussed in section 7.3.2.5. A strong point in favour of these methods was that they could be modified to estimate results at larger displacement, in addition to linear elastic analysis.

The finite element solution generally predicted the behaviour of the site tests to within some 15% and in addition induced axial forces were estimated. Consequently the results were superior to the theoretical solutions for linear analysis. The reason for this was that the model of the pile/soil system was constructed according to the site conditions and pile geometry. The finite element solutions were able to predict the Ktan, bending moments, axial force and lateral soil pressures. The problem of using the three dimensional finite element analysis is its expense and the need for a correct and complex model of pile/soil system to predict the behaviour. A particular advantage of using three dimensional finite element analysis was the prediction of axial forces in the piles. The axial forces obtained by finite element analysis were close to the axial forces obtained from the field tests series. Whilst it is possible to modify a finite element solution to include plasticity, this was not possible in this work because of the size of the matrix of 3 dimensional elements.

7.5-Conclusions

In the this chapter comparisons have been made between the field tests series, predictive methods and finite element analysis. Conclusions are as follows;

1 -Load/deflection curves and maximum bending moment/horizontal load ratios for single pile field test results were used effectively to back analyse soil stiffness profiles. These showed fair agreement with soil stiffness tests.

2 -The field test results were clearly affected by seasonal variations in ground conditions. In particular, pile shaft moment/lateral load ratios showed major variations with wet/dry seasons.

3 -The predictive methods did not allow for pile cap tilting which introduced some error in comparison with site results.

4 -The finite element analysis provided reasonable agreement with the two-pile group field tests, for the linear elastic condition.

5 -An important feature of the 3 dimensional finite element analysis was the satisfactory estimation of induced axial forces in two-pile groups.

6 -Non-linear finite element analysis could not be undertaken because of cost and computer storage limits. The "predictive" methods were capable of estimating nonlinear behaviour.
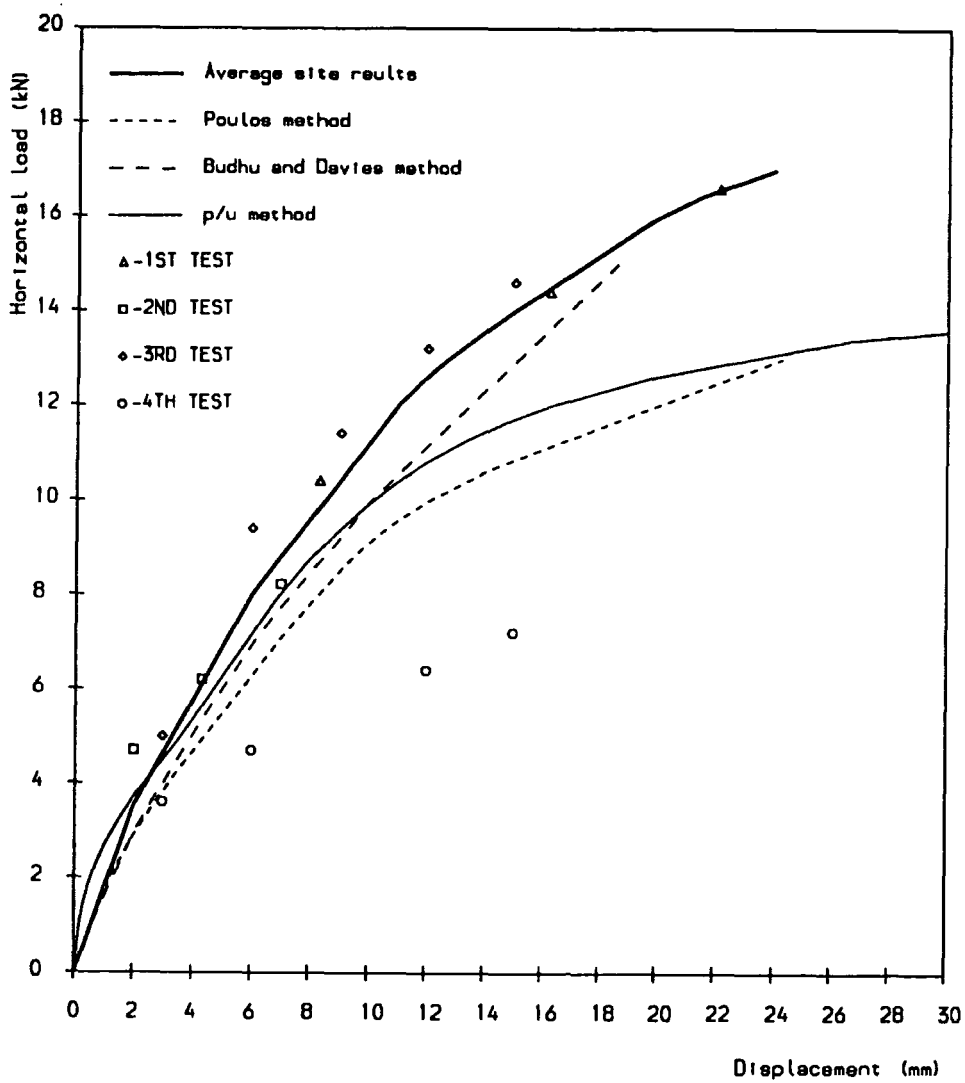
Figure 7.1 Load/deflection curves for single pile.
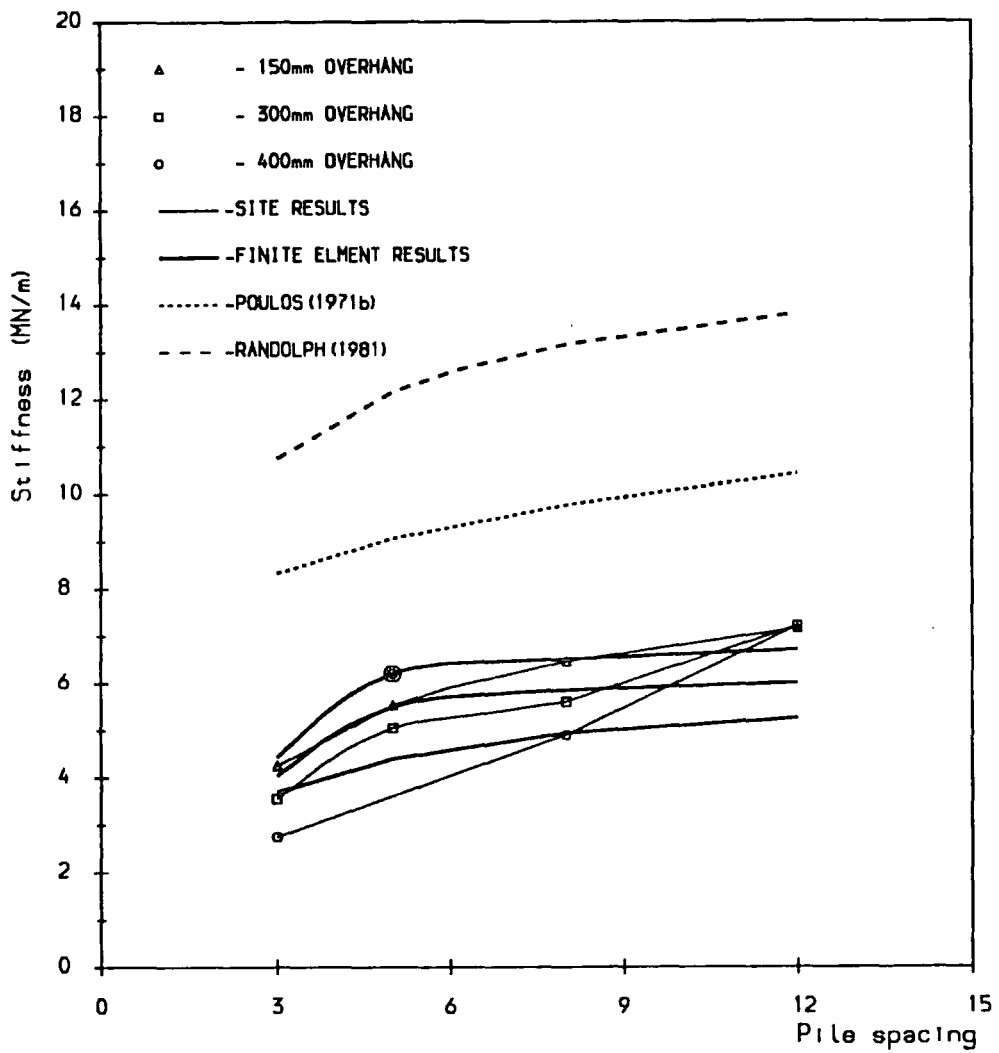
Figure 7.2 Tangent stiffness of two-pile groups against pile spacing.
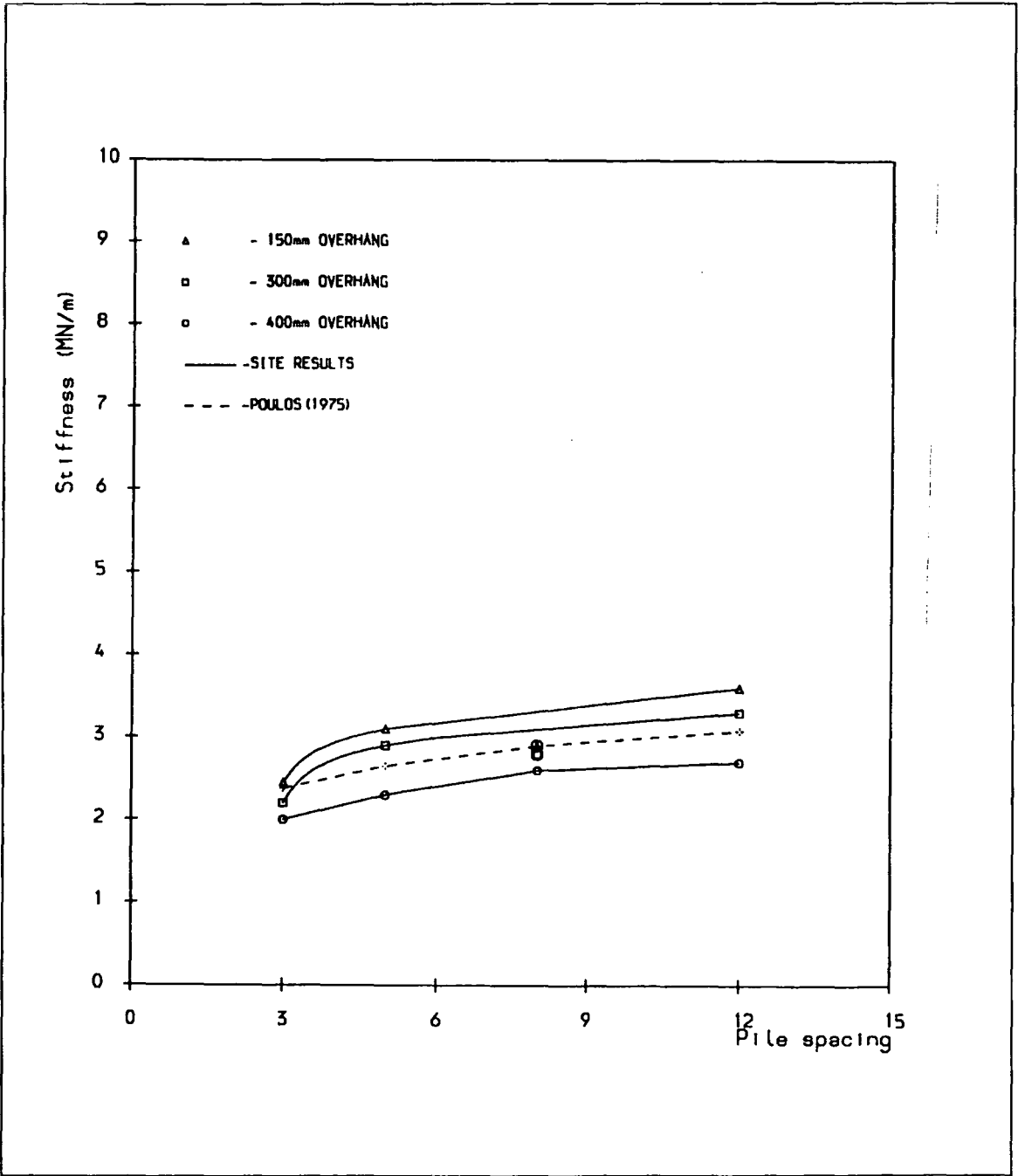
Figure 7.3   Secant stiffness of two-pile groups against pile spacing.
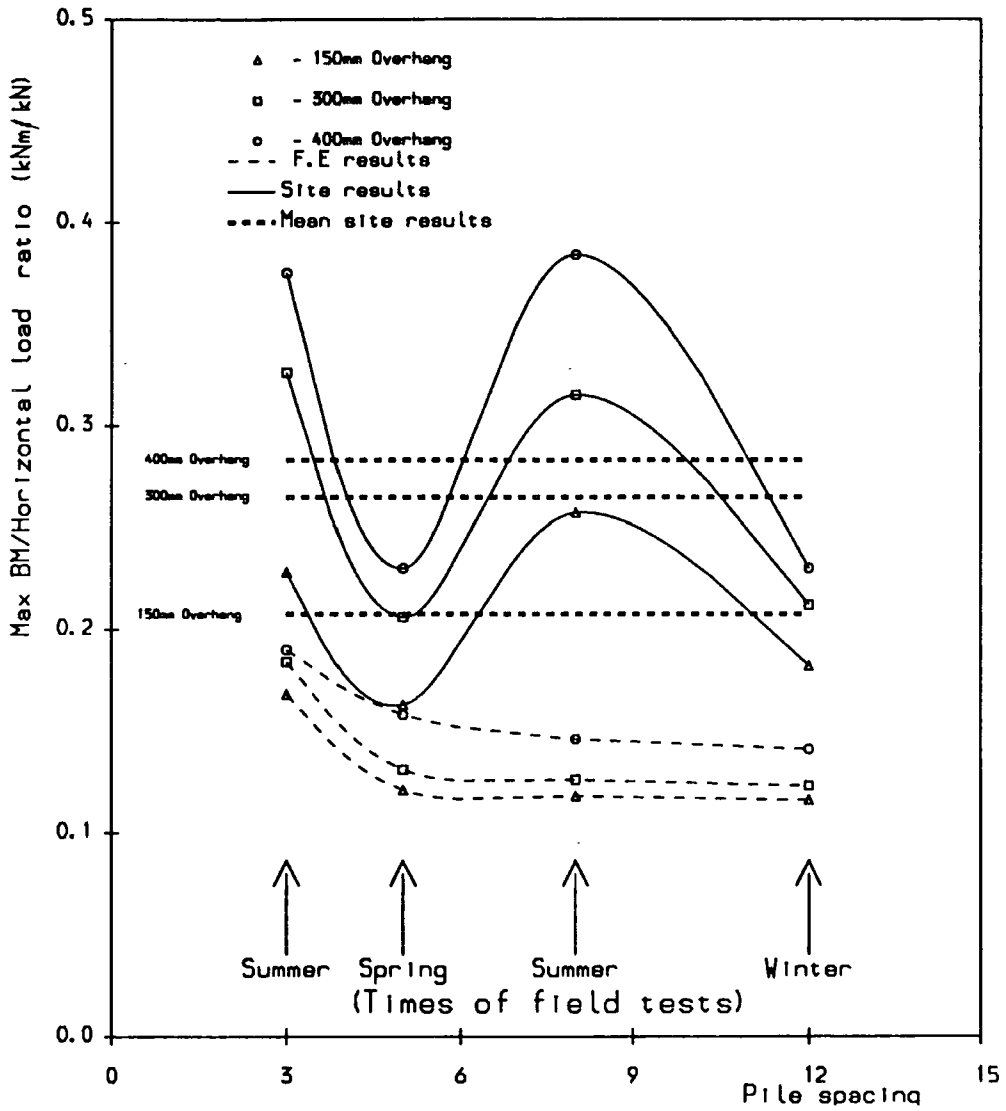
Figure 7.4 Plot of maximum bending moment/horizontal load ratio against pile spacing.
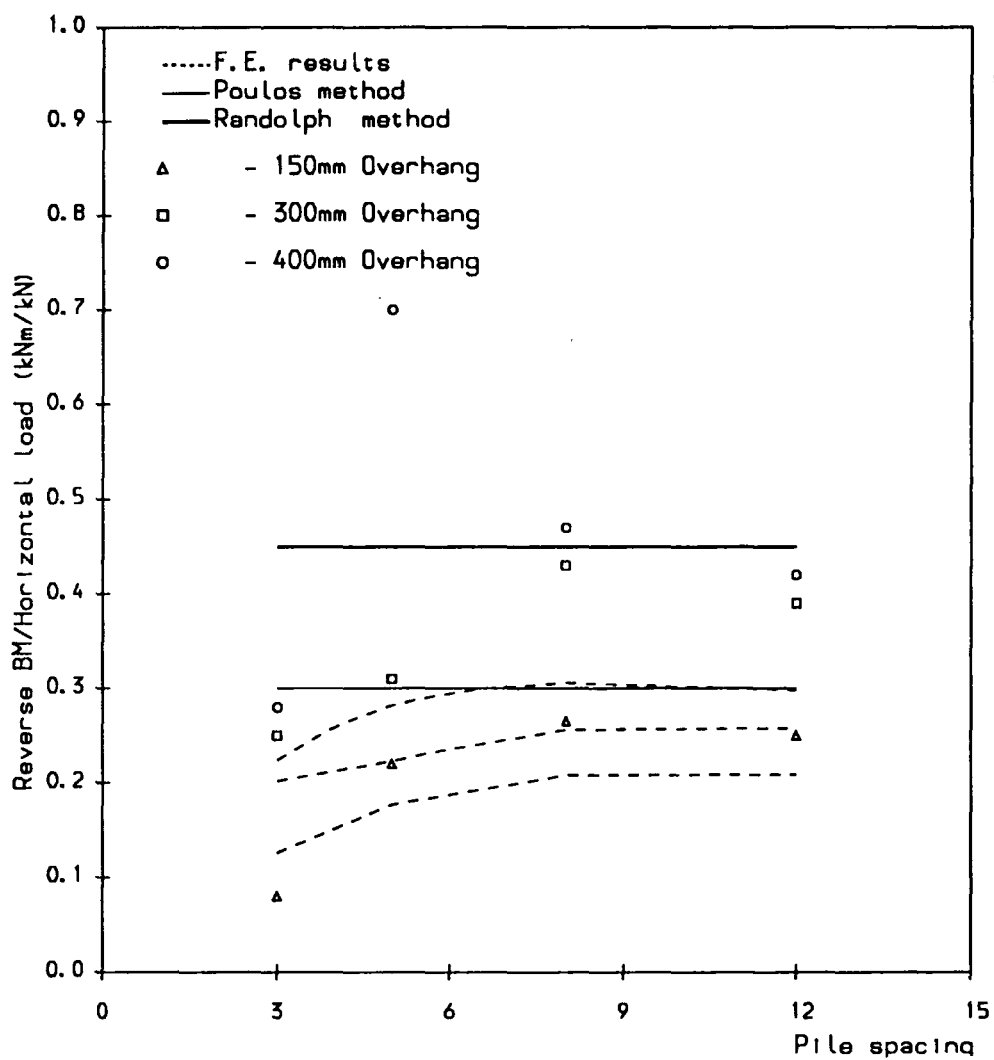
Figure 7.5 Reverse bending moment/horizontal load ratio against pile spacing.
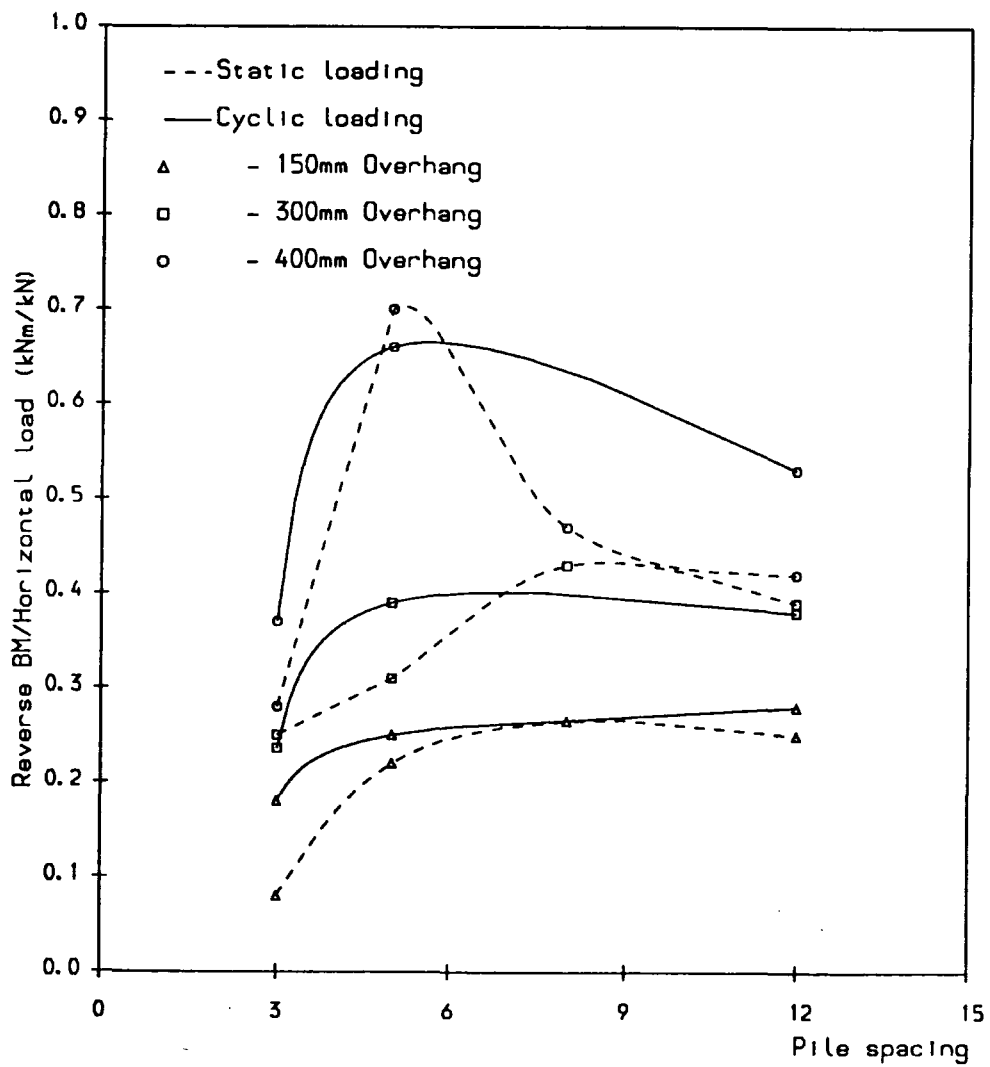
Figure 7.6 Reverse bending moment/horizontal load ratio for static and cyclic loading against pile spacing.
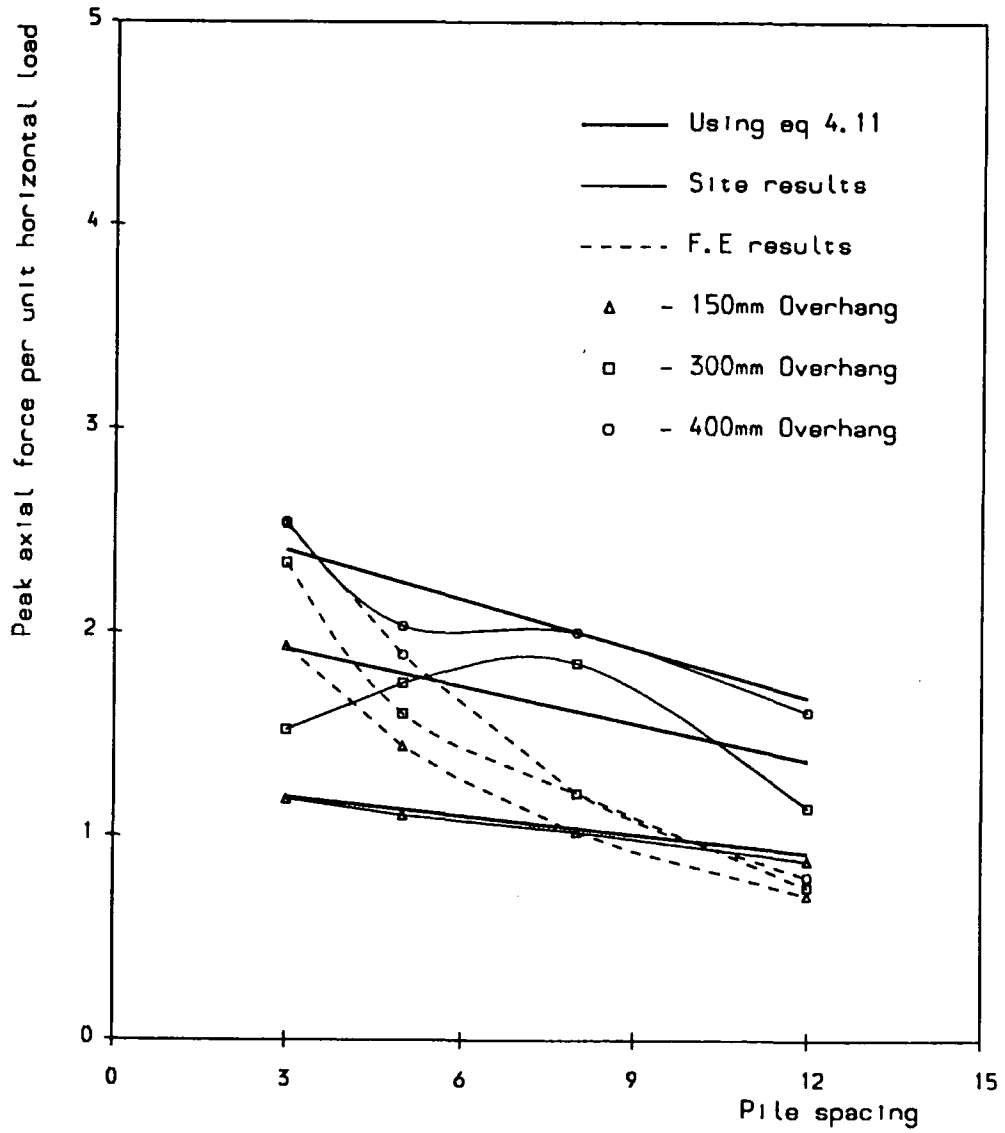
Figure 7.7 Plot of peak axial force per unit horizontal load against pile spacing .

Table T7.1 Interaction Factors (after Poulos (1971b) & Randolph (1981)

Method	3 pile width spacing	5 pile width spacing	8 pile width spacing	12 pile width spacing
Poulos	0.50	0.38	0.28	0.20
Randolph	0.42	0.25	0.16	0.11

Table T7.2 Comparison of tangent stiffnesses of two-pile groups

Method	overhang (mm)	3 pile width spacing	5 pile width spacing	8 pile width spacing	12 pile width spacing
Site	150.0	4.25	5.53	6.45	7.15
Site	300.0	3.55	5.05	5.60	7.20
Site	400.0	2.75	6.20	4.9	7.20
Poulos	0.0	8.33	9.06	9.76	10.41
Randolph	0.0	10.74	12.15	13.15	13.80
F.E	150.0	4.43	6.20	6.50	6.70
F.E	300.0	4.04	5.50	5.85	6.00
F.E	400.0	3.7	4.40	4.94	5.25

Table T7.3 Comparison of secant stiffnesses of two-pile groups

Method	overhang (mm)	3 pile width spacing	5 pile width spacing	8 pile width spacing	12 pile width spacing
Site	150.0	2.45	3.10	2.90	3.60
Site	300.0	2.20	2.90	2.80	3.30
Site	400.0	1.90	2.30	2.60	2.70
Poulos	0.0	2.38	2.65	2.90	3.08

Table T7.4 Secant stiffnesses for first and final cyclic loading

Loading condition	overhang (mm)	3 pile width spacing	5 pile width spacing	8 pile width spacing	12 pile width spacing
First	150.0	2.45	3.10	2.90	3.60
Final	150.0	1.60	2.65	-	2.02
First	300.0	2.20	2.90	2.80	3.30
Final	300.0	1.55	2.50	-	3.06
First	400.0	1.90	2.30	2.60	2.70
Final	400.0	1.73	1.30	-	2.45

Table T7.5 Comparison of maximum bending moment/horizontal load ratios

Method	overhang (mm)	3 pile width spacing	5 pile width spacing	8 pile width spacing	12 pile width spacing
Site	150.0	0.228	0.163	0.257	0.182
Site	300.0	0.326	0.206	0.315	0.212
Site	400.0	0.375	0.230	0.384	0.230
F.E	150.0	0.168	0.121	0.118	0.116
F.E	300.0	0.184	0.131	0.126	0.123
F.E	400.0	0.190	0.158	0.146	0.141

Table T7.6 Comparison of maximum reverse bending moment/horizontal load ratios

Method	overhang (mm)	3 pile width spacing	5 pile width spacing	8 pile width spacing	12 pile width spacing
Site	150.0	0.08	0.22	0.265	0.25
Site	300.0	0.25	0.31	0.43	0.39
Site	400.0	0.28	0.70	0.47	0.42
F.E	150.0	0.126	0.177	0.208	0.209
F.E	300.0	0.202	0.223	0.256	0.258
F.E	400.0	0.224	0.282	0.306	0.298
Randolph	0.0	0.450	0.450	0.450	0.450
Poulos	0.0	0.301	0.301	0.301	0.301

Table T7.7 Comparison of peak axial force per unit horizontal load

Method	overhang (mm)	3 pile width spacing	5 pile width spacing	8 pile width spacing	12 pile width spacing
Site	150.0	1.18	1.10	1.02	0.88
Site	300.0	1.52	1.75	1.85	1.14
Site	400.0	2.54	2.03	2.00	1.61
F.E	150.0	1.93	1.44	1.02	0.71
F.E	300.0	2.34	1.60	1.21	0.75
F.E	400.0	2.53	1.89	1.21	0.80

CHAPTER EIGHT

Conclusions and Recommendations
For Further Work

8.1-Conclusions

Based upon this research the following conclusions are drawn;

1 -The lateral stiffness of a two-pile group tends towards an upper limit value as the pile spacing increased in both the field results and theoretical analyses. The tangent stiffness reflecting the elastic behaviour of the soil at a small strain generally exceeded the secant stiffness which allows for some plastic deformation of the soil.

2 -As the overhang height of the pile cap increased the lateral stiffness of the two-pile group decreased.

3 -In the field tests, resistance to the applied lateral load was developed partly by tilting of the pile cap, causing axial loads in the piles, and partly by bending deflections and soil resistance, causing bending moments in the piles.

4 -The maximum positive bending moment occurred in the pile shaft typically at some 1.3m depth, and the maximum reverse bending moment occurred directly beneath the pile cap; and both increased with respect to an increase in pile spacing or overhang for a given cap displacement.

5 -For a given cap displacement, an increase in overhang and pile spacing both caused increases in pile axial forces.

6 -For agiven horizontal force, an increase in cap overhang caused larger moments and axial forces. However an increase in pile spacing decreased the axial forces and also the moment slightly.

7 -During cyclic loading of two-pile groups the magnitude of the bending moments increased and tangent stiffness was reduced by some 20% after five load cycles.

8 -The load and moment effects were not shared equally between the front and rear in a two-pile group. The front pile generally attracted 8% more than the rear pile, a fairly insignificant difference.

9 -One of the significant achievements in the field tests on the two-pile groups was the determination of axial loads in the front and rear piles in addition to the bending moment diagrams. The axial load in the pile reaches its maximum between the pile cap and 1.0m below the ground level. The axial loads in the front and rear piles were found to be nearly equal but of opposite sign. They increased with pile cap overhang and decreased with increase in pile spacing for agiven cap displacement. An equation was derived (eq No 4.11) to describe the axial forces in the two-pile groups. Axial forces have rarely been measured in field tests on laterally loaded pile groups. The measured axial forces in the piles were substantial and so they should not be ignored in analysis or design.

10 -Of the predictive analyses of two-pile groups the Poulos solution for both linear and non-linear cases agreed most consistently with the field test results.

11 -The lateral stiffness obtained from the linear 3-dimensional finite element analysis was in close agreement with the field test values for small displacements.

12 -No published method was available to predict the axial forces in the piles. The finite element analysis predicted these forces in the piles at low strain, and showed the same trends as the site results.

13 -Throughout this research it was concluded that the finite element analysis pre-

dicted the site values better than the theoretical methods because the pile/soil models were constructed in accordance with the site geometry and the pile cap was allowed to tilt.

14 -The soil moduli calculated from the back analysis of a single pile gave a more reliable estimate of the soil stiffness than the laboratory tests.

15 -Seasonal variations of rainfall were found to have a direct affect on the lateral stiffness of the two-pile groups and the induced bending moments. No such effects on axial forces in the piles were observed.

16 -The conducting of tests at a realistic scale proved to be very difficult in comparison to model tests the in laboratory. Field tests are rare, expensive and time consuming. Such tests are valuable because of the lack of field test data, and because of their direct application to the understanding of the behaviour of laterally load pile groups.

8.2-Recommendations For Further Work

The following recommendations cover the design of laterally loaded pile groups and for further research:

1 -It is apparent that selection of an appropriate soil stiffness profile is a central element in any analysis of laterally loaded pile groups. This is best achieved by single pile tests, and back analysis. Where this is impractical, then laboratory testing of soil samples and a conservative estimate of a soil stiffness range is appropriate.

2 -Designers should use the Poulos solution to predict the behaviour of laterally loaded pile groups.

3 -A designer should take into account the axial forces in the piles. The finite element method proved to be a very expensive method and consequently equation 4.11 could be used.

4 -Further confirmation (repeats) is desirable. Ideal tests of pile groups should involve longer piles (e.g 6.0m) and tests should be conducted in fully saturated soils. Large isolated pressure cells may be used to measure change in soil pressure. Future work should incorporate the use of more sophisticated data collection and analysis by computer

5 -Theoretical methods are needed to predict axial forces in the piles in a group with respect to pile spacing and overhang heights.

6 -Since estimation of the soil stiffness profile is such an important aspect, it would be of considerable value to undertake simple tests on a number of full scale piling installations. Where piles are installed in groups, especially steel H or tube section, lateral load tests could be undertaken, using a simple manual hydraulic jack and dial gauges, on single piles. If many such measurements could be taken, a database could be established which would be of value when trying to ascribe a stiffness profile in the design of a laterally loaded pile group.

List of References

Alizadeh, M. (1969), *Lateral Load Tests on Instrumented Timber Piles.*, ASTM, STP 444: pp 379-394.

Alizadeh, M. & Davisson, M. T. (1970), *Lateral Load Tests on Piles-Arkansas River Project.*, J.S.M.F.D., ASCE, vol. 96, SM5: pp 1583-1604.

Allen . B. & Reese L. C., (1980), *Full Scale Lateral Load Tests of Pile Groups.* J. Geot. Div. ASCE 102, pp 643-653.

Arta. M. R. (1986), *Lateral Loading of Linear Model Pile Groups in Non-Cohesive Soil.*, M.Sc. Dissertation. University of Durham, U.K.

Audibert, J. M. E. & Nyman, K. J., (1977) *Soil Restraint Against Horizontal Motion of Piles.*, Proc. Geot. Eng. Div. ASCE. vol. 103 No GT 10 pp 1119-1142.

Baguelin, F., & Je'Ze'quel, J. F., & Shields, D. H., (1978), *The Pressuremeter and Foundation Engineering.*, Clausthal, Trans. Tech. Pubications.

Banerjee, P. K. & Driscoll, (1976), *Three Dimensional Analysis of Raked Pile Groups.*, Proc. Instn. Civ. Engrs. Part 2, vol. 61, pp 653-671.

Banerjee, P. K. (1978), *Analysis of Axially and Laterally Loaded Pile Groups.*, Developments in Soil Mechanics, Ed. C. R. Scott, London, Applied Science Publishers.

Banerjee, P. K. & Davies, T. G. (1978), *The Behaviour of Axially and Laterally Loaded Single Piles Embedded in Non-Homogeneous Soils.*, Geot., Vol. 28, No. 3: pp 309-326.

Banerjee, R., (1980), *An Approach to the Design of Vertical Piles Subjected to Lateral Loads.*, J. IE(India) CI vol 60 pp 249-253.

Barber, E. S., (1953), *Discussion on paper by S. M. Gleser.*, ASTM, STP 154: pp 96-99.

Barton, Y. O., (1982), *Laterally Loaded Model Piles in Sand: Centrifuge Tests and Finite Element Analysis.*, Ph.D. Thesis, Univ. of Cambridge.

Bhushan, K. & Askari, S., (1968), *Lateral-Load Tests on Drilled Pier Foundations for Solar Plant Heliostats.*, Laterally Loaded Deep Foundations: Analysis and Performance, ASTM STP 835.

Bogard, D. & Matlock, H., (1983), *Procedures for Analysis of Laterally Loaded Pile Groups in Soft Clay.*, Proc. of the Conf. on Geotechnical Practice in Offshore Eng., Univ. of Texas at Austin, Texas, pp 499-553

Bowles, J. E., (1982), *Foundation Analysis and Design.*, McGraw Hill, New York.

Broms, B. B. (1964a), *Lateral Resistance of Piles in Cohesive Soils.*, J.S.M.F.D., ASCE, vol. 90, SM2: pp 27-963

Broms, B. B. (1964b), *Lateral Resistance of Piles in Cohesionless Soils.*, J.S.M.F.D., ASCE, vol. 90, SM3: pp 123-156

Broms, B. B. (1981), *Pre-cast Piling Practice.*, Thomas Telford, London.

Brown D. A., O'Neill M. and Reese L. C. (1987), *Cyclic Lateral Loading of a Large Scalr Pile Group.* J. Geot. Eng. ASCE, vol 113, pp 1326-1343.

Brown D. A., Morrison C. and Reese L. C. (1988), *Lateral Load Behaviour of Pile Group in Sand.*, J. Geot. Eng. ASCE, vol 114, pp 1261-1276.

Brown D. A., Morrison C. and Reese L. C. (1990), *Lateral Load Behaviour of Pile Group in Sand. Clousre.*, J. Geot. Eng. ASCE, vol 116, pp 1282-1283.

Brinch Hansen, J. (1961), *The Ultimate Resistance of Rigid Piles Against Transversal Forces.* Geotechnisk Institut. Bull. No. 12, Copenhagen.

BS. 1377:Part 4: 1975, *Method of Test for Soils for Civil Engineering Purposes* ; Compaction Related Tests.

BS. 1377:Part 2: 1990, *Method of Test for Soils for Civil Engineering Purposes* ; Classification Tests.

BS. 1377:Part 9: 1990, *Method of Test for Soils for Civil Engineering Purposes* ; Insitu Tests.

BS. 4395:Part 1: 1969, *The Specification for High Strength Friction Grip Bolts.*, General Grade.

BS. 4395:Part 2: 1969, *The Specification for High Strength Friction Grip Bolts.*, High Grade Bolts and Nuts and General Grade Washers.

Budhu, M. & Davies, T. G., (1987), *Analysis of Laterally Loaded Piles in Soft Clay.*, J. Geot. Eng. ASCE vol. 114, pp 21-39.

Budhu, M. & Davies, T. G., (1988), *Nonlinear Analysis of Laterally Loaded Piles in Cohesionless soil.*, Can. Geot. J. vol 24, pp 289-296.

Butterfield, R. & Banerjee P.K., (1971), *The Elastic Analysis of Compressible Piles and Pile Groups.*, Geotechnique, 21.

Butterfield, R. & Douglas, R. A., (1981), *Flexibility Coefficients For The Design of Piles and Pile Groups.*, CIRIA. Technical Note 108. London.

Butterfield, R. & Ghosh, N., (1980), *A Linear Elastic Interpretation of Model Tests on Single piles and Groups of Piles in Clay.*, ICE, Numerical Methods in offshore piling, London. pp 109-118.

Carter, J. P. & Booker, J. R., (1981), *Consolidation Due to Lateral Loading of Piles.*, Proc 10th Int. Conf. on S.M. and F.E. Stockholm, pp 647-650.

Davisson, M. T., (1970), *Lateral Load Capacity of Piles.* Highway research Report No 333 Transportation Research Board, Washington D.C.

Davisson, M. T. & Gill, H. L. (1963), *Laterally Loaded Single Piles in a*

Layered Soil Systems., J.S.M.F.D., ASCE, vol. 89, pp 63-94

Davisson, M. T. & Robinson, K. E. (1965), *Bending and Buckling of Partially Embedded Piles.*, Proc. 6th Int. Conf. S.M. & F.E., vol. 2 pp 253-246.

De'court, L., (1991), *Load Deflection Prediction for Laterally loaded Piles Based on N-SPT values.*, 4th Int. DFI Conf. Balkema, Rotterdam, pp 549-555.

Druery, B. M. & Ferguson, R. A., (1969), *An Experimental Investigation of the Behaviour of Laterally Loaded Piles.*, B. E. thesis, Dept. Civil Eng., Univ. of Sydney, Aust.

Elson, W. K. (1985), *Design of Laterally Loaded Piles.*, CIRIA Report 103, London.

Fleming W, Weltman A, Randolph M and Elson W. (1985), *Piling Engineering.*, Surrey University Press, London.

Focht, J. A. & Koch, K. J., (1973), *Rational Analysis of the Lateral Performance of Offshore Pile Groups.*, Proc. 5th Offshore Tech. Conf., Houston, vol 2, paper OTC 1896: pp 701-708.

Francis, A. J., (1964), *Analysis of Pile Groups with Flexural Resistance.*, Proc. ASCE. vol. 90, Sm.3

Frydman, S., Sha'al, B. & Mazurik, A., (1975), *Analysis of Instrumented Laterally Loaded Piles.*, Proc. 5th Asian Reg. Conf. S.M. and F.E., India.

Garassino, A., Jamiolkowski, M. & Pasqualini, E., (1976), *Soil Modulus for Laterally Loaded Piles in Sand and Clay.*, Proc 6th Eurp. Conf. on S.M. and F.E., Vienna, vol 1.2 Part III and 18 pp 429-434.

Gazioglu, S. M. & O'Neill M. W., (1985), *Evaluation of p/y Relationships in Cohesive Soils.*, Proc of Symp. ASCE Geot. Eng. Div 'Analysis and Design of Pile Foundations.*, pp 192-213.

Gleser, S. M., (1953), *Lateral Load Tests on Vertical Fixed-head and Free-Head*

Piles., ASTM, STP 154 pp 75-93.

Gleser, S. M., (1976), *Discussion on Kim & Brungraber (1976).*, J. Geot. Eng. ASCE. pp 1288-1291

Hage-Chehade F., Meimon Y. and Shahrour I. (1991), *Validation of FEM Calculation For Piles Under Lateral Loading,* Comput & Struct. Tech. 1st Int. Conf on Compt. and Struct. Technology, Heriot-Watt University, Edinburgh, vol. I, pp 249-256.

Hetenyi, M. (1946), *Beams on Elastic Foundations.*, Ann Arbor, Mich.: University of Mich. Press.

Holloway D. M., Moriwaki Y., Stevens J. B. and Perez J. Y. (1981), *Response of a Pile Group to Combined Axial and Lateral Loading.*, Proc. of the 10th Conf. on Soil Mech. and Found. Eng., Stockholm, pp 731-734.

Hotoinh, M. & Nakatani, S., (1991), *Laterally loaded Piles Under Large Deflection.*,, Proc. 4th Int. D.F.I. Conf. Rotterdam., pp 431-434.

Horowitz, P. & Hill, W. (1989), *The Art of Electronics.* Camb. University Press, Second Edition. pp 1001-1004.

Hughes J. M. O., Fendall H. D. W. & Goldsmith P. R., (1980) *Model pile Groups subjected to Lateral Loading.* 3rd Australia-New Zealand conf. on Geotechanics, Wellington, vol. 1 pp 79-85.

Ismael N. F., (1990), *Discussion on Lateral Load Behaviour of Pile Groups in Sand.*, J. Geot. Eng. ASCE, vol. 116, pp 1277-1278

Jamiolkowski, M. & Lancelotta, R., (1977), *Remarks on the Use of the Selfboring Pressuremeter Test in Three Italian Clays.*, Riv. Ital. Geotecnica 11 (No. 3).

Kim, J. B. & Brungraber, R. J. (1976), *Full Scale Lateral Load Tests of Pile Groups.* J. Geot. Div. ASCE 102, pp 87-105.

Kim, J. B., Singh P. L. & Brungraber, R. J. (1979), *Full Scale Lateral Load Tests of Pile Groups.* J. Geot. Div. ASCE 102, pp 643-653.

Kubo, J., (1965), *Experimental Study of the Behaviour of Laterally Loaded Piles.*, Proc. 6th Int. Conf. S.M. and F.E., vol 2 pp 275-279.

Lee, K. L., (1968), *Buckling of Partially Embedded Piles in Sand.* J. S.M and F.E. Div. ASCE, vol 94, SM1: pp 255-270.

Leyden, ir. W.van., (1971), *Plastic-Elastic Analysis of Laterally Loaded Free-Standing Piles.*, Angenieur Hague, V. 83, Vol 82 pp B101-111.

Long, N. C. M, (1987), *Lateral Loading of Linear Model Pile Groups.*, Final Year B.SC. Proj. Univ. of Durham, U.K.

Lord, J. A. & Davies J.A.G., (1979), *Lateral Load and Tension Tests On Driven Cased Piles In Chalk.*, Proc. of the Conf. at IEE London. pp 113-120.

Madhav, M. R. & Rao, N. S. V. K., (1971a), *Model for Machine-Pile Foundation System.*, J. S.M.F.D., ASCE, vol 97 SM1 pp 295-299.

Matlock, H. (1970), *Correlation for Design of Laterally Loaded Piles in Soft Clay..*, Proc. 2nd Offshore Tech. Conf. Houston, vol I pp 577-594.

Matlock, H., (1976), *Discussion on Kim & Brungraber (1976).*, J. Geot. Eng. ASCE. pp 1291-1292

Matlock, H. (1980), *Field Tests of the Lateral Loaded Behaviour of Pile Groups in Soft Clay.*, Offshore Tech. Conf. 12th Ann. Proc vol 4 Houston Texas pp 163-174.

Matlock, H. & Reese, L. C., (1961), *Foundation Analysis of Offshore Pile Supported Structures.*, Proc. 5th Int. Conf. S.M. and F.E., vol 2 pp 91-97.

McClelland, B. & Focht, J. A., (1958), *Soil Modulus for Laterally Loaded*

Piles., Trans, ASCE, vol 123: pp 1049-1063.

Menard, L., Bourdon, G. & Gambin, M., (1968), *General Method to Calculate a Pile or a Diaphram Subject to Horizontal Loading in Terms of Pressuremeter Tests.*, Sols. Soil VI (22/23), pp 16-40.

Mindlin R. D., (1936), *Force at a Point in the Interior of a Semi-Infinite Soild.*, Physics 7: 195.

Murchison, J. M. & O'Neill M. W., (1985), *Evaluation of p/y Relationships in Cohesionless Soils.*, Proc of Symp. ASCE Geot. Eng. Div. Analysis and Design of Piled Foundations' pp 174-191.

Navy Design Manual., (1982), *Foundation and Earth Structures Design Manual 7.2.*, Department of the Navy, Naval Facilities Engineering Command.

Odone A. J., Paterson K. W. & Hooper D. J., (1979), *The Lateral Load Testing of Two Offshore Single Point Mooring (SPM) Tower Piles.*, Proc of the Conf. ICE. London, pp 95-111.

Oteo, C. S., (1972), *Displacements of Vertical Pile Groups Subjected to Lateral Loads.*, Proc. 5th Eurp. Conf. S.M. and F.E., Madrid, vol 1 pp 397-405.

Ottaviani, M., (1975), *Three Dimensional Finite Element Analysis of Vertically Loaded Pile Groups.* Geotechnique 25, pp 159-174.

PAFEC 75 , *PAFEC 75 Manual.*, PAFEC Limited., Nott. U.K.

Parikh, S.K. & Pal, S. C., (1981), *Coefficient of Subgrade Reaction for Pile Systems.*, Proc. 10th Int. Conf. on S.M & F.E. Stockholm, pp 209-212.

Pise, P. J. , (1977), *Experimental Coefficients for Laterally Loaded Piles.*, Int. Symp. on Soil Struct. Interact. India Univ. of Roorkee, pp 327-333.

Pise, P. J. , (1982), *Lateral Load Deflection Behaviour of Pile Groups.*, Int. Symp. on Soil Struct. Interact. India Univ. of Roorkee, pp 37-51.

Poulos, H. G. (1971a), *Behaviour of Laterally loaded piles: I-Single Piles.*,

J.S.M.F.D., ASCE, vol. 97, No. SM5: pp 711-731.

Poulos, H. G. (1971b), *Behaviour of Laterally loaded piles: II-Pile Groups.*, J.S.M.F.D., ASCE, vol. 97, No. SM5: pp 733-751.

Poulos, H. G. (1971c), *Discussion on "Load-Deformation Mechanism for Bored Piles.*, by R. D. Ellison, E. D'Appolonia, & G. R. Thiers. J. Soil Mechs. & Fndns. Div., ASCE, vol 97, No. SM12 pp1716

Poulos, H. G. (1972a), *Behaviour of Laterally Loaded Piles: III-Socketed Piles.*, J.S.M.F.D., ASCE, vol 98, No. SM4: pp 341-360.

Poulos, H. G. (1972c), *Difficulties in Prediction of Horizontal Deformations of Foundations.*, J.S.M.F.D., ASCE, vol 98, No. SM8: pp 343-348.

Poulos, H. G. (1973), *Load-Deflection Prediction for Horizontal Laterally Loaded Piles.*, Aust. Geomechs. J., Vol. G3, No. 1 pp 1-8.

Poulos, H. G. (1974), *Analysis of Pile Groups Subjected to Vertical and Horizontal loads.*, Aust. Geomechs. J., Vol. G4, No. 1 pp 26-32.

Poulos, H. G. (1975), *Lateral Load-Deflection Prediction for Pile Groups.*, J. Geot. Eng. Div., ASCE, vol 101, No. GT1: pp 19-34.

Poulos, H. G. (1976), *Behaviour of Laterally Loaded Piles Near a Cut Slope.*, Aust. Geomechs. J. vol. G6, No. 1: pp 6-12.

Poulos, H. G. (1979), *Group Factors for Pile Deflection Estimation.*, J. Geot. Eng. Div., ASCE, vol 105, No. GT12: pp 1489-1509.

Poulos, H. G. (1980), *An Approach for Analysis of Offshore Pile Groups.*, ICE. Numerical methods in offshore piling, London, pp 119-126.

Poulos, H. G., (1989), *Pile Behaviour-Theory and Application.*, The 29th Rankine Lecture, Geotechnique 39, No. 3, pp 365-415.

Prakash, S., (1982), *Behaviour of Pile Groups Subjected to Lateral Loads.*, Ph.D. Thesis, Univ. of Illinois, Urbana.

Prakash, S., (1990), *Lateral Behaviour of Pile Group in Sand. Discussion*, J. Geot. Eng. ASCE, vol 116, pp 1278-1282.

Prakash, S. & Saran, D. (1967), *Behaviour of Laterally loaded Piles in Cohesive Soil.*, Proc. 3rd. Asian Conf. S.M.: pp 235-238.

Price, C. & Wardle, I. F., (1979), *The Deformation of Vertical Piles in London Clay Under Static And Cyclic Horizontal Working Loads.*, Proc. of the Conf. at IEE. London pp 87-94.

Price, C. & Wardle, I. F., (1981), *Horizontal Load Tests on Steel Piles in London Clay.*, Proc. 10th Conf. on S.M. & F.E. pp 803-808

Ramasamy, G., (1989), *Estimation of Lateral Capacity of Piles From Load Tests - A Note of Caution.*, Piletalk Inter. Malaysia, pp 261-273

Randolph, M. F. (1981), *The Response of Flexible Piles to Lateral Loading.*, Geotechnique, 31, pp 247-259.

Randolph, M. F. & Poulos, H. G. (1982), *Estimating the Flexibility of Off-shore Pile Groups.*, Proc. of 2nd Inter. Conf. on Num. Method in Offshore Piling, the Univ. of Texas, Austin, pp 313-328.

Ranjan, G., Ramasamy, G. & Rao, B. G., (1977), *Model Study of the Time-Dependent Deflection of Laterally Loaded Piles in Saturated Clays.*, Proc. 5th Southeast Asian Conf. S.M., Bangkok, Thailand, pp 141-152.

Reddaway A. L. & Elson W. K., (1982), *The Performance of a Piled Bridge Abutment at Newhaven.*, CIRIA, Tech. Note 109.

Reddy, A. S. & Valsangkar, A. J., (1968), *An Analytical Solution for Laterally Loaded Piles in Layered Soils.*, Sols-Soils, No. 21: pp 23-28

Reddy, A. S. & Ramasamyar, A. J., (1976), *Flexural Behaviour of Group of Piles in Elasyo-Plasto Soil.*, Int. Inst. Eng. C. Indias. CIE. End. Div. 57 PT. CI. pp-1-6.

Reddy, A. S. & Valsangkar, A. J., (1970), *Buckling of Fully and Partially Embedded Piles.*, J.S.M.F.D., ASCE, vol. 96, SM6: PP 1951-1965.

Reese, L. C. (1971), *The Analysis of Piles Under Lateral Loading,* Proc. Symp. Inter. of Struct, and Found. Midland Soil Mechanics and Foundation (Engineering society Birmiingham) pp 206-218.

Reese, L. C., (1977), *Lateral Loaded Piles: Program Documentation.*, J. Geot. Eng. Div., ASCE, vol 103 No. GT4: pp 287-305.

Reese, L. C., (1979), *Design and Evaluation of Load Tests on Deep Foundations.*, ASTM. Spec. Techn. Pub. Behaviour of Deep Found. Symp. Boston, pp 4-26

Reese, L. C., Cox, W. R., & Koop, F. D., (1974), *Analysis of Laterally Loaded Piles in Sand.*, Proc. 6th Offshore Tech. Conf., Houston, Paper OCT 2080 pp 473-483.

Reese, L. C., Cox, W. R., & Koop, F. D., (1975), *Field Testing and Analysis of Laterally Loaded Piles in Stiff Clay.*, Proc. 7th Offshore Tech. Conf., Houston, Paper OCT 2312 pp 671-690.

Reese, L. C. & Matlock, H. (1956), *Non-Dimensional Solutions for Laterally Loaded Piles with Soil Modulus Assumed Proportional to Depth.*, Proc. 8th Texas Conf. S.M. and F.E., Spec. Pub. 29, Bureau of Engr. Res., University of Texas, Austin. pp 1-30.

Reese, L. C. & Welch, R. C. (1975), *Lateral Loading of Deep Foundations in Stiff Clay.*, J. Geot. Eng. Div., ASCE, vol 101 No. GT7: pp 633-649.

Robinson, K. E., (1979), *Horizontal Subgrade Reaction Estimated from Lateral Loading Tests on Timber Piles.*, behaviour of Deep Found., STP 670, ASTM, pp 520-536.

Rockey, K. C., Evans, H. R., Griffith, D. W. & Nethercot, D. A., (1975),

The Finite Element Method., William Clowes & Sons, Limited, London.

Sawko, F., (1968), *Simple Approach to the Analysis of Piling Systems.* Struct. Eng. 46(3) pp 83-86.

Selby, A. R. & Parton G. M., (1985), *The Use of Models to Identify Treends in Laterally Loaded Pile Groups..* Mexican Geo. Tech. J. Eng. Aust. pp 365-385.

Selby, A. R. & Poulos, H. G. (1985), *Lateral Load Tests on Model Pile Groups.* Civ. Eng. Trans., Instn. Eng. Aust. pp 281-285.

Selby, A. R. & Wallace P. D. (1985), *Microcomputer Analysis of Pile Groups Under General Loading.*, Ground Eng. pp 33-39.

Selby, A. R. & Arta, M. R. (1991), *Three Dimensional Finite Element Analysis of Pile Groups Under Lateral Loading,* Comput & Struct. Tech. 1st Int. Conf. on Compt. and Struct. Technology Edinburgh, vol. 40, No. 5 pp 1329-1336.

Singh, A., (1979), *Experimental Study and Analysis of Pile Groups.*, J. Indian Road Congr. vol 40 No. 2 pp 439-461.

Smith I. M. & Griffiths D. V., (1988), *Programming the Finite Element Method.*, Second Edition. John Willy & Sons Ltd.

Sung, Ho. & Maddison, B. H., (1989), *Load Distribution in Pile Groups in Cohessionless Soils, Subject to Lateral Loads.*, Piletalk, Int. Conf. Malaysia, pp 177-194.

Sullivan, W. R., Reese, L. C., & Fenske, C. W., (1979), *Unified Method for Analysis of Laterally Loaded Piles in Clay.'* Conf. on Num. Methods in Offshore Piling, London ICE., Paper no. 17.

Sogge, R. L., (1981), *Laterally Loaded Pile Design.*, Proc ASCE, vol. 107 GT 9 pp 1179-1199.

Terzaghi, K. (1955), *Evaluation of Coefficient of Subgrade Reaction.*, Geot., vol 5: pp 297- 326.

Timoshenko, S. & Woinowsky-Krieger, S., (1959), *Theory of Plates and Shells.* McGraw-hill, New York.

Tomlinson, M. J., (1977), *Pile Design and Construction Practice.* Viewpoint Publ. London.

Toolan, F. E. & Coutts, J. S. , (1979), *The Application of Laboratory and In-situ Data to the Design of Deep Foundations.*, Offshore Site Invest. Int. Conf. Soc. of Underwater Tech., London pp 231-245.

Uromeihy, A. (1986), *In-Situ Lateral Load Tests on Pairs of Piles,* M.Sc. Dissertation, University of Durham, U.K.

Verruijt, A. & Kooijman, P. A., (1989), *Laterally Loaded Piles in a Layered Elastic Medium.*, Geotechnique 39, No. 1, pp 39-46.

Winkler, E. (1867), *Die Lehre Von Elastizitat und Festigkeit (on elasticity and fixity.* Prague, P. 182. Geot., vol 5: pp 297- 326.

Wolters J. G. & Marcon N. V., (1937), *Lateral Load Capacity of Piles In Offshore Structures.*, The Hague Neth. JPT. Technol. vol 25 pp 487-498.

Wood. L. A. , (1979), *A Program For The Analysis of Laterally Loaded Pile Groups, Sheet Piles and Diaphragm Walls.*, Proc. 1st Int. Conf. on Eng. Software, Southampton University, Vol. 1.4, pp 614-632.

Zienkiewics, O. C. & Taylor, R. L. (1989), *The Finite Element Method.*, vol. 1. Basic Formulation and Linear Problems. Fourth Edition. McGraow Hill Ltd. London.

Appendix A

A1-Content

Appendix A contains a summary of site results presented in graphical form for the following properties and relationships:

A.1a - A.35a Load and deflection.

A.1b - A.35b Bending moments.

A.1c - A.4c Soil pressure distributions for single pile tests.

A.1d - A.4d Load and rotation for single pile tests.

A.5c - A.35c Axial forces.

A.36 - A.39 Maximum bending moment ratios.

A.40a - A.40d Average bending moments and horizontal load ratios.

A.41 - A.47 Load and rotation for two-pile groups.

It should be noted that in some tests it was not always possible to obtain a full set of reliable and repeatable results.
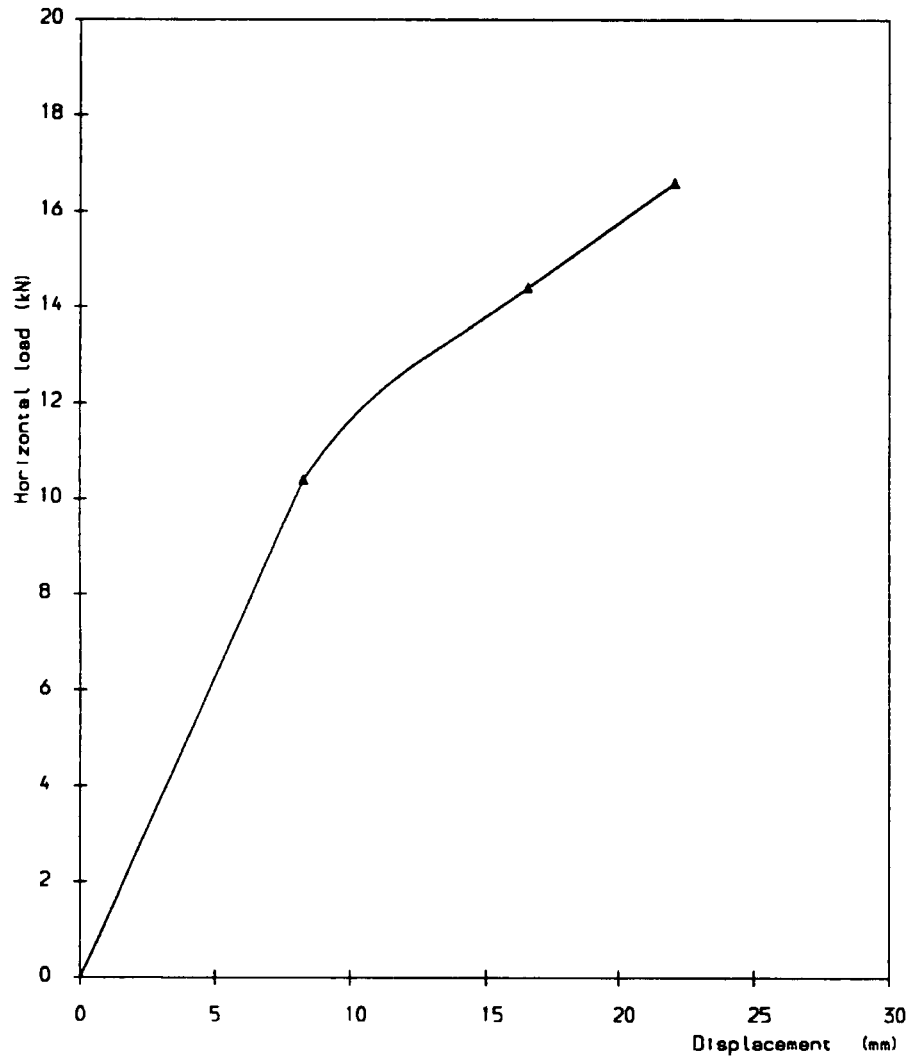
Figure A.1 Load/deflection curve first single pile test

1 = 8.30mm Pile head defl.
2 = 16.22mm Pile head defl.
3 = 22.10mm Pile head defl.
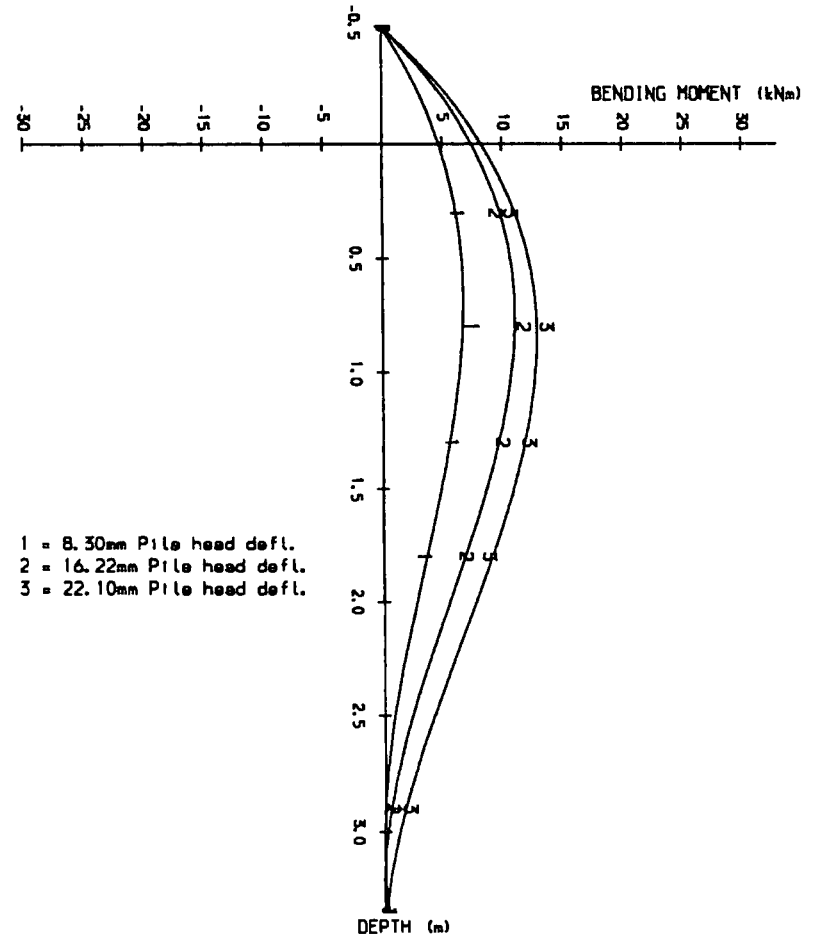
Figure A.1b Bending Moment Diagram for single pile (first test)
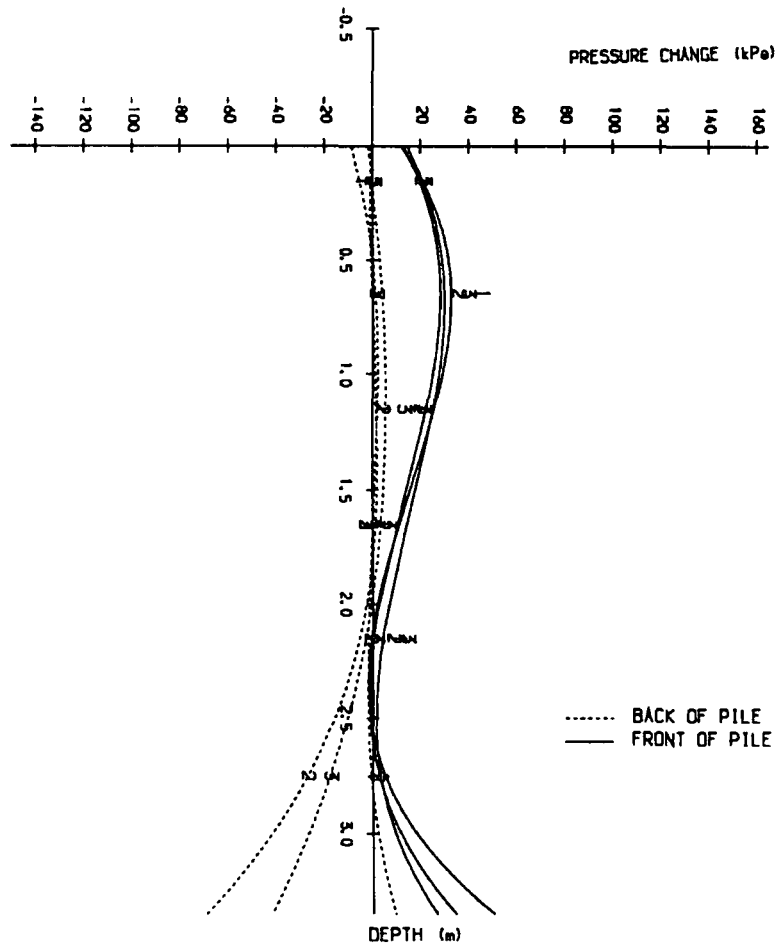
Figure A.1c Pressure distribution diagram for single (first test)
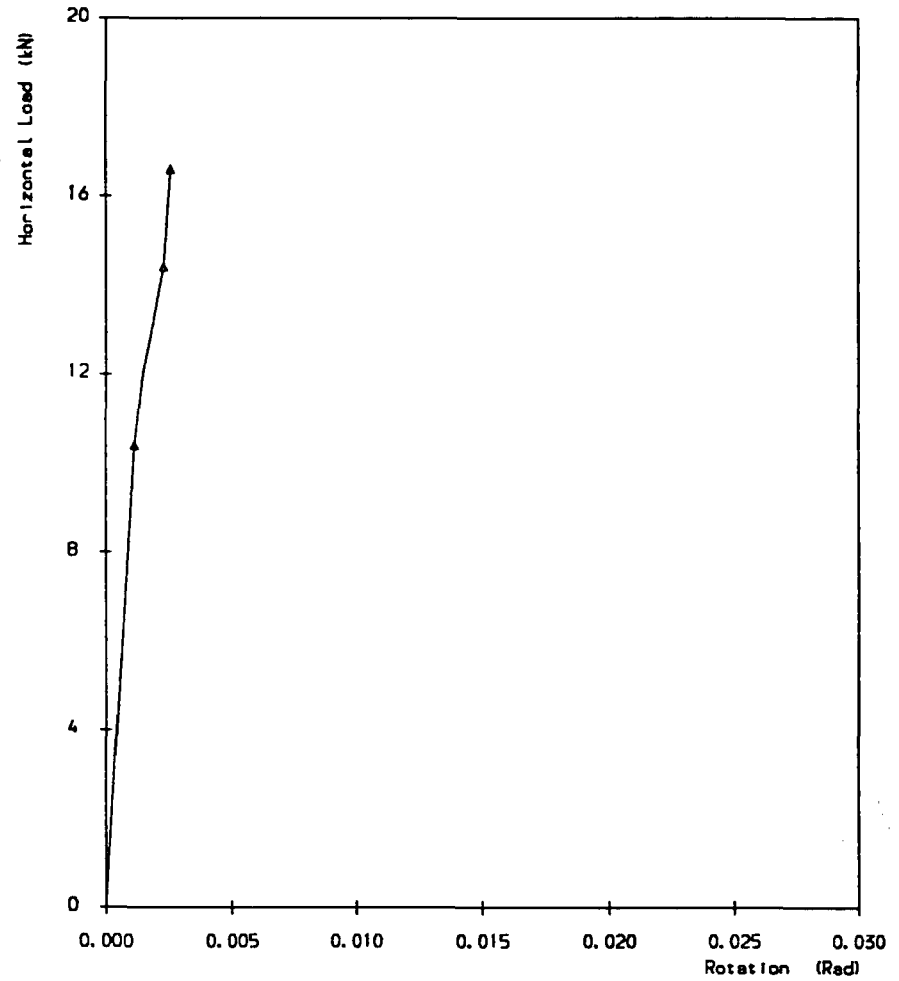
Figure A.1d Load/rotation curve for first single pile test.
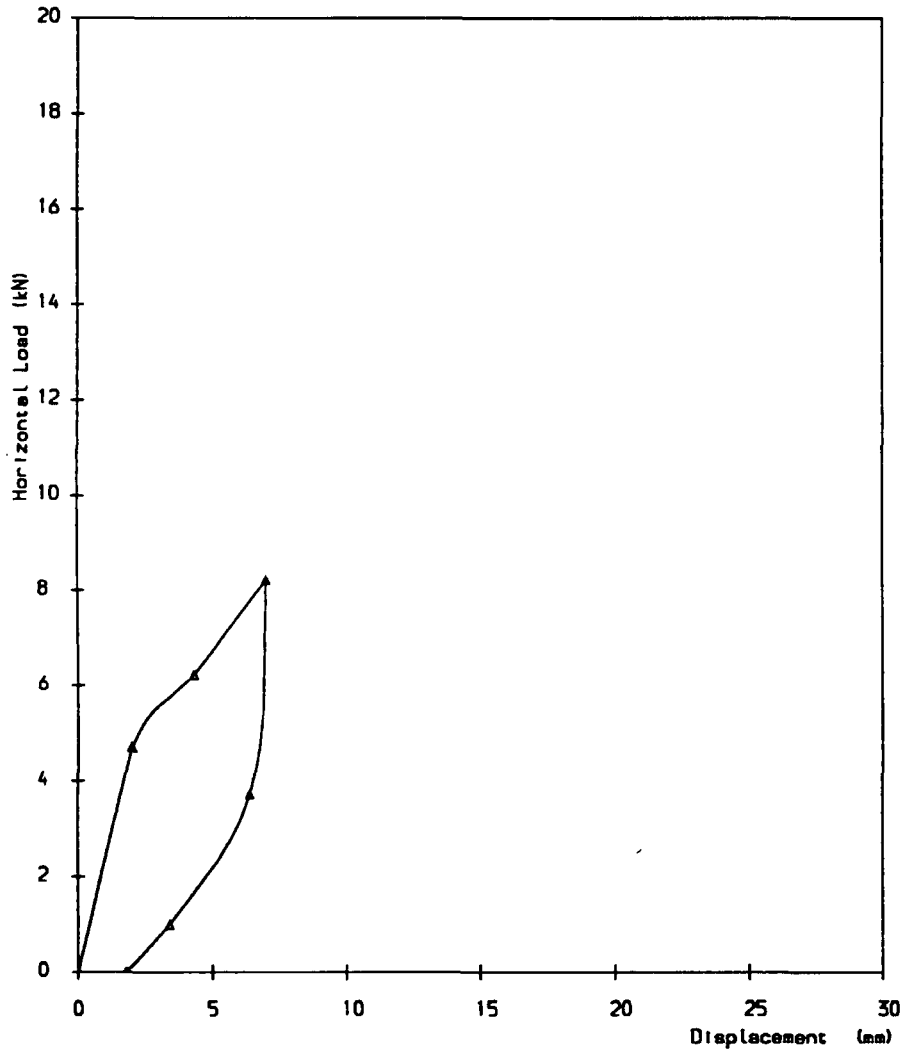
Figure A.2 Load/deflection curve for second single pile test.

1 = 2.00mm Pile head defl.
2 = 4.30mm Pile head defl.
3 = 7.00mm Pile head defl.
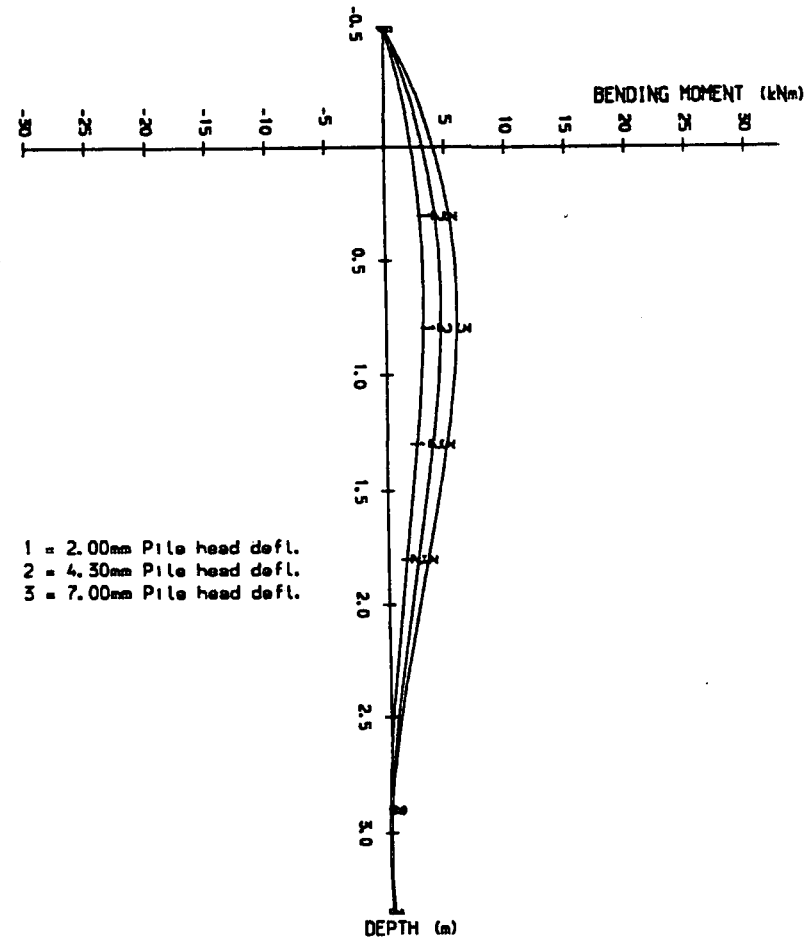
Figure A.2b Bending Moment Diagram for single pile (second test)

PRESSURE CHANGE (kPa)

BACK OF PILE
FRONT OF PILE

DEPTH (m)
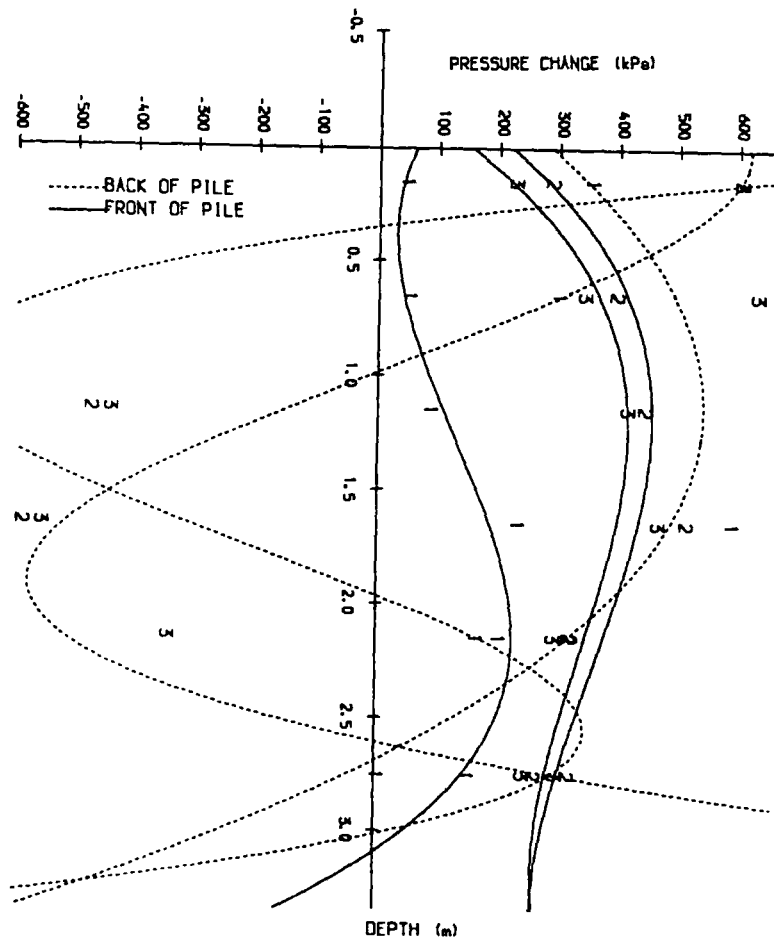
Figure A.2c Pressure distribution diagram for single (second test)
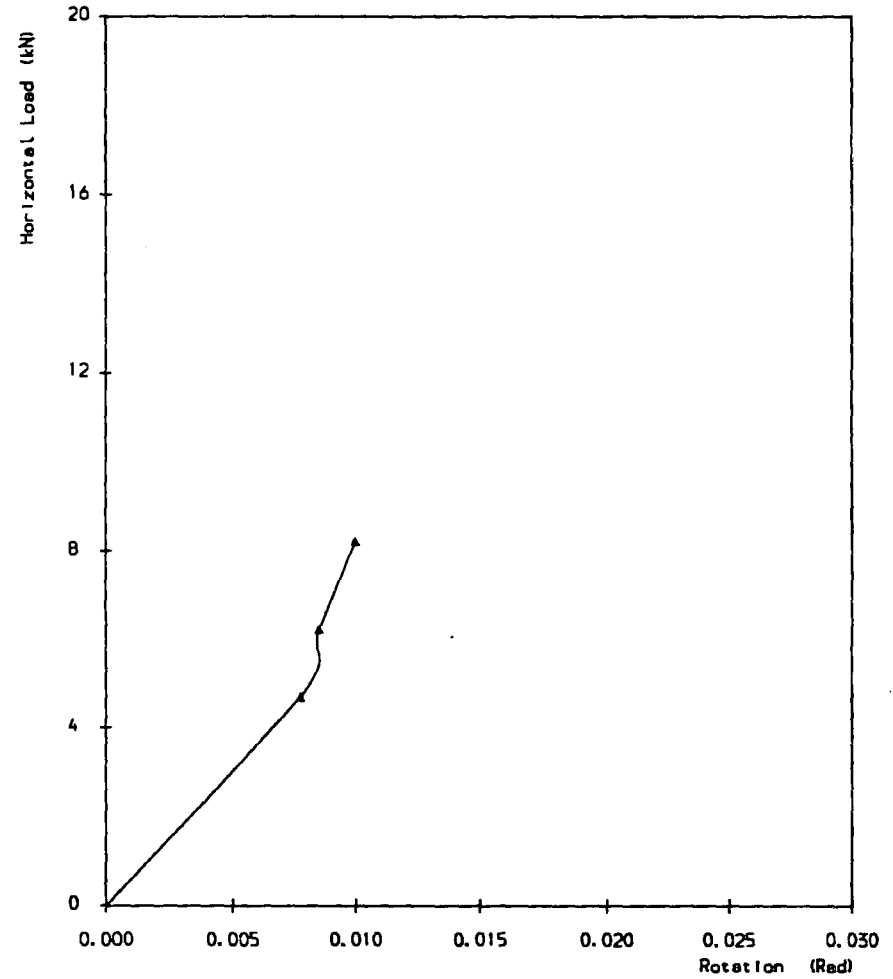
Figure A.2d Load/rotation curve for second single pile test.
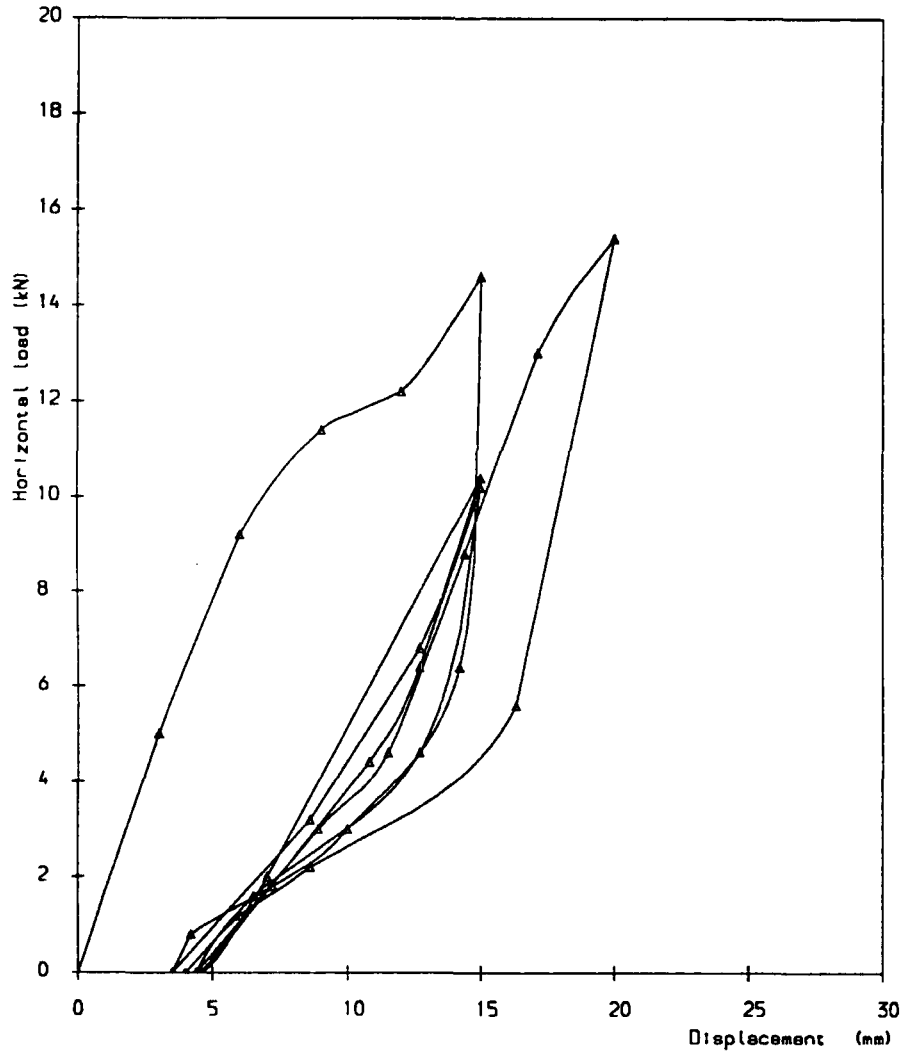
Figure A.3 Load/deflection curve third single pile test

1 = 3.00mm Pile head defl.
2 = 6.00mm Pile head defl.
3 = 9.00mm Pile head defl.
4 = 12.00mm Pile cap Defl.
5 = 15.00mm Pile cap Defl.
6 = 20.00mm Pile cap Defl.
Cyclic loading.
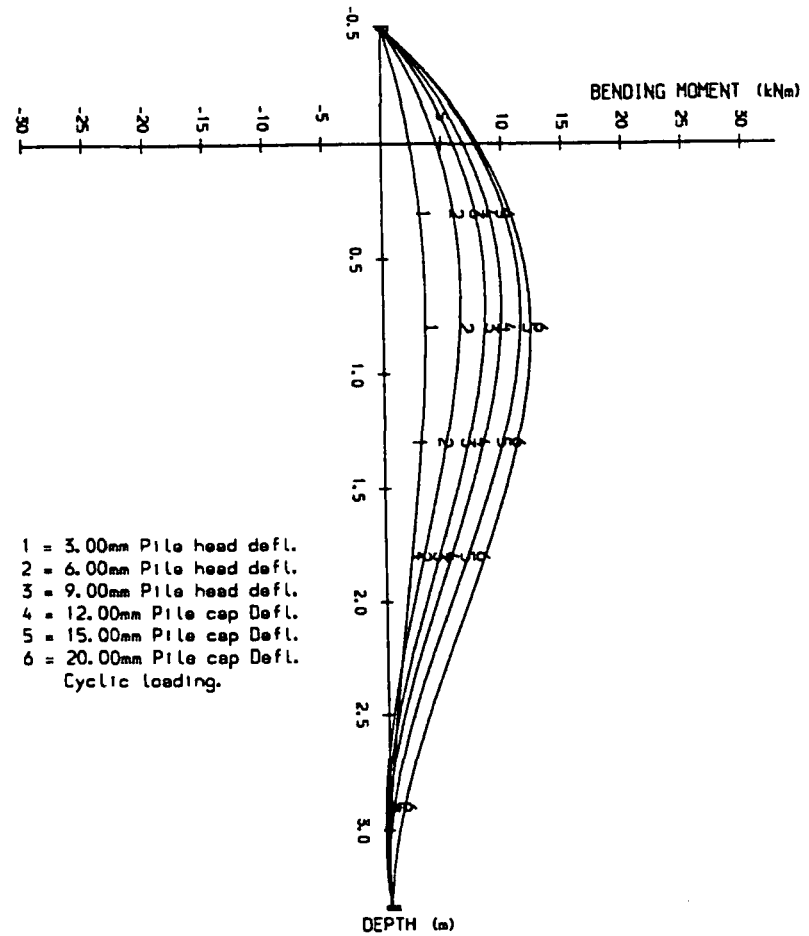
Figure A.3b Bending Moment Diagram for single pile (third test)
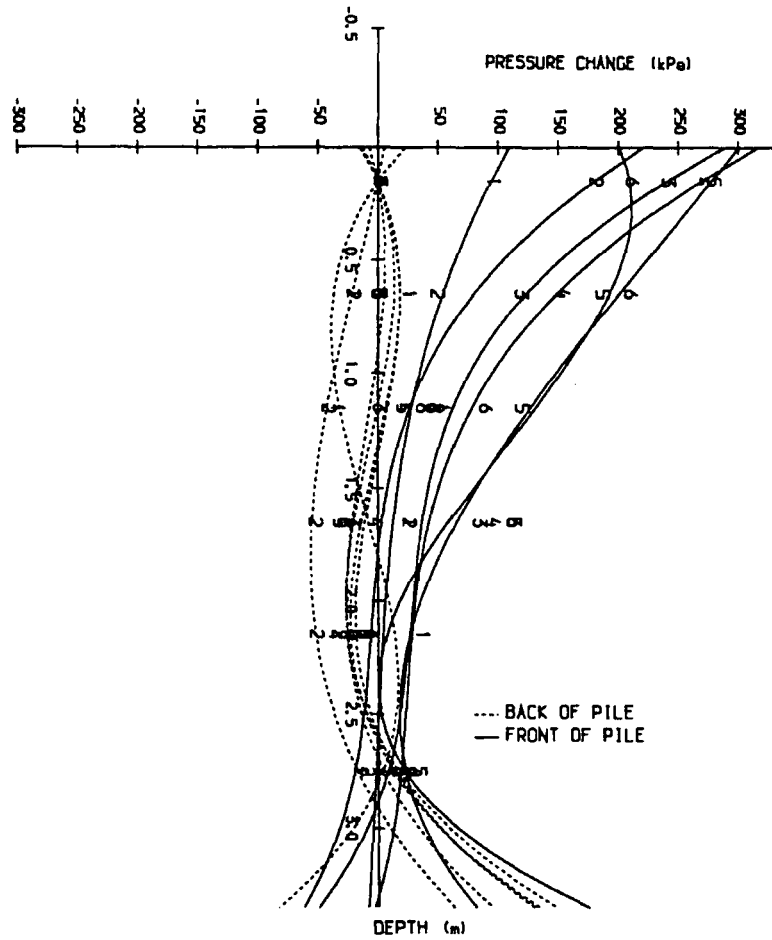
Figure A.3c Pressure distribution diagram for single (third test)
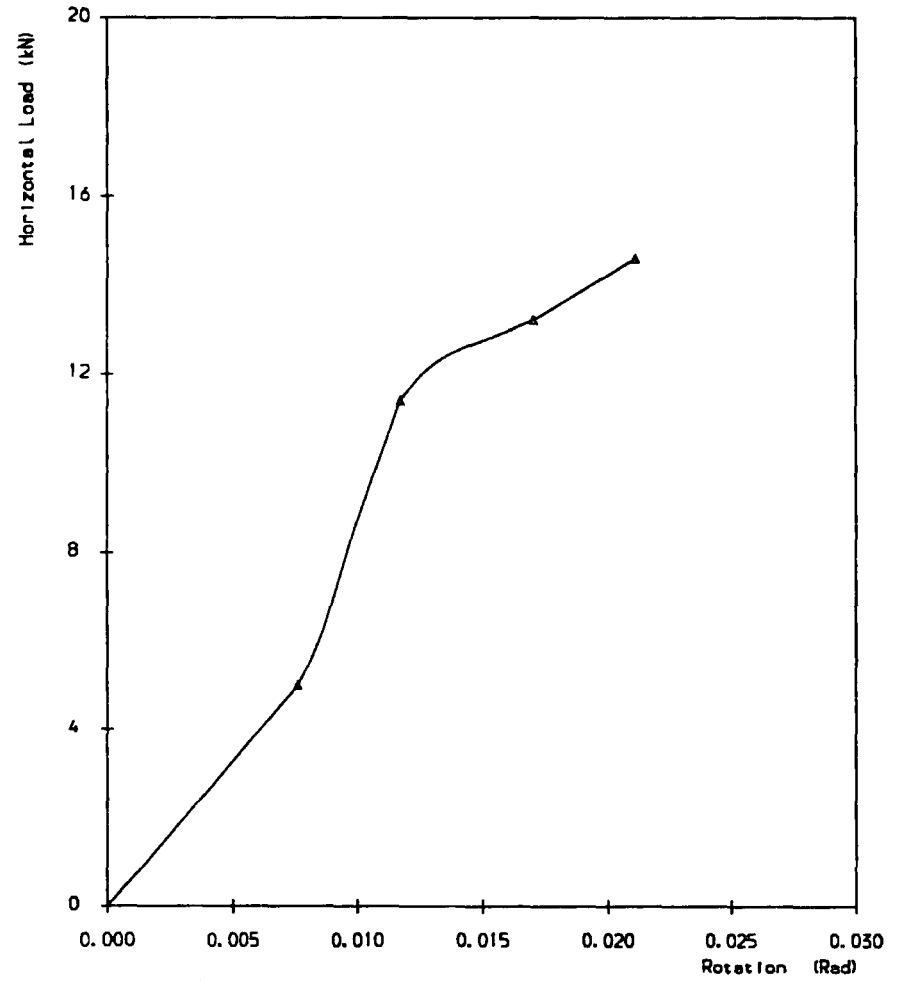
Figure A.3d Load/rotation curve for third single pile test.
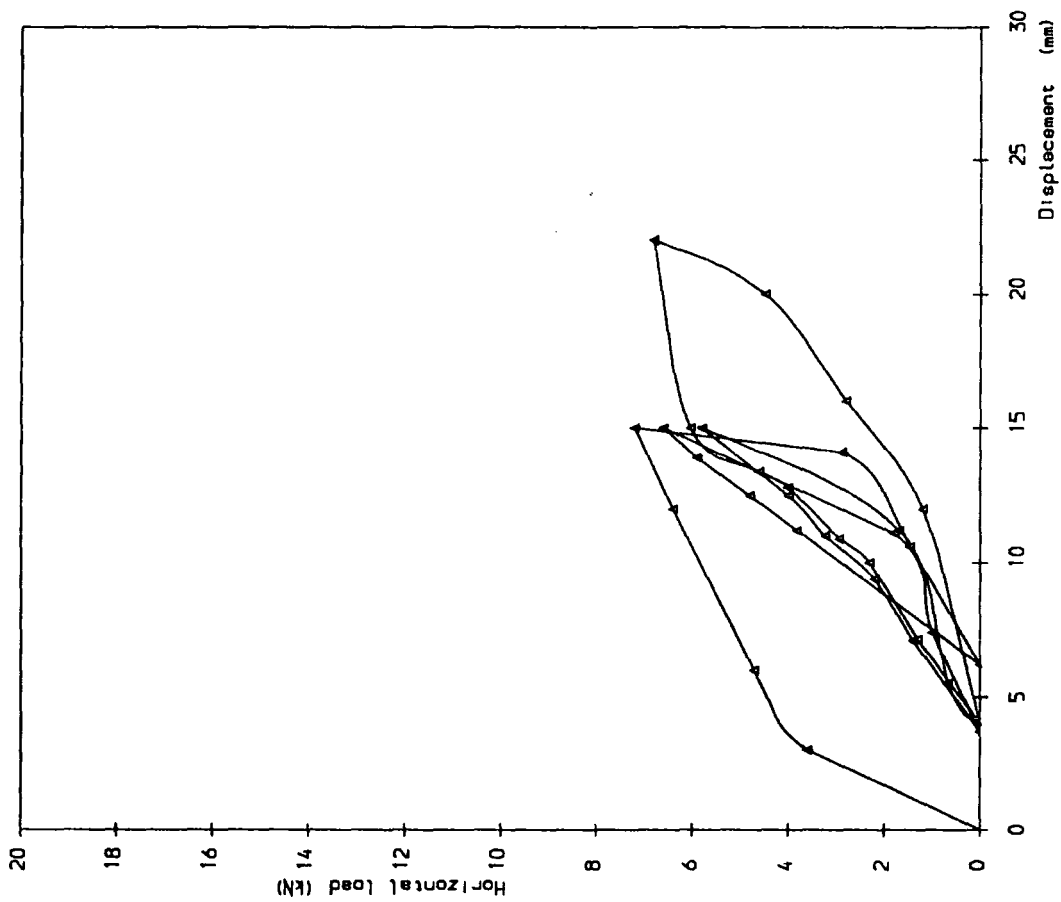
Figure A.4 Load/deflection curve fourth single pile test

BENDING MOMENT (kNm)

1 = 3.00mm Pile head defl.
2 = 6.00mm Pile head defl.
3 = 12.00mm Pile head defl.
4 = 15.00mm Pile cap Defl.
5 = 22.00mm Pile cap Defl.
Cyclic loading.

DEPTH (m)
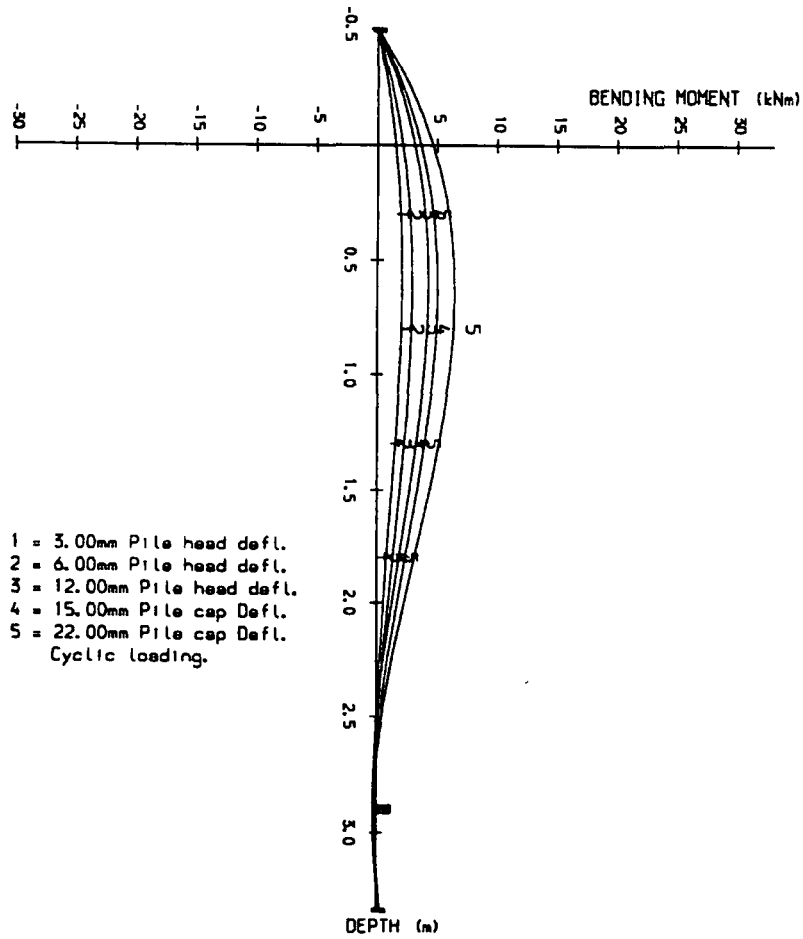
Figure A.4b Bending Moment Diagram for single pile (fourth test)

PRESSURE CHANGE (kPa)

------BACK OF PILE
——FRONT OF PILE

DEPTH (m)
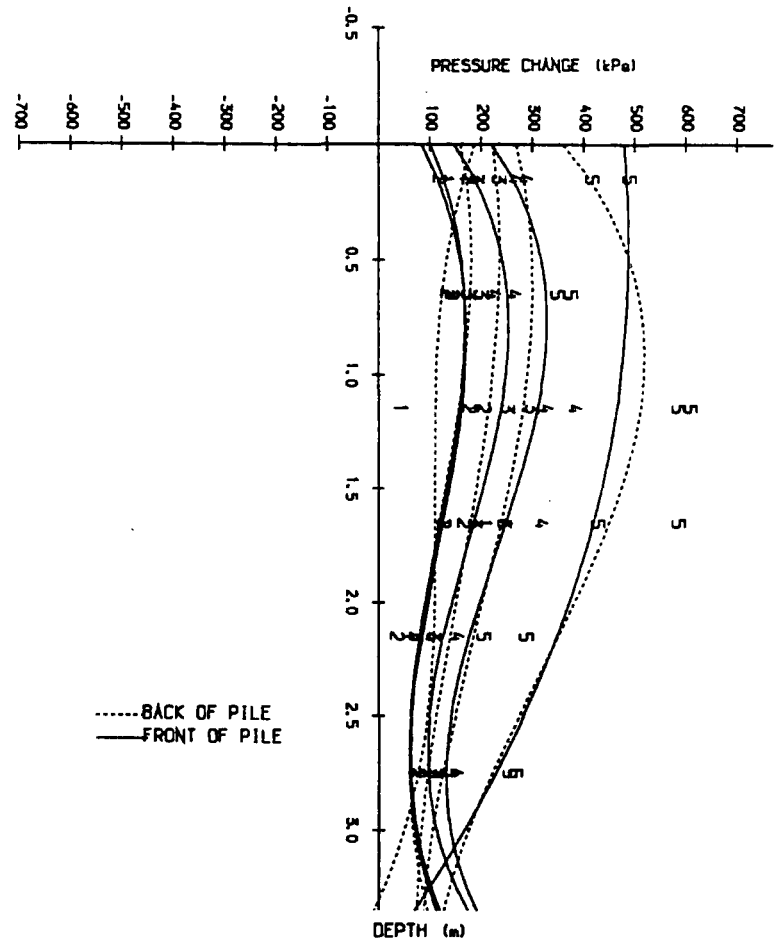
Figure A.4c Pressure distribution diagram for single (fourth test)
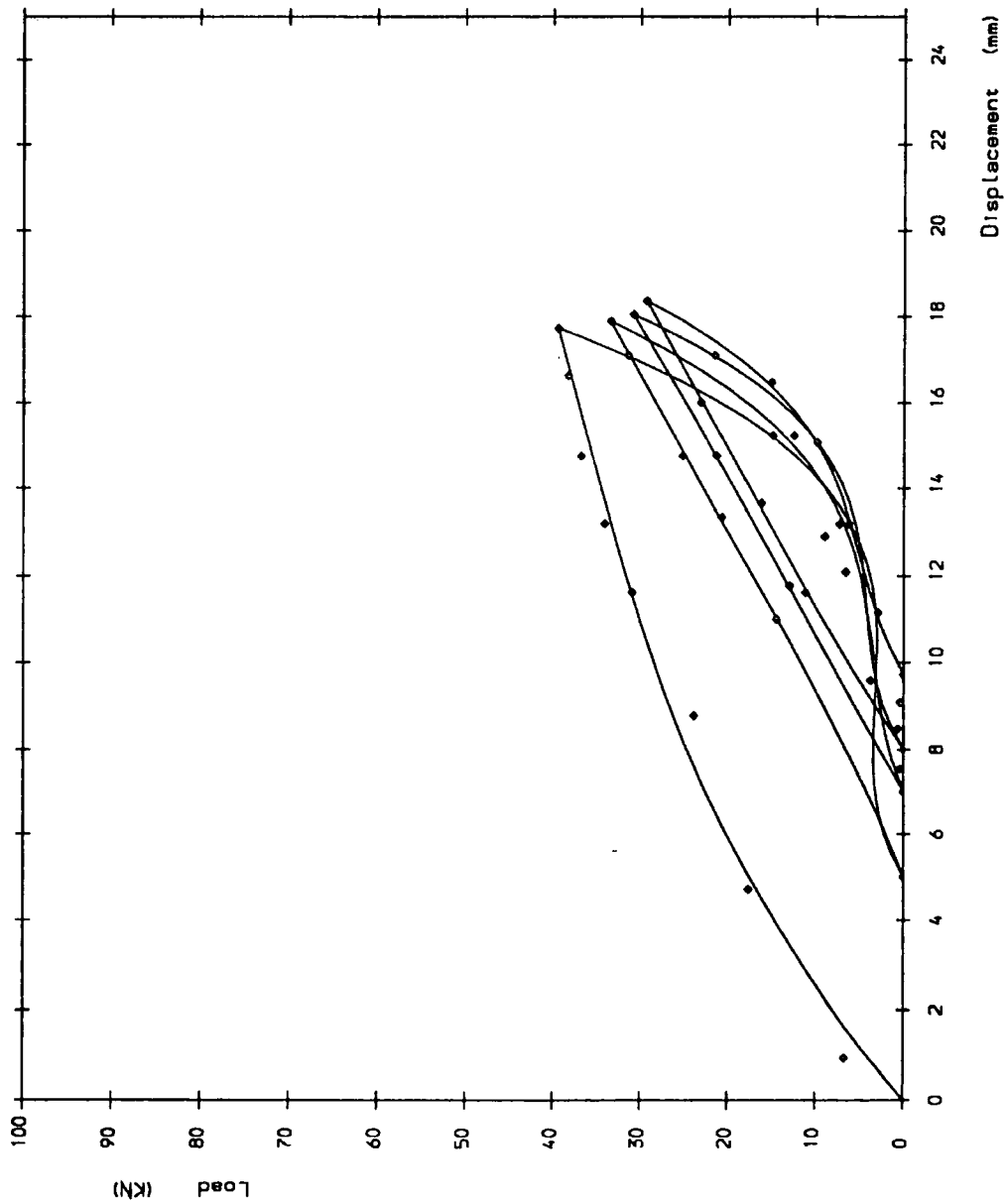
Figure A.5a Load/deflection curve 1st test 3 pile width spacing at 150mm overhang
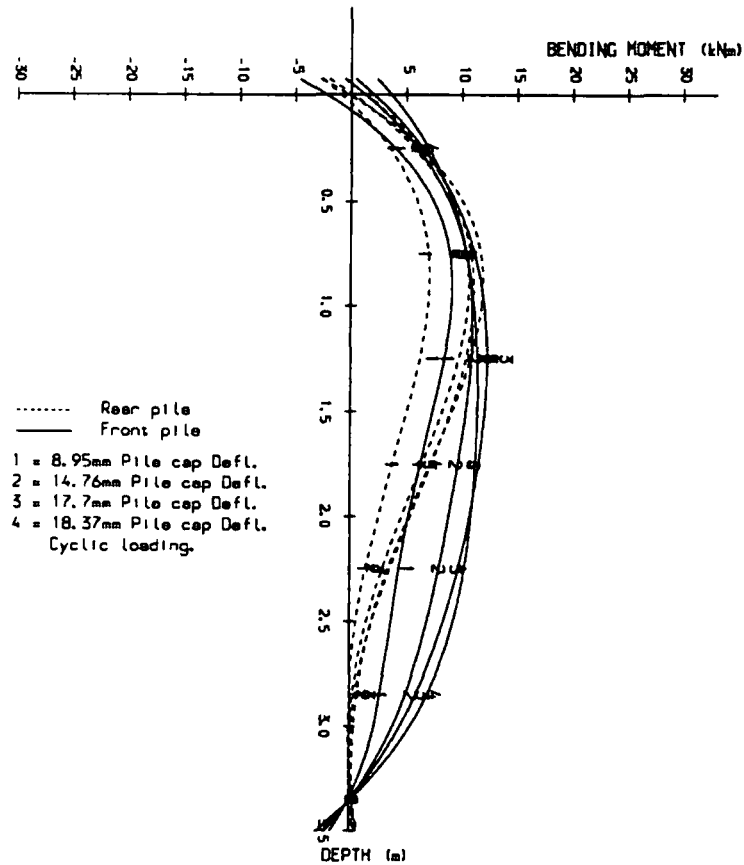
Figure A.5b Bending Moment Diagram for 2 pile group (first
test piles at 3 pile width spacing with 150mm overhang).
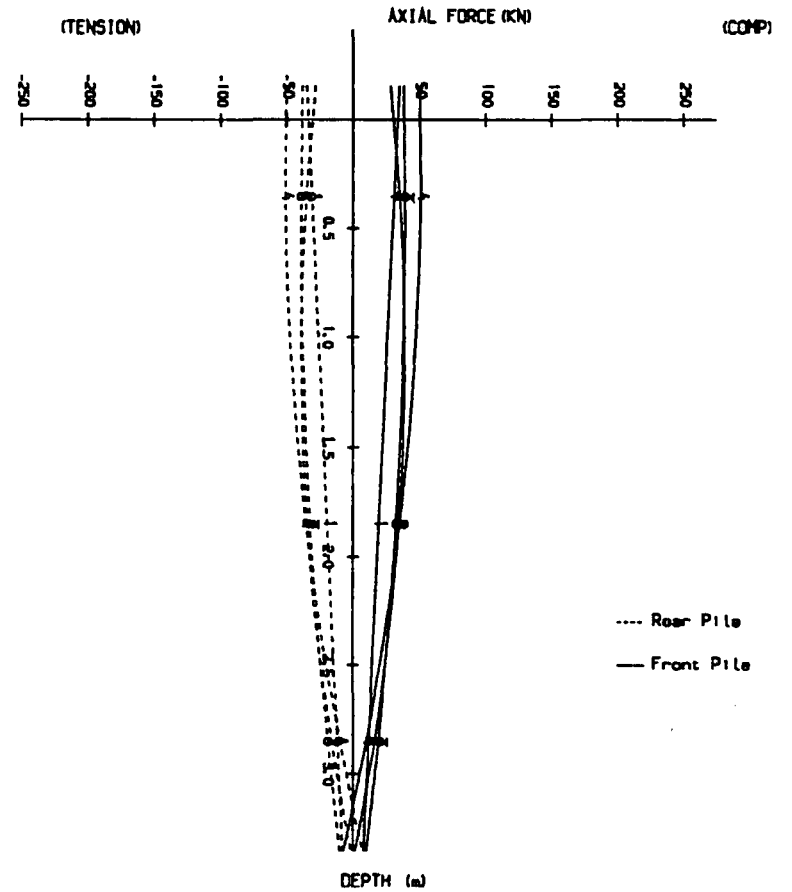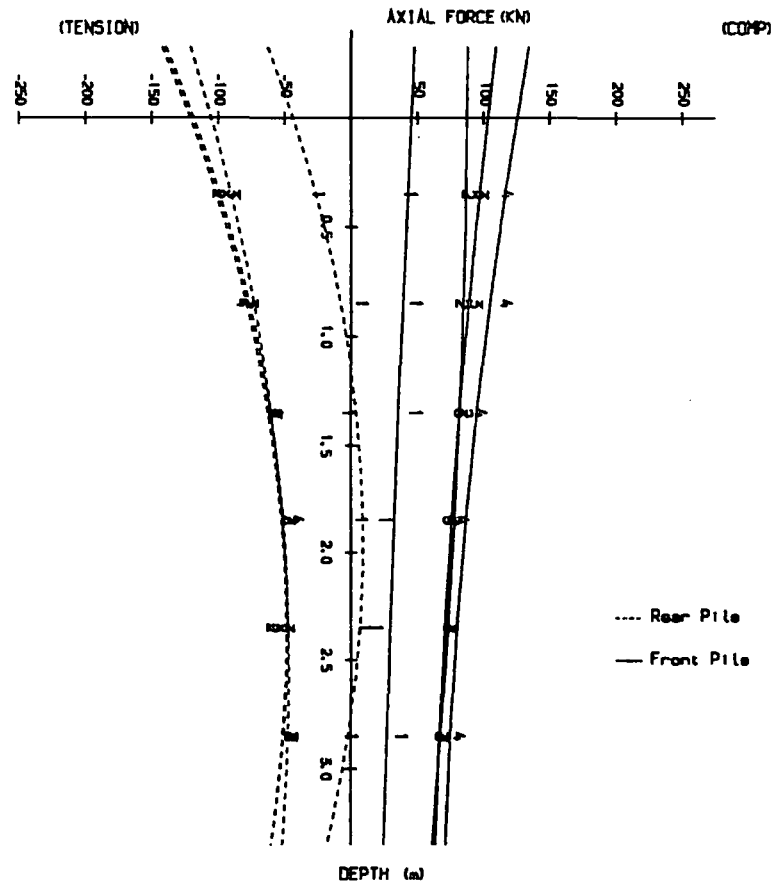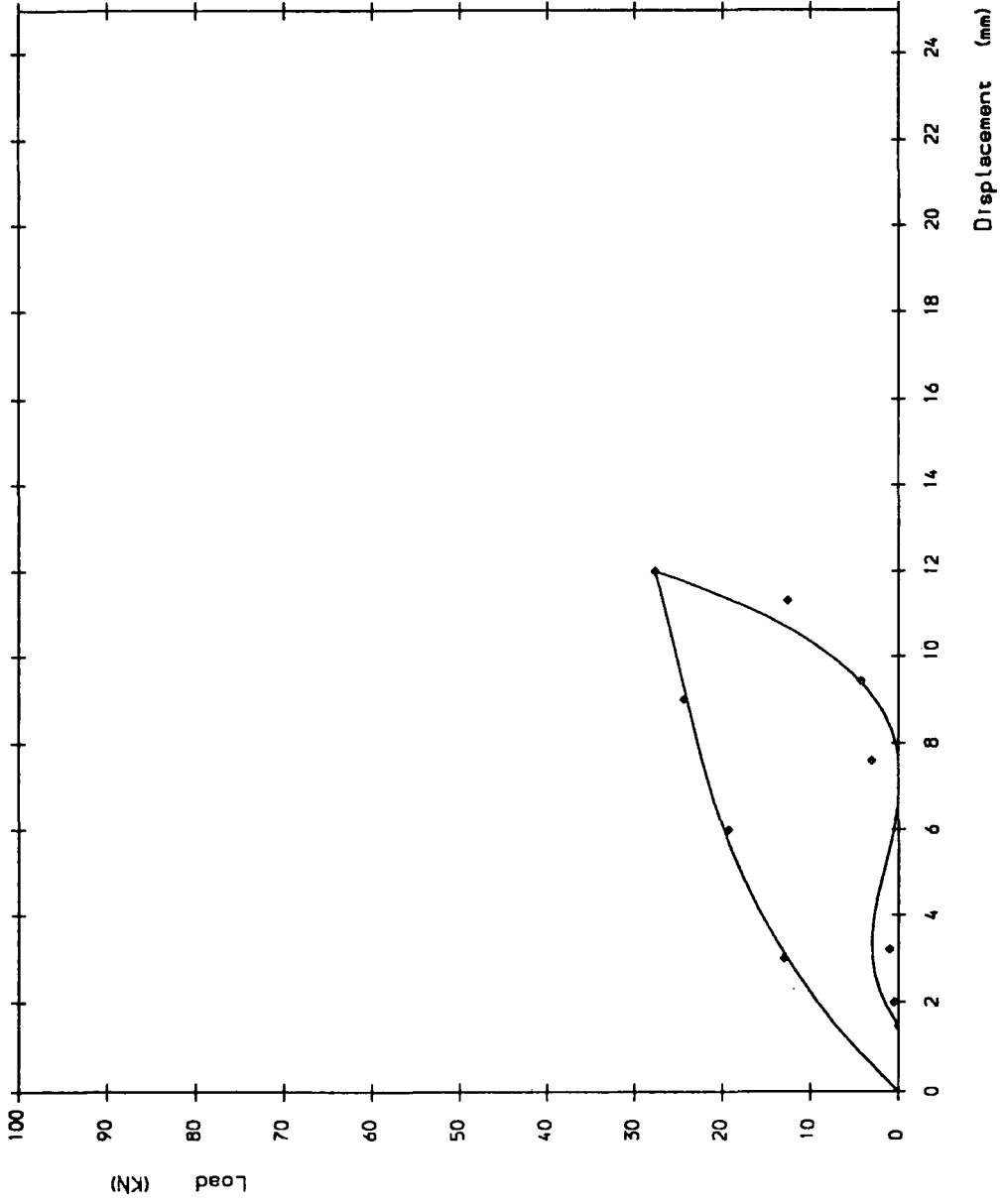

Figure A.5C Axial Force Diagram for 2 pile group (first
test piles at 3 pile width spacing with 150mm overhang).
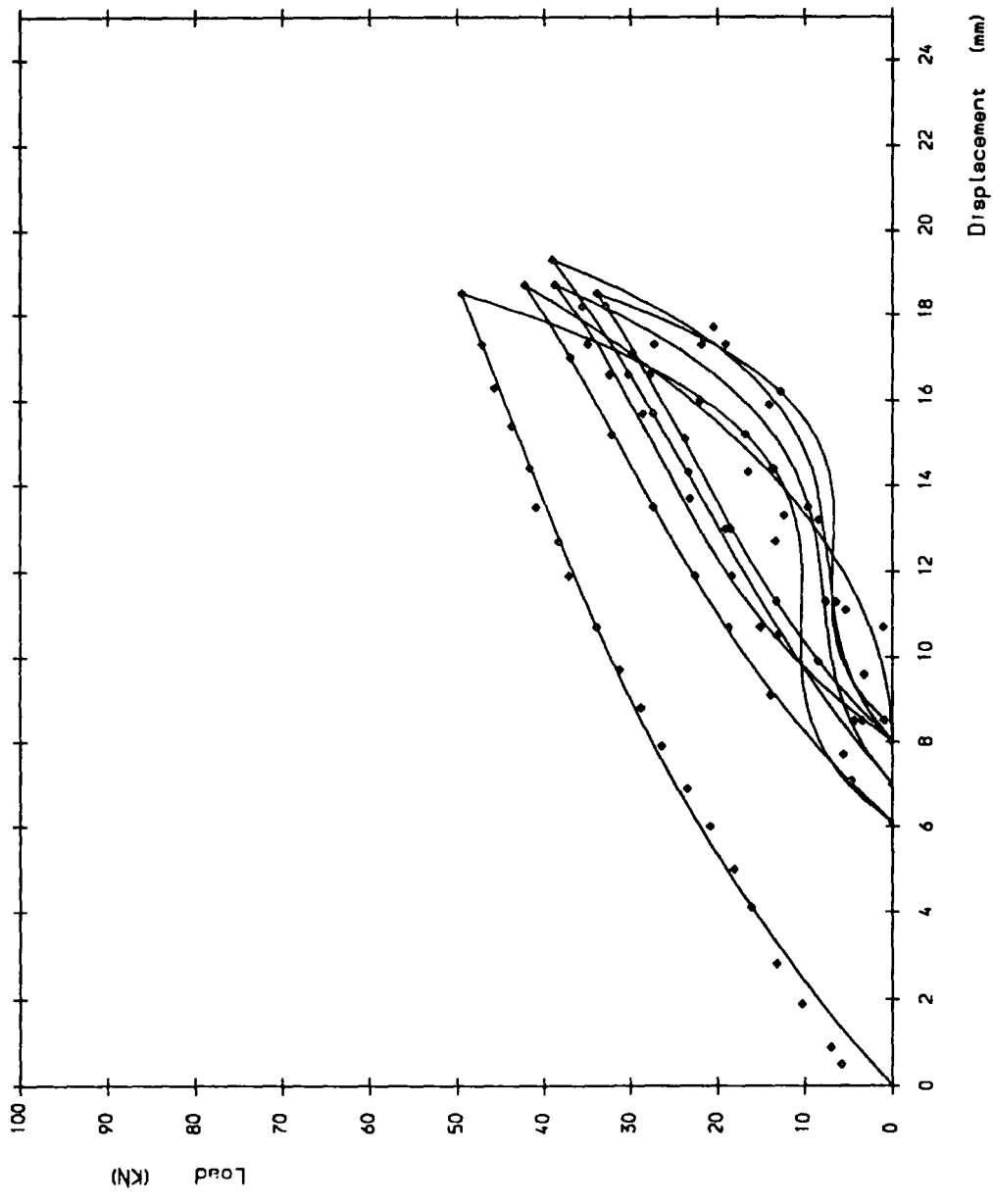
Figure A.6a Load/deflection curve 2nd test 3 pile width spacing 150mm overhang
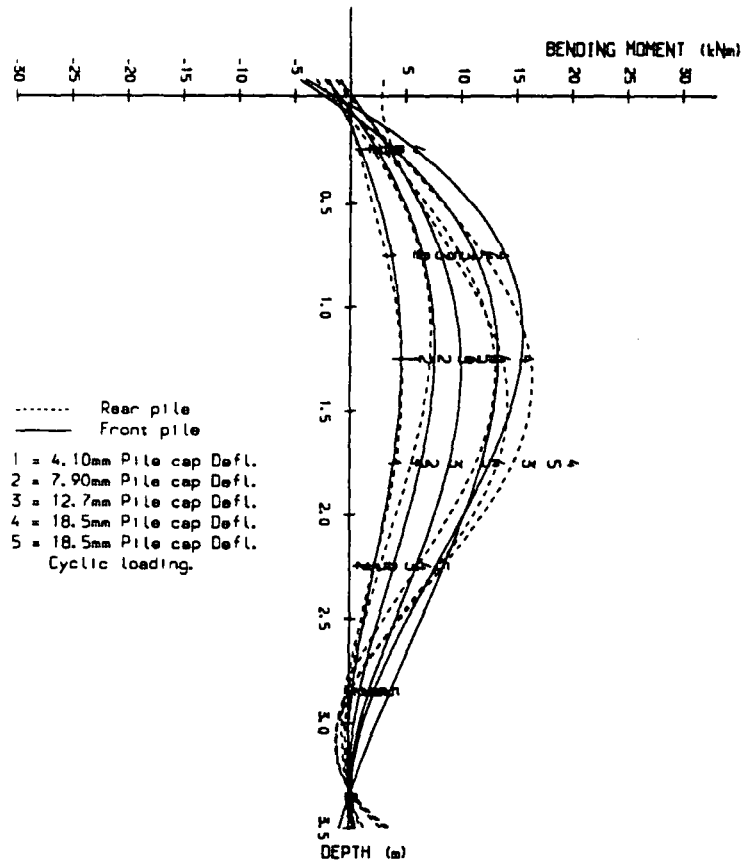
Figure A.6b Bending Moment Diagram for 2 pile group (second
test piles at 3 (pile width) spacing with 150mm overhang).
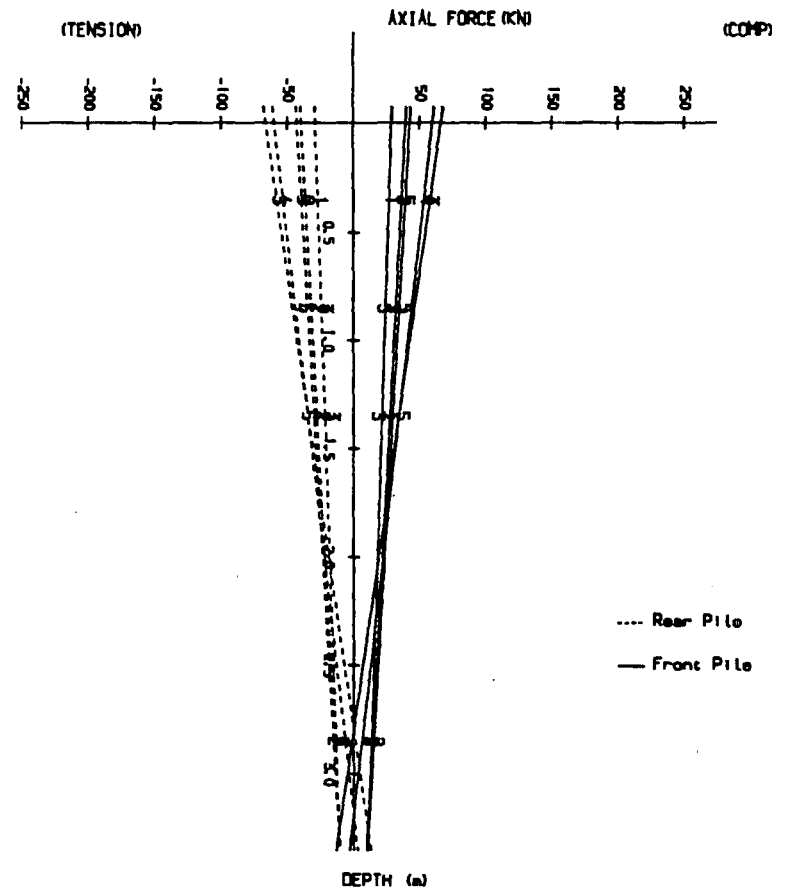
Figure A.6C Axial Force Diagram for 2 pile group (second
test piles at 3 (pile width) spacing with 150mm overhang).
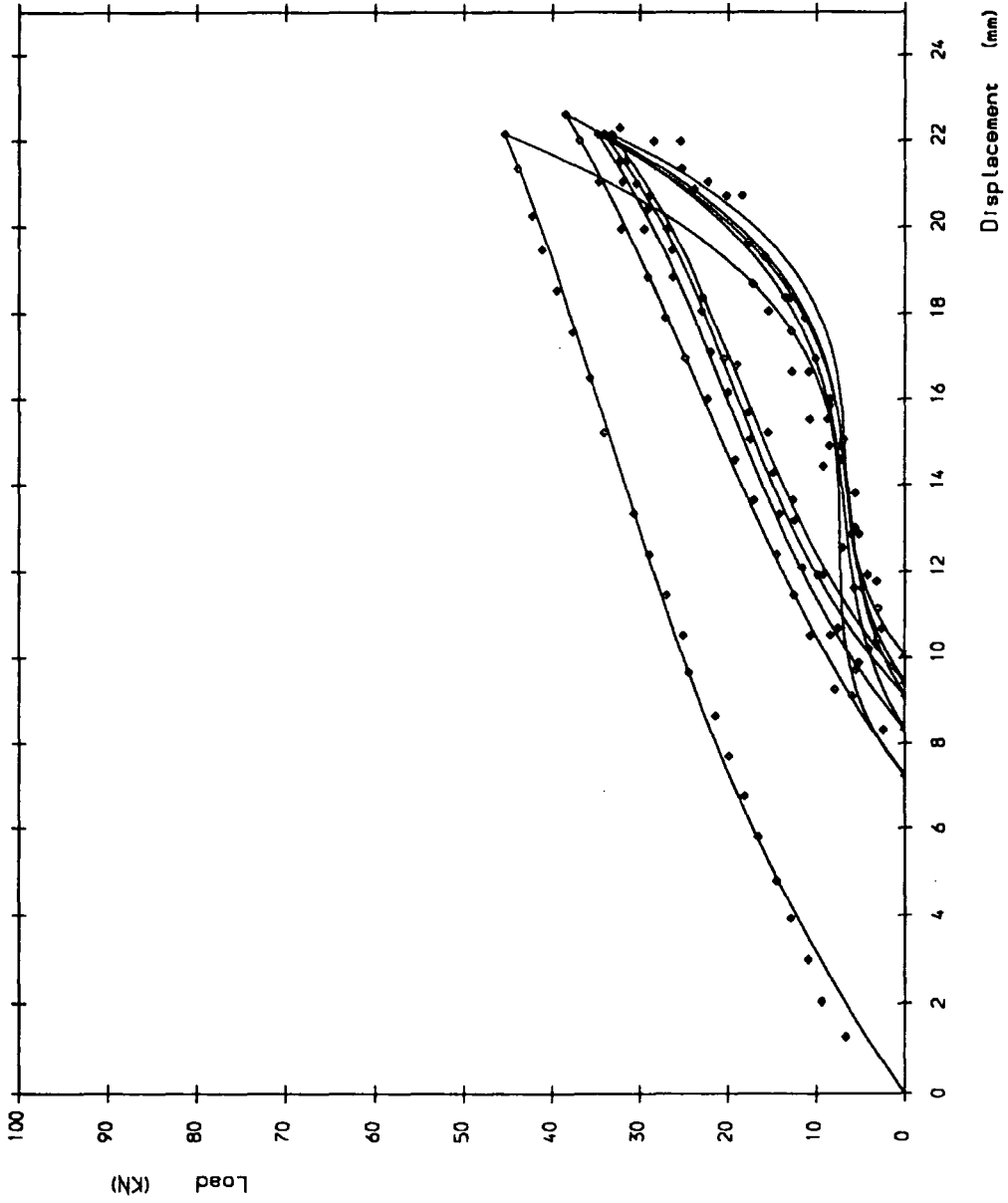
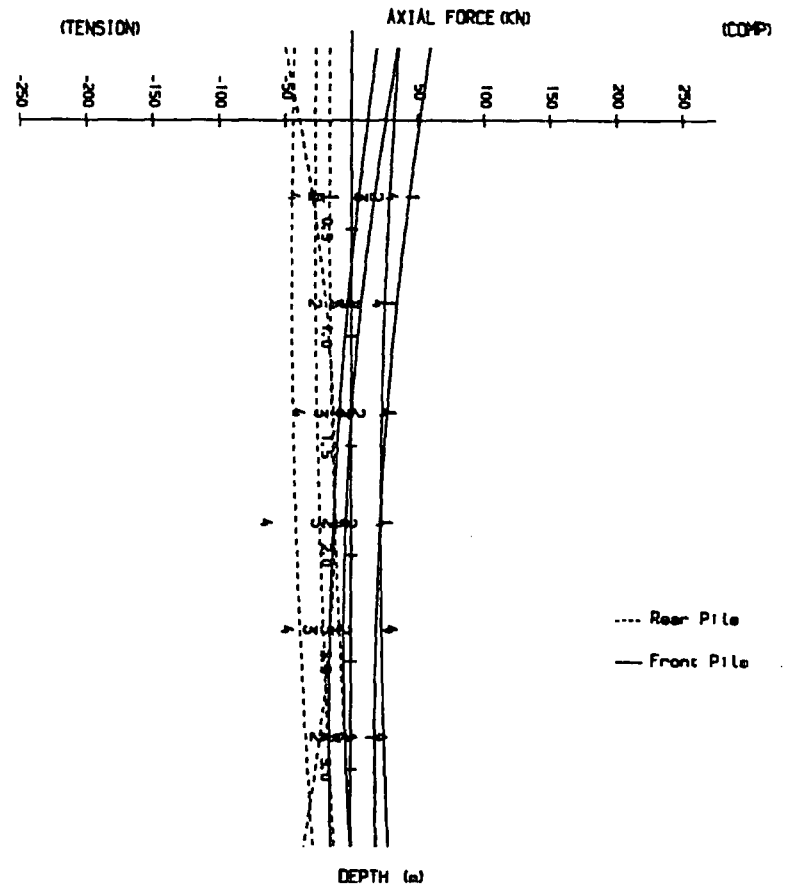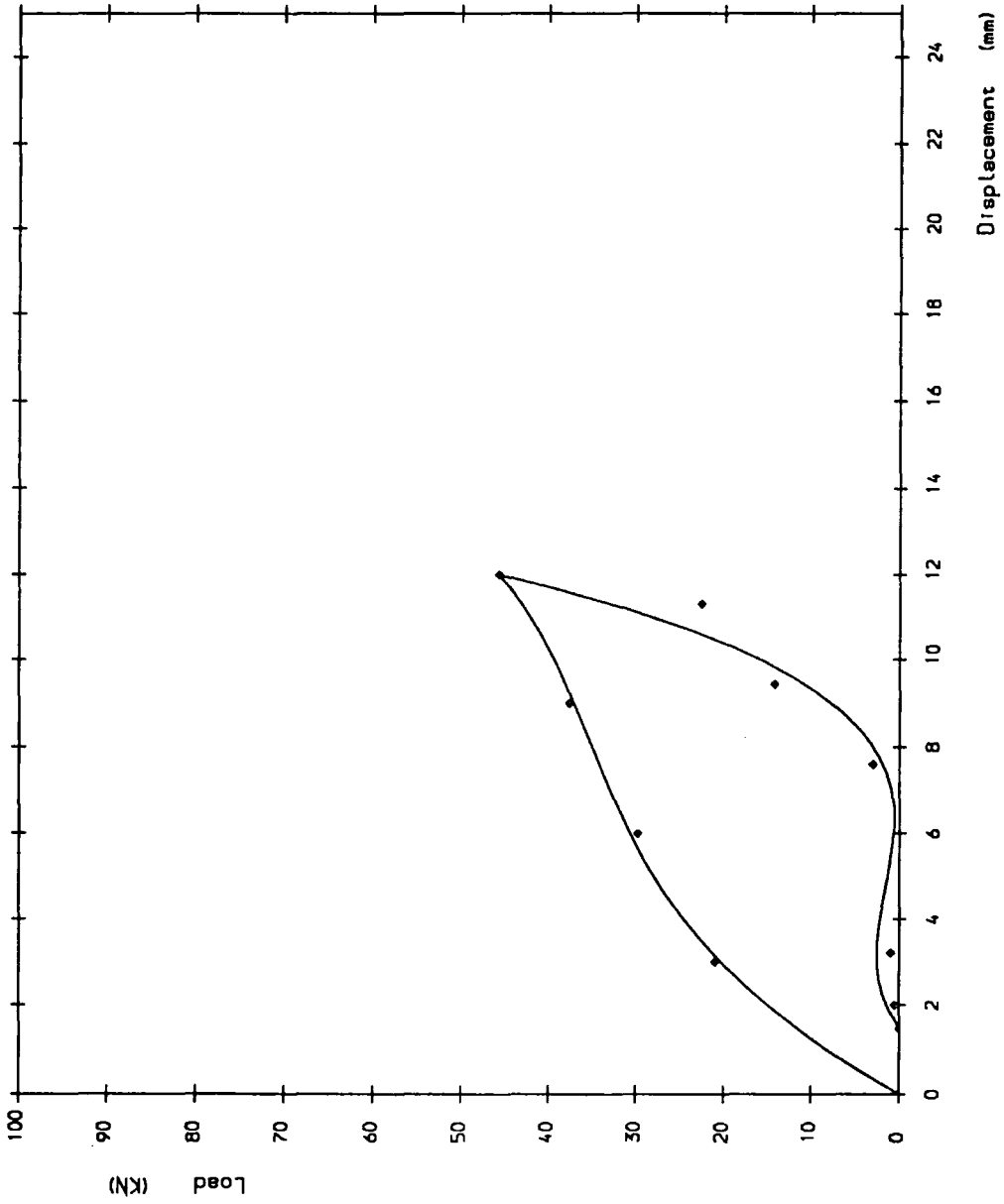Figure A.7a Load/deflection curve 1st test 3 pile width spacing at 300mm overhang

BENDING MOMENT (kNm)

-30 -25 -20 -15 -10 -5   5   10   15   20   25   30

DEPTH (m)

.... Rear pile
———— Front pile

1 = 4.79mm Pile cap Defl.
2 = 9.66mm Pile cap Defl.
3 = 16.5mm Pile cap Defl.
4 = 22.14mm Pile cap Defl.
5 = 22.0mm Pile cap Defl.
    Cyclic loading.
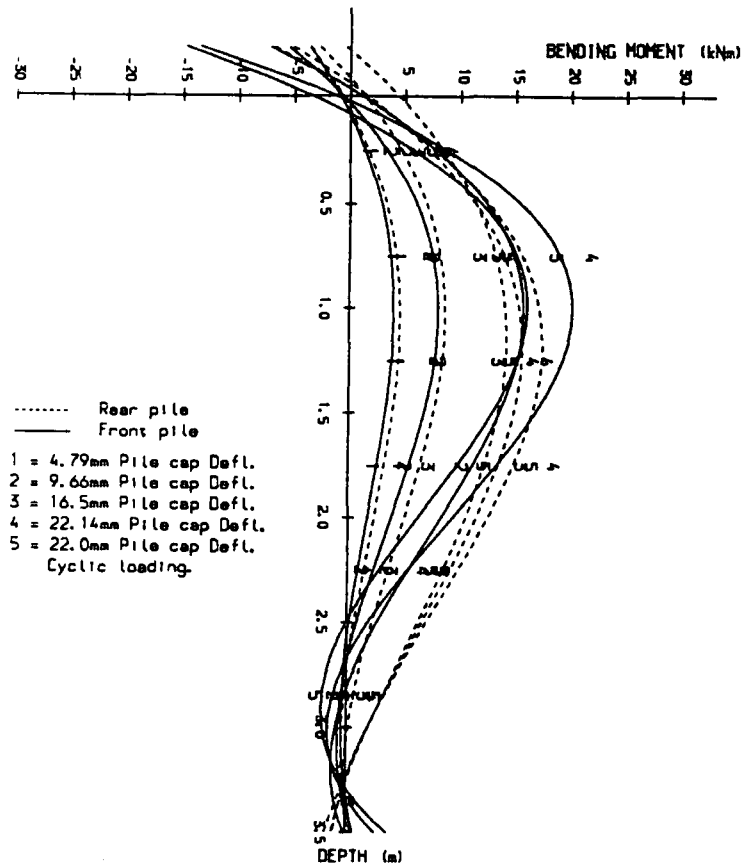
Figure A.7b Bending Moment Diagram for 2 pile group (first
test piles at 3 pile width spacing with 300mm overhang).

(TENSION)   AXIAL FORCE (KN)   (COMP)

-250 -200 -150 -100 -50   50   100   150   200   250

DEPTH (m)

---- Rear Pile
—— Front Pile
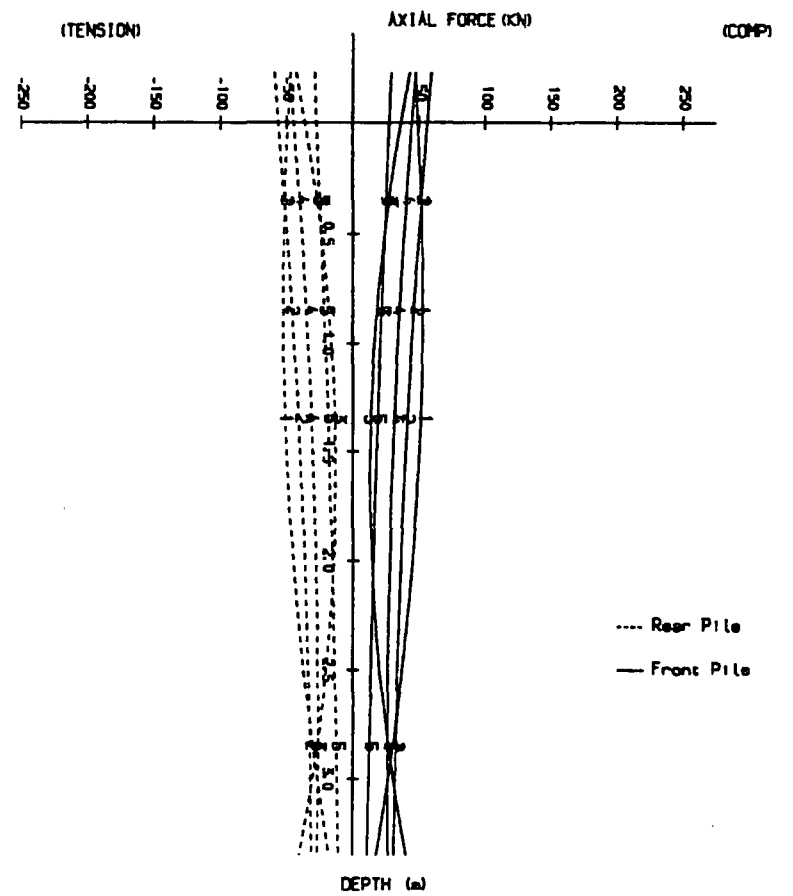
Figure A.7C Axial Force Diagram for 2 pile group (first
test piles at 3 pile width spacing with 300mm overhang).
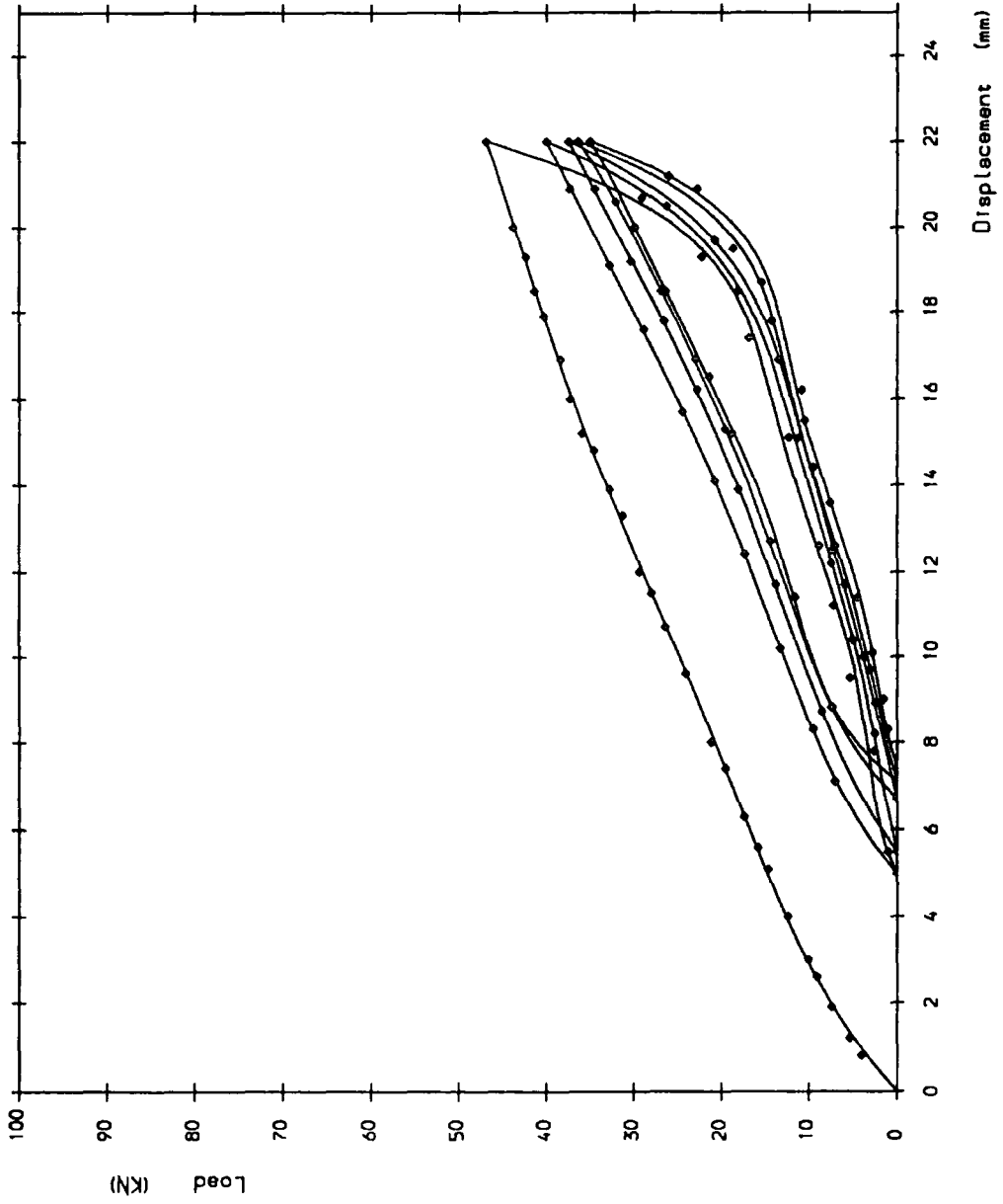
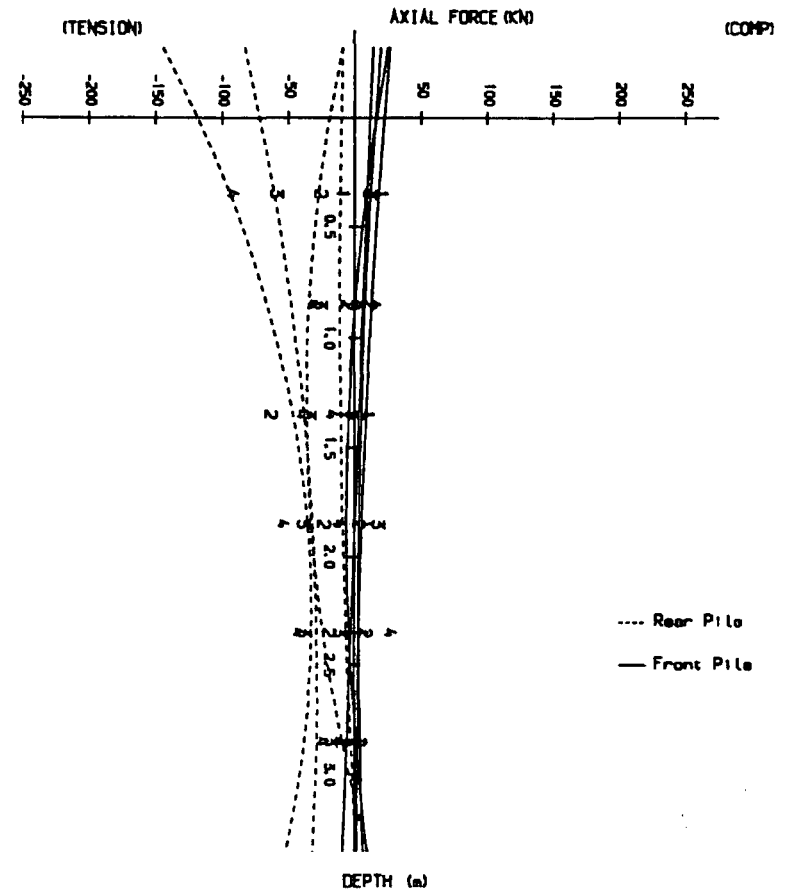Figure A.8a Load/deflection curve 2nd test 3 pile width spacing at 300mm overhang

BENDING MOMENT (kN·m)

-30 -25 -20 -15 -10 -5 5 10 15 20 25 30

-------- Rear pile
———— Front pile

1 = 4.00mm Pile cap Defl.
2 = 8.00mm Pile cap Defl.
3 = 12.00mm Pile cap Defl.
4 = 16.00mm Pile cap Defl.
5 = 22.00mm Pile cap Defl.
6 = 22.00mm Pile cap Defl.
     Cyclic loading.

DEPTH (m)
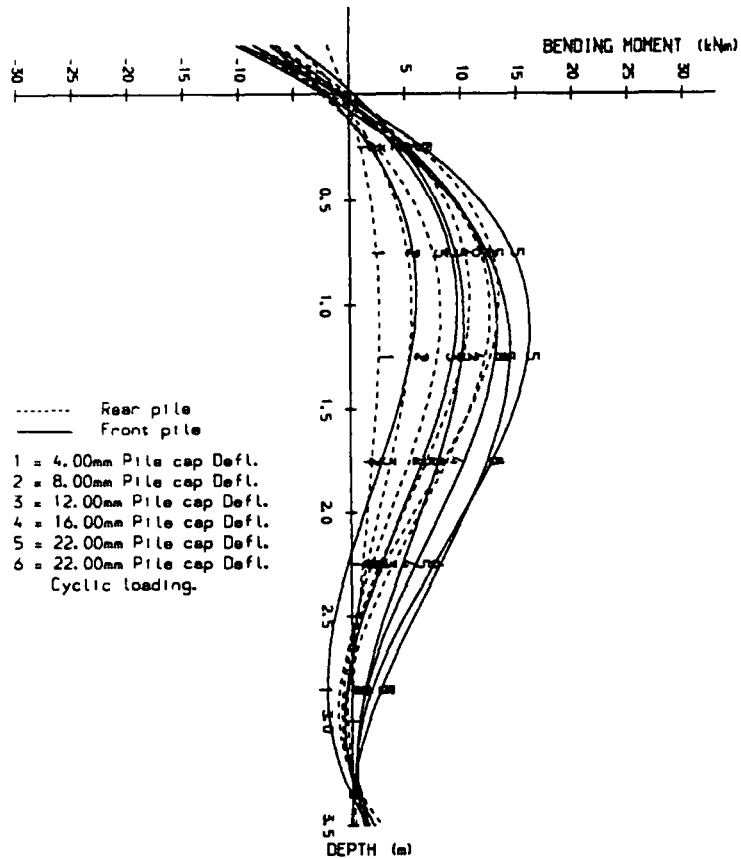
Figure A.8b Bending Moment Diagram for 2 pile group (second test piles at 3 pile width spacing with 300mm overhang).

(TENSION)   AXIAL FORCE (KN)   (COMP)

-250 -200 -150 -100 -50 50 100 150 200 250

-------- Rear Pile
———— Front Pile

DEPTH (m)
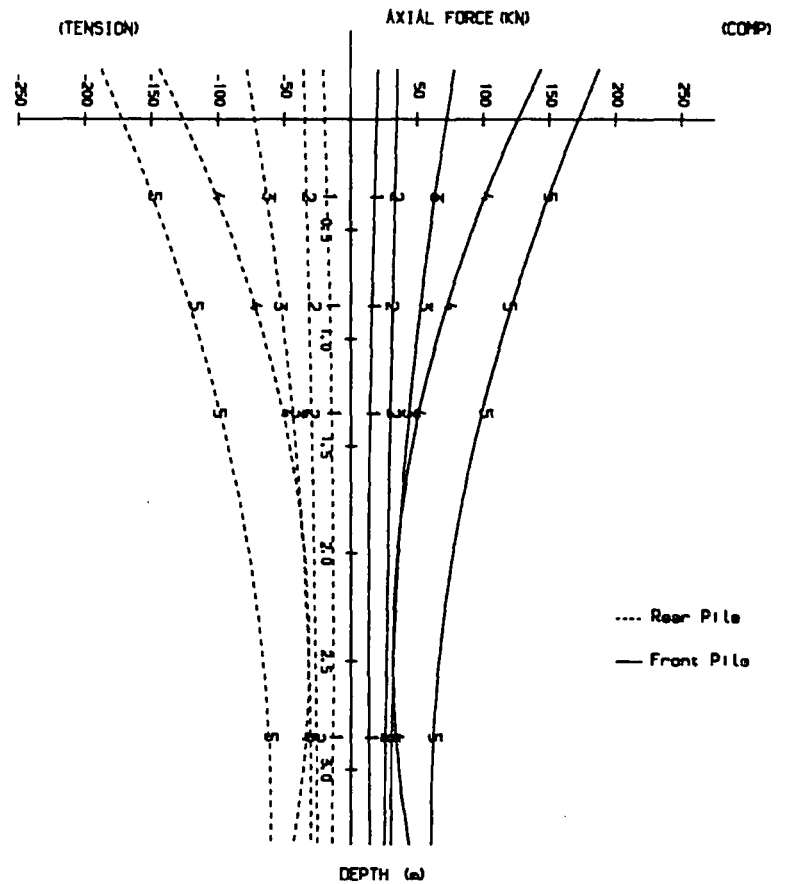
Figure A.8C Axial Force Diagram for 2 pile group (second test piles at 3 pile width spacing with 300mm overhang).
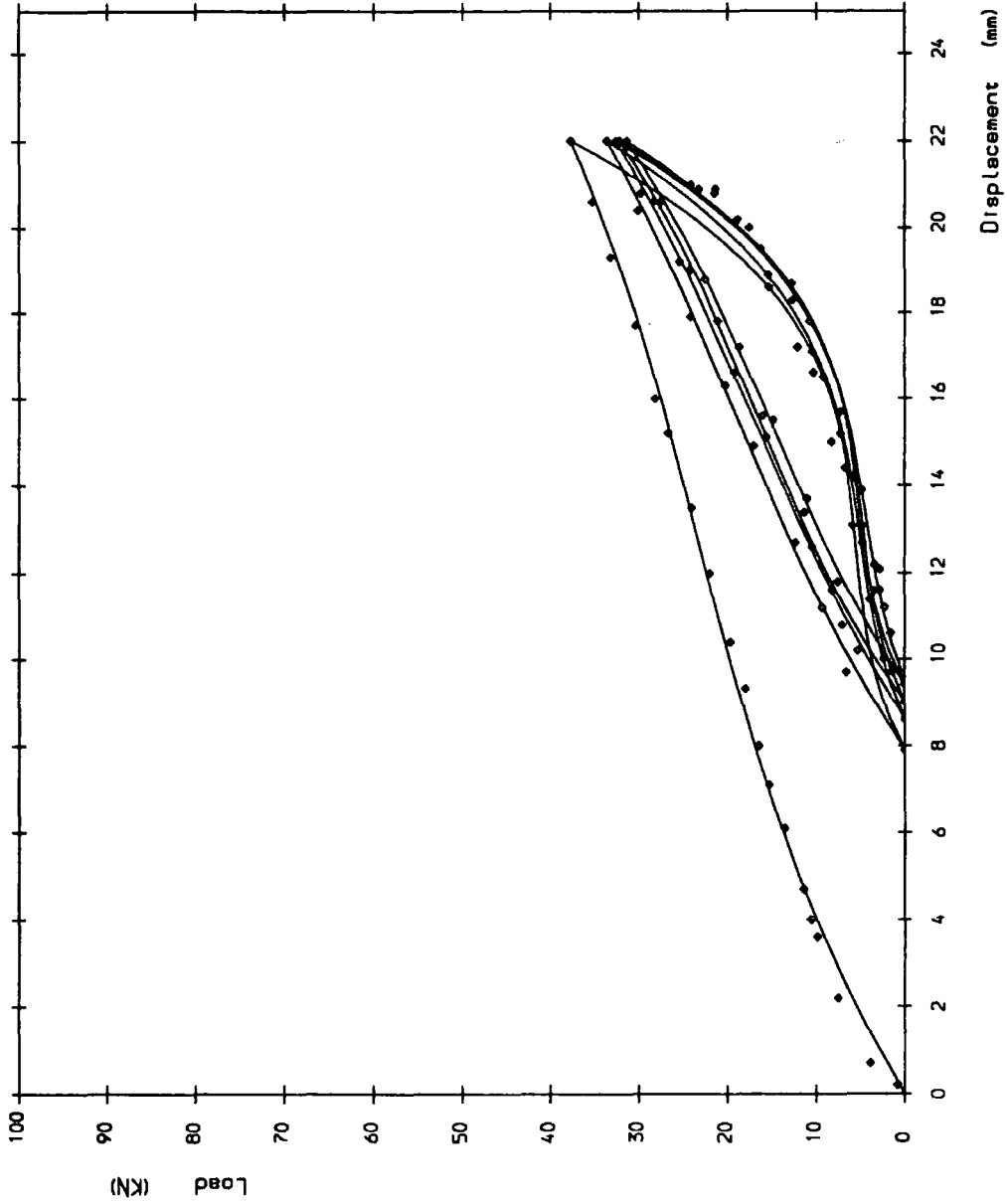
Figure A.9a Load/deflection curve 1st test 3pile widthspacing at 400mm overhang
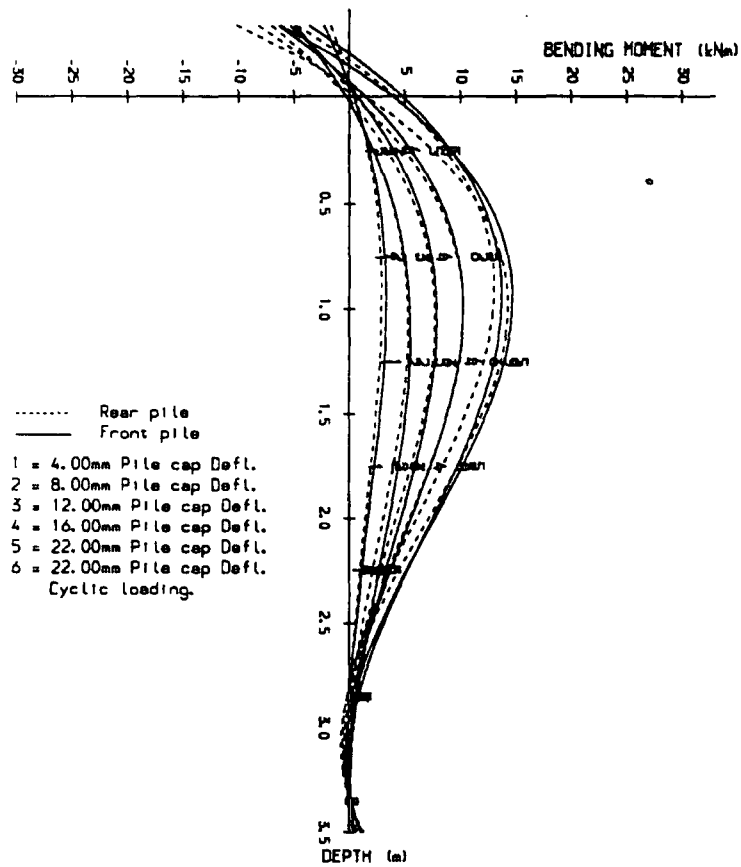
Figure A.9b Bending Moment Diagram for 2 pile group (first test piles at 3 pile width spacing with 400mm overhang).
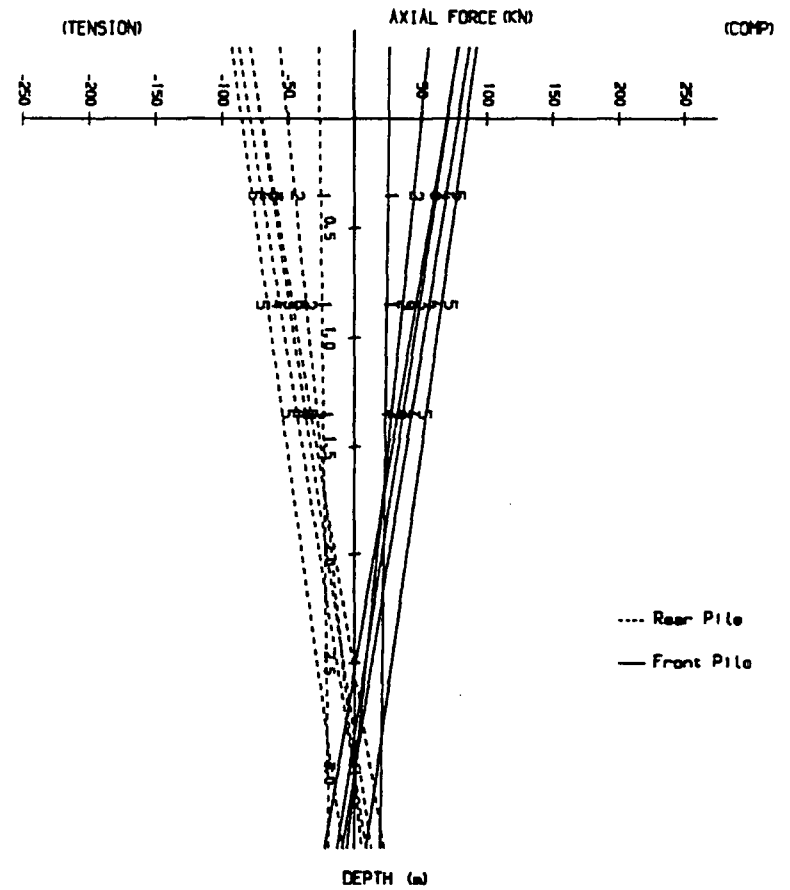
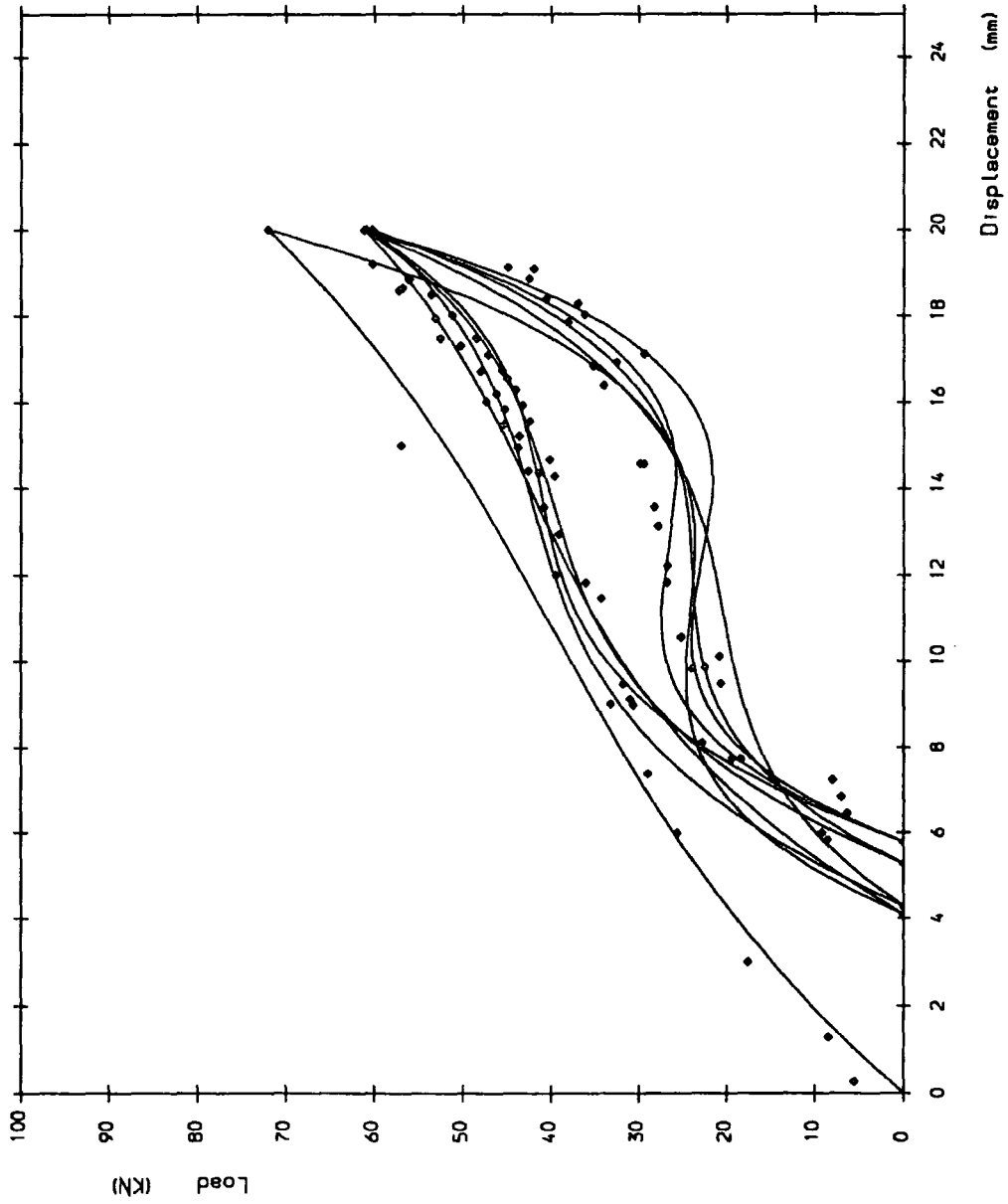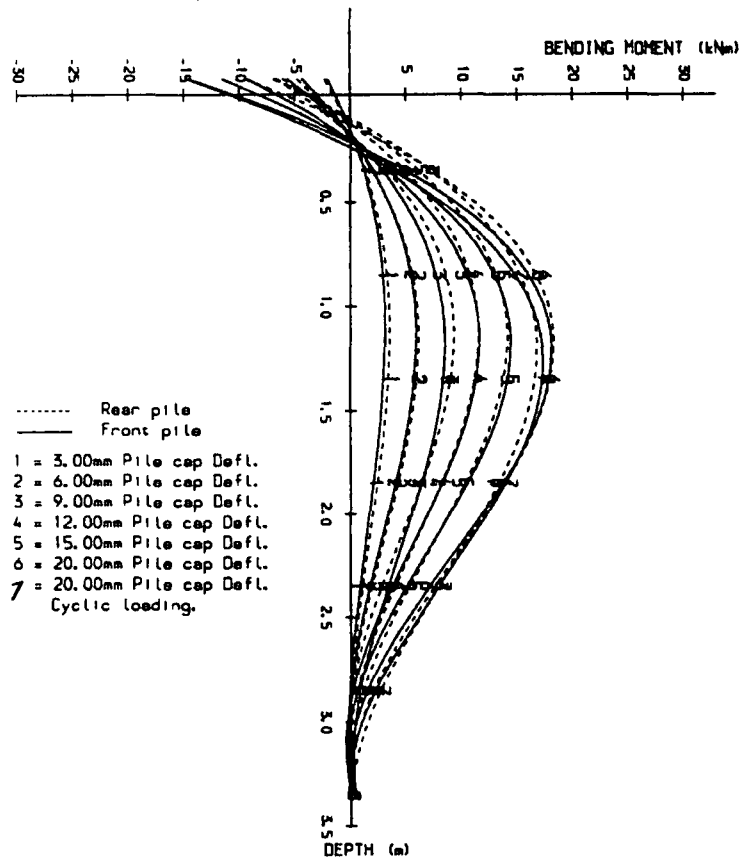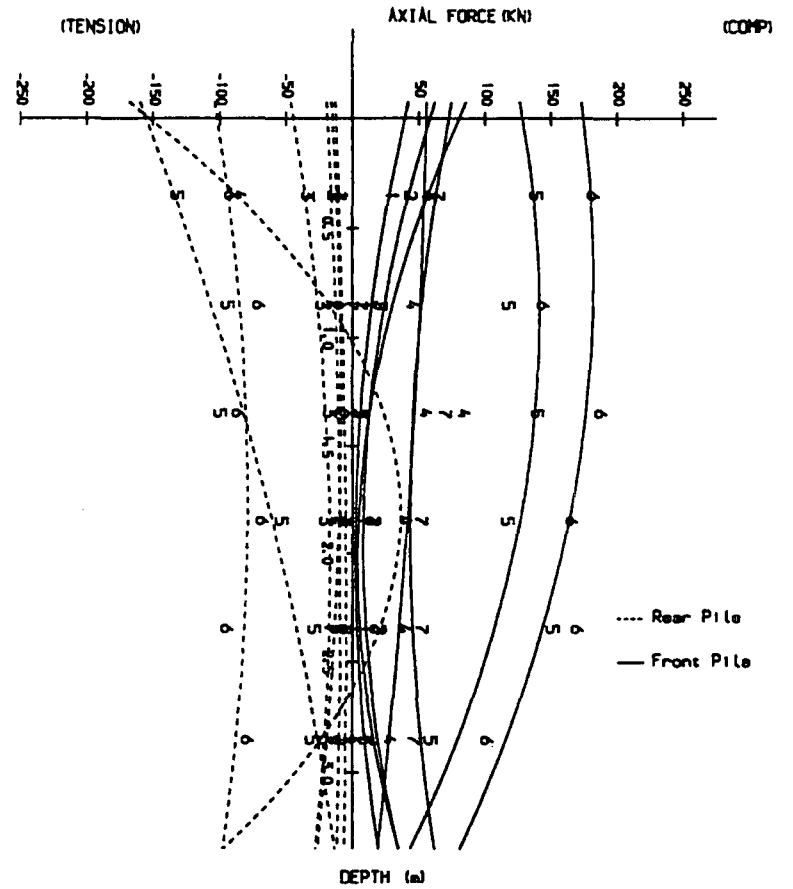Figure A.9C Axial Force Diagram for 2 pile group (first test piles at 3 pile width spacing with 400mm overhang).
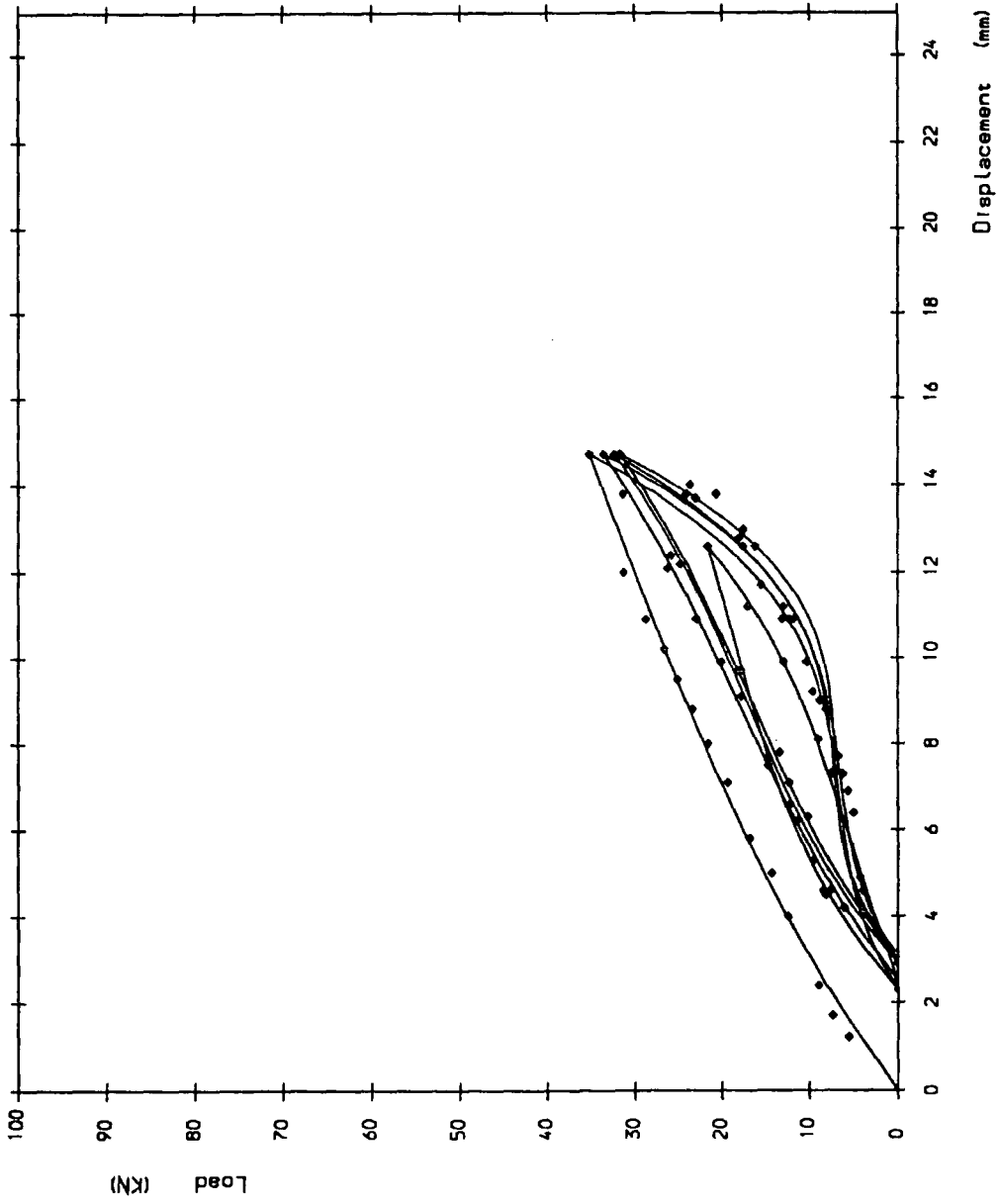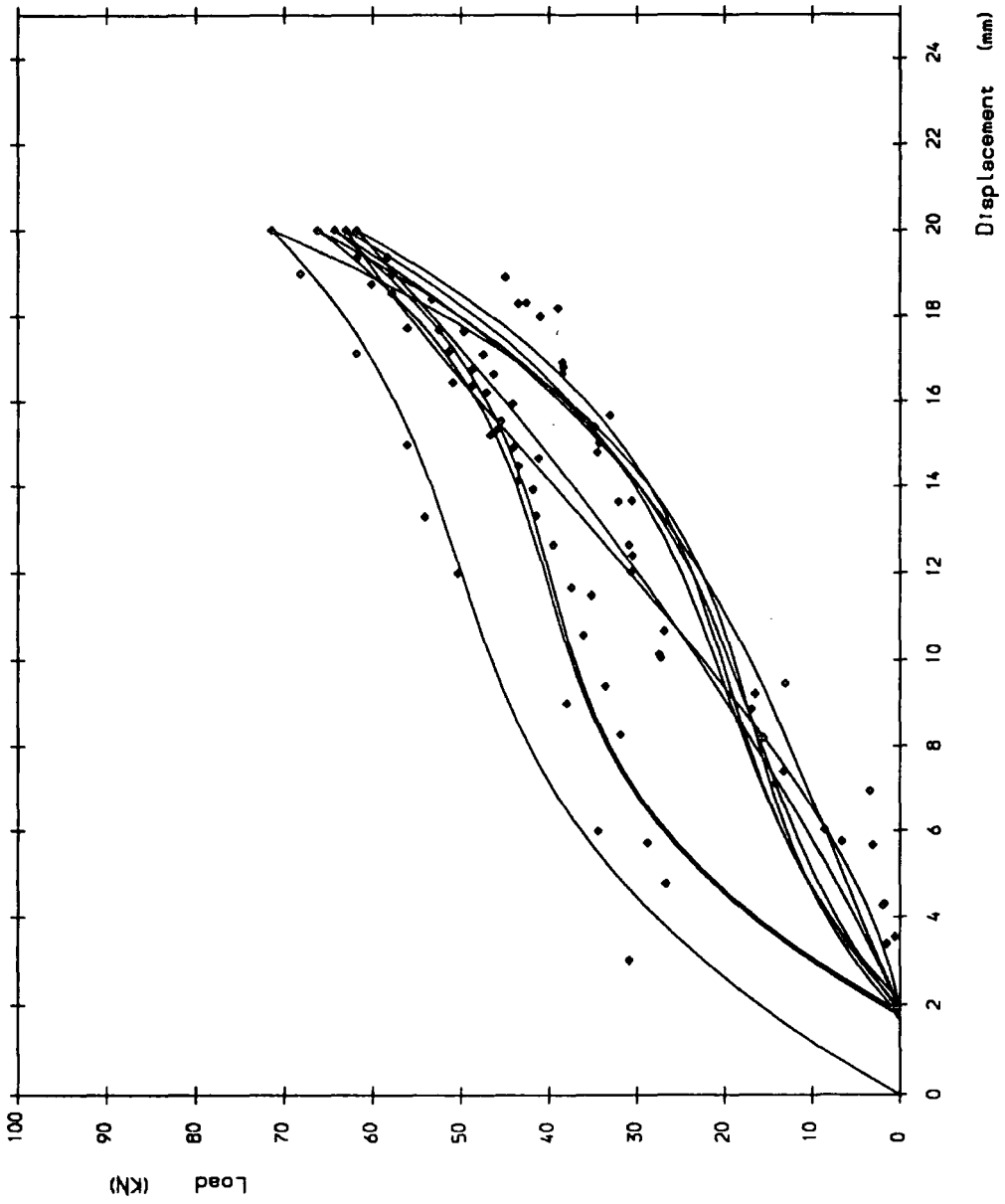
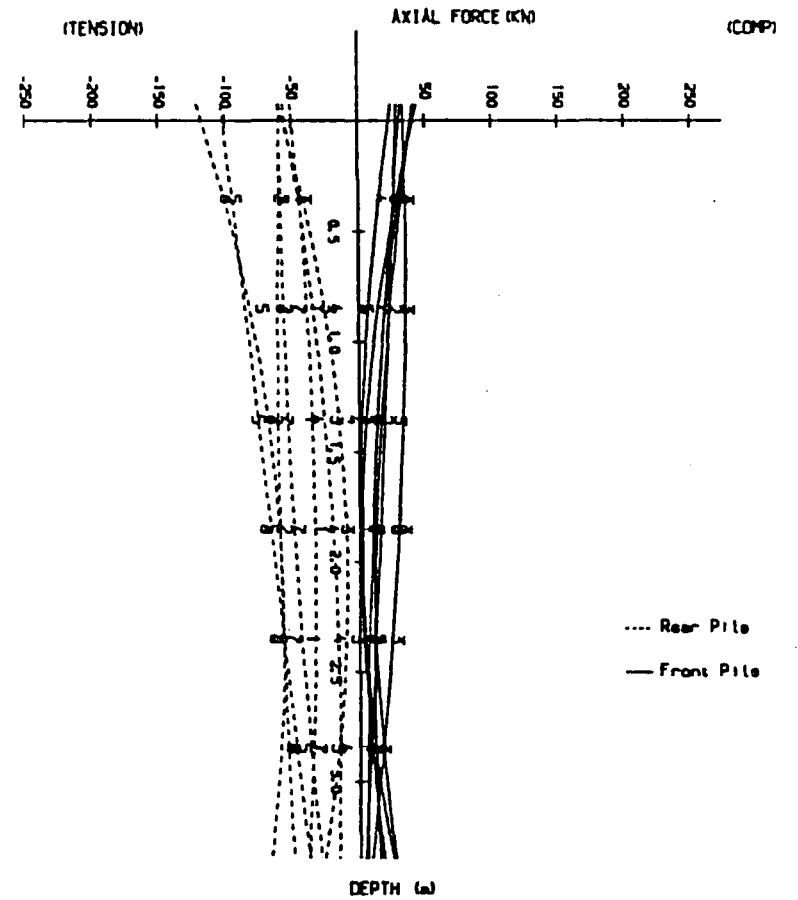Figure A.10a Load/deflection curve 2nd test 3 pile width spacing at 400mm overhang

BENDING MOMENT (kNm)

-30 -25 -20 -15 -10   5   10   15   20   25   30

0.5

1.0

1.5

-------- Rear pile
———— Front pile

1 = 4.00mm Pile cap Defl.
2 = 8.00mm Pile cap Defl.
3 = 12.00mm Pile cap Defl.
4 = 14.70mm Pile cap Defl.
5 = 15.00mm Pile cap Defl.
   Cyclic loading.

2.0

2.5

3.0

3.5

DEPTH (m)
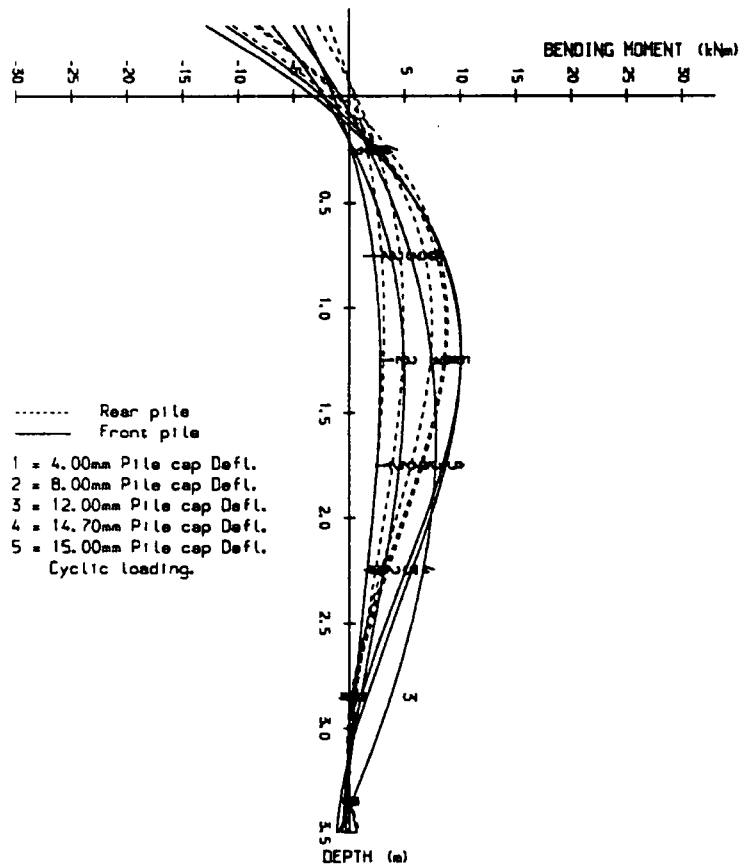
Figure A.10b Bending Moment Diagram for 2 pile group (second

test piles at 3 pile width spacing with 400mm overhang).
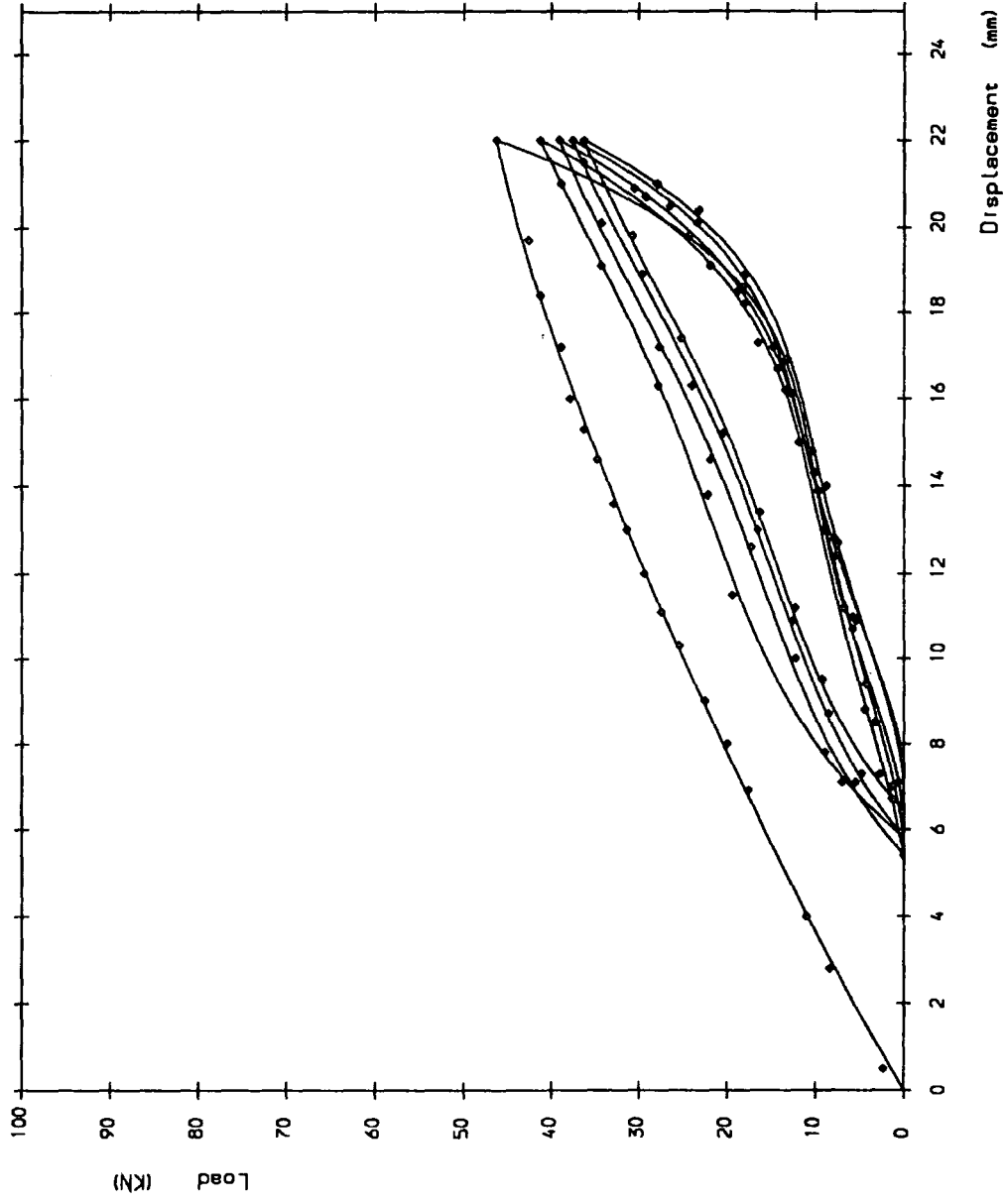
Figure A.11a Load/deflection curve 3rd test 3 pile width spacing at 400mm overhang

BENDING MOMENT (kN·m)

Rear pile
Front pile

1 = 4.00mm Pile cap Defl.
2 = 8.00mm Pile cap Defl.
3 = 12.00mm Pile cap Defl.
4 = 14.70mm Pile cap Defl.
5 = 15.00mm Pile cap Defl.
Cyclic loading.

DEPTH (m)
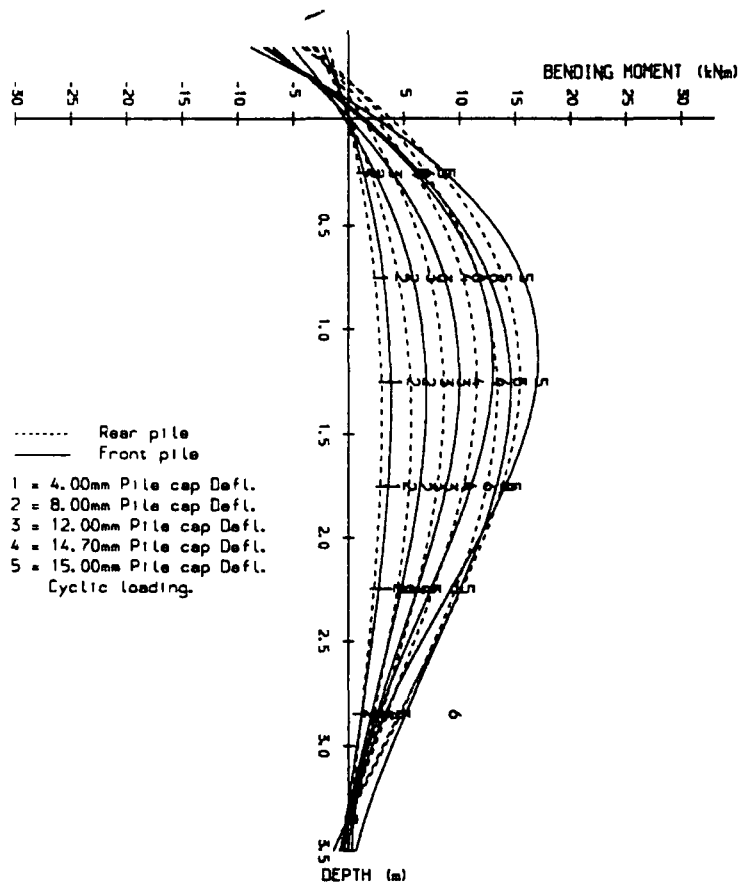
Figure A.11b Bending Moment Diagram for 2 pile group (third
test piles at 3 pile width spacing with 400mm overhang).
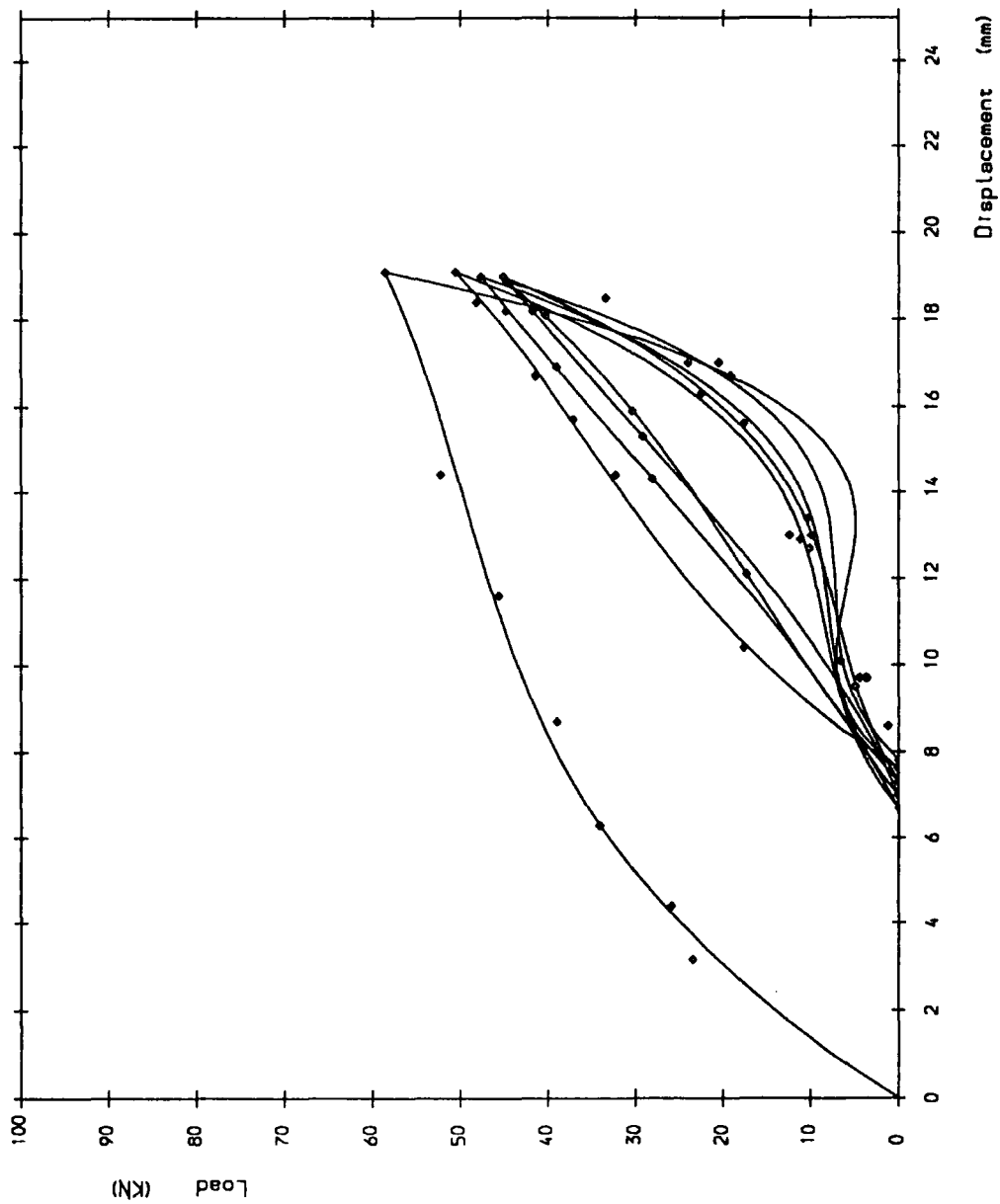
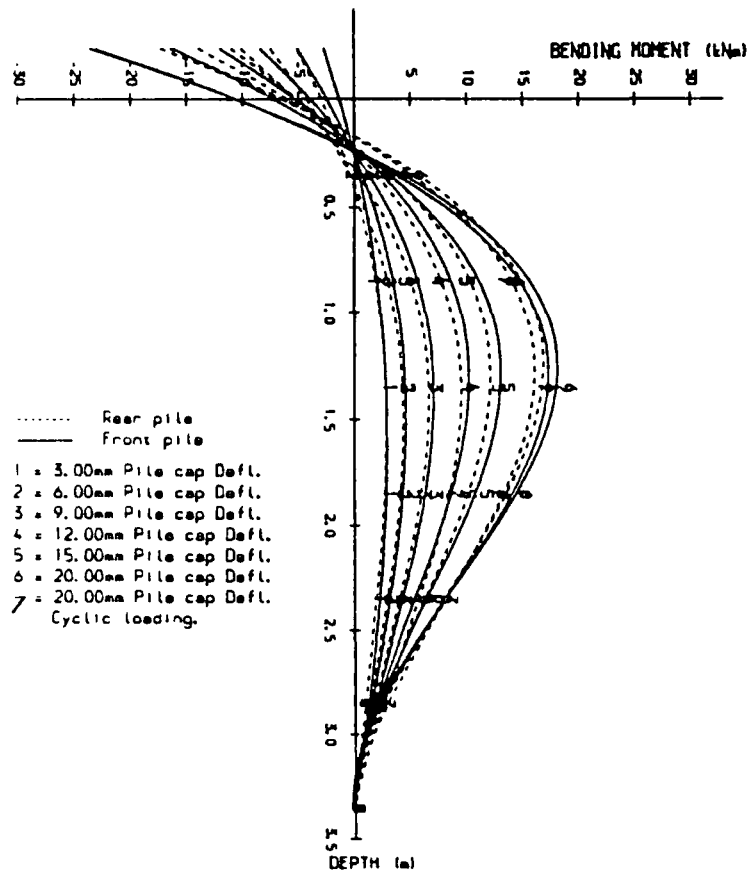Figure A.12a Load/deflection curve 1st test 5 pile width spacing at 150mm overhang

BENDING MOMENT (kN·m)

-30 -25 -20 -15 -10 -5 5 10 15 20 25 30

-------- Rear pile
———— Front pile

1 = 3.15mm Pile cap Defl.
2 = 6.30mm Pile cap Defl.
3 = 8.70mm Pile cap Defl.
4 = 11.60mm Pile cap Defl.
5 = 14.40mm Pile cap Defl.
6 = 19.10mm Pile cap Defl.
7 = 18.90mm Pile cap Defl.
   Cyclic loading.

DEPTH (m)
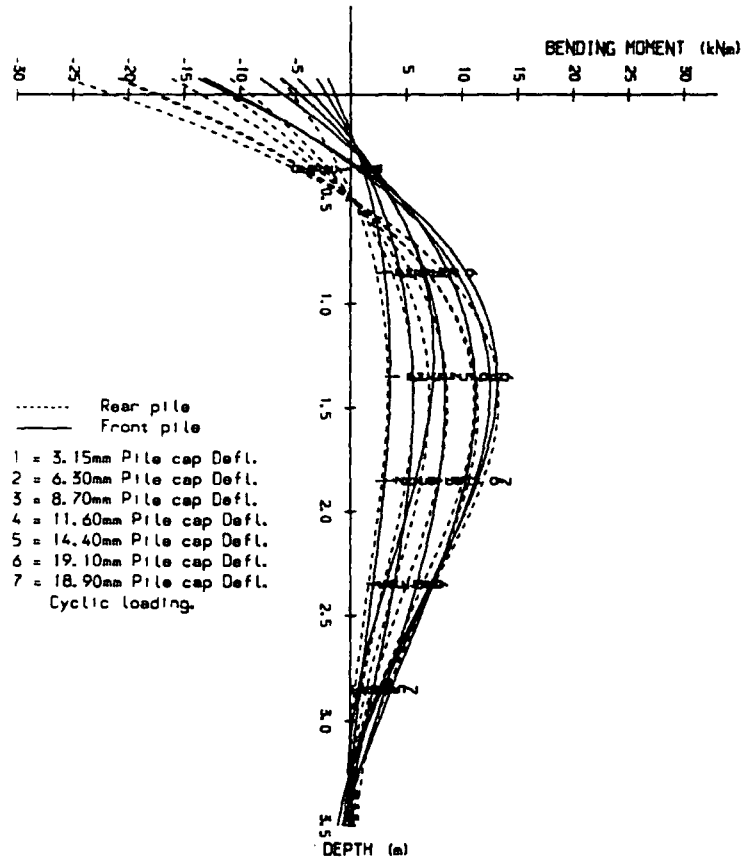
Figure A.12b Bending Moment Diagram for 2 pile group (first
test piles at 5 (pile width) spacing with 150mm overhang).
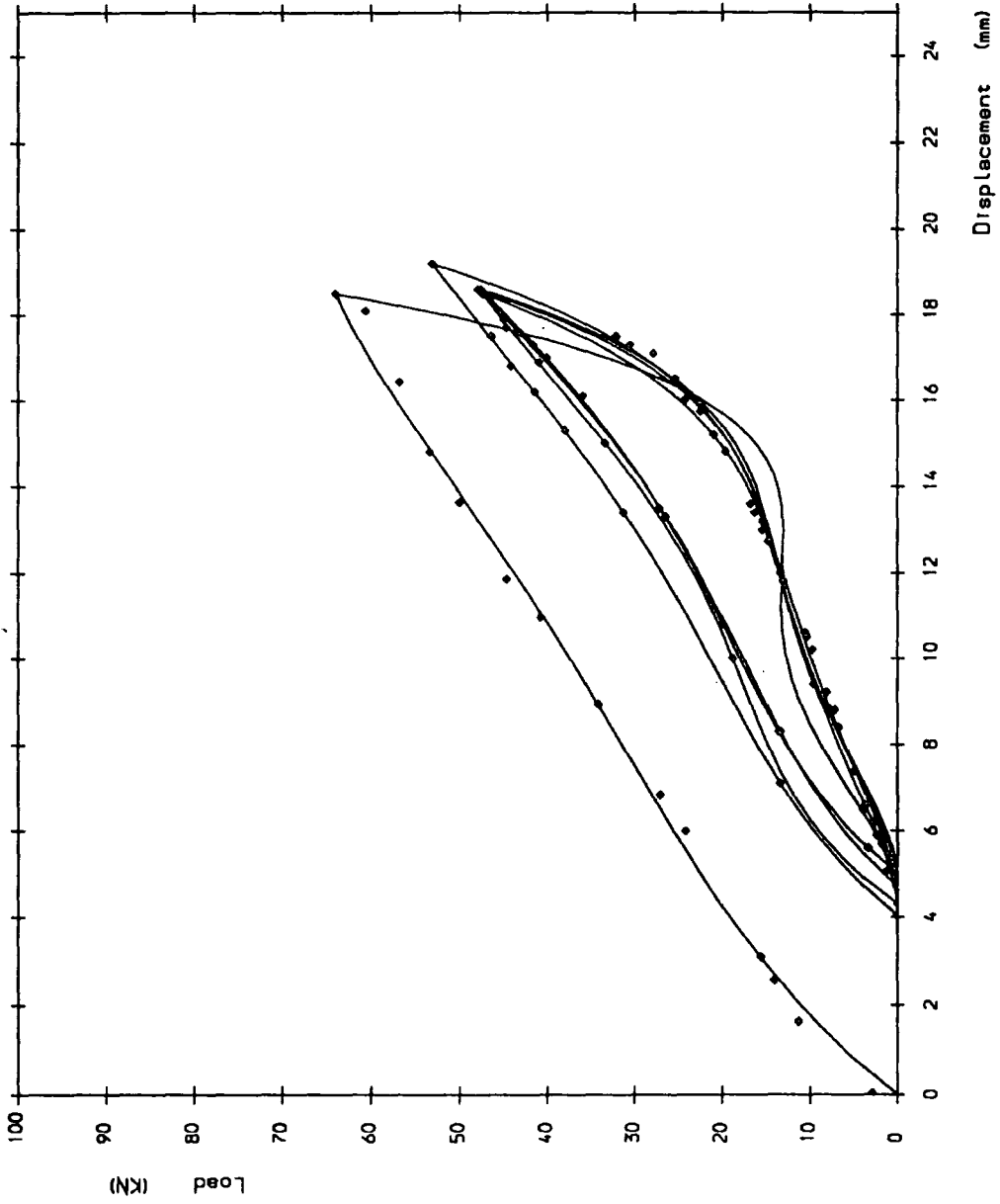
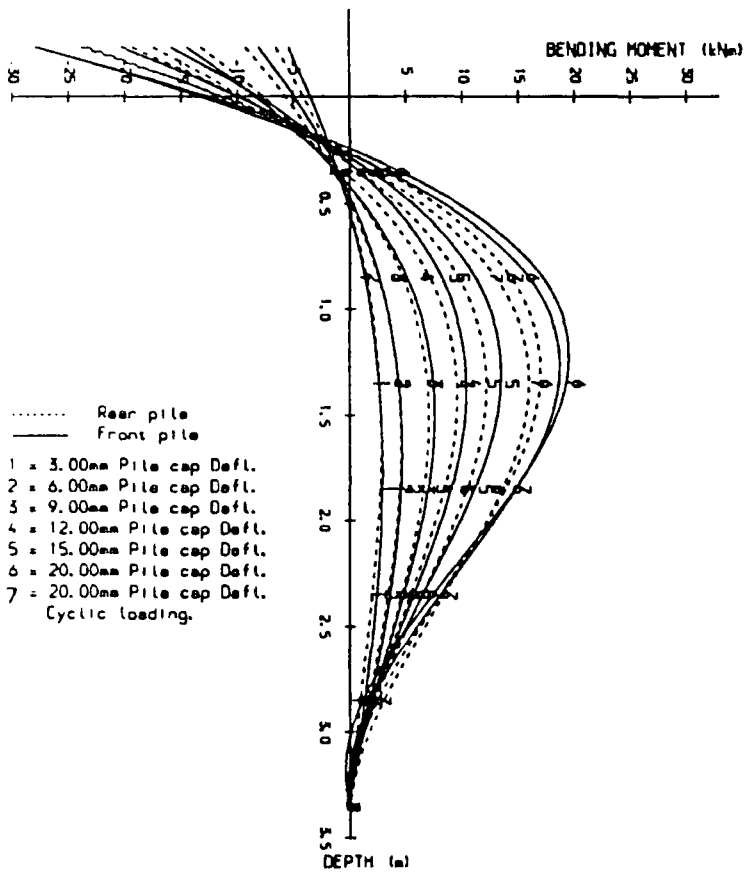Figure A.13a Load/deflection curve 2nd test 5 pile width spacing at 150mm overhang
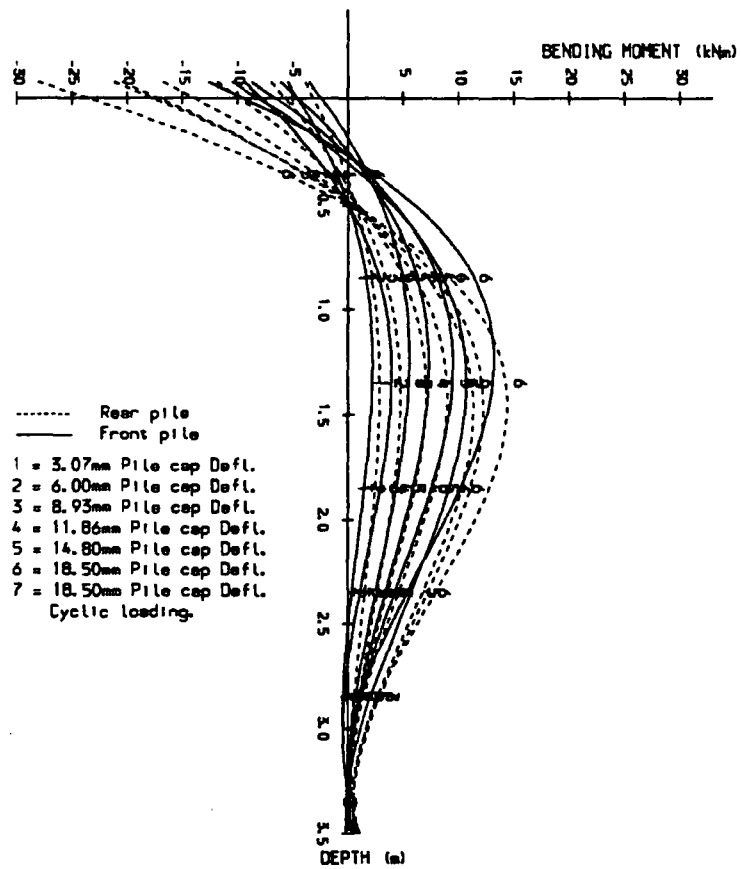
BENDING MOMENT (kN·m)

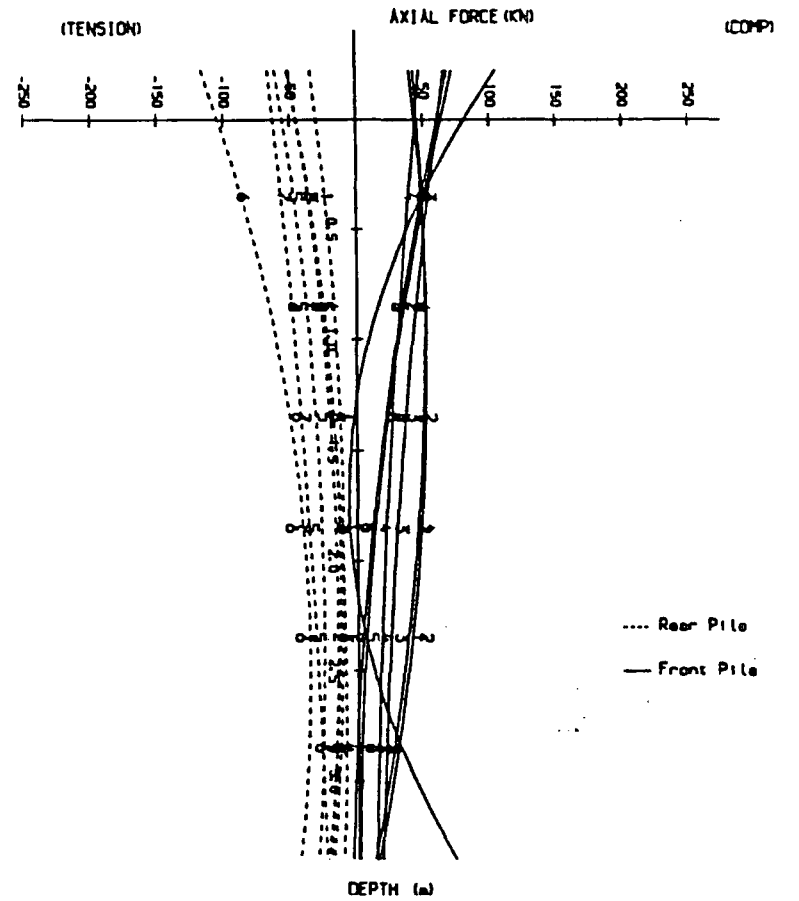Figure A.13b Bending Moment Diagram for 2 pile group (second test piles at 5 pile width spacing with 150mm overhang).

Rear pile
Front pile

1 = 3.07mm Pile cap Defl.
2 = 6.00mm Pile cap Defl.
3 = 8.93mm Pile cap Defl.
4 = 11.86mm Pile cap Defl.
5 = 14.80mm Pile cap Defl.
6 = 18.50mm Pile cap Defl.
7 = 18.50mm Pile cap Defl.
   Cyclic loading.

DEPTH (m)
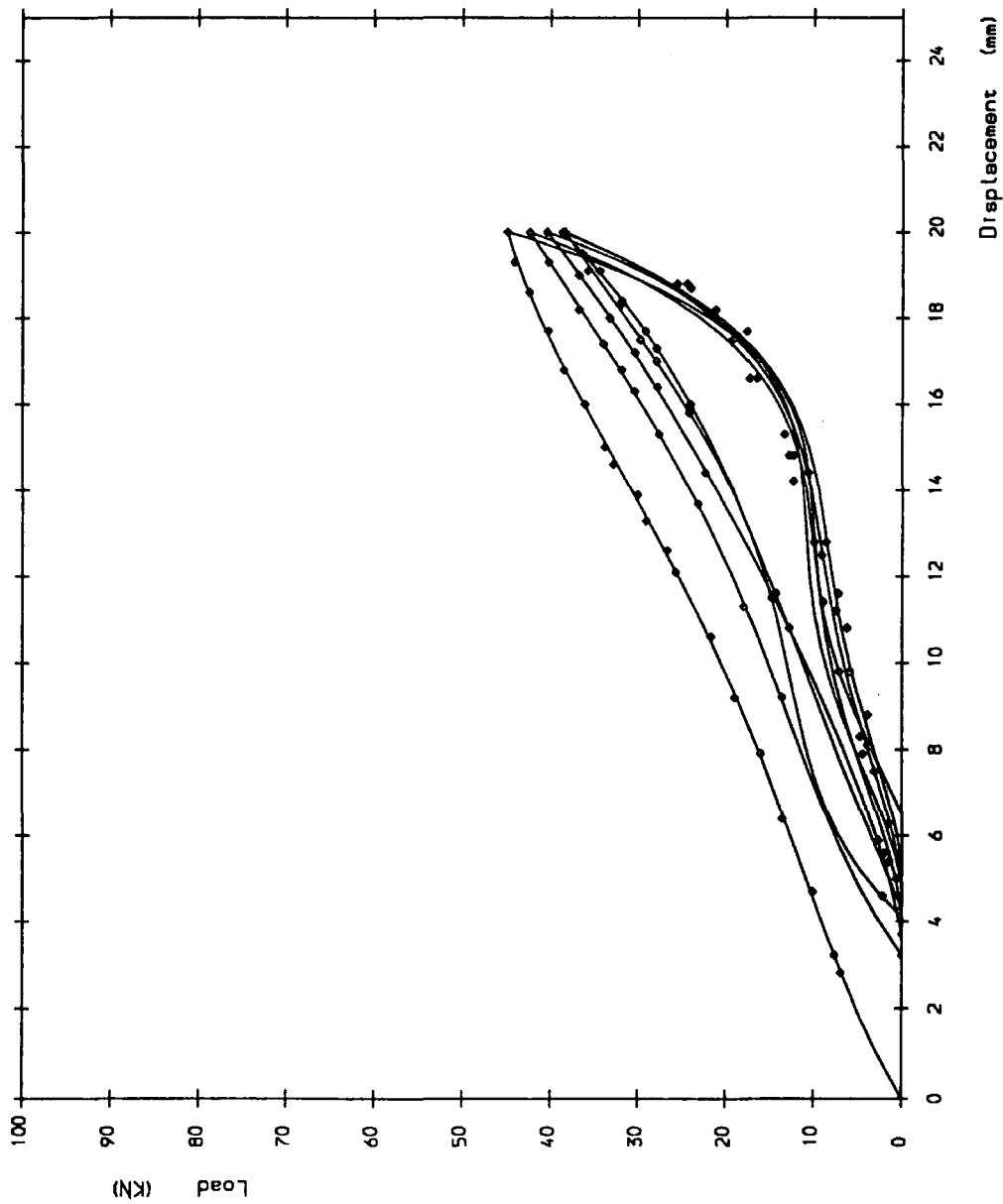
Figure A.14a Load/deflection curve 3rd test 5 pile width spacing at 150mm overhang

BENDING MOMENT (kNm)

-30 -25 -20 -15 -10 -5 5 10 15 20 25 30

Rear pile
Front pile

1 = 3.20mm Pile cap Defl.
2 = 6.40mm Pile cap Defl.
3 = 9.20mm Pile cap Defl.
4 = 12.16mm Pile cap Defl.
5 = 15.00mm Pile cap Defl.
6 = 20.00mm Pile cap Defl.
7 = 20.00mm Pile cap Defl.
  Cyclic loading.

0.5
1.0
1.5
2.0
2.5
3.0
3.5

DEPTH (m)
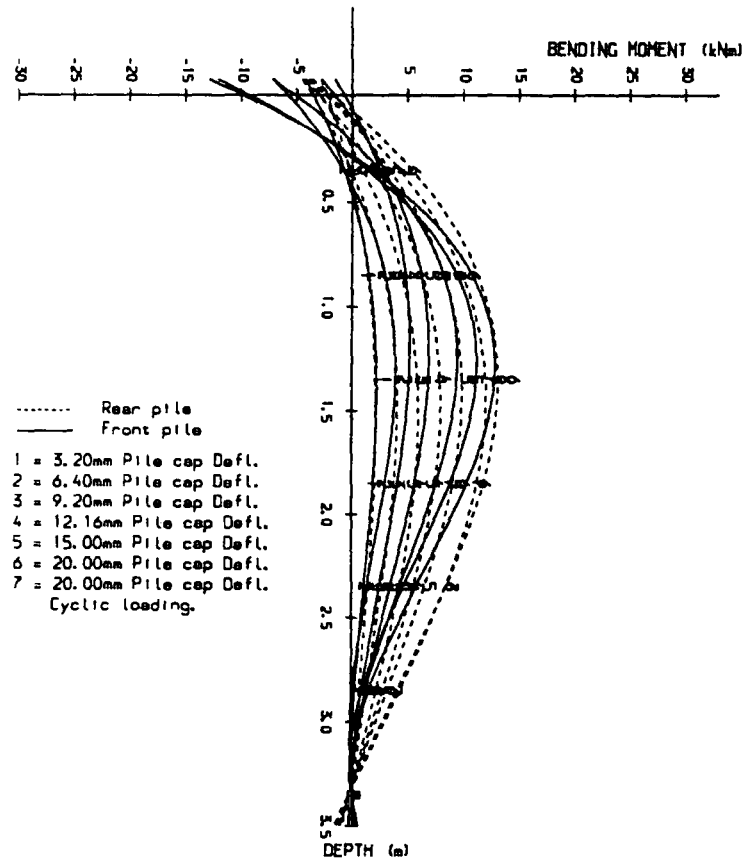
Figure A.14b Bending Moment Diagram for 2 pile group (third test piles at 5 pile width spacing with 150mm overhang).

(TENSION)   AXIAL FORCE (KN)   (COMP)

-250 -200 -150 -100 -50 50 100 150 200 250

Rear Pile
Front Pile

DEPTH (m)
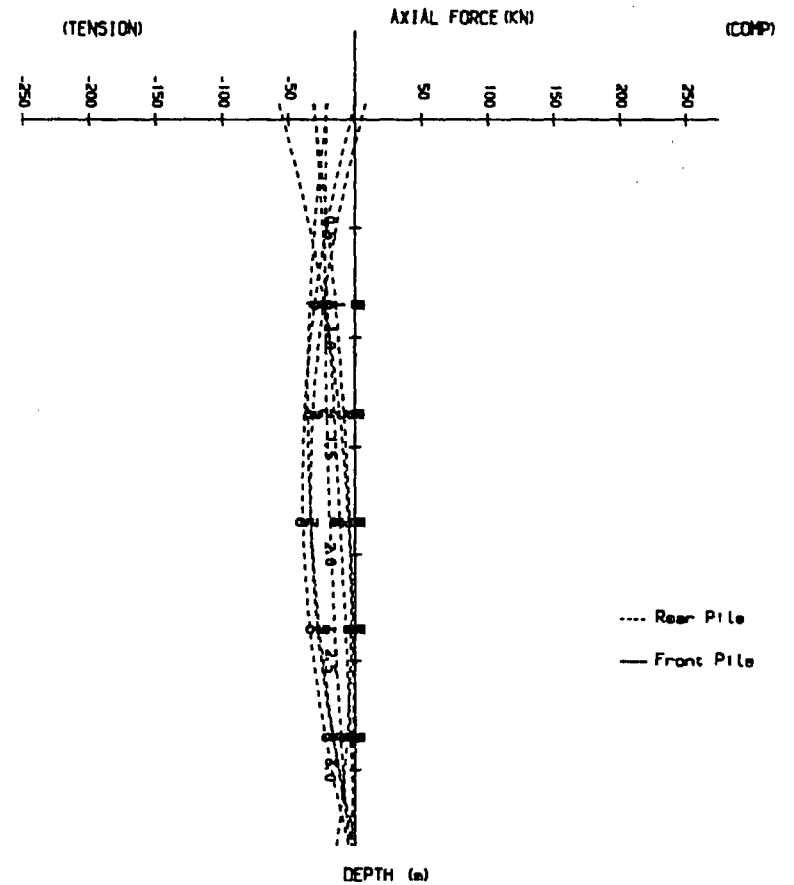
Figure A.14C Axial Force Diagram for 2 pile group (third test piles at 5 pile width spacing with 150mm overhang).
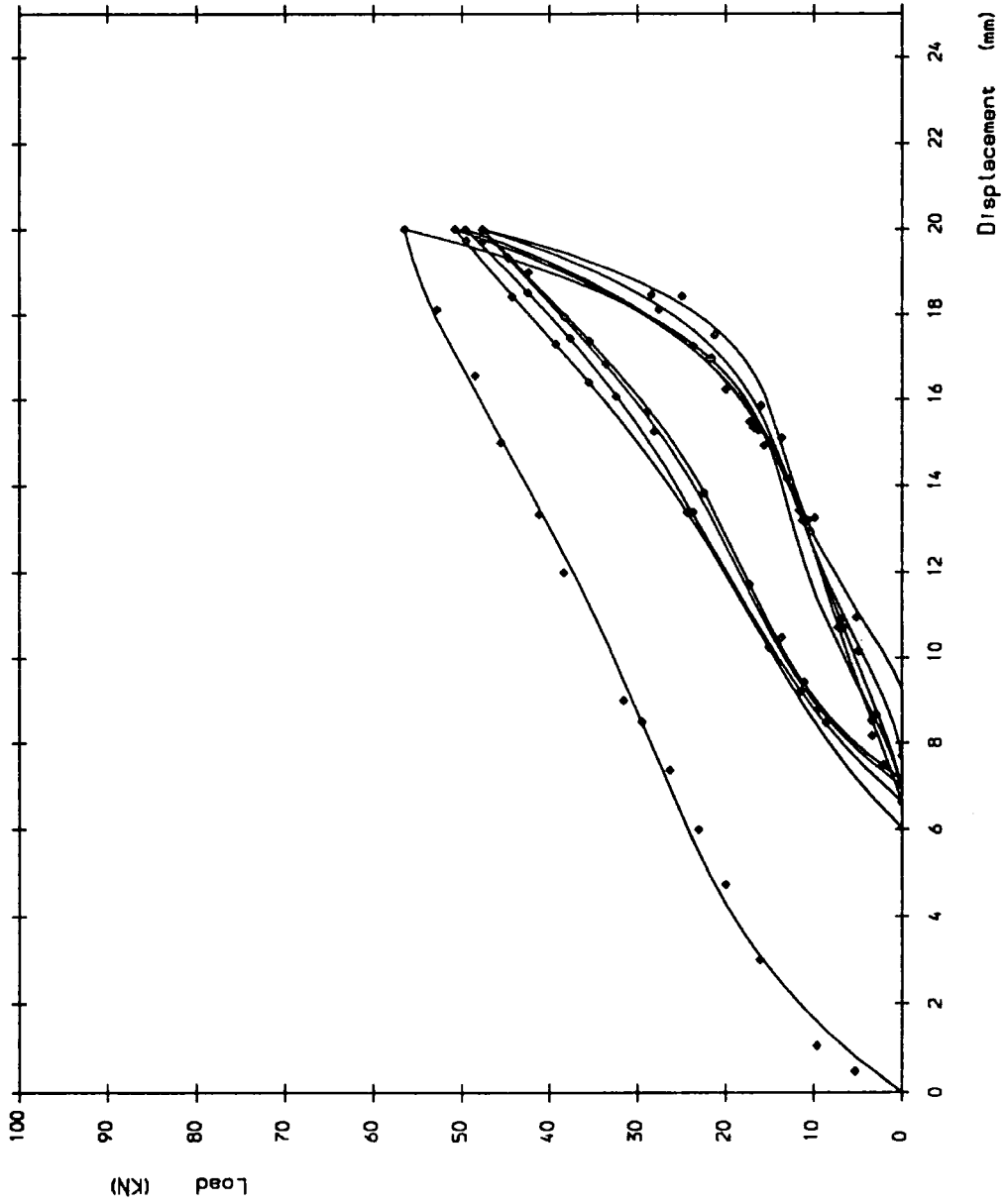
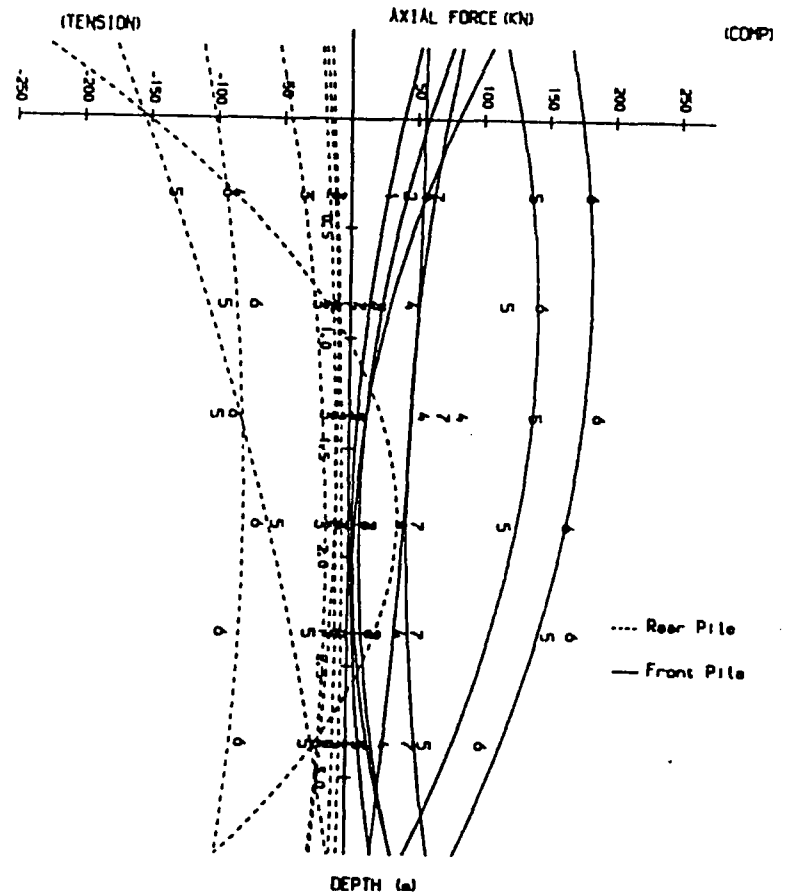Figure A.15a Load/deflection curve 4th test 5 pile width spacing at 150mm overhang
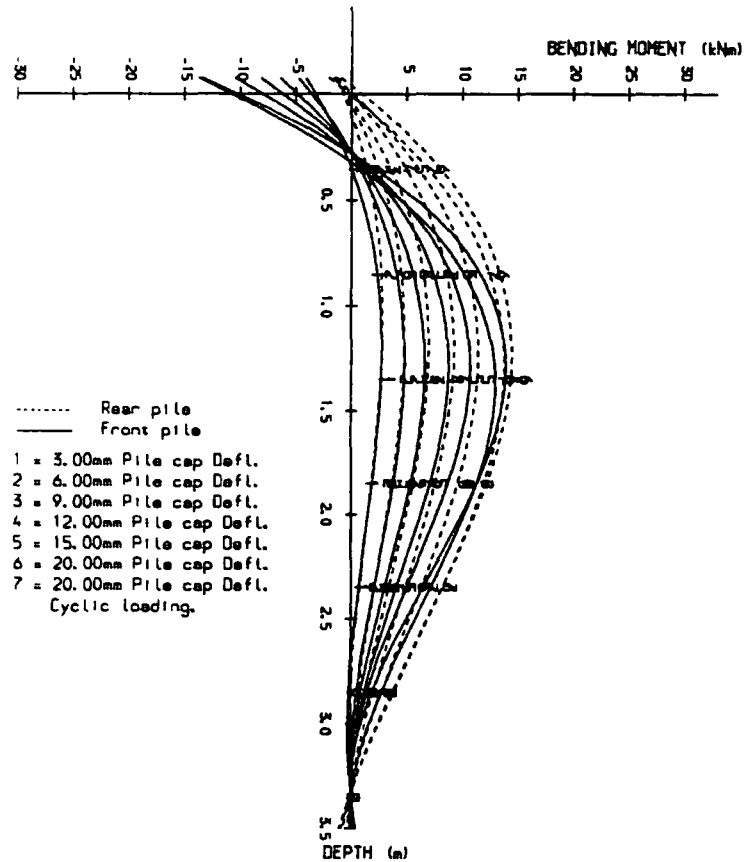
BENDING MOMENT (kNm)

-30 -25 -20 -15 -10 -5 5 10 15 20 25 30

-------- Rear pile
———— Front pile

1 = 3.00mm Pile cap Defl.
2 = 6.00mm Pile cap Defl.
3 = 9.00mm Pile cap Defl.
4 = 12.00mm Pile cap Defl.
5 = 15.00mm Pile cap Defl.
6 = 20.00mm Pile cap Defl.
7 = 20.00mm Pile cap Defl.
   Cyclic loading.

0.5 1.0 1.5 2.0 2.5 3.0 3.5

DEPTH (m)

Figure 4.15b Bending Moment Diagram for 2 pile group (fourth test piles at 5 pile width spacing with 150mm overhang).

(TENSION)   AXIAL FORCE (KN)   (COMP)

-250 -200 -150 -100 -50 50 100 150 200 250

-------- Rear Pile
———— Front Pile

0.5 1.0 1.5 2.0 2.5 3.0

DEPTH (m)
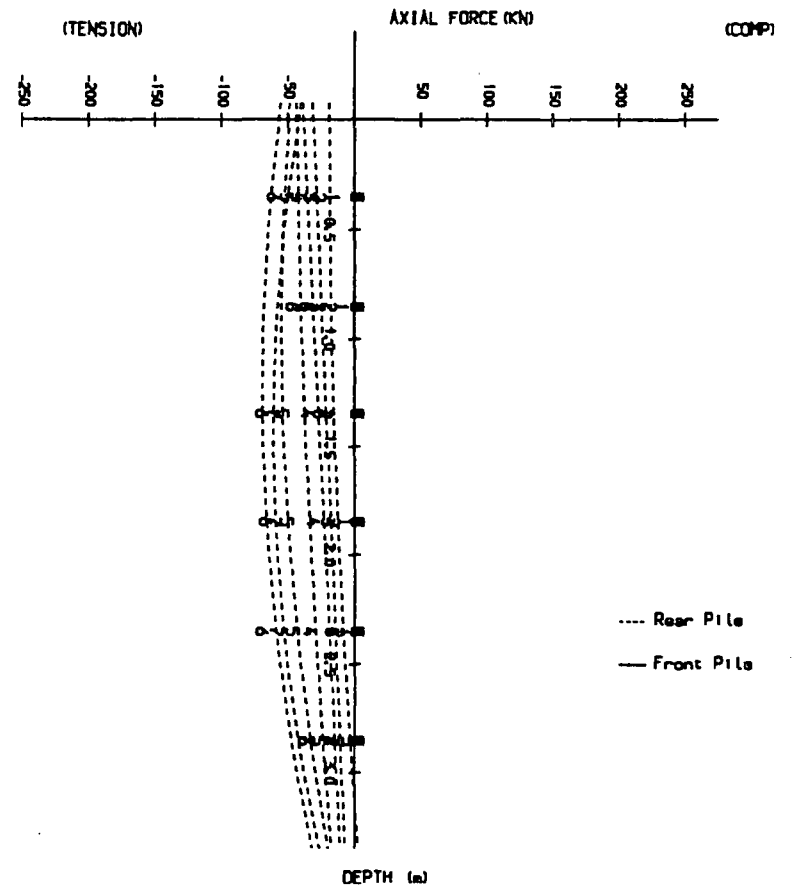
Figure 4.15C Axial Force Diagram for 2 pile group (fourth test piles at 5 pile width spacing with 150mm overhang).
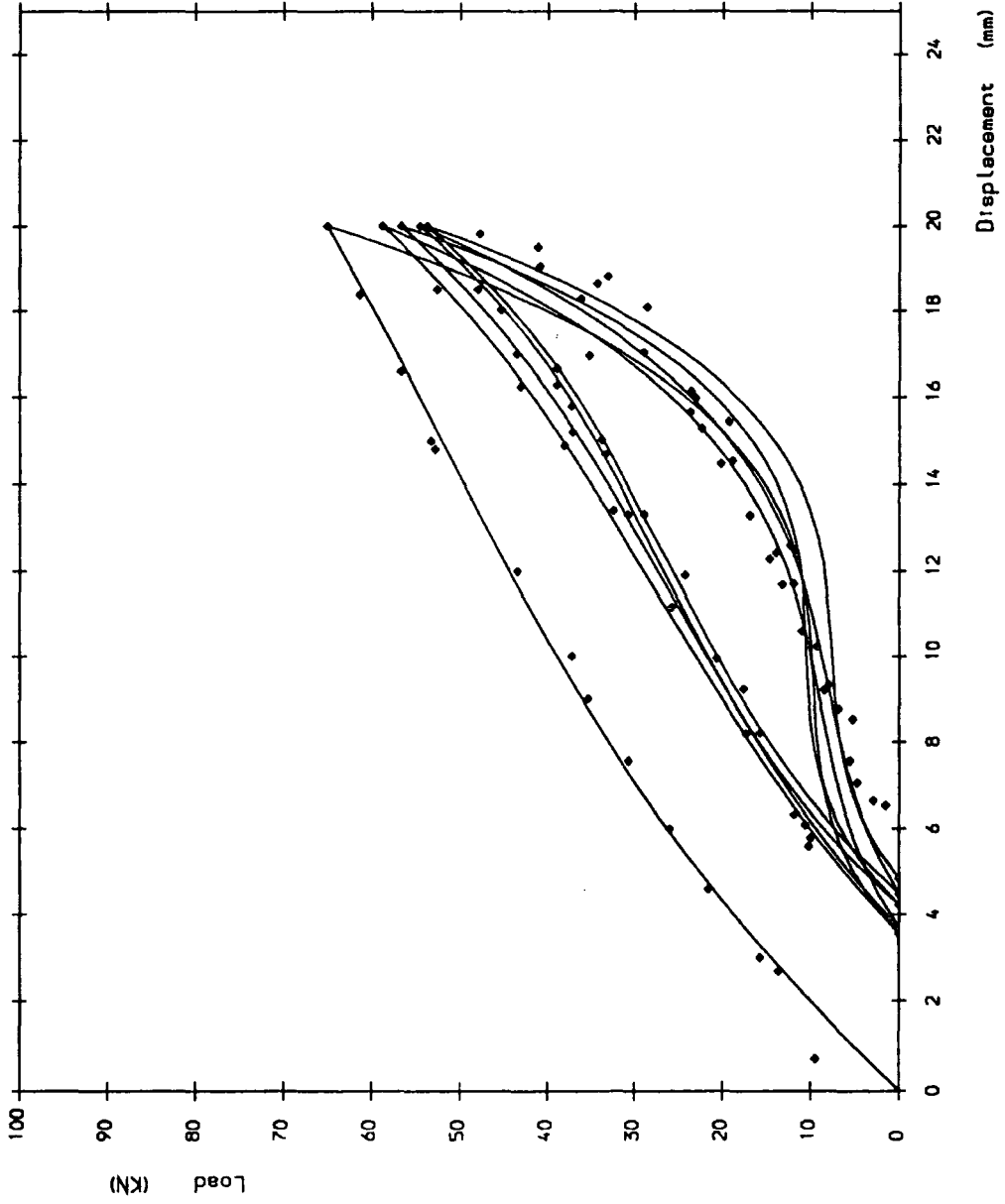
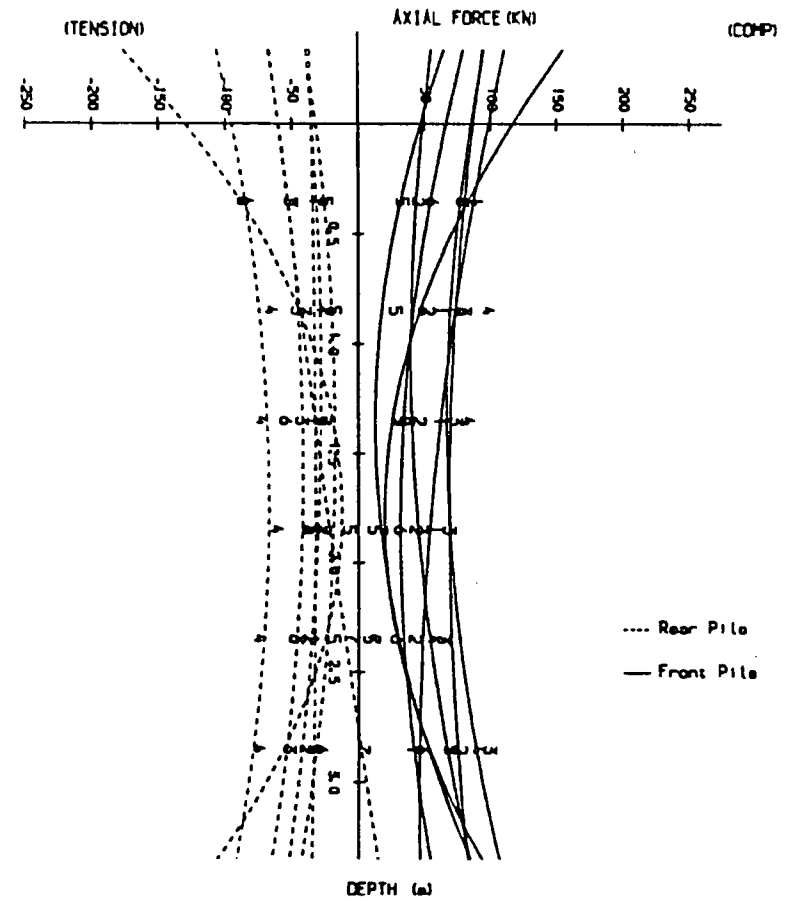Figure A.16a Load/deflection curve 5th test 5 pile width spacing at 150mm overhang

BENDING MOMENT (kNm)

-30 -25 -20 -15 -10 -5   5   10   15   20   25   30

-------- Rear pile
———— Front pile

1 = 3.00mm Pile cap Defl.
2 = 6.00mm Pile cap Defl.
3 = 9.00mm Pile cap Defl.
4 = 12.00mm Pile cap Defl.
5 = 15.00mm Pile cap Defl.
6 = 20.00mm Pile cap Defl.
7 = 20.00mm Pile cap Defl.
    Cyclic loading.

0.5   1.0   1.5   2.0   2.5   3.0   3.5

DEPTH (m)
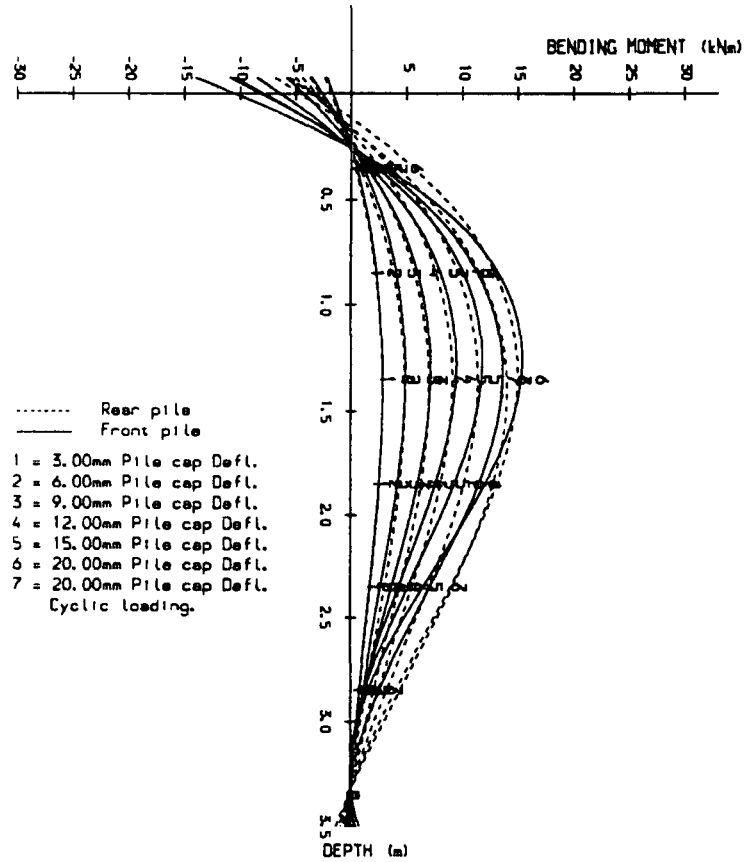
Figure A.16b Bending Moment Diagram for 2 pile group (fifth
test piles at 5 pile width spacing with 150mm overhang).
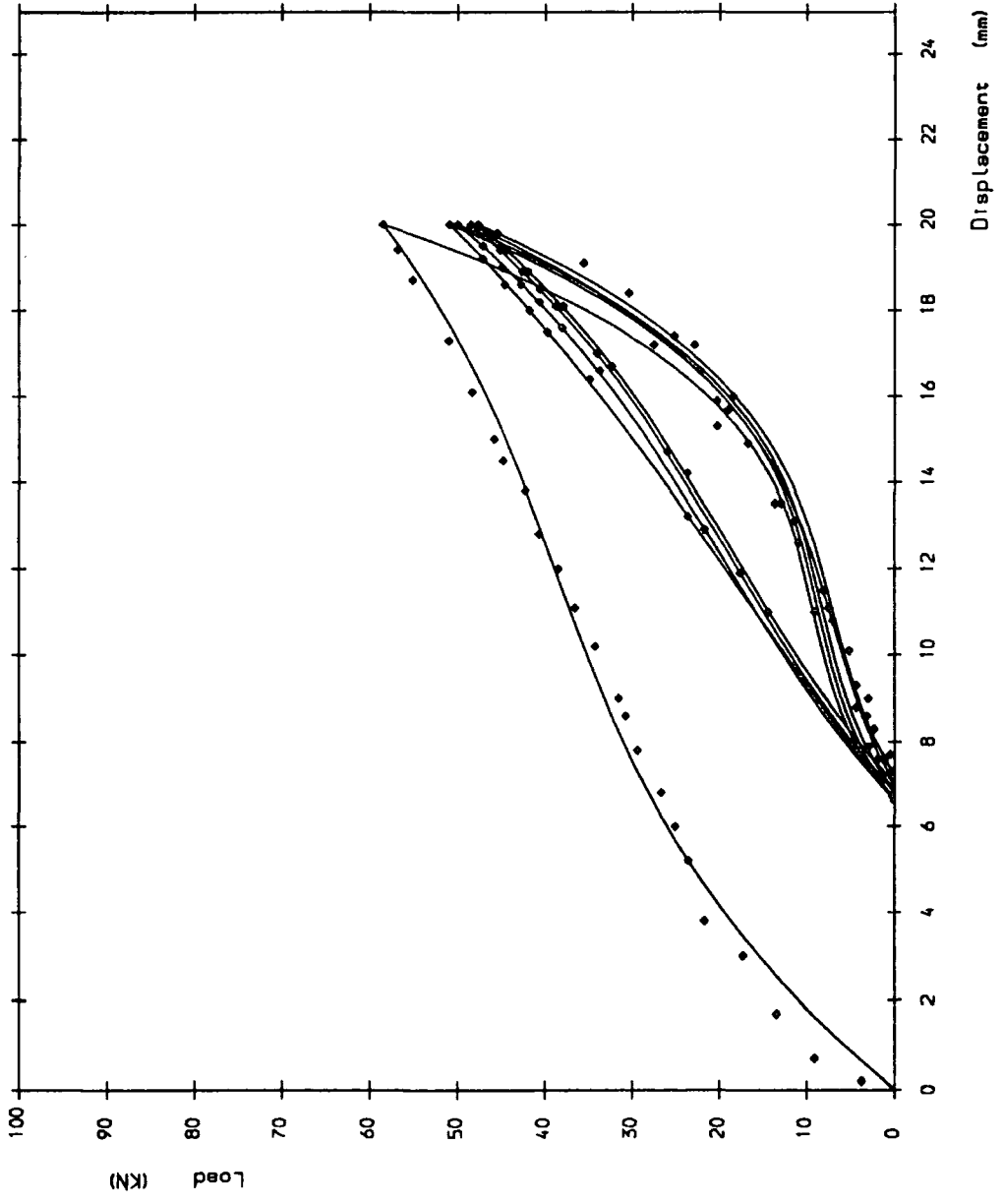
Figure A.17a Load/deflection curve 1ST test 5 pile width spacing at 300mm overhang
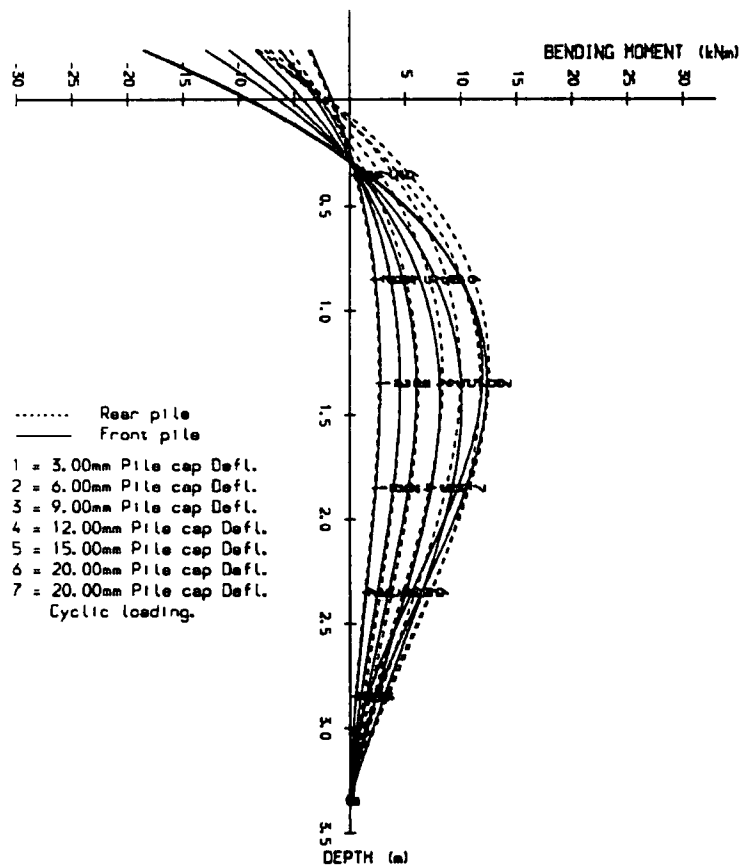
Figure A.17b Bending Moment Diagram for 2 pile group (first test piles at 5 pile width spacing with 300mm overhang).
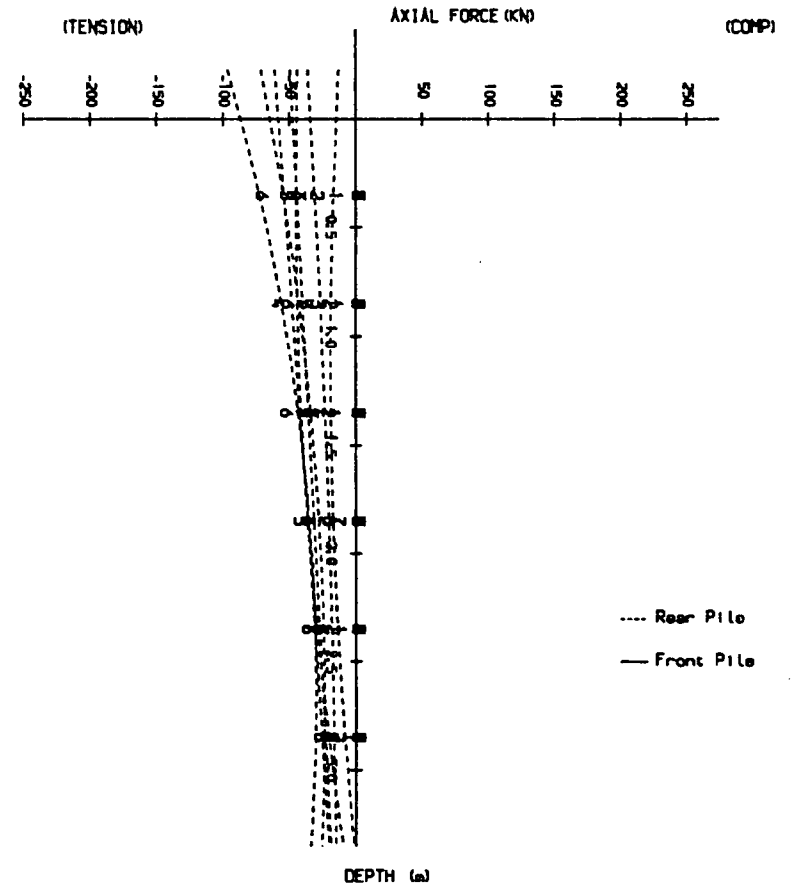
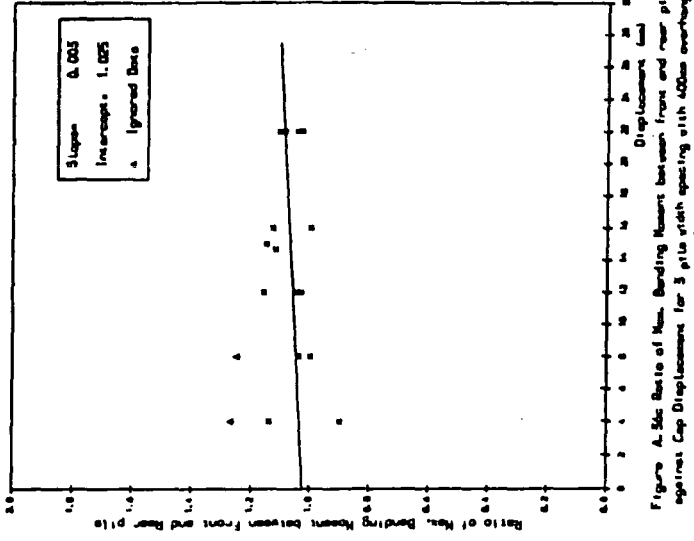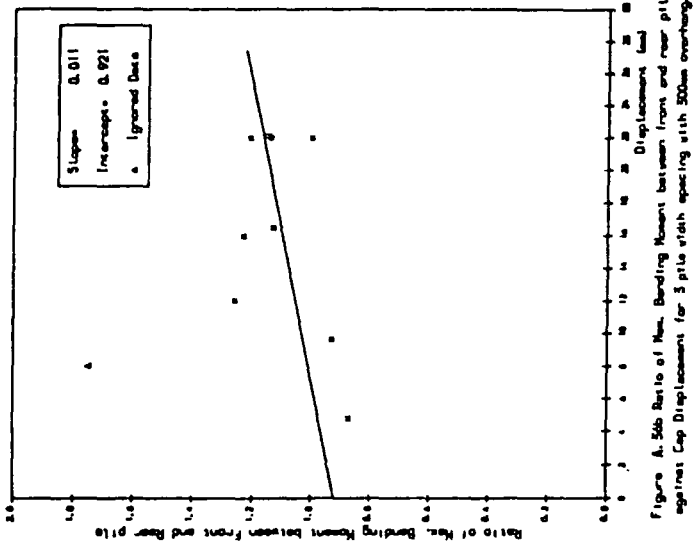Figure A.17C Axial Force Diagram for 2 pile group (first test piles at 5 pile width spacing with 300mm overhang).
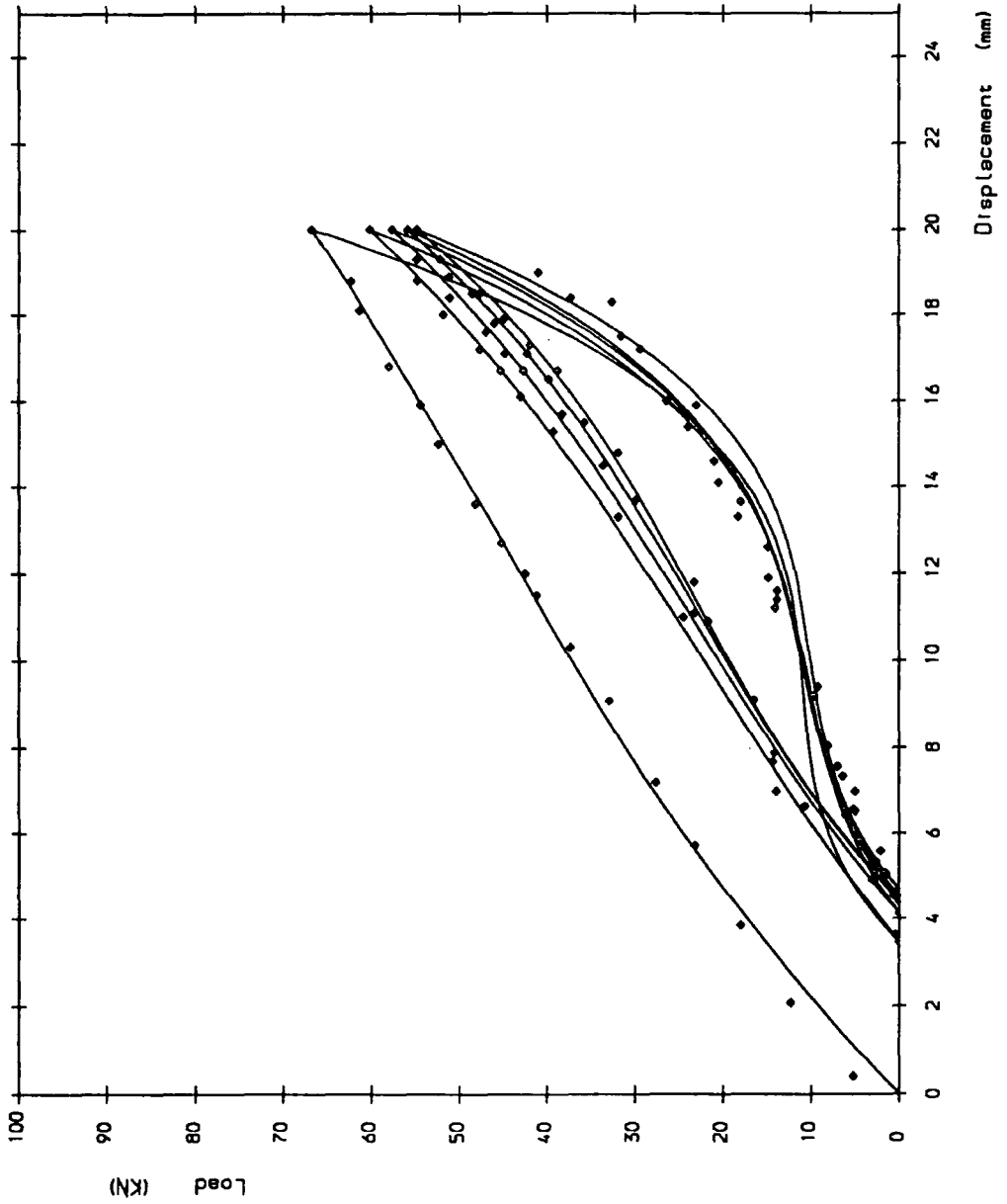
Figure A.18a Load/deflection curve 2nd test 5 pile width spacing at 300mm overhang
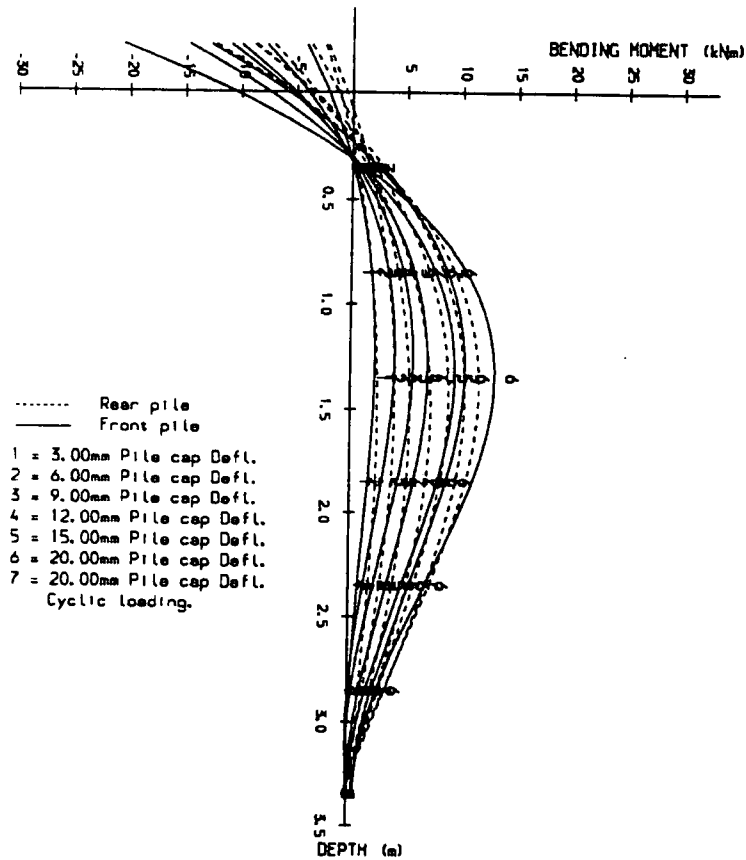
BENDING MOMENT (kNm)

-30 -25 -20 -15 -10 -5 5 10 15 20 25 30

DEPTH (m)
0.5 1.0 1.5 2.0 2.5 3.0 3.5

-------- Rear pile
———— Front pile

1 = 3.00mm Pile cap Defl.
2 = 6.00mm Pile cap Defl.
3 = 9.00mm Pile cap Defl.
4 = 12.00mm Pile cap Defl.
5 = 15.00mm Pile cap Defl.
6 = 20.00mm Pile cap Defl.
7 = 20.00mm Pile cap Defl.
    Cyclic loading.

Figure A.18b Bending Moment Diagram for 2 pile group (second
test piles at 5 pile width spacing with 300mm overhang).

(TENSION) AXIAL FORCE (kN) (COMP)

-250 -200 -150 -100 -50 50 100 150 200 250

DEPTH (m)
0.5 1.0 1.5 2.0 2.5 3.0

---- Rear Pile
———— Front Pile
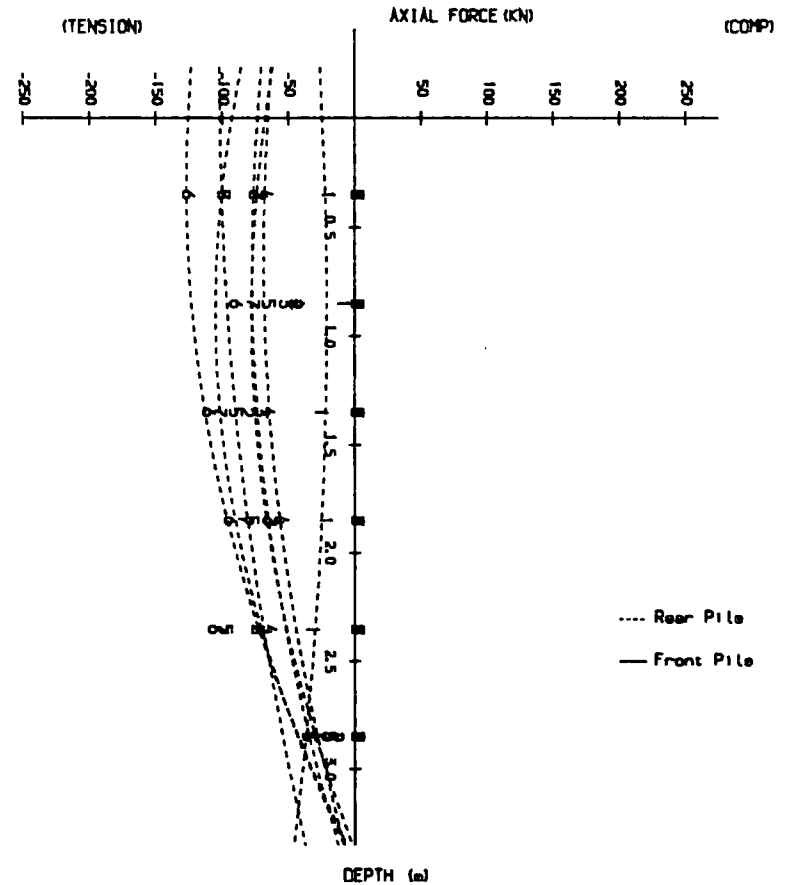
Figure A.18C Axial Force Diagram for 2 pile group (second
test piles at 5 pile width spacing with 300mm overhang).
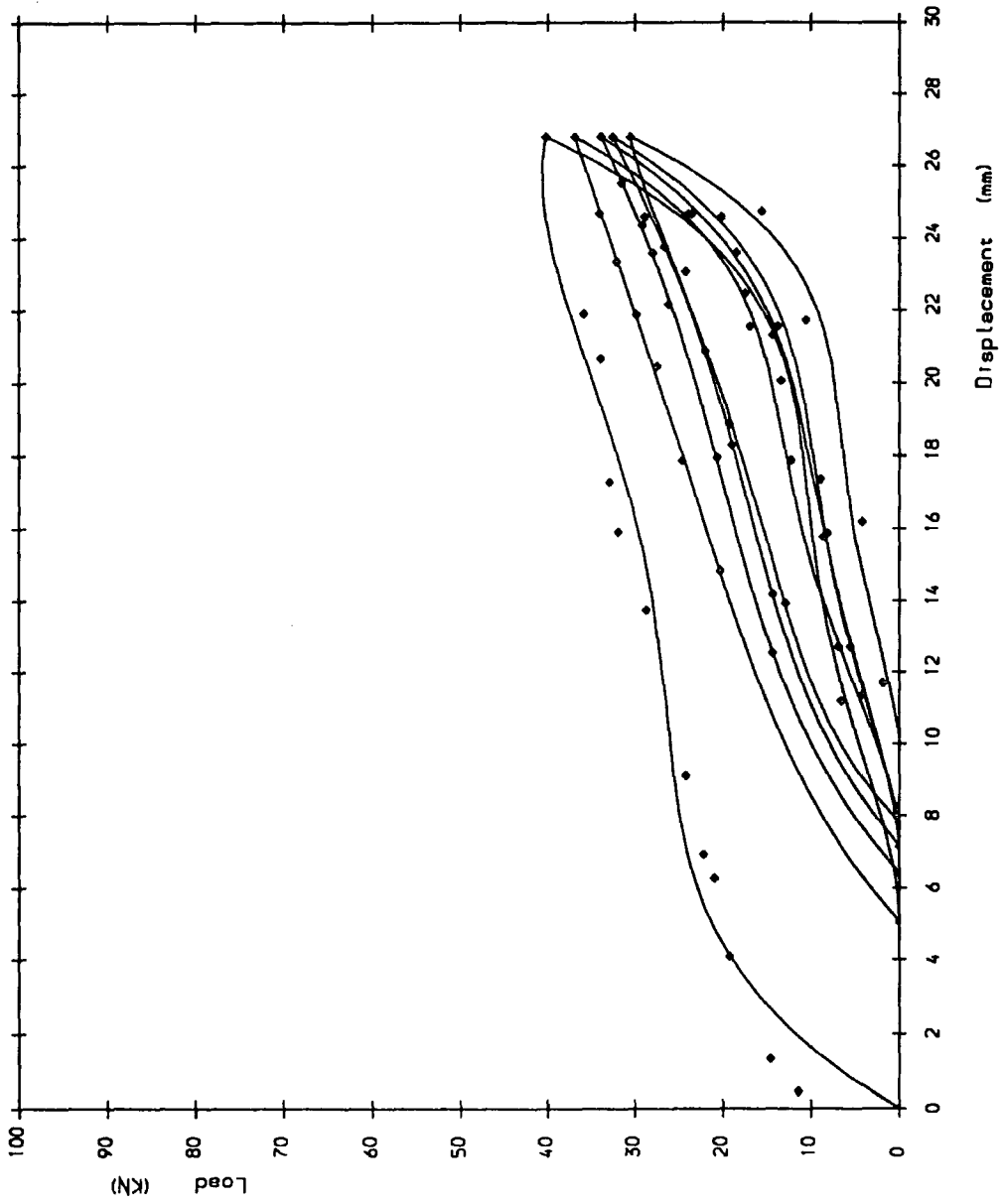
Figure A.19a Load/deflection curve 1st test 5 pile width spacing at 400mm overhang

BENDING MOMENT (kNm)

-30 -25 -20 -15 -10 -5   5 10 15 20 25 30

0.5

1.0

1.5

2.0

2.5

3.0

3.5

DEPTH (m)

.... Rear pile
———— Front pile

1 = 4.08mm Pile cap Defl.
2 = 6.93mm Pile cap Defl.
3 = 13.74mm Pile cap Defl.
4 = 17.27mm Pile cap Defl.
5 = 20.67mm Pile cap Defl.
6 = 26.80mm Pile cap Defl.
7 = 26.80mm Pile cap Defl.
  Cyclic loading.
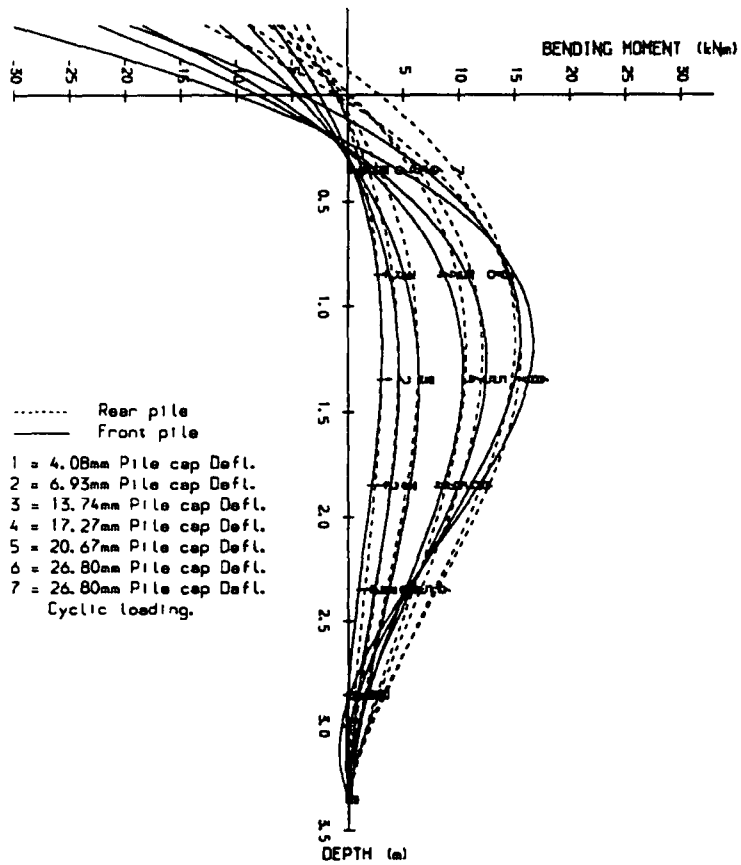
Figure A.19b Bending Moment Diagram for 2 pile group (first
test piles at 5 pile width spacing with 400mm overhang).

(TENSION)   AXIAL FORCE (KN)   (COMP)

-250 -200 -150 -100 -50   50 100 150 200 250

DEPTH (m)

.... Rear Pile
—— Front Pile
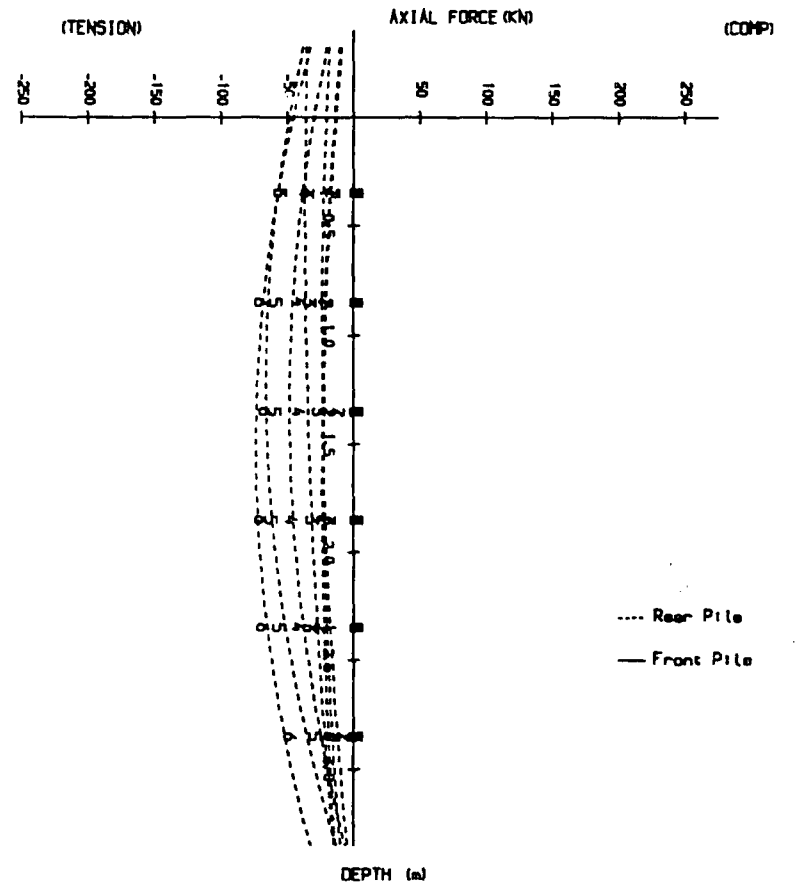
Figure A.19C Axial Force Diagram for 2 pile group (first
test piles at 5 pile width spacing with 400mm overhang).
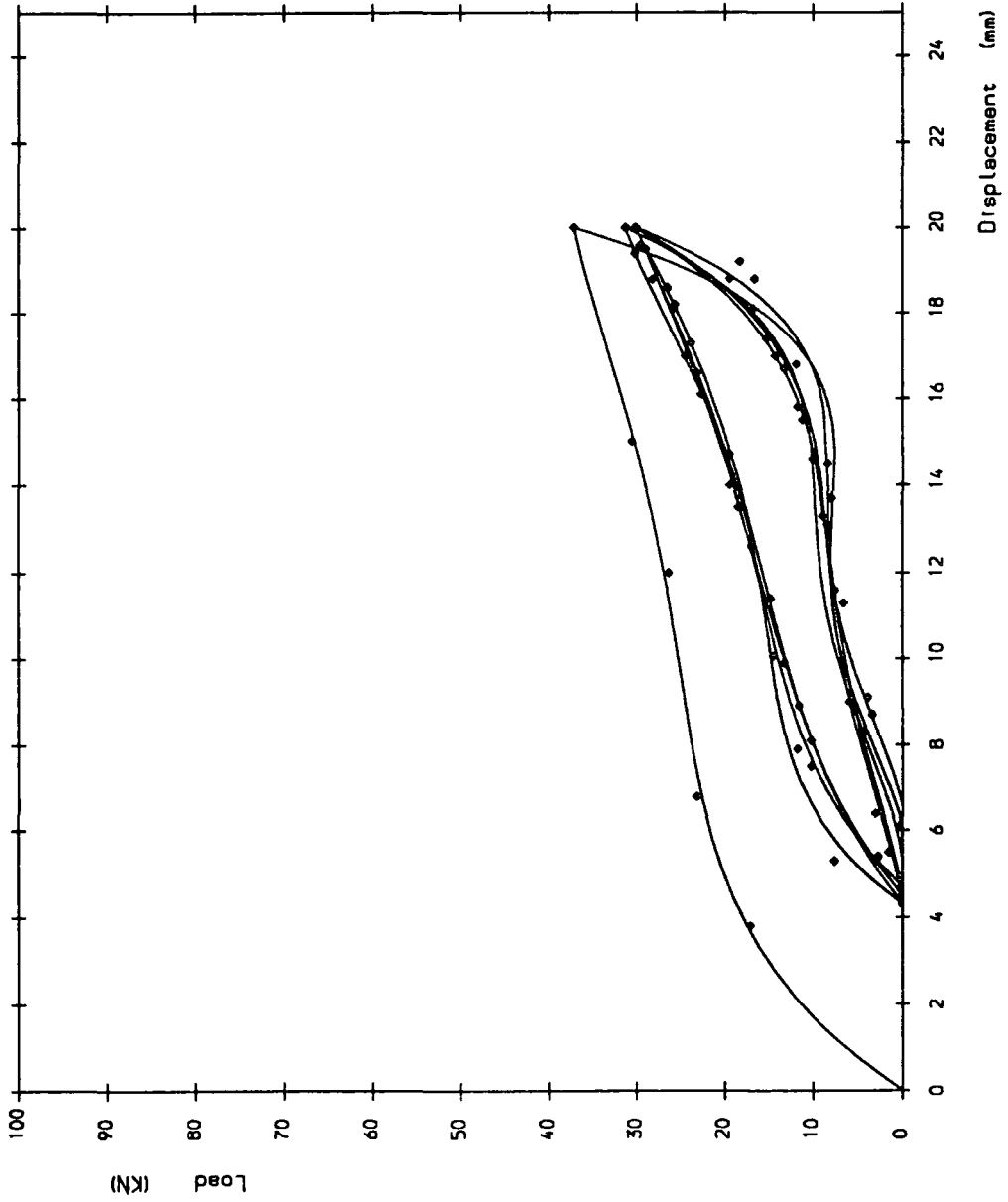
Figure A.20a Load/deflection curve 2nd test 5 pile width spacing at 400mm overhang
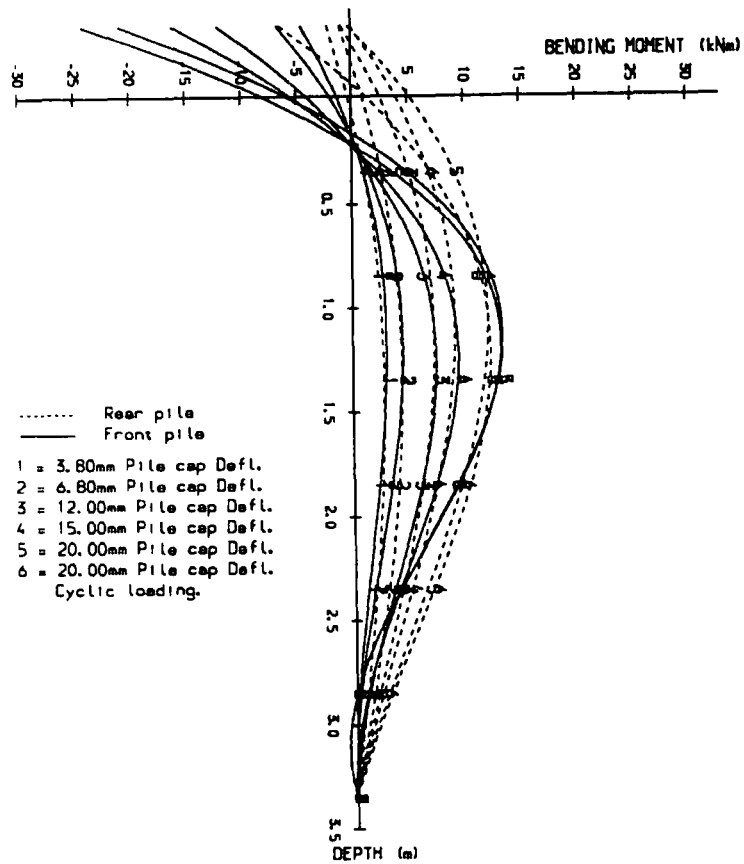
Figure A.20b Bending Moment Diagram for 2 pile group (second test piles at 5 pile width spacing with 400mm overhang).

BENDING MOMENT (kNm)

DEPTH (m)

.... Rear pile
———— Front pile

1 = 3.80mm Pile cap Defl.
2 = 6.80mm Pile cap Defl.
3 = 12.00mm Pile cap Defl.
4 = 15.00mm Pile cap Defl.
5 = 20.00mm Pile cap Defl.
6 = 20.00mm Pile cap Defl.
    Cyclic loading.
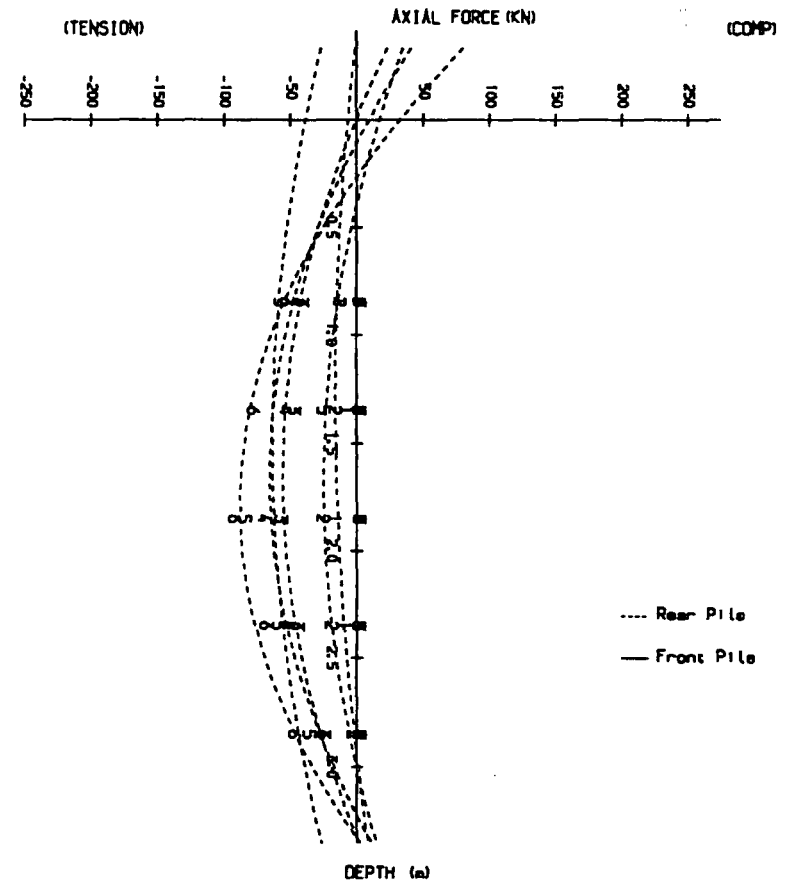
Figure A.20C Axial Force Diagram for 2 pile group (second test piles at 5 pile width spacing with 400mm overhang).

(TENSION)   AXIAL FORCE (KN)   (COMP)

DEPTH (m)

---- Rear Pile
—— Front Pile

308
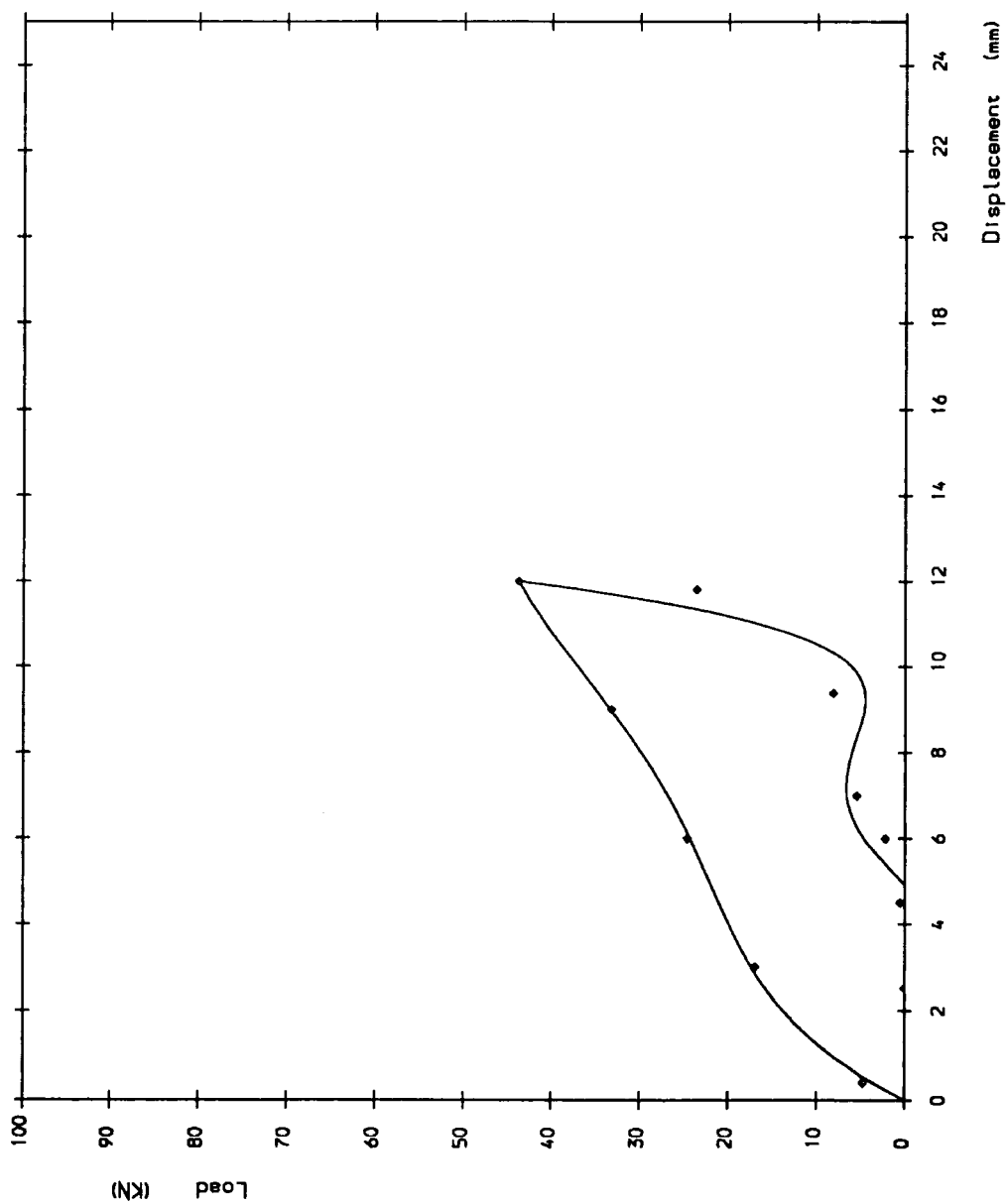
Figure A.21a Load/deflection curve 1st test 8 pile width spacing at 150mm overhang
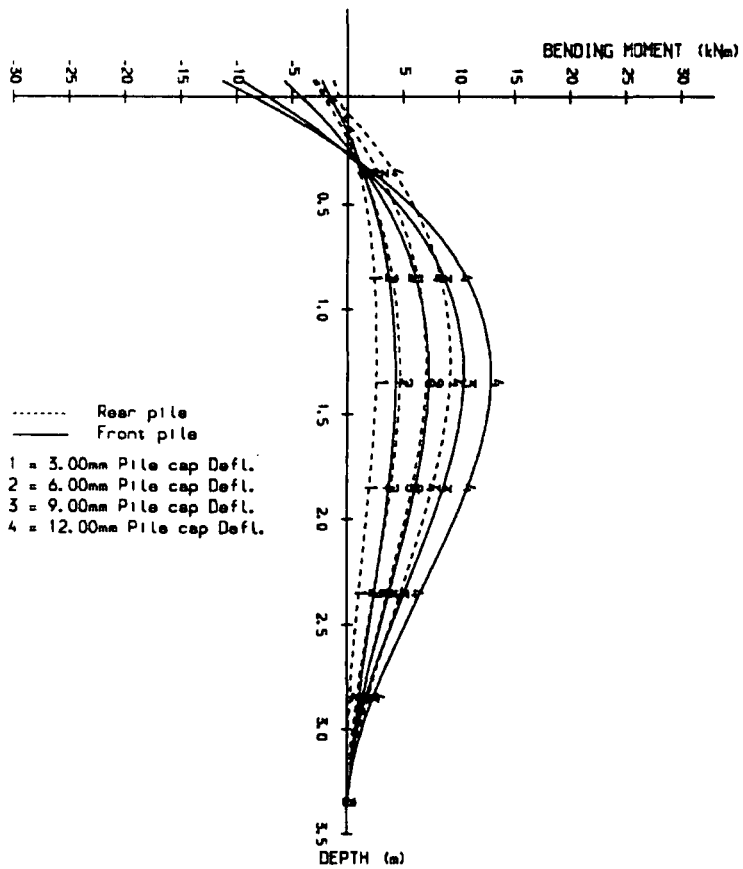
Figure A.21b Bending Moment Diagram for 2 pile group (first

test piles at 8 pile width spacing with 150mm overhang).
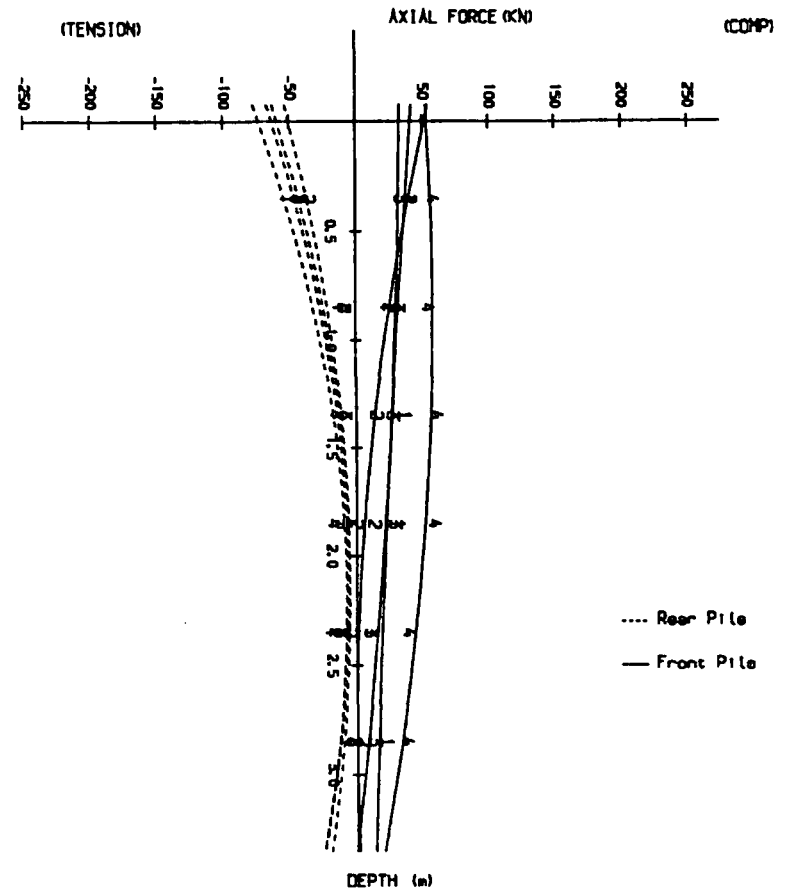
Figure A.21C Axial Force Diagram for 2 pile group (first

test piles at 8 pile width spacing with 150mm overhang).
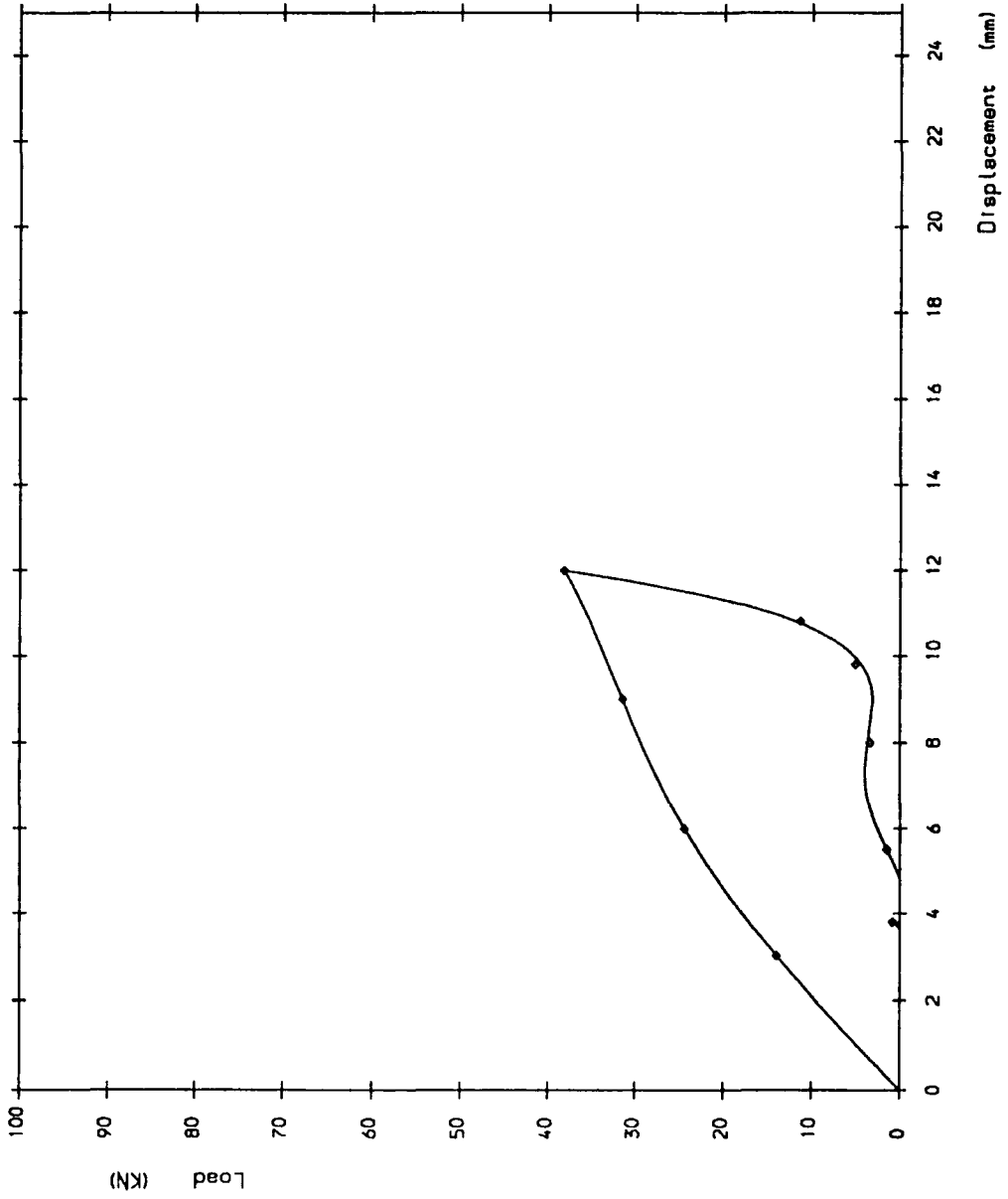
Figure A.22a Load/deflection curve 2nd test 8 pile width spacing at 150mm overhang
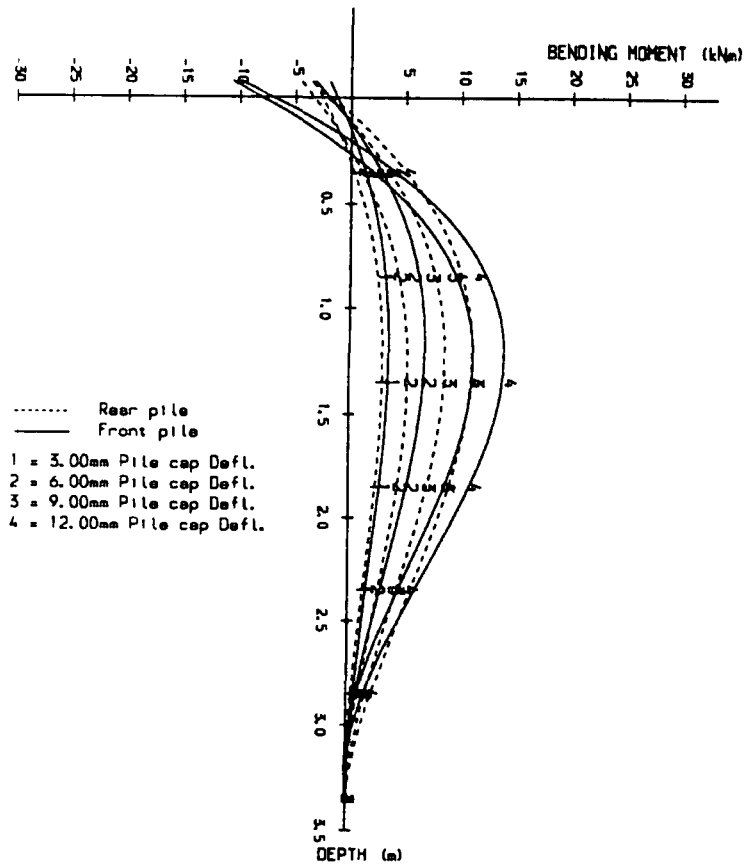
Figure 4.22b Bending Moment Diagram for 2 pile group (second test piles at 8 pile width spacing with 150mm overhang).

Rear pile
Front pile

1 = 3.00mm Pile cap Defl.
2 = 6.00mm Pile cap Defl.
3 = 9.00mm Pile cap Defl.
4 = 12.00mm Pile cap Defl.
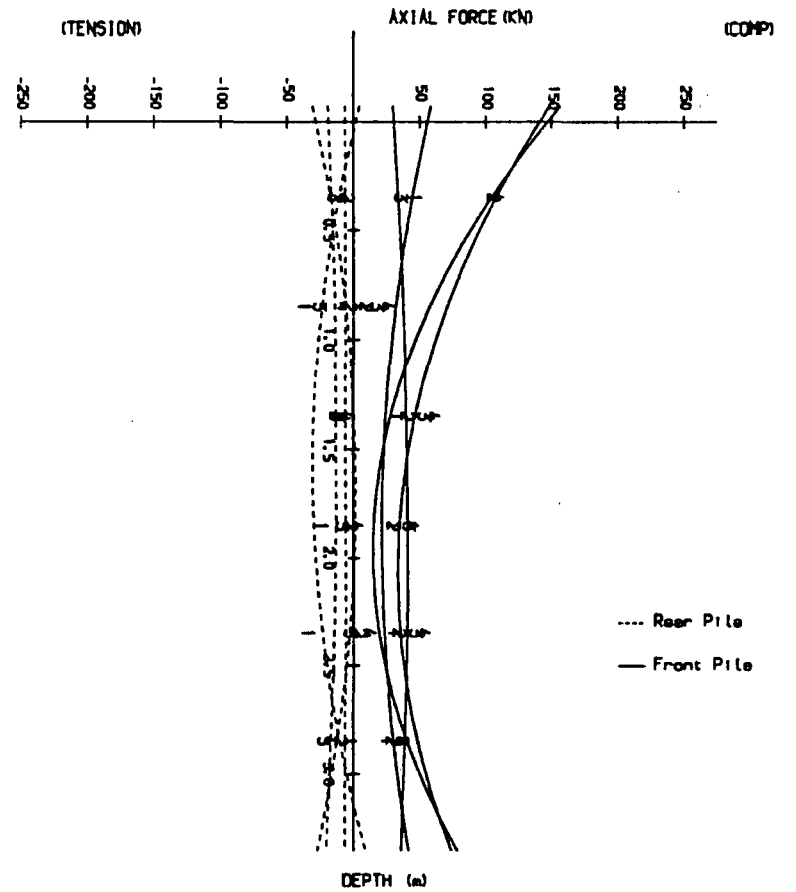
Figure 4.22C Axial Force Diagram for 2 pile group (second test piles at 8 pile width spacing with 150mm overhang).

Rear Pile
Front Pile
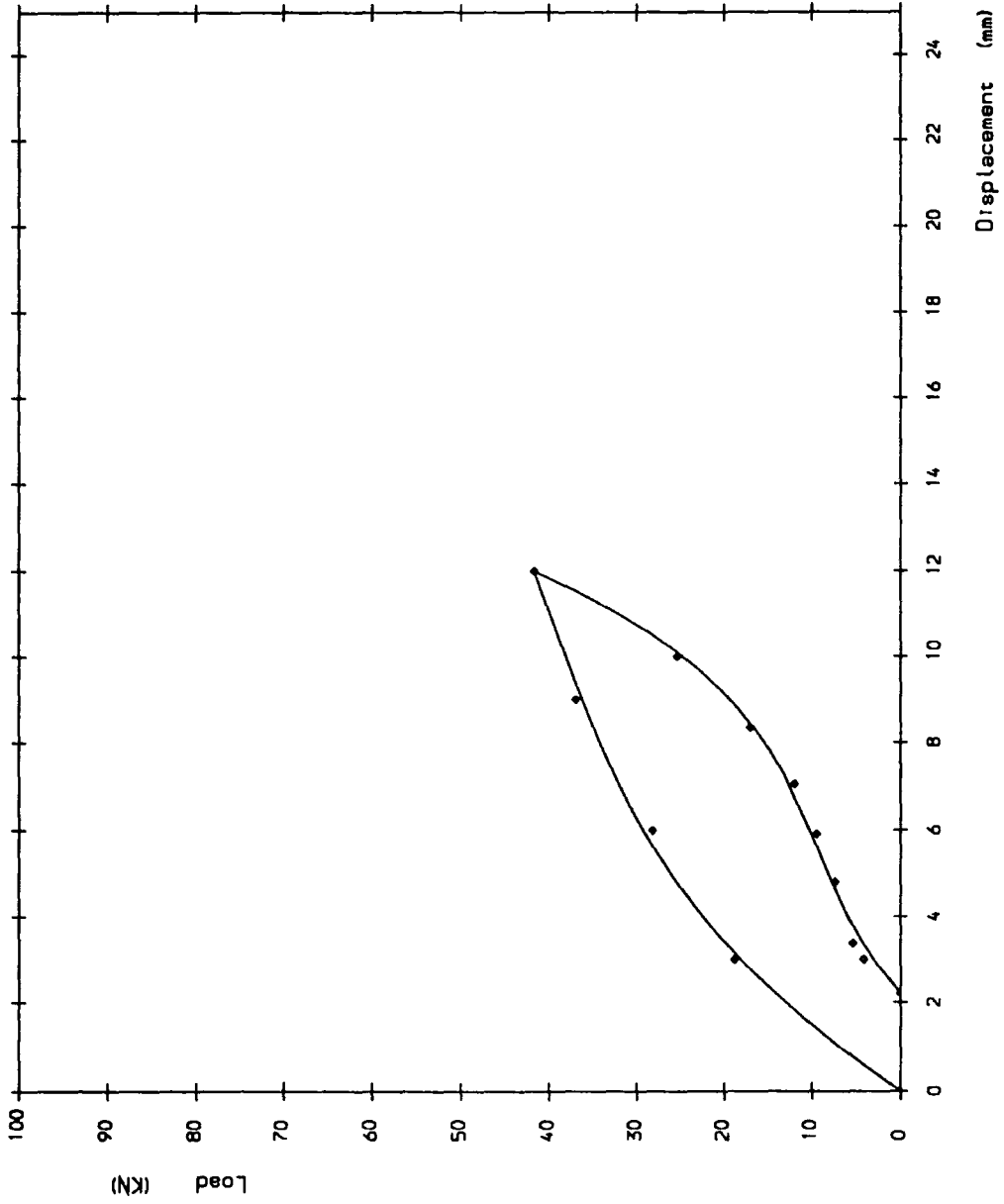
Figure A.23a Load/deflection curve 3rd test 8 pile width spacing at 150mm overhang
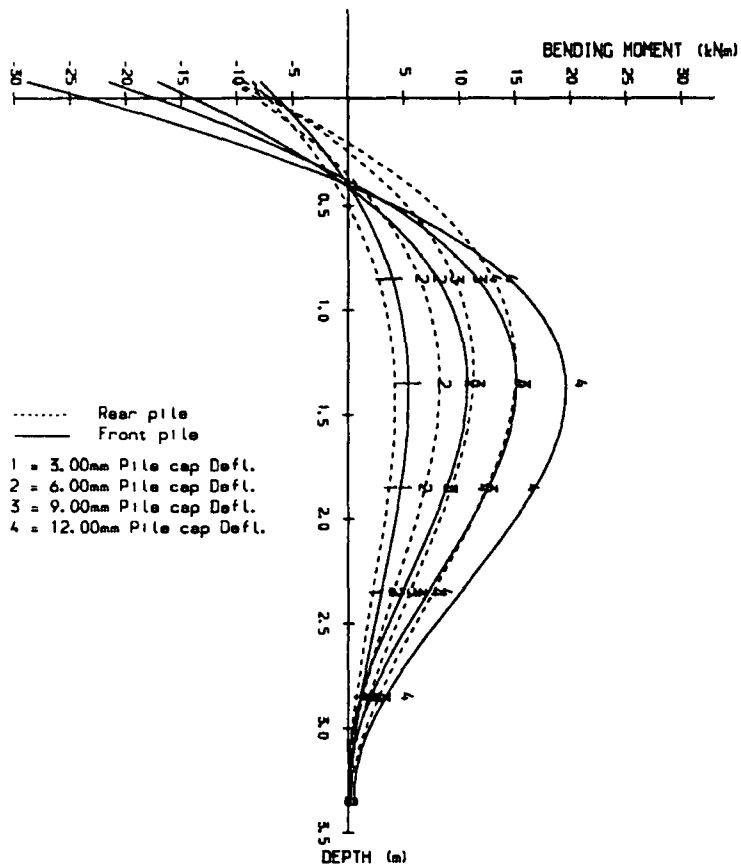
Figure A.23b Bending Moment Diagram for 2 pile group (third test piles at 8 pile width spacing with 150mm overhang).

Rear pile

Front pile

1 = 3.00mm Pile cap Defl.
2 = 6.00mm Pile cap Defl.
3 = 9.00mm Pile cap Defl.
4 = 12.00mm Pile cap Defl.

BENDING MOMENT (kNm)

DEPTH (m)
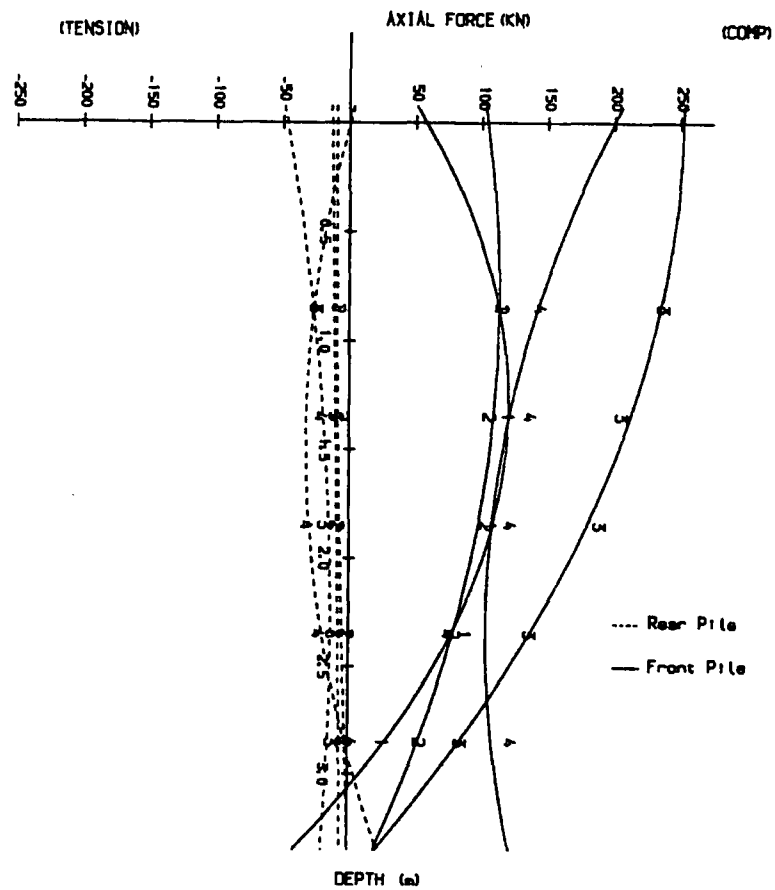
Figure A.23c Axial Force Diagram for 2 pile group (third test piles at 8 pile width spacing with 150mm overhang).

(TENSION)

AXIAL FORCE (KN)

(COMP)

Rear Pile

Front Pile

DEPTH (m)
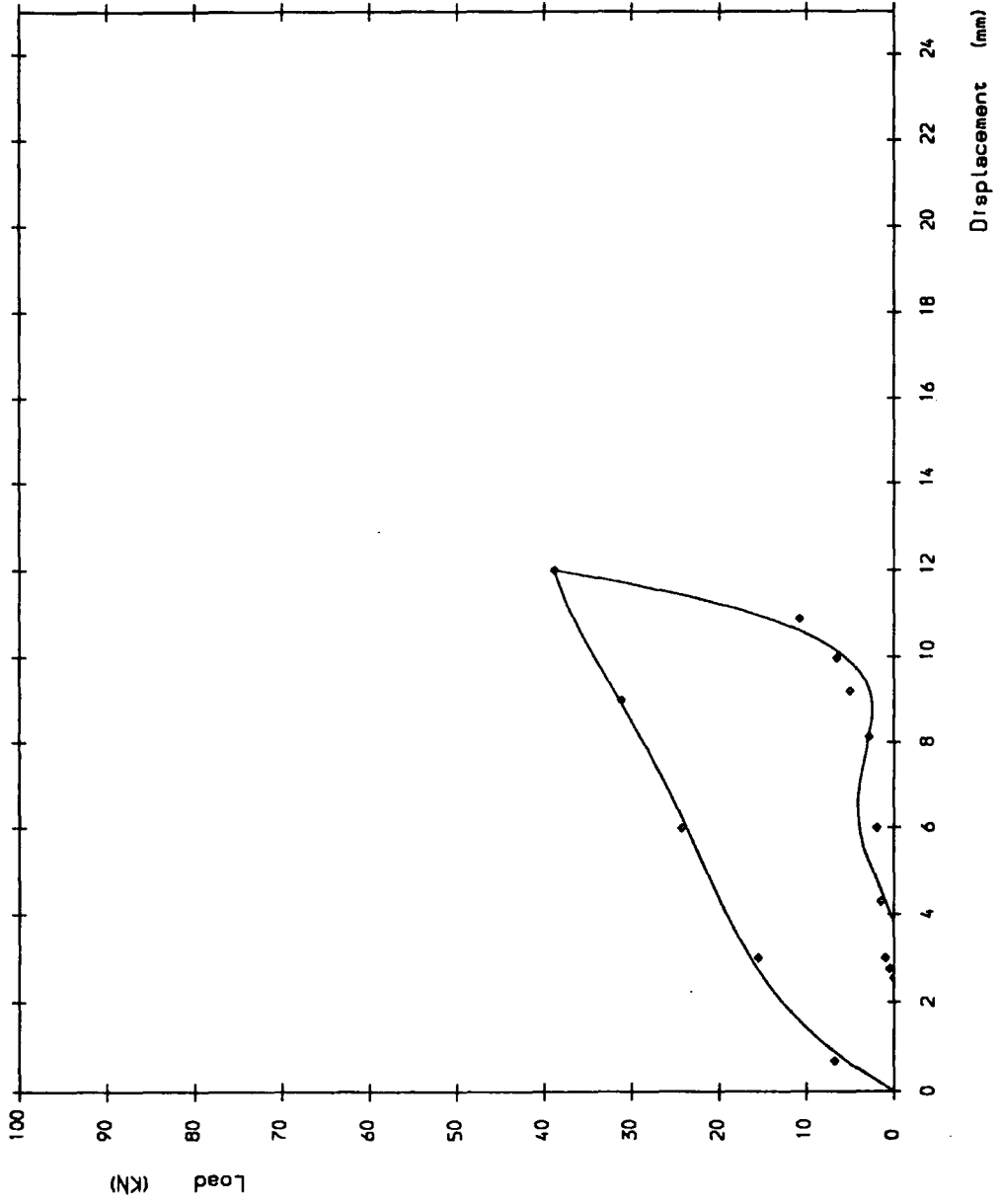
Figure A.24a Load/deflection curve 1st test 8 pile width spacing at 300mm overhang
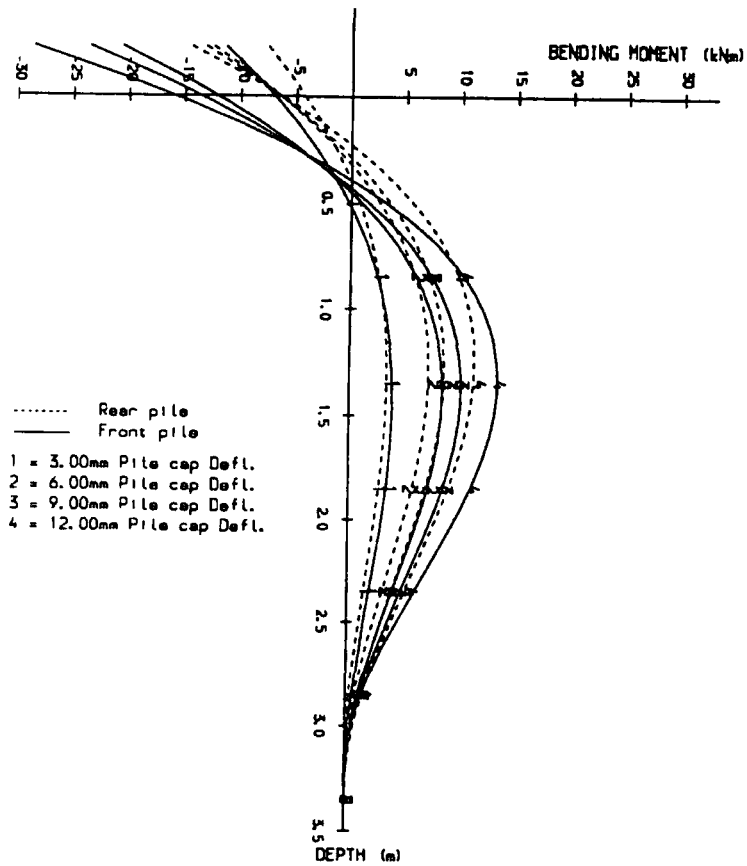
Figure A.24b Bending Moment Diagram for 2 pile group (first test piles at 8 pile width spacing with 300mm overhang).
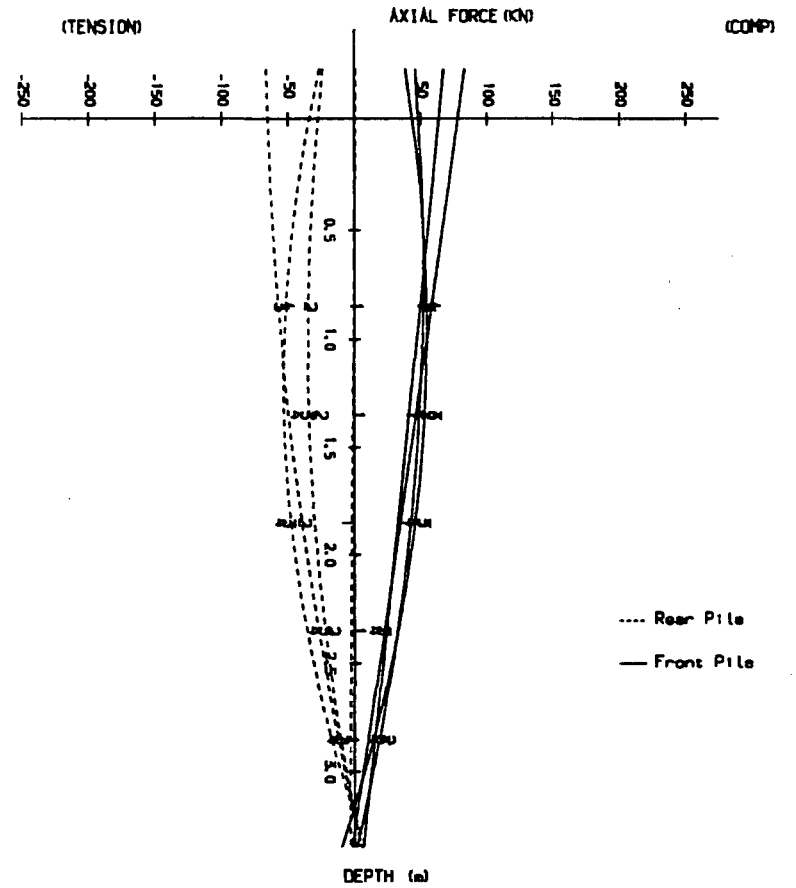
Figure A.24C Axial Force Diagram for 2 pile group (first test piles at 8 pile width spacing with 300mm overhang).
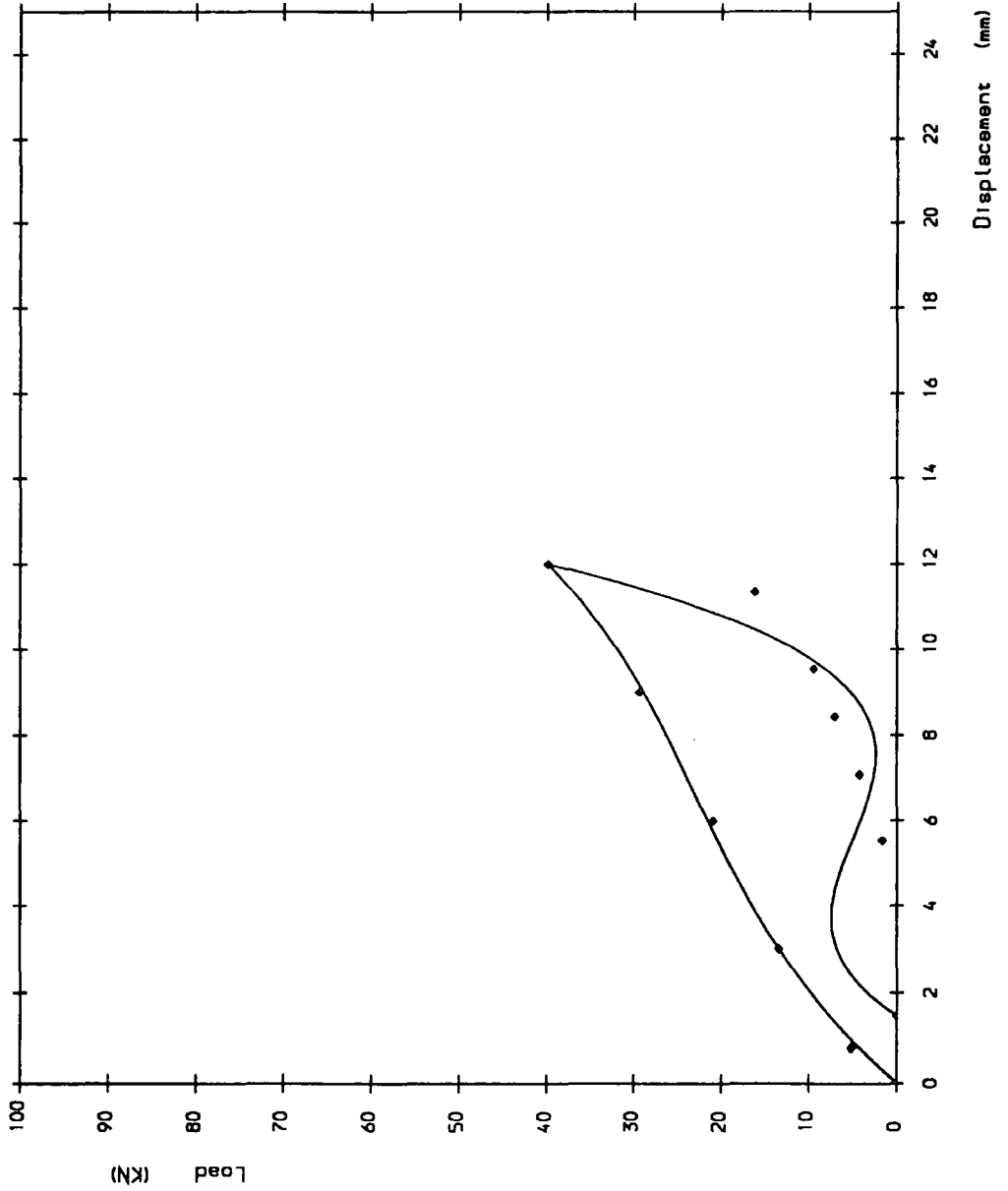
Figure A.25a Load/deflection curve 2nd test 8 pile width spacing at 300mm overhang
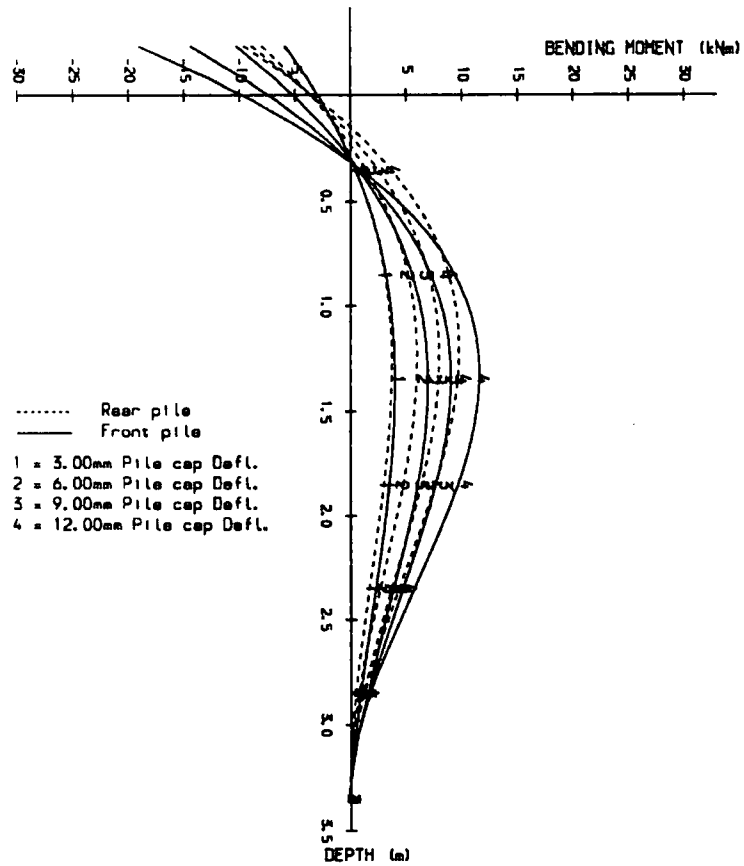
Figure A.25b Bending Moment Diagram for 2 pile group (second
test piles at 8 pile width spacing with 300mm overhang).
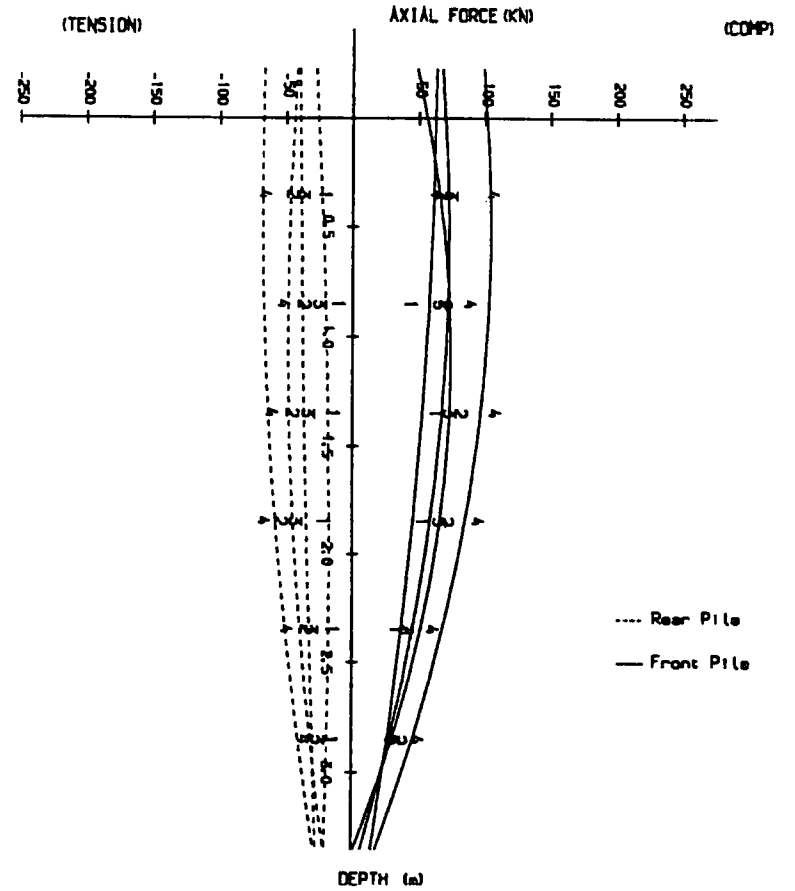
Figure A.25C Axial Force Diagram for 2 pile group (second
test piles at 8 pile width spacing with 300mm overhang).
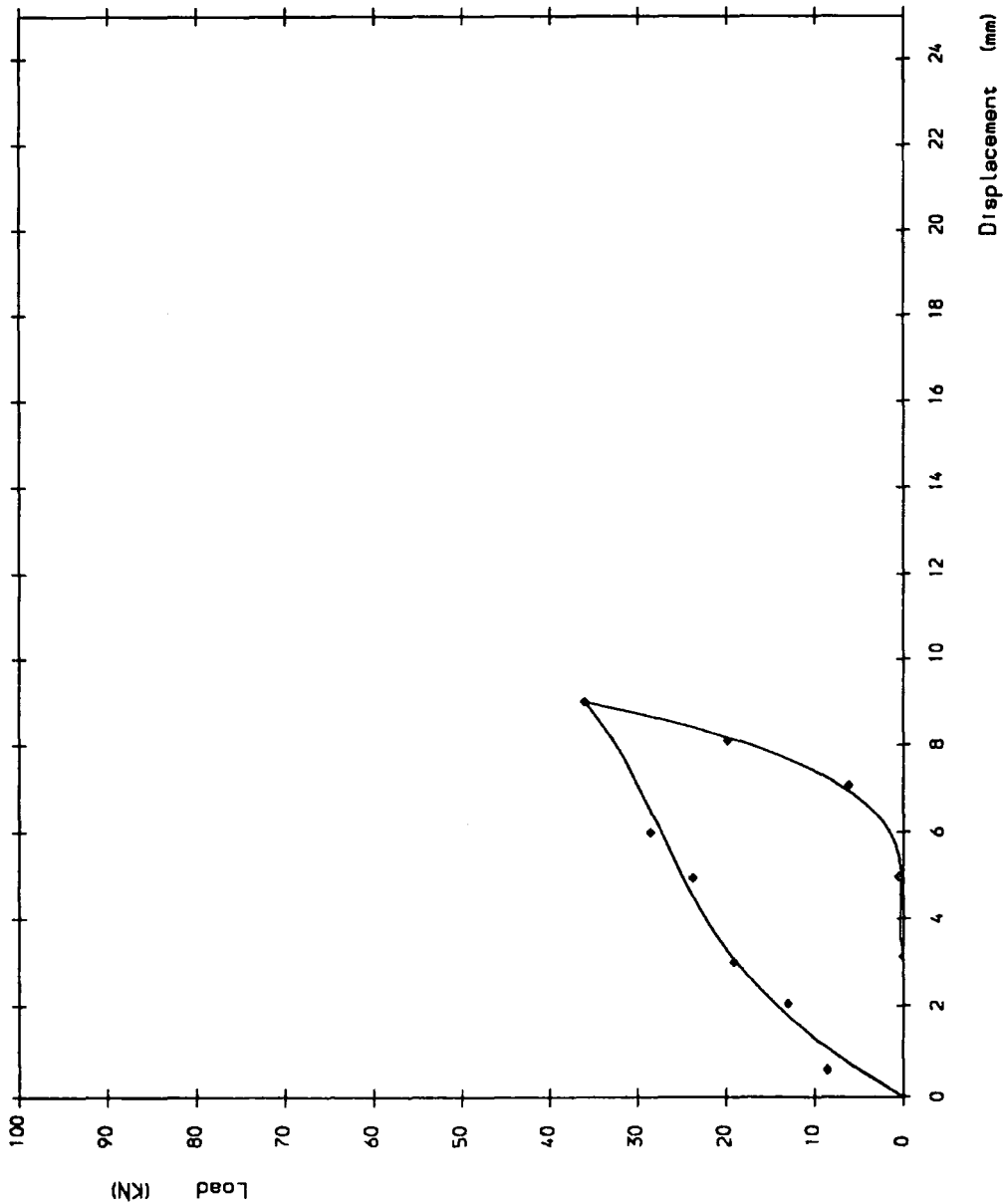
Figure A.26a Load/deflection curve 1st test 8 pile width spacing at 400mm overhang

BENDING MOMENT (kNm)

-30 -25 -20 -15 -10   5   10   15   20   25   30

DEPTH (m)

------- Rear pile
———— Front pile

1 = 3.00mm Pile cap Defl.
2 = 6.00mm Pile cap Defl.
3 = 9.00mm Pile cap Defl.
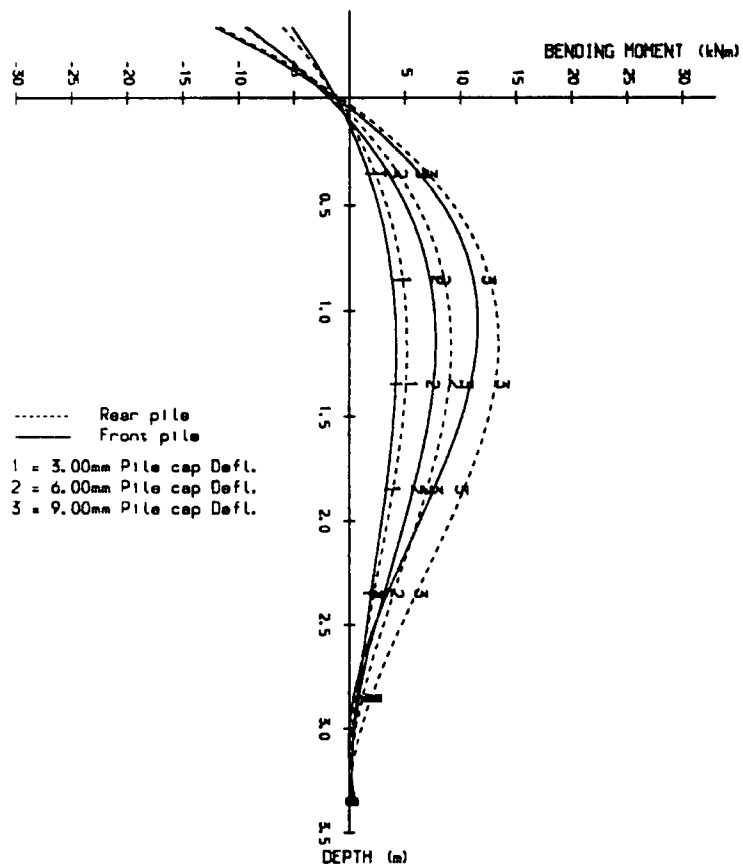
Figure A.26b Bending Moment Diagram for 2 pile group (first

test piles at 8 pile width spacing with 400mm overhang).

(TENSION)   AXIAL FORCE (KN)   (COMP)

-250 -200 -150 -100 -50   50   100   150   200   250

DEPTH (m)

····· Rear Pile
——— Front Pile
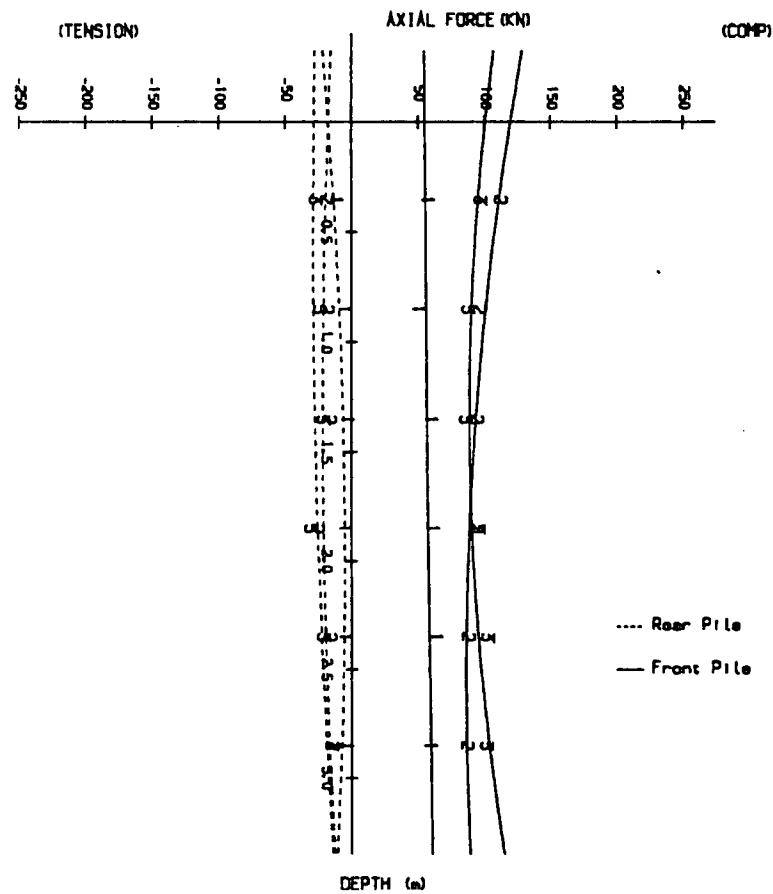
Figure A.26C Axial Force Diagram for 2 pile group (first

test piles at 8 pile width spacing with 400mm overhang).
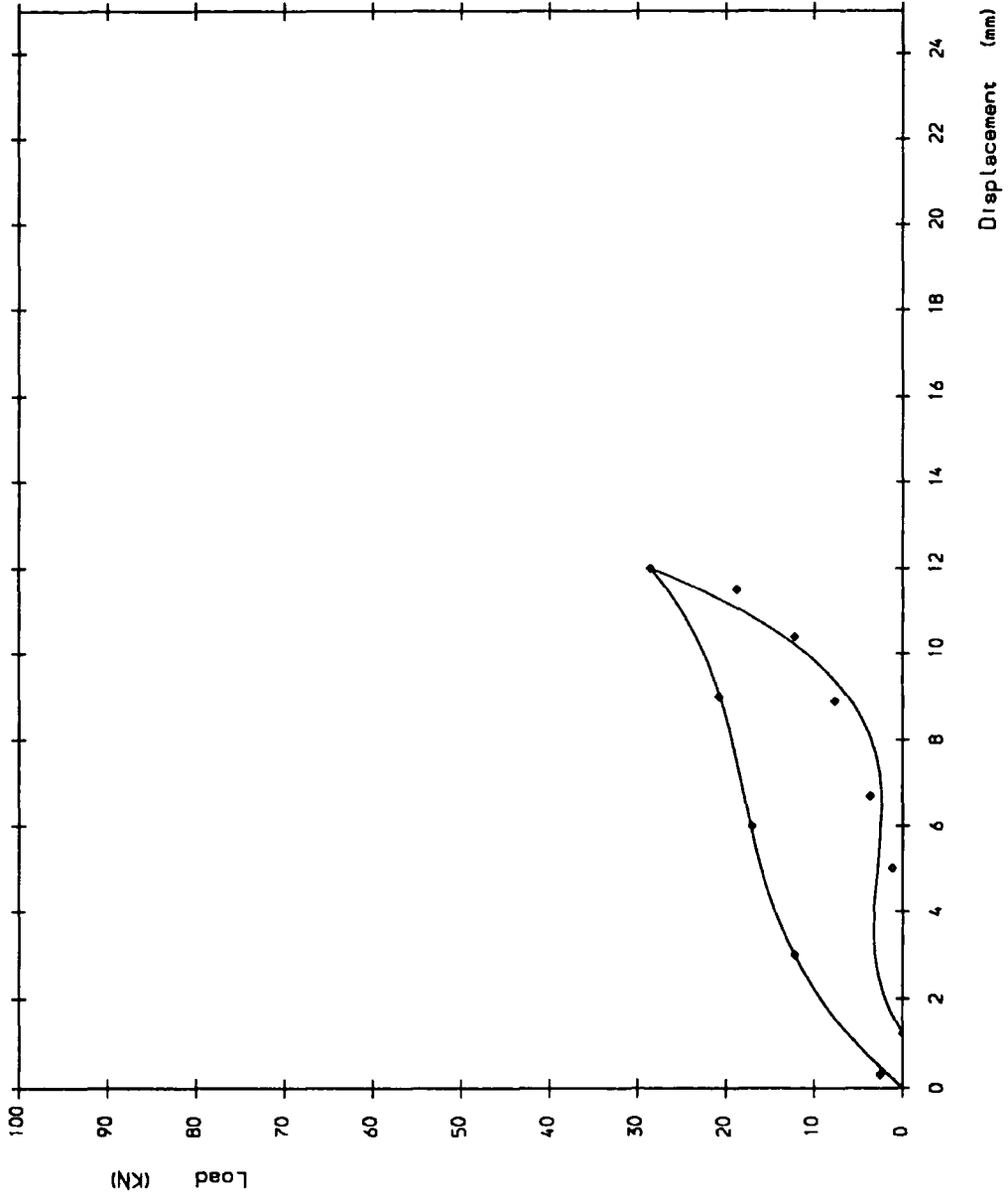
Figure A. 27a Load/deflection curve 2nd test 8 pile width spacing at 400mm overhang
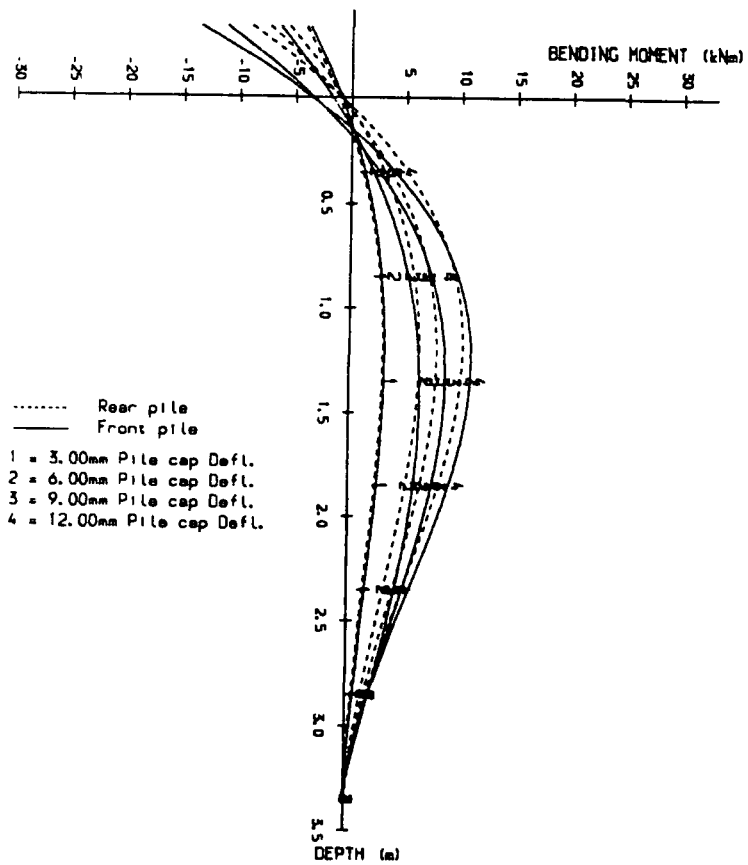
Figure A.27b Bending Moment Diagram for 2 pile group (second test piles at 8 pile width spacing with 400mm overhang).

Figure A.27C Axial Force Diagram for 2 pile group (second test piles at 8 pile width spacing with 400mm overhang).

Figure A.28a Load/deflection curve 3th test 8 pile width spacing at 400mm overhang
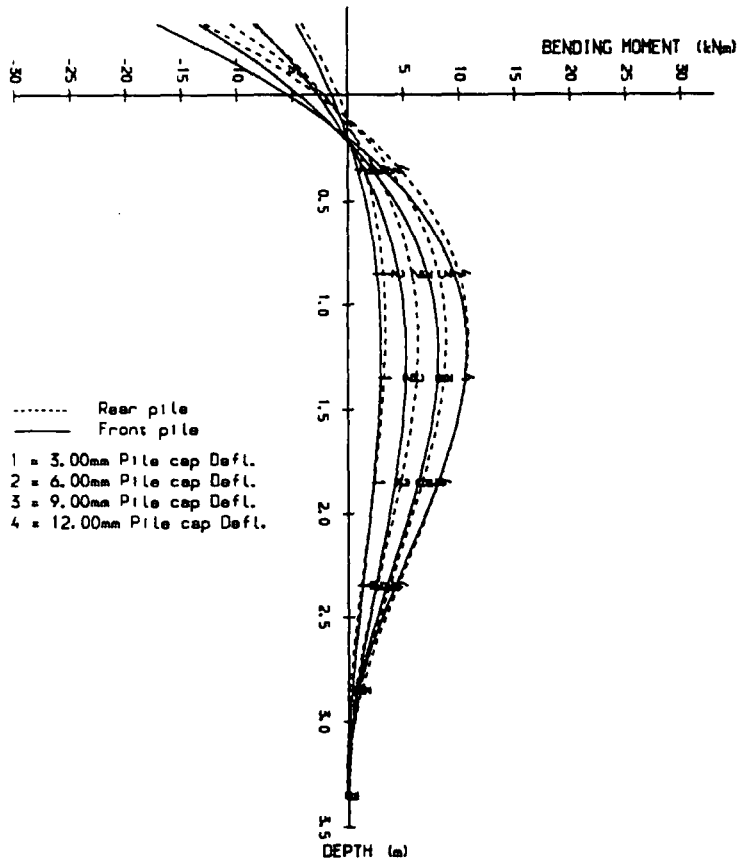
BENDING MOMENT (kNm)

Figure A.28b Bending Moment Diagram for 2 pile group (third test piles at 8 pile width spacing with 400mm overhang).

-------- Rear pile
———— Front pile

1 = 3.00mm Pile cap Defl.
2 = 6.00mm Pile cap Defl.
3 = 9.00mm Pile cap Defl.
4 = 12.00mm Pile cap Defl.

DEPTH (m)

(TENSION)　　　AXIAL FORCE (KN)　　　(COMP)

---- Rear Pile
—— Front Pile

DEPTH (m)

Figure A.28C Axial Force Diagram for 2 pile group (third test piles at 8 pile width spacing with 400mm overhang).

Figure A.29a Load/deflection curve 4th test 8 pile width spacing at 400mm overhang
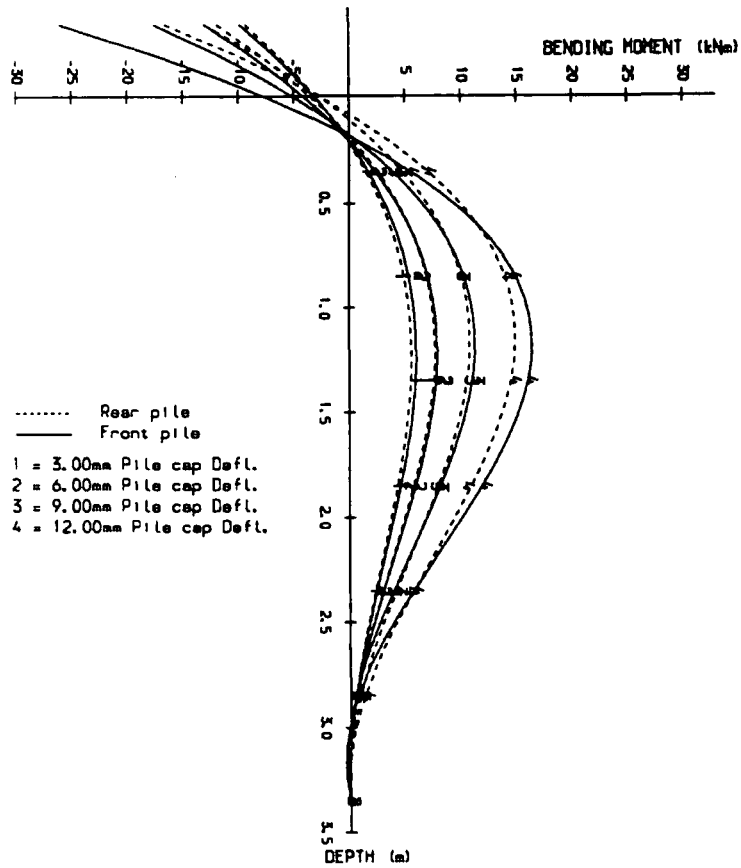
Figure A.29b Bending Moment Diagram for 2 pile group (forth

test piles at 8 pile width spacing with 400mm overhang).

Figure A.29C Axial Force Diagram for 2 pile group (fourth

test piles at 8 pile width spacing with 400mm overhang).

Figure A.30a Load/deflection curve 1st test 12 pile width spacing at 150mm overhang

Figure A.30b Bending Moment Diagram for 2 pile group (first
test piles at 12 pile width spacing with 150mm overhang).

BENDING MOMENT (kNm)

-------- Rear pile
———— Front pile

1 = 3.00mm Pile cap Defl.
2 = 6.00mm Pile cap Defl.
3 = 9.00mm Pile cap Defl.
4 = 12.00mm Pile cap Defl.
5 = 15.00mm Pile cap Defl.
6 = 20.00mm Pile cap Defl.
7 = 20.00mm Pile cap Defl.
    Cyclic loading.

DEPTH (m)

Figure A.30C Axial Force Diagram for 2 pile group (first
test piles at 12 pile width spacing with 150mm overhang).

(TENSION)   AXIAL FORCE (kN)   (COMP)

----- Rear Pile
——— Front Pile

DEPTH (m)

329

Figure A.31a Load/deflection curve 2nd test 12 pile width spacing at 150mm overhang
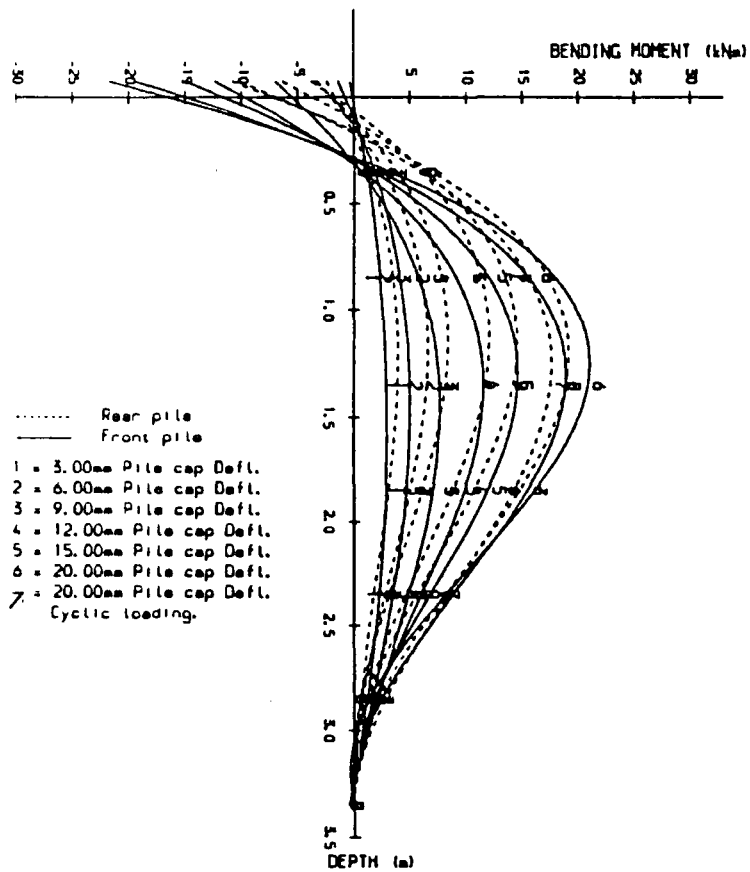
Figure A.31b Bending Moment Diagram for 2 pile group (second test piles at 12 pile width spacing with 150mm overhang).

Figure A.31C Axial Force Diagram for 2 pile group (second test piles at 12 pile width spacing with 150mm overhang).

Legend for Figure A.31b:

.... Rear pile
——— Front pile

1 = 3.00mm Pile cap Defl.
2 = 6.00mm Pile cap Defl.
3 = 9.00mm Pile cap Defl.
4 = 12.00mm Pile cap Defl.
5 = 15.00mm Pile cap Defl.
6 = 20.00mm Pile cap Defl.
7 = 20.00mm Pile cap Defl. Cyclic loading.

Legend for Figure A.31C:

···· Rear Pile
—— Front Pile
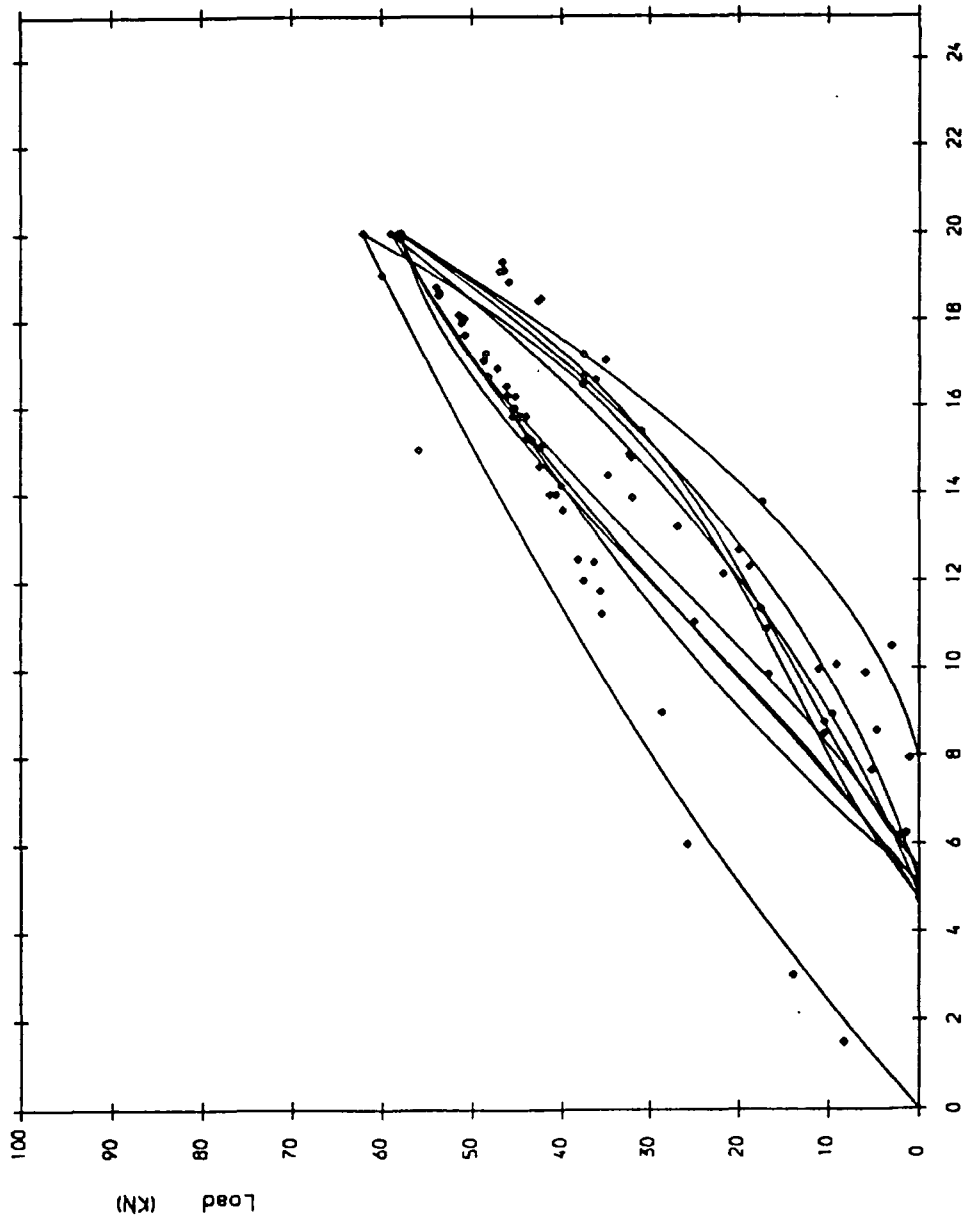
Figure A. 32a Load/deflection curve 1st test 12 pile width spacing at 300mm overhang

Figure 4.32b Bending Moment Diagram for 2 pile group (first test piles at 12 pile width spacing with 300mm overhang).
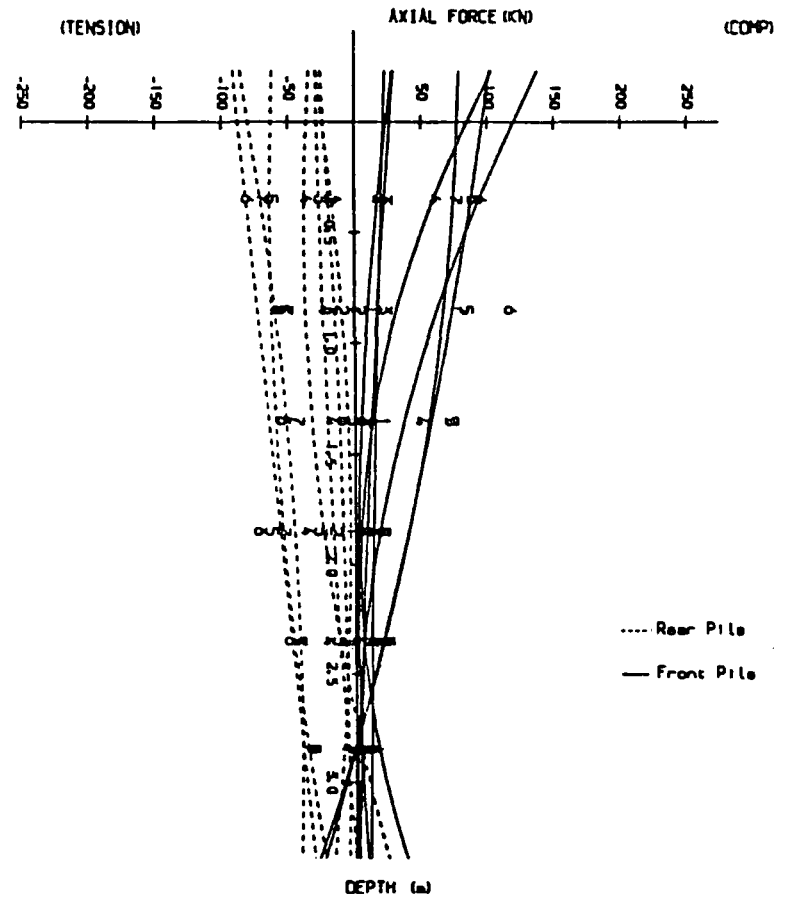
Figure A.32C Axial Force Diagram for 2 pile group (first test piles at 12 pile width spacing with 300mm overhang).
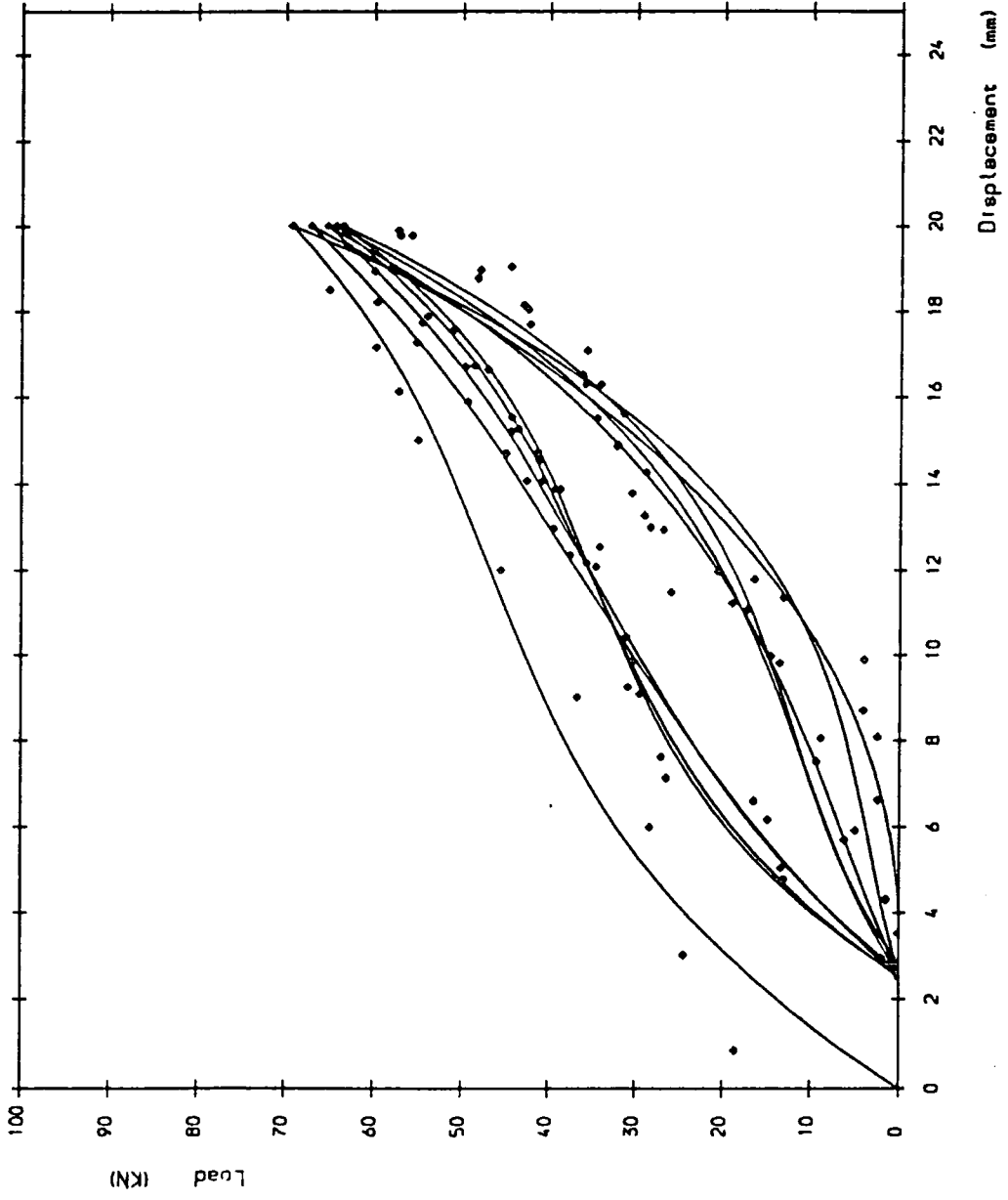
Figure A.33a Load/deflection curve 2nd test 12 pile width spacing at 300mm overhang

BENDING MOMENT (kNm)

(TENSION)　　　　AXIAL FORCE (kN)　　　　(COMP)

.... Rear pile
———— Front pile

1 = 3.00mm Pile cap Defl.
2 = 6.00mm Pile cap Defl.
3 = 9.00mm Pile cap Defl.
4 = 12.00mm Pile cap Defl.
5 = 15.00mm Pile cap Defl.
6 = 20.00mm Pile cap Defl.
7 = 20.00mm Pile cap Defl.
     Cyclic loading.

.... Rear Pile
—— Front Pile

DEPTH (m)

DEPTH (m)

Figure A.33b Bending Moment Diagram for 2 pile group (second
test piles at 12 pile width spacing with 300mm overhang).

Figure A.33C Axial Force Diagram for 2 pile group (second
test piles at 12 pile width spacing with 300mm overhang).
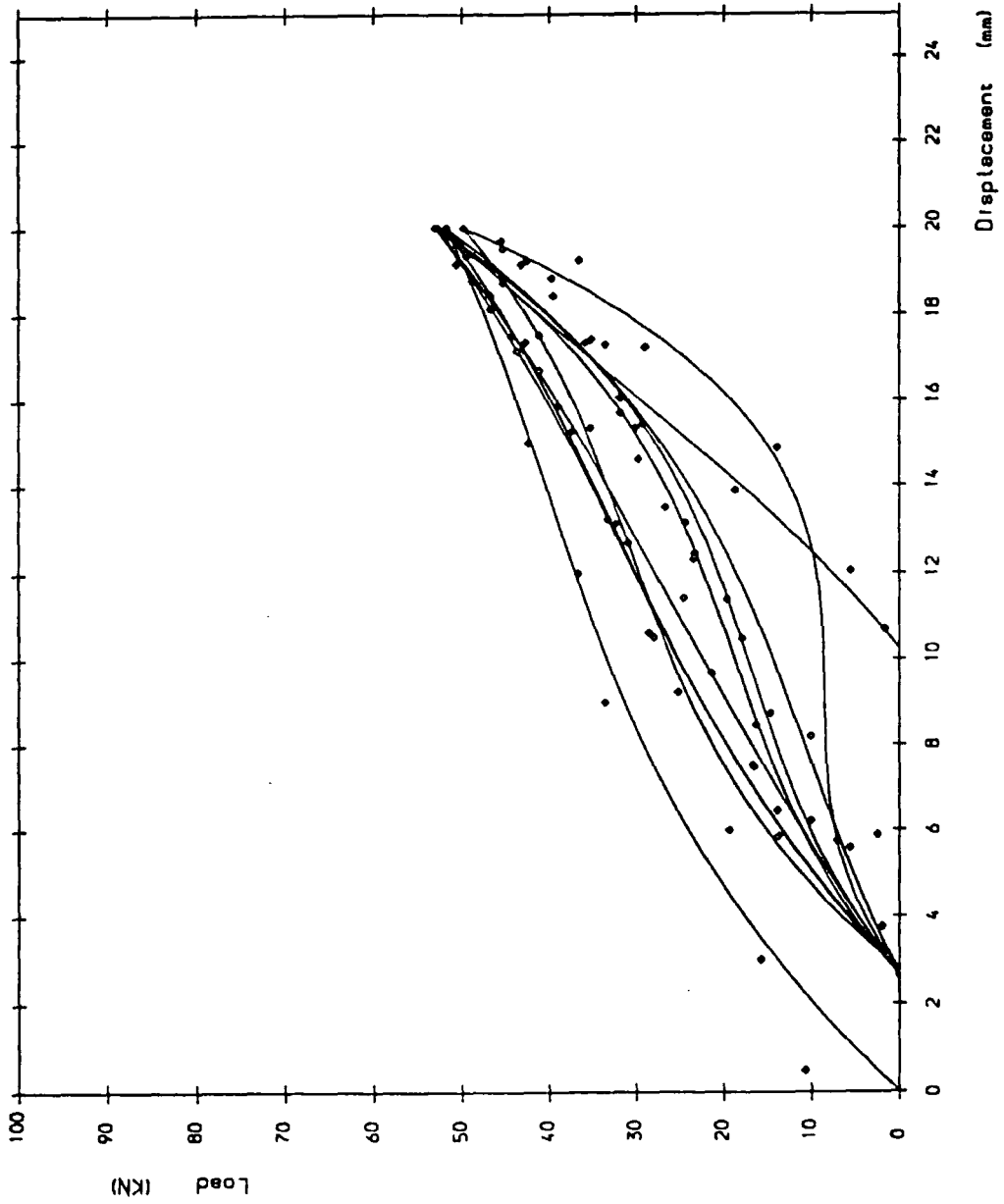
Figure A.34a Load/deflection curve 1st test 12 pile width spacing at 400mm overhang
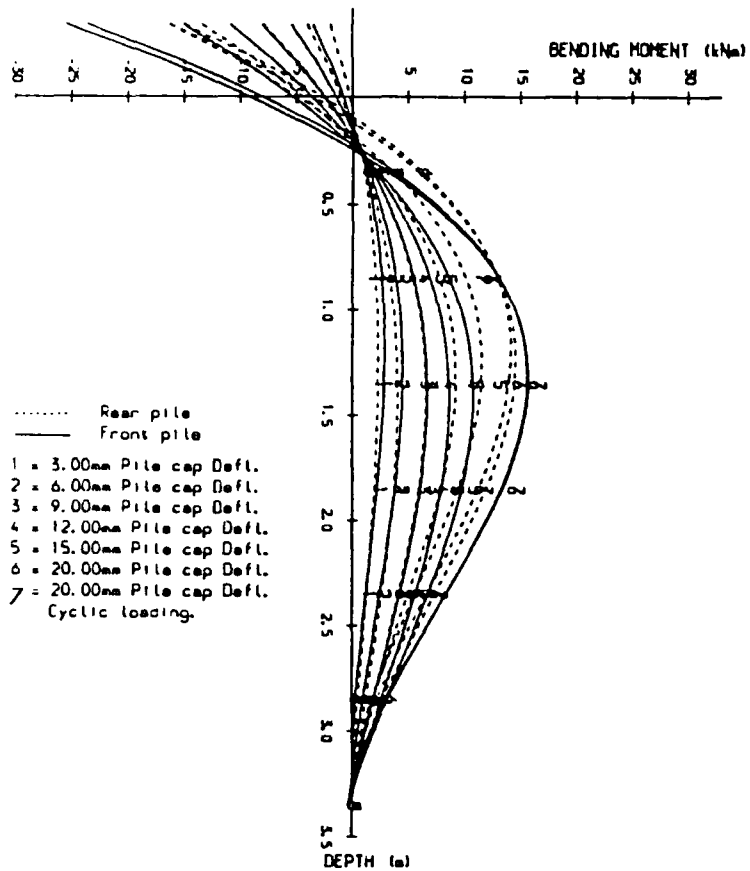
Figure A.34b Bending Moment Diagram for 2 pile group (first test piles at 12 pile width spacing with 400mm overhang).

Figure A.34C Axial Force Diagram for 2 pile group (first test piles at 12 pile width spacing with 400mm overhang).
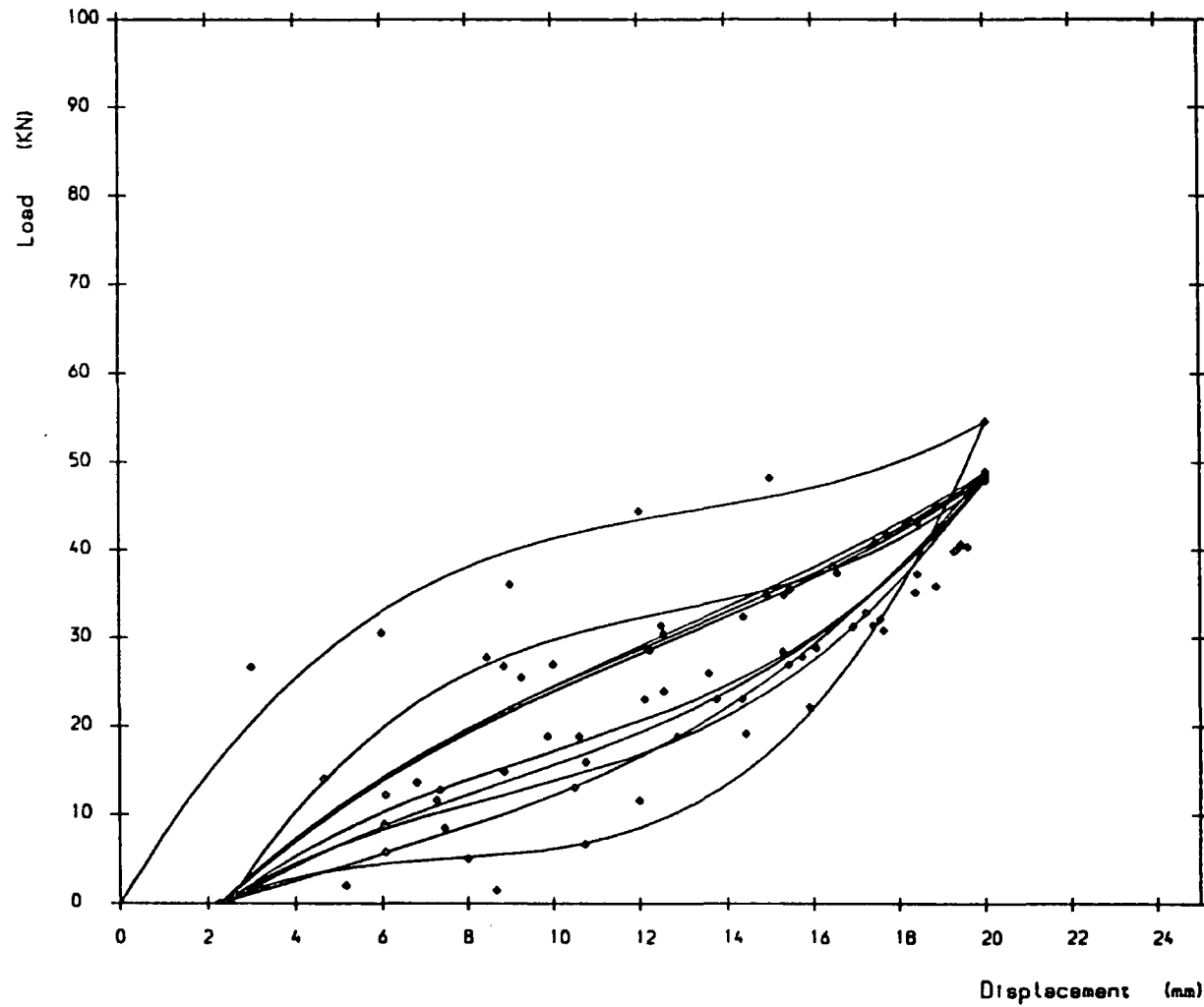
Figure A.35a Load/deflection curve 2nd test 12 pile width spacing at 400mm overhang
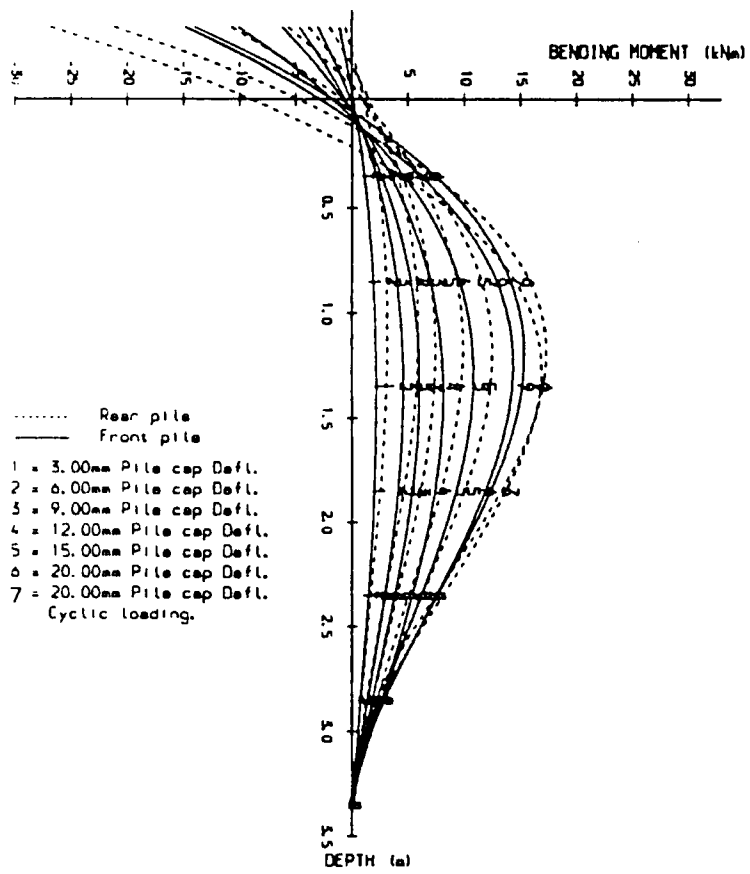
Figure A.35b Bending Moment Diagram for 2 pile group (second test piles at 12 pile width spacing with 400mm overhang).

BENDING MOMENT (kNm)

DEPTH (m)

.... Rear pile
———— Front pile

1 = 3.00mm Pile cap Defl.
2 = 6.00mm Pile cap Defl.
3 = 9.00mm Pile cap Defl.
4 = 12.00mm Pile cap Defl.
5 = 15.00mm Pile cap Defl.
6 = 20.00mm Pile cap Defl.
7 = 20.00mm Pile cap Defl.
    Cyclic loading.

Figure A.35C Axial Force Diagram for 2 pile group (second test piles at 12 pile width spacing with 400mm overhang).

(TENSION)   AXIAL FORCE (kN)   (COMP)

DEPTH (m)

..... Rear Pile
——— Front Pile

Figure A.34a Ratio of Max. Bending Moment between front and rear pile against Cap Displacement for 3 pile width spacing with 400mm overhang.

Figure A.34b Ratio of Max. Bending Moment between front and rear pile against Cap Displacement for 3 pile width spacing with 300mm overhang.

Figure A.34c Ratio of Max. Bending Moment between front and rear pile against Cap Displacement for 3 pile width spacing with 150mm overhang.
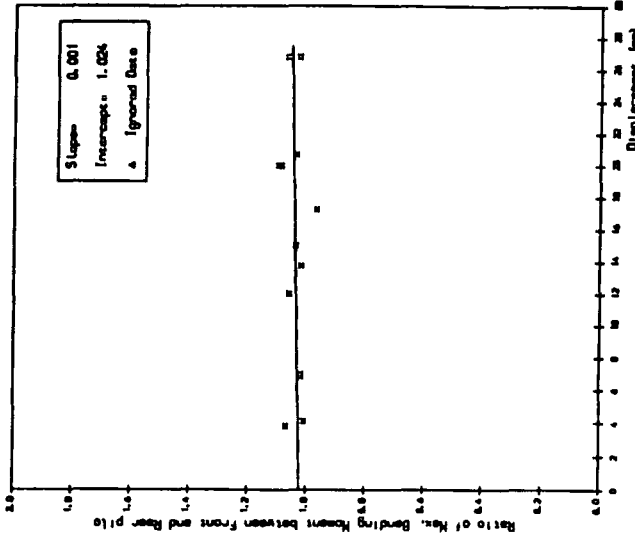
Figure A.57c Ratio of Max. Bending Moment between front and rear pile against Cap Displacement for 5 pile width spacing with 400mm overhang.
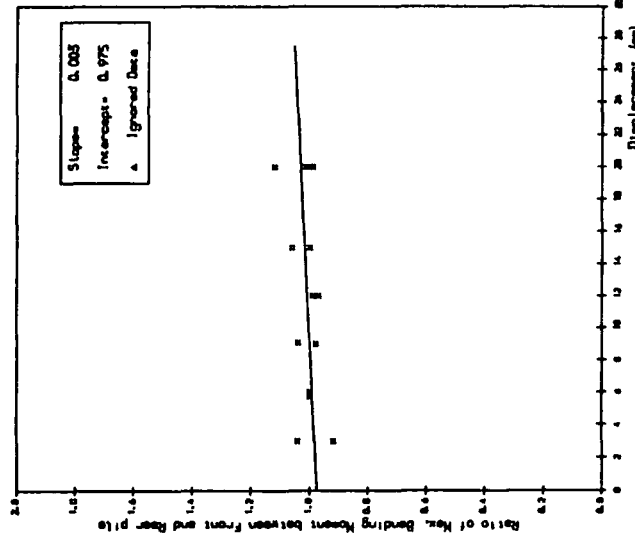
Figure A.57b Ratio of Max. Bending Moment between front and rear pile against Cap Displacement for 5 pile width spacing with 300mm overhang.
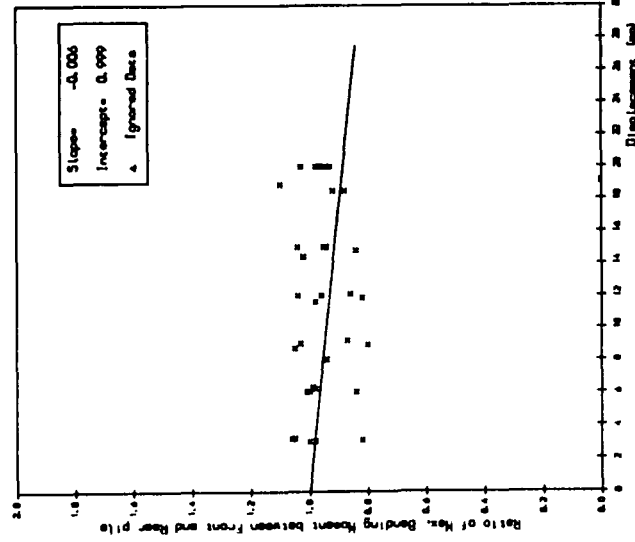
Figure A.57a Ratio of Max. Bending Moment between front and rear pile against Cap Displacement for 5 pile width spacing with 150mm overhang.

Figure A.35c Ratio of Max. Bending Moment between front and rear pile against Cap Displacement for 8 pile with spacing with 400m overhang.
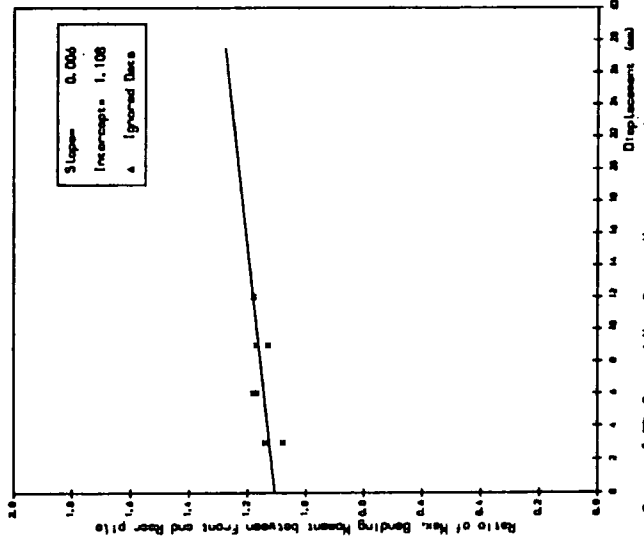
Figure A.35b Ratio of Max. Bending Moment between front and rear pile against Cap Displacement for 8 pile with spacing with 300m overhang.
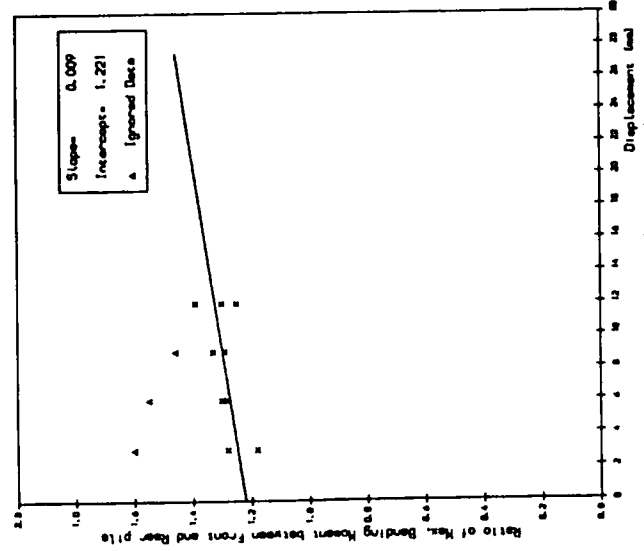
Figure A.35a Ratio of Max. Bending Moment between front and rear pile against Cap Displacement for 8 pile with spacing with 150m overhang.
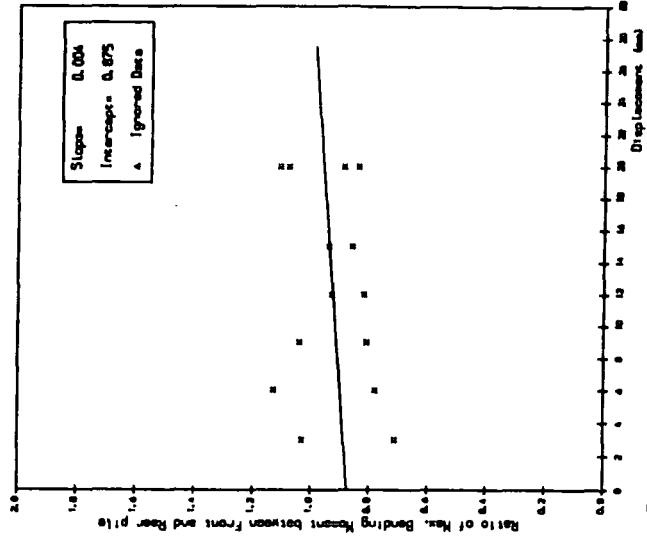
Figure A.39c Ratio of Max. Bending Moment between front and rear pile against Cap Displacement for 12 pile slash spacing with 400mm overhang.
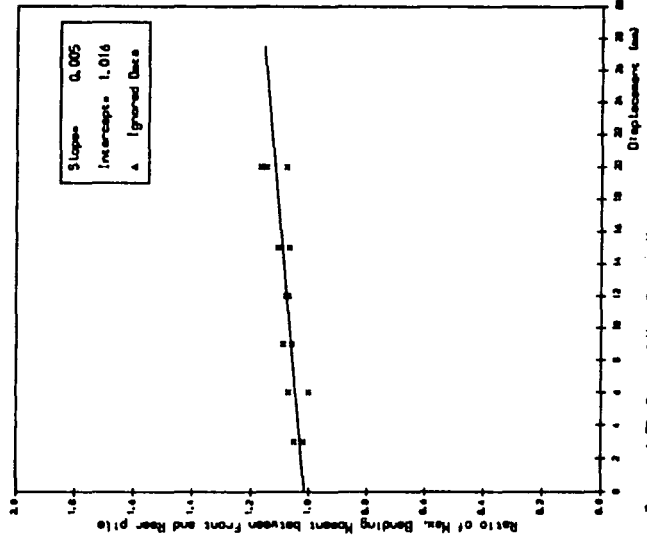
Figure A.39b Ratio of Max. Bending Moment between front and rear pile against Cap Displacement for 12 pile slash spacing with 300mm overhang.
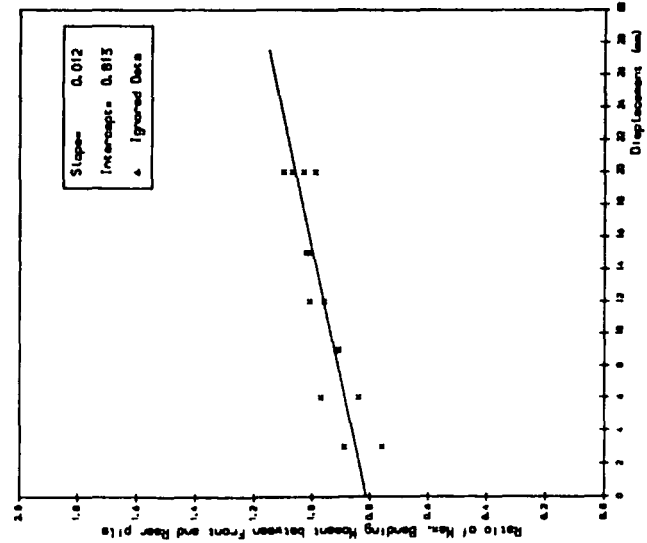
Figure A.39a Ratio of Max. Bending Moment between front and rear pile against Cap Displacement for 12 pile slash spacing with 150mm overhang.

Figure A. 40a Av. Maximum bending moment against horizontal load for 2pile width spacing.
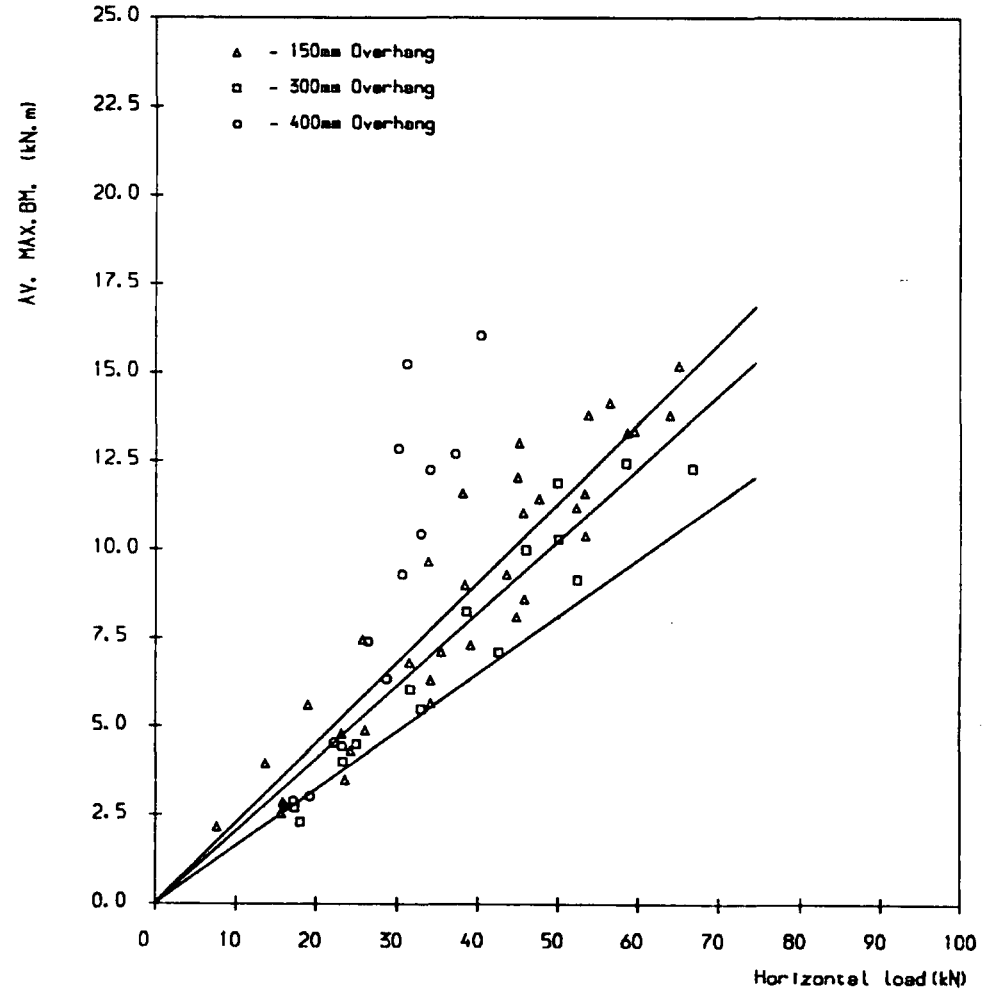
Figure A. 40b Av. Maximum bending moment against horizontal load for 5pile width spacing.
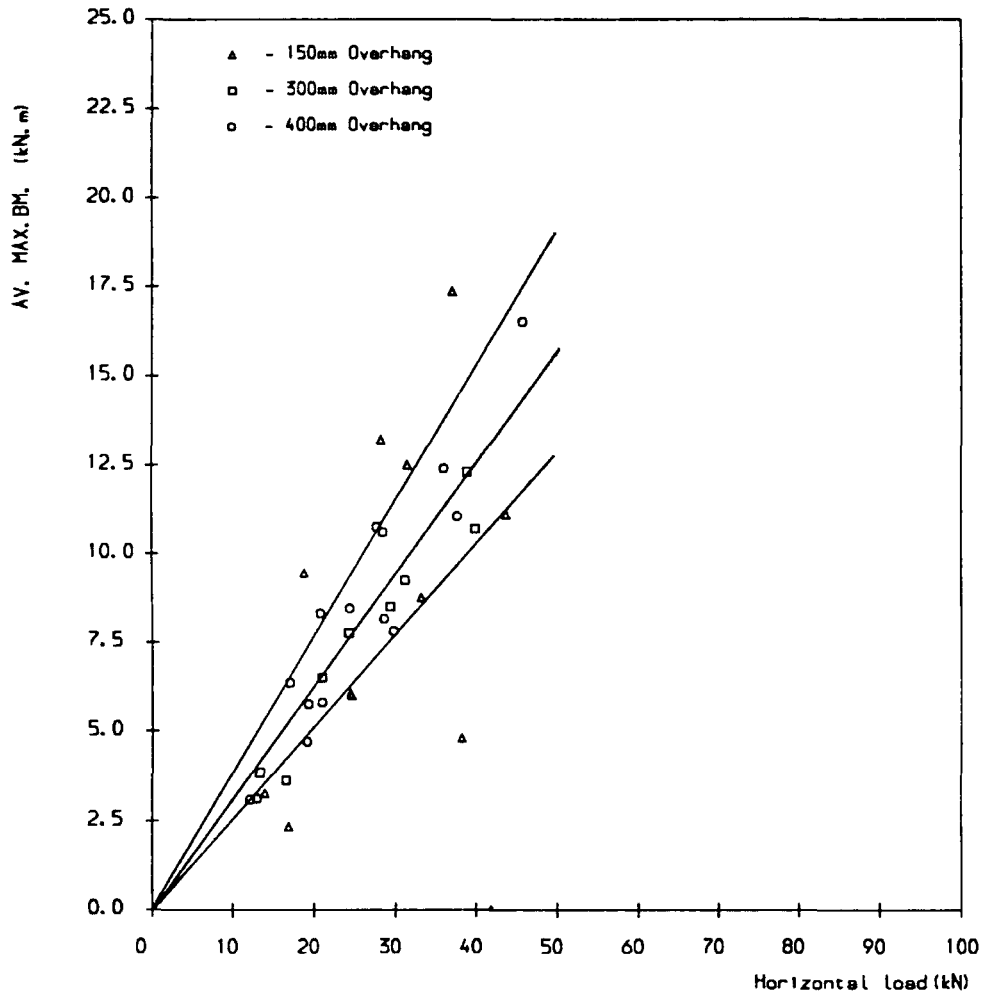
Figure A. 40c Av. Maximum bending moment against horizontal

load for 8pile widthspacing.
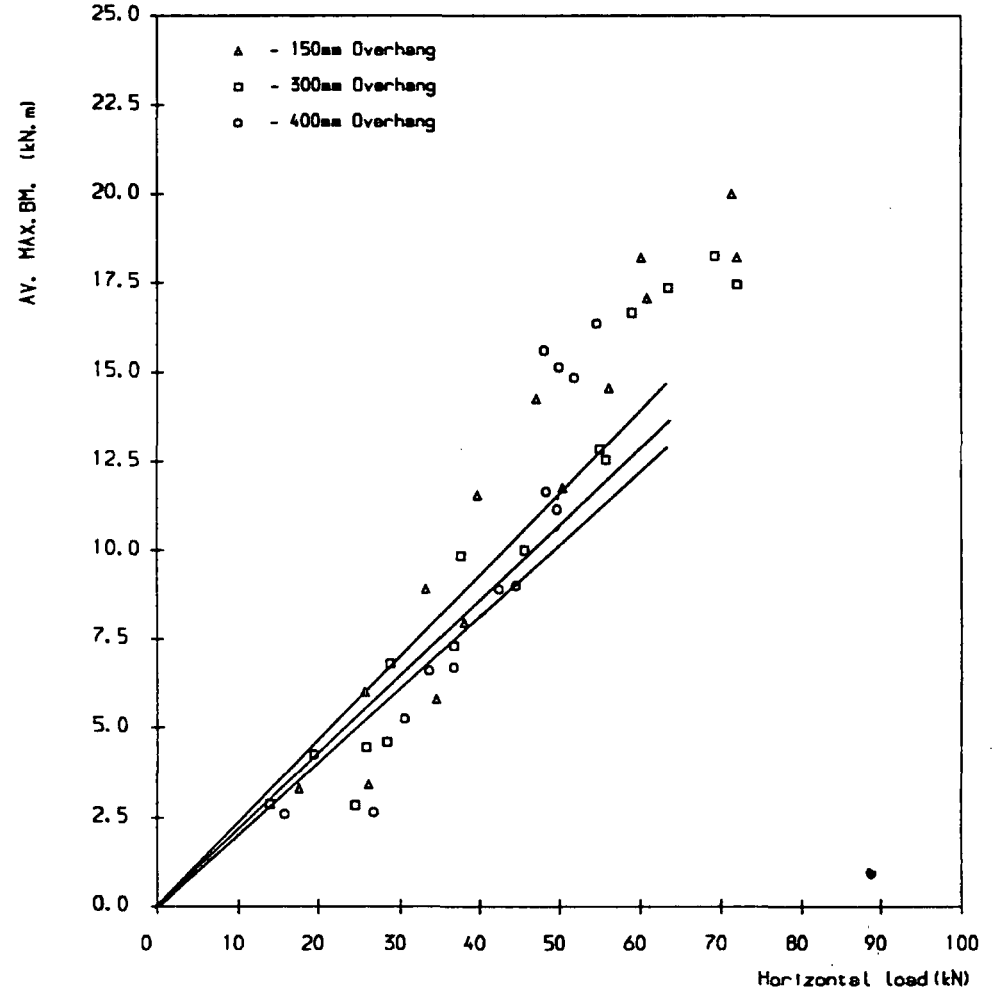
Figure A. 40d Av. Maximum bending moment against horizontal

load for 12pile widthspacing.
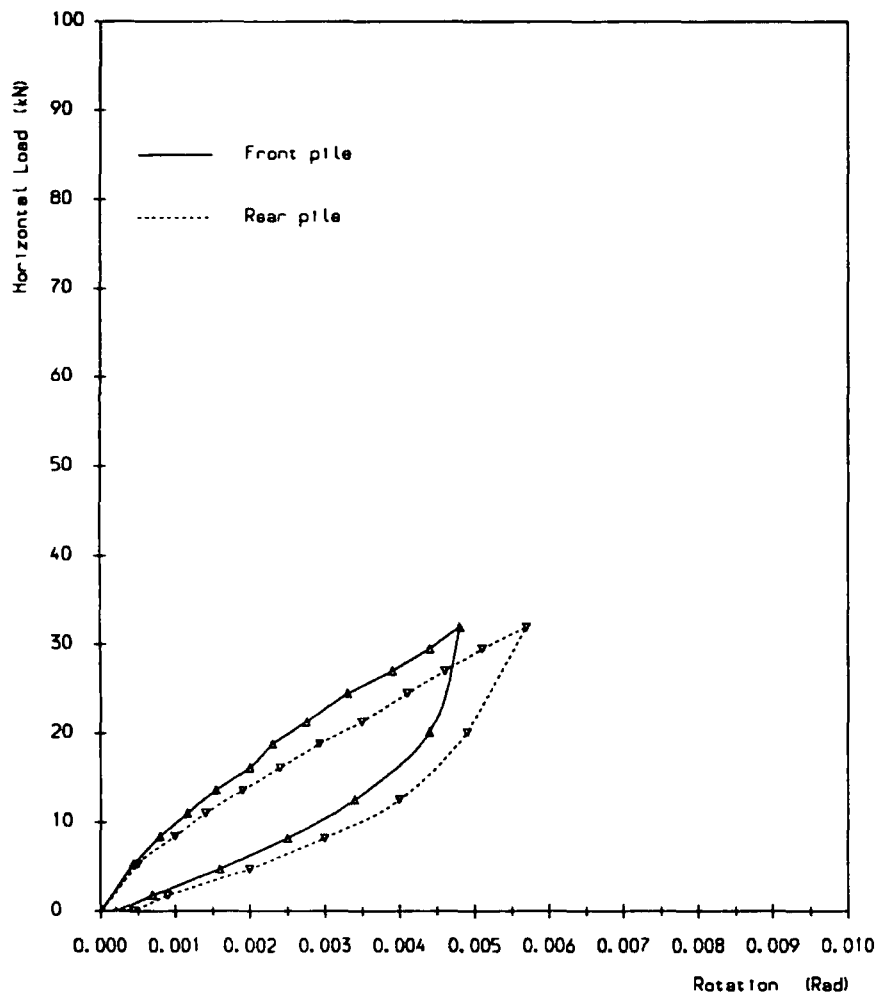
Figure A.41 Load/rotation curve for forth test on 3 width 400mm overhang.
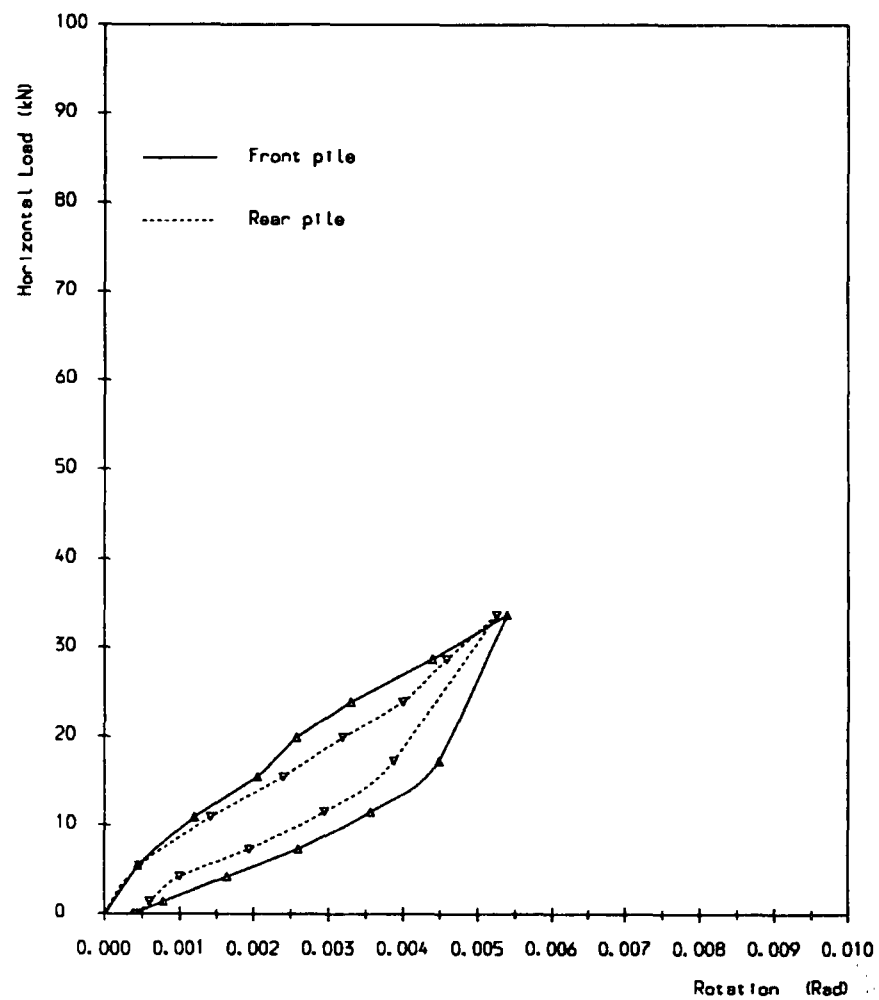
Figure A.42 Load/rotation curve for fifth test on 3 width 400mm overhang.
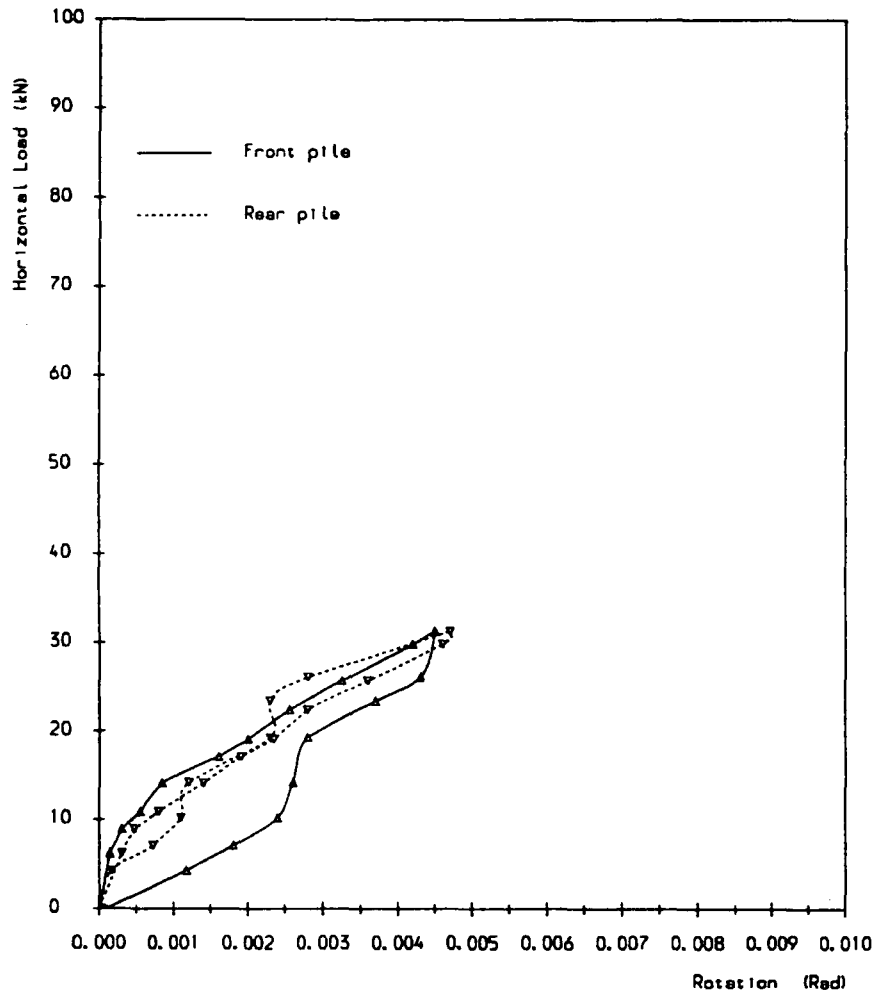
Figure A.43 Load/rotation curve for third test on 5 width,400mm overhang.
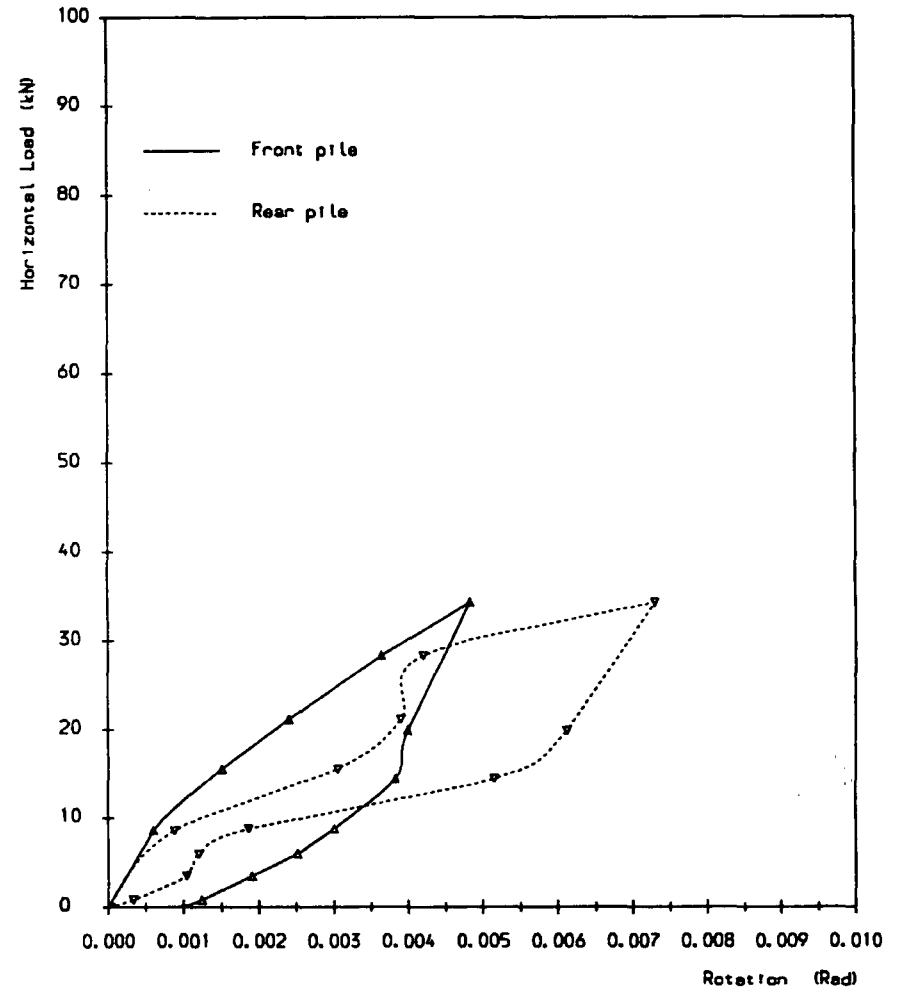
Figure A.44 Load/rotation curve for fourth test on 5 width,400mm overhang.

347
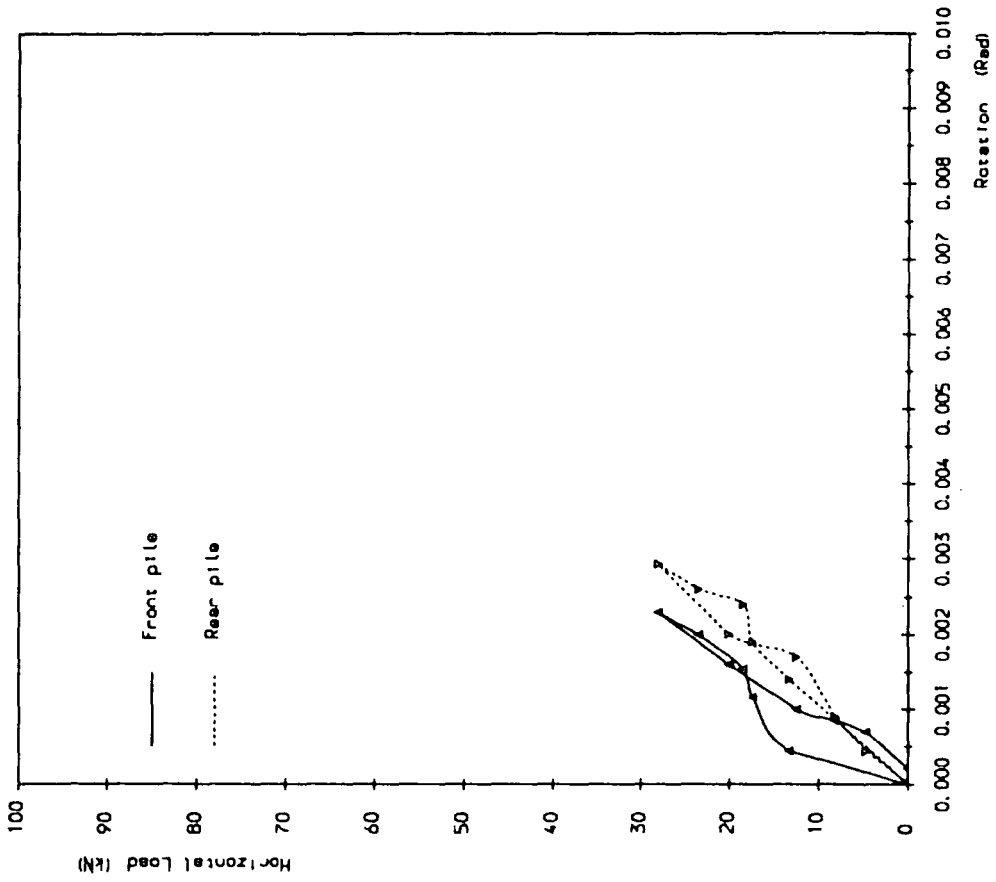
Figure A.45 Load/rotation curve for fifth test on 8 width 400mm overhang.
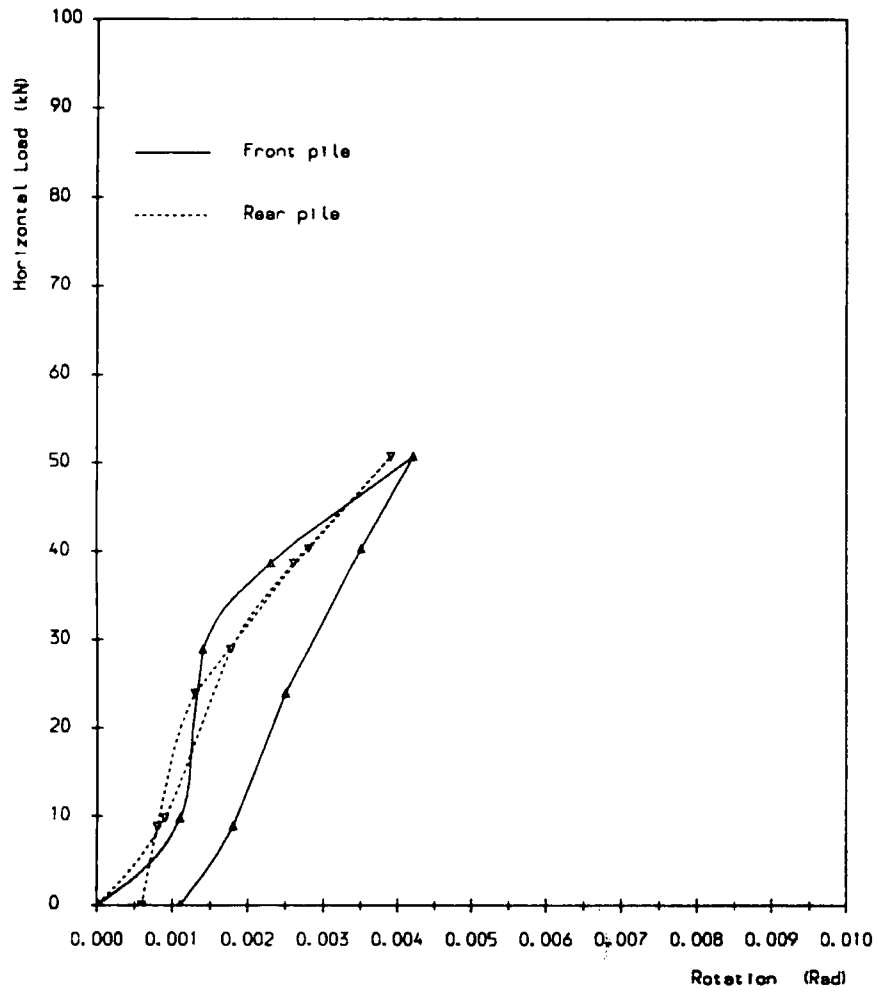
Figure A.46 Load/rotation curve for third test on 12 width 400mm overhang.
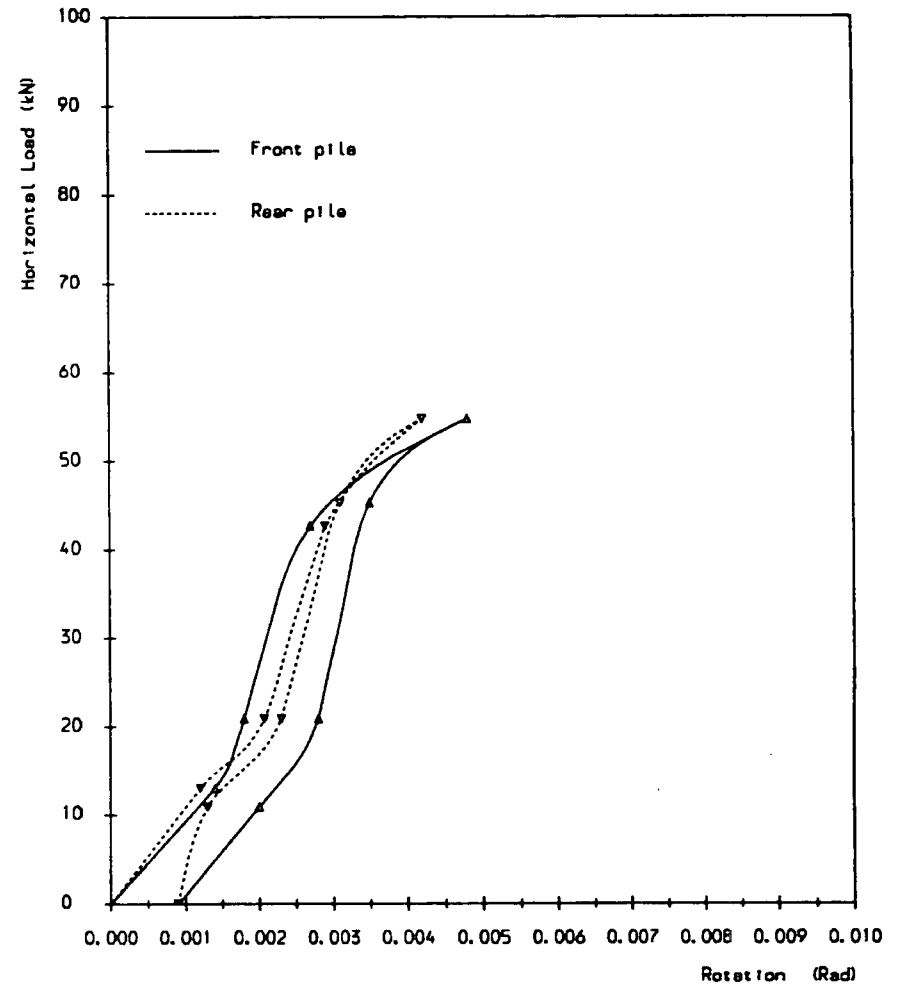
Figure A.47 Load/rotation curve for fourth test on 12 width 400mm overhang.

Appendix B

B1-Content

Appendix B contains a summary of finite element results presented in graphical form for the following properties and relationships:

B.1a - B.14a Pile deflections.

B.1b - B.14b Bending moments.

B.1c - B.2c Soil pressure distributions for the single pile.

B.3c - B.14c Axial forces.

B.3d - B.14d Soil pressure distributions for two-pile groups.

A.15a Bending moment for reduced pile cap stiffness.
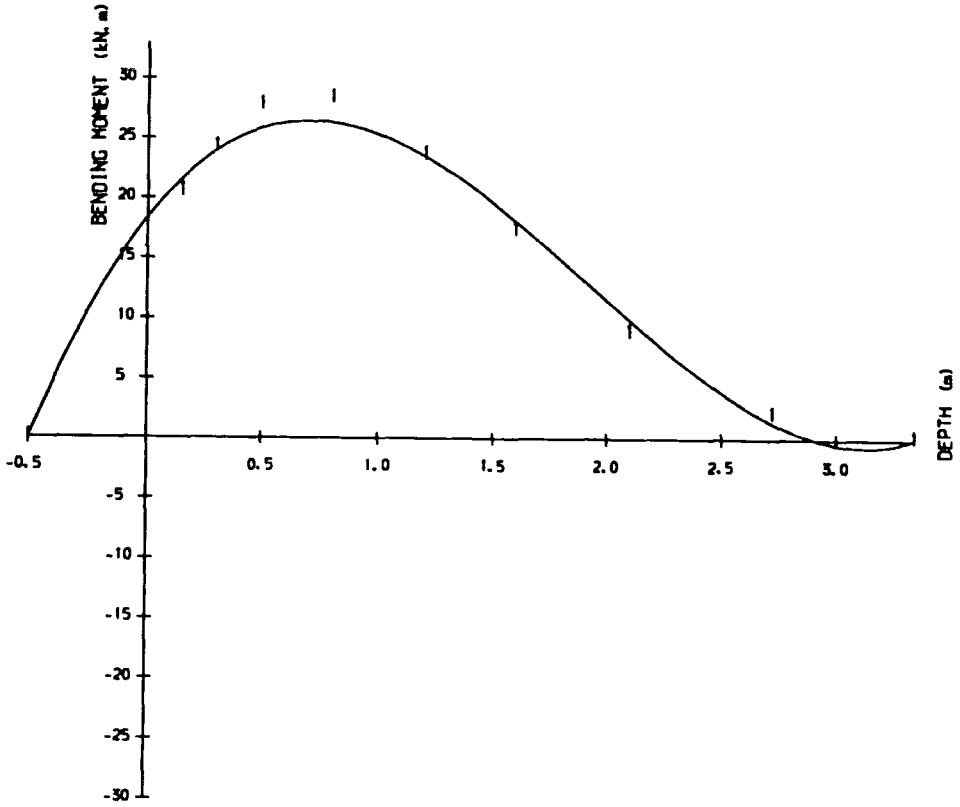
Figure B.1b Bending moment diagram for single pile (free head)
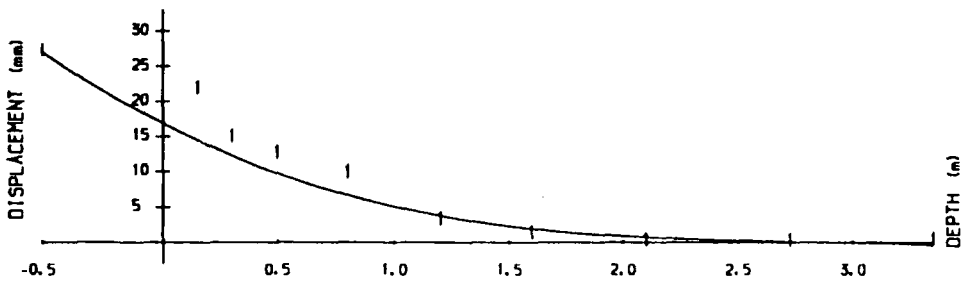
Figure B.1a Pile deflection diagram
for single free head pile, lateral
load 36.9kN at 500mm above the ground
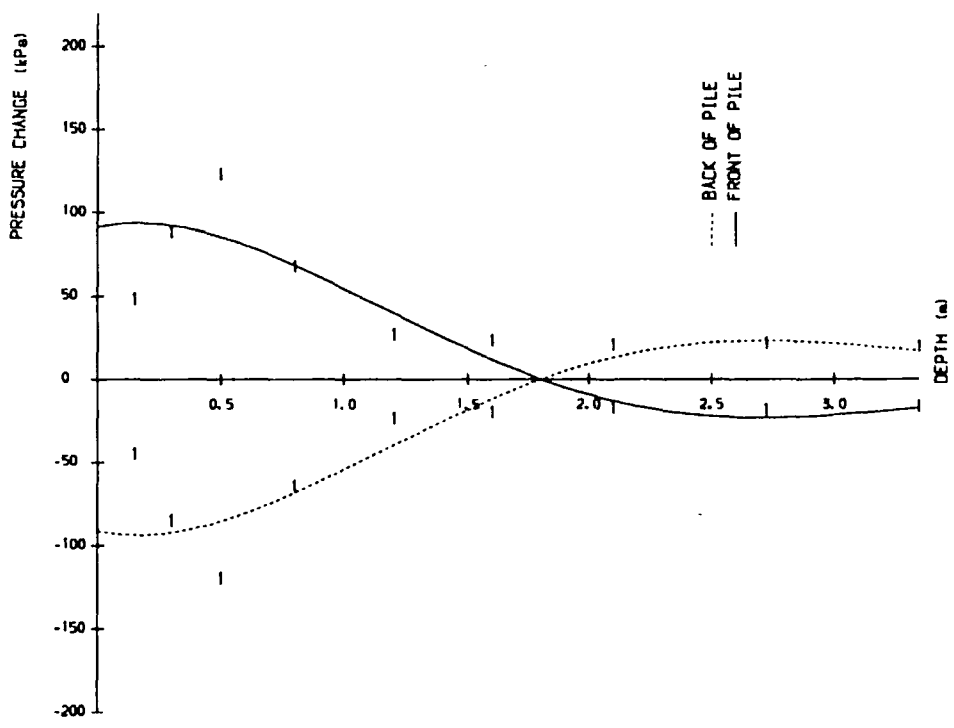
Figure B.1c Pressure distribution diagram for single pile (free head)

DISPLACEMENT (mm)
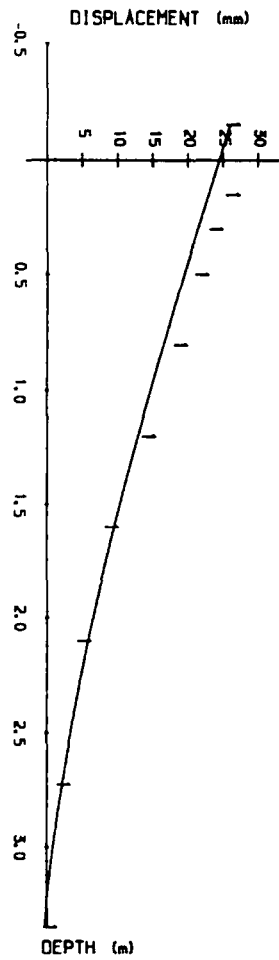
Figure B.2a Pile deflection diagram
for single fix head pile, lateral
load 103.4kN at ground line.

DEPTH (m)

BENDING MOMENT (kN.m)

DEPTH (m)
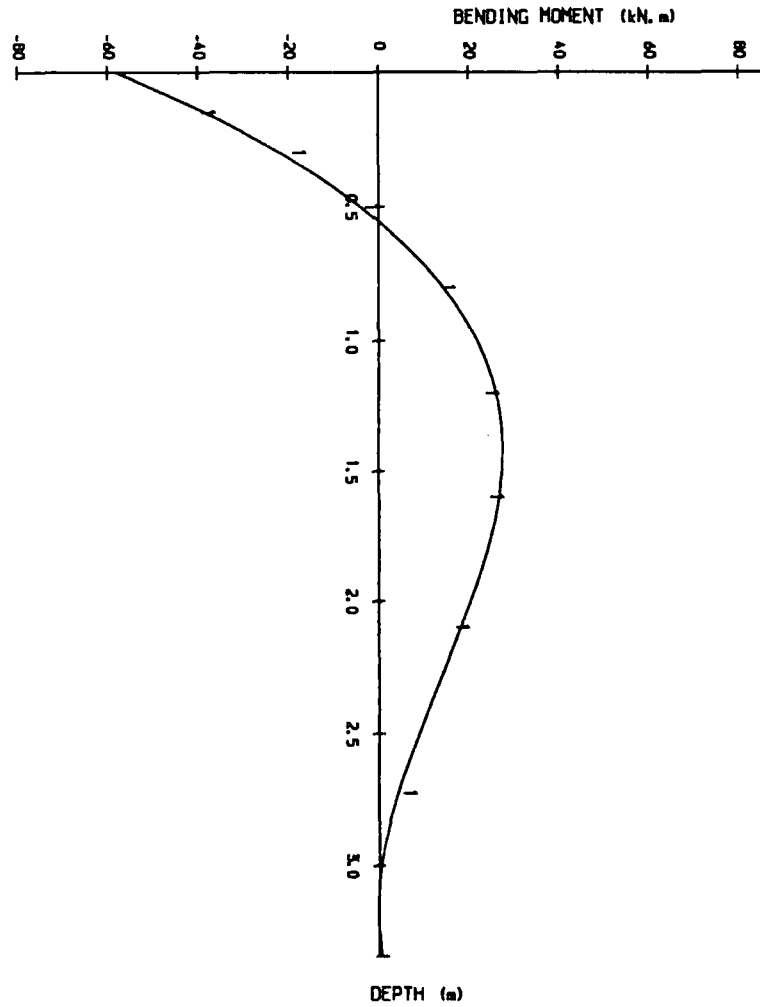
Figure B.2b Bending moment diagram for single pile (fix head)
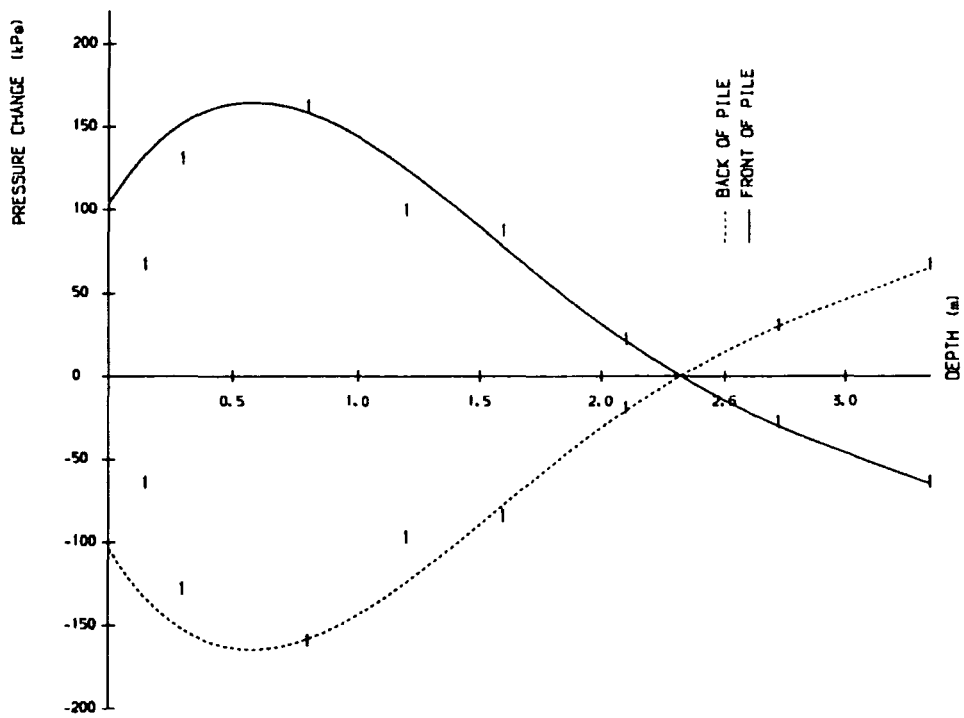
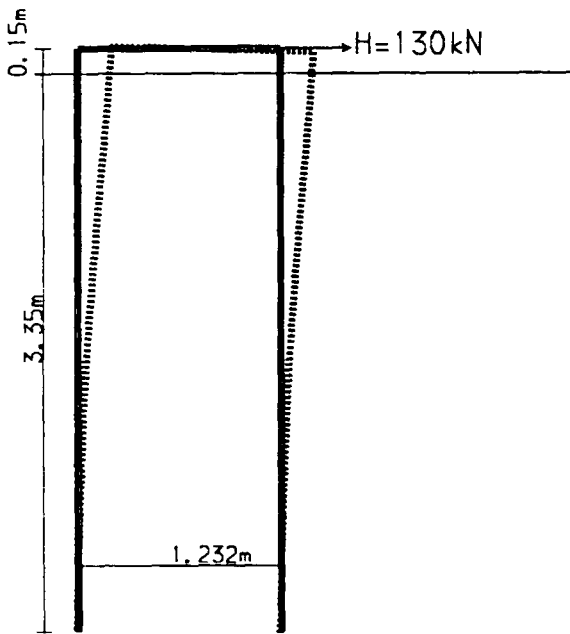Figure B.2c Pressure distribution diagram for single pile (fix head)
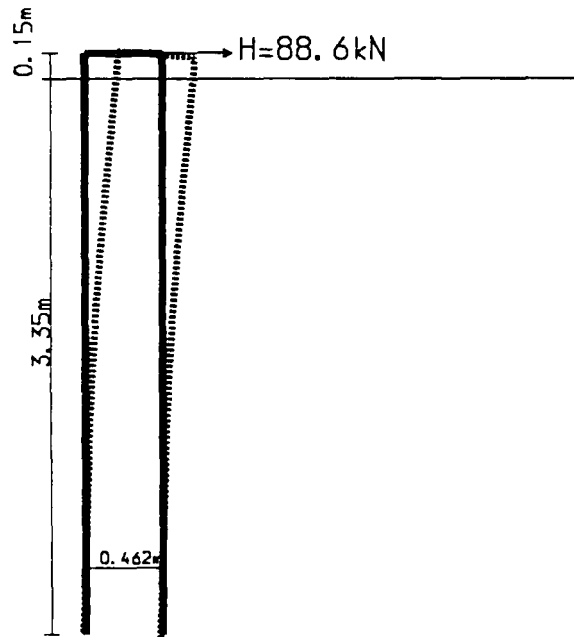
Figure B.3a Deflected shape of two-pile group at 3
pile width spacing 150mm overhang for 20mm pile cap defl.
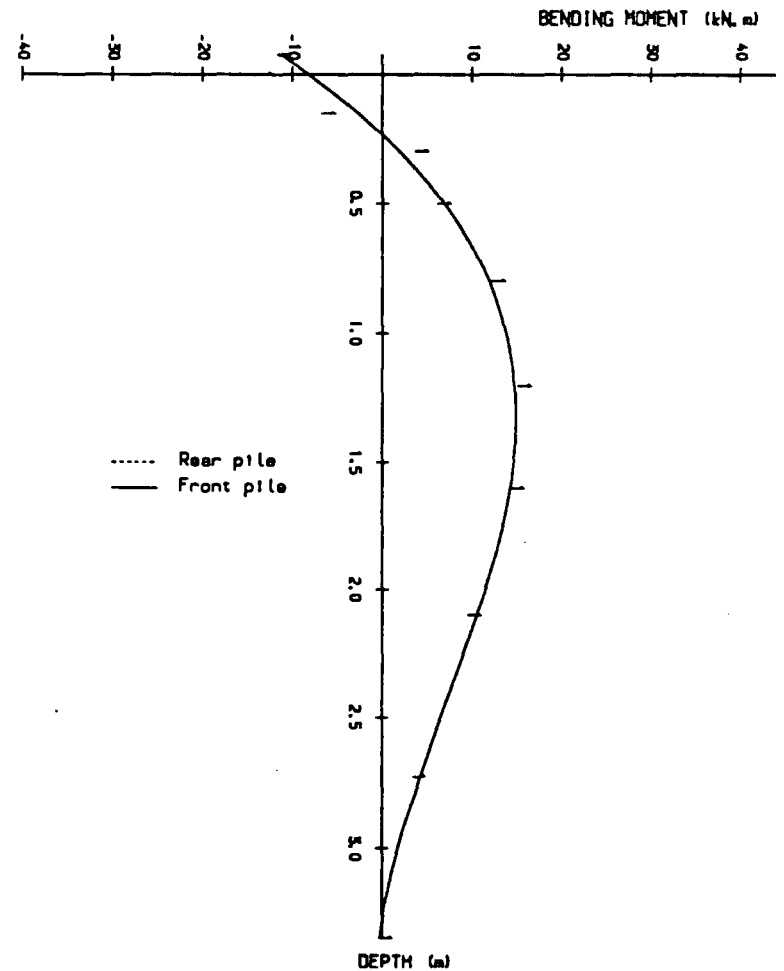
Figure B.3b Bending moment diagram for two-pile group
(3 pile width spacing 150mm overhang).
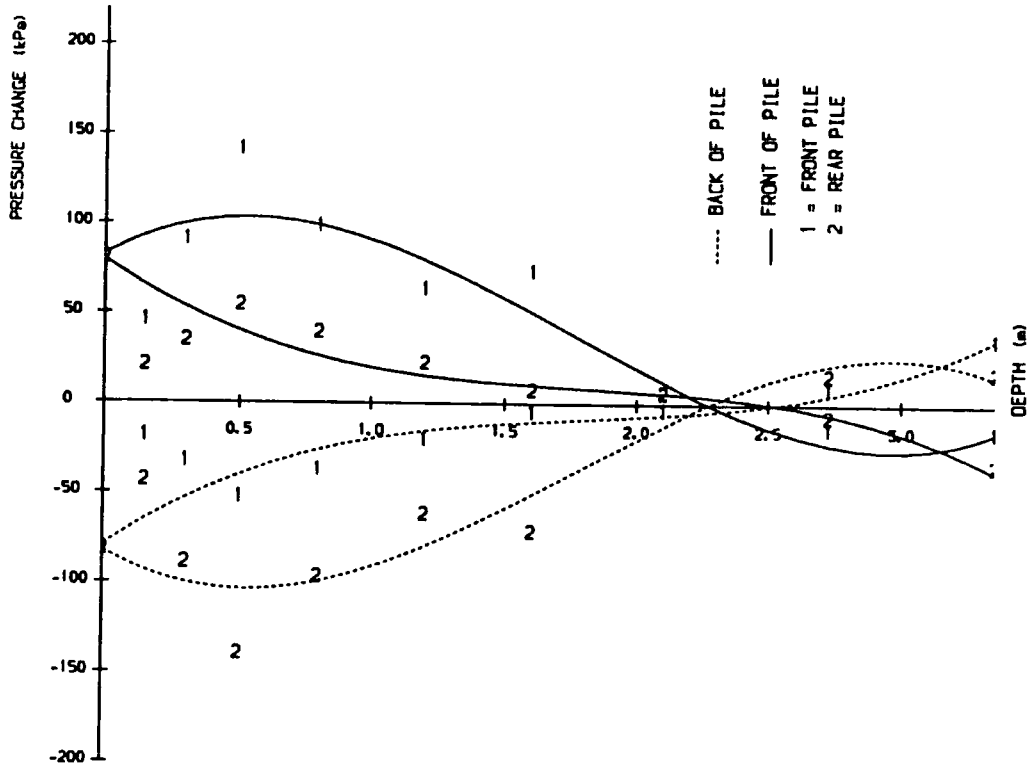
Figure B.3d Pressure distribution diagram for two-pile group
(3 pile dish spacing 150mm overhang)
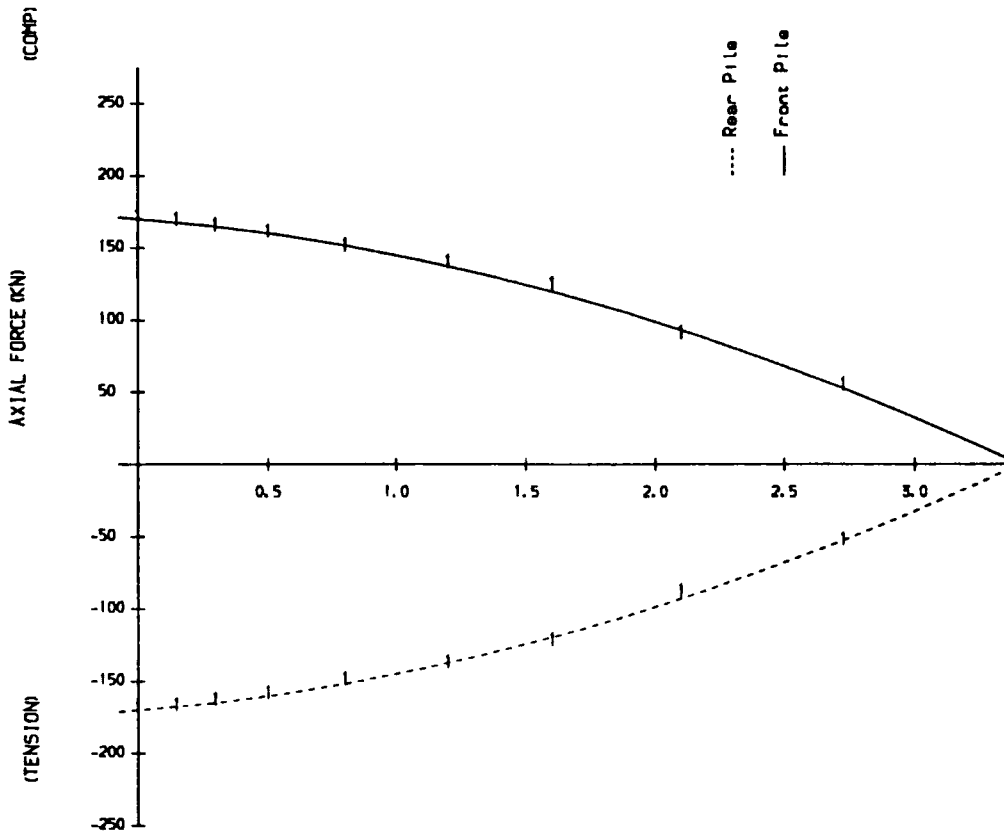
Figure B.3c Axial force diagram for two pile group
(3 pile dish, spacing 150mm overhang)
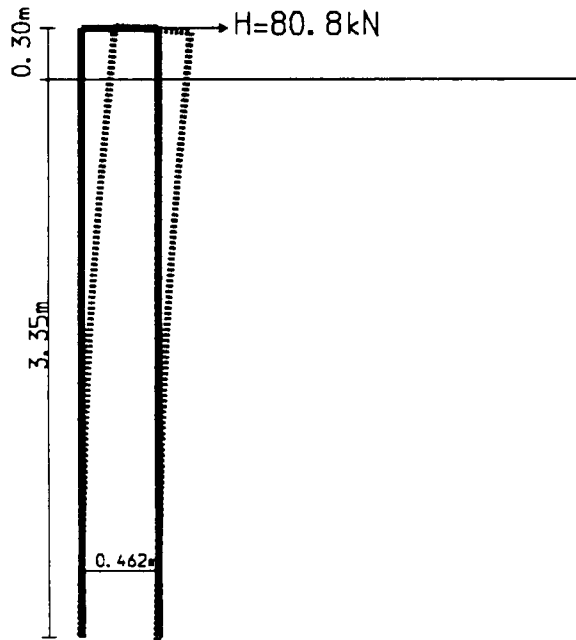
Figure B.4a Deflected shape of two-pile group at 3
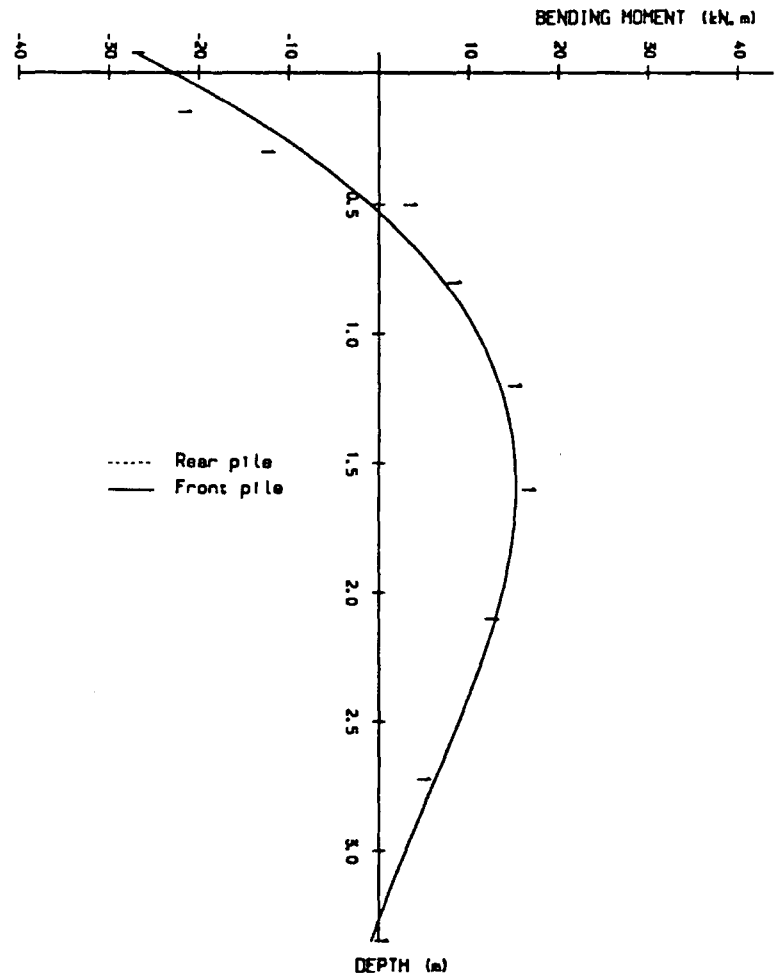pile width spacing 300mm overhang for 20mm pile cap defl.
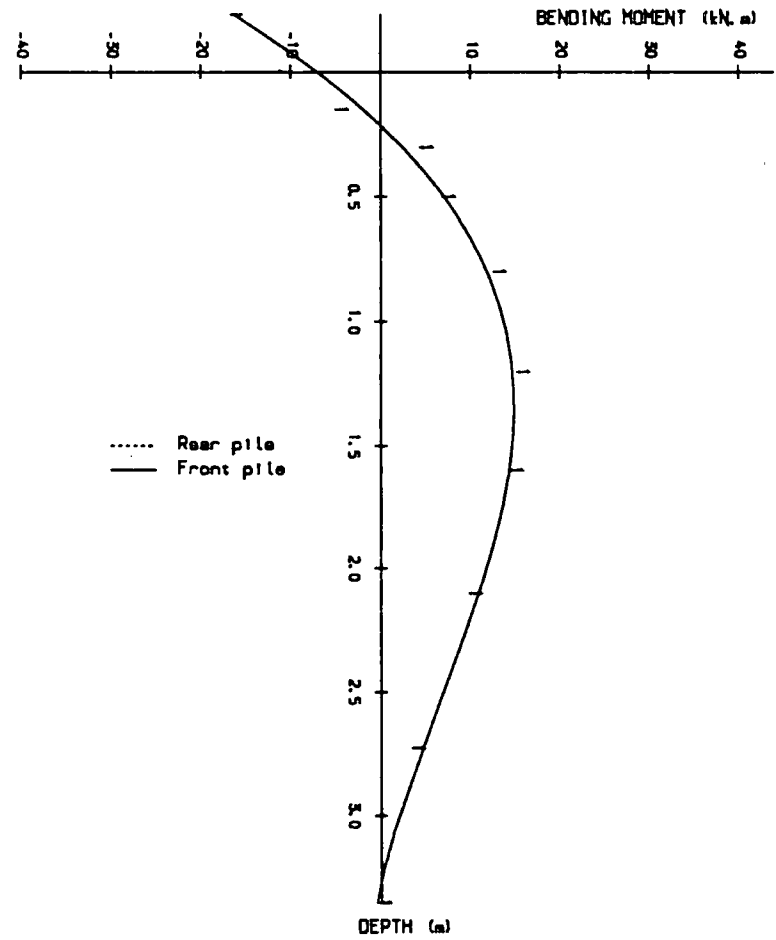
Figure B.4b Bending moment diagram for two-pile group
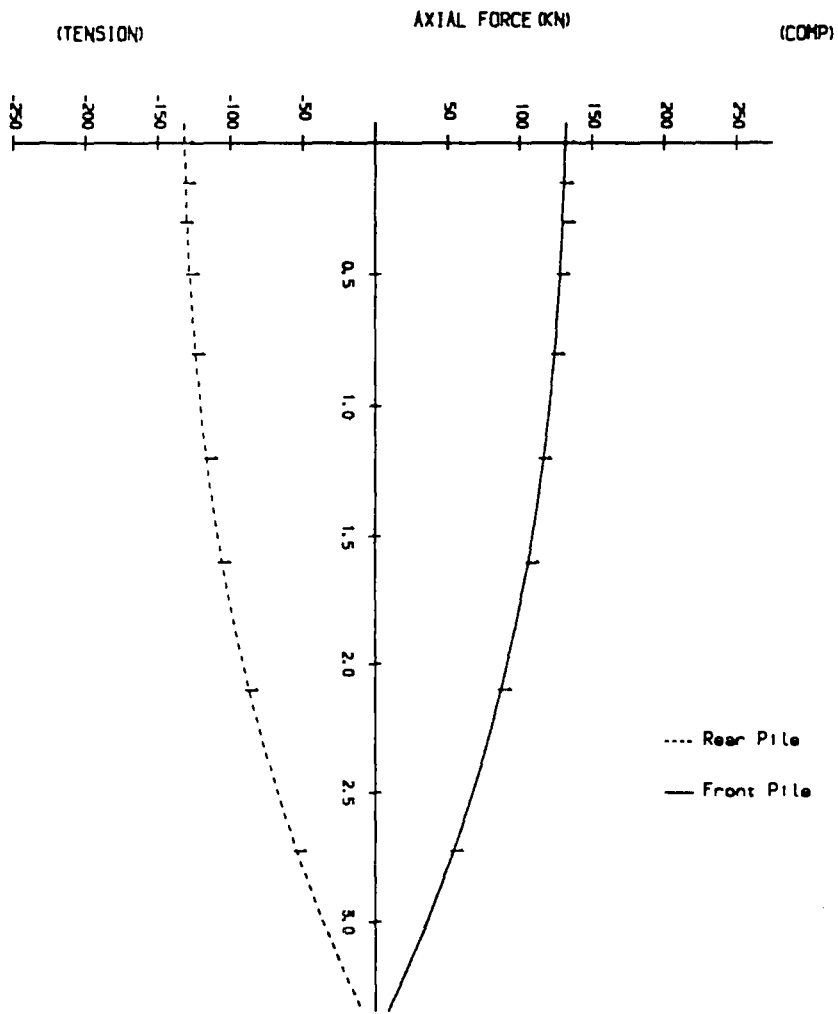(3 pile width spacing 300mm overhang).
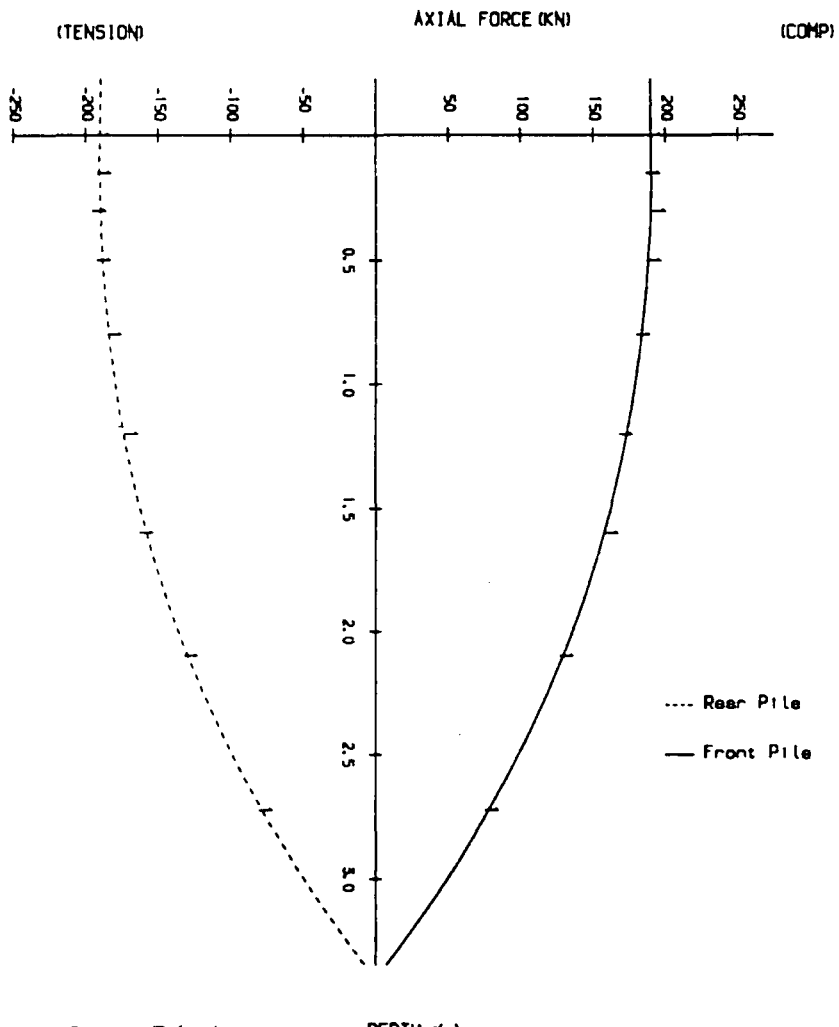
Figure B.4c Axial force diagram for two pile group
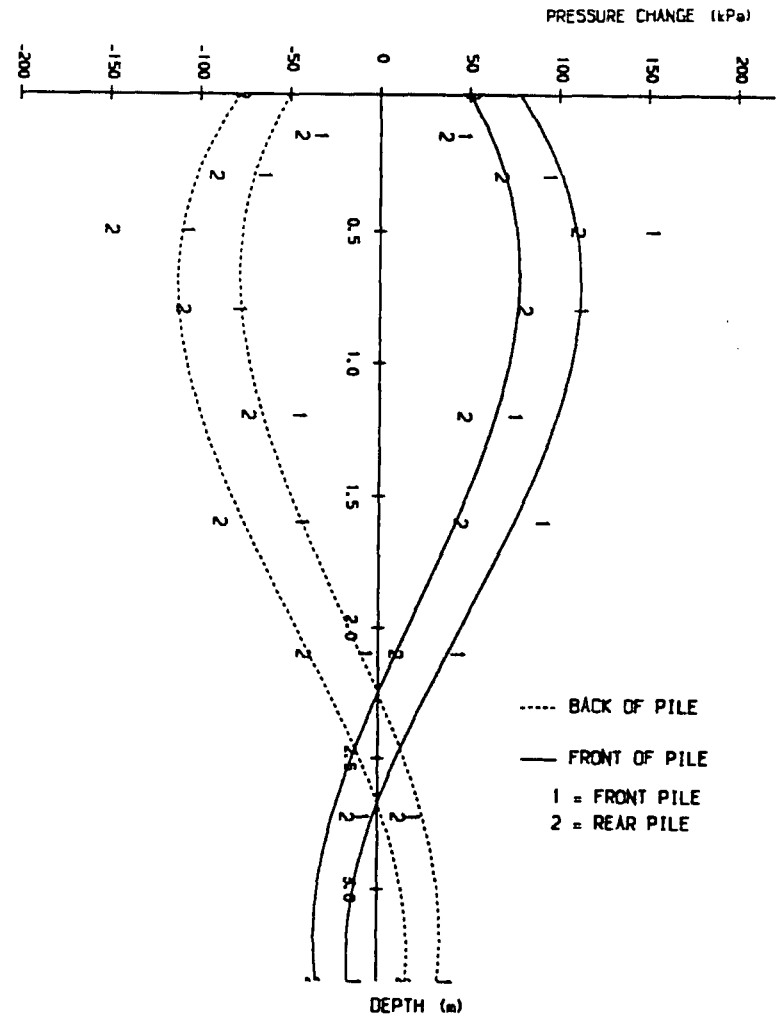(3 pile width spacing 300mm overhang)
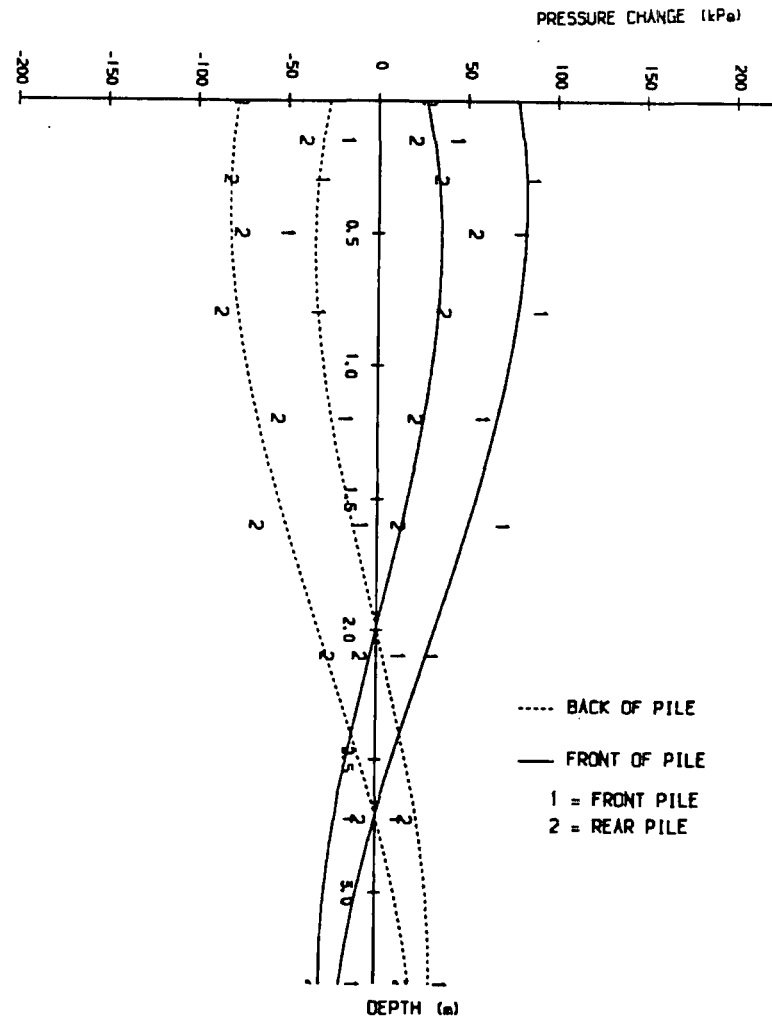
Figure B.4d Pressure distribution diagram for two-pile group
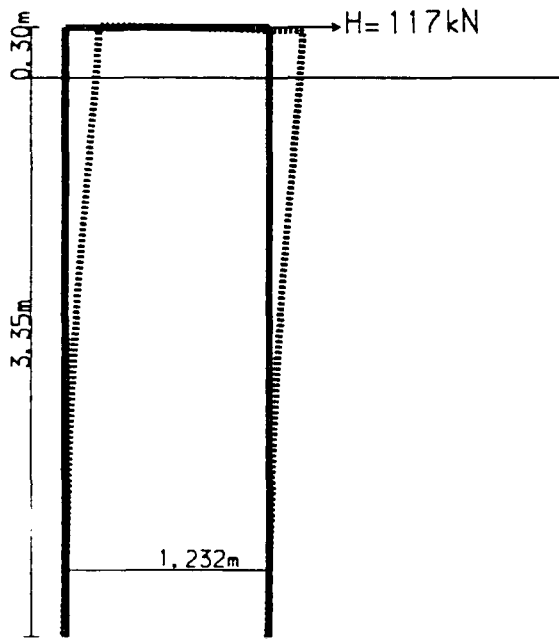(3 pile width spacing 300mm overhang)
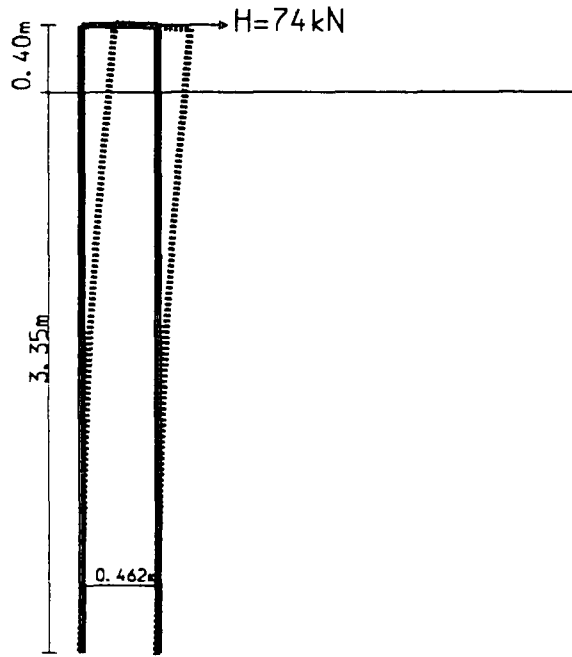
Figure B.5a Deflected shape of two-pile group at 3
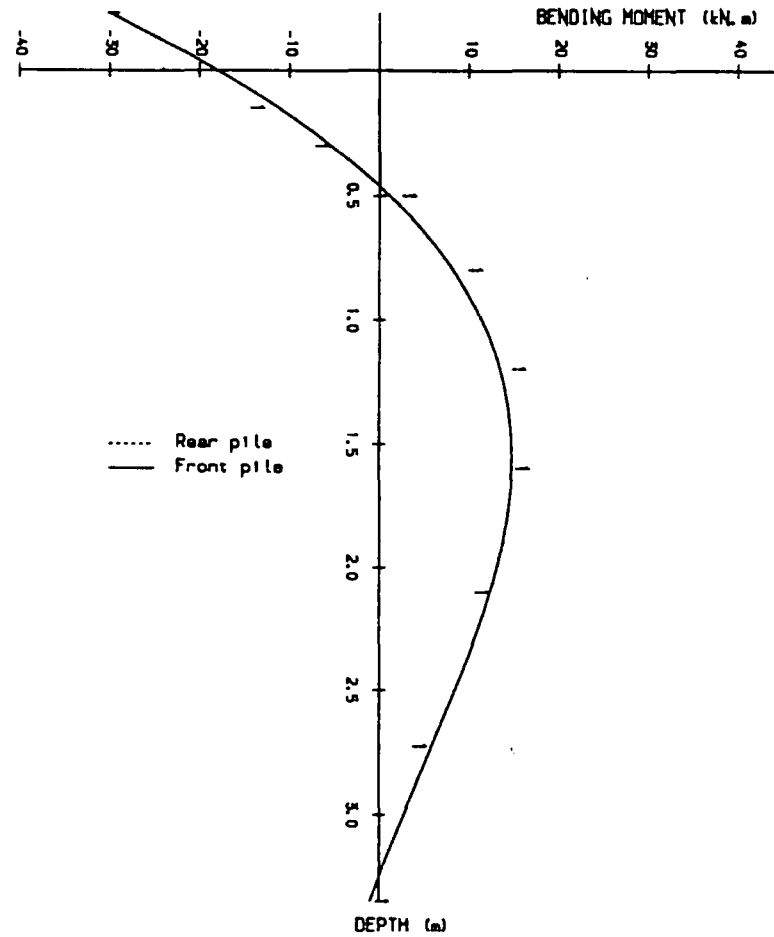pile width spacing 400mm overhang for 20mm pile cap defl.
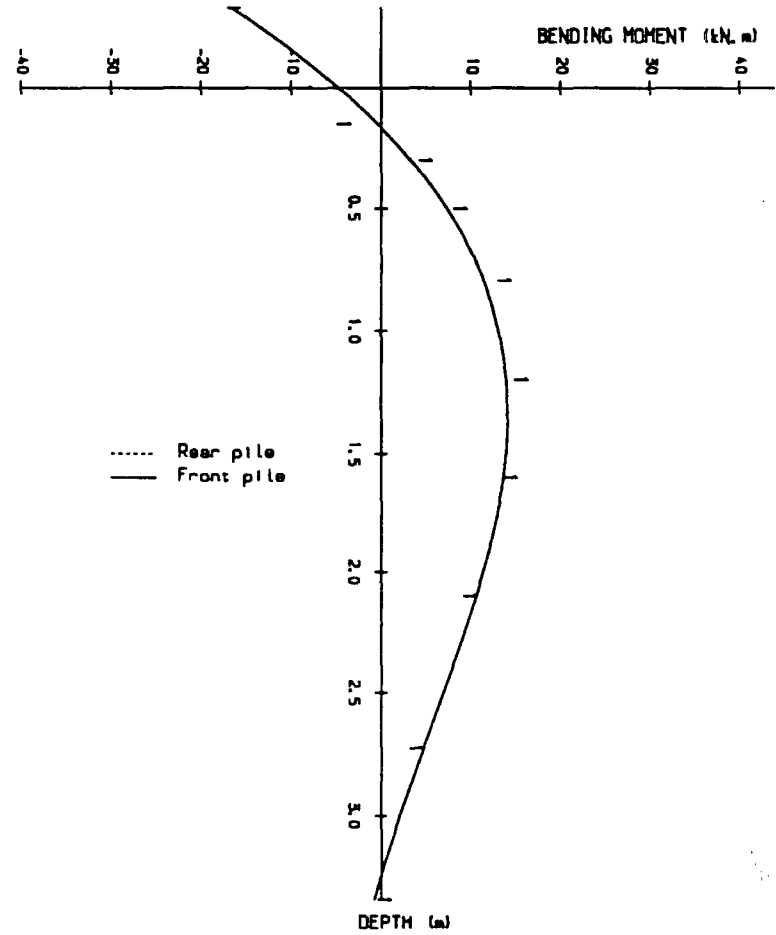
Figure B.5b Bending moment diagram for two-pile group
(3 pile width spacing 400mm overhang).
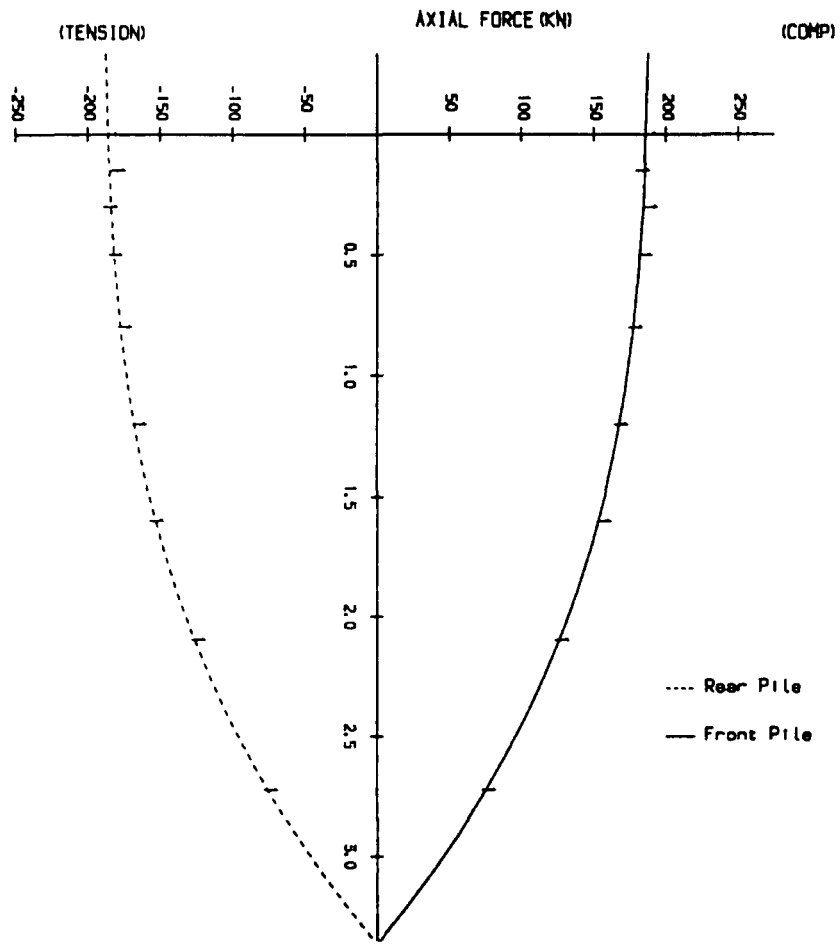
Figure B.5c Axial force diagram for two pile group
(3 pile width spacing 400mm overhang)
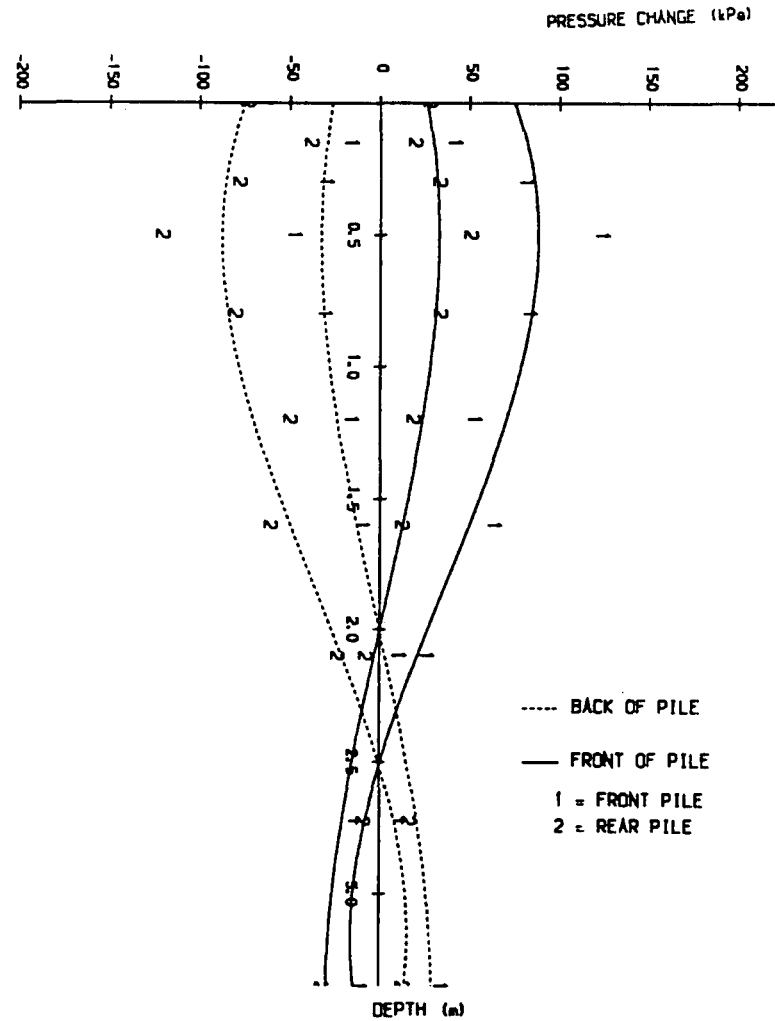
Figure B.5d Pressure distribution diagram for two-pile group
(3 pile width spacing 400mm overhang)

H=124kN

0.15m

3.35m

0.77m
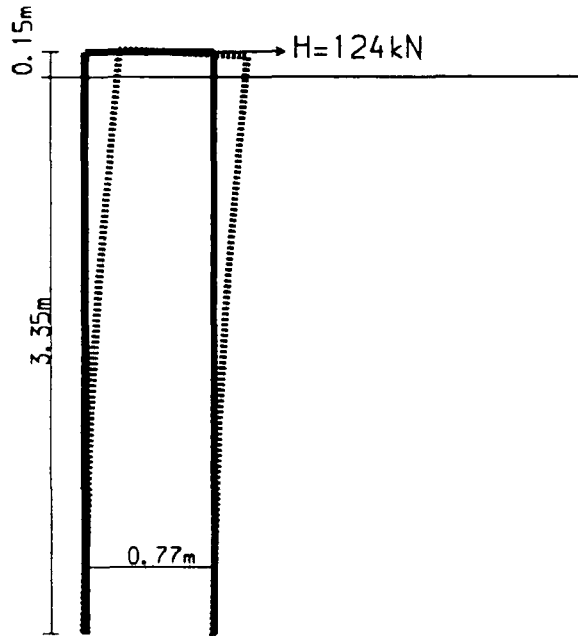
Figure B. 6a Deflected shape of two-pile group at 5
pile width spacing 150mm overhang for 20mm pile cap defl.

BENDING MOMENT (kN. m)

-40   -30   -20   -10   0   10   20   30   40

0.5

1.0

1.5

2.0

2.5

3.0

...... Rear pile
—— Front pile

DEPTH (m)
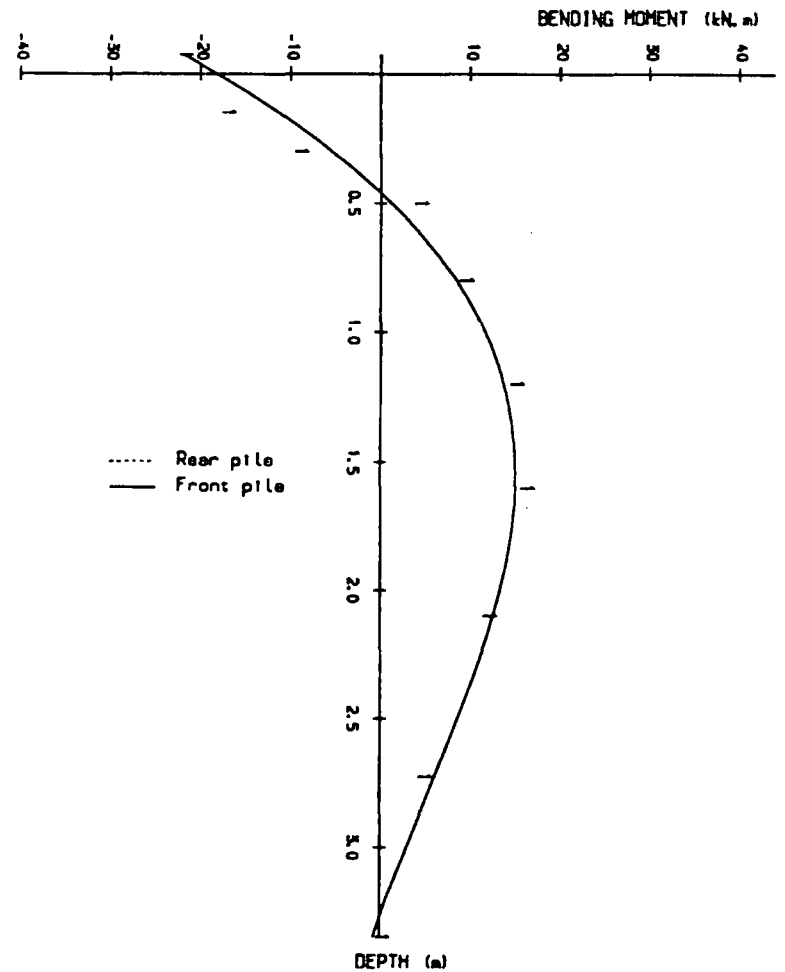
Figure B.6b Bending moment diagram for two-pile group
(5 × pile width spacing 150mm overhang).

Figure B.6c Axial force diagram for two pile group
(5 : pile width spacing 150mm overhang)

Figure B.6d Pressure distribution diagram for two-pile group
(5 : pile width spacing 150mm overhang)

Figure B.7a Deflected shape of two-pile group at 5 pile width spacing 300mm overhang for 20mm pile cap defl.
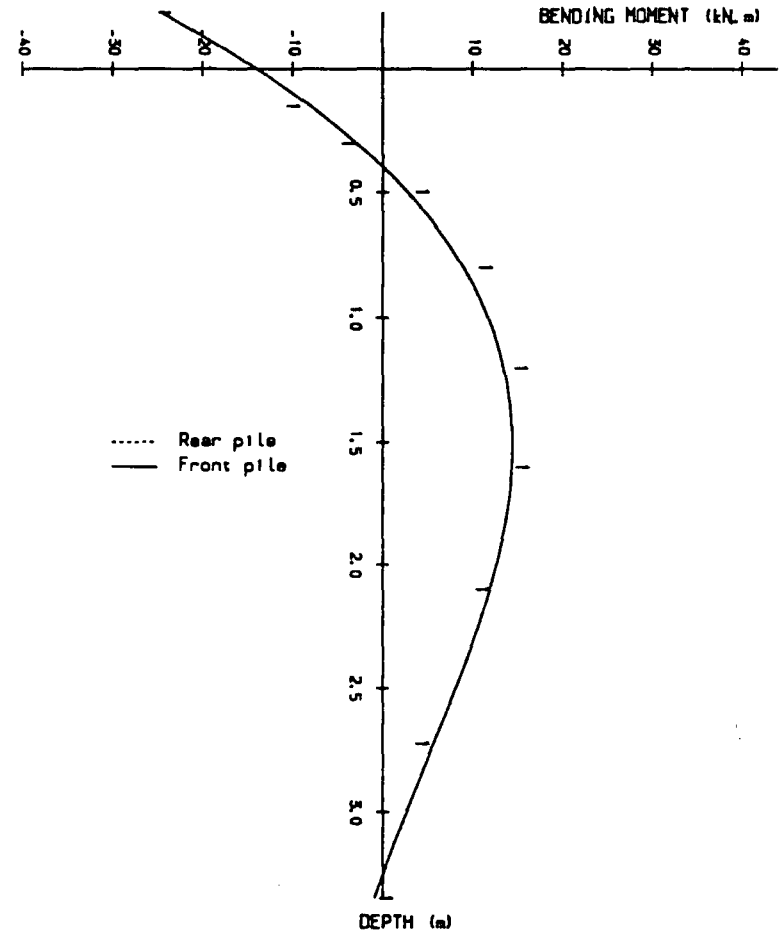
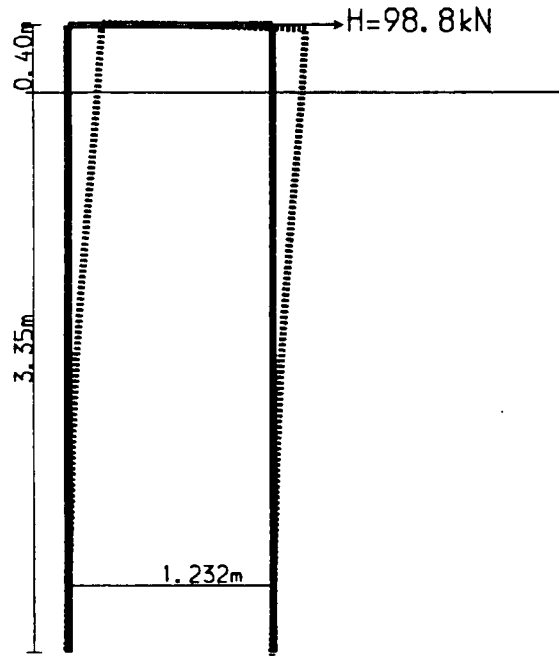Figure B.7b Bending moment diagram for two-pile group (5 pile width spacing 300mm overhang).

(TENSION)   AXIAL FORCE (KN)   (COMP)

..... Rear Pile

——— Front Pile
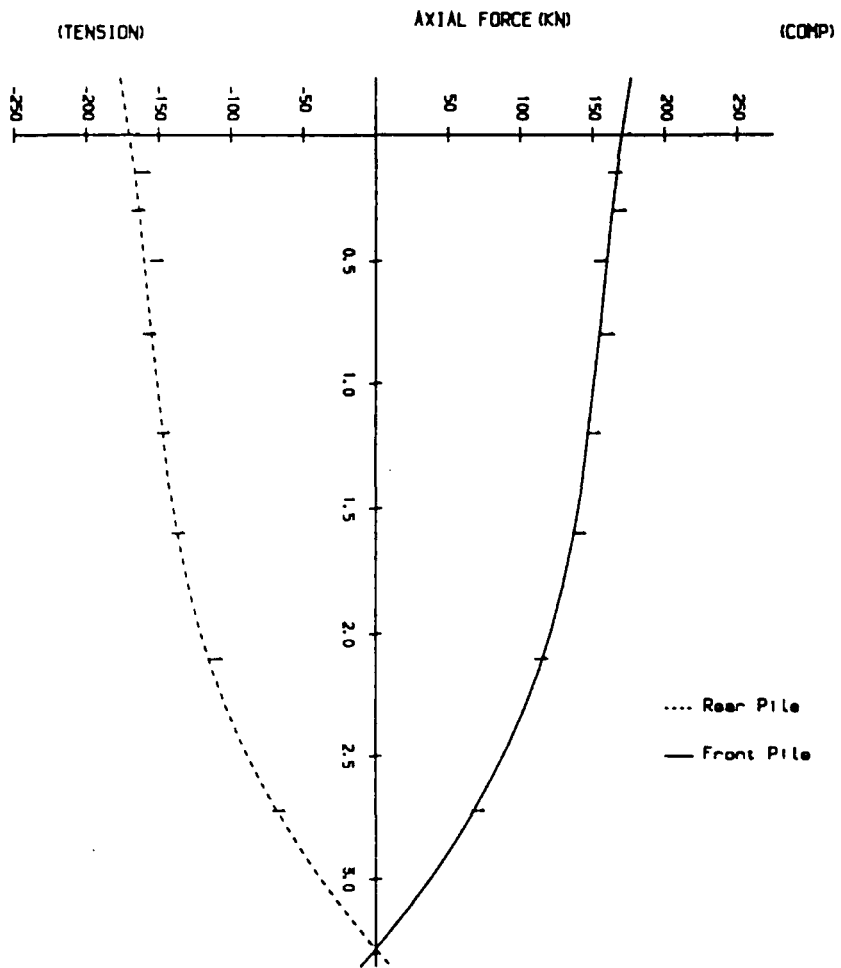
Figure B.7c Axial force diagram for two pile group
(5 pile width spacing 300mm overhang)

PRESSURE CHANGE (kPa)

..... BACK OF PILE

——— FRONT OF PILE

1 = FRONT PILE

2 = REAR PILE

DEPTH (m)
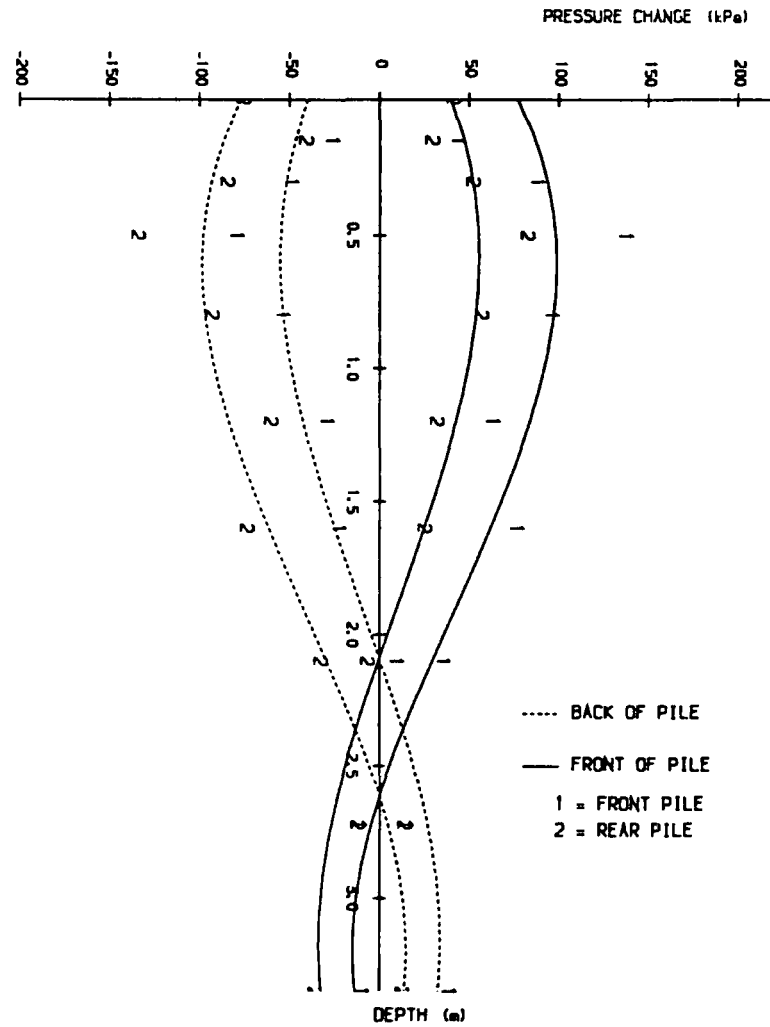
Figure B.7d Pressure distribution diagram for two-pile group
(5 pile width spacing 300mm overhang)

H=88kN

0.40m

3.35m

0.77m
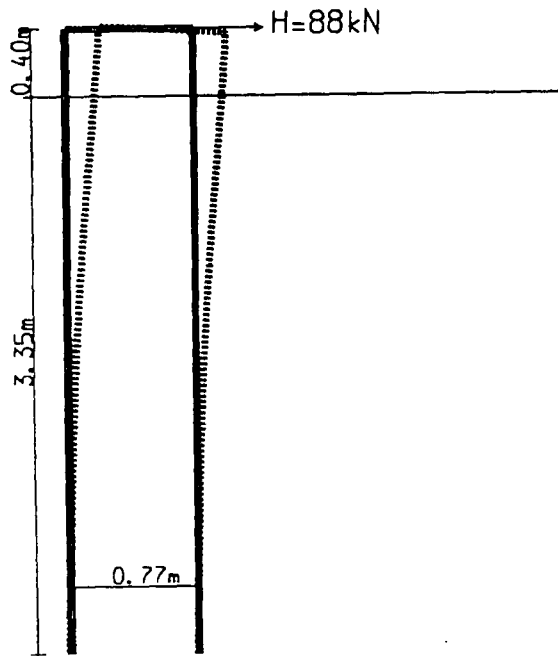
Figure B.8a Deflected shape of two-pile group at 5
pi width spacing 400mm overhang for 20mm pile cap defl.

BENDING MOMENT (kN.m)

-40 -30 -20 -10   10 20 30 40

0.5

1.0

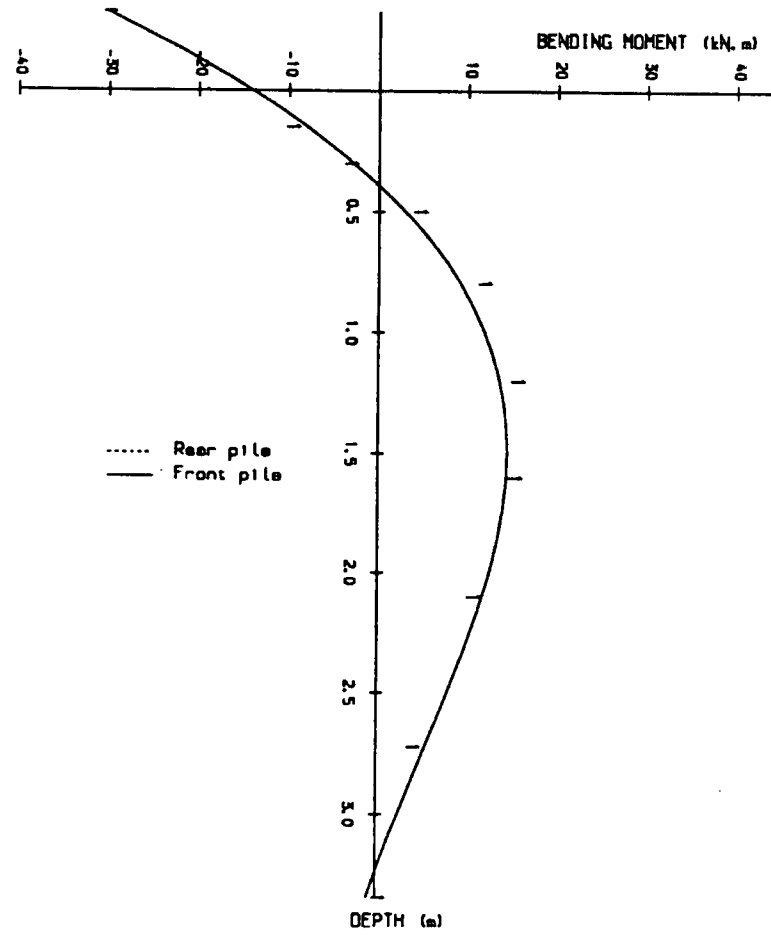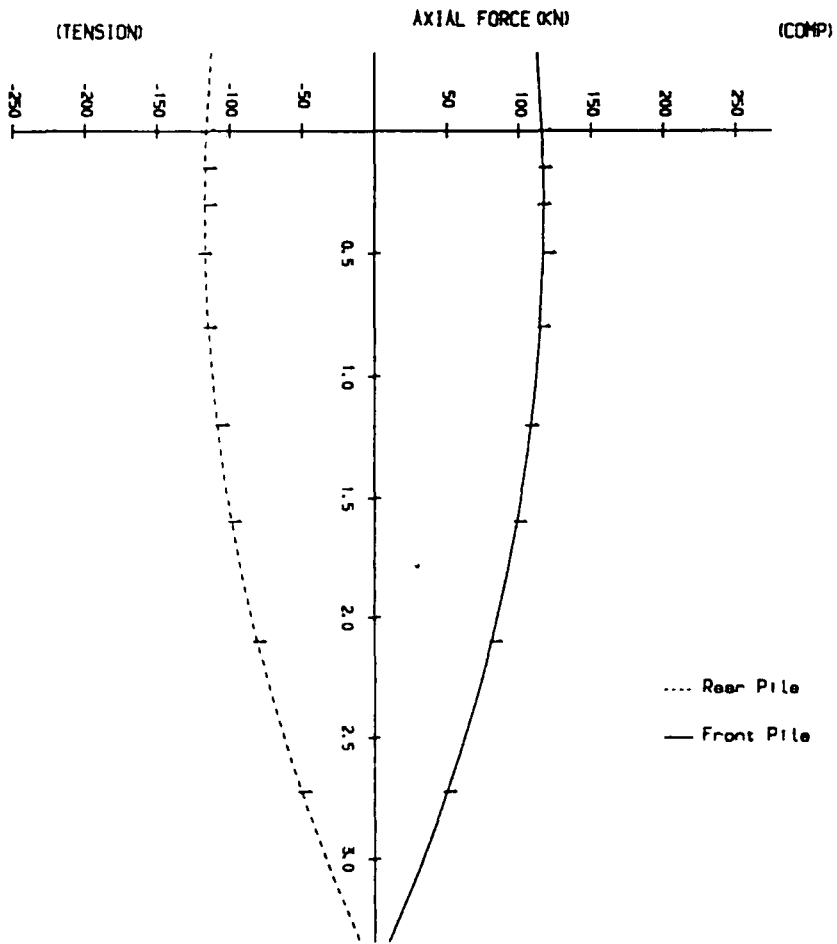...... Rear pile
―― Front pile

1.5

2.0

2.5

3.0

DEPTH (m)
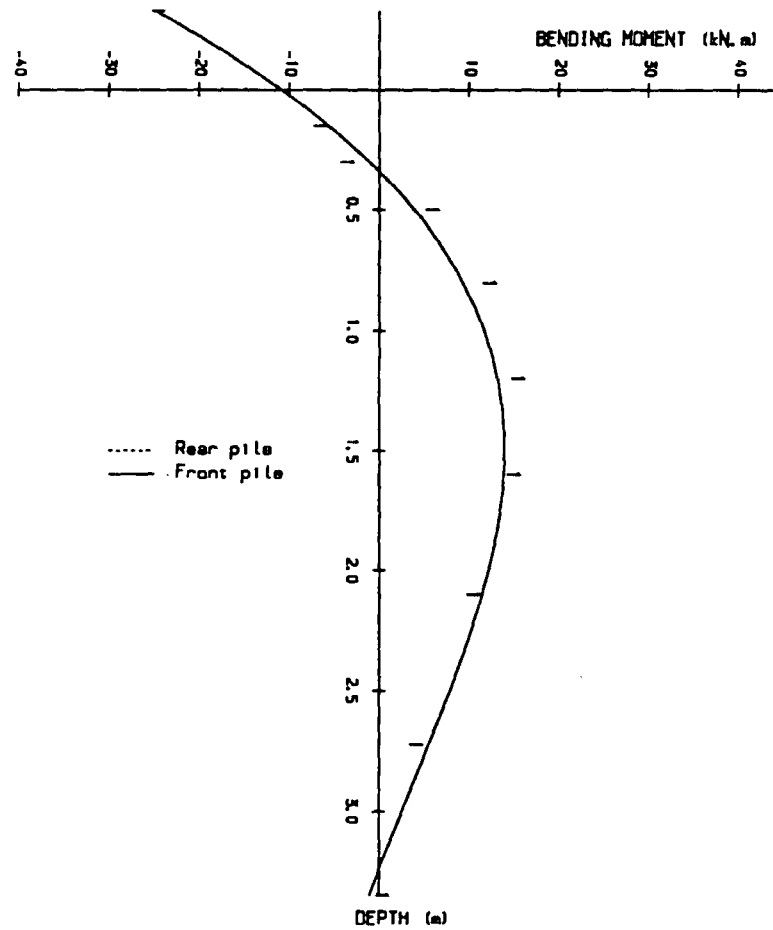
Figure B.8b Bending moment diagram for two-pile group
(5 pile width spacing 400mm overhang).

364
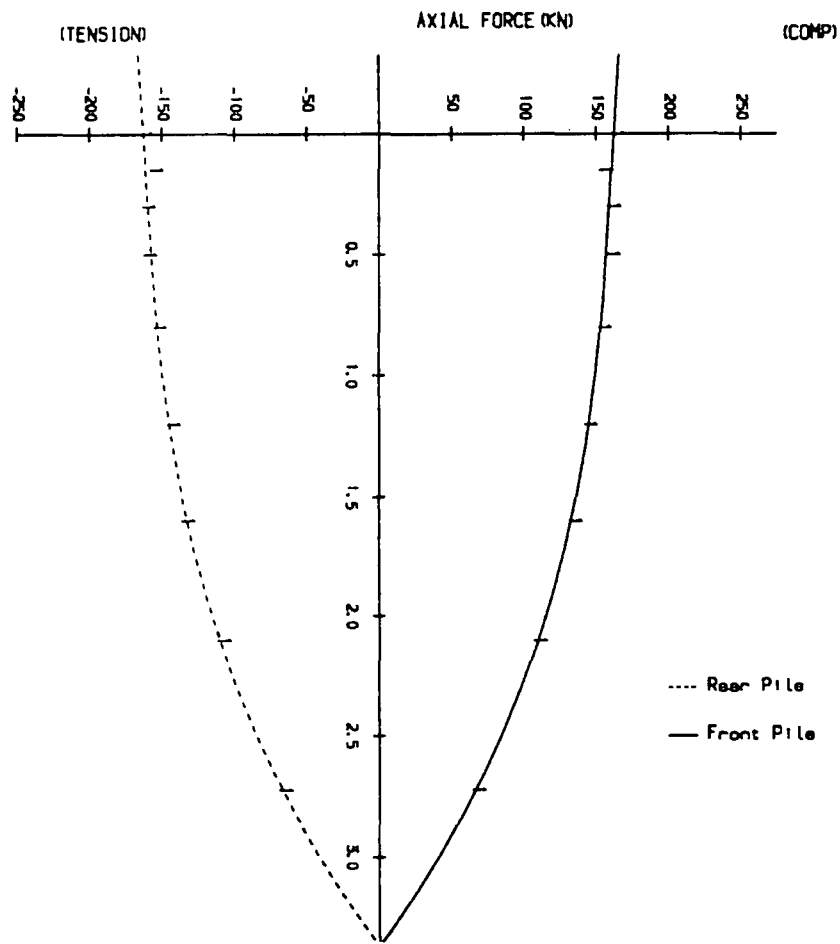
Figure B.8c Axial force diagram for two pile group
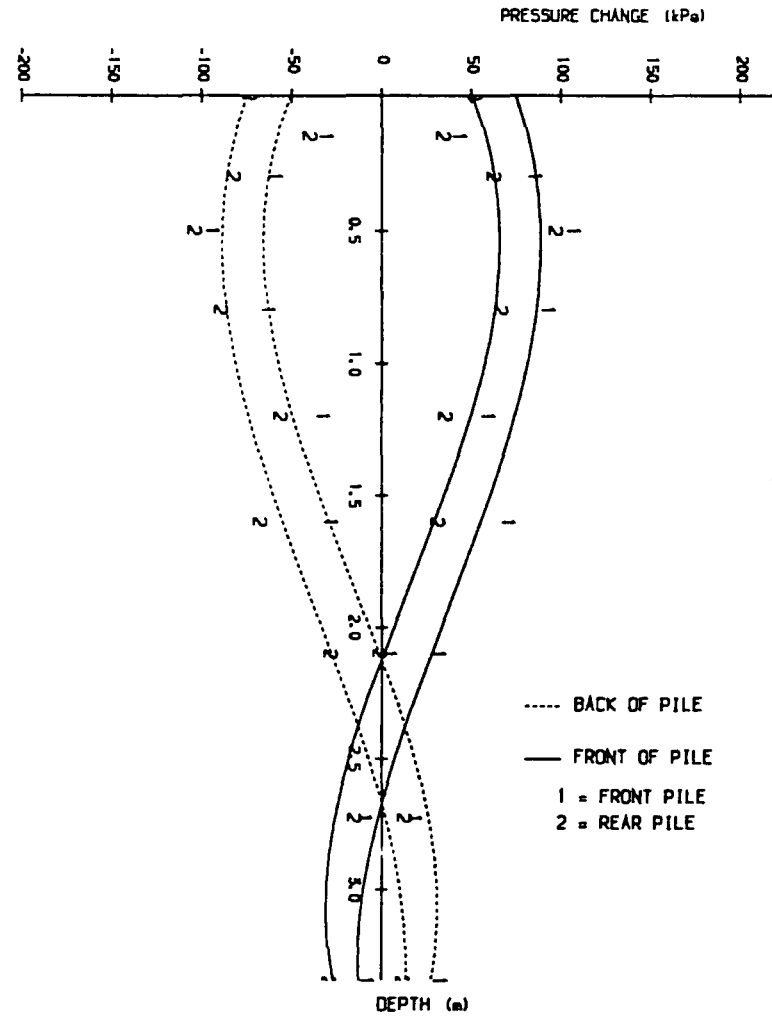(5 pile width spacing 400mm overhang)
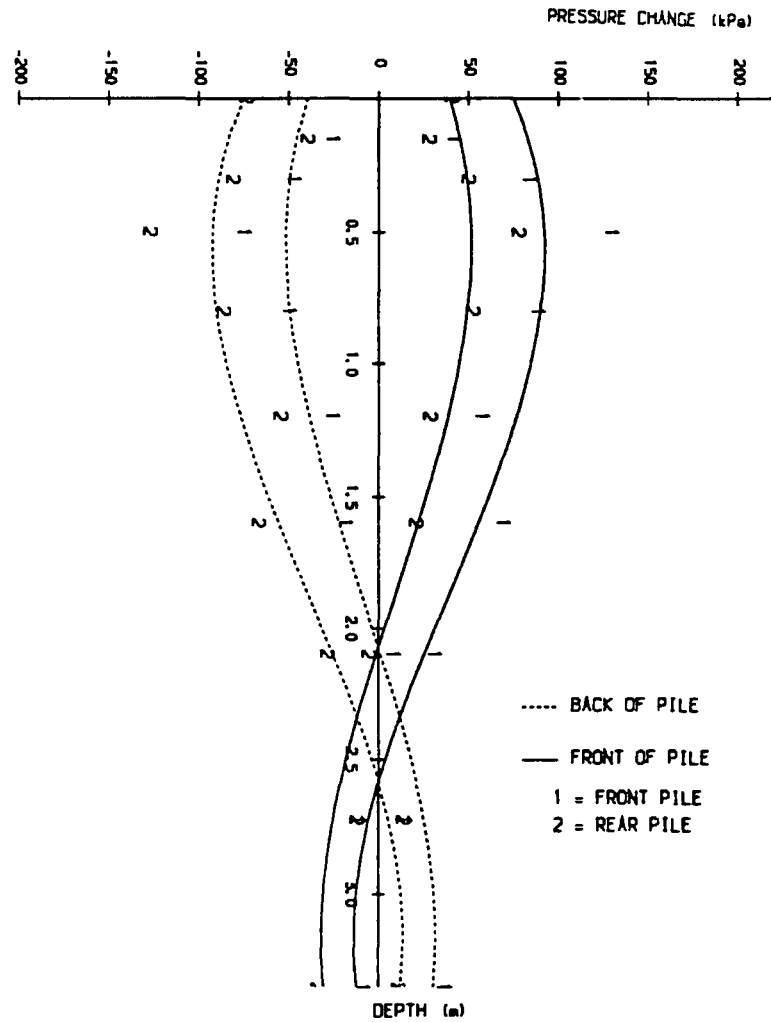
Figure B.8d Pressure distribution diagram for two-pile group
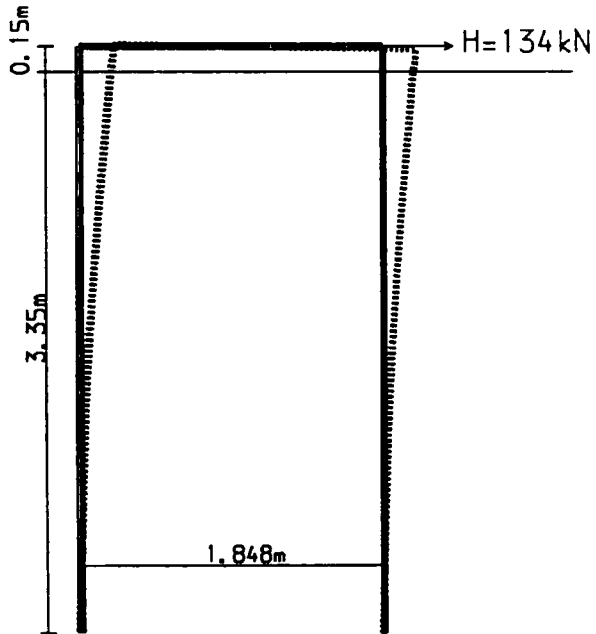(5 pile width spacing 400mm overhang)

$0.15m$

$\rightarrow H=130\,kN$

$3.35m$

$1.232m$

Figure B.9a Deflected shape of two-pile group at 8
pile width spacing 150mm overhang for 20mm pile cap defl.

BENDING MOMENT (kN.m)

-40   -30   -20   -10   10   20   30   40

0.5

1.0

1.5

2.0

2.5

3.0

······ Rear pile
——— Front pile

DEPTH (m)

Figure B.9b Bending moment diagram for two-pile group
(8 pile width spacing 150mm overhang).

Figure B.9c Axial force diagram for two pile group
(8 pile width spacing 150mm overhang)

Figure B.9d Pressure distribution diagram for two-pile group
(8 pile width spacing 150mm overhang)

Figure B. 10a Deflected shape of two-pile group at 8
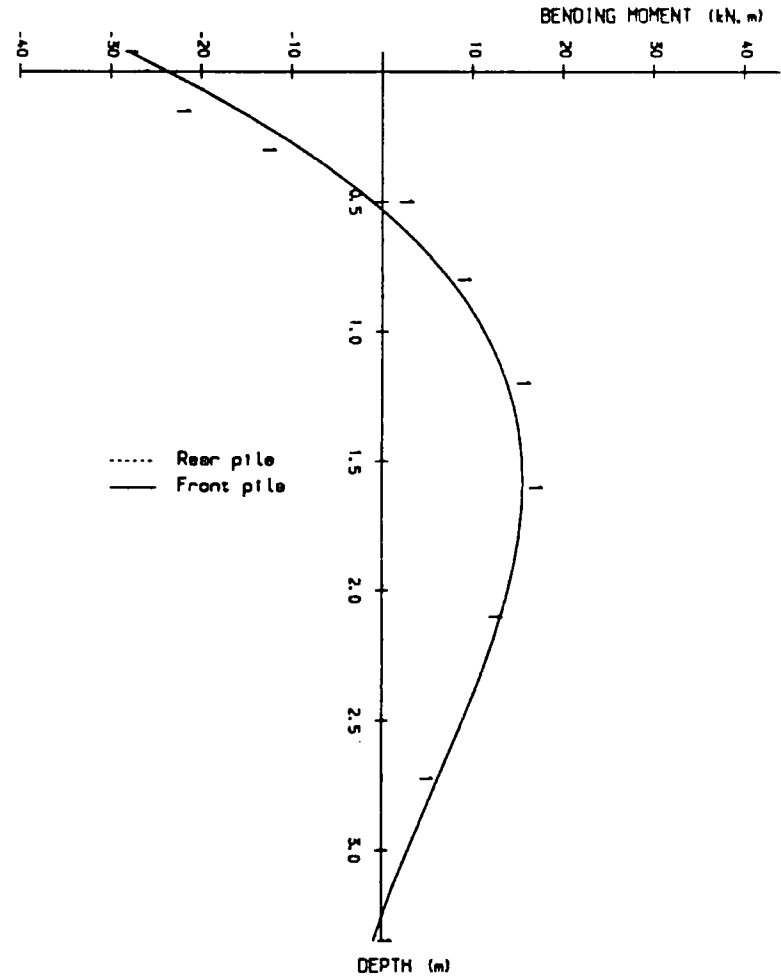pile width spacing 300mm overhang for 20mm pile cap defl.

Figure 6.18a Bending moment diagram for two-pile group
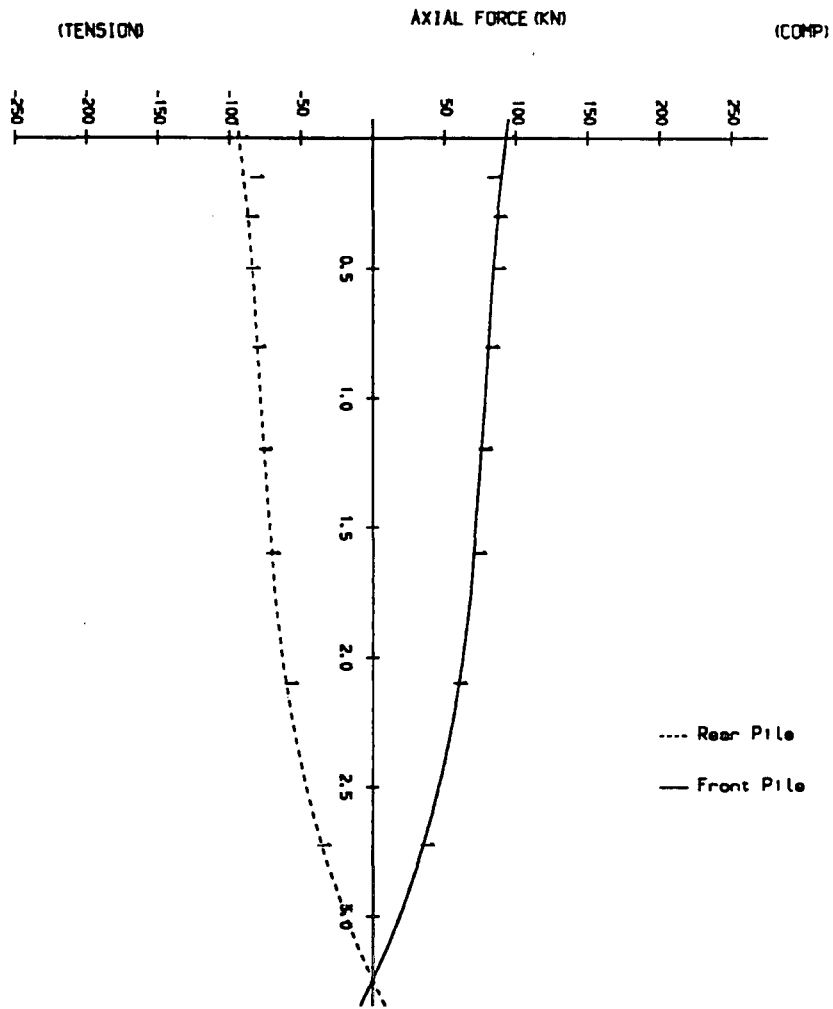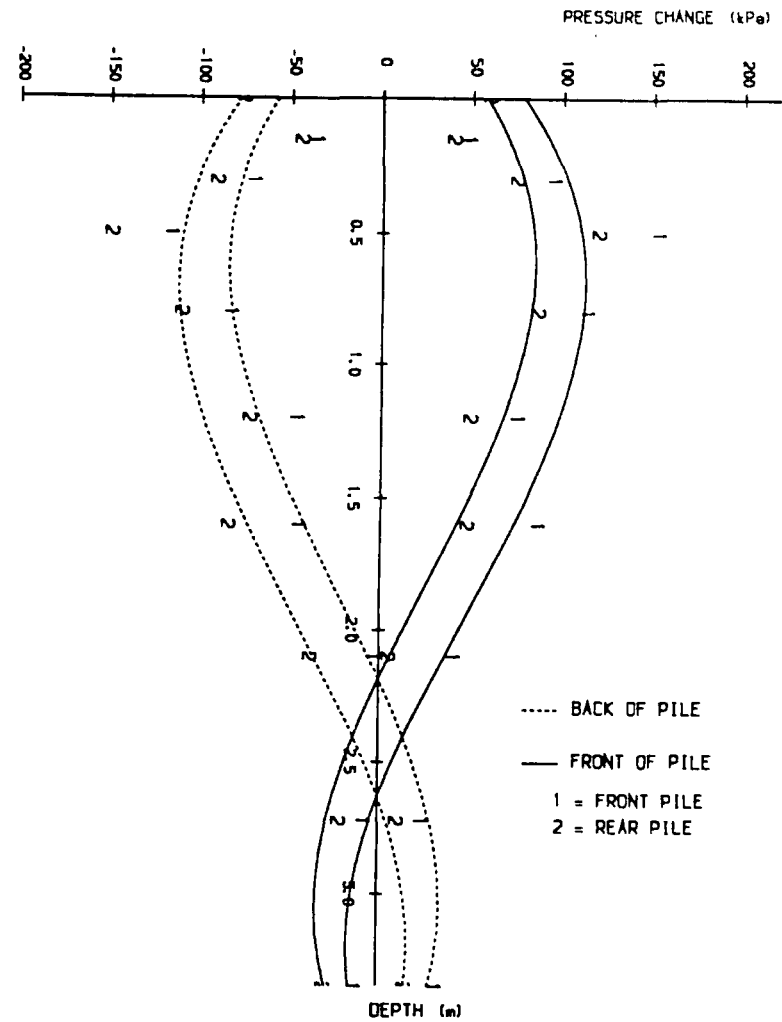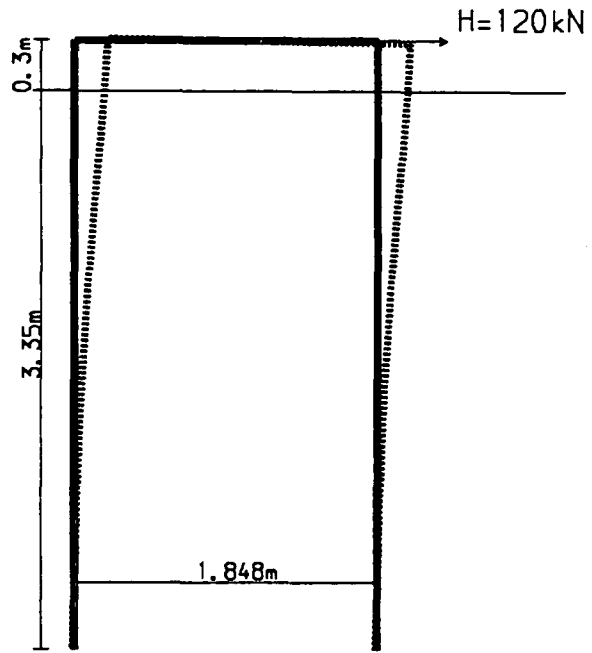(8 pile width spacing 300mm overhang).

Figure B.10d Pressure distribution diagram for two-pile group
(8 pile spacing 300mm overhang)
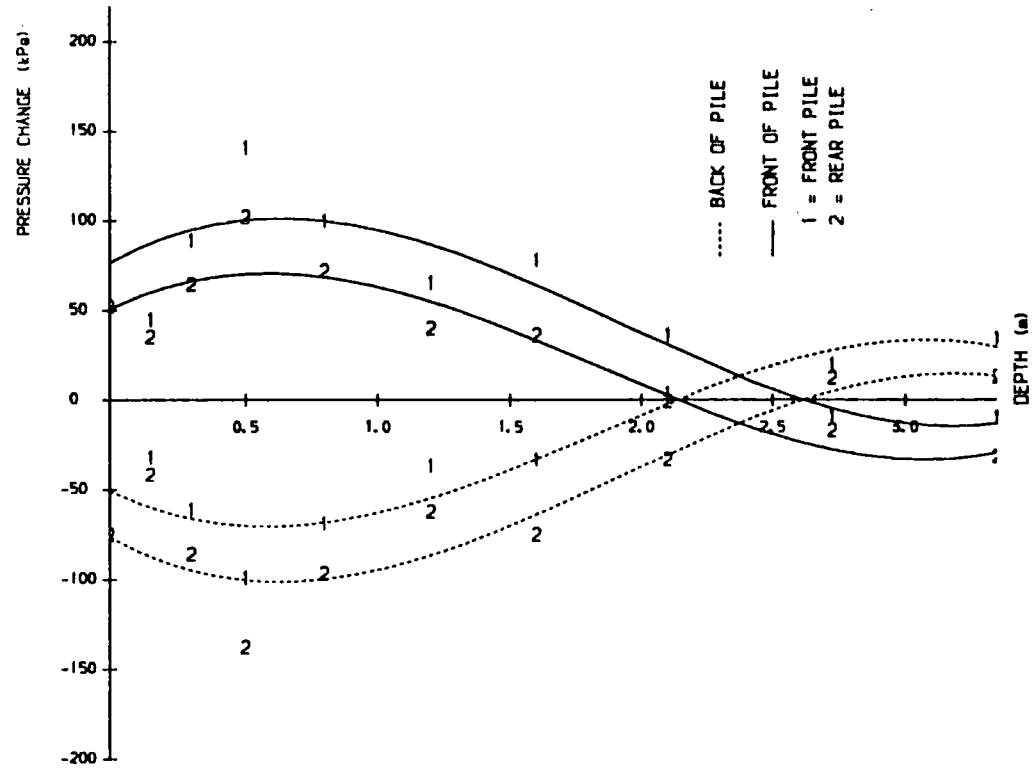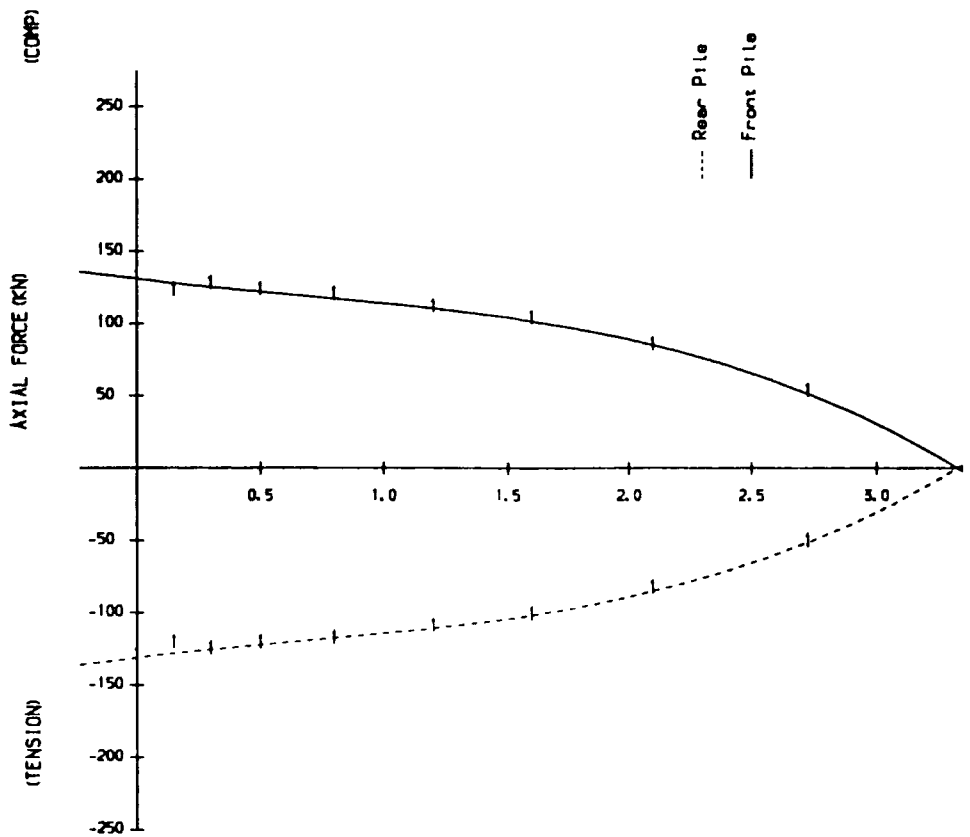
Figure B.10c Axial force diagram for two pile group
(8 pile spacing 300mm overhang)

H=98.8kN

0.40m

3.35m

1.232m

Figure B.11a Deflected shape of two-pile group at 8
pile width spacing 400mm overhang for 20mm pile cap defl.

BENDING MOMENT (kN.m)

-40 -30 -20 -10   10   20   30   40

0.5

1.0

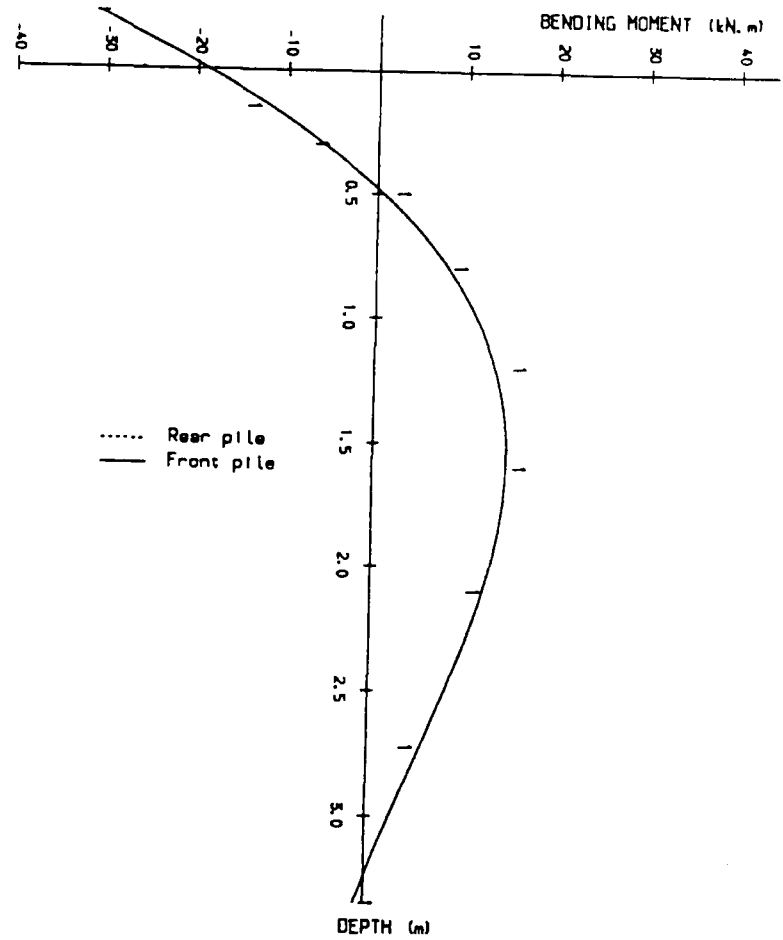...... Rear pile
—— Front pile

1.5

2.0

2.5

3.0

DEPTH (m)

Figure B.11b Bending moment diagram for two-pile group
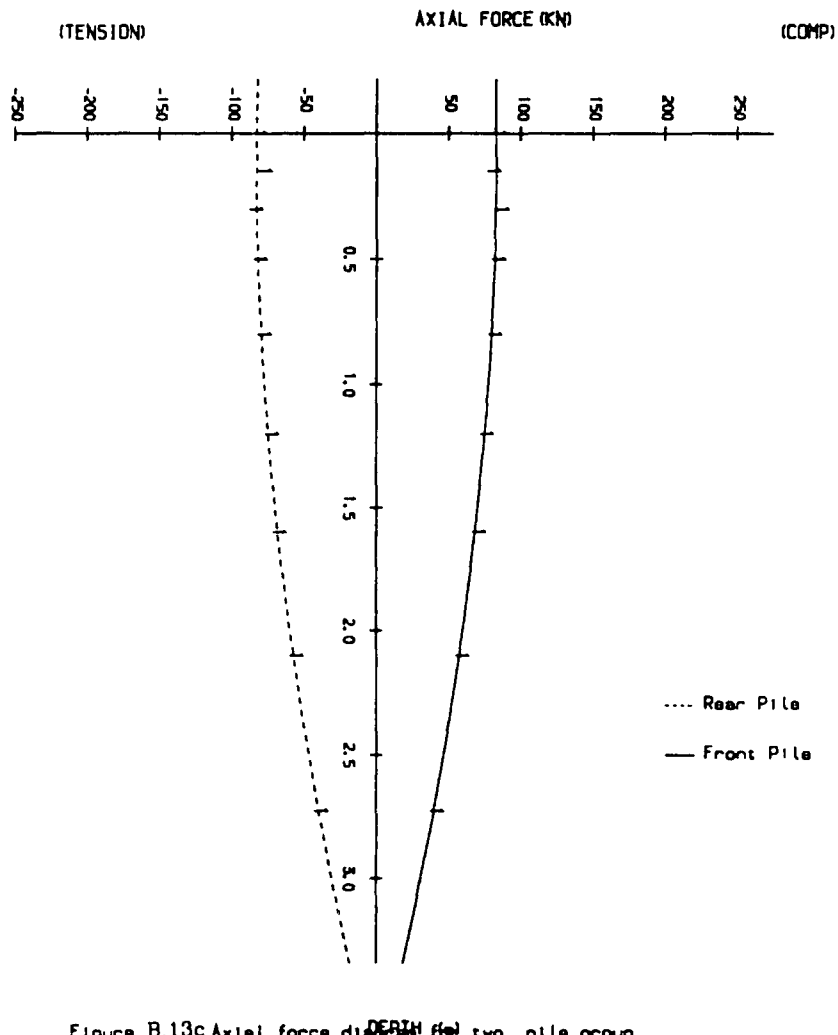(8 pile width spacing 400mm overhang).

Figure B.11c Axial force diagram for two pile group
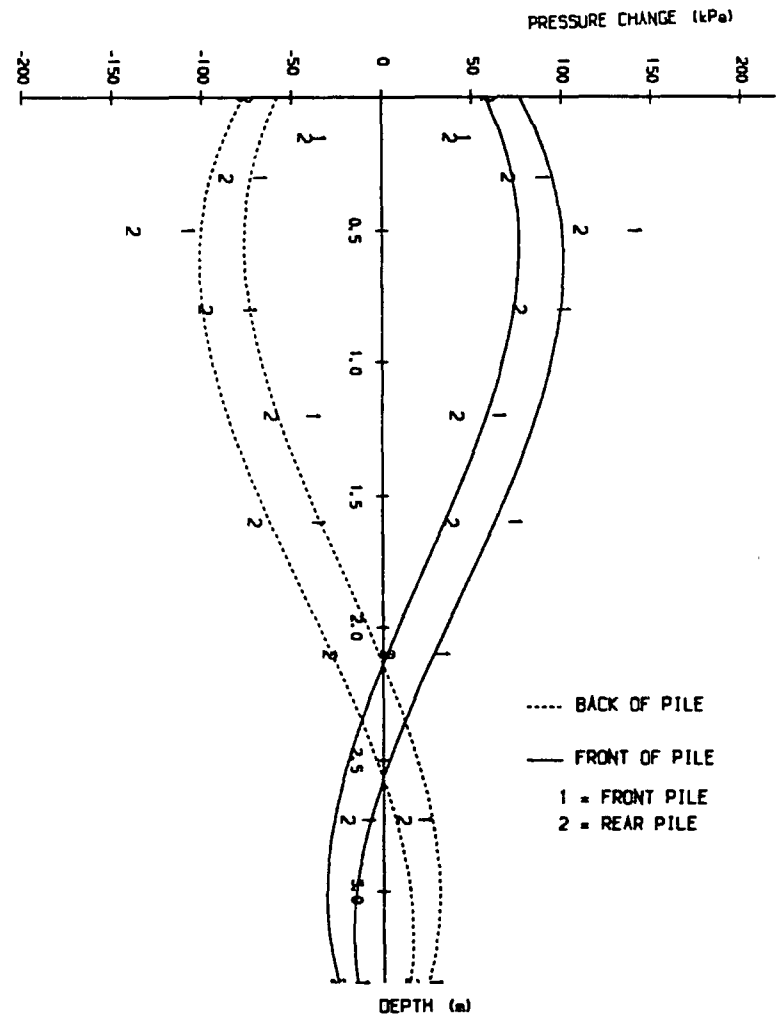(8 pile width spacing 400mm overhang)

Figure B.11d Pressure distribution diagram for two-pile group
(8 pile width spacing 400mm overhang)

Figure B.12a Deflected shape of two-pile group at 12
pile width spacing 150mm overhang for 20mm pile cap defl.

H=134kN

0.15m

3.35m

1.848m

BENDING MOMENT (kN.m)

DEPTH (m)

...... Rear pile
—— Front pile

Figure B.12b Bending moment diagram for two-pile group
(12 pile width spacing 150mm overhang).

Figure B.12c Axial force diagram for two pile group
(12 pile width spacing 150mm overhang)

Figure B.12d Pressure distribution diagram for two-pile group
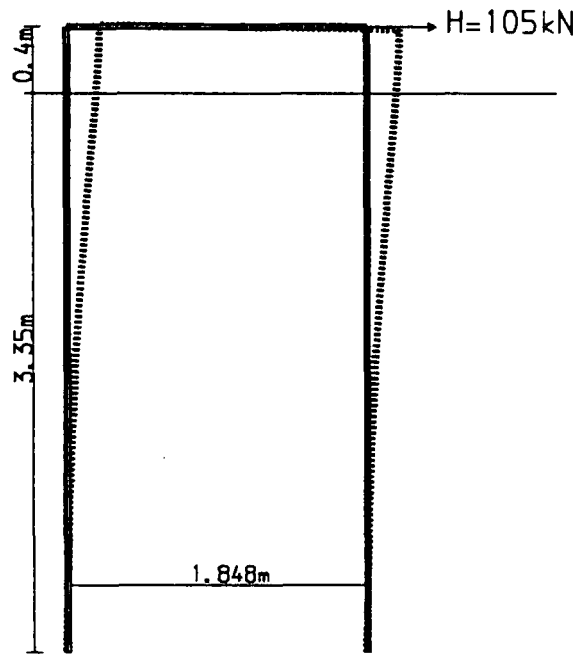(12 pile width spacing 150mm overhang)

Figure B.13a Deflected shape of two-pile group at 12 pile width spacing 300mm overhang for 20mm pile cap defl.

BENDING MOMENT (kN.m)

...... Rear pile
——— Front pile

DEPTH (m)

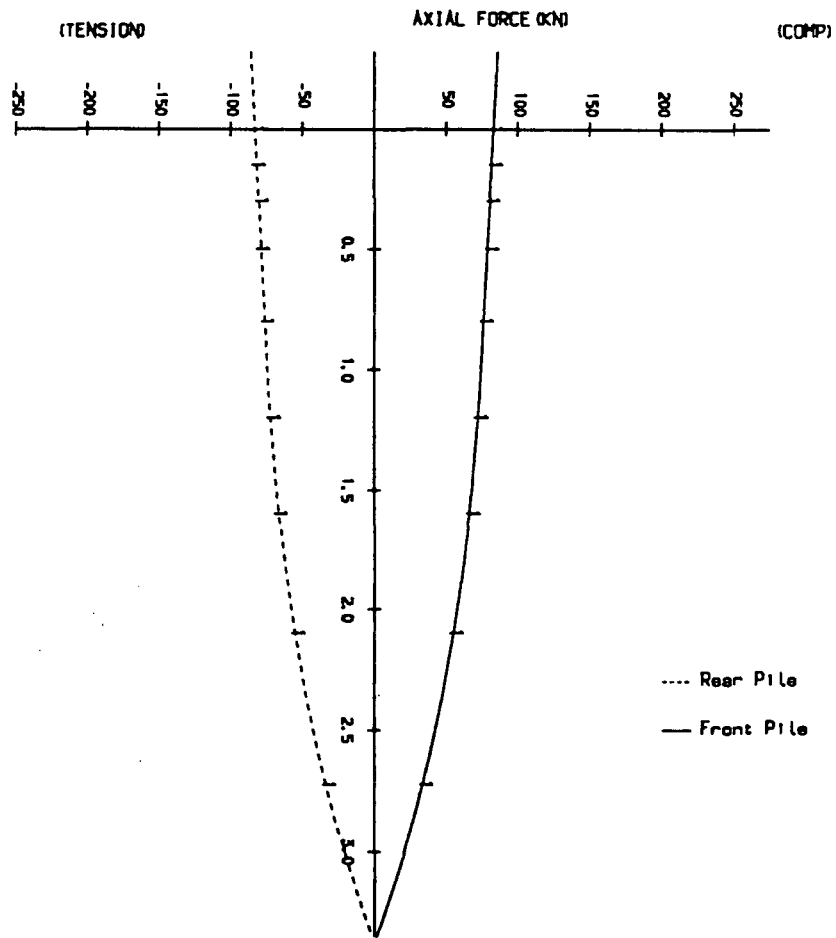Figure B.13b Bending moment diagram for two-pile group (12 pile width spacing 300mm overhang).

Figure B.13c Axial force diagram for two pile group
(12 pile width spacing 300mm overhang)

Figure B.13d Pressure distribution diagram for two-pile group
(12 pile width spacing 300mm overhang)

Figure B.14a Deflected shape of two-pile group at 12
pile width spacing 400mm overhang for 20mm pile cap defl.

BENDING MOMENT (kN.m)

.... Rear pile
——— Front pile

DEPTH (m)
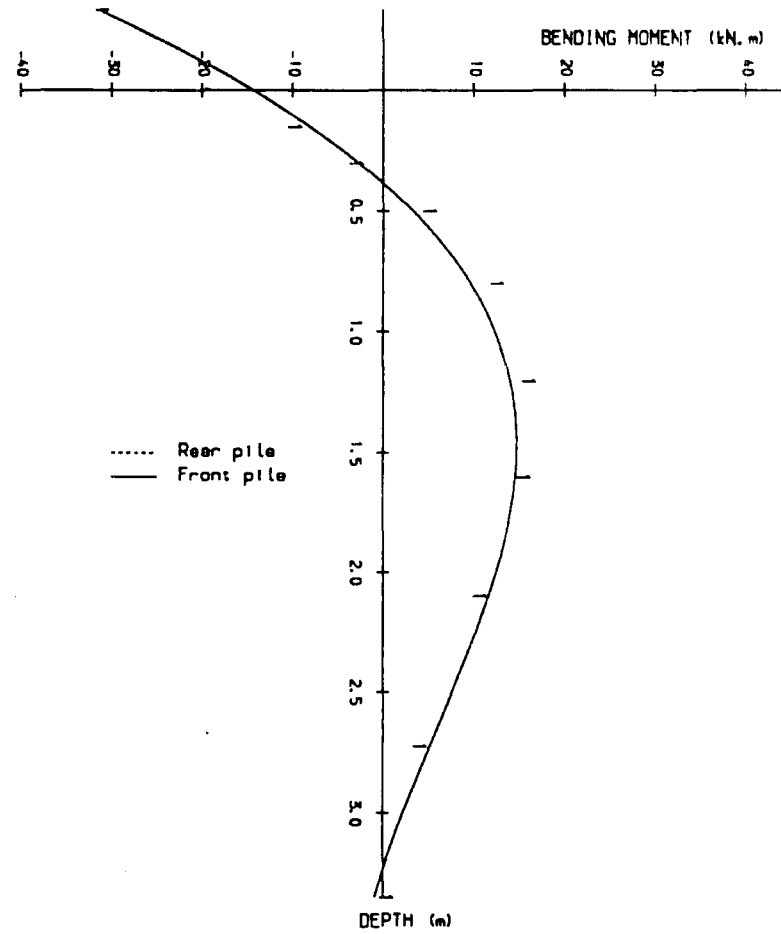
Figure B.14b Bending moment diagram for two-pile group
(12 pile width spacing 400mm overhang).

Figure B.14c Axial force diagram for two-pile group
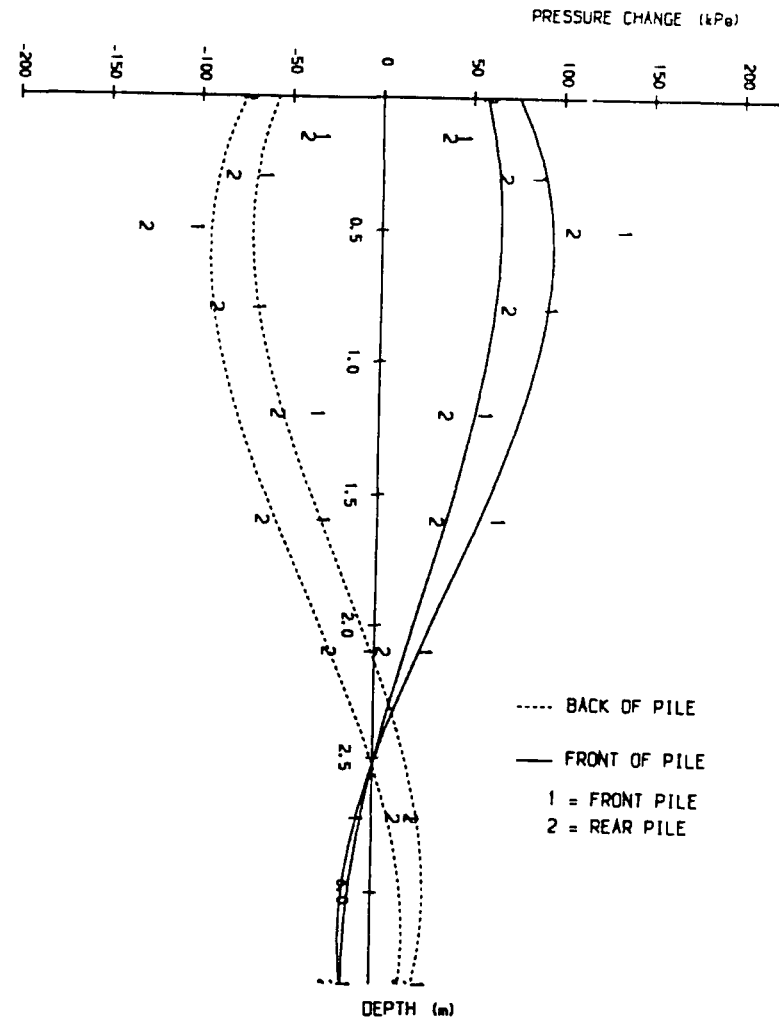(12 pile width spacing 400mm overhang)

Figure B.14d Pressure distribution diagram for two-pile group
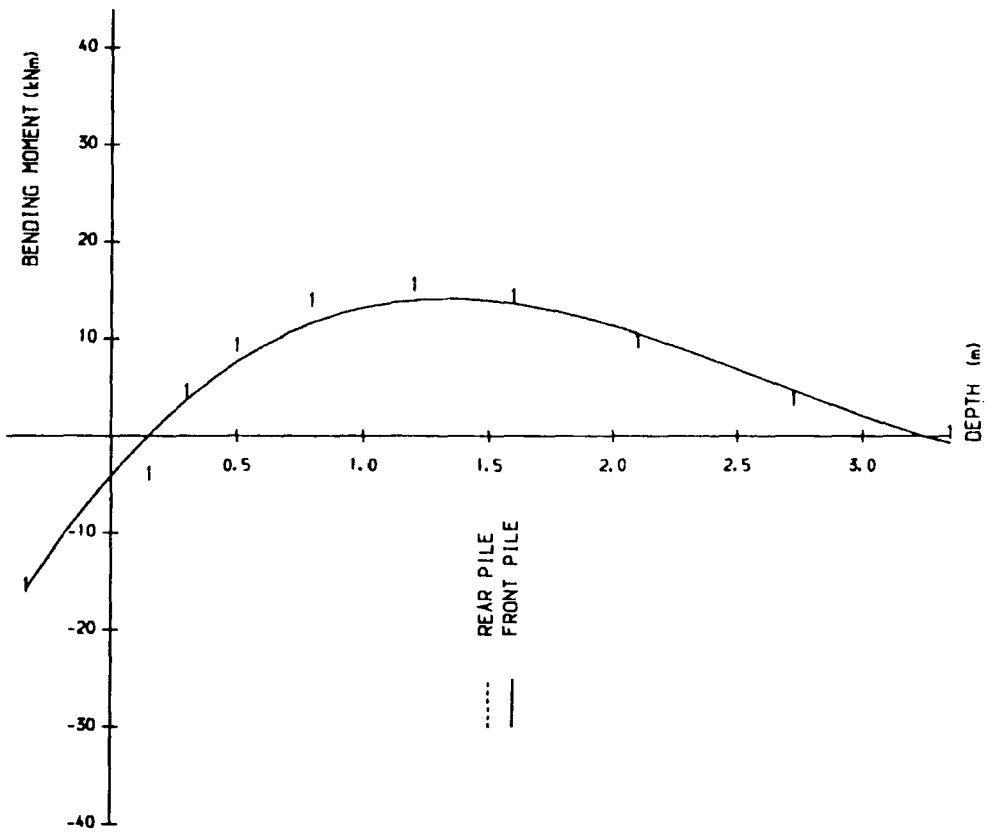(12 pile width spacing 400mm overhang)

Figure B.15e Bending moment diagram for two-pile group 3 pile width spacing 40mm overhang (reduced stiffness)